NREL/TP-230-4634 • UC Category: 243 • DE92010583

Hawaii Integrated Biofuels Research Program

Final Subcontract Report Phase III

Hawaii Natural Energy Institute
Honolulu, Hawaii

NREL technical monitor: R. Overend

National Renewable Energy Laboratory
(formerly the Solar Energy Research Institute)
1617 Cole Boulevard
Golden, Colorado 80401-3393
A Division of Midwest Research Institute
Operated for the U.S. Department of Energy
under Contract No. DE-AC02-83CH10093

Prepared under Subcontract No. XN-0-19164-1

May 1992

May 1992 • NREL/TP-230-4634

Hawaii Integrated Biofuels Research Program

Final Subcontract Report
Phase III

Hawaii Natural Energy Institute
Honolulu, Hawaii

On September 16, 1991 the Solar Energy Institute was designated a national laboratory, and its name was changed to the National Renewable Energy Laboratory.

Printed in the United States of America
Available from:
National Technical Information Service
U.S. Department of Commerce
5285 Port Royal Road
Springfield, VA 22161

Price: Microfiche A01
Printed Copy A23

Codes are used for pricing all publications. The code is determined by the number of pages in the publication. Information pertaining to the pricing codes can be found in the current issue of the following publications which are generally available in most libraries: *Energy Research Abstracts (ERA)*; *Government Reports Announcements* and Index (*GRA* and I); *Scientific and Technical Abstract Reports (STAR)*; and publication NTIS-PR-360 available from NTIS at the above address.

FOREWORD

Hawaii is uniquely suited to serve as a showcase for the production, conversion, and utilization of biofuels. Hawaii has no indigenous fossil fuels and spends more than $1 billion per year for imported oil to provide more than 90% of the state's total energy use. Almost two-thirds of this total energy is consumed in the transportation sector. Environmental conditions for plant growth in Hawaii are ideal year-round to maximize biomass yields. In addition, a wealth of experience and expertise in both herbaceous and woody crop production, as well as in thermochemical and biochemical conversion processes, exists in the agricultural industry and university community. Either methanol or ethanol from biomass may be the most cost-effective, indigenous, renewable liquid fuel that can be readily available to replace gasoline and diesel fuel for ground transportation in Hawaii.

The goal of the U.S. Department of Energy's (DOE) Hawaii Biofuels Program is to provide a technology data base for converting indigenous biomass feedstocks to liquid fuels for transportation and to electricity that can be used to produce liquid fuels. The objectives of this work are to develop an integrated set of strategies for the development of renewable energy technologies in Hawaii. This will be done primarily by evaluating the potential of several biomass resources, including sugarcane, energy cane, eucalyptus, and leucaena, for utilization in thermochemical and biochemical conversion processes to produce methanol and ethanol as transportation fuels. Intrinsic to the program objectives is a strong educational component to create an infrastructure of skilled personnel in biofuels systems research and development for technology transfer.

As you read this report you will also become aware of another aspect of integration of effort that is unique to the Hawaiian situation–the work of the Hawaii Natural Energy Institute (HNEI) is often in collaboration with other organizations such as the Hawaiian Sugar Planters' Association, or DOE's Oak Ridge National Laboratory and National Renewable Energy Laboratory.

This close coordination with other ongoing DOE research ensures that the work has broad-based applicability to the entire United States. This program also provides a vehicle for the coordination of activities within Hawaii. Because of Hawaii's unique location, it is also a center for Pacific Rim activities in renewables, which will result in significant technology transfer and training in biofuels activities.

CONTENTS

Page

Cooperators and Advisors vii

Introduction ix

Task 1—Biomass Resource Assessment and System Modeling 1

Task 2—Short Rotation Woody Biomass Research 4

Task 3—Energy Grasses 7

Task 4—Biomass Productivity Studies 9

Task 5—Fundamental Solvolysis Research 12

Task 6—Feedstock and Process Testing 14

Task 7—Postharvest Handling and Processing 17

Task 8—Study of Methanol Conversion Systems 20

Task 9—Biomass Plantation Studies 21

Task 10—Gasification of West Biomass in Supercritical Water 22

Appendix A—Biomass Resource Assessment and System Modeling

Land Available for Biomass Crop Production in Hawaii A-1

Identifying Land Potentially Available for Biomass Plantations in Hawaii A-29

Appendix B—Short Rotation Woody Biomass Research

Estimation of Biological Dinitrogen Fixation by ^{15}N-dilution in Tree Plantation B-1

Biomass Energy Plantation—Root Response to Coppicing and Tree Root Interaction B-18

CONTENTS (concluded)

Page

Appendix C—Biomass Productivity Studies

Establishment of Biomass-to-Energy Research Facilities C-1

Performance and Management of Fast-Growing Tropical Trees in Diverse Hawaiian Environments C-31

Appendix D—Fundamental Solvolysis Research

Productive and Parasitic Pathways in Dilute Acid-Catalyzed Hydrolysis of Cellulose D-1

Uncatalyzed Solvolysis of Whole Biomass Hemicellulose by Hot Compressed Liquid Water D-35

Appendix E—Feedstock and Process Testing

Chemical Equilibrium Computation for Gasification of Biomass to Produce Methanol E-1

Parametric Bench-Testing of an Indirectly Heated, Steam/Oxygen-Blown Biomass Gasifier E-9

Temperature Field and Reaction Zones in Biomass Gasification E-13

Experimental Analysis of Biomass Gasification with Steam and Oxygen E-17

Appendix F—Gasification of Wet Biomass in Supercritical Water

Pyrolytic Gasification of Glucose and Wet Biomass in Supercritical Water to Produce Hydrogen F-1

Hydrogen Production by Gasification of Wet Biomass in Supercritical Water F-180

COOPERATORS AND ADVISORS

BioEnergy Development Corporation

Thomas Crabb
Thomas Schubert
Aileen Yeh

University of Hawaii

James Brewbaker
James Fownes
Russell Yost
Susan Miyasaka

U.S. Department of Agriculture, Forest Service Institute of Pacific Islands

Robert Strand
Craig Whitesell
Tom Cole

State of Hawaii, Department of Land and Natural Resources, Forestry and Wildlife Division

Patrick Costales
Karl Masaki
Robert Meriam
Masayoshi Takaoka

U.S. Department of Agriculture, Soil Conservation Service

John Beddish
Robert Joy

Hawaiian Research, Ltd.

Peter Eichhorn

Hamakua Sugar Company, Inc.

M. Owen Sheets

Hawaiian Commercial & Sugar Company, Ltd.

Mae Nakahata
John Sakuma
Robert Warzecha

The Lihue Plantation Company, Ltd.

Mike Furukawa

Amfac/JMB-Hawaii, Inc.

Charles Wallace

Hawaiian Sugar Planters' Association

Win Bui
Stephen Haller
Yuki Inouye
Tsutomu Yamamoto
Frederick Meinzer
Geroge Mikami
Lance Santo
Alvin Tadani

Hawaii Natural Energy Institute

Vic Philips
Charles Kinoshita

INTRODUCTION

Experimental plots were installed at five Hawaiian sites beginning in 1985 to study the relative productivity of grasses and trees. The sites are located at Mountain View, Hawaii; Honokaa, Hawaii; Puunene, Maui; Hoolehua, Molokai; and Kilohana, Kauai. The sites represent upland and lowland conditions with a wide variation in soil and weather. Replicated small-plot species trials planted at 1x1 m and large-plot tree production trials planted at 2x2 m were established at each site. The yield of the trees is compared to the yield of either sugarcane (*Saccharum* spp. hybrids) or napiergrass (*Pennisetum purpureum*).

We previously presented the methods used in the studies and preliminary results in reports to the Department of Business, Economic Development and Tourism in 1986, 1987, and 1988. This report summarizes the work completed through 1989. Reports appearing in the appendix include the M.S. thesis of N. S. Dudley and a paper titled "Performance of Fast Growing Trees in Diverse Environments."

STATUS OF BIOMASS RESEARCH FACILITIES

Mountain View Site

Small-plot species trials

The small-plot species trial was completed in 1988; however, we have maintained portions of the site in order to collect vegetative propagation material from selected elite trees. Vegetative offshoots from the elite trees have been placed in micropropagation culture at the HSPA Experiment Station in Aiea. In addition, conventional vegetative cuttings from the trees are being grown at the Waiakea Experiment Station, University of Hawaii. We are hopeful that these potentially improved clones will be used in future biomass experiments.

Based on the percent survival rate and the dry weight of harvested trees, we have determined the yield per hectare for 24-month-old trees at the Mountain View site (Table 2). The most productive species was *Eucalyptus urophylla* at 35.9 tons/ha/yr. Height and diameter measurements for tree species are summarized by site in Table 5.

Large-plot production trials

Data collection continued for the large-plot production trials. Only tree diameter is reported since it was determined that tree height was not required to estimate biomass. Tree growth at the Mountain View site is compared to growth at other sites at 36 months after planting in Table 1. *Eucalyptus urophylla* and *E. grandis* performed better than *E. saligna*. *Eucalyptus* growth at Mountain View was better than at Honokaa and about the same as at Kilohana, the other upland sites. The equations developed for biomass estimation in the small-plot tests (Table 7) were not applicable to the large plots at 36 months because the diameters were out of the range achieved in the small-plot trials. New equations will be developed for larger trees at greater spacing when the large plots are harvested five years after planting (1991).

Sugarcane yield at Mountain View at 40.1 months was 3.2 tons/ha/mo (Table 3). At the conclusion of the experiment the yield of sugarcane will be compared to the yield of the trees in the large plots. Currently, the only tree harvest data are from the small plots where, at two years, the dry matter accumulation of the most productive tree, *E. urophylla*, was 2.9 tons/ha/mo. Sugarcane and tree dry biomass yields in the small plots were comparable; however, we estimate that the large-plot tree yields are considerably less productive than sugarcane at three years since the planting density of the trees is only one-fourth of that in the small plots. Larger per-tree biomass cannot compensate for the reduction in tree population. Actual tree dry matter production in the large-plot trials will not be determined until the termination of the experiment.

Kilohana Site

Small-plot species trial

The small-plot species trial was completed in 1988 and is being maintained to obtain propagation material of selected elite trees. As at the Mountain. View site, trees were felled to determine dry biomass produced per tree (Table 2). The Kilohana site was considerably more productive than the Mountain View site. The most productive species was *Acacia mangium* (51.2 tons/ha/yr). The highest yielding *Eucalyptus* was *E. urophylla* (47.4 tons/ha/yr). The higher yields at Kilohana reflect better growing conditions and better early weed control. A different picture emerged for the large-plot trials because better weed control was provided at the Mountain View site.

Large-plot production trial

Data collection continued in the large production plots. Although Kilohana is a better site for tree growth, performance was not better in the large plots compared to Mountain View. We believe the reason for the poorer-than-expected performance of *E. urophylla* and *E. grandis* in the large plots was related to less-than-adequate early weed control.

Sugarcane yield at Kilohana was 3.1 tons/ha/mo at 36 months (Table 3). At the conclusion of the experiment, tree dry biomass yield will be determined. At present we only have the harvest data from the small plots with which to estimate tree yield. The highest yield obtained was 4.3 tons/ha/mo with *Acacia mearnsii*. *Eucalyptus urophylla* produced 3.9 tons/ha/mo. Both tree species in the small plots produced considerably more biomass than the sugarcane. Large-plot tree biomass yields will be compared to grass yields at the five year harvest.

Hoolehua Site

Small-plot species trial

The small-plot species trial at the Hoolehua site was completed in 1988 and data were presented in the 1988 report to DBED. The most productive tree was *Eucalyptus camaldulensis*. Plots of selected species are being maintained as a source of seed.

Large-plot production trials

Data collection continues in the large plot production trials. Diameters for 36 month old trees are given in Table 1. Based on these data, the most productive tree is *Leucaena leucocephala* although *E. calmaldulensis* and *Casurina equisetifolia* are also growing at about the same rate.

Seed are being collected at the Hoolehua site from *L. leucocephala* for distribution to other researchers. Problems with the irrigation system have plagued the Hoolehua site. Water with high solids content has been supplied from a reservoir, but the filtration system installed has not been able to handle the water being delivered. Additional filters were installed; however, problems have persisted, affecting the growth of the trees. Harvest is planned for 1991.

Napiergrass production at the Hoolehua site was 4.1 tons/ha /mo, the highest of any grass species in the five test sites. Grass dry matter yields will be compared to tree dry matter yields at the termination of the experiment in 1991.

Puunene Site

Small-plot species trials

The Puunene small-plot trials were completed in 1988 and the data were presented in the 1988 report to DBED. The most productive species measured by height and diameter was *Eucalyptus grandis* although *Casurina equisetifolia* and *Leucaena leucocephala* appeared better adapted to the site. Mortality was considerably higher for the *Eucalyptus*. Several plants of two Aracruz eucalyptus clones planted at the site appeared especially well adapted and were placed into micropropagation for increase. This material, selected for sea level conditions in Brazil, appears well adapted to central Maui. The material has been placed into micropropagation and seed was collected. Tree height and diameter data are summarized in Table 5.

Large-plot production trial

Data collection is continuing in the large-plot production trial. Three-year diameter data are presented in Table 1. *Leucaena leucocephala* and *Casurina equisetifolia* performed better than *Eucalyptus grandis*. Although the average diameter for *E. grandis* was greater, mortality was also greater, indicating poor adaptability under the conditions of the experiment. There were problems with both over and under irrigation, and individual trees were infected with a fungus. Severe mortality was observed near the ends of the lines where water ponded. Harvest is planned for early 1991.

Problems with the sugarcane plots forced abandonment of the grass yield trial. Dry matter estimates of sugarcane cut for seed in the area of the trial are 3.4 tons/ha/mo; this value will be used in a comparison with tree dry matter yield at the termination of the experiment.

Honokaa Site

Small-plot species trial

The Honokaa trial was initiated a year later than the other trials; therefore, the two-year performance data were not published in earlier reports to DBED. Two-year height and diameter data are given in Table 4. The *Eucalyptus* species--*E. grandis, E. saligna, E. urophylla* and *E. robusta*--performed well at the site. *Casurina equisetifolia* adapted.poorly. *Acacia mangium* and *Acacia mearnsii* were well-adapted and deserve more attention as fast-growing biomass trees at this location. *Leucaena leucocephala* performed well at Honokaa compared to the other upland sites. Trees in the small-plot trial at Honokaa generally performed well, reflecting the location of the trial. The trial was located at the bottom of a hill and had a deep soil. Nutrients were washed into the site from the large-plot trials located above the site.

Large-plot production trials

Data collection continued in the large-plot trial. Tree diameter data for the Honokaa site are presented in comparison with data from the other sites (Table 1). Growth in the large plots was poor compared to the small plots for the reasons given above. All the *Eucalyptus* species tested performed equally in the large-plot production trials at the Honokaa site.

Sugarcane cv. H65-7052 grew poorly at the Honokaa site. The rate of dry matter production over a three-year period was 2.8 tons/ha/mo, lower than the other upland sites. Tree dry matter production will be compared to the sugarcane production at completion of the experiment.

SUMMARY OF THE SMALL-PLOT SPECIES TRIAL

Since the data for the small plot species trial have been spread over two progress reports, we have summarized the tree height and diameter data for the five sites (Table 5). A statistical analysis follows (Table 6). There was an interaction between species and location, indicating that the species performed

differently at the sites. At the upland sites of Mountain View, Kilohana, and Honokaa, *Eucalyptus grandis* performed better than *Casurina equisetifolia* or *Leucaena leucocephala*. At the lowland sites of Puunene and Hoolehua, *E. Grandis* performed about equal to *C. equisetifolia* and *L. leucocephala.*

DRY MATTER PREDICTION EQUATIONS

Equations based on tree diameter for prediction of dry matter in two-year-old trees were developed for the Mountain View site. Both total and stem-only biomass equations are presented in Table 7. Care must be taken to use the equations should not be used for trees older than two years of age and for trees growing under conditions varying from those where the relationships were developed.

Table 1. Tree Diameters in the Large-Plot Production Trials at 36 months*

Species	Tree Diameter (cm)				
	Mountain View	Kilohana	Hoolehua	Puunene	Honokaa*
E. grandis	8.4	8.2	---	8.4	6.6
E saligna	7.9	---	---	---	6.4
E. urophylla	8.6	8.7	---	---	6.5
E. calmaldulensis	---	---	8.2	---	---
C. equisetifolia	---	---	7.5	7.5	---
L. leucocephala	---	---	8.6	8.5	---

* Tree spacing 2x2 m.

Table 2. Mean Annual Dry Weight for Several Tree Species at the Mountain View and Kilohana Sites at 24 months

Species	Population (trees/ha)	Weight (kg/tree)	Yield (ton/ha/yr)
Mountain View			
Acacia mangium	6,675	3.09	10.3
Acacia mearnsii	7,025	7.25	25.5
Casurina equisetfolia	8,375	2.90	12.1
Eucalyptus grandis	9,375	6.25	29.3
Eucalyptus urophylla	8,675	8.29	35.9
Leucaena leucocephala	9,400	2.26	10.6
Kilohana			
Acacia mangium	7,125	4.41	15.7
Acacia mearnsii	7,775	13.16	51.2
Casurina equisetfolia	7,750	3.93	15.3
Eucalyptus grandis	9,275	8.83	40.9
Eucalyptus urophylla	9,500	9.99	47.4

Table 3. Grass Biomass Yields from Five Sites at Ages 33 to 40 months

Site	Grass	Age (mo.)	Dry Matter Yield (tons/ha) Total	Per Month
Mountain View	Sugarcane '68-1158'	40.1	129	3.2
Kilohana	Sugarcane '68-1158'	36	112	3.1
Puunene*	Sugarcane '65-7052'	---	---	3.4*
Hoolehua	Napiergrass 'banagrass'	35	144	4.1
Honokaa	Sugarcane '65-7052'	33.2	94	2.8

* Previously reported values were inaccurate. The current value is obtained from seed cane yields for Hawaiian Commercial & Sugar Company and dry matter values obtained previously.

Table 4. Height and Diameter for Trees at Honokaa at 24 months

Species	Height (m)		Diameter (cm)	
C. equisetifolia	3.3	e	1.9	d
E. grandis	10.1	a	5.8	a
L. leucocephala	6.1	ed	4.0	bc
A. mangium	5.8	e	5,6	a
A. mearnsii	8.0	bc	5.5	a
E. robusta	7.6	dc	5.0	ab
E. saligna	9.3	ab	5.9	a
E. urophylla.	8.9	abc	5.6	a

Means with same letter are not signifcantly different at 5% level.
Note: -Two-year data for the other sites were reported in the 1988 report to DBED.

Table 5. Summary of Tree Height and Diameter for Small Plots at 24 Months

Species	Mountain View	Honokaa	Puunene	Hoolehua	Kilohana
			Height (m)		
C. equisetifolia	4.3b	5.8b	5.6b	5.8b	5.0b
L. leucocephala	5.0b	6.1b	7.1a	6.1b	4.6b
E. grandis	9.2a	10.1a	7.9a	7.2a	10.8a
			Diameter (cm)		
C. equisetifolia	2.5b	1.9c	4.6b	3.6b	2.4b
L. leucocephala	2.9b	4.0b	5.5a	4.1a	2.0b
E. grandis	5.5a	5.9a	6.4a	4.3a	6.6a

Values in columns with same letter are not significantly different.
p = .05

Table 6. Combined Anova for Diameter for Three Tree Species at Five Locations

Source of Variation	D.F.	SS	MS	F
Location	4	26.2	6.55	11.4*
Replication	15	8.61	0.574	
Species	2	74.29	37.15	9.28*
Spp. X Location	8	32.00	4.00	13.42*
Pooled Error	49	17.58	298	

* Significant at 5% level.

Table 7. Equations Relating Biomass to Diameter Derived from Harvest at Mountain View Site

Species	Regression Equation	R^2
Acaia mangium		
DW stem	$0.02235 * D^{2.736}$	.88
DW total	$0.09815 * D^{2.142}$	.97
A. mearnsii		
DW stem	$0.0572 * D^{2.631}$	.97
DW total	$0.0585 * D^{2.729}$	.97
Casuarina equisetifolia		
DW stem	$0.7839 * D^{3.683}$	.83
DW total	$0.1168 * D^{2.524}$	.93
Eucalyptus grandis		
DW stem	$0.07425 * D^{2.294}$	.94
DW total	$0.06998 * D^{2.439}$	.94
E. robusta		
DW stem	$0.03943 * D^{2.636}$	.96
DW total	$0.04768 * D^{2.756}$	.98
E saligna		
DW stem	$0.06407 * D^{2.467}$	.94
DW total	$0.08765 * D^{2.443}$	.96
E. urophylla		
DW stem	$0.05836 * D^{2.563}$	.98
DW total	$0.07501 * D^{2.534}$	.98
Leucaena Leucocephala c.v. K636		
DW stem	$0.06744 * D^{2.694}$	.86
DW total	$0.10048 * D^{2.391}$	.89

BIOMASS RESOURCE ASSESSMENT AND SYSTEM MODELING
PHASE 3, TASK 1

Task Leader: Dr. Victor D. Phillips
Hawaii Institute of Tropical Agriculture and Human Resources
University of Hawaii at Manoa

Dr. Devindar Singh
Department of Agricultural Engineering
University of Hawaii at Manoa

Dr. M. Akram Khan
Department of Agricultural Engineering
University of Hawaii at Manoa

Ms. Wei Liu
Department of Agricultural Engineering
University of Hawaii at Manoa

Mr. Robert A. Merriam
Forestry Consultant
Kailua, Hawaii

The development of informational and analytical tools needed to plan for large-scale biomass feedstock production and its conversion to gaseous and liquid biofuels is the focus of this task. This requires the integration of field and laboratory data on biomass crop production and thermochemical conversion developed within the Hawaii Integrated Biofuels Research Program. The approach calls for developing and utilizing a land resource data base to match appropriate biomass species and sites according to land availability and land suitability. After potential biomass plantation species and sites are identified, appropriate biomass yield and economic models are developed to estimate the cost of feedstock production, including the costs of cultivation, harvesting, processing, storage, and transport. The resulting biomass yield and delivered cost data will ultimately be used in process-specific conversion and economic models to determine the cost of gaseous and liquid biofuels at the plant gate.

GENERAL TECHNICAL OR SCIENTIFIC PROGRESS

Methodologies for determining the suitability of potential lands for siting biomass plantations were developed in earlier stages of this project using biomass productivity data from field trials in Hawaii. Land suitability refers to the intrinsic and manageable environmental conditions of a given site necessary for a given species to achieve a targeted biomass yield economically. Using the Hawaii Natural Resource Information System (HNRIS) geographical information system and data base developed at the University of Hawaii, we extended the estimated yields and costs of promising biomass species in experimental plots to other land areas

where field trials have not been conducted. Some of these promising species are *Eucalyptus grandis*, *Eucalyptus saligna*, and *Leucaena leucocephala*. Subsequently, the critical issue of land availability for biomass crop production was addressed. Given the limited land area and intense competition for alternative land use in Hawaii, in Phase 3 we developed methodologies for evaluating how much and where land exists for potential biomass plantations. Land availability refers to the legal (e.g., zoning and ownership), economic (e.g., present land use versus alternative land uses, and rent or price), and environmentally sound (e.g., avoiding essential habitats for threatened and endangered species and sensitive cultural or archeological areas) access to parcels of land to establish biomass energy plantations. By integrating the results of our land suitability and land availability analyses, we hope to provide accurate information to private landowners, governmental officials, and other decision-makers regarding the biomass resource potential of Hawaii.

SIGNIFICANT ACHIEVEMENTS

A methodology for determining the availability of specific parcels of potential biomass energy plantations was developed (see appendix A). A classification system of five levels of land availability, ranging from "unavailable" under any conceivable situation to "available" with no concern identified in this study, was developed. The island of Molokai was featured as a case study of the methodology, with more than 38,000 ha identified as "available" (class 5) or "probably available" (class 4) for biomass plantations. We then extended the analysis to the islands of Hawaii, Kauai, and Maui (see appendix A). We believe that classifying the land in Hawaii into land availability classes for biomass plantations, coupled with the consideration of land suitability and economic constraints, will greatly facilitate realistic planning for Hawaii's biomass energy future.

SCIENTIFIC PUBLICATIONS

1. Phillips, V.D., R.A. Merriam, D. Singh, M.A. Khan, and P.K. Takahashi. 1991. "Land Available for Biomass Crop Production in Hawaii." Submitted to *Biomass and Bioenergy.*

2. Singh, D., V.D. Phillips, R.A. Merriam, M.A. Khan, and P.K. Takahashi. 1991. "Identifying Land Potentially Available for Biomass Plantations in Hawaii." *Agric. Systems* (to appear).

SUMMARY ASSESSMENT AND FORECAST FOR COMPLETION

As information becomes available, we are integrating biomass yield data within an economic framework to estimate the costs of biomass feedstock production, including establishment and maintenance, harvesting, and postharvesting processing and transport to specific conversion facility sites on a $/dry tonne delivered basis. The biomass feedstock production and economic models will be coupled to process-specific energy conversion and economic models for methanol and ethanol fuel production to provide an overall, integrated cost analysis for the manufacture of alternative energy products in Hawaii. We project that accurate

cost estimates for methanol from biomass, manufactured from locally grown feedstocks, could be made by the end of FY 1991. However, because this research task serves as the critical technical and economic link, integrating the biomass production and biomass conversion components of the Hawaii Integrated Biofuels Research Program (and perhaps other research and development (R&D) biomass energy initiatives), we envision the work continuing through the demonstration phases of methanol-, ethanol-, and electricity-from-biomass production as advanced technologies come on-line during the next 5 to 10 years.

SHORT ROTATION WOODY BIOMASS RESEARCH
PHASE 3, TASK 2

Task Leader: Dr. James L. Brewbaker
Department of Horticulture
University of Hawaii at Manoa

Mr. Robert A. Wheeler
Department of Horticulture
University of Hawaii at Manoa

GENERAL TECHNICAL OR SCIENTIFIC PROGRESS

The short rotation biomass (SRB) trial at the Waimanalo Experiment Station was established in fields I and K in January 1989. This trial was designed to provide woody biomass yield information for three species of nitrogen-fixing trees (NFT) (*Leucaena* hybrid, *Enterolobium cyclocarpum,* and *Paraserianthes falcataria*) and *Eucalyptus grandis,* a non-nitrogen-fixing tree. These species were planted in pure plots and 50/50 mixes of NFT and non-NFT. The trial was designed to evaluate coppice yields for pure plots and mixed plots under four harvest cycles (1, 2, 3, and 4 years) after an initial coppice 1 year after planting. The initial coppice of the SRB trial was made in December 1989. The subsequent 1-year growth was measured during Phase 3 in December 1990 at the time of the cutting of the 1-year coppice cycle plots. Results from these measurements were presented at the Short Rotation Biomass Conference in March 1991, in Idaho and are summarized in Table 1.

Table 1. Biomass yields per species and species mixes for 1-year growth before and after coppicing. Short Rotation Trial, Waimanalo Experiment Station.

Species/mixed Spp.	1 yr. precoppice (dry tonnes/ha)	1 yr. postcoppice (dry tonnes/ha)
Eucalyptus	9.3	7.1
Leucaena/Euc.	7.1	8.1
Falcataria	4.3	9.5
Leucaena	8.3	12.5
Falactaria/Euc.	8.2	13.5
Enterolobium/Euc.	10.6	14.3
Enterolobium	14.8	16.7

The results indicate that the superior initial rapid growth observed in *Enterolobium cyclocarpum* continues even after a coppice; however, the advantage is expected to diminish as the other species, which have slower initial growth, become established. Additionally, two separate studies were initiated within the SRB trial: one to evaluate the rates of nitrogen fixation

occurring within the mixed species plots and another to evaluate root biomass development and nodulation activity.

Nitrogen Fixation Study

During the initial establishment of the SRB trial, three replicates of the mixed species plots within the trial were selected for trenching. (See appendix B for more details about this study.) The boundaries of these plots were lined with heavy gauge plastic and backfilled. The plastic was used to prevent penetration of roots beyond the plot boundaries and limit penetration of nutrients into the plots. During Phase 3, N15 was applied to the plots, and leaf samples were collected using two different sampling intensities. Results from the analysis of these leaf samples indicated that the level of nitrogen fixation occurring within these plots, measured with the N15 dilution method, was accurately estimated by the simplified sampling strategy. This simplified method involved the random collection of small numbers of leaves from selected trees. This was an important discovery because traditional nitrogen-fixing estimation procedures are laborious and costly, limiting the extent to which the N15 dilution method can be used.

Short Rotation Root Biomass Study

During each December, both D. and K. Vogt visited the SRB trial to assist in the collection of soil cores for estimation of total tree root biomass and estimations of root nodulation activity by NFT. Initial root samples from the trial indicate significant differences in root biomass development and rates of nodulation. As the root biomass has grown, these relationships are becoming more significant in relation to the aboveground biomass accumulation. Initial species belowground biomass interaction has been limited, but these findings are expected to change as the root zones become more fully occupied.

SCIENTIFIC PUBLICATIONS

1. Baker, D., R.A. Wheeler, and M. Fried. 1990. Estimation of Biological Dinitrogen Fixation by N15-dilution in Tree Plantation: I Sampling Strategies and First Harvest Results for Three Legume Species (in press).

2. Vogt, D., K. Vogt, R. Wheeler, J. Brewbaker, and V. Phillips. 1990. "Biomass Energy Plantation-Root Response to Coppicing and Tree Root Interaction." *Belowground Ecology* 1(2).

SUMMARY ASSESSMENT AND FORECAST FOR COMPLETION

The upcoming December 1991 biomass measurements will be very important for both the aboveground and belowground biomass measurements. This will be the second regrowth after coppicing for the 1-year cycle plots, which are crucial for understanding sustainability of these short rotation systems. The second year after coppice plots will indicate whether the slower establishing canopy species are now substantially increasing their growth contribution as their

canopies and leaf areas have expanded. The species interaction between the NFT and the eucalyptus are becoming more pronounced. The eucalyptus in some plots have grown more than 8 m in the last year and a half. Results from the SRB trial are crucial for a comprehensive view of short rotation biomass plantations in Hawaii.

ENERGY GRASSES
PHASE 3, TASK 3

Task Leader: Dr. William C. Wells
Hawaiian Sugar Planters' Association
Aiea, Hawaii

Dr. K.K. Wu
Hawaiian Sugar Planters' Association
Aiea, Hawaii

GENERAL TECHNICAL OR SCIENTIFIC PROGRESS

Growth measurements and chemical analyses of cane samples were made on 6-month-old cane on Maui and 8-month-old cane on Kauai. As a group, hybrids from crosses between commercial sugarcane produced more dry biomass and more sucrose than hybrids produced from crosses between commercial sugarcane and *Saccharum spontaneum* clones.

Results of this study suggest that hybrids derived from crosses between commercial parents tend to have greater stalk weight, soluble solids content, sucrose content, dry biomass yield, and sucrose yield than hybrids derived from commercial cane ¥ *S. spontaneum* crosses. Differences in fiber content between the two groups are expected to be small.

The six hybrids with the highest biomass yield included hybrids produced from both commercial sugarcane ¥ commercial sugarcane and commercial sugarcane ¥ *S. spontaneum* crosses. The distribution of character values for the two groups of hybrids overlapped for all the characters studied.

SCIENTIFIC PUBLICATIONS

A paper describing the performance of hybrids derived from crosses between commercial canes and from crosses between commercial canes and *Saccharum spontaneum* clones is being prepared. It will be submitted to the journal *Sugar Cane* in 1991.

SUMMARY ASSESSMENT AND FORECAST FOR COMPLETION

The results of this study suggest that including a large number of commercial sugarcane × *S. spontaneum* crosses in the breeding program at the Hawaiian Sugar Planters' Association Experiment Station would not have much value in the production of either sugarcane or energy cane varieties. However, keep in mind that these results are based on a very limited number of hybrids, and that the growth measurements upon which the character values were calculated were

obtained at an early age. In a commercial sugar or biomass production program, cane would probably be harvested at 12 to 36 months of age. Data from older cane will be available from this experiment late in 1991, when an additional report will be prepared.

BIOMASS PRODUCTIVITY STUDIES
PHASE 3, TASK 4

Task Leader: Dr. Robert V. Osgood
Hawaiian Sugar Planters' Association
Aiea, Hawaii

Mr. Nick S. Dudley
Hawaiian Sugar Planters' Association
Aiea, Hawaii

The biomass productivity studies, funded primarily by the State of Hawaii, Department of Business, Economic Development and Tourism, with supplemental funding from the Hawaii Natural Energy Institute (HNEI) through the National Renewable Energy Laboratory (NREL), formerly the Solar Energy Research Institute, are divided into four areas of research: (1) small plot species productivity trials, (2) large plot yield trials, (3) clonal propagation method development, and (4) germplasm introduction. (For more details about this study, see appendix C.)

GENERAL TECHNICAL OR SCIENTIFIC PROGRESS

Small Plot Species Productivity Trials

Yield was determined 2 years after planting for three species of fast-growing tropical trees in closely spaced (1×1 m), small (0.01 ha), replicated plots. *Eucalyptus grandis* (EUC) was more productive than *Leucaena leucocephala* (LEU) and *Casuarina equisetifolia* (CAS) at all sites. LEU and CAS were the most productive in the warmer lowland sites, whereas EUC was most productive in the cooler upland sites. EUC produced 2.4 tonnes/ha/month at Mountain View, and 3.3 tonnes/ha/month at Kilohana, reflecting better site conditions and better initial weed control.

Large Plot Yield Trials

Adjacent to the small plots, but not comparable because of different agronomic practices, large replicated tree plots (0.4 ha) were planted at 2×2 m spacing. Thirty-six months after planting, *Eucalyptus urophylla* had the largest diameter in the unirrigated plots, and *Leucaena leucocephala* had the largest diameter in irrigated plots. Dry matter yield per hectare will be measured commencing in 1991.

Associated with each tree planting, a 0.4-ha block of either sugarcane (*Saccharum* spp. hybrid) or napiergrass (*Pennisetum purpureum*) was grown. Thirty-three to forty months following planting, grass yields ranged from 2.8 tonnes/ha/month at Honokaa, Hawaii, to 4.1 tonnes/ha/month at Hoolehua, Molokai. The grass plot yields will be compared to the tree plot yields 5 years after planting.

Vegetative Propagation of *Eucalyptus*

The biomass trials reported above were conducted with unselected seedling trees. However, to maximize the biomass yield potential, it is clear that the seedling populations should be screened and then vegetatively propagated on a large scale in commercial plantings. We have taken two approaches following tree selection: conventional vegetative propagation and micropropagation. Both techniques show promise in increasing the number of attractive trees. Micropropagation is of particular interest because maintenance of field blocks of propagation material is not required. Micropropagation techniques were developed for *Eucalyptus*, and we are presently increasing several selected elite trees with this method.

Introduction of New Germplasm

The germplasm currently available from *Eucalyptus* in Hawaii is narrowly based, and new material is required if yield improvements are to be achieved. New material from Indonesia and Australia was introduced during the current project, and plantings have been made in the Hilo region of Hawaii.

SIGNIFICANT ACHIEVEMENTS

In Phase 3, we performed the following:

1. Determined growth rates and yields of fast-growing trees in several locations.

2. Developed equations to describe biomass yield based on diameter measurement.

3. Developed procedures for micropropagation of *Eucalyptus* and conditions for optimum growth.

4. Introduced and began evaluating new *Eucalyptus* germplasm.

SCIENTIFIC PUBLICATIONS

1. Osgood, R.V. and Dudley, N.S. 1990. *Establishment of Biomass-to-Energy Research Facilities*. Report to the Alternate Energy Branch, Department of Business, Economic Development, and Tourism, State of Hawaii.

2. Dudley, N.S. May 1990. Performance and Management of Fast-Growing Tropical Trees in Diverse Hawaiian Environments. Master's Thesis, Department of Agronomy and Soil Science, University of Hawaii at Manoa.

SUMMARY ASSESSMENT AND FORECAST FOR COMPLETION

Significant progress has been made in the evaluation of several fast-growing trees for biomass production in varying environments. Selection and micropropagation of elite individual trees from seedling stands are recommended for future trials. The project is scheduled for completion in mid-1992, following the harvest of the large plot biomass yield trials. Comparisons will be made of the productivity of grass and tree crops, and an economic assessment will be presented.

FUNDAMENTAL SOLVOLYSIS RESEARCH
PHASE 3, TASK 5

Task Leader: Dr. Michael J. Antal
Hawaii Natural Energy Institute
Department of Mechanical Engineering
University of Hawaii at Manoa

Mr. William S. Mok
Hawaii Natural Energy Institute
University of Hawaii at Manoa

GENERAL TECHNICAL OR SCIENTIFIC PROGRESS

During Phase 3 of this program, a study detailing the reaction pathways of cellulose hydrolysis was completed. The study showed how the classical mechanism is unable to model low-temperature hydrolysis and provided a new explanation for the less-than-perfect yield of glucose from cellulose. A study of the solvolysis of biomass in hot, compressed liquid water was also completed. This work showed extremely high efficiency in extracting hemicellulose from 10 biomass species. This could lead to the development of a new method for biomass fractionation, which could enjoy many advantages over the established steam explosion process. (See appendix D for more details about this study.)

SIGNIFICANT ACHIEVEMENTS

Cellulose hydrolysis experiments were conducted in a percolating reactor at 34.5 MPa. A glucose yield of 71% of the theoretical maximum was obtained at 215° C with 0.05% by weight of sulfuric acid in the percolating solution. The classical model of glucose formation from cellulose followed by secondary sugar degradation did not describe the reaction chemistry under these conditions. A parasitic pathway that leads to the formation of nonhydrolyzable oligomer was discovered in the absence of acid. In the presence of acid, kinetic modeling of the measured, temperature-dependent rates of glucose evolution indicated that an acid-catalyzed parasitic pathway operates in competition with the glucose production pathway. No chemical changes were detected in the solid phase during the course of reaction.

Samples of six woody and four herbaceous biomass feedstocks were washed with compressed, liquid water at 200° to 230° C to determine the extent of hemicellulose solvolysis. In the case of sweet gum, 100% of the hemicellulose was solubilized in 1 min at 230° C and was completely recoverable as sugar after hydrolysis. Concurrently, up to 20% of the cellulose and 40% of the lignin were also solubilized. These values were almost invariant over wide ranges of temperatures and residence times. In most other cases, more than 90% of the hemicellulose was solubilized and was recoverable as sugar. High lignin content somewhat reduced the effectiveness of the solvolysis process.

SCIENTIFIC PUBLICATIONS

1. Mok, W.S., M.J. Antal, and G. Varhegyi. 1991. Productive and Parasitic Pathways in Dilute Acid-Catalyzed Hydrolysis of Cellulose. Submitted to I&EC Research for publication.

2. Mok, W.S. and M.J. Antal. 1991. Uncatalyzed Solvolysis of Whole Biomass Hemicellulose by Hot Compressed Liquid Water. Submitted to I&EC Research for publication.

3. Mok, W.S. and M.J. Antal. 1991. Method and Apparatus of Uncatalyzed Solvolysis of Biomass Hemicellulose. Invention disclosure filed with the University of Hawaii, Office of Technology Transfer and Economic Development, for consideration of a U.S. patent application.

SUMMARY ASSESSMENT AND FORECAST FOR COMPLETION

The commercial opportunities for utilization of the whole biomass solvolytic process could be large. Potential applications include the manufacture of ethanol and many other commercial products. Future developmental work will focus on the design, fabrication, and testing of a prototype reactor that can be readily scaled up to industrial size.

FEEDSTOCK AND PROCESS TESTING
PHASE 3, TASK 6

Task Leader: Dr. Charles M. Kinoshita
Hawaii Natural Energy Institute
University of Hawaii at Manoa

Mr. Yue Wang
Agricultural Engineering Department and
Hawaii Natural Energy Institute
University of Hawaii at Manoa

Methanol, produced from gasification of biomass, has the potential to make a substantial contribution to the future supply of alternative transportation fuels. Because methanol production is strongly affected by the composition of the gas used in its synthesis, it is important to determine, *a priori*, the gas composition for different gasification conditions and to identify the optimal gasification conditions for methanol synthesis. This research — a parametric analysis of biomass gasification leading to methanol production — attempts to achieve those goals. The objective of this research is the correlation of the thermochemical conversion behavior with theoretical predictions in biomass gasification leading to methanol production. (Appendix E contains more details about this study.)

GENERAL TECHNICAL OR SCIENTIFIC PROGRESS

A bench-scale, indirectly heated, fluidized-bed gasifier was designed and fabricated. A computer test system for biomass gasification was developed with automatic control of biomass feed rate, oxygen and nitrogen flow rates, and gasification temperature. The gasifier can be operated under different conditions — varying temperature, equivalence ratio, steam:biomass ratio, and residence time. Computer programs were developed to facilitate data acquisition and reduction. Mass balance calculations were performed to determine important performance indices for gasification. Experimental and related errors were analyzed.

Parametric tests for biomass gasification were performed to investigate the effects of varying key parameters on product gas composition and on gasifier performance. Parameters selected for variation in this study include (1) residence time, (2) equivalence ratio, (3) temperature, and (4) steam:biomass ratio. The trends in the test results agree with those predicted by equilibrium computations. Differences between actual and theoretical results are primarily due to the influences of chemical kinetics.

The following are salient findings of the parametric test:

1. Residence time has significant influence on the product gas composition and gasifier performance — the longer the residence time, the more the product gas composition approaches equilibrium.

2. The parametric test results for varying equivalence ratio have trends similar to those predicted by equilibrium computations. Gasification at lower equivalence ratio produces a gas with higher H_2 and CO concentrations and higher gross heating value, while gasification at higher equivalence ratio results in increased carbon conversion efficiency.

3. Gasification temperature plays an important role in biomass gasification, affecting chemical kinetics more than chemical equilibrium. The product gas composition approaches equilibrium as temperature increases. Gasifier performance improves significantly with increasing temperature.

4. The parametric test results indicate that the H_2:CO ratio increases as the steam:biomass ratio increases. Carbon conversion efficiency and gas yield increase and gross heating value decreases as the steam:biomass ratio increases.

Comparisons of theoretical computations with test data for different gasification systems indicate that none of the current gasification systems can produce a gas with near equilibrium composition without employing catalytic or secondary-oxygen reforming processes. In all cases, the actual concentrations of hydrogen and carbon monoxide are lower than theoretically predicted, whereas the actual concentrations of carbon dioxide and methane are higher than theoretically predicted. Increasing the residence time or gasification temperature would improve the extent of the gasification reactions, and thereby bring the product gas composition closer to equilibrium.

SIGNIFICANT ACHIEVEMENTS

In Phase 3, the following were achieved:

1. Design and fabrication of an indirectly heated, fluidized-bed gasifier.
2. Development of a computer test system for biomass gasification.
3. Parametric testing and analyses of biomass gasification.
4. Comparison of theoretical and experimental data.

SCIENTIFIC PUBLICATIONS

1. Kinoshita C.M. and Y. Wang. 1991. "Chemical Equilibrium Computation for Gasification of Biomass to Produce Methanol." *Energy Sources* 13: 361–368.

2. Wang, Y. and C.M. Kinoshita. 1991. "Parametric Bench-Testing of an Indirectly Heated, Steam/Oxygen-Blown Biomass Gasifier." *ISES Solar World Congress.*

3. Wang, Y. and C.M. Kinoshita. 1991. "Temperature Field and Reaction Zones in Biomass Gasification." *ASME Journal of Solar Energy Engineering* (in press).

4. Wang, Y. and C.M. Kinoshita. 1991. "Experimental Analyses of Biomass Gasification with Steam and Oxygen." *Solar Energy* (to appear).

SUMMARY ASSESSMENT AND FORECAST FOR COMPLETION

We have completed all planned work and have achieved all stated objectives on schedule in Phase 3. Follow-on work, pursuing new objectives, continues in Phase 4.

POSTHARVEST HANDLING AND PROCESSING
PHASE 3, TASK 7

Task Leader: Dr. Devindar Singh
Department of Agricultural Engineering
University of Hawaii at Manoa

The objectives of this task are to determine the drying rate of nitrogen-fixing tropical energy trees (*Leucaena*) under different weather conditions and to determine energy requirements for converting whole *Leucaena* trees into chips.

GENERAL TECHNICAL OR SCIENTIFIC PROGRESS

Drying experiments were conducted outdoors, in the open, at the Waimanalo Experiment Station, and in a specially constructed drying chamber. For in-field drying, five to six trees were cut every 2 weeks, bunched together, and left in the field to dry. Figure 1 displays the process of drying for bunches cut between November 11, 1990, and April 26, 1991. Figure 2 depicts the recorded evaporation at a nearby weather station. Drying was faster during warmer periods. In-field drying experiments were started on January 11, 1990, and are continuing.

A drying chamber was constructed to determine the drying rate of *Leucaena leucocephala* under controlled conditions to establish drying equations. Figure 3 displays the progress of drying in this chamber during one such test. Figure 4 depicts the controlled weather conditions that were maintained inside the chamber during the test period. These tests are also continuing.

SIGNIFICANT ACHIEVEMENTS

It was found that the following form of equation best describes the drying process:

$$Wt = 1/(a+b\ e^{-t/c})$$

where Wt is the weight of the tree bunch inside the drying chamber in kilograms, t is time in days, and a, b, and c are constants. For test no. 2, depicted in Figure 3, the values of the constant a, b, and c were 0.0296, –0.0055, and 100, respectively. The R^2 value was 0.9909.

To determine the energy requirements for converting whole *Leucaena* trees into chips, a commercial chipper was specially instrumented for power measurement. Measurements were made during chipping of freshly cut and field-dried logs of *Leucaena*. Figure 5 presents the results of one such test. Energy requirements were calculated from these measurements. Multiple regression of the data reveals that energy consumption for chipping *Leucaena* is strongly influenced by moisture content. It takes more energy to chip field-dried tree logs than green logs. The multiple regression equation is given below.

$$EC = 8.901 - 0.036 * MC - 0.064 * Dia - 0.140 * L$$
$$(0.590)\ (0.004)\qquad (0.085)\qquad (0.107)$$

where

EC = Energy consumption/weight, ft-lb/lb
MC =Moisture content, dry weight basis, %
Dia = Log diameter, cm
L = Log length, ft

The numbers in parentheses below the equation give the standard error of the coefficients above. The R^2 value for this equation was 0.76. Figure 6 depicts the relationship between the moisture content and chipping energy consumption per unit weight.

SUMMARY ASSESSMENT AND FORECAST FOR COMPLETION

The results from the drying chamber will be used to develop drying equations for *Leucaena* that predict the effect of different weather patterns on the drying rate of *Leucaena.* These equations will be verified by the in-field drying experiments. The equations developed will be used in conjunction with a geographic information system to predict the drying rate of *Leucaena* in different parts of the state of Hawaii.

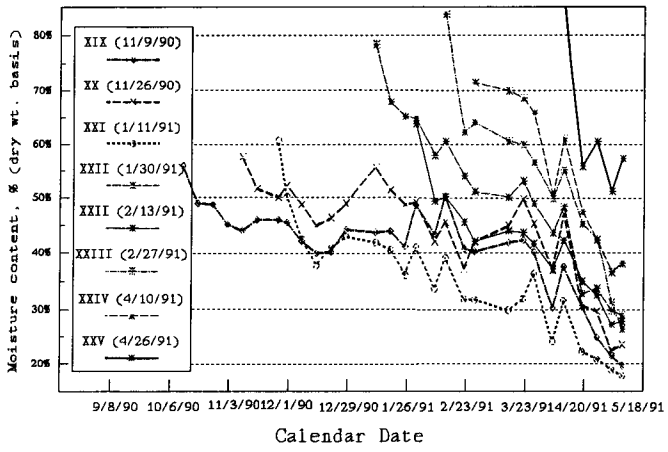

Figure 1. Field drying of *leucaena* tree bunches (experiments initiated from 11/9/90 to 4/26/91).

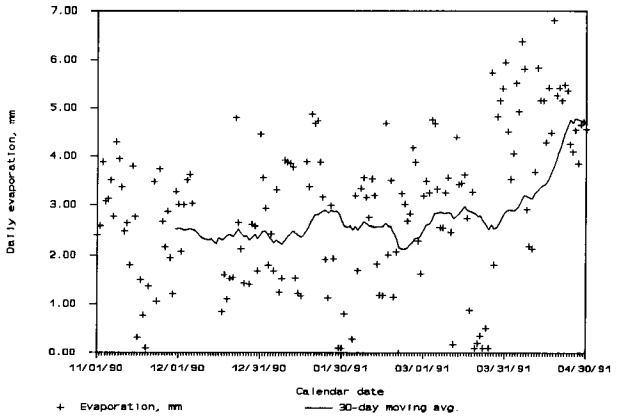

Figure 2. Evaporation at a nearby weather station during in-field drying of *leucaena.*

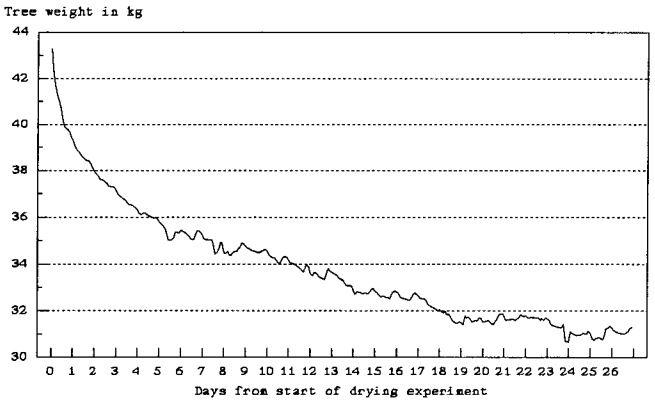

Figure 3. Chamber drying of *leucaena* under controlled conditions (test no. 2).

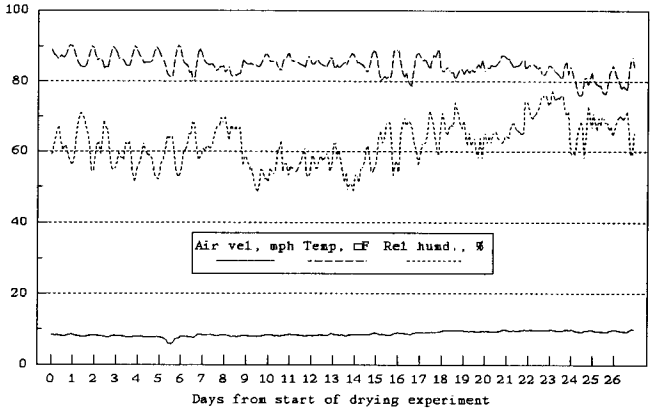

Figure 4. Environmental conditions in the drying chamber during *leucaena* drying (test no. 2).

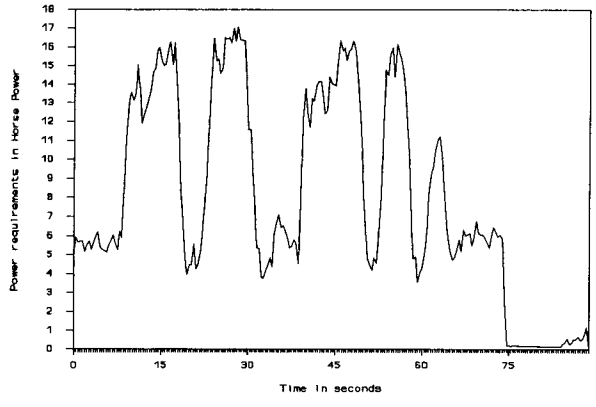

Figure 5. Power requirement curve for chipping field dried logs of *leucaena leucocephala.*

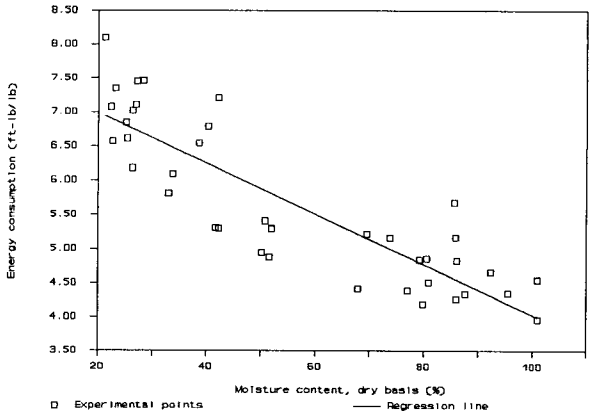

Figure 6. Chipping energy requirements for *Leucaena* tree logs as affected by moisture content.

STUDY OF METHANOL CONVERSION SYSTEMS
PHASE 3, TASK 8

Task Leader: Dr. Victor D. Phillips
Hawaii Institute of Tropical Agriculture and
Human Resources

University of Hawaii at Manoa

Dr. Devindar Singh
Department of Agricultural Engineering
University of Hawaii at Manoa

Dr. M. Akram Khan
Department of Agricultural Engineering
University of Hawaii at Manoa

Ms. Wei Liu
Department of Agricultural Engineering
University of Hawaii at Manoa

Mr. Robert A. Merriam
Forestry Consultant
Kailua, Hawaii

Task 8 is an ongoing continuation of Task 1.

BIOMASS PLANTATION STUDIES
PHASE 3, TASK 9

Task Leader: Dr. Victor D. Phillips
Hawaii Institute of Tropical Agriculture and
Human Resources
University of Hawaii at Manoa

Dr. Devindar Singh
Department of Agricultural Engineering
University of Hawaii at Manoa

Dr. M. Akram Khan
Department of Agricultural Engineering
University of Hawaii at Manoa

Ms. Wei Liu
Department of Agricultural Engineering
University of Hawaii at Manoa

Mr. Robert A. Merriam
Forestry Consultant
Kailua, Hawaii

No work was performed on this task. Because contingent cost-matching for task 9 did not materialize, approval was granted to reallocate funds budgeted for this task to procure electrophoresis equipment required in other work.

GASIFICATION OF WET BIOMASS IN SUPERCRITICAL WATER
PHASE 3, TASK 10

Task Leader: Dr. Michael J. Antal
Hawaii Natural Energy Institute
Department of Mechanical Engineering
University of Hawaii at Manoa

Ms. Supaporn Manarungson
Department of Mechanical Engineering
University of Hawaii at Manoa

Mr. William S. Mok
Hawaii Natural Energy Institute
University of Hawaii at Manoa

GENERAL TECHNICAL OR SCIENTIFIC PROGRESS

Substantial improvements were made to the existing supercritical flow reactor (SCFR) system to accommodate the severe reaction conditions that prevail. The improvements, identified in earlier phases of this research as necessary for effective gasification of wet biomass, include the fabrication of a new Hastelloy coil reactor (0.32 mm OD x 0.14 mm ID x 6.2 m long) immersed in a fluidized sand bath to provide the necessary temperature (650°C) and residence time (up to 2 min), a magnetic driven pressurized stirred tank (500 mL) to hold the reactants, and a water displacement balloon system to feed the wet biomass slurry. A new gas sampling system was also developed, which collects all of the effluent from the reactor over a measured time period.

After shakedown testing of the new equipment and establishing agreement with earlier data, experiments were conducted for a systematic study of the effects of temperature, residence time, quenching, feedstock type, and concentration.

SIGNIFICANT ACHIEVEMENTS

The major products of wet biomass gasification in supercritical water (SCW) are hydrogen and carbon dioxide, followed by carbon monoxide and methane. Small amounts of ethene and ethane are also observed. The following reactions are used as a working model for wet biomass gasification in SCW:

$$C_xH_yO_z + (x - z)\ H_2O \rightarrow x\ CO + \{x + (y/2) - z\}\ H_2$$

$$x\ CO + x\ H_20 \rightarrow x\ H_2 + x\ CO_2$$

Employing this model, the theoretical hydrogen yield (mole of hydrogen per mole of feed carbon) is $2 + (y/2x) - z/x$, which for gracilera (algae), water hyacinth, and kelp are 2.22, 2.29, and 1.47, respectively (x, y, z were determined from proximate analyses performed by an independent commercial laboratory).

Our experimental results show that gasification efficiency (carbon in gas:carbon in feedstock) increases with increasing temperature and residence time. In the temperature range of 550° to 600° C, longer residence times enhance H_2 and CO_2 formation and reduce the formation of CH_4 and CO. At 650° C, longer residence time shifts the product distribution from H_2 and CO to CH_4 and CO_2, in molar proportions that are consistent with the following reactions:

$$CO + 3\ H_2 \rightarrow CH_4 + H_20$$

$$2\ CO + 2\ H_2 \rightarrow CH_4 + CO_2$$

When the product stream is rapidly quenched, the above reactions are inhibited somewhat, resulting in improved yields of hydrogen. In the limited range of low initial concentrations (0.7 to 4.9 g/L) studied so far, no significant effect of concentration on gas yield was observed. Of the three wet biomass feedstocks studied, gasification of kelp results in hydrogen yields that are near the theoretical limit, about twice the yields from water hyacinth and algae. Complete experimental data are available in appendix F.

SCIENTIFIC PUBLICATIONS

1. Manarungson, Supaporn. May 1991. Pyrolytic Gasification of Glucose and Wet Biomass in Supercritical Water to Produce Hydrogen. Master's Thesis, Department of Mechanical Engineering, University of Hawaii at Manoa.

2. Manarungson, S., W.S. Mok, and M.J. Antal. 1990. Hydrogen Production from Gasification of Wet Biomass in Supercritical Water. Presented at the World Hydrogen Energy Conference 8, Honolulu, Hawaii, July 22-27, 1991.

3. Antal, M.J., W.S. Mok, and S. Manarungson. 1990. Hydrogen Production by Pyrolytic Gasification of Wet Biomass in Supercritical Water. Invention disclosure filed with the University of Hawaii, Office of Technology Transfer and Economic Development, for consideration of a U.S. patent application.

SUMMARY ASSESSMENT AND FORECAST FOR COMPLETION

The efficiency of the wet biomass gasification process is clearly demonstrated by the achievement of close to theoretical yield of hydrogen from kelp. In parallel with a commercial assessment of the process, further fundamental research is needed to study the effect of higher reactant concentrations, wall and catalytic effects, and product gas separation by controlled pressure reduction.

Appendix A

Biomass Resource Assessment and System Modeling

LAND AVAILABLE FOR BIOMASS CROP PRODUCTION IN HAWAII

Victor D. Phillips [1,2], Devindar Singh [2], Robert A. Merriam [3], M. Akram Khan [2], & Patrick K. Takahashi [1]

Hawaii Natural Energy Institute [1], 2540 Dole Street, Holmes Hall 246, University of Hawaii at Manoa, Honolulu, Hawaii, USA 96822
Department of Agricultural Engineering [2], University of Hawaii at Manoa
Forestry Consultant, Kailua, Hawaii [3]

ABSTRACT

A geographical information system is being used to facilitate the evaluation of land available for consideration as biomass production areas in Hawaii. The methodology developed by the authors to assess land availability was tested previously in a case study of the island of Molokai. This paper extends the analysis to the islands of Hawaii, Kauai, Maui, and Molokai. The results are applicable to private landowners, governmental officials, and others involved in land use decisions on the potential of biomass crops. The concept of establishing a statewide "Strategic Biomass Reserve" of dedicated energy plantations to offset interruptions in imported oil supply is proposed.

KEYWORDS

Biomass crops; energy plantation; *eucalyptus*; *leucaena*; methanol.

INTRODUCTION

Because Hawaii is over 90% dependent on imported oil at an annual cost exceeding $1 000 000 000 and extremely vulnerable to interruptions in oil supply or to international oil price shocks, alternative energy supplies, preferably based on abundant, indigenous, renewable resources, are critically needed. Almost two-thirds of the state's total annual energy use is in the transportation sector, with approximately half of this amount as gasoline and diesel fuels for surface transportation. Hawaii, by taking advantage of its ideal conditions for plant growth, has the potential to grow sufficient biomass feedstocks for conversion to alcohol fuels to make the state self-sufficient in surface transportation fuels (Fig. 1). Only 5% of the land area would be required to produce the 3 300 million liters (880 million gallons) per year of methanol to replace all the gasoline and diesel fuel consumed annually [1,2].

The Hawaii Natural Energy Institute (HNEI) and the Department of Agricultural Engineering (AGENG) at the University of Hawaii are presently working to identify the necessary 67 000 hectares that are both suitable (i.e., soil, climate, and productivity) and potentially available (i.e., appropriate zoning, ownership, present use, and lack of environmental or other constraints) (Fig. 2) [3,4].

Previous efforts have focused on the use of the Hawaii Natural Resource Information System (HNRIS), a geographic information system and database developed at AGENG, for evaluating cropland suitability [5]. The extensive soil, climate, and other information available in the system makes HNRIS time- and cost efficient for such a purpose.

In this paper HNRIS is used to evaluate land availability based on the environmental and/or social characteristics of four Hawaiian islands — Hawaii, Kauai, Maui, and Molokai. Each of these islands has had extensive agricultural and forestry operations historically and holds promise for future short-rotation biomass crop production, especially as traditional crops such as sugarcane and pineapple decline and the trend towards crop diversification increases. The results of this study are the identification of land potentially available to grow biomass energy crops.

In parallel, analyses based on methodologies to determine land suitability (i.e., matching biomass species requirements with appropriate environmental and soil conditions to achieve a targeted biomass yield economically in Hawaii) are in progress [3,6]. The ultimate goal of this biomass resource assessment is to identify land *potentially available and suitable* for biomass crop production and conversion to liquid or gaseous fuels to enhance the energy, economic, and environmental security of the state [7].

HAWAII'S LAND SITUATION [8]

Hawaii is renowned as a tropical paradise, resplendent with beautiful beaches, a comfortable climate, the world's most unique biota, and inhabited by a cultural mix of some one million people. Hawaii's appeal has, as in other gathering places, resulted in an exponential increase in its population and the attendant infrastructure, services, and trappings of an affluent society, which require ever greater amounts of energy and natural resources. So great is the demand for the basic necessities of space, energy, food, and construction materials, plus such lifestyle amenities as automobiles and golf courses, that intense competition for alternative land uses (with associated inflated land prices) exists. Brief descriptions of the geographical and demographic features of the four islands used in this study are provided below.

Hawaii County

The island of Hawaii is not only the largest island in the state, it is also the only single island county (discounting off-shore rocks). It is also the only growing island, with lava reaching the shore and enlarging Hawaii's coastline on an almost daily basis for the last several years. With an area of 1 044 806 hectares, the "Big Island" is almost twice the combined size of all the other islands in the state. It measures 150 by 122 kilometers. It was formed by five volcanoes, two of which are still active and one of which is currently adding to its size. Ka Lae (South Point) is the southernmost point in the United States.

There are wide variations in temperature and rainfall on the Big Island, due primarily to the range of elevation and location rather than to seasonal change. Along the coastal regions the climate is warm and semitropical. Average temperatures in Hilo range from about 21·7° C in February to about 24·4° C in August. In the higher areas the temperatures are lower due to adiabatic cooling. The average annual temperature at the 3 355 meter level of Mauna Loa is 6·7° C. Frost occurs above the 1 220 meter level, and snow often covers the almost 4 270 meter peaks of Mauna Loa and Mauna Kea in the winter. Rainfall varies markedly between regions of the county, ranging from an annual rainfall of 762 cm at the 915 meter level northwest of Hilo to 15 cm near Kawaihae. The annual average has been 328 cm for the city of Hilo and 64 cm for Kailua-Kona.

Agriculture is one of the major industries in Hawaii County. Sugar acreage is expected to decline substantially during the next decade from the 26 993 hectares in 1988.

However, Hawaii is expected to remain the state's largest sugar producer; three sugar companies produced 2 087 000 Mg of unprocessed cane in 1988. Big Island cattle ranches, including Parker Ranch, one of the largest singly-owned ranches in the United States, produce over 65% by volume of the livestock marketed in the state. The bulk of the state's macadamia nuts and papaya and all of its Kona coffee are grown on Hawaii. Farm crops, including diversified agriculture, tropical foliage and flowers, and livestock sales totaled nearly $200 million in 1988.

The estimated resident population of Hawaii County in 1989 was 122 300. Hilo is the county seat and the fourth most populous city in the state. In addition to Hilo, the main population center of the county is the Kailua-Kona area on the leeward side.

City and County of Honolulu

The City and County of Honolulu is the center of business and government for the state of Hawaii. Although smallest of the four counties in geographical size, it has approximately three-fourths of the state's population. Legally, the City and County of Honolulu includes most of the northwestern Hawaiian islands, stretching beyond Niihau to tiny Kure Atoll, 2 201 km from the Honolulu Airport. For most purposes, the City and County of Honolulu is defined as the island of Oahu, an area of 153 846 hectares. The other islands and reefs included in the county add about 777 hectares to the total area.

Honolulu's climate is close to ideal with very little seasonal variation. In Waikiki, the center of tourism, the average temperature is 22·2° C in the coolest month of February and only 27·2° C in the warmest month of August. Average annual rainfall ranges from 50·8 cm in the low, dry leeward areas to about 381 cm in the wetter residential areas near the mountains. Higher elevations may receive nearly 762 cm.

Although the City and County of Honolulu is the most industrialized area in the state, one-fifth of its land is used for agricultural purposes. In 1989 there were two pineapple plantations and one pineapple cannery; two sugar cane plantations and one sugar refinery. The total value of all crops and livestock produced on Oahu was over $175 million in 1988.

The resident population of the City and County of Honolulu was estimated to be 841 600 in mid-1989, including military personnel stationed or home-ported on Oahu. Tourism added another 60 000 persons, on average, each day.

Kauai County

Kauai County includes the islands of Kauai and Niihau, the two northernmost islands of the Hawaiian chain, plus the tiny uninhabited island of Lehua. Geologically Kauai is the oldest of the major islands of Hawaii and was the site of the first Hawaii landing by Captain James Cook in 1778. Kauai is the state's third largest but least populous of the four counties. The "Garden Island" of Kauai is 142 295 hectares in area while Niihau and uninhabited Lehua are together 18 130 hectares. Lihue, the county seat, is on Kauai and is 166 km from Honolulu. It is the center of major economic activities for the county and the location of the two most important transportation facilities, the Lihue Airport, which handles most the passenger arrivals to Kauai, and Nawiliwili Harbor, a deep water port.

Niihau is a privately-owned, entirely rural island and is only accessible to the general public through helicopter landings at uninhabited sites. Niihau is the last

community in Hawaii where native Hawaiians, secluded from the outside world, preserve the heritage of old Hawaii.

Kauai has an almost ideal climate with average temperatures near the coast of 21·7° C in February and March, and 26·1° C in August and September. Cooler temperatures in mountain areas such as Kokee offer a pleasant contrast. Rainfall usually varies widely depending on location with the county. The summit of Waialeale is the wettest spot in the United States with an average rainfall of 1 128 cm per year. At the Poipu Beach resort area on the southern coast, rainfall averages only 89 cm per year.

Sugar is the major agricultural product on Kauai. Unprocessed cane was valued at more than $50 million in 1988. Other crops and livestock brought the total to nearly $65 million.

Kauai County had an estimated total resident population of only 51 000, including about 200 on Niihau.

Maui County

Maui County is the second largest county in the state. Made up of four major islands — Maui, Lanai, Kahoolawe, and most of Molokai — it has a total land area of 300 958 hectares, approximately the size of Rhode Island. Kalawao County (a state-administered hospital settlement for Hansen's disease patients) on Molokai is an additional 3 445 hectares. The island of Maui is the largest (188 707 hectares) of the four islands. It is the center of trade and tourism and the seat of the county government.

On Molokai's 67 573 hectares the long standing pineapple growing and packing industry was phased out in 1988. There has been some increase in tourism, diversified agriculture, and cattle ranching, but Molokai continues to have the highest unemployment in the state.

Raising pineapple is currently the major industry on the privately-owned 36 364 hectares of Lanai, but construction of two hotels and the promised phase out of pineapple is a dramatic, and for many people, traumatic change.

Uninhabited Kahoolawe (11 655 hectares) has been used as a bombing range by the U.S. Navy and Marine Corps, although it is hoped by many that such abusive use will no longer continue.

Throughout Hawaii the weather is generally warm and pleasant year-round; Maui is no exception. Variations in temperature and rainfall depend more on location than season. The average temperature in Lahaina in February is 21·7° C, and in August and September, 25·5° C. At the other extreme, the top of Haleakala (elevation of 3 057 meters), temperatures occasionally drop below freezing in the winter, and snow covers the summits for brief periods. Rainfall in Lahaina averages 38·1 cm per year, while portions of the East Maui rainforest receive more than 635 cm.

Sugar and pineapple are the two major crops in the county, followed by dairy and beef herds. The three sugar companies on Maui — one of them among the largest cane sugar plantations in the country — occupied more than 16 997 hectares in 1988. Pineapple is grown on another 8 499 hectares. With Hawaii's only commercial winery and a valuable diversified agriculture and flower industry, the gross value of agriculture in Maui County is almost $140 million per year.

With an estimated 97 100 residents in 1989, Maui (including Kalawao) is the third most populous county in the state. With visitors included, the 1988 de facto population was 125 000.

LAND AVAILABILITY ANALYSIS CRITERIA

Land availability refers to the legal (e.g., zoning and ownership), economic (e.g., present land use versus alternative land uses and rent or price), and environmentally and socially acceptable (avoid native forests and essential habitats for threatened and endangered species) access to parcels of land for the purpose of establishing biomass energy plantations [3,6]. It includes a recognition that the potential for commercial development of biomass energy plantations is more a land use problem than a technological challenge [9]. There is limited land area in our island state, which significantly aggravates conflicts over alternative land uses and inflates land prices.

The use of much land in Hawaii is constrained by laws and administrative rules. We have assumed land to be available if the landowner is freely able to consider the establishment of a biomass plantation on the land. We have made no effort at this stage to evaluate profitability or the wishes of any owner(s) to engage in commercial biomass production for energy or other purposes. A statewide system of land use zoning has existed in Hawaii since the early 1960s. The land ownership patterns stem from a variety of sources, including the history of Hawaii as a kingdom, republic, territory, and finally as a state, and the early acquisition of lands by plantation agriculture companies.

Land Use Zoning

The state of Hawaii is the only state with a statewide system of land use zones, designated as the Conservation, Agricultural, Urban, and Rural Districts. Boundaries of the districts are determined by an appointed body, the Land Use Commission, following strict legislative guidelines (Table 1). The regulation of uses of Conservation District lands rests with the State Board of Land and Natural Resources. Each of the four counties regulates the Agricultural District lands under guidelines established by the Land Use Commission. Other parcels, zoned for urban or rural (small farm lot) uses, are regulated by each county. Thus, the zone in which a parcel lies has a great deal to do with its availability. All urban and rural zoned lands are considered unavailable for any conceivable use as biomass plantations and are therefore eliminated from our analysis. In this study only lands classified within the Conservation and Agricultural Districts are considered as potential sites.

Land Ownership

Land ownership, or its effective control through long-term leases or other legal mechanisms, is a major factor in land availability in Hawaii (Table 2). Of slightly more than 1 664 200 hectares in the state, nearly 623 700 hectares are owned by federal, state and county governments. The 136 800 hectares in federal ownership are almost exclusively in the National Park or National Wildlife Refuge systems or under the control of the U.S. Department of Defense. The 480 900 hectares of state lands are put to many uses, including agricultural and commercial and lands set aside for environmental protection. The 6 030 hectares of county lands are principally in park and watershed parcels, generally unavailable for any other use.

A special segment of lands often included in totals of state land are the Hawaiian Homes Lands. These lands, some 77 700 hectares, are set aside by federal and state laws for the benefit of native Hawaiians and their descendents. Private land ownership is dominated by large landowners. The six largest owners control nearly a quarter of the state. Only 6% of the land is controlled by owners with fewer than 2 000 hectares. These latter owners are not individually identified in HNRIS.

LAND AVAILABILITY METHODOLOGY

The methodology used to derive the land availability statistics and maps has been reported previously [10]. The key to analytical success using the methodology was the maximum utilization of an available database with land ownership and land zoning information, minimum input of new data, and a relatively simple scale of availability categories (Table 3).

The principal elements of the rationale behind the system are threefold: (1) public lands are less available for intensive culture than are private lands (this is certainly true for an outside entrepreneur, if not for government itself); (2) lands zoned as Conservation are less available than lands zoned as Agriculture; and (3) shoreline lands are almost always not available. An availability scale was derived from the recognition of these assumptions (Table 4).

Preliminary Analyses

The matrix illustrated in Table 3 was applied to the information (base data) in HNRIS to determine the initial availability rating for the islands of Hawaii, Maui, Kauai, and Molokai (Figures 3, 4, 5, and 6). As can be seen, lands presently zoned for agricultural purposes are generally available. What is surprising to many people is the fact that lands now forested are largely unavailable, even where tree crops are the focus. This is because conservation-zoned lands are valued primarily for factors other than their capacity to produce wood fiber.

Environmental Concerns

Following this analysis, information not previously contained within the HNRIS system was added to the database so that an indication of lower availability was recorded. The new information (modified data) was primarily about environmentally sensitive areas.

Environmental concerns about land use in Hawaii are not the purview of any single governmental agency or private group. Relatively large blocks of land are protected for environmental purposes by the federal and state governments and by private parties. Information about such areas has not been centralized and is not readily available. It was decided that the nature of this study did not require specific, parcel-by-parcel information regarding the character of the protection provided or the agency or party providing the protection. It was only important to know that it was, in fact, in a protected status. For planning purposes, a private reserve is just as "unavailable" as a national park [10].

LAND AVAILABILITY RESULTS

Land "Available" and "Probably Available" Statewide

The initial analysis using base data stored in HNRIS indicated clearly that there is nothing inherent in the Hawaiian land use situation that would preclude the consideration of a biomass plantation of up to several tens of thousands of hectares in any of the counties. However, we have chosen to eliminate from early consideration the islands of Oahu, because of its dominant urban orientation, and Lanai, because of its single ownership and low rainfall. No uninhabited island is considered. Results of the follow-on analysis using modified data of land "*probably available*" and "*available*" in classes #4 and #5 respectively are presented below.

Hawaii

As the largest of the islands it is not surprising that Hawaii has the largest land area available or probably available for consideration as biomass plantation sites. Of the 472 700 hectares identified, all but 75 100 hectares are in the Agricultural District.

Kauai

Kauai has 68 600 hectares identified as probably available, which includes 54 700 hectares zoned for agriculture.

Maui

Maui has the second largest land area considered available or probably available for biomass plantations, 109 800 hectares. Of this potential all but 13 100 hectares are in the Agricultural District.

Molokai

Molokai has 32 400 hectares in these two availability classes; all but 200 hectares are zoned for agriculture.

Land "Unavailable" and "Availability Unlikely" Statewide

As mentioned earlier, the principal reason for developing this land availability methodology is the recognition that the HNRIS database does not contain information that specifically identifies several large categories of environmentally sensitive areas. It is not surprising then, that when those areas are considered, many more hectares of each of the islands are classified as unavailable or unlikely to be available. The increase statewide in these two categories combined was 382 900 hectares, from 175 800 to 558 700 hectares.

Hawaii

On Hawaii 413 100 hectares are both unavailable and unlikely to be available. Without the addition of information about environmentally sensitive areas, only 127 900 hectares would have been identified in classes #1 and #2. Slightly more than 50 000 hectares of the total are zoned for agriculture. Much of this land is located in the new Hakalau National Wildlife Refuge where efforts are underway to re-establish a native forest on lands grazed for almost 100 years, in areas recommended for critical habitat for threatened and endangered birds, and in areas controlled by the federal government for military training.

Kauai

Kauai, although smaller than Maui by about one-third, has 57 700 hectares in the two least available categories.

Maui

Some 67 100 hectares on Maui, largely in the Haleakala National Park and adjoining East Maui watersheds as well as in the West Maui Mountains, are in the unavailable and unlikely to be available categories. Of this amount, about one-half (30 900 hectares) was recognized before the new data input.

Molokai

Molokai has roughly one-third of its area, or 20 800 hectares, in the two least available categories. As anyone familiar with the island could attest, the entire Kaulapapa-North Shore area is clearly unavailable due to its historical preservation as a leper colony and inaccessibly rugged terrain. In addition to the environmental concerns expressed in the Protected subzone of the Conservation District, Natural Area Reserves, and Reserves of the Natural Conservancy, access is severely limited throughout the area because there is no motorized access to much of the area. About 5 800 hectares were identified as unavailable in the initial data processing.

Land "Possibly Available" Statewide

Another large block of land statewide, consisting of 173 800 hectares in the Conservation District and 63 600 hectares in the Agricultural District, is identified as possibly available in land availability class #3. As noted in the definition, it is recognized that there are significant environmental concerns on many of these lands. These lands should be considered unavailable in the initial planning process, but some parcels might be available to complete the plantation area required for a nearby or adjacent project on lands identified as available.

STRATEGIC BIOMASS RESERVE

As biomass crops continue to grow over time, a valuable stockpile of energy feedstocks accumulates. One dry Mg of biomass, roughly equal to one barrel of oil on an energy basis, can provide approximately 1 000 kWh of electricity or 1 456 liters (386 gallons) of methanol fuel with full conversion of carbon from biomass to methanol via hydrogen addition. At a production rate of 34 dry Mg hectare $^{-1}$ year $^{-1}$, which has been achieved with fast-growing, high-yielding grasses like sugarcane and banagrass as well as trees such as *eucalyptus* and *leucaena* in Hawaii, potentially 23 239 000 dry Mg of biomass could be grown on 683 500 hectares of land identified on four islands as available and probably available.

This amount of biomass feedstocks could be converted into 23 239 million kWh of electricity or 34 000 000 000 liters (8 966 million gallons) of methanol annually. For comparison, the total annual consumption of electricity and liquid fuels for surface transportation in the state are approximately 9 000 million kWh and 3 300 million liters (880 million gallons) of methanol fuel equivalent, respectively. Even if only 10% of this potential biomass energy plantation area (68 350 hectares) meets strict land suitability and economic requirements for commercial biomass energy production, over 25% of the

state's electricity use (2 324 million kWh) or virtually all of its liquid fuels for surface transportation (3 384 million liters or 897 million gallons of methanol) could be provided locally, with positive economic and environmental results.

We are in the process of conducting land suitability and economic analyses for biomass energy plantations in the state. By integrating the results of our land suitability and land availability analyses, we hope to provide private landowners, governmental officials, and other decision-makers with accurate information on the biomass resource potential of the state of Hawaii. Conceptually, a *Strategic Biomass Reserve* for the state of Hawaii of dedicated energy plantations to offset interruptions in imported oil supply or crippling oil price shocks is possible. Our study indicates that as much as 683 500 hectares are potentially available (this land area is presently being evaluated for its suitability in achieving targeted biomass crop yields economically) to enhance the energy, economic, and environmental security of the state of Hawaii.

REFERENCES

1. Phillips, V.D., Neill, D.R., & Takahashi, P.K. (1988). Methanol plantations in Hawaii. In *Proceedings of the VIII International Symposium on Alcohol Fuels*, Tokyo, Japan, November 13–16.

2. Takahashi, P.K., Neill, D.R., Phillips, V.D., & Kinoshita, C.M. (1990). Hawaii: an international model for methanol from biomass. *Energy Sources* **12**, 421–28.

3. Phillips, V.D., Singh, D., Khan, M.A., & Takahashi, P.K. (1989). Geographical information system for site selection of biomass energy crops. In *Hawaiian Sugar Technologists' 1989 Annual Report*, Honolulu, Hawaii.

4. Phillips, V.D., Merriam, R.A., Takahashi, P.K., Singh, D., & Khan, M.A. (1990a). Methodology for determining land availability for biomass plantations in Hawaii. Presented at the *U.S. Department of Energy Biofuels and Municipal Waste Technology Division Management Review Meeting FY1990*, Washington, D.C., April 11–12.

5. Liang, T. & Khan, M.A. (1986). A natural resource information system for agriculture. *Agricultural Systems* **21**, 81–105.

6. Phillips, V.D., Singh, D., Khan, M.A., & Takahashi, P.K. (1990b). Matching species and sites for biomass plantations in Hawaii. In *Proceedings of the IGT Energy from Biomass and Wastes XIV Conference*, Paper #8, Lake Buena Vista, Florida, January 29–February 2.

7. Hawaii Natural Energy Institute (1990). *Final Report of the Hawaii Integrated Biofuels Research Program- Phase 2*, ed. V.D. Phillips. Subcontract No. XK-8-18000-1 to the Solar Energy Research Institute/U.S. Department of Energy.

8. Hawaii, State of (1990). *Facts and Figures* (Series on state of Hawaii and each county of the state). Department of Business, Economic Development and Tourism, Honolulu, Hawaii.

9. Phillips, V.D. & Merriam, R.A. (1988). Biofuel production in Hawaii: appropriate species, sites, sizes, and scenarios. Presented at *Hawaii Forestry and Wildlife Conference*, Hilo, Hawaii, February 10–13.

10. Singh, D., Phillips, V.D., Merriam, R.A., Khan, M.A., & Takahashi, P.K. (1991). Identifying land potentially available for biomass plantations in Hawaii. In *Annual Report of the Hawaii Integrated Biofuels Research Program--Phase 3*, ed. V. Phillips. Subcontract No. XN-0-19164-1 to the Solar Energy Research Institute.

11. Hawaii, State of (1989). *Data Book*. Department of Planning and Economic Development, p. 651.

LAND AVAILABLE FOR BIOMASS CROP PRODUCTION IN HAWAII

V. D. Phillips, D. Singh, R. A. Merriam, M. A. Khan, & P. K. Takahashi

Tables

1. Estimated Area of Land Use Districts on Hawaii, Kauai, Maui, and Molokai, 1989 (Source: Hawaii 1989)

2. Estimated Area of Land Ownership on Hawaii, Kauai, Maui, and Molokai, 1989 (Source: Hawaii 1989)

3. Conceptual Land Availability Classes for Biomass Plantations

4. Initial Land Availability Classification for Biomass Plantations by Location, Ownership, and Land Zoning Districts

5. Summary of Land Availability for Biomass Crops on Agricultural and Conservation District Lands on Hawaii, Kauai, Maui, and Molokai

6. Comparison of Results using Base Data and Modified Data on Land Availability for Biomass Crops on Hawaii, Kauai, Maui, and Molokai

LAND AVAILABLE FOR BIOMASS CROP PRODUCTION IN HAWAII

V. D. Phillips, D. Singh, R. A. Merriam, M. A. Khan, & P. K. Takahashi

Figures

1. Land Required to Grow Methanol for Surface Transportation in Hawaii

2. Biomass Decision Tree

3. Land Availability for Biomass on Hawaii, Base Data

4. Land Availability for Biomass on Kauai, Base Data

5. Land Availability for Biomass on Maui, Base Data

6. Land Availability for Biomass on Molokai, Base Data

7. Land Availability for Biomass on Hawaii, Modified Data

8. Land Availability for Biomass on Kauai, Modified Data

9. Land Availability for Biomass on Maui, Modified Data

10. Land Availability for Biomass on Molokai, Modified Data

Table 1
ESTIMATED AREA (HECTARES) OF LAND USE DISTRICTS ON HAWAII, KAUAI, MAUI, AND MOLOKAI, 1989

Island	*Total*	*Urban*	*Rural*	*Conservation*	*Agricultural*
Hawaii	1 041 440	17 900	250	526 460	496 830
Kauai	143 220	5 010	500	80 430	57 280
Maui	188 510	6 950	1 520	78 360	101 680
Molokai	67 100	1 010	760	20 140	45 190
Total	1 440 270	30 870	3 030	705 390	700 980

Source: Hawaii 1989, p. 172

Table 2
ESTIMATED AREA (HECTARES) OF LAND OWNERSHIP ON HAWAII, KAUAI, MAUI, AND MOLOKAI, 1989

Island	*Total*	*Federal*	*State*	*County*	*Private*
Hawaii	1 010 540	93 020	330 790	520	586 210
Kauai	142 170	1 280	61 100	250	79 540
Maui	181 370	10 880	41 420	630	128 440
Molokai	69 170	90	19 260	110	49 710
Total	1 403 250	105 270	452 570	1 510	843 900

Source: Hawaii 1989, p. 172

Table 3
CONCEPTUAL LAND AVAILABILITY CLASSES FOR BIOMASS PLANTATIONS

Land Availability Class	*Description*
Unavailable (1)	Not available under any conceivable situation
Availability unlikely (2)	Little likelihood of availability, extremely sensitive
Availability possible (3)	Possibly available in part, but major concerns exist
Availability probable (4)	Probably available in part, but concerns exist in specific areas
Available (5)	No concern identified in this study

Table 4
INITIAL LAND AVAILABILITY CLASSIFICATION FOR BIOMASS PLANTATIONS BY LOCATION, OWNERSHIP, AND LAND ZONING DISTRICTS

		Land Availability Class	
Location	*Ownership*	*Conservation District*	*Agricultural District*
Shoreline	All	1	2
Not shoreline	Federal	2	3
Not shoreline	Hawaiian Homes Commission	2	3
Not shoreline	State	3	4
Not shoreline	Private	4	5

Table 5
SUMMARY OF LAND AVAILABILITY FOR BIOMASS CROPS ON AGRICULTURAL AND CONSERVATION DISTRICT LANDS ON HAWAII, KAUAI, MAUI, AND MOLOKAI

	Land Availability Class (Hectares)*				
Island	*(1) Unavailable*	*(2) Unlikely*	*(3) Possible*	*(4) Probable*	*(5) Available*
Hawaii					
Agricultural	7 800	42 800	36 600	74 000	323 500
Conservation	252 300	91 100	122 400	75 100	0
Kauai					
Agricultural	400	1 300	8 100	11 100	43 600
Conservation	45 600	3 900	23 800	13 900	0
Maui					
Agricultural	400	2 100	9 600	9 800	87 000
Conservation	49 000	6 300	22 300	13 100	0
Molokai					
Agricultural	1 800	0	9 600	900	32 800
Conservation	14 600	400	5 300	800	0
Total					
Agricultural	10 400	46 200	63 900	95 800	486 900
Conservation	361 500	101 700	173 800	102 900	0

* Rounded to nearest 100 hectares

Note: Lands zoned urban and rural are included in land availability class #1 (unavailable).

Table 6
COMPARISON OF RESULTS USING BASE DATA AND MODIFIED DATA ON LAND AVAILABILITY FOR BIOMASS CROPS ON HAWAII, KAUAI, MAUI, AND MOLOKAI

	Land Availability Class (Hectares)*				
Island	*(1) Unavailable*	*(2) Unlikely*	*(3) Possible*	*(4) Probable*	*(5) Available*
Hawaii					
Base Data	8 000	100 600	319 200	242 200	355 500
Modified Data	260 100	133 900	159 000	149 100	323 500
Kauai					
Base Data	2 100	2 500	56 400	46 900	43 700
Modified Data	46 000	5 200	31 900	25 000	43 600
Maui					
Base Data	2 900	18 500	53 700	36 900	87 400
Modified Data	49 400	8 400	31 900	22 900	87 000
Molokai					
Base Data	2 000	2 100	27 600	2 000	32 400
Modified Data	16 400	400	14 900	1 700	32 800
Total					
Base Data	15 000	123 700	456 900	328 000	519 000
Modified Data	371 900	147 900	237 700	198 700	486 900

* Rounded to nearest 100 hectares

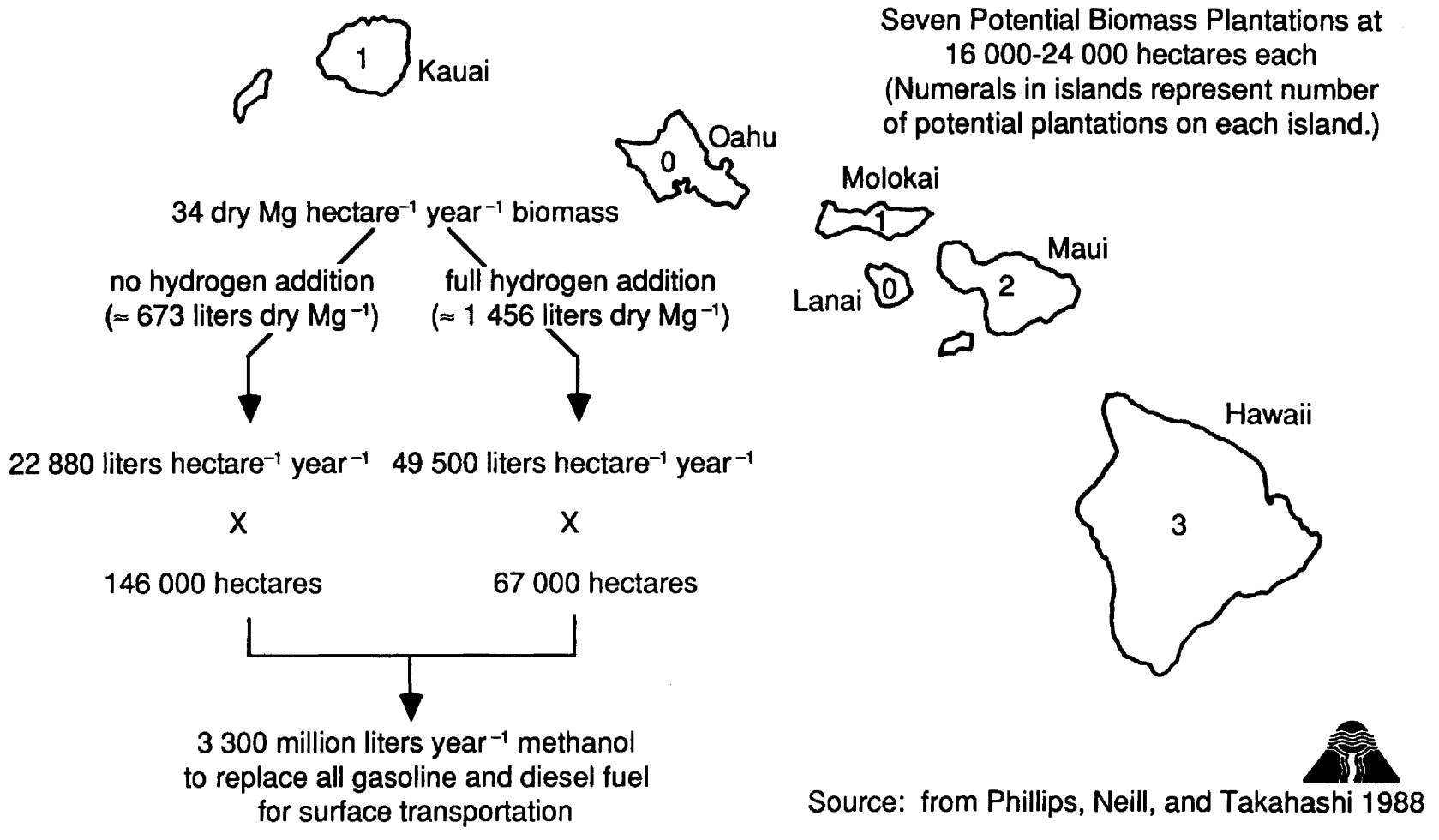

Fig. 1. Land Required to Grow Methanol for Surface Transportation in Hawaii

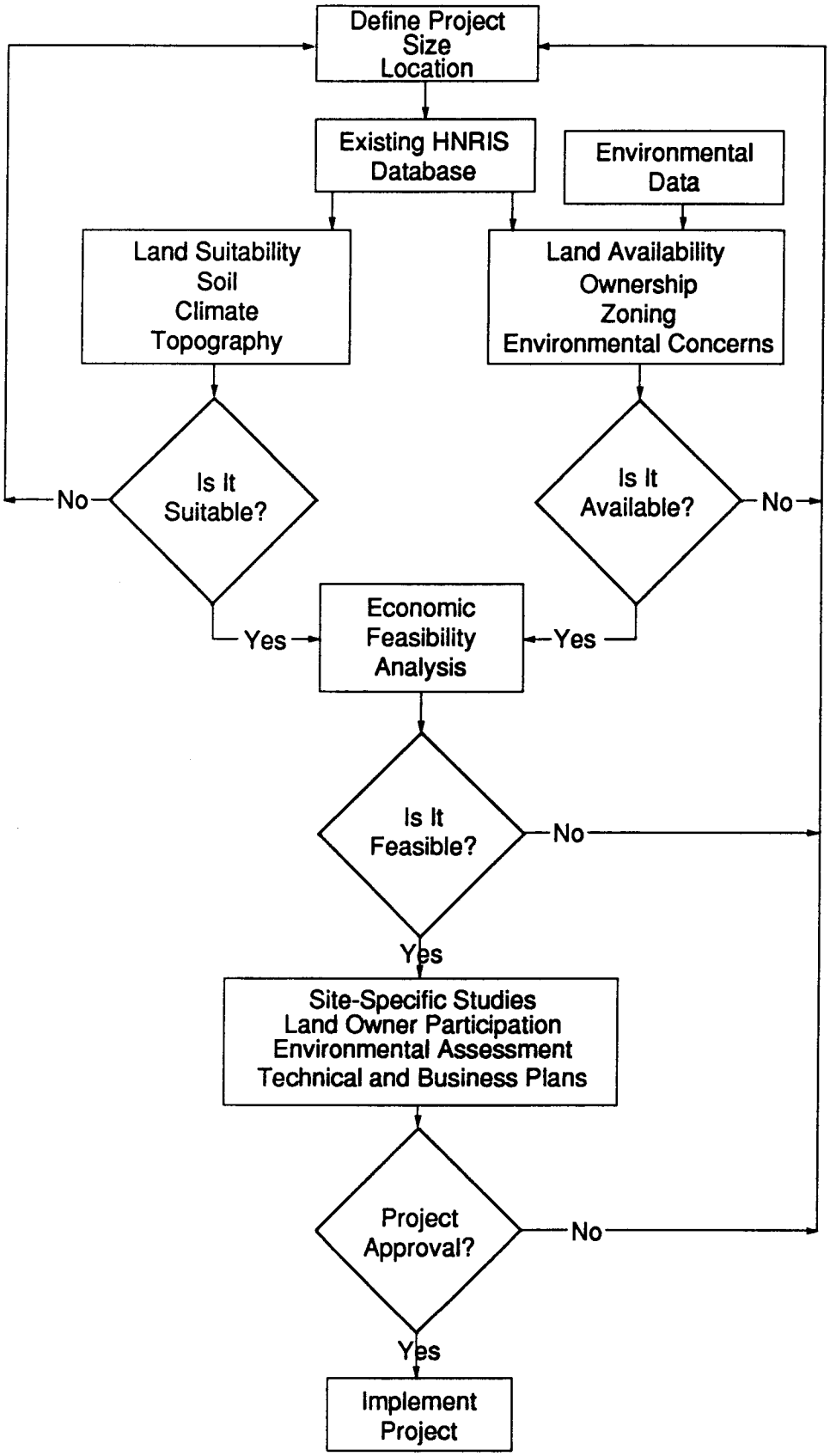

Fig. 2. Biomass Decision Tree

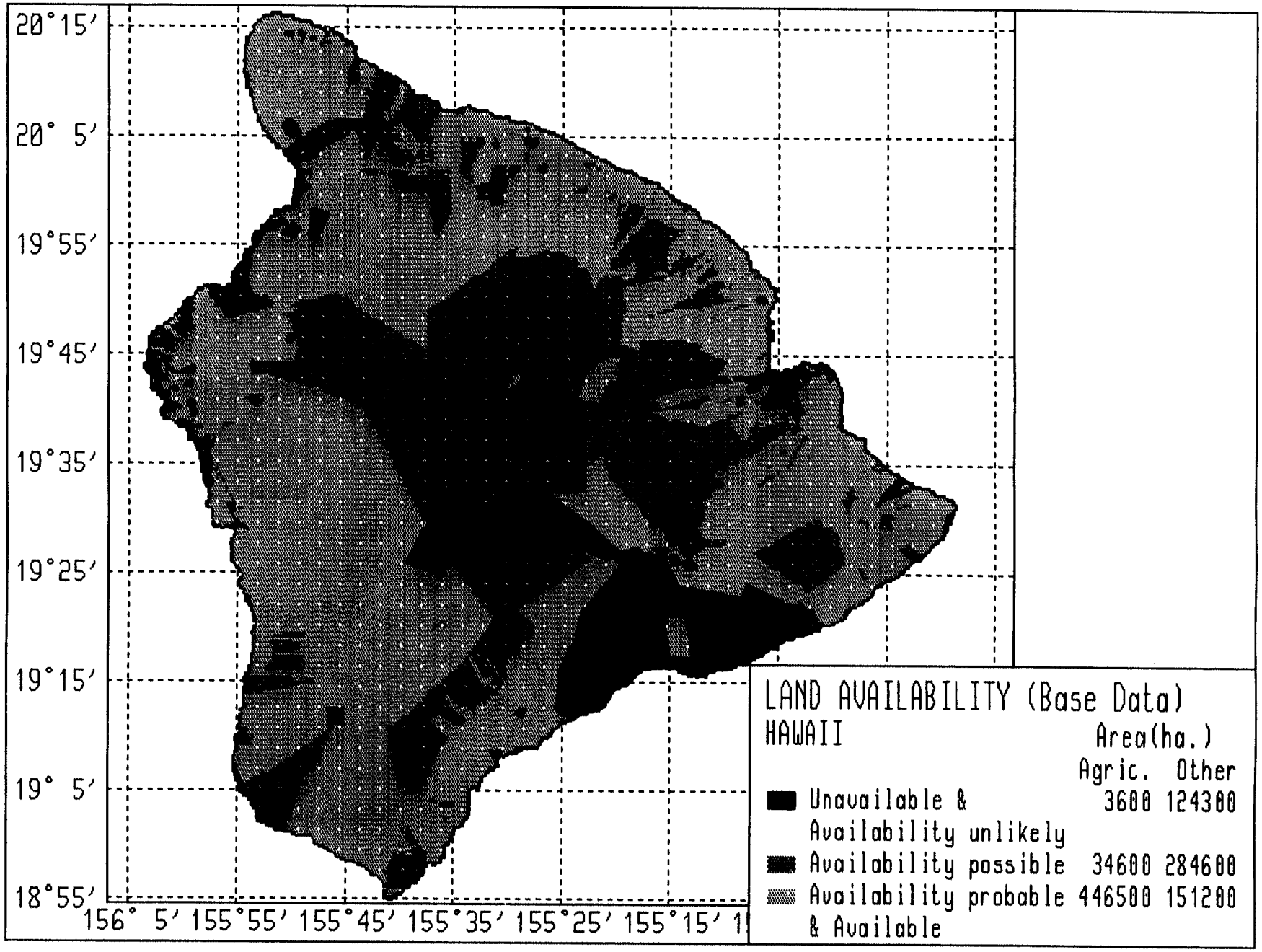

Fig. 3. Land Availability for Biomass on Hawaii, Base Data

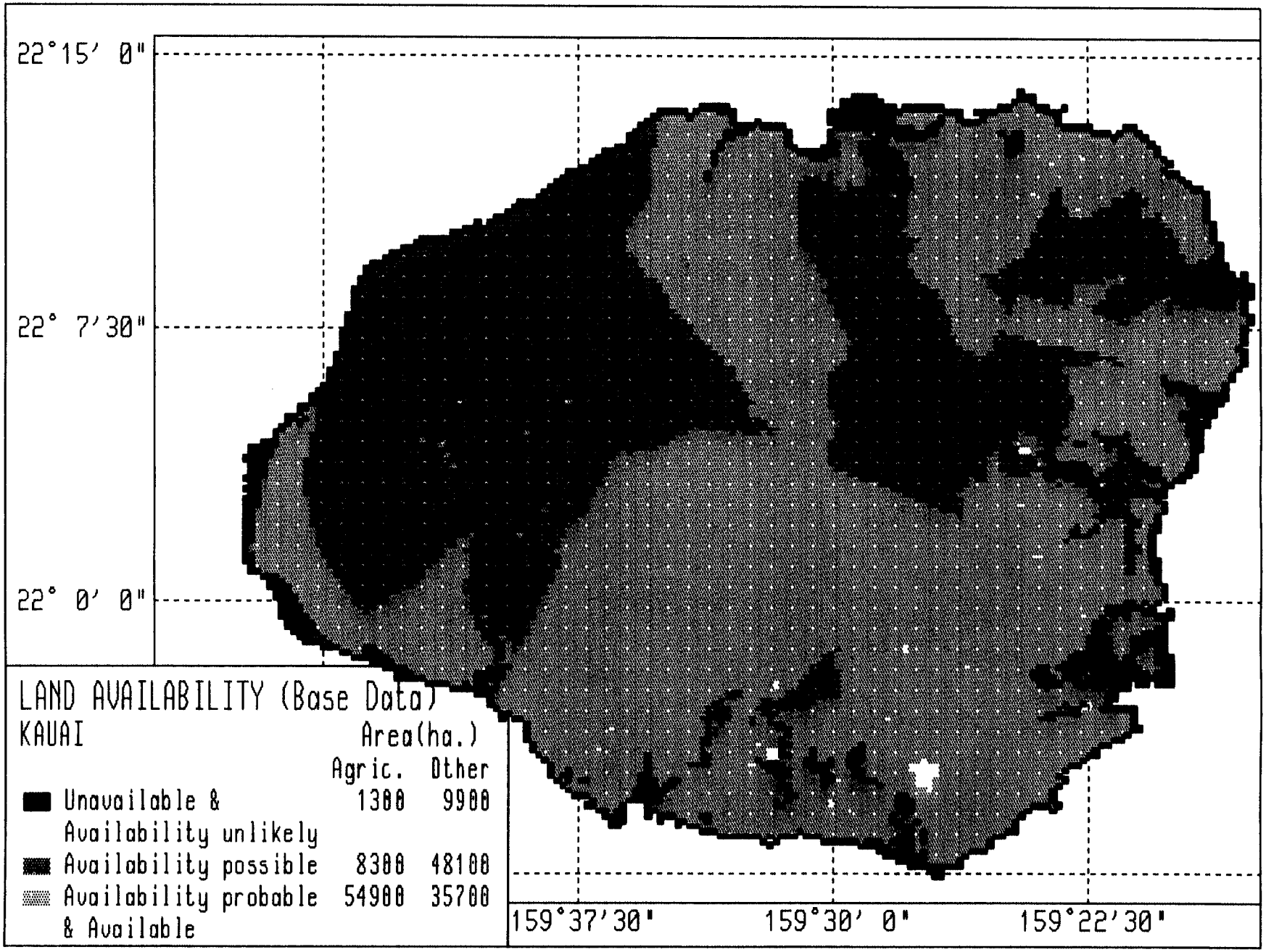

Fig. 4. Land Availability for Biomass on Kauai, Base Data

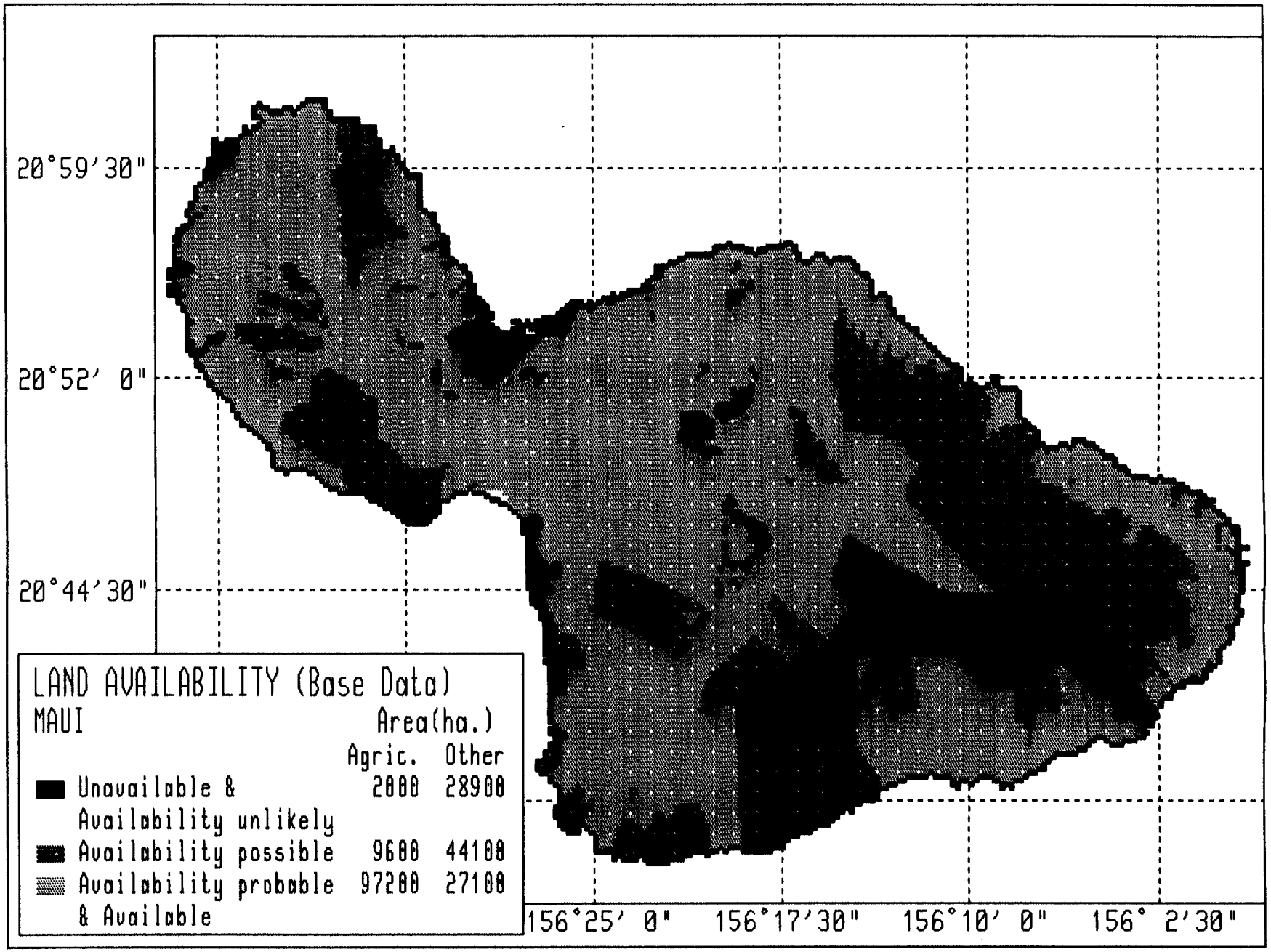

Fig. 5. Land Availability for Biomass on Maui, Base Data

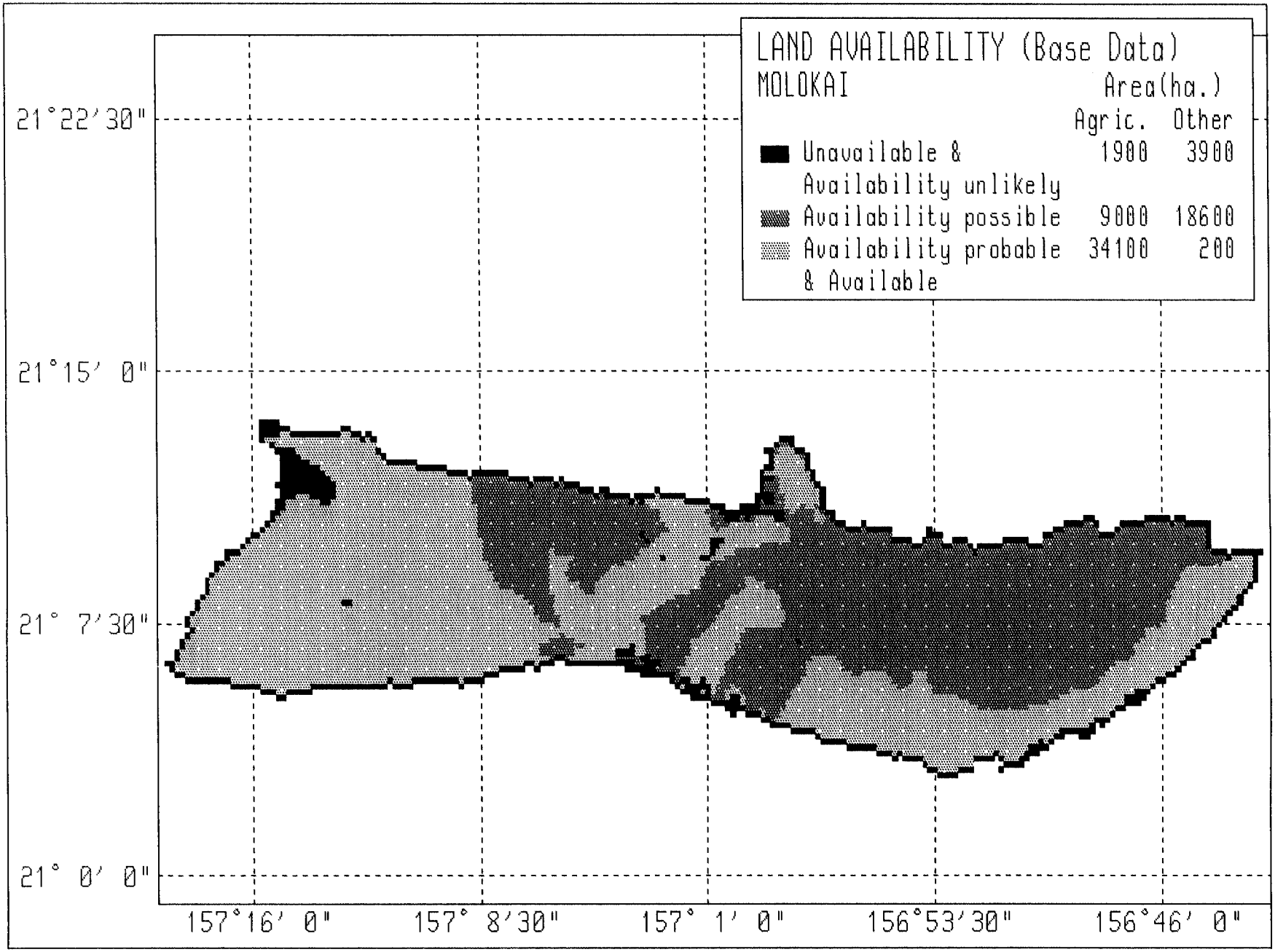

Fig. 6. Land Availability for Biomass on Molokai, Base Data

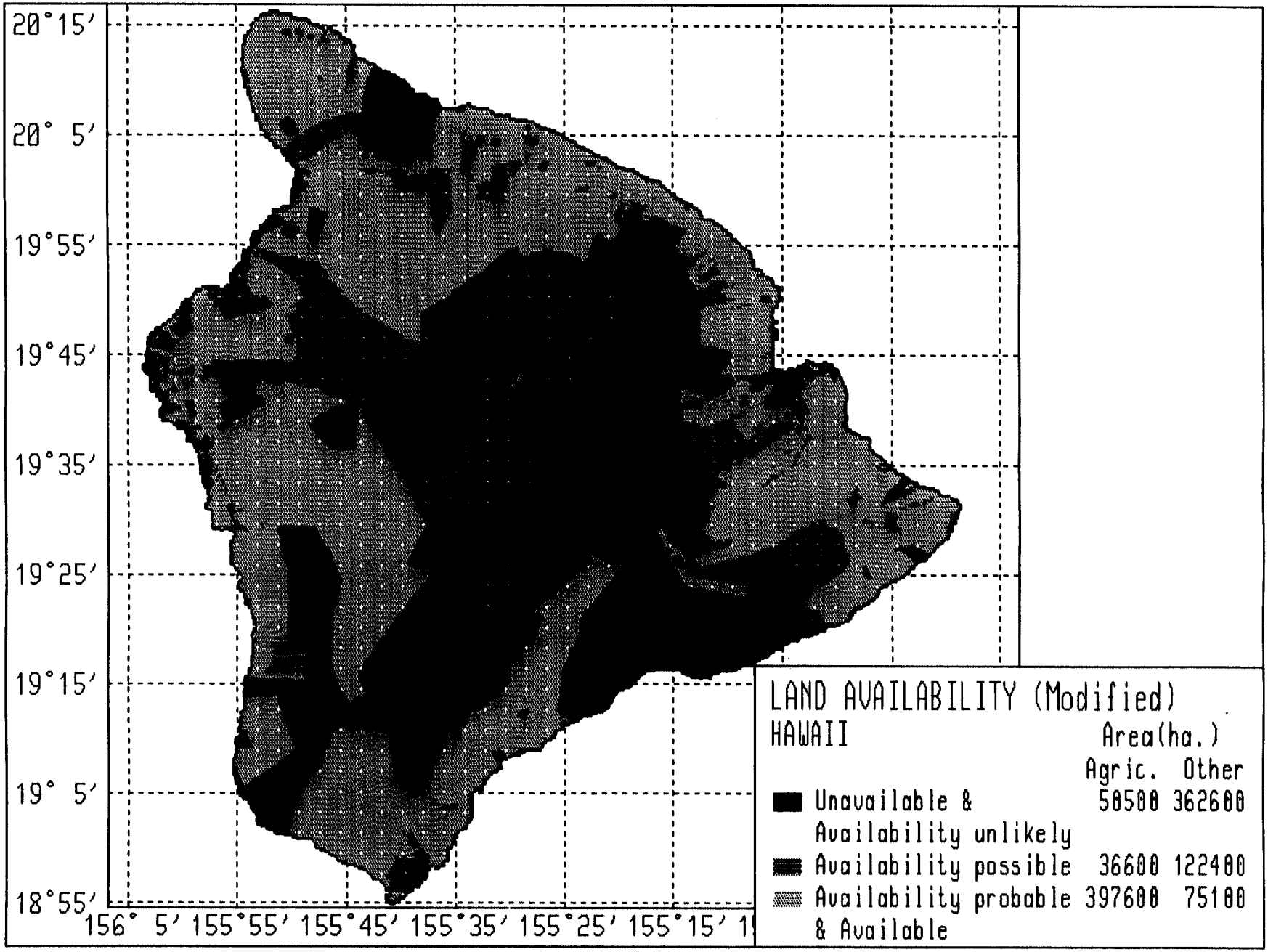

Fig. 7. Land Availability for Biomass on Hawaii, Modified Data

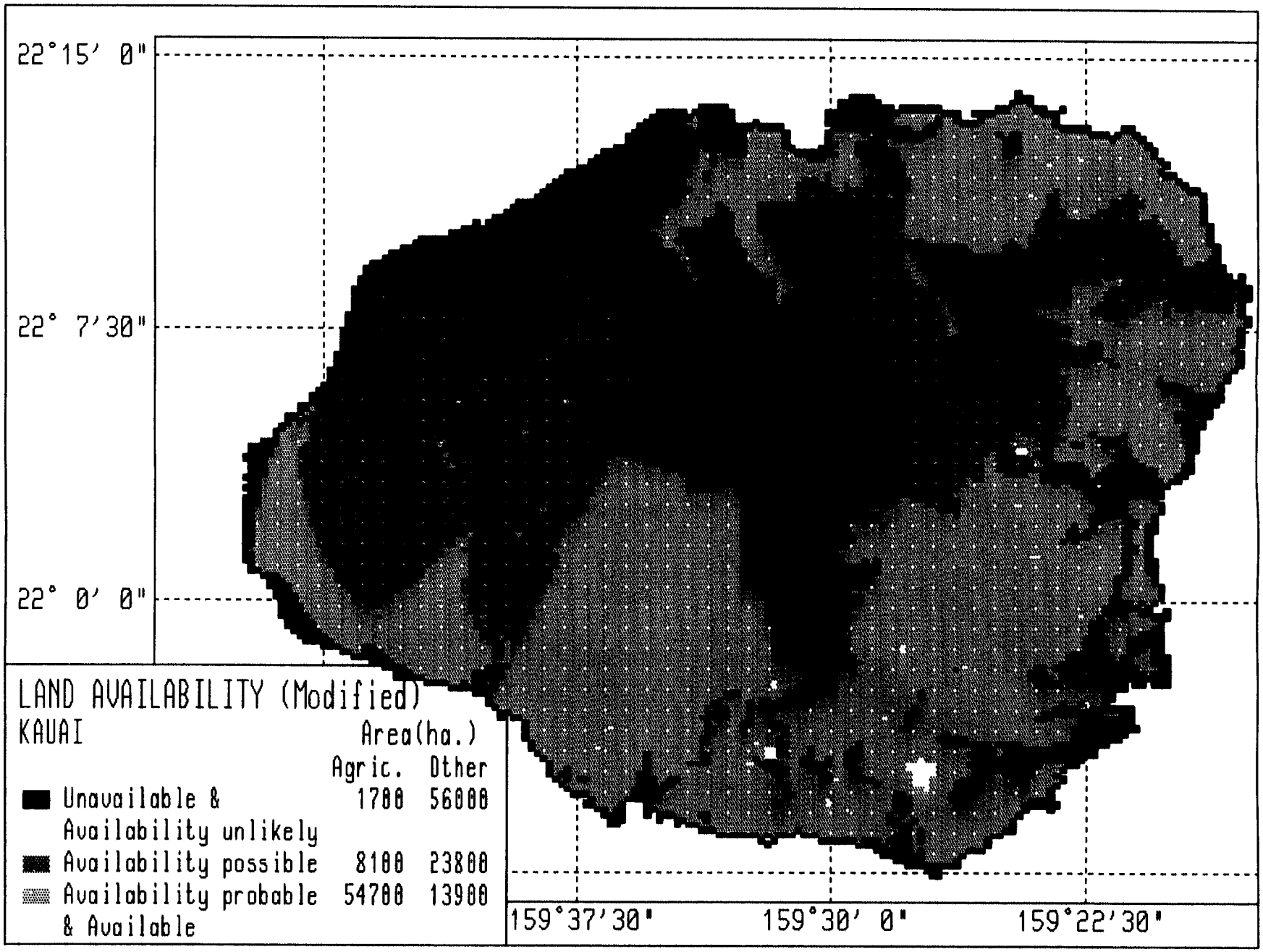

Fig. 8. Land Availability for Biomass on Kauai, Modified Data

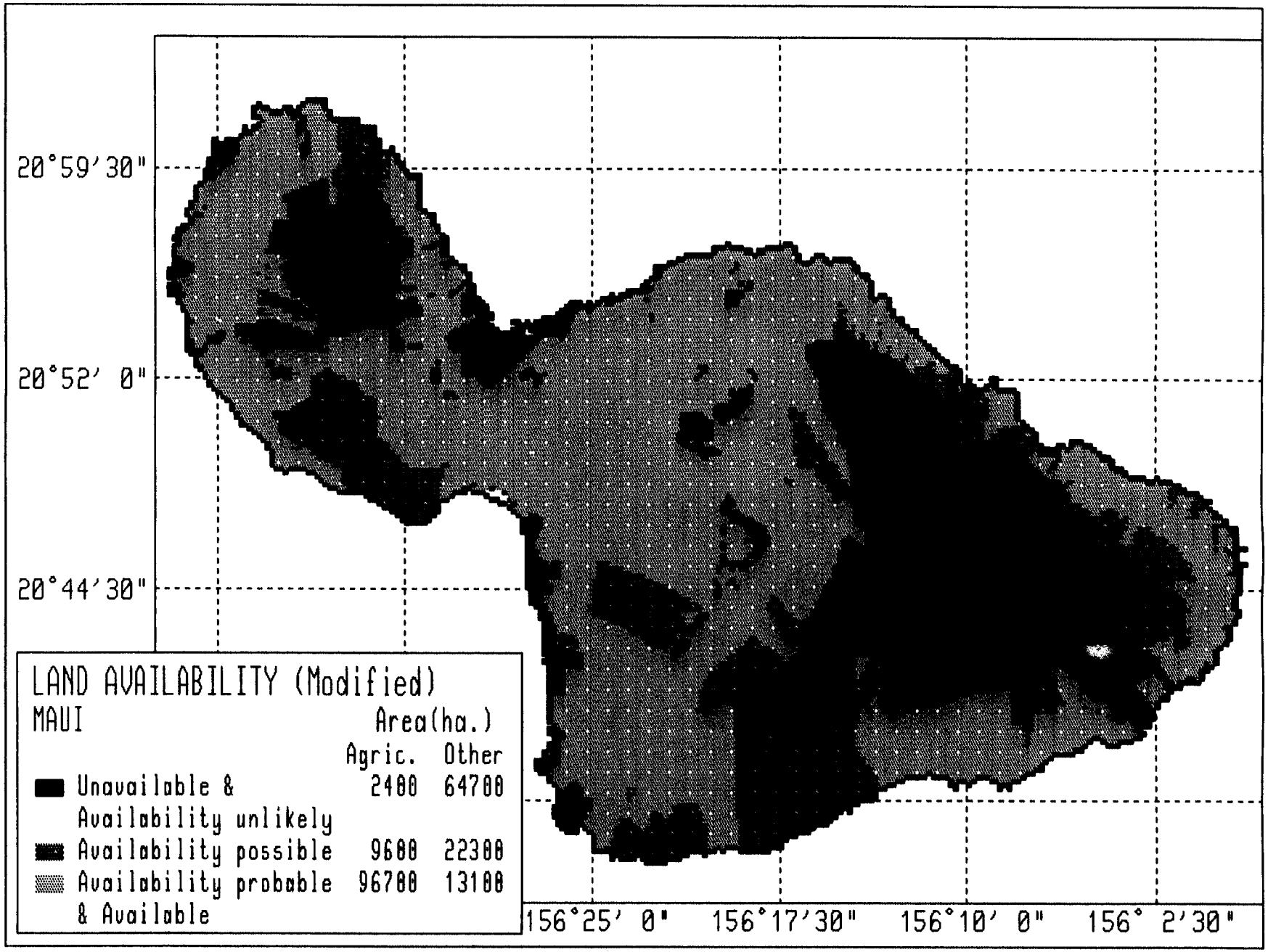

Fig. 9. Land Availability for Biomass on Maui, Modified Data

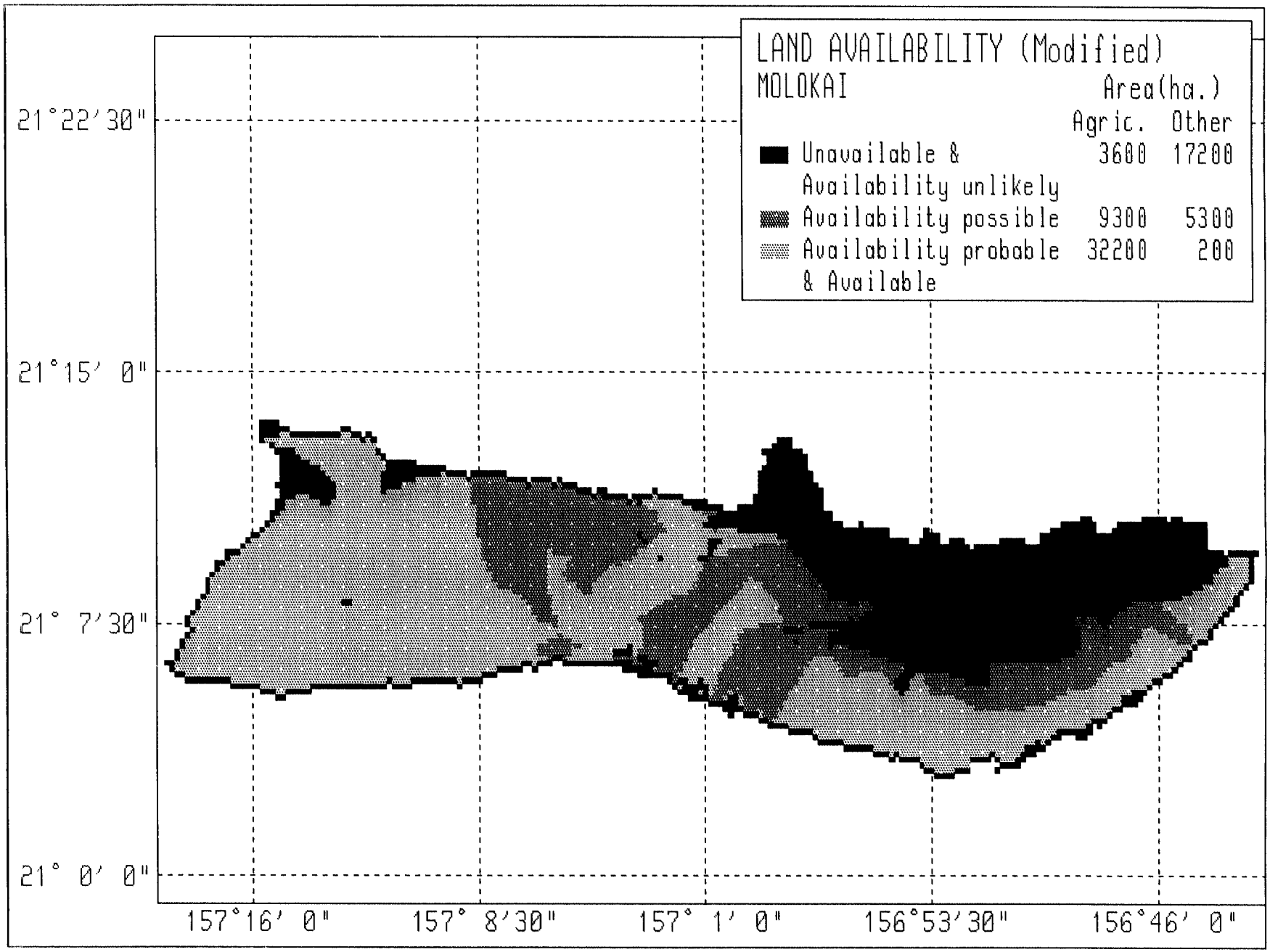

Fig. 10. Land Availability for Biomass on Molokai, Modified Data

IDENTIFYING LAND POTENTIALLY AVAILABLE FOR BIOMASS PLANTATIONS IN HAWAII

Devindar Singh [1]
Victor D. Phillips [1,2]
Robert A. Merriam [3]
M. Akram Khan [1]
Patrick K. Takahashi [2]

Department of Agricultural Engineering [1]
Hawaii Natural Energy Institute [2]
University of Hawaii at Manoa
2540 Dole St., Holmes Hall 246
Honolulu, Hawaii 96822
Consulting Forester [3]
Kailua, Hawaii

ABSTRACT

A geographical information system is used to expedite the site selection process for biomass energy crops in Hawaii. The G.I.S. and database, Hawaii Natural Resources Information System, has been used previously to identify agriculturally suitable land for biomass crop production. A methodology is presented that extends the use of HNRIS to identify land potentially available for biomass plantations. As a test case, the island of Molokai is used to demonstrate the methodology for determining land availability in the site selection process.

KEYWORDS

Biomass crops; biomass plantations; energy plantations; methanol.

INTRODUCTION

Hawaii, by taking advantage of its ideal conditions for plant growth, has the potential to grow sufficient biomass feedstocks for conversion to alcohol fuels to make the state self-sufficient in ground transportation fuels (Fig. 1). Only five percent of the land area would be required to produce the 3 300 million liters (880 million gallons) per year of methanol to replace all the gasoline and diesel fuel consumed annually (Phillips *et al.* 1988; Takahashi *et al.* 1990).

The Hawaii Natural Energy Institute (HNEI) and the Department of Agricultural Engineering (AGENG) at the University of Hawaii are presently working to identify the necessary 67 000 hectares that are both suitable (i.e., soil, climate, and productivity) and potentially available (i.e., appropriate zoning, ownership, present use, and lack of environmental or other constraints) (Fig. 2) (Phillips *et al.* 1989; Phillips *et al.* 1990).

Previous efforts have focused on the use of the Hawaii Natural Resource Information System (HNRIS), a geographic information system and database developed at AGENG,

for evaluating cropland suitability (Liang & Khan 1986). The extensive soil, climate, and other information available in the system makes HNRIS time- and cost efficient for such a purpose.

This paper uses HNRIS to evaluate land availability based on the environmental and/or social characteristics of rather large areas of land. These characteristics bear a strong relation to the availability of land for any proposed large-scale intensive culture plantation of any crop and are key criteria for evaluating the feasibility of any such venture.

LAND AVAILABILITY

Land availability, within the context of this paper, refers to a recognition that the potential for commercial development of biomass energy plantations is more a land use problem than a technological challenge (Phillips & Merriam 1988). There is limited land area in our island state, which significantly aggravates conflicts over alternative land uses and inflates land prices. The use of much land in Hawaii is constrained by laws and administrative rules. We have assumed land to be available if landowners can freely consider the establishment of a biomass plantation on their land. We have made no effort at this stage to evaluate profitability or the wishes of any owner(s) to engage in commercial biomass production for energy or other purposes.

A statewide system of land use zoning has existed in Hawaii since the early 1960s. The land ownership patterns stem from a variety of sources, including the history of Hawaii as a kingdom, republic, territory, and finally as a state, and the early acquisition of lands by plantation agriculture companies.

Land Use Zoning

The state of Hawaii is the only state with a statewide system of land use zones, designated as the Conservation, Agricultural, Urban, and Rural Districts. Boundaries of the districts are determined by an appointed body, the Land Use Commission, following strict legislative guidelines (Table 1). The regulation of uses of Conservation District lands rests with the State Board of Land and Natural Resources. Each of the four counties regulates the Agricultural District lands under guidelines established by the Land Use Commission. Other parcels, zoned for urban or rural (small farm lot) uses, are regulated by each county. Thus, the zone in which a parcel lies has a great deal to do with its availability. In this study, all urban and rural zoned lands are considered unavailable for any conceivable use as biomass plantations. Only lands classified within the Conservation and Agricultural Districts are considered as potential sites for analysis.

Land Ownership

Land ownership, or its effective control through long-term leases or other legal mechanisms, is a major factor in land availability in Hawaii (Table 2). Of slightly more than 1 664 200 hectares in the state, nearly 623 700 hectares are owned by federal, state and county governments. The 136 800 hectares in federal ownership are almost exclusively in the National Park or National Wildlife Refuge systems or under the control of the U.S. Department of Defense. The 480 900 hectares of state lands are put to many uses including agricultural and commercial, and lands set aside for environmental protection. The 6 030 hectares of county lands are principally in park and watershed parcels, generally unavailable for any other use.

A special segment of lands often included in totals of state land are the Hawaiian Homes Lands. These lands, some 77 700 hectares, are set aside by federal and state laws for the benefit of native Hawaiians and their descendents. Private land ownership is dominated by large landowners. The six largest owners control nearly a quarter of the state. Only six percent of the land is controlled by owners with fewer than 2 000 hectares. These latter owners are not individually identified in HNRIS.

Environmental Concerns

Environmental concerns about land use in Hawaii are not the purview of any single governmental agency or private group. Relatively large blocks of land are protected for environmental purposes by the federal and state governments and by private parties. Information about such areas has not been centralized and readily available.

It was decided that the nature of this study did not require specific, parcel-by-parcel information regarding the character of the protection provided or the agency or party providing the protection. It was only important to know that it was, in fact, in a protected status. For planning purposes, a private reserve is just as "unavailable" as a national park.

Conceptual Land Availability Classes

A classification system of five levels of land availability, ranging from clearly unavailable (Class 1) to imminently available (Class 5) was developed (Table 3). Such a system seemed appropriate in the context of using HNRIS in preliminary considerations of potential sites for biomass plantations. As mentioned earlier, land availability as used here means that there are no known and recognized constraints due to environmental and social concerns about a given parcel of land.

METHODOLOGY

The Hawaii Natural Resource Information System

The Hawaii Natural Resource Information System is a geographic information system developed in the Department of Agricultural Engineering, University of Hawaii at Manoa. It has, and continues to undergo modifications and improvements. However, the problem of updating and maintaining current information in a database, inherent in any GIS system, exists in HNRIS. Basic data on land ownership and land zoning have not been updated except in the case of a few large land transactions for which information was readily available. Because cell resolution in HNRIS is 8 hectares (based on contract work, some specific areas have 1-hectare resolution), small changes are inherently not recognizable.

Basic information in the system is in five major types of data files, a set of resource retrieval, interpretation and display programs/models and a database maintenance/management program (Liang & Khan 1986). The data files consist of site characteristics such as elevation, soil physical and chemical properties, as well as soil series designation, climatic variables, and selected census and land use information including ownership, zoning (but not subzoning within the Conservation District) and present use.

Initial Availability Classification

Given the desire to provide broadly based availability classes, the initial land availability classification matrix was developed (Table 4). It uses information already in HNRIS to arrive at the initial availability class. As indicated, Class 1 is considered to be unavailable under any conceivable situation. Class 5 has no known land use constraints among those considered in this study and is available at the preliminary planning stage.

What rationale supports this matrix? As an island state, the ocean shoreline is a part of everyday life as well as the location of many important cultural and historic sites. It is the focus of tourism, Hawaii's largest industry. Use of shoreline lands is always a community concern, and these lands are extremely sensitive to intensive development of any kind.

Land use zoning has created another category of lands that can be readily identified. Nearly one-half the state, 796,100 hectares, is in the Conservation District. It is known that nearly 25 percent of the Conservation District is subzoned for protection (Table 5), although the subzones are not identified in HNRIS. In fact, much of the balance of the Conservation District is available only with a difficult-to-obtain permit.

The prominent role of public lands and their control, now recognized to be that of a public trust rather than as a land disposal opportunity, makes them more sensitive than lands in private ownership. There are no "general use" federal lands in Hawaii, such as the lands under the control of the Bureau of Land Management on the U.S. mainland. In Hawaii, nearly all federal lands are committed to their present use, and are therefore unavailable for consideration for alternative uses.

Use of lands under the control of the Department of Hawaiian Homes Lands is limited to programs that benefit native Hawaiians and their descendants. Such a restriction would not necessarily rule out a biomass plantation, and, in fact, such a plantation might be the best use of Hawaiian Homes Commission lands in some instances. However, serious constraints on the availability of such lands make large scale development unlikely.

This ranking cannot take, nor is it intended to take the place of specific, site-by-site evaluations, especially where environmental concerns may be prominent but not clearly delineated. The initial availability class ranking provides no more than a broad picture of availability for the lands within the Agricultural District and all subzones of the Conservation District. The initial class boundaries can and will be refined as new information develops.

Refining the Initial Availability Class

Two major considerations in the decision to use HNRIS and to develop a land availability classification based on information already available within a database that was not "state-of-the-art," were the lack of well-documented alternatives and the capability of the HNRIS system to accept updated data without expensive and time-consuming effort. Given the long-range planning and land use decisions inherent in using HNRIS, the critically important features of HNRIS as an effective decision-making tool are the ease and speed of use as well as the development of a fail-safe method of updating information.

Fail-Safe Addition of New Information

Assuring that any new data entry is fail-safe is necessary so that a highly sensitive area, based on a given set of factors, will not be down-graded based on the lower sensitivity of a different factor(s). We have chosen to implement the following procedure to assure the security of all previous information entered at an earlier date.

The proposed new availability class data is first entered into a temporary field. That field is then checked, cell by cell, against the existing availability classification. If the new availability class is equal to or less than that already in the system based on previous information, then there is no reason for a change. However, if the temporary field indicates a lower availability class than that previously believed to be appropriate, then the new classification is used.

Thus, the computer is programmed to change an availability class only when the new information indicates lesser availability (greater sensitivity) than was previously believed to be appropriate. If changes must be made toward more availability, the deliberate act of entering the system to change a particular cell is required.

Data Entry by Blocks

Any initial attempt to modify the original classification should be made using data already available in HNRIS. It is entirely possible that pertinent information about some limiting factor, which applies generally to a major geographic area, already exists in the HNRIS database, but is associated with another recognized category. When this is the case, a change in the original classification could be made by reference to the alternative or surrogate factor (Fig. 3).

Several prominent descriptive characteristics of land units already within the HNRIS system were considered to be reliable and accurate identifiers of lands of a particular availability class. Ownership was considered in the initial classification, but a major landowner with such a concern for other land values could refuse to consider establishing biomass or other crops. Certainly the lands with elevations above tree level could be excluded, but we would expect these to be eliminated using land suitability criteria. As will be demonstrated in the case of Molokai, a watershed (hydrographic) boundary can be used to delineate a large area as probably unavailable for further consideration.

New Data Entry

The ease of updating information is related to the way in which new data is entered into HNRIS. Because HNRIS uses AutoCAD (a registered trademark name of Autodesk, Inc.; mention of this trade name is for the understanding of the reader only and does not imply any recommended use by the authors) for data entry, a stylus must be moved around the boundary of the property in question on a map of known scale. This procedure mandates that as much information as possible be entered on one map of an appropriate scale, and, when possible, with common boundaries defined.

It will be quite common for areas to be classified the same for more than one reason. As previously noted, ownership and land zoning are two factors that affect all land parcels. In Hawaii there are large areas known to contain rare plant and animal species, many of which are listed as threatened and endangered. Large parcels are proposed for designation as critical habitat for forest or water birds. Many land areas are culturally sensitive because

of archaeological and religious importance and are recognized nationally as valuable historic sites. There are also valuable watersheds.

Our decision was to start with maps of the subzones within the Conservation District because one major boundary delineation was already done. Such maps had been updated during 1988, were available on blue-line copies of U.S.G.S. maps of 1:24 000 scale, and also contained much additional information such as park boundaries. On these subzone maps additional boundaries were added from information obtained from one or more of the cooperating agencies listed in our acknowledgements. All known public and private parties managing land and/or having a major concern with the environment were contacted for maps or descriptive data. The resultant boundaries were entered into the system by the fail-safe method outlined above.

Site-Specific Planning

A more accurate and meaningful approximation of land availability has thus been achieved by using data previously within HNRIS as augmented by map information from many sources. Data entry has been minimized by consolidating map information onto one standard base map before entry.

The next step is to identify suitable lands within the areas most likely to be available. One computer run combining suitability and availability criteria should be adequate to indicate whether there is enough suitable land in availability class 5 or perhaps classes 4 and 5 so that further detailed analysis is desirable. Such an additional analysis would be to investigate present land uses, conduct discussions with landowners, and pursue further cultural and environmental surveys. Pertinent persons and agencies would be those who could provide information beyond that available on maps, such as cultural and historic experts and natural scientists.

Finally, of course, a site-specific reconnaissance or field examination of a given parcel by qualified persons is necessary if a formal environmental assessment or environmental impact statement is required for the action being considered.

MOLOKAI AS A CASE STUDY

The island of Molokai (Fig. 4) is used as a test case for several reasons. It is small, 67 800 hectares, has few landowners, and yet has very diverse geographical and environmental characteristics. It is the only island that has had a single biomass-burning power plant (approximately 3 MWe normal operating capacity) as its primary source of electricity. It contains large blocks of land controlled by the federal and state governments, including the Hawaiian Homes Commission (Fig. 5). Molokai has a single private party, Molokai Ranch, Inc., as the third major landowner.

Molokai contains a national park, a state park, state natural area reserves, a national wildlife refuge, and a reserve of the Nature Conservancy, a private conservation organization. Hydrographic Area #1, including Kalaupapa point and the north shore of Molokai (Fig. 6) is convenient to illustrate the block change procedure because it contains large environmentally sensitive areas and is extremely remote.

Initial Availability Classification

Land zoned in the Conservation and Agricultural Districts dominate Molokai (Fig. 7). The recognition that a significant part of the Conservation District lands (Protective subzones) are unavailable for the intensive culture of biomass is a major reason for the development of the land availability classification system.

The initial availability classification of these lands is shown in Figs. 8 and 9. At this stage, with this analysis and no other to consider, we have only a rough picture of potential availability. Agricultural zoned lands are clearly more likely to be available than conservation lands.

Block Change of Data

A casual inspection of a map of Molokai is sufficient to determine that overwhelming problems exist for developing the land in Hydrographic Area #1. It is remote, essentially roadless, and is known to be environmentally sensitive in large part. Some parcels will show up as unavailable in the initial (base data) classification because of the shoreline, if for no other reason (Fig. 10). It would be fair and perhaps obvious from the start to state that the entire area is unlikely to be available.

The block change procedure was used to test this concept. All data in Hydrographic Area #1 was changed to class 2 unless previous information indicated they belonged in class 1. The change in availability class from the initial level to the level after the block change is shown in Fig. 11.

Adding New Data

Next, quadrangle sheets with the information collected from many sources (see acknowledgements) were digitized and entered into the system through the fail-safe method described above. The effect of the new data modification on the availability classification of Hydrographic Area #1 is seen in Fig. 12. The effect of the modified data on the availability classification for all Agricultural and Conservation lands on Molokai can be seen in Fig. 13 (map format) and Figs. 14, 15, and 16 (bar charts that illustrate significant changes in hectares of land availability classes between Agricultural and Conservation lands as well as between base data and modified data).

A Final Look at Molokai

Table 6 indicates that more than 38 000 hectares of land are identified as "available" and "probably available" for biomass plantations on Molokai. What is the significance of this analytical result? First, it clearly shows that planning for any sizeable biomass plantation on Molokai must begin with lands that are already zoned for agriculture. There are no vast areas of Conservation land awaiting biomass development. Secondly, the preliminary nature of this analysis and the importance of other factors is apparent. Principal among those factors are the suitability of the land for the desired crop, the land use choice of the landowner(s), and the economic return on investment considerations.

THE NEXT STEP

Molokai was selected as a case study because of its relatively small size and considerable physiognomic diversity. Completing this analysis for the rest of the state of Hawaii will be the next step. By deciding at the outset that the islands of Kahoolawe, Lanai, Niihau, and Oahu do not have enough available land at the very earliest and fundamental level of analysis to warrant this type of study will simplify the process. The remainder of the state is covered by about 100 U.S.G.S. quad sheets that will expedite the analysis of land availability in the remainder of Hawaii.

We believe that the classification of the lands in Hawaii into land availability classes for biomass plantations, coupled with the consideration of land suitability and economic reality, will greatly facilitate realistic planning for Hawaii's biomass energy future.

REFERENCES

Hawaii, State of. 1989. *Data Book.* Department of Planning and Economic Development, 651 p.

Liang, T. and M.A. Khan. 1986. A natural resource information system for agriculture. *Agricultural Systems* 21: 81-105.

Phillips, V.D. and R.A. Merriam. 1988. Biofuel production in Hawaii: appropriate species, sites, sizes, and scenarios. Presented at *Hawaii Forestry and Wildlife Conference*, Hilo, Hawaii, February 10–13.

Phillips, V.D., D.R. Neill, and P.K. Takahashi. 1988. Methanol plantations in Hawaii. In *Proceedings of the VIII International Symposium on Alcohol Fuels*, Tokyo, Japan, November 13–16.

Phillips, V.D., D. Singh, M.A. Khan, and P.K. Takahashi. 1989. Geographical information system for site selection of biomass energy crops. In *Hawaiian Sugar Technologists' 1989 Annual Report*, Honolulu, Hawaii.

Phillips, V.D., R.A. Merriam, P.K. Takahashi, D. Singh, and M.A. Khan. 1990. Methodology for determining land availability for biomass plantations in Hawaii. Presented at the *U.S. Department of Energy Biofuels and Municipal Waste Technology Division Management Review Meeting FY1990*, Washington, D.C., April 11–12.

Takahashi, P.K., D.R. Neill, V.D. Phillips, and C.M. Kinoshita. 1990. Hawaii: an international model for methanol from biomass. *Energy Sources* 12: 421–428.

Thomassin, P.J. and H.L. Baker. 1985. Estimating the impacts of increased forest industry outputs on the Hawaiian economy by using input-output analysis. *Research Series 019*, HITAHR, College of Tropical Agriculture and Human Resources, University of Hawaii, Honolulu, Hawaii.

ACKNOWLEDGEMENTS

This work was supported by the U.S. Department of Energy through the "Hawaii Integrated Biofuels Research Program – Phase 3" (Subcontract No. XN-0-19164-1) to the Hawaii Natural Energy Institute administered by the Solar Energy Research Institute.

Many people have contributed to the development of this system of land availability classification. Particularly helpful were those who generously provided map information and advice for using this information efficiently. We thank the following agencies listed alphabetically.

Department of Land and Natural Resources, State of Hawaii. *Recreation Map, Island of Molokai*, September 1988. Indicates many of the features of concern, including public hunting areas that are very hard to identify on other maps.

_____. *Guide to Hawaii's State Parks*, January 1984. A basic reference for park locations.

_____. *Conservation District Inventory, Island of Molokai*, 1977. A set of 8 maps and related text about uses of Conservation District lands only.

_____. *Conservation District Plan*, 1977. A single map and accompanying text showing many projects planned by the several Divisions of DLNR.

Environmental Center, University of Hawaii at Manoa. John Harrison and Jacquelin Miller were particularly helpful with discussions about geographic information systems and their use and application with environmental information.

Fish and Wildlife Service, U.S. Department of the Interior. Provided a map of Kakahaia National Wildlife Refuge. Mr. Jerry Leinecke, Supervisor, Refuge and Wildlife, was particularly helpful.

Hawaii Stream Assessment, Commission on Water Resources Management, State of Hawaii. Provided a working draft map of all perennial streams on Molokai. Discussions with Sallie Edmunds were particularly helpful.

Hawaiian Homes Commission, State of Hawaii. Charles Ice provided helpful information about HHC lands on Molokai.

National Park Service, U.S. Department of the Interior. *Kalaupapa National Historical Park.* A brochure with map and text information.

The Natural Area Reserves System Commission, State of Hawaii. Executive Secretary Robert E. Lee provided boundary maps of Natural Area Reserves on Molokai.

The Nature Conservancy of Hawai'i. Provided boundary maps of preserves and a watershed management area under TNCH control. Ms. Audrey Newman, Coordinator, Hawai'i Heritage Program, was particularly helpful.

Office of State Planning, State of Hawaii. Mary Lou Kobayashi and Craig Tasaka provided helpful discussions about the OSP efforts to utilize environmental data in a geographic information system they plan to use in conjunction with their Conservation District boundary review.

IDENTIFYING LAND POTENTIALLY AVAILABLE FOR BIOMASS PLANTATIONS IN HAWAII

Devindar Singh, Victor D. Phillips, Robert A. Merriam, M. Akram Khan, and Patrick K. Takahashi

Tables

1. Estimated Area of Land Use Districts by Islands, 1989 (Source: Hawaii 1989, p. 172)

2. Estimated Area of Land Ownership by Islands, 1989 (Source: Hawaii 1989, p. 177)

3. Conceptual Land Availability Classes for Biomass Plantations

4. Initial Land Availability Classification for Biomass Plantations by Location, Ownership, and Land Zoning Districts

5. Conservation District Land by Island and Sub-Zone (Source: Thomassin and Baker 1985)

6. Summary of Land Availability Class by Area on Molokai Using Modified Data

IDENTIFYING LAND POTENTIALLY AVAILABLE FOR BIOMASS PLANTATIONS IN HAWAII

Devindar Singh, Victor D. Phillips, Robert A. Merriam, M. Akram Khan, and Patrick K. Takahashi

Figures

1. Land Required to Grow Methanol for Surface Transportation in Hawaii

2. Biomass Decision Tree

3. Flow Chart for Block Change of Availability Class using HNRIS

4. Geographic Location of the Hawaiian Islands and the Island of Molokai (insert).

5. Land Ownership on Molokai

6. Hydrographic Areas on Molokai

7. Land Zoning Districts on Molokai

8. Land Availability Classes on Molokai based on Environmental and Social Sensitivity using Base Data

9. Land Availability for Biomass by Hydrographic Areas on Molokai using Base Data

10. Land Availability in Hydrographic Area 1 using Base Data

11. Land Availability in Hydrographic Area 1 with Block Change

12. Land Availability in Hydrographic Area 1 after Block Change using Modified Data

13. Land Availability Classes on Molokai based on Block Change and Modified Data

14. Land Availability for Biomass by Hydrographic Areas on Molokai using Block Change and Modified Data

15. Effect of Block Change and Modified Data on Land Availability for Biomass on Agricultural Land on Molokai

16. Effect of Block Change and Modified Data on Land Availability for Biomass on Conservation District Land on Molokai

Table 1. Estimated Area of Land Use Districts by Islands, 1989

	(Hectares)*				
Island	Total	Urban	Rural	Conservation	Agricultural
Hawaii	1 041 400	17 900	300	526 400	496 800
Maui	188 500	7 000	1 500	78 400	101 700
Molokai	67 100	1 000	800	20 100	45 200
Lanai	36 600	900	800	15 500	19 100
Oahu	156 300	37 500	---	62 700	56 100
Kauai	143 200	5 000	500	80 400	57 300
Niihau	18 500	---	---	---	18 500
Uninhabited Isles	12 600	---	---	12 600	---
State Total	1 664 200	69 300	4 100	796 100	794 700

* Rounded to the nearest 100 hectares.
Source: Hawaii 1989, p. 172

Table 2. Estimated Area of Land Ownership By Islands, 1989

	(Hectares)*				
Island	Total	Federal	State	County	Private
Hawaii	1 003 200	93 000	330 800	500	586 200
Maui	1 181 400	10 900	41 400	600	128 400
Molokai	69 100	Δ	19 300	100	49 700
Lanai	36 000	Δ	Δ	Δ	36 000
Oahu	163 200	19 800	28 100	4 500	110 800
Kauai	142 100	13 000	61 100	200	79 500
Niihau	18 900	Δ	Δ	Δ	18 900
State Total	1 633 200	136 800	480 900	6 000	1 009 500

* Rounded to the nearest 100 hectares
Δ Less than 100 hectares
Source: Hawaii 1989, p. 177

Table 3. Conceptual Land Availability Classes for Biomass Plantations

Land Availability Class	Description
Unavailable (1)	Not available under any conceivable situation
Availability unlikely (2)	Little likelihood of availability, extremely sensitive
Availability possible (3)	Possibility available in part, but major concerns exist
Availability probable (4)	Probably available in part, but concerns exist in specific areas
Available (5)	No concern identified in this study

Table 4. Initial Land Availability Classification for Biomass Plantations By Location, Ownership, and Land Zoning Districts

		Land Availability Class	
Location	Ownership	Conservation District	Agricultural District
Shoreline	All	1	2
Not shoreline	Federal	2	3
Not shoreline	Hawaiian Home Commission	2	3
Not shoreline	State	3	4
Not shoreline	Private	4	5

Table 6. Summary of Land Availability Class By Area on Molokai Using Modified Data

	Area (Hectares)		
Land Availability Class	Conservation District	Agricultural District	Totals
Unavailable (1)	15 523	1 785	17 308
Availability unlikely (2)	53	1 820	1 873
Availability possible (3)	5 390	3 775	9 165
Availability probable (4)	160	6 439	6 599
Available (5)	0	31 269	31 269
Total	21 126	45 088	66 214

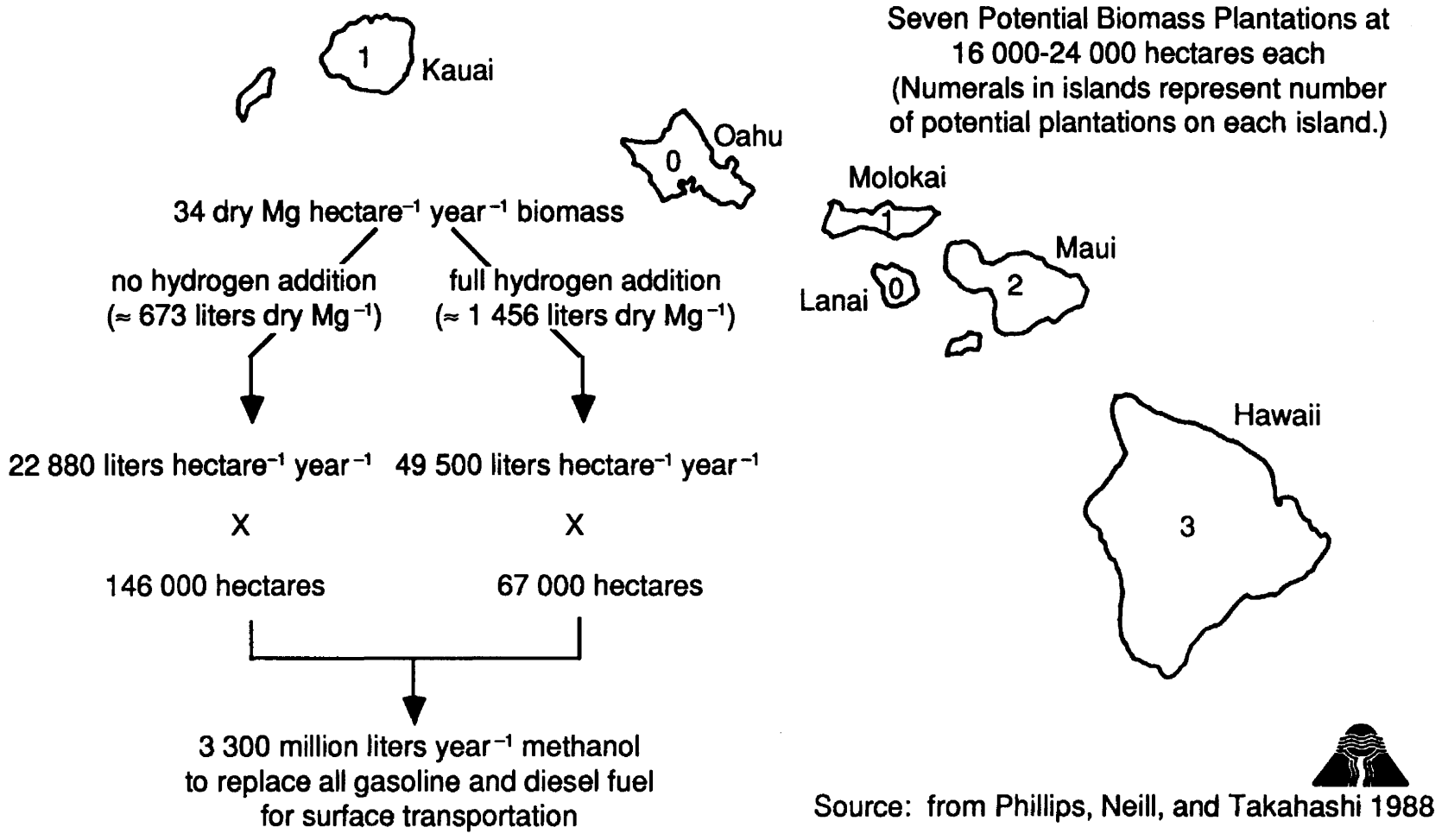

Fig. 1. Land Required to Grow Methanol for Surface Transportation in Hawaii

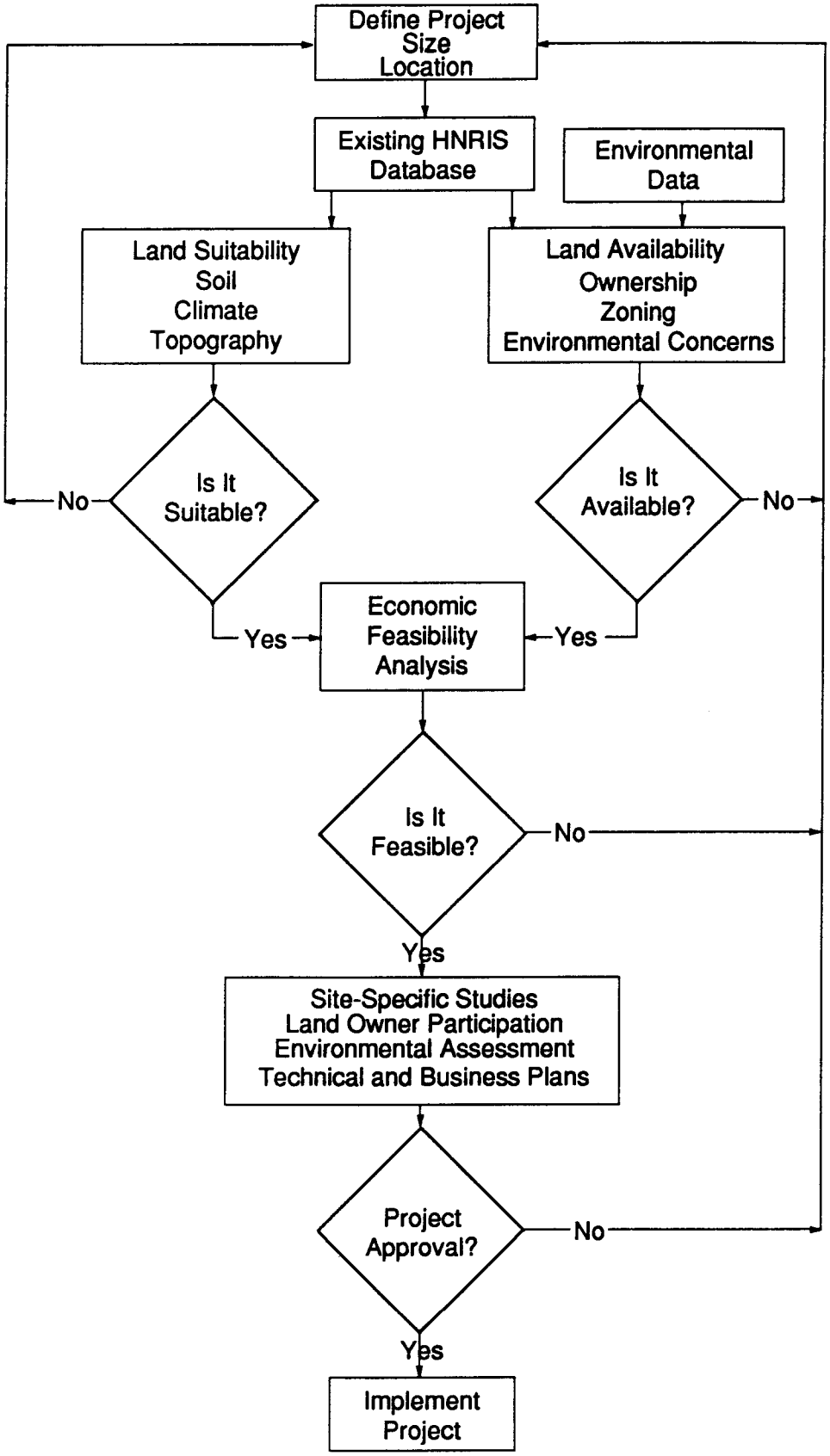

Fig. 2. Biomass Decision Tree

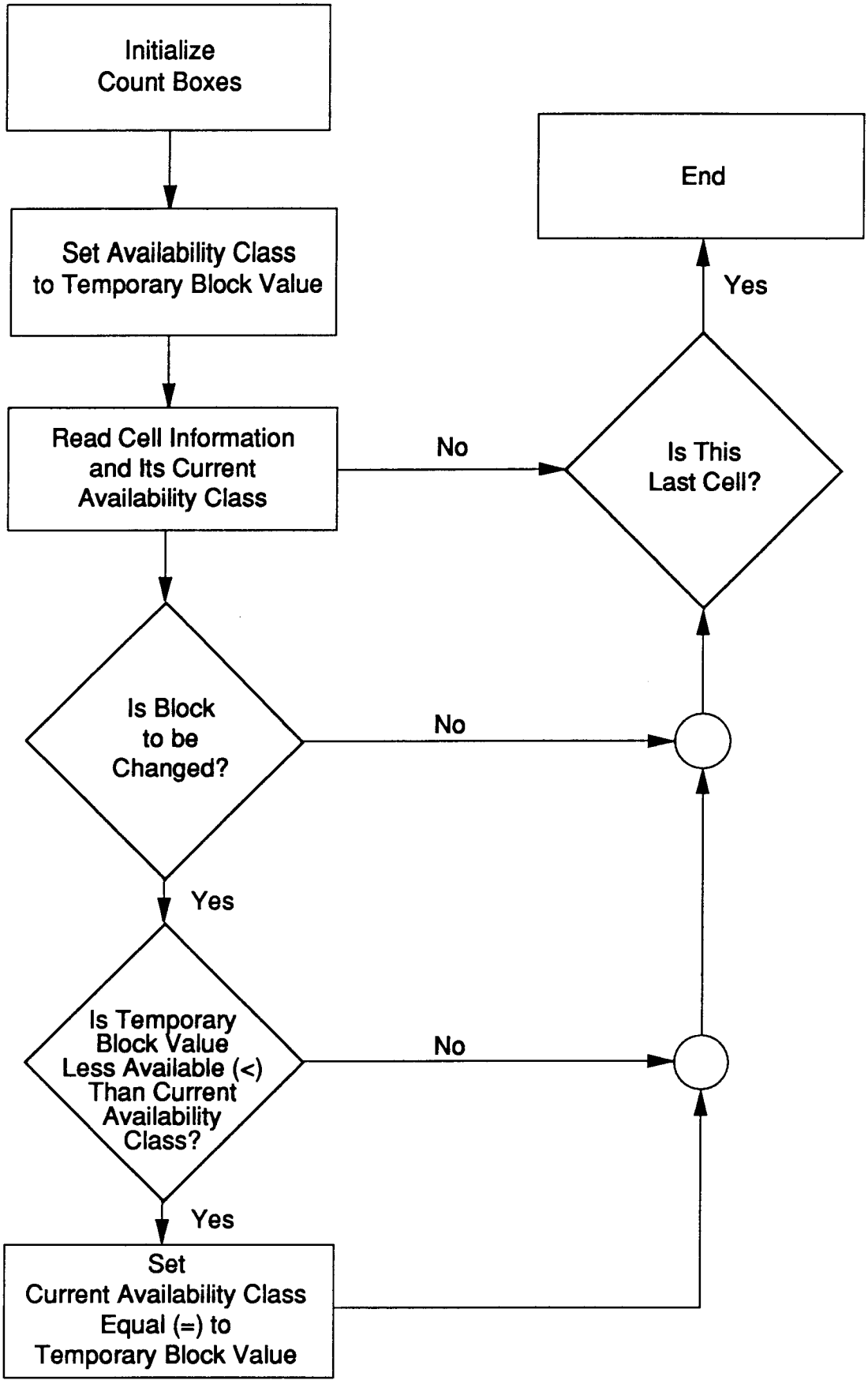

Fig. 3. Flow Chart for Block Change of Availability Class

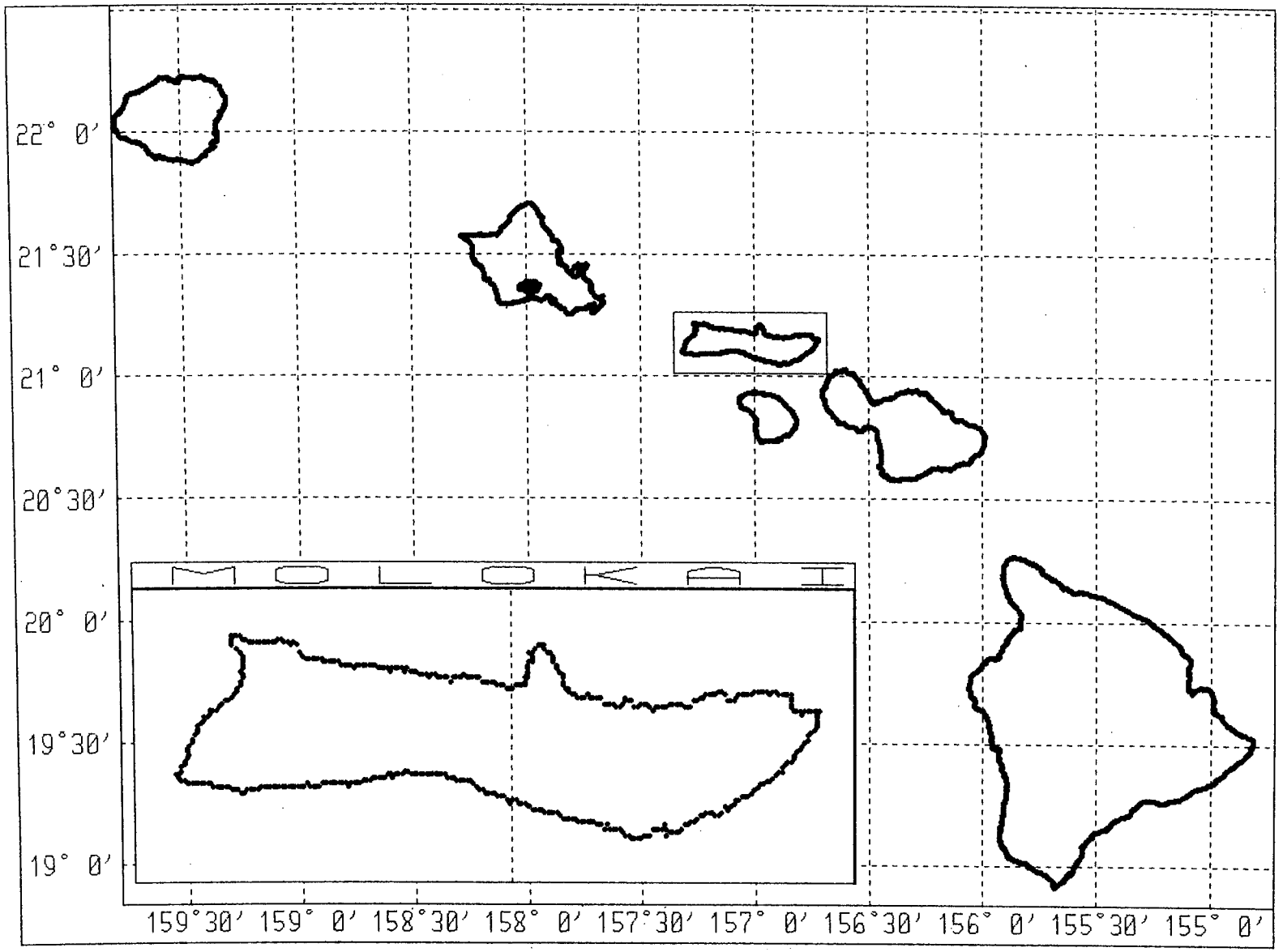

Fig. 4. Geographic Location of the Hawaiian Islands and the Island of Molokai (inset)

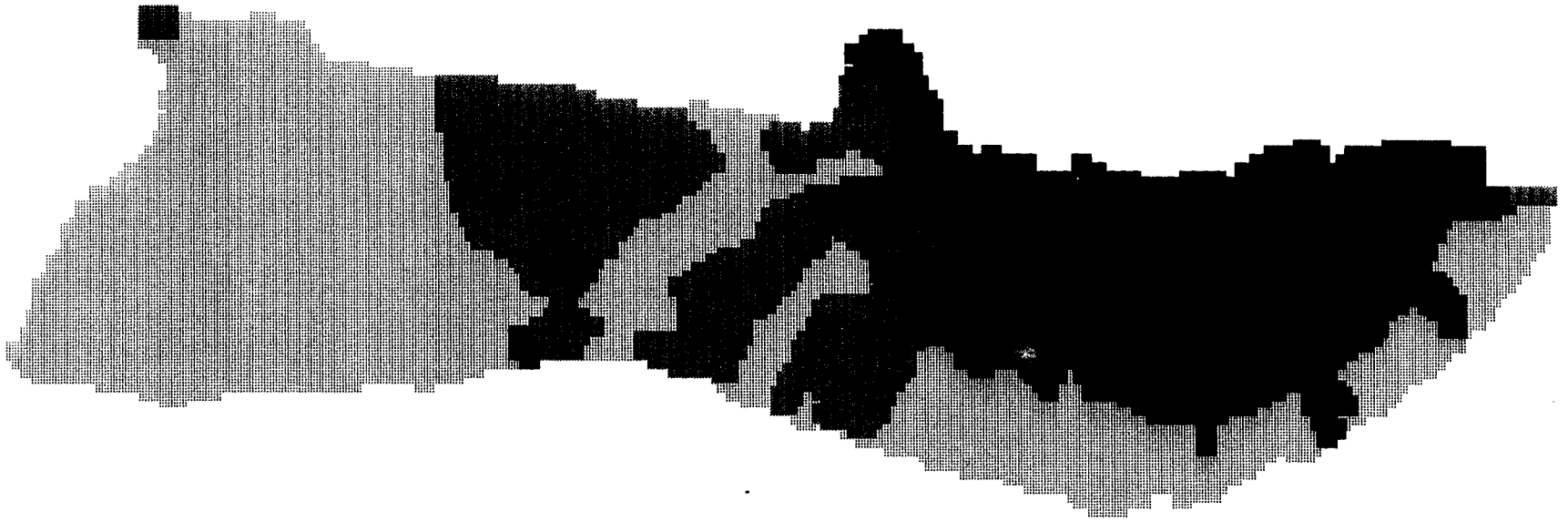

STATE	21,278	hectares
FEDERAL	107	hectares
HHC	10,159	hectares
PRIVATE	36,269	hectares

Fig. 5. Land Ownership on Molokai

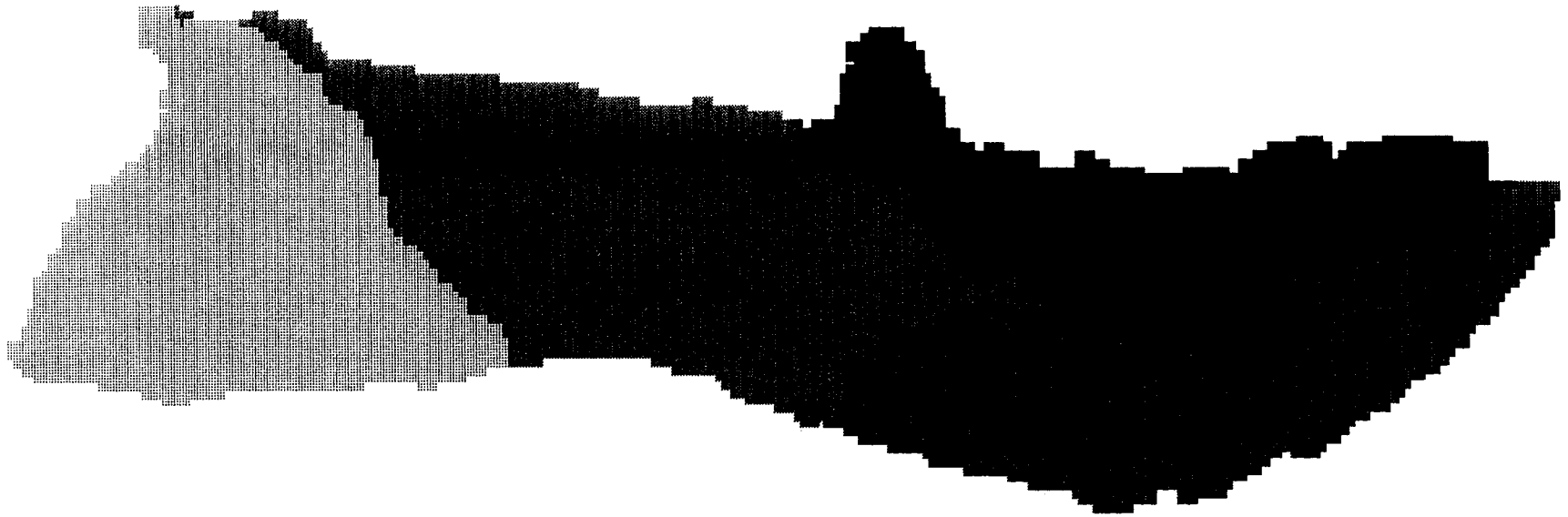

Watershed 1	14,165	hectares
Watershed 2	15,301	hectares
Watershed 3	22,139	hectares
Watershed 4	16,207	hectares

Fig. 6. Hydrographic Areas on Molokai

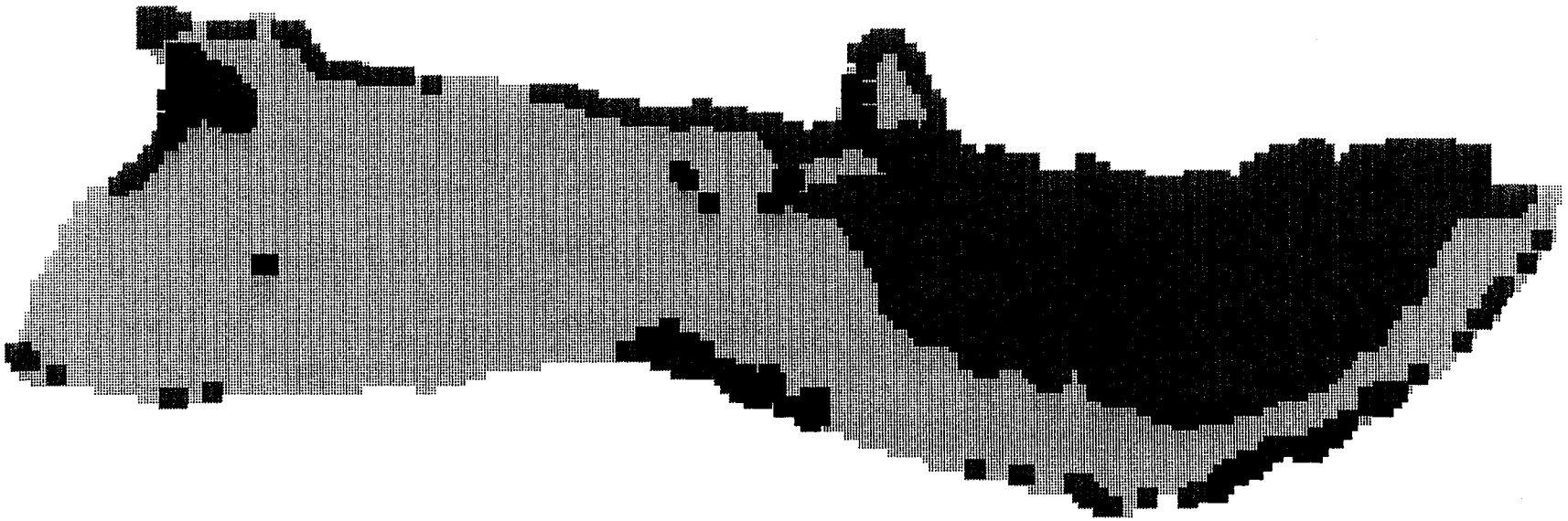

URBAN	799	hectares
RURAL	799	hectares
CONSERVATION	21,127	hectares
AGRICULTURAL	45,087	hectares

Fig. 7. Land Zoning Districts on Molokai

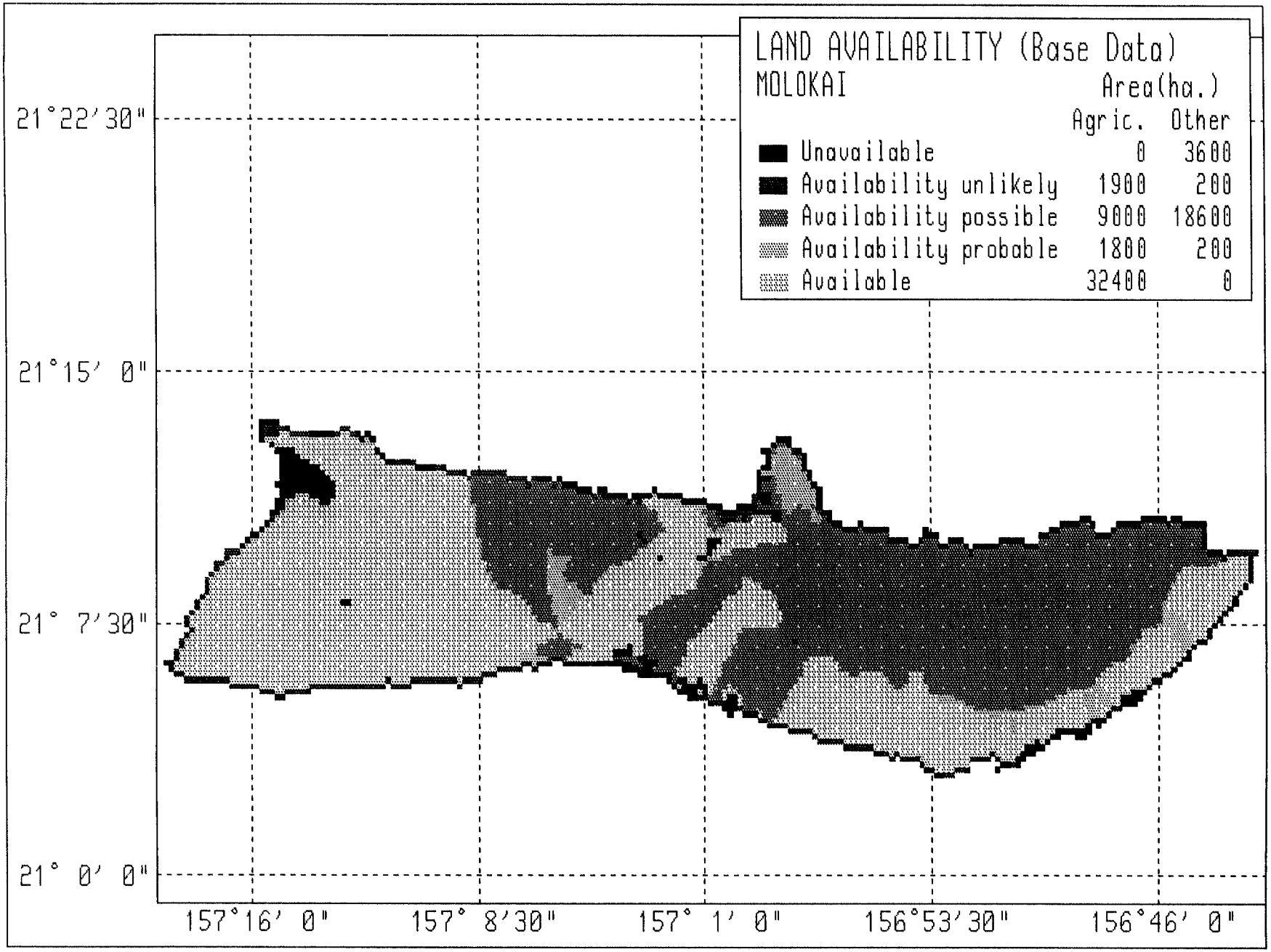

Fig. 8. Land Availability Classes on Molokai based on Environmental and Social Sensitivity using Base Data

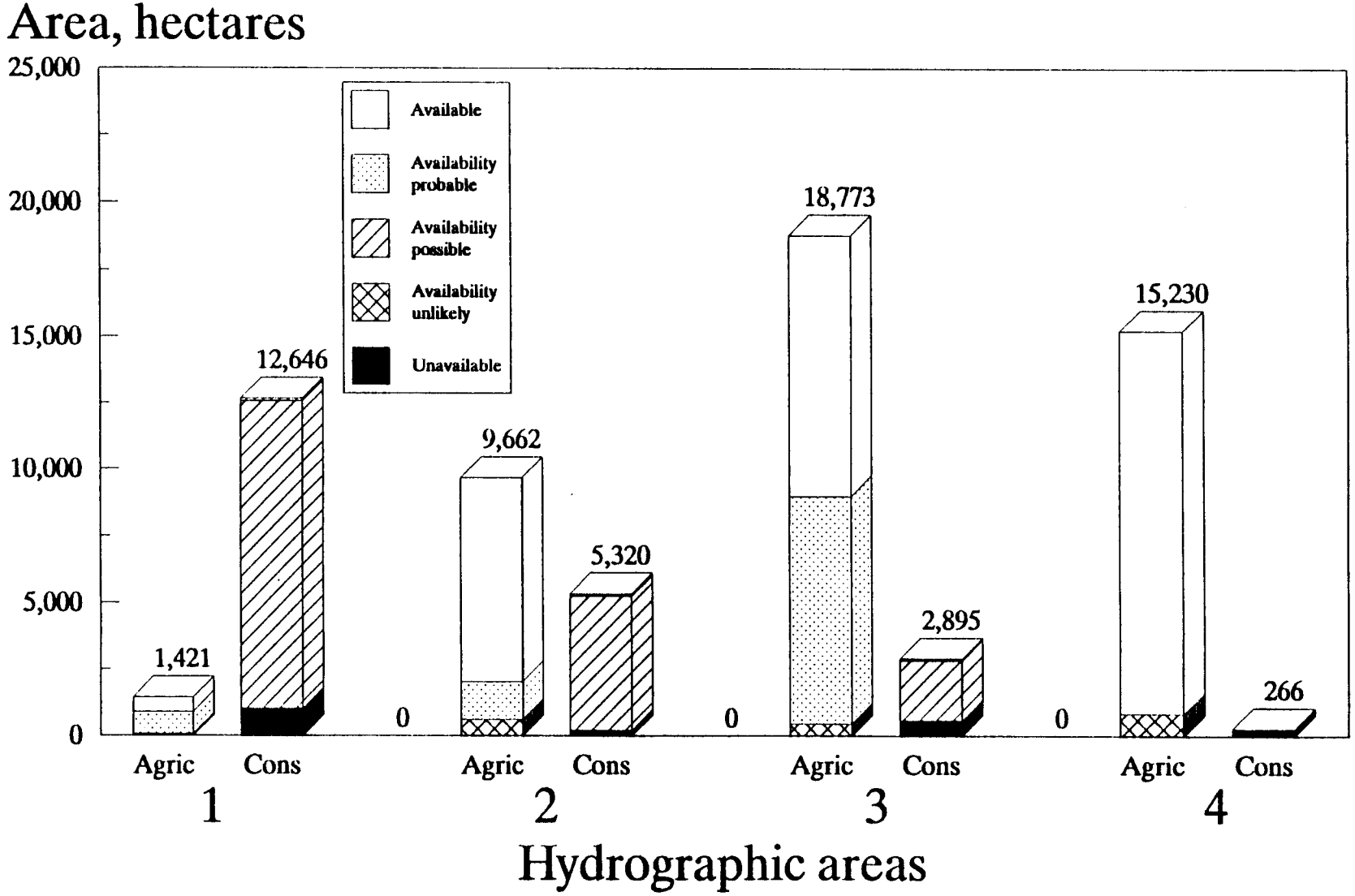

Fig. 9. Land Availability for Biomass by Hydrographic Areas on Molokai using Base Data

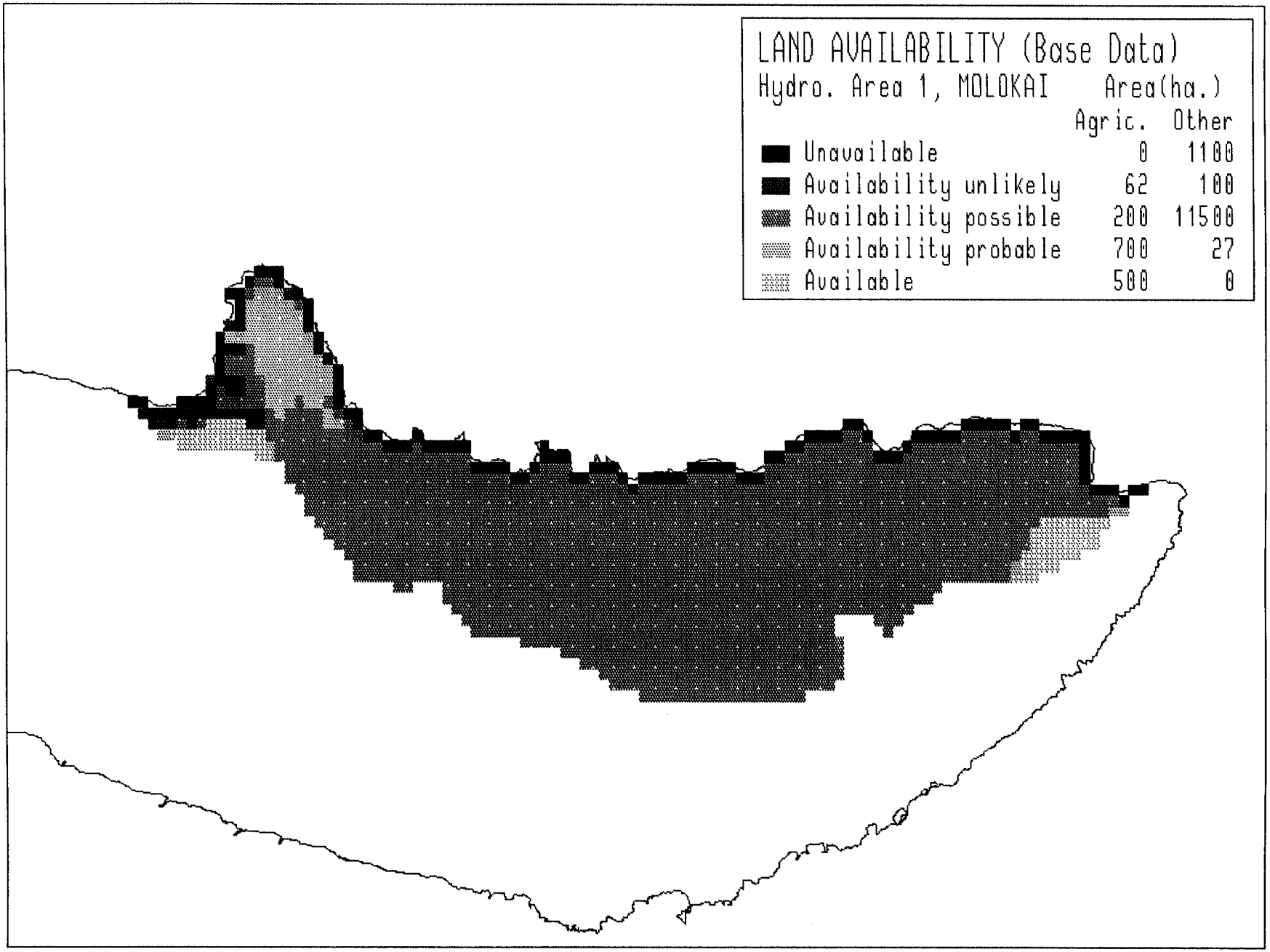

Fig. 10. Land Availability in Hydrographic Area 1 using Base Data

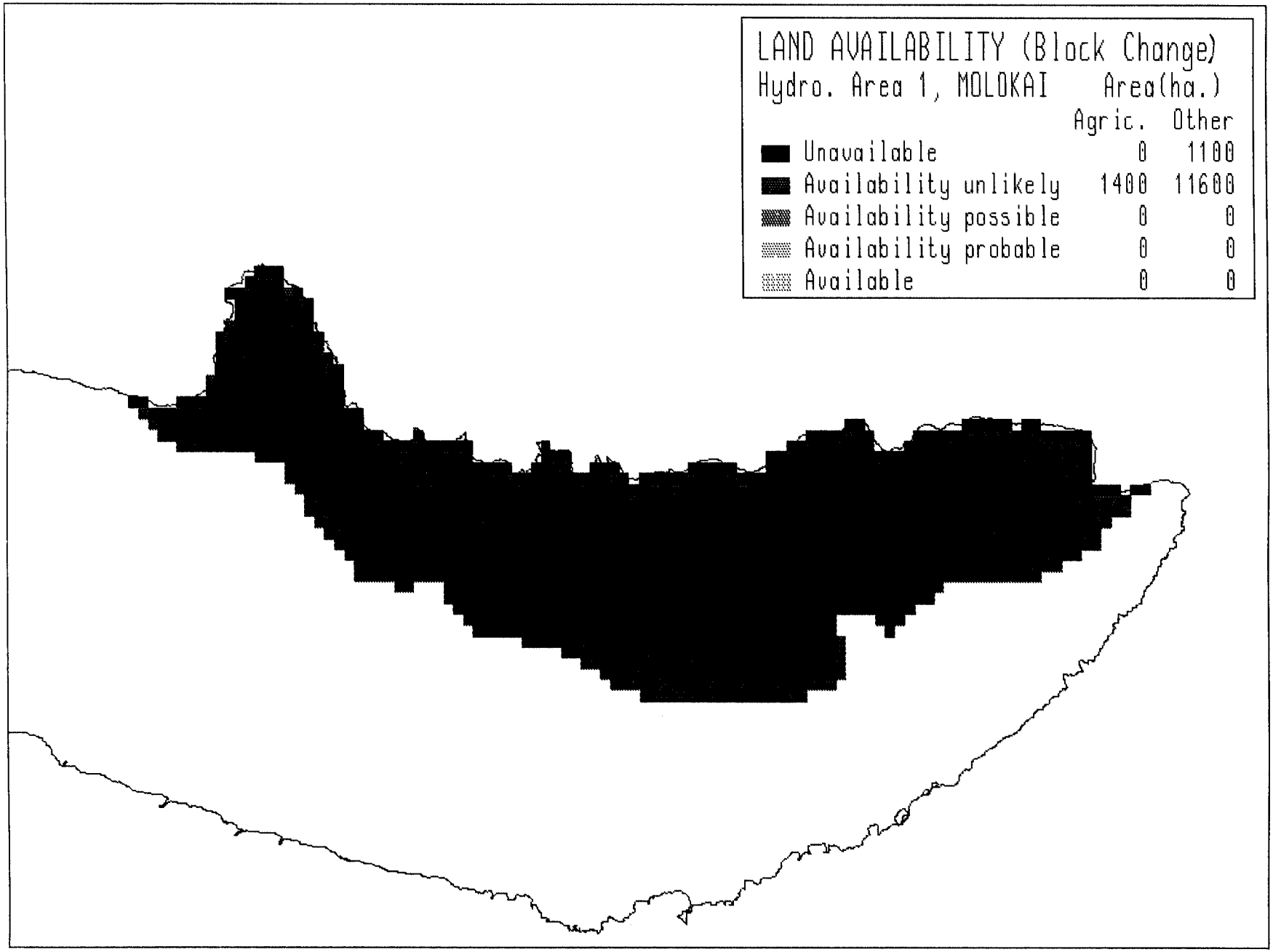

Fig. 11. Land Availability in Hydrographic Area 1 with Block Change

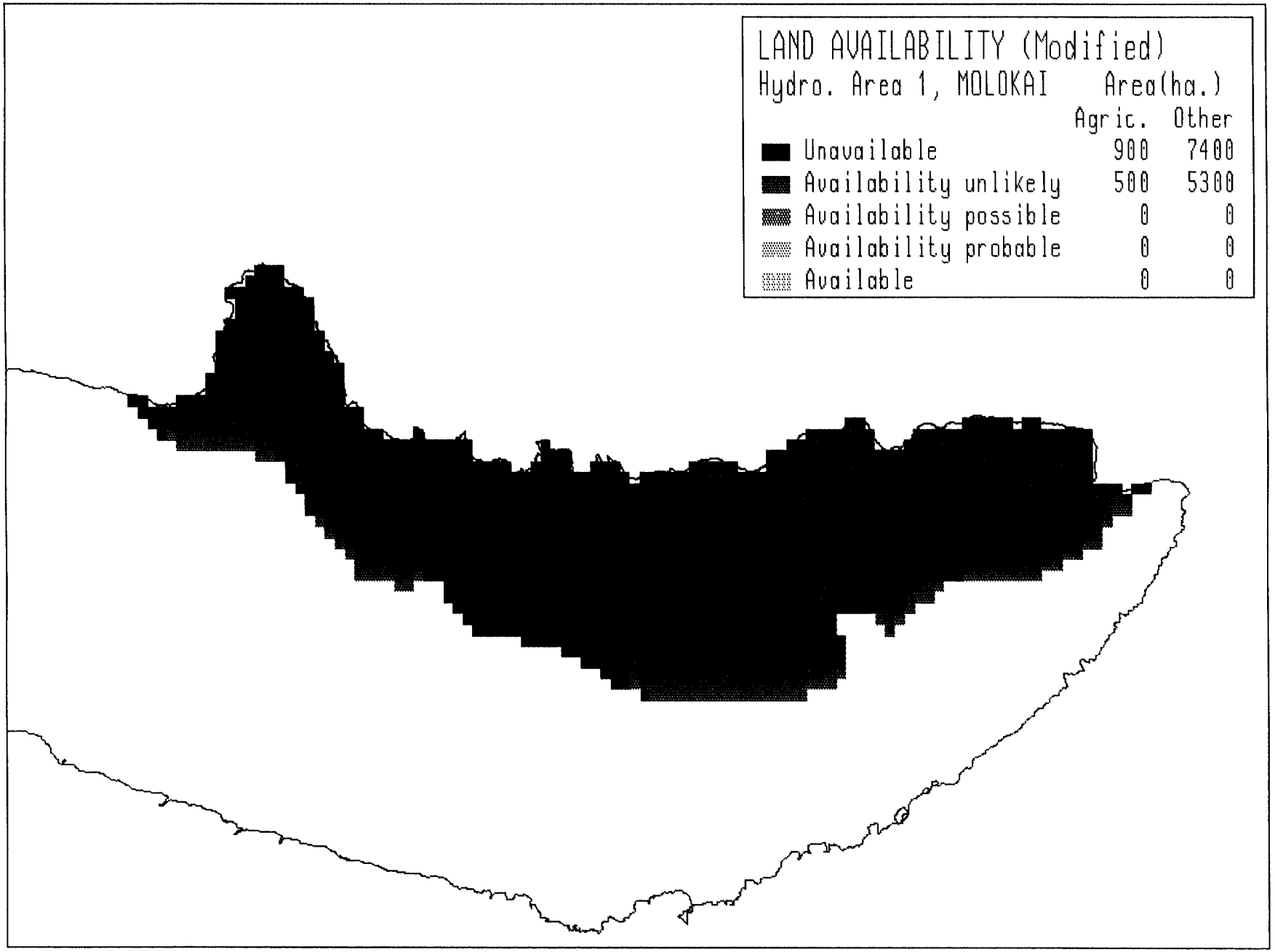

Fig. 12. Land Availability in Hydrographic Area 1 after Block Change using Modified Data

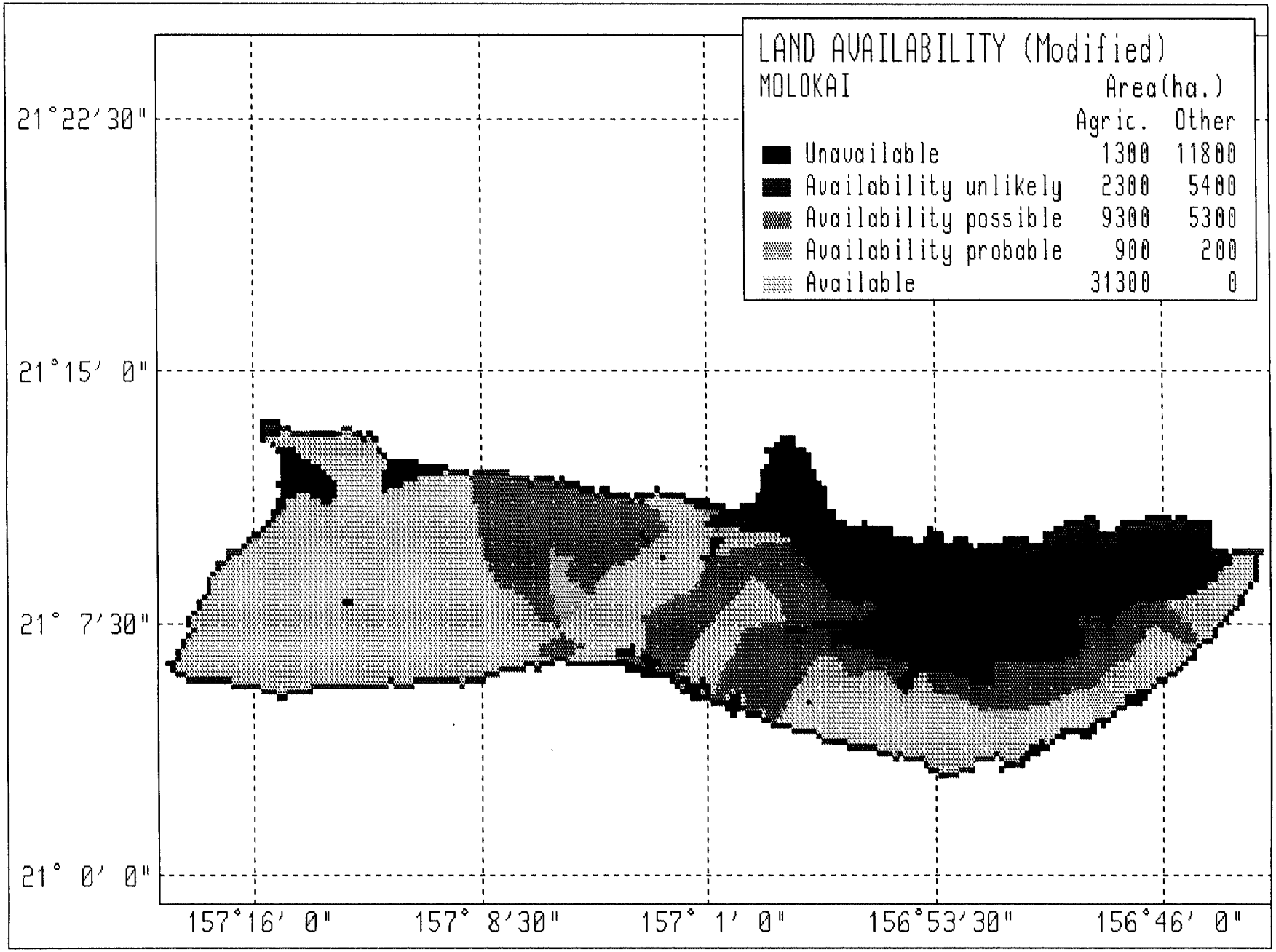

Fig. 13. Land Availability Classes on Molokai based on Block Change and Modified Data

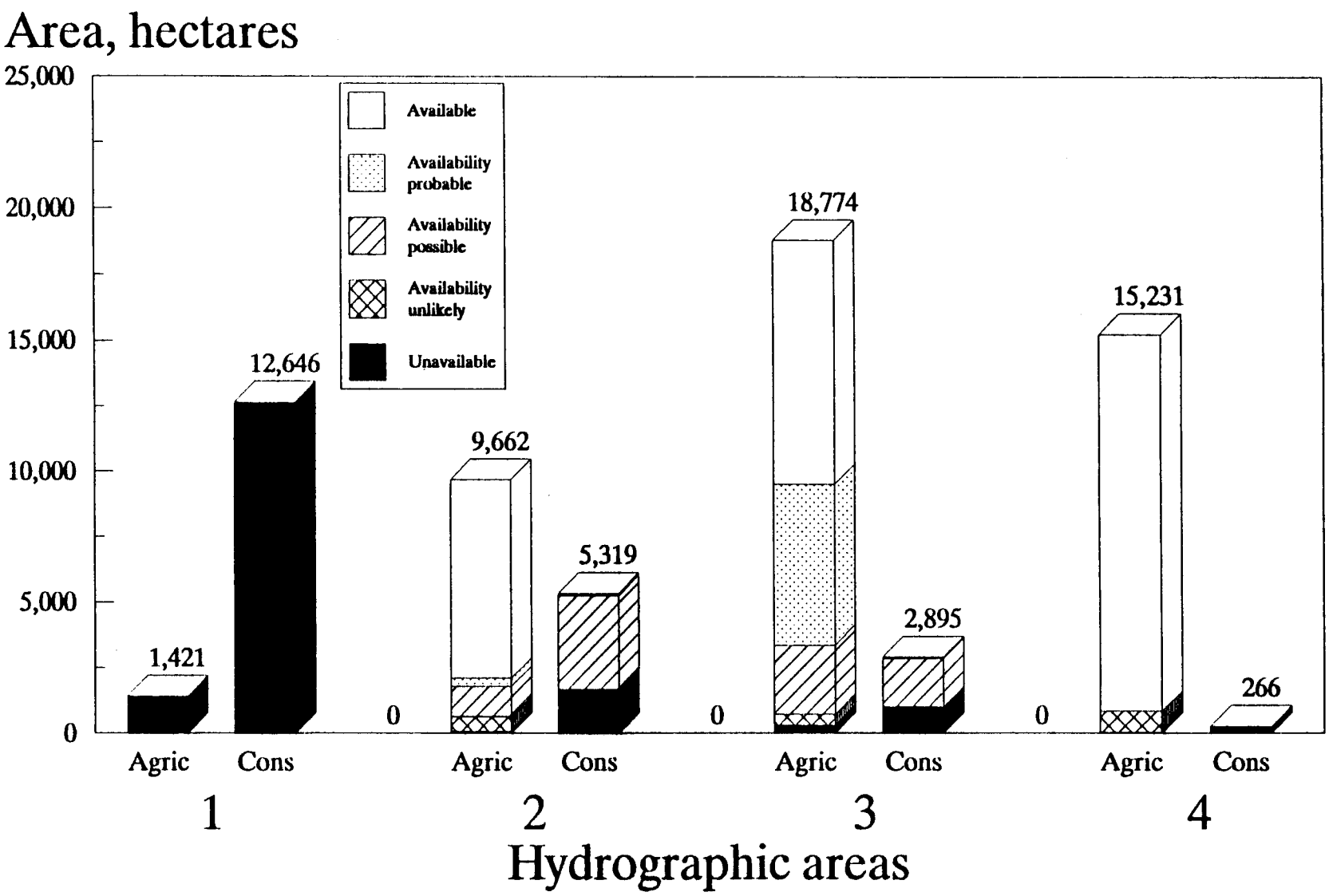

Fig. 14. Land Availability for Biomass by Hydrographic Areas on Molokai using Block Change and Modified Data

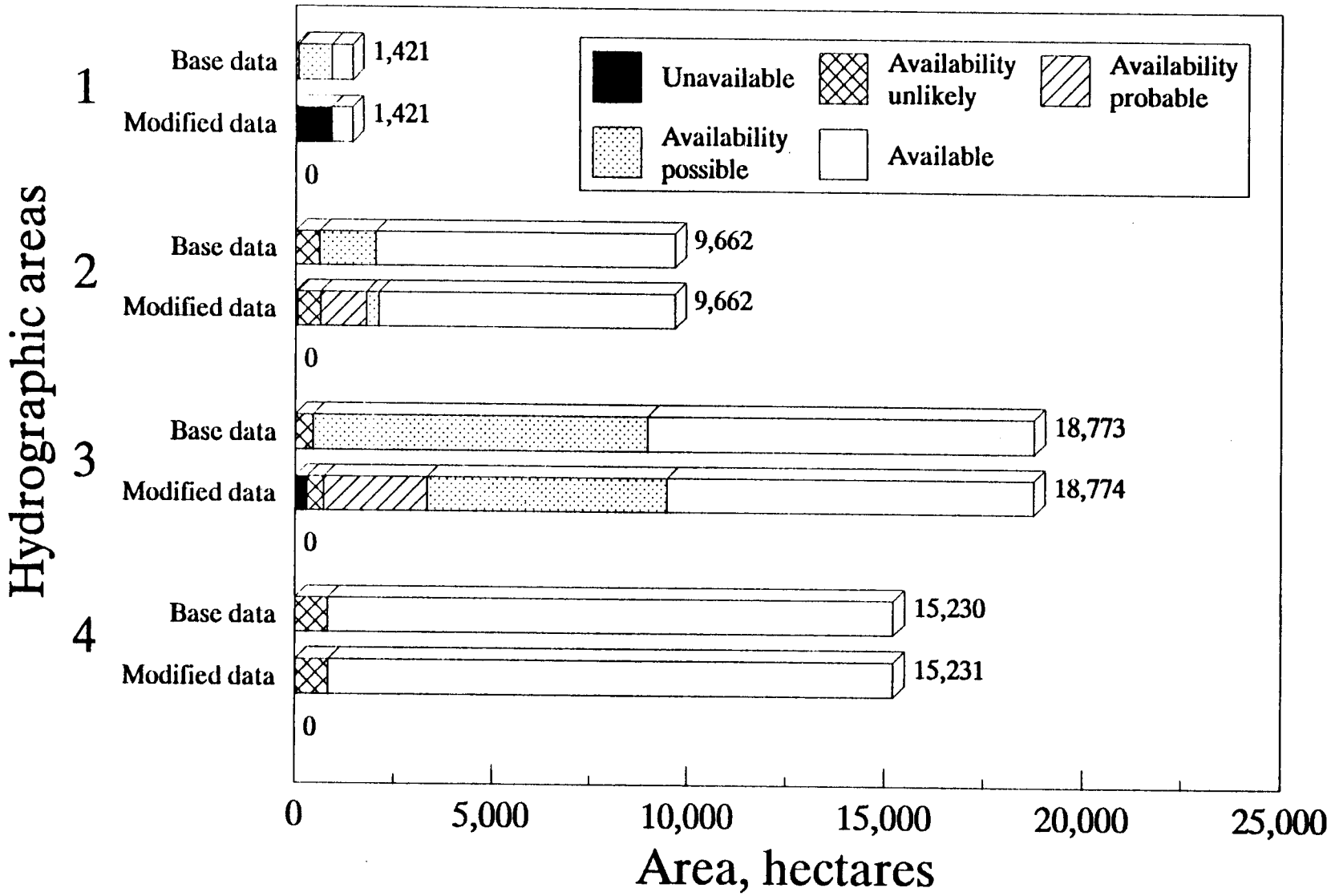

Fig. 15. Effect of Block Change and Modified Data on Land Availability for Biomass on Agricultural Land on Molokai

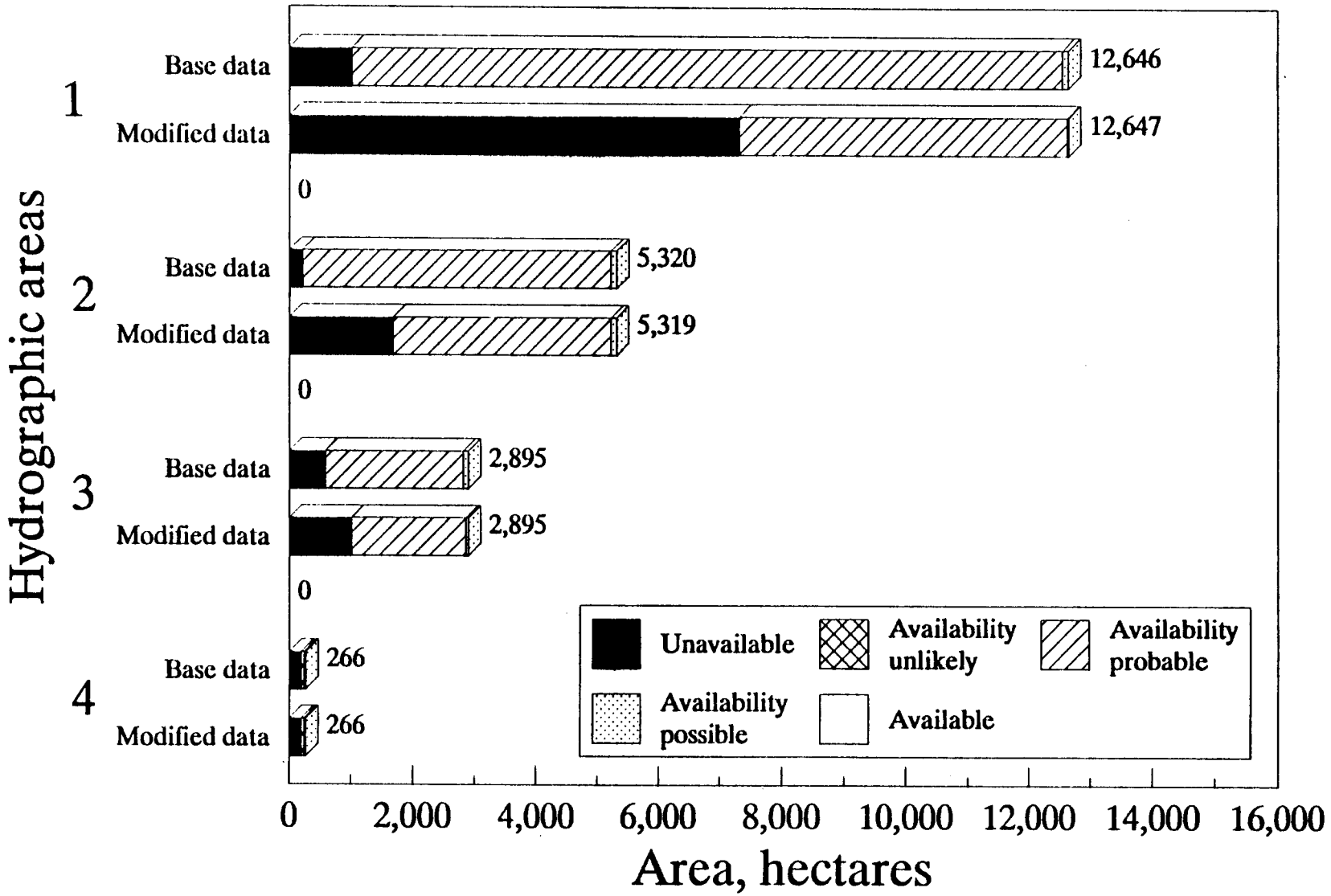

Fig. 16. Effect of Block Change and Modified Data on Land Availability for Biomass on Conservation District Land on Molokai

Appendix B

Short Rotation Woody Biomass Research

Estimation of biological dinitrogen fixation by ^{15}N-dilution in tree plantations: I. Sampling strategies and first harvest results for three legume species.

DWIGHT D. BAKER
School of Forestry and Environmental Studies, Yale University, New Haven, Connecticut, USA,

ROBERT A. WHEELER
University of Hawaii, Department of Horticulture, and the Nitrogen Fixing Tree Association, Waimanalo, Hawaii, USA,

and MAURICE FRIED
National Research Council, Board on Science and Technology for International Development, Washington, DC, USA

Keywords: nitrogen fixation, estimation, ^{15}N-dilution, trees

Summary: Mixed-species tree plantations of Eucalyptus grandis in combination with Enterolobium cyclocarpum, Leucaena hybrid KX3, or Paraserianthes falcataria were established in two fields at the University of Hawaii Experiment Station at Waimanalo, Oahu. The perimeter of each 75 m^2 replication block was trenched and a multi-layered plastic film barrier installed to a depth of 1.5 m. A liquid solution of ^{15}N-enriched ammonium sulfate was applied to each block at three months after seedling establishment. Leaf tissue samples were collected using two sampling strategies after

seven months of growth and ^{15}N-concentrations were measured. From our results we determined that significant amounts of nitrogen were derived from fixation during this period. However, we observed a significant inhibition of nitrogen fixation in one of the fields attributable to differences in available soil nitrogen.

The experimental design which we used in this field situation proved adequate to estimate nitrogen fixation. A simplified sampling strategy involving random collection of small numbers of leaves from trees was as accurate for measuring leaf ^{15}N-concentrations as a more comprehensive, large-scale strategy. From these results on a young tree plantation, we have concluded that the estimation of tree nitrogen fixation by ^{15}N-dilution methodology is feasible and should be applied more broadly in the future.

Acknowledgements: The Waimanalo Short Rotation Bioenergy Trial located at the Waimanalo Experiment Station of the University of Hawaii was established and continues to operate through support of the Hawaii Energy Institute under the direction of Dr. Victor Phillips. The trial field allocation and guidance for the trial establishment and monitoring have been provided by Dr. James L. Brewbaker of the Department of Horticulture, University of Hawaii. Additional funds for the completion of this study were obtained from the Andrew W. Mellon Foundation through a grant to the Program for Forest Microbiology at Yale University School of Forestry and Environmental Studies.

Introduction

The estimation of symbiotic dinitrogen fixation by tree species in plantations or mature forest ecosystems is difficult. Methods for estimation are limited and all have significant margins of error (Baker 1990).

^{15}N-isotopic dilution methodology using enriched ^{15}N holds promise as an effective and straightforward approach for measuring nitrogen fixation of trees in plantations under field conditions. The basic principles of this methodology have been discussed in several publications (e.g. Fried and Middelboe 1977, Rennie 1986, Hauck and Weaver 1986). A small amount of ^{15}N-enriched fertilizer is applied to the soil and the $^{15}N/^{14}N$ ratio of the nitrogen-fixing and non-fixing plants is measured. The fixation of atmospheric nitrogen by the nitrogen-fixing plant species results in lower enrichments of ^{15}N, when compared to a non-fixing reference species. This is because atmospheric nitrogen has a lower enrichment of ^{15}N than that in the enriched available soil nitrogen. Thus a dilution of ^{15}N is observed, if the plant indeed is fixing nitrogen. The greater the fixation, the greater the dilution and the greater the proportion of nitrogen derived from atmosphere (pNdfa).

^{15}N-dilution methods have been applied to tree seedlings in the laboratory (D. Baker and M. Fried, unpublished results), the greenhouse (Gauthier et al. 1985, van Kessel and Nakao 1986) and under simulated field conditions (Cornet et al. 1985), but only recently in large tree plantations (Sanginga et al. 1989). We feel that this methodology is potentially more accurate in esti-

mating actual contribution of dinitrogen fixation of trees under field conditions. However, much of the methodology is yet to be worked out. We undertook a preliminary study to 1) assess problems of sampling in a large biomass production plantation, and 2) measure nitrogen fixation of trees using ^{15}N-enriched procedures.

Materials and Methods

Plantation establishment

A set of mixed plantations of three legumes species (*Enterolobium cyclocarpum*, *Leucaena* hybrid KX3, and *Paraserianthes falcataria*) with *Eucalyptus grandis* were established in January-March 1989 in fields I and K at the University of Hawaii Experiment Station at Waimanalo, Oahu. Three 75 m^2 replicate plots were established for each of the three combinations of one legume and Eucalyptus within a larger plantation of trees for short-rotation biomass production. Because of the size of the entire plantation, two of the replications were placed in I field and the third in K field. I field had been the site of a Leucaena provenance trial, whereas K field had been unused and was covered with a mixture of perennial grasses.

Previous to planting, the fields were plowed and broad spectrum pre-emergent herbicide applied. The treatment plots were laid out and the perimeter of each plot was trenched and a multi-layered plastic film barrier installed to a depth of 1.5 m to prevent lateral flow of water and fertilizer and restrict root growth to the experimental plot. The tree seedlings were planted on a 1.0 m by 1.5 m spacing interval. The peripheral two rows of each plot were considered border rows and were not used for the collection of data.

Enriched fertilizer application

In May 1989, ^{15}N-enriched ammonium sulfate was applied to each trenched plot at a rate of 10 kg N ha^{-1} (3.06% atom excess). To uniformly spread the label over the field plots, the fertiliz-

er was applied as an aqueous solution using a calibrated pressurized applicator.

Harvesting and biomass estimation

In December 1989, estimates of above-ground biomass were made by measuring height and basal diameter on all trees within the plot, except the border rows. At the same time, leaf samples were collected for nitrogen and ^{15}N analysis.

Leaf sampling strategies

Two sampling strategies were used to collect leaf material from the trees for ^{15}N analysis. The first strategy involved removing half of all the leaves from the selected trees. For Eucalyptus, this meant removing all of the leaves from the right side of each branch. For the legume species, all the pinnae were removed from the right side of each leaf rachis. In each plot, eight trees (four of Eucalyptus and four of the legume) were selected at random for sampling. Because of time limitations, this strategy was applied only to one replication plot of the Eucalyptus/Enterolobium and Eucalyptus/Leucaena treatments, but to all replication plots of the Eucalyptus/Periserianthes treatment.

The second strategy involved collecting only twenty leaves (or pinnae for the legumes) at random from the tree. Because of the small size of Leucaena leaves, we collected 60 rather than 20 pinnae. In each plot, twelve trees (six of Eucalyptus and six of the legume) were selected at random for sampling. For direct comparisons of the two sampling strategies, the same trees were sampled both ways.

^{15}N analysis

Leaf tissue samples were dried at 70°C and ground in a Tecator sample mill. ^{15}N and percent nitrogen analyses were performed using an automated Dumas procedure at the Waikato Stable Isotope Unit in Hamilton, New Zealand. Statistical analyses of the biomass data were performed using SAS-JMP on a MacIntosh computer and of the ^{15}N data using SYSTAT on an IBM PS/2 computer.

Results and Discussion

Biomass

Total above-ground biomass accumulations for the three mixed plantations are shown in Table 1. Significant differences were observed between the different species combinations. At the time of the December 1989 harvest, the majority of trees had attained heights of approximately 2-4 m.

Nitrogen and ^{15}N

Significant differences were observed in nitrogen and ^{15}N enrichments between treatments as well as between the replications in the two fields. Table 2 shows the mean values for percent nitrogen and percent ^{15}N atom excess for all of the replicate blocks and all species. In almost all cases, the legume leafy biomass was higher in nitrogen than that of the interplanted Eucalyptus.

We were surprised to observe the large differences in percent N and ^{15}N concentration between the replicate blocks of the two fields (Table 2). Eucalyptus showed a lower percent N when grown in K field, indicating a lower level of available soil nitrogen in this field. The ^{15}N enrichment of Eucalyptus grown in K field was considerably higher than I field. This again reflects a lower level of available soil N. From the amount and ^{15}N-enrichment of the ammonium sulfate, A values were calculated in accordance with the concept of Fried and Dean (1952). The A value for I field was 268, while that of K field was 199. Thus, our data indicated that the available soil nitrogen content in I field was 30% higher than that of K field. The history of the

use of these two fields provides insight into the observed results. Because I field was most recently used for Leucaena trials, a nitrogen-fixing species, the amounts of soil nitrogen undoubtedly were elevated over that of K field, which was covered with perennial grasses. These differences were observed in standard analyses of available soil nitrogen also.

As a result of these field differences, we observed an inhibition of nitrogen fixation by the higher soil nitrogen levels in I field. In Table 3, we provide values for pNdfa calculated from the atom excess data. Nitrogen fixation (estimated from the pNdfa) was almost two times greater in K field than in I field. This is an impressive demonstration of nitrogen inhibition of nitrogen fixation under field conditions.

In comparing the results of the two sampling strategies, we observed no significant differences in ^{15}N concentration. Table 4 illustrates the similarity of data obtained using the two strategies. From our results, we feel that the more simple procedure of collecting smaller numbers of leaves at random from the trees is sufficient to estimate pNdfa.

Although we have not directly measured total biomass accumulation of these mixed plantations, we feel we can make estimations of total nitrogen fixation (tNdfa) from our above-ground biomass measurements and the pNdfa calculated from leaf tissue samples. In Table 5 our estimations of tNdfa for the three species in the two fields in Hawaii are listed. Our values are comparable to those obtained by Sanginga et al. (1989) for Leucaena, and suggest that the contribution of these nitrogen-fixing

trees is considerable, at least during the first year of growth. Harvesting and export of the above-ground biomass and its nitrogen could result in net negative balances for nitrogen, especially in I field where the pNdfa was estimated at less than 50%. For example, if all of the above-ground biomass were harvested from the Eucalyptus/Leucaena treatment, the result would be a net loss of nitrogen from the site. This is due to the fact that harvesting would remove a greater amount of nitrogen than was contributed by fixation. Other studies have correctly pointed out that harvesting nitrogen-fixing trees is not as nitrogen-depleting as harvesting non-fixing species (Bormann and Gordon 1989, Baker 1990), but it should be fully understood that even the use of nitrogen-fixing tree species can result in nutrient (and nitrogen) export from the site. The amounts of nitrogen fixation estimated in this study are considerable, perhaps due to the young age of the trees. We will be following this plantation over the next three years to determine whether the levels of nitrogen fixation are sustained.

References

Baker, D D 1990 Optimizing actinorhizal nitrogen fixation and assessing actual contribution under field conditions. In Fast Growing Trees and Nitrogen Fixing Trees Eds. D. Werner. Gustav Fischer Verlag, Stuttgart. (in press)

Bormann, B T and Gordon J C 1989 Can intensively managed forest ecosystems be self-sufficient in nitrogen? Forest Ecol. Management 29, 95-103.

Cornet, F, Otto, C, Rinaudo, G, Diem, H G and Dommergues, Y R 1985 Nitrogen fixation by Acacia holosericea grown in field-simulating conditions. Acta Oecologica 6, 211-218.

Fried, M and Dean, 1952 A concept concerning the measurement of available soil nutrients. Soil Science 73, 263-271.

Fried, M and Middelboe, V 1977 Measurement of amount of nitrogen fixed by a legume crop. Plant and Soil 47, 713-715.

Gauthier, D, Diem H G, Dommergues Y R and Ganry F 1985 Assessment of N_2 fixation by Casuarina equisetifolia inoculated with Frankia ORS021001 using ^{15}N methods. Soil Biol. Biochem. 17, 375-379.

Hauck, R D and Weaver R W 1986 Field Measurement of Dinitrogen Fixation and Denitrification. Soil Science Society of America, Madison, Wisconsin, 115pp.

Rennie, R J 1986 Comparison of methods of enriching a soil with nitrogen-15 to estimate dinitrogen fixation by isotope dilution. Agronomy Journal 78, 158-163.

Sanginga, N, Mulongoy, K and Ayanaba, A 1989 Nitrogen fixation of field-inoculated Leucaena leucocephala (Lam.) de Wit estimated by the ^{15}N and the difference methods. Plant and Soil 117, 269-274.

van Kessel, C and Nakao, P 1986 The use of nitrogen-15-depleted ammonium sulfate for estimating nitrogen fixation by leguminous trees. Agronomy Journal 78, 549-551.

Table 1. Above-ground biomass accumulation

Treatment	Biomass yield[1]		
	Eucalyptus	Legume	Total
Eucalyptus/Enterolobium	21.63	32.96	54.59
Eucalyptus/Leucaena	20.40	52.68	73.08
Eucalyptus/Paraserianthes	15.68	42.40	58.08

[1]expressed as Mg/ha fresh weight

Table 2. Nitrogen and ^{15}N content

Treatment	Rep.	Field	% N		^{15}N (% atom excess)	
			Eucalyptus	Legume	Eucalyptus	Legume
Eucalyptus/	1	I	2.99±0.43	3.22±0.13	0.086±0.030	0.050±0.015
Enterolobium	2	I	2.92±0.21	3.12±0.27	0.117±0.027	0.067±0.010
	3	K	2.32±0.27	3.58±0.28	0.125±0.037	0.031±0.016
Eucalyptus/	1	I	2.96±0.27	3.76±0.45	0.094±0.040	0.047±0.018
Leucaena	2	I	2.99±0.26	3.75±0.14	0.089±0.010	0.088±0.024
	3	K	2.19±0.34	2.92±0.33	0.145±0.023	0.048±0.026
Eucalyptus/	1	I	3.34±0.41	3.05±0.35	0.118±0.031	0.062±0.020
Paraserianthes	2	I	2.93±0.36	3.45±0.22	0.158±0.041	0.097±0.027
	3	K	2.68±0.47	3.39±0.44	0.168±0.020	0.022±0.011

each data point represents 6 individuals (± S.D.)

Table 3. Calculations of pNdfa based on field data

Treatment	pNdfa	
	I field	K field
Eucalyptus/ Enterolobium	43.1	75.2
Eucalyptus/ Leucaena	26.4	66.9
Eucalyptus/ Paraserianthes	42.8	86.9

Table 4. Comparison of data obtained with different sampling strategies

Treatment	Rep.[a]	% ^{15}N atom excess[b]			
		small samples		large samples	
		Eucalyptus	Legume	Eucalyptus	Legume
Eucalyptus/ Enterolobium	1	0.091	0.055	0.095	0.055
Eucalyptus/ Leucaena	1	0.109	0.039	0.115	0.042
Eucalyptus/ Paraserianthes	1	0.106	0.057	0.113	0.057
	2	0.141	0.096	0.149	0.101
	3	0.160	0.025	0.168	0.023
	mean	0.136	0.059	0.143	0.060

[a] because of time limitations no samples were collected in the 2nd and 3rd replications of the first two treatments

[b] each data point represents 4 individuals

Table 5. Estimations of tNdfa for legume trees in two fields after seven months of growth

Treatment	tNdfa[a]	
	foliage[b]	total[c]
Eucalyptus/ Enterolobium	65.5	158.6
Eucalyptus/ Leucaena	29.3	202.8
Eucalyptus/ Paraserianthes	48.6	220.7

[a] kg N/ha

[b] calculated from measured dry weight of leaf biomass

[c] calculated by estimating total dry biomass as 0.35 X total biomass fresh weight X pNdfa X %N (0.025)

Biomass Energy Plantation — Root Response to Coppicing and Tree Root Interaction

Daniel Vogt, Kristiina Vogt, Robert Wheeler†, James Brewbaker†, Victor Phillips‡.

†*University of Hawaii, Oahu,* ‡ *Hawaii Natural Energy Institute*

There is general agreement that tropical forests are being depleted faster than they are being regenerated (Myers 1984; Nambiar 1984). Attention regarding potential effects of this deforestation has focused on four concerns: (1) change in local climate, (2) contribution to build-up of atmospheric CO_2, (3) species loss, and (4) degradation of land through increased soil erosion, salinization and desertification (Crosson, 1986). Equally critical as a social issue is increasing fuelwood deficits in developing countries where deforestation is occurring most rapidly. Half of all wood harvested annually is used as fuel for cooking and heating, most of this (at least four-fifths) in the developing countries (Meyers 1984). Time and/or financial resources devoted to fuelwood collection or purchasing can be as much as one-quarter of an urban family's income in the arid and semi-arid areas of Africa, the populous areas of southern Asia, and the arid and mountainous regions of Latin America (Myers, 1984).

In meeting this biomass crisis and to relieve pressure on natural forests, attention has increasingly focused on the role of plantations to meet fuelwood needs. The World Bank predicted that 20-25 million hectares of new plantations would have to be established by the year 2000 to meet future firewood needs alone, doubling the total area of plantations currently in the tropics (Nambiar 1984). Establishment of more tree plantations, especially in moist tropical environments, as well as more intensive management of natural forests would be a major step towards keeping pace and eventually satisfying the world's demand for forest products and wood-derived energy.

Selection of species for monoculture or polyculture plantations depends on recognition of a variety of kinds of benefits that may be associated with particular species, including modification of soil nitrogen status, production of browse material as well as woody biomass, and the possibility of shortening rotation times and reducing the need for large harvesting equipment by utilizing species that will vegetatively sprout following harvest (coppicing).

Species selection and stand management methods to maximize soil amendment and minimize generational decline in coppiced stands are currently being tested in experimental plots in Hawaii. Previous research in Hawaii conducted by DeBell et al. (1989) established plantations of *Albizia*, a N_2-fixing tree, and *Eucalpytus*. *Eucalpytus* when planted alone was found to grow rapidly, but many sites required supplemental nitrogen. In mixed species plantings, however, *Albizia* was able to provide the amount of nitrogen needed by *Eucalyptus* in a high-yielding bioenergy plantation.

With this in mind we have designed a study with the following goals: (1) to examine the feasibility of interplanting other Nitrogen Fixing Trees (NFTs) with *Eucalyptus* to increase wood productivity on N-poor sites for biomass energy plantations; (2) to test coppice regrowth and wood quality derived from short- rotation harvests of 1, 2, 3, and 4 year cycles; (3) to monitor the effects of coppicing on root biomass; and, (4) to determine whether we can distinguish any root interaction between tree species under field conditions. This research is being conducted at the Waimanalo Experiment Station of the University of Hawaii on Oahu.

Four different tree species are being tested in this study: 3 NFTs — *Leucaena* hybrid, *Paraserianthes falcataria* and *Enterolobium cyclocarpum* , and 1 non-NFT — *Eucalyptus grandis*. All are capable of vegetative

In the thick clay soils at this site, it was impossible to dig the necessary trenches using light - weight equipment. Ultimately a back hoe was used to create the one-meter deep trenches dividing the experimental plots. These trenches were lined with plastic and then back filled. Trenches were dug in 1988.

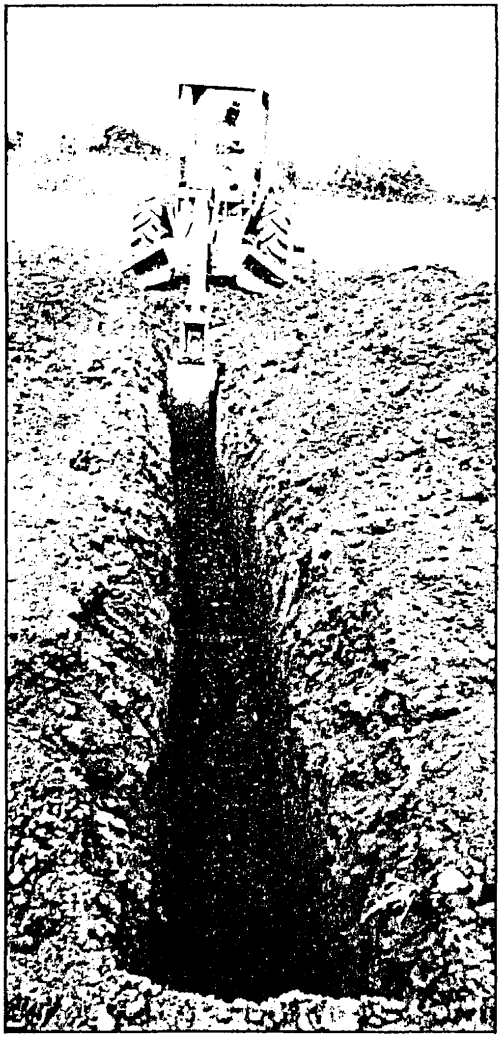

regeneration. Plots are either monoculture or a NFT mixed (50/50) with *Eucalyptus*. Seedlings of each species were planted in the field January 1988.

There are three blocks for replication. Each block is divided into four sections that represent the four different harvest cycles of 1, 2, 3 and 4 years. Within each harvest section there are at least 7 plots representing the 4 monoculture and 3 mixed species treatments. Each plot is 8.5 x 11 m with a tree spacing of 1 x 1.5 m (5 rows of 10 trees per row). The outside rows and ends of each plot are buffer strips (data will be obtained only from inside the middle three rows). The initial tree stocking density was 50 per plot or 5,348 stems per hectare. Some plots were trenched to at least a 1-m depth using a backhoe (a trench was dug around the perimeter of the plot, the trench was lined with thick plastic and back-filled to stop different species' roots from entering the plot). This was done to see if root encroachment would affect adjacent tree biomass and productivity. There was also an additional block established to use as a control in which the trees were not coppiced in January 1990 and would not be harvested until the end of the study. Within this control block the plots were only half the size of the other plots but these plots were all trenched.

Each year in December all the trees will be measured for stem diameter and height. Individual and/or plot tree biomass can be non-destructively determined using tree biomass regression equations developed for each tree species as well as for their components (leaves, branches, and stemwood). For each appropriate year the harvest cycle sections will be coppiced and weighed. Also soil cores for root analysis will be taken in all the control plots, all the trenched plots, and all the 1-year harvest cycle plots.

After four years we will be much further along in understanding not only how productive these nitrogen-fixing trees are and how they affect the aboveground growth of *Eucalyptus* on short-rotations but also how roots interact between different tree species and how they are affected by coppicing.❑

A view of the research site at the Waimanalo Experiment Station of the University of Hawaii on Oahu. In the foreground, plastic lining of the back-filled trenches peeks from the ground. Regrowth following coppicing of four different species of trees are being studied. Three of these are nitrogen fixing. Fast-growing plantations of monocultures or mixed plantations of a nitrogen-fixing species with Eucalyptus *may provide both fuel for energy generation and fodder for livestock.*

REFERENCES

Crosson, P. 1986. Agricultural development — looking to the future. pp. 104-139. In W.C. Clark & R.E. Munn (eds.) Sustainable development of the biosphere. Published for International Institute for Applied Systems Analysis, Laxenburg, Austria by Cambridge University Press, Cambridge. 491 p.

DeBell, D.S., C.D. Whitesell and T.H. Schubert. 1989. Using N2-fixing *Albizia* to increase growth of *Eucalyptus* plantations in Hawaii. Forest Science 35(1):64-75.

Kio, P.R.O. and S.A. Ekwebelan. 1987. IV. Economic, social, and political aspects of management: Plantations versus natural forests for meeting Nigeria's wood needs. In F. Mergen and J.R. Vincent (eds.) Natural management of tropical moist forests: Silvicultural and management prospects of sustained utilization. Yale University, School of Forestry and Environmental Studies, New Haven, CT 06511, USA.

Myers, Norman. 1984. GAIA, an atlas of planet management. Anchor Press/Doubleday & Company Inc. Garden City, New York. 272p.

Nambiar, E.K.S. 1984. Plantation forests: their scope and a perspective on plantation nutrition. pp. 1-15. In G.D. Bowen and E.K.S. Nambiar (eds.) Nutrition of plantation forests. Academic Press, London. 516 p.

UNESCO. 1978. Tropical forest ecosystems: a state-of- knowledge report prepared by UNESCO/UNEP/FAO. Natural Resources Research XIV, UNESCO, Paris.

ACKNOWLEDGEMENTS

This study was initiated in 1988 by Dr. James Brewbaker and Robert Wheeler of the U. of Hawaii and the Nitrogen Fixing Tree Association (NFTA). It is funded by the Hawaii Natural Energy Institute (HNEI) and the Andrew W. Mellon Foundation through the Program in Belowground Ecology at Yale University School of Forestry and Environmental Studies.

Appendix C

Biomass Productivity Studies

ESTABLISHMENT OF
BIOMASS-TO-ENERGY RESEARCH FACILITIES

HSPA Project No. 36-5252

HAWAIIAN SUGAR PLANTERS' ASSOCIATION, 99-193 AIEA HEIGHTS DRIVE, AIEA, HAWAII
MAILING ADDRESS: P.O. BOX 1057, AIEA, HAWAII 96701-1057, TELEPHONE: (808) 487-5561
FAX: (808) 486-5020 TELEX: 7430262

Completion Report of the

ESTABLISHMENT OF BIOMASS-TO-ENERGY RESEARCH FACILITIES

Contract 25059
October 1988 to October 1989

Prepared for the

Alternate Energy Branch
Department of Business, Economic Development, and Tourism
State of Hawaii

by

R. V. Osgood, Project Leader
and
N. S. Dudley, Biomass Specialist

December 1990

HSPA Project 36-5252

About the authors

R. V. Osgood is the department head and an Agronomist and N. S. Dudley is a biomass specialist in the Crop Science Department, Experiment Station, Hawaiian Sugar Planters' Association, P. O. Box 1057, Aiea, Hawaii 96701. Telephone: (808) 487-5561; FAX: (808) 486-5020.

The Hawaiian Sugar Planters' Association is a nonprofit association organized for the maintenance, advancement, improvement, and protection of the sugar industry in Hawaii and for the support of a sugarcane research station.

Any commercial product or tradename mentioned herein is not to be construced as an endorsement by the authors or the Hawaiian Sugar Planters' Association.

TABLE OF CONTENTS

Page

LIST OF TABLES iv

COOPERATORS AND ADVISORS v

EXECUTIVE SUMMARY vii

INTRODUCTION 1

STATUS OF BIOMASS RESEARCH FACILITIES 2

Mountain View , Hawaii Site 2
Kilohana, Kauai Site 3
Hoolehula, Molokai Site 4
Puunene, Maui Site 5
Honokaa, Hawaii Site 6

SUMMARY OF THE SMALL-PLOT SPECIES TRIAL 6

APPENDIX 15

LIST OF TABLES

Page

1. Tree Diameters in The Large Plot Production Trials at 36 Months 8

2. Mean Annual Dry Weight for Several Species at the Mt. View and Kilohana Sites at 24 Months 9

3. Grass Biomass Yield from Five Sites 10

4. Height and Diameter for Trees at Honokaa at 24 Months 11

5. Summary of Tree Height and Diameter for Small Plots at 24 Months 12

6. Combined Anova for Tree Diameter at 24 Months 13

7. Equations Relating Biomass to Diameter Derived from Harvest at Mt. View 14

COOPERATORS AND ADVISORS

BioEnergy Development Corporation

Thomas Crabb
Thomas Schubert
Aileen Yeh

University of Hawaii

James Brewbaker
James Fownes
Russell Yost
Susan Miyasaka

U.S. Department of Agriculture, Forest Service Institute of Pacific Islands

Robert Strand
Craig Whitesell
Tom Cole

State of Hawaii, Department of Land and Natural Resources, Forestry and Wildlife Division

Patrick Costales
Karl Masaki
Robert Meriam
Masayoshi Takaoka

U.S. Department of Agriculture, Soil Conservation Service

John Beddish
Robert Joy

Hawaiian Research, Ltd.
Peter Eichhorn

Hamakua Sugar Company, Inc.

M. Owen Sheets

Hawaiian Commercial & Sugar Company, Ltd.

Mae Nakahata
John Sakuma
Robert Warzecha

The Lihue Plantation Company, Ltd.

Mike Furukawa

Amfac/JMB-Hawaii, Inc.

Charles Wallace

Hawaiian Sugar Planters' Association

Win Bui
Stephen Haller
Yuki Inouye
Tsutomu Yamamoto
Frederick Meinzer
George Mikami
Lance Santo
Alvin Tadani

Hawaii Natural Energy Institute

Vic Philips
Charles Kinoshita

EXECUTIVE SUMMARY

Highlights of the 1989 work include completion of the small-plot species evaluations and initiation of the clonal propagation of selected, elite *Eucalyptus* cultivars. Data collection continued for the third year in the large plot production trials where tree and grass yields are compared.

In the small-plot (1x1 meter spacing) tree species evaluation trials, we found *Eucalyptus grandis* to be more productive than *Leucaena leucocephala* and *Casurina equisetifolia* at all sites. Among the replicated species, *E. grandis* performed best in the upland locations and *L. leucocephala* and *C. equisetifolia* in the lowland locations. The highest tree dry biomass yield was obtained at Kilohana, Kauai, with *Acacia mearnsii* (4.3 ton/ha/mo). Allometric equations were developed for determination of tree dry weight based on the stem diameter. Individual trees having superior growth were selected and techniques are being developed to increase the selections by micropropagation and conventional vegetative propagation.

For the large-plot trial trees planted at 2x2 m growth measurements through 36 months are presented. The most productive trees in the upland sites were the *Eucalyptus* species. In lowland sites, *L. leucocephala* and *C. equisetfolia* were productive, having growth comparable to *Eucalyptus* species.

The grass species plots planted in conjunction with the large tree plots have given an average dry matter yield of 3.26 tons/ha/mo at 33 to 40 months across five sites. Napiergrass grown at Hoolehua, Molokai, was the most productive grass species, yielding 4.1 tons/ha/mo. Densely planted trees (1x1 m spacing) on the upland sites can approach or even exceed grass yields; however, yields in lowland sites exceeded tree yields. At the more practical (2x2 m) tree spacing used in the production trials, tree yields are estimated to be considerably lower than yields achieved by the grasses. Actual tree yield in the large plots will be compared to grass yield at the completion of the experiments in 1991 and 1992.

ESTABLISHMENT OF BIOMASS TO ENERGY RESEARCH FACILITIES

INTRODUCTION

Experimental plots were installed at five Hawaiian sites beginning in 1985 to study the relative productivity of grasses and trees. The sites are located at Mountain View, Hawaii; Honokaa, Hawaii; Puunene, Maui; Hoolehua, Molokai; and Kilohana, Kauai. The sites represent upland and lowland conditions with a wide variation in soil and weather. Replicated small-plot species trials planted at 1x1 m and large-plot tree production trials planted at 2x2 m were established at each site. The yield of the trees is compared to the yield of either sugarcane (*Saccharum* spp. hybrids) or napiergrass (*Pennisetum purpureum*).

We previously presented the methods used in the studies and preliminary results in reports to the Department of Business, Economic Development and Tourism in 1986, 1987, and 1988. This report summarizes the work completed through 1989. Reports appearing in the appendix include the M.S. thesis of N. S. Dudley and a paper titled "Performance of Fast Growing Trees in Diverse Environments."

STATUS OF BIOMASS RESEARCH FACILITIES

Mountain View Site

Small-plot species trials

The small-plot species trial was completed in 1988; however, we have maintained portions of the site in order to collect vegetative propagation material from selected elite trees. Vegetative offshoots from the elite trees have been placed in micropropagation culture at the HSPA Experiment Station in Aiea. In addition, conventional vegetative cuttings from the trees are being grown at the Waiakea Experiment Station, University of Hawaii. We are hopeful that these potentially improved clones will be used in future biomass experiments.

Based on the percent survival rate and the dry weight of harvested trees, we have determined the yield per hectare for 24-month-old trees at the Mountain View site (Table 2). The most productive species was *Eucalyptus urophylla* at 35.9 tons/ha/yr. Height and diameter measurements for tree species are summarized by site in Table 5.

Large-plot production trials

Data collection continued for the large-plot production trials. Only tree diameter is reported since it was determined that tree height was not required to estimate biomass. Tree growth at the Mountain View site is compared to growth at other sites at 36 months after planting in Table 1. *Eucalyptus urophylla* and *E. grandis* performed better than *E. saligna. Eucalyptus* growth at Mountain View was better than at Honokaa and about the same as at Kilohana, the other upland sites. The equations developed for biomass estimation in the small-plot tests (Table 7) were not applicable to the large plots at 36 months because the diameters were out of the range achieved in the small-plot trials. New equations will be developed for larger trees at greater spacing when the large plots are harvested five years after planting (1991).

Sugarcane yield at Mountain View at 40.1 months was 3.2 tons/ha/mo (Table 3). At the conclusion of the experiment the yield of sugarcane will be compared to the yield of the trees in the large plots. Currently, the only tree harvest data are from the small plots where, at two years, the dry matter accumulation of the most productive tree, *E. urophylla*, was 2.9 tons/ha/mo. Sugarcane and tree dry biomass yields in the small plots were comparable; however, we estimate that the large-plot tree yields are considerably less productive than sugarcane at three years since the planting density of the trees is only one-fourth of that in the small plots. Larger per-tree biomass cannot compensate for the reduction in tree population. Actual tree dry matter production in the large-plot trials will not be determined until the termination of the experiment.

Kilohana Site

Small-plot species trial

The small-plot species trial was completed in 1988 and is being maintained to obtain propagation material of selected elite trees. As at the Mountain. View site, trees were felled to determine dry biomass produced per tree (Table 2). The Kilohana site was considerably more productive than the Mountain View site. The most productive species was *Acacia mangium* (51.2 tons/ha/yr). The highest yielding *Eucalyptus* was *E. urophylla* (47.4 tons/ha/yr). The higher yields at Kilohana reflect better growing conditions and better early weed control. A different picture emerged for the large-plot trials because better weed control was provided at the Mountain View site.

Large-plot production trial

Data collection continued in the large production plots. Although Kilohana is a better site for tree growth, performance was not better in the large plots compared to Mountain View. We believe the reason for the poorer-than-expected performance of *E. urophylla* and *E. grandis* in the large plots was related to less-than-adequate early weed control.

Sugarcane yield at Kilohana was 3.1 tons/ha/mo at 36 months (Table 3). At the conclusion of the experiment, tree dry biomass yield will be determined. At present we only have the harvest data from the small plots with which to estimate tree yield. The highest yield obtained was 4.3 tons/ha/mo with *Acacia mearnsii*. *Eucalyptus urophylla* produced 3.9 tons/ha/mo. Both tree species in the small plots produced considerably more biomass than the sugarcane. Large-plot tree biomass yields will be compared to grass yields at the five year harvest.

Hoolehua Site

Small-plot species trial

The small-plot species trial at the Hoolehua site was completed in 1988 and data were presented in the 1988 report to DBED. The most productive tree was *Eucalyptus camaldulensis*. Plots of selected species are being maintained as a source of seed.

Large-plot production trials

Data collection continues in the large plot production trials. Diameters for 36 month old trees are given in Table 1. Based on these data, the most productive tree is *Leucaena leucocephala* although *E. calmaldulensis* and *Casurina equisetifolia* are also growing at about the same rate.

Seed are being collected at the Hoolehua site from *L. leucocephala* for distribution to other researchers. Problems with the irrigation system have plagued the Hoolehua site. Water with high solids content has been supplied from a reservoir, but the filtration system installed has not been able to handle the water being delivered. Additional filters were installed; however, problems have persisted, affecting the growth of the trees. Harvest is planned for 1991.

Napiergrass production at the Hoolehua site was 4.1 tons/ha /mo, the highest of any grass species in the five test sites. Grass dry matter yields will be compared to tree dry matter yields at the termination of the experiment in 1991.

Puunene Site

Small-plot species trials

The Puunene small-plot trials were completed in 1988 and the data were presented in the 1988 report to DBED. The most productive species measured by height and diameter was *Eucalyptus grandis* although *Casurina equisetifolia* and *Leucaena leucocephala* appeared better adapted to the site. Mortality was considerably higher for the *Eucalyptus*. Several plants of two Aracruz eucalyptus clones planted at the site appeared especially well adapted and were placed into micropropagation for increase. This material, selected for sea level conditions in Brazil, appears well adapted to central Maui. The material has been placed into micropropagation and seed was collected. Tree height and diameter data are summarized in Table 5.

Large-plot production trial

Data collection is continuing in the large-plot production trial. Three-year diameter data are presented in Table 1. *Leucaena leucocephala* and *Casurina equisetifolia* performed better than *Eucalyptus grandis*. Although the average diameter for *E. grandis* was greater, mortality was also greater, indicating poor adaptability under the conditions of the experiment. There were problems with both over and under irrigation, and individual trees were infected with a fungus. Severe mortality was observed near the ends of the lines where water ponded. Harvest is planned for early 1991.

Problems with the sugarcane plots forced abandonment of the grass yield trial. Dry matter estimates of sugarcane cut for seed in the area of the trial are 3.4 tons/ha/mo; this value will be used in a comparison with tree dry matter yield at the termination of the experiment.

Honokaa Site

Small-plot species trial

The Honokaa trial was initiated a year later than the other trials; therefore, the two-year performance data were not published in earlier reports to DBED. Two-year height and diameter data are given in Table 4. The *Eucalyptus* species--*E. grandis, E. saligna, E. urophylla* and *E. robusta*--performed well at the site. *Casurina equisetifolia* adapted.poorly. *Acacia mangium* and *Acacia mearnsii* were well-adapted and deserve more attention as fast-growing biomass trees at this location. *Leucaena leucocephala* performed well at Honokaa compared to the other upland sites. Trees in the small-plot trial at Honokaa generally performed well, reflecting the location of the trial. The trial was located at the bottom of a hill and had a deep soil. Nutrients were washed into the site from the large-plot trials located above the site.

Large-plot production trials

Data collection continued in the large-plot trial. Tree diameter data for the Honokaa site are presented in comparison with data from the other sites (Table 1). Growth in the large plots was poor compared to the small plots for the reasons given above. All the *Eucalyptus* species tested performed equally in the large-plot production trials at the Honokaa site.

Sugarcane cv. H65-7052 grew poorly at the Honokaa site. The rate of dry matter production over a three-year period was 2.8 tons/ha/mo, lower than the other upland sites. Tree dry matter production will be compared to the sugarcane production at completion of the experiment.

SUMMARY OF THE SMALL-PLOT SPECIES TRIAL

Since the data for the small plot species trial have been spread over two progress reports, we have summarized the tree height and diameter data for the five sites (Table 5). A statistical analysis follows (Table 6). There was an interaction between species and location, indicating that the species performed

differently at the sites. At the upland sites of Mountain View, Kilohana, and Honokaa, *Eucalyptus grandis* performed better than *Casurina equisetifolia* or *Leucaena leucocephala*. At the lowland sites of Puunene and Hoolehua, *E. Grandis* performed about equal to *C. equisetifolia* and *L. leucocephala.*

DRY MATTER PREDICTION EQUATIONS

Equations based on tree diameter for prediction of dry matter in two-year-old trees were developed for the Mountain View site. Both total and stem-only biomass equations are presented in Table 7. Care must be taken to use the equations should not be used for trees older than two years of age and for trees growing under conditions varying from those where the relationships were developed.

Table 1. Tree Diameters in the Large-Plot Production Trials at 36 months*

Species	Tree Diameter (cm)				
	Mountain View	Kilohana	Hoolehua	Puunene	Honokaa*
E. grandis	8.4	8.2	---	8.4	6.6
E saligna	7.9	---	---	---	6.4
E. urophylla	8.6	8.7	---	---	6.5
E. calmaldulensis	---	---	8.2	---	---
C. equisetifolia	---	---	7.5	7.5	---
L. leucocephala	---	---	8.6	8.5	---

* Tree spacing 2x2 m.

Table 2. Mean Annual Dry Weight for Several Tree Species at the Mountain View and Kilohana Sites at 24 months

Species	Population (trees/ha)	Weight (kg/tree)	Yield (ton/ha/yr)
Mountain View			
Acacia mangium	6,675	3.09	10.3
Acacia mearnsii	7,025	7.25	25.5
Casurina equisetfolia	8,375	2.90	12.1
Eucalyptus grandis	9,375	6.25	29.3
Eucalyptus urophylla	8,675	8.29	35.9
Leucaena leucocephala	9,400	2.26	10.6
Kilohana			
Acacia mangium	7,125	4.41	15.7
Acacia mearnsii	7,775	13.16	51.2
Casurina equisetfolia	7,750	3.93	15.3
Eucalyptus grandis	9,275	8.83	40.9
Eucalyptus urophylla	9,500	9.99	47.4

Table 3. Grass Biomass Yields from Five Sites at Ages 33 to 40 months

Site	Grass	Age (mo.)	Dry Matter Yield (tons/ha) Total	Per Month
Mountain View	Sugarcane '68-1158'	40.1	129	3.2
Kilohana	Sugarcane '68-1158'	36	112	3.1
Puunene*	Sugarcane '65-7052'	---	---	3.4*
Hoolehua	Napiergrass 'banagrass'	35	144	4.1
Honokaa	Sugarcane '65-7052'	33.2	94	2.8

* Previously reported values were inaccurate. The current value is obtained from seed cane yields for Hawaiian Commercial & Sugar Company and dry matter values obtained previously.

Table 4. Height and Diameter for Trees at Honokaa at 24 months

Species	Height (m)		Diameter (cm)	
C. equisetifolia	3.3	e	1.9	d
E. grandis	10.1	a	5.8	a
L. leucocephala	6.1	ed	4.0	bc
A. mangium	5.8	e	5,6	a
A. mearnsii	8.0	bc	5.5	a
E. robusta	7.6	dc	5.0	ab
E. saligna	9.3	ab	5.9	a
E. urophylla.	8.9	abc	5.6	a

Means with same letter are not signifcantly different at 5% level.
Note: -Two-year data for the other sites were reported in the 1988 report to DBED.

Table 5. Summary of Tree Height and Diameter for Small Plots at 24 Months

Species	Mountain View	Honokaa	Puunene	Hoolehua	Kilohana
		Height (m)			
C. equisetifolia	4.3b	5.8b	5.6b	5.8b	5.0b
L. leucocephala	5.0b	6.1b	7.1a	6.1b	4.6b
E. grandis	9.2a	10.1a	7.9a	7.2a	10.8a
		Diameter (cm)			
C. equisetifolia	2.5b	1.9c	4.6b	3.6b	2.4b
L. leucocephala	2.9b	4.0b	5.5a	4.1a	2.0b
E. grandis	5.5a	5.9a	6.4a	4.3a	6.6a

Values in columns with same letter are not significantly different.
p = .05

Table 6. Combined Anova for Diameter for Three Tree Species at Five Locations

Source of Variation	D.F.	SS	MS	F
Location	4	26.2	6.55	11.4*
Replication	15	8.61	0.574	
Species	2	74.29	37.15	9.28*
Spp. X Location	8	32.00	4.00	13.42*
Pooled Error	49	17.58	298	

* Significant at 5% level.

Table 7. Equations Relating Biomass to Diameter Derived from Harvest at Mountain View Site

Species	Regression Equation	R^2
Acaia mangium		
DW stem	$0.02235 * D^{2.736}$	.88
DW total	$0.09815 * D^{2.142}$	.97
A. mearnsii		
DW stem	$0.0572 * D^{2.631}$	.97
DW total	$0.0585 * D^{2.729}$	.97
Casuarina equisetifolia		
DW stem	$0.7839 * D^{3.683}$	.83
DW total	$0.1168 * D^{2.524}$	.93
Eucalyptus grandis		
DW stem	$0.07425 * D^{2.294}$	.94
DW total	$0.06998 * D^{2.439}$	.94
E. robusta		
DW stem	$0.03943 * D^{2.636}$	.96
DW total	$0.04768 * D^{2.756}$	.98
E saligna		
DW stem	$0.06407 * D^{2.467}$	.94
DW total	$0.08765 * D^{2.443}$	.96
E. urophylla		
DW stem	$0.05836 * D^{2.563}$	.98
DW total	$0.07501 * D^{2.534}$	.98
Leucaena Leucocephala c.v. K636		
DW stem	$0.06744 * D^{2.694}$	.86
DW total	$0.10048 * D^{2.391}$	.89

Appendix

Nick Dudley, Hawaiian Sugar Planters' Association, P.O. Box 1057, Aiea, Hawaii 96701, USA.

Performance of Fast Growing Trees in Diverse Hawaiian Environments

Abstract

Biomass productivity was compared for 14 species of fast growing tropical trees in Hawaii. Five locations representing diverse ecosystems on four islands were selected. Three core species with a reputation for fast growth in Hawaii were planted at all sites: *Casuarina equisetifolia* Forst. & Forst.; *Eucalyptus grandis Hill* ex Maiden; and *Leucaena leucocephala* (Lam.) de Wit cv. K636. Eleven species were planted only at selected sites as augments.

A randomized complete block design was used with four replications. Tree density was 10,000 stems per hectare with a spacing of 1 x 1 m. A standard fertilizer treatment of 50 g/tree or 500 kg/ha of 14N-14P-14K was applied at planting, and at 6, 12 and 18 months. At 24 months, the trees were felled and weighed, and wood samples taken. *Eucalyptus grandis* performed well across all sites. *Casuarina equisetifolia* and *Leucaena leucocephala* showed strong site preference.

Introduction

There is a history of tree crop experimentation in Hawaii from which a number of promising fast growing species have been identified (Schubert and Whitesell 1985, Skolmen 1986, Brewbaker et al. 1981). Most of these tree species have the potential for use as energy, fiber or feedstock. These species have been known for many years, but have not been well studied in short rotation, intensively cultured plantings, or evaluated across diverse environments for maximum biomass production. Clearly, matching the proper species with the optimal growing environment is important. The objective of the following study was to evaluate growth (height and diameter) of 14 fast growing tropical trees in different Hawaiian environments.

Materials and Methods

A core of three species were included in each of the five trials sites with a varied selection of 11 species planted as augments at each site. The core species were *Casuarina equisetifolia*

Table 1. Site descriptions.

SITE	RAINFALL (mm)	ELEVATION (m)	SOIL TYPE
Mountain View Hawaii	4,570	389	Dysic, isohyperthermic Lithic Tropofolist
Honokaa Hawaii	2,030	305	Thixotropic, isothermic Hydric Dystrandept
Puunene* Maui	(48)	10	Clayey, kaolinitic, isohyperthermic, Typic Torrox
Hoolehua** Molokai	(70)	100	Clayey, kaolinitic isohyperthermic, Typic Torrox
Kilohana Kauai	2,980	337	Clayey, ferritic isothermic Typic Gibbsihumox

*furrow irrigation, **drip irrigation

Forst. & Forst. (CAS), *Eucalyptus grandis* Hill ex Maid (GRA) and *Leucaena leucocephala* (Lam.) de Wit (LEU). The augment species were *Acacia mangium, A. meamsii, Casuarina cunninghamiana, Eucalyptus alba, E. camaldulensis, E. citriodora, E.*robusta, E. saligna, E. urophylla, Leucaena diversifolia cv. K156, and *L. leucocephala* x *diversifolia* hybrid KX3. Environmental data are listed for each of the five experimental sites in Table 1. Irrigation water was applied as needed at the Puunene. The Molokai site was drip irrigated every day, automatically. Other sites were rainfed.

Eight tree species were compared in a randomized complete block design with four replications. Individual plots were 100 m^2 and consisted of 100 trees. Three-month-old containerized seedling were planted at 1 x 1 m spacing (10,000 trees per ha) in the summer of 1986 using a dibble bar to prepare a hole in the soil the shape and size of the root mass. Fifty grams of fertilizer with $N:P_2O_5:K_2O$ analysis of 16:16:16 was placed by each tree just after planting and every six months throughout the experiment. Data was collected from the interior 20 trees which were bordered on all sides by trees of the same species. Experimental data on the growth rates of these species were collected for a period of 24 months at each site. A simple growth response to fertilizer test was also included in the experiment. There were two treatments, a standard fertilizer treatment of N,P,K, and an unfertilized control. Only the results of fertilizer treatment will be reported in this chapter.

Results and Discussion

Eucalyptus grandis was the most productive core species in height and diameter growth at all sites (Table 2, Figures 1-5). The environmental plasticity of *E. grandis* is well known, when grown as an exotic it loses its ecological sensitivity (FAO 1979). At Kilohana, *E. grandis* attained the greatest measure of both height (10.8 m) and diameter (6.6 cm). High rainfall and cooler soil temperatures of upland sites appear to favor the growth performance of *E. grandis*. At Puunene, stand mortality was highest for this species. This may be due to periodic flooding of the level-level ditch system and adverse site conditions. *E. grandis* prefers well-drained soil and is intolerant of flooded conditions (Turnbull and Pryor 1984).

Leucaena leucocephala ranked second in growth performance over all sites. This species was severely limited by soil acidity and cool temperatures of the upland sites of Mountain View and Kilohana (Table 3 and Figures 1, 5). Poor growth performance of *L. leucaena* at cooler sites has been verified by Brewbaker and Sorensson (1987). Also at Kilohana, Leucaena was accidentally browsed by cattle before the 12-month measurement, and so its growth is not recorded in Figure 5). The best growth performance of *L. leucocephala* was at Puunene where

Table 2. Height and diameter measurements at 24 months after transplanting.

Species	Mt. View	Honokaa	Puunene	Hoolehua	Kilohana	Mean
			Height (m)			
CAS	4.3b	5.8b	5.6b	5.8b	5.0b	4.9b
LEU	5.0b	6.1b	7.1a	6.1b	4.6d	5.6b
GRA	9.2a	10.1a	7.9a	7.2a	10.8a	8.7a
			Diameter (cm)			
CAS	2.5b	1.9c	4.6b	3.6b	2.4b	3.0b
LEU	2.9b	4.0b	5.5a	4.1a	2.0b	3.6b
GRA	5.5a	5.9a	6.4a	4.3a	6.6a	5.6a

NOTE: Values not followed by a common letter are significantly different at p = 0.05.

Table 3. Best performing tree species at 24 months.

Species	Height (m)	Diameter (cm)
Mountain View		
Eucalyptus grandis	9.2	5.5
E. robusta	8.8	5.3
E. urophylla	8.2	5.1
Kilohana		
Eucalyptus grandis	10.8	6.6
E. urophylla	10.2	6.2
Acacia mearnsii	7.6	5.4
Hoolehua		
Eucalyptus camaldulensis	7.5	4.7
E. grandis	7.1	4.2
E. saligna	6.1	4.2
Leucaena leucocephala	6.1	4.1
Honokaa		
Eucalyptus grandis	10.1	6.0
E. saligna	9.3	5.9
E. urophylla	8.9	5.6

NOTE: Values for each site are not significantly different at p=0.05.

Figure 1. Tree heights and diameters at Mountain View.

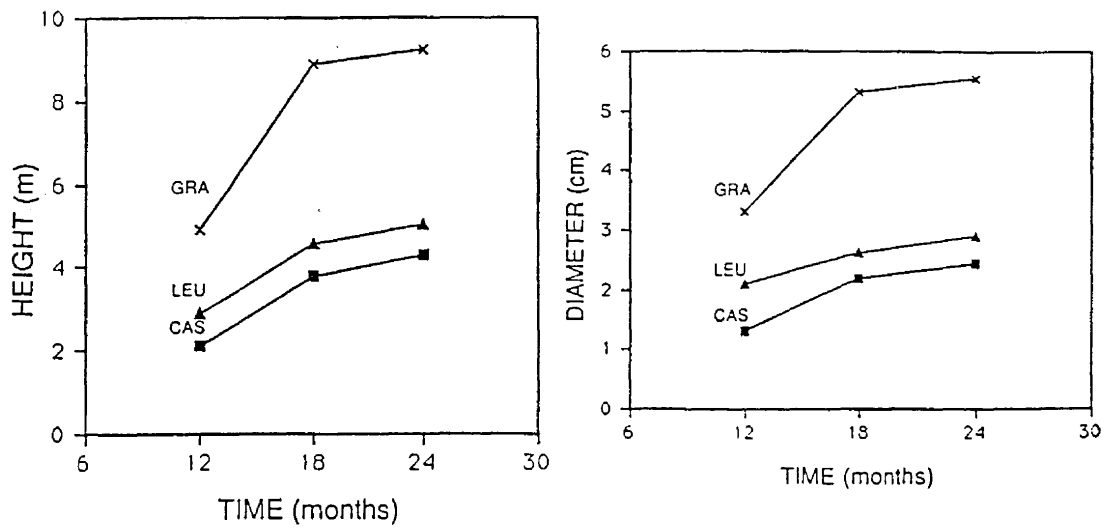

height and diameter recorded were 7.1 m and 5.5 cm, respectively. At Hoolehua and Puunene, *L. leucocephala growth performance was significantly better than that of Casuarina equisetifolia* (Table 2 and Figures 2, 3).

C. equisetifolia showed strong site preference. It performed poorly at Mountain View, Kilohana and Honokaa. Growth was noticeably better, however, at the sea level and mid-lands irrigated sites of Puunene and Hoolehua (Figures 3, 4). The growth performance of *C. equisetifolia*, which ranked third among the core species, was never better than that of *L. leucocephala*

Figure 2. Tree heights and diameters at Honokaa.

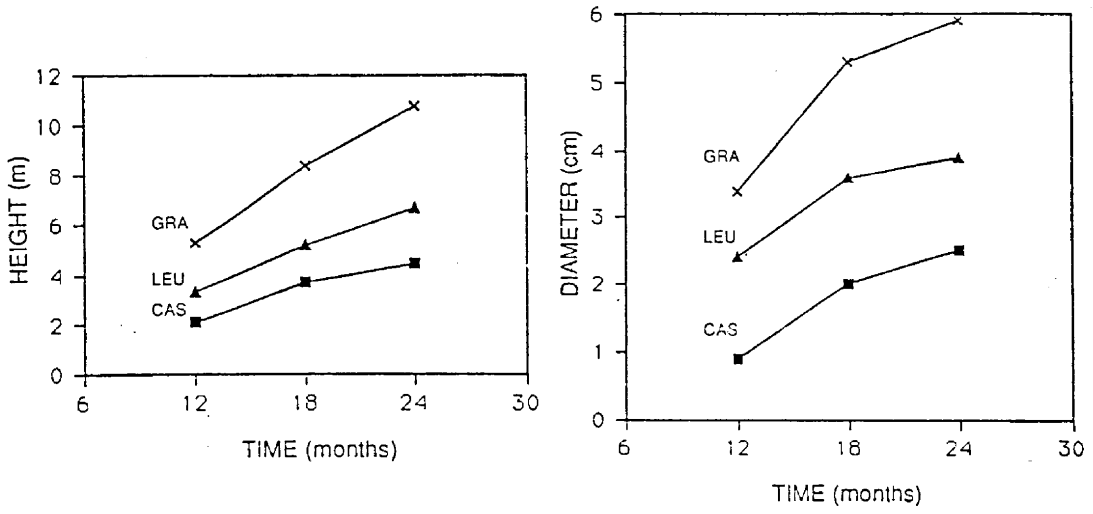

Figure 3. Tree heights and diameters at Puunene.

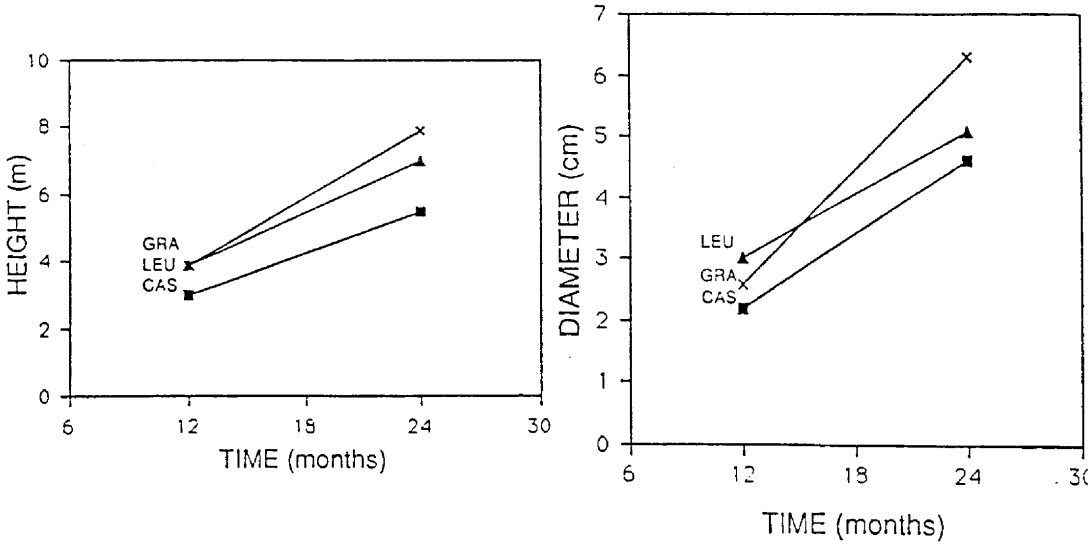

Honokaa is another upland site somewhat drier than the Kilohana site. Tree growth results indicate that eucalyptus were the most productive genus. Specifically, *Eucalyptus grandis, E. urophylla, E. saligna* and *Acacia mearnsii* performed best in terms of height and diameter (Table 2). A combined analysis of variance of diameter growth indicated highly significant differences (P = .01) between locations and species. The location times species interaction was also highly significant, demonstrating variation in environmental requirements among the five species.

Augmented Species Comparison by Location

At the Mountain View site, *Eucalyptus grandis, E. robusta, E. urophylla* and *E. saligna* were most productive in terms of height and diameter (Table 3). This upland site is cool and very wet with extreme soil variability. Kilohana was the most productive site overall with nearly

Figure 4. Tree heights and diameters at Hoolehua.

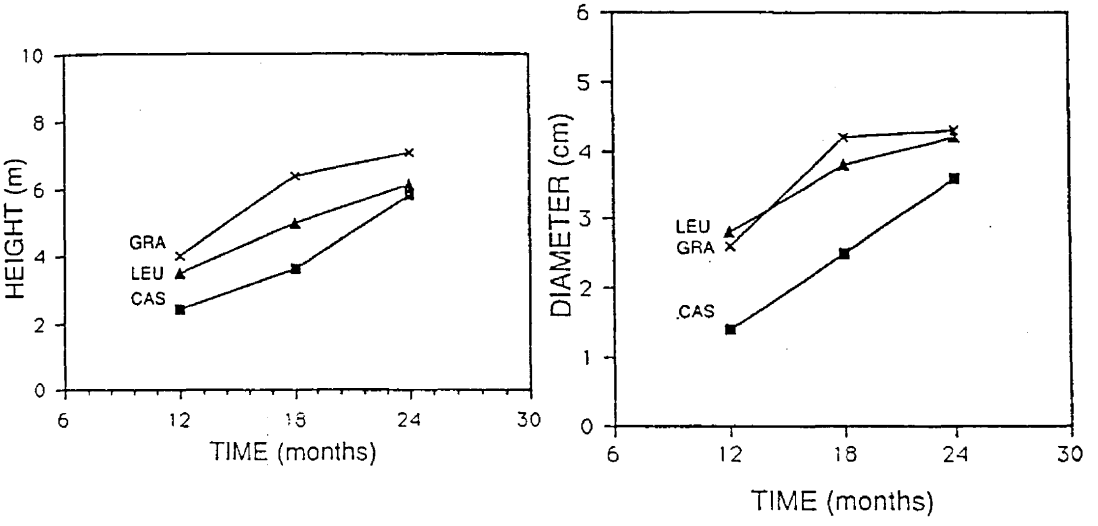

Figure 5. Tree heights and diameters at Kilohana.

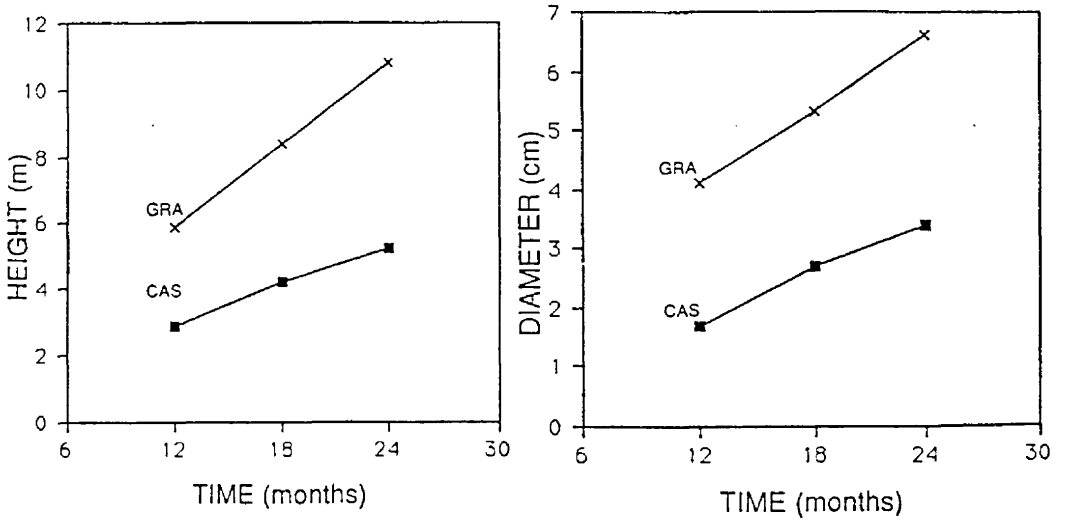

ideal growing conditions for *Eucalyptus grandis, E. urophylla* and *Acacia meamsii* (Table 3). Diameter measurements for *Acacia mangium* and *E. robusta* were not significantly different from the previously stated tree species. Hoolehua is a mid-elevation, drip-irrigated site with hot day and cool night temperatures. There is a strong trade wind effect at this site. The outstanding tree species in terms of both height and diameter were *Eucalyptus grandis, E. camaldulensis, E. saligna* and *Leucaena leucocephala* (Table 3).

The experimental design at the Puunene site was adjusted to accommodate the irregular spacing of the ditch irrigation system that supplied sugarcane mill water effluent to the site. Because of problems created by these design differences, only the growth performance of core species is reported here.

Summary

Of the core species tested, *Eucalyptus grandis* performed well across a range of environmental conditions. Best growth was recorded at the upland sites of Kilohana, Honokaa and Mt. View, respectively. *Casuarina equisetifolia* and *Leucaena* leucocephala showed strong site preference, performing well in lowland and midland sites of Puunene and Hoolehua under irrigated conditions. Of the augmented species: *Eucalyptus urophylla* and *Acacia mearnsii* growth was outstanding at higher elevations sites and merit further testing. *Eucalyptus camaldulensis* grew well under the demanding conditions of the Hoolehua site.

Literature Cited

Brewbaker, J.L., R.J. VanDenBelt and K.G. MacDicken. 1981. Nitrogen-fixing tree resources: potentialities and limitations. Paper presented at Conference on Biological Nitrogen Fixation, Cali, Colombia, 1981.

Brewbaker, J.L. and C.T. Sorensson. 1987. *Leucaena diversifolia* and its hybrids for the highlands. Leucaena Research Reports 8:66-67.

FAO (Food and Agriculture Organization). 1979. Eucalyptus for planting. FAO Forestry and Forest Products Studies, No. 11. Rome, Italy.

Schubert, T.H. and C.D. Whitesell. 1985. Species trials for biomass plantation in Hawaii: A first appraisal. Res. Pap. PSW-176. Pacific Southwest Forest and Range Experiment Station, U.S. Forest Service, USDA, Berkeley, CA.

Skolmen, R.G. 1986. Performance of Australian provenances of *Eucalyptus grandis* and *Eucalyptus saligna* in Hawaii. Res. Pap. PSW-181. Pacific Southwest Forest and Range Experiment Station, U.S Forest Service, USDA, Berkeley, CA.

Turnbull, J.W. and L.D. Prior. 1984. Choice of species and seed sources. *In* W.E. Hillis and A.G. Brown (eds), Eucalyptus for wood production. Academic Press, Sydney, Australia.

PERFORMANCE AND MANAGEMENT OF FAST-GROWING TROPICAL TREES IN DIVERSE HAWAIIAN ENVIRONMENTS

A THESIS SUBMITTED TO THE GRADUATE DIVISION OF THE UNIVERSITY OF HAWAII IN PARTIAL FULFILLMENT OF THE REQUIREMENTS FOR THE DEGREE OF

MASTER OF SCIENCE

IN AGRONOMY AND SOIL SCIENCE

MAY 1990

By

Nicklos Sandor Dudley

Thesis Committee:

James L. Brewbaker, Chairman
Robert V. Osgood
James H.Fownes

We certify that we have read this thesis and that in our opinion it is satisfactory in scope and quality as a thesis for the degree of Master of Science in Agronomy.

THESIS COMMITTEE

James L. Brewbaker
Chairman

Robert V. Osgood

James H. Fowler

ACKNOWLEDGEMENTS

I would like to thank the members of my committee for their support, guidance, and commentary. I am especially grateful to Dr. James L. Brewbaker for expertise in tree species selection, experimental design and analysis, and his global view which greatly strengthens this thesis. I would also like to acknowledge Dr. Robert V. Osgood for his timely advice and the Hawaiian Sugar Planters' Association for allowing me to incorporate my graduate work into the biomass productivity study. Additionally, thanks to Dr. James Fownes for teaching me how to look critically at a tree and for providing counsel when interpretation of experimental data reached final stages of writing.

I am most appreciative for funding of this work provided by the State of Hawaii Department of Business and Economic Development, Energy Division.

My wife Kristen deserves special appreciation for emotional support and financial sacrifice during my master's program. Finally, special thanks to my parents Darwin and Mary Dudley who instilled in me a respect for the natural world and love of trees.

ABSTRACT

Biomass productivity was compared for 14 species of fast-growing tropical trees in Hawaii. Five locations representing diverse environments on four islands were selected. Three core species with a reputation for fast growth in Hawaii were planted at all sites: Casuarina equisetifolia Forst. & Forst.; Eucalyptus grandis Hill ex Maiden; Leucaena leucocephala (Lam.) de Wit var. K636. Eleven species were planted only at selected sites as aguments; Acacia mangium, A. mearnsii, Casuarina cunninghamiana, Eucalyptus camaldulensis, E. citriodora, E. robusta,E. saligna, E. urophylla, Leucaena diversifolia var.K156,L. leucocephala x diversifolia var. K743. Heights and diameters were recorded at 3,6,9,12,18, and 24 months. At 24 months, the trees were felled and weighed, and wood samples were taken.

Of the core species tested, Eucalyptus grandis performed well across a wide range of environmental conditions. Best growth was recorded at upland sites of Kilohana, Honokaa, and Mtn. View. Casuarina equisetifolia and Leucaena leucocephala showed strong site preference, performing best at lowland and midland sites of Puunene and Hoolehua under irrigated conditions. Of the augment species, Eucalyptus urophylla and Acacia mearnsii growth was outstanding at higher elevations. Eucalyptus camaldulensis grew well at the Hoolehua site.

Regression equations based on diameter or diameter and height were obtained from a destructive harvest at Mtn. View. These equations were compared to published equations for accuracy in predicting actual tree harvest weights for both the Mtn. View and Kilohana sites. In general, the dry weight yields agreed with the growth performance data for Eucalyptus as a group and A. mearsii. Casuarina equisetifolia, Acacia mangium, and Leucaena leucocephala grew poorly at the Mtn. View site, reflected in both yield and measurement results. Performance of the published biomass equations varied. The Leucaena volume equation worked well. The published equations for Eucalyptus tended to over-estimate biomass by 20-25%. The published equation for Acacia mangium preformed poorly. However, the specific biomass equation worked well for predicting biomass yields at the Mtn. View site as expected. At the Kilohana site, the prediction performance was quite variable. Problems developed when the regression equations were applied beyond the range of height and diameter. These findings illustrate the preliminary nature of these equations.

The economic feasibility of commercial Eucalyptus woodchip production was outlined. Alternative woodchip markets were analyzed. The production of woodchips for energy was not economical under the condition of this study. The chief contributing factor was the low value of the end product.

In contrast, the production of woodchips for the paper pulp market at high prices was economically viable within the parameters of this study.

TABLE OF CONTENTS

Acknowledgements.....iii
Abstract.....iv
List of Tables.....ix
List of Figures.....x

Chapter 1. INTRODUCTION AND LITERATURE REVIEW. 1
1.1 Biomass production for energy in Hawaii.....1
1.2 Tree species for short-rotation energy production.. 4
1.2.1 Casuarina equisetifolia..... 5
1.2.2 Eucalyptus grandis..... 6
1.2.3 Leucaena leucocephala..... 7
1.2.4 Other tree species..... 8
1.3 Thesis objectives..... 12

Chapter 2. MATERIALS AND METHODS..... 14

2.1 Experimental sites.....14
2.2 Experimental designs.....15
2.3 Establishment of experiments.....16
2.3.1 Seed treatments.....16
2.3.2 Nursery methods.....17
2.3.3 Field establishment.....17
2.3.4 Weed control.....18
2.4 Data collection and analysis.....19

Chapter 3. PERFORMANCE OF FAST GROWING TREES.....25

3.1 Introduction and objectives.....25
3.2 Tree performance at the five locations.....25
3.2.1 Mtn. View, Hawaii.....26
3.2.2 Honokaa, Hawaii.....28
3.2.3 Puunene, Maui.....29
3.2.4 Hoolehua, Molokai.....30
3.2.5 Kilohana, Kauai.....31
3.3 Performance of the three core species.....32
3.4 Summary.....33

Chapter 4. ESTIMATING AND PREDICTING WOODY BIOMASS YIELDS..42

4.1 Introduction 42
4.2 Equation comparison.....44
4.3 Objectives.....46
4.4 Materials and methods.....47
4.2.1 Study area.....47
4.4.2 Destructive harvest data collection.....47
4.4.3 Moisture content and Specific gravity.....48
4.4.4 The choice of regression variables.....49
4.4.5 Tree biomass equations.....49
4.5 Results.....51
4.5.1 Tree survival rates.....51

4.5.2 Wood characteristics.....51
4.5.3 Regression equations.....52
4.5.4 Dry weight yields at Mtn. View.....52
4.5.5 Equation comparison Mtn. View.....53
4.5.6 Equation comparison Kilohana.....53
4.5.7 Mean Annual Increment.....55
4.6 Discussion.....56

Chapter 5. ECONOMIC ASSESSMENT OF EUCALYPTUS FOR WOODCHIP PRODUCTION.....69
5.1 Introduction.....69
5.2 Alternate markets for woodchips.....72
5.2.1 Biomass for energy.....72
5.2.2 Woodchips for paper-pulp.....72
5.3 Methodology.....73
5.4 Results.....74
5.5 Discussion.....76

Literature Cited.....83

Appendices 92

Appendix Table 1 Tree growth data at Mtn. View 92
Appendix Table 2 Tree growth data at Honokaa.....95
Appendix Table 3 Tree growth data at Puunene.....97
Appendix Table 4 Tree growth data at Hoolehua.....98
Appendix Table 5 Tree growth data at Kilohana.....100
Appendix Table 6 Mtn. View weather data.....102
Appendix Table 7 Honokaa weather data.....103
Appendix Table 8 Puunene weather data.....104
Appendix Table 9 Hoolehua weather data.....105
Appendix Table 10 Kilohana weather data.....106
Appendix 11 Illustrative costs and calculations for wood chip production.....107
Appendix 12 Illustrative NPV calculations 108

LIST OF TABLES

2.1 Sites of fuelwood experiments.....20

2.2 Environmental characteristics of sites of fuelwood experiments averaged over 24 months of trial.....20

2.3 Tree species included in experiments.....21

3.1 Height and Diameter Measurements at 24 months after transplanting.....35

3.2 Combined Anova for DBH of 3 Core tree species at five locations.....36

4.1 Published biomass estimation equations.....58

4.2 Tree survival rates at Mtn. View and Kilohana.....59

4.3 Wood Characteristics.....60

4.4 Equations relating biomass todiameter derived from harvest at Mtn View site.....61

4.5 Mtn. View equations: D^2H.....62

4.6 Mtn. View equations: D.....63

4.7 Measured versus estimated mean total dry weight per tree.....64

4.8 Mean annual increment (t/ha/yr) at Mtn. View.....65

5.1 Production costs for the establishment and maintenance of eucalyptus plantations for wood chip production.....79

5.2 Gross revenue per rotation per hectare at varying prices.....80

5.3 Net revenue per rotation per hectare.....81

5.4 Net Present Value per rotation per hectare.....82

LIST OF FIGURES

2.1 Map of Sites.....22

2.2 Site Preparation at Mtn. View.....22

2.3 Tree Planting at Puuene.....23

2.4 Drip Irrigation at Hoolehua.....23

2.5 Eucalyptus grandis Kilohana site after planting.....24

2.6 Installing Experiment at Kilohana.....24

3.1 Tree Height and Diameter (Mtn. Veiw).....37

3.2 Tree Height and Diameter (Honokaa).....38

3.3 Tree Height and Diameter (Puunene).....39

3.4 Tree Height and Diameter (Hoolehua).....40

3.5 Tree Height and Diameter (Kilohana).....41

4.1 Wet Weight to Diameter Comparison (Acacia mangium).....66

4.2 Wet Weight to Diameter Comparison (Acacia mearnsii)....66

4.3 Wet Weight to Diameter Comparison (Eucalyptus grandis).67

4.4 Wet Weight to Diameter Comparison (E. urophylla).....67

4.5 Wet Weight to Diameter Comparison (C. equisetifolia)...68

CHAPTER 1

1. INTRODUCTION AND LITERATURE REVIEW

1.1 Biomass production for energy in Hawaii

As early as 1870 fast-growing trees were introduced to meet fuelwood (energy) needs in Hawaii. By 1915 growing trees for fuelwood represented 44 percent of the total tree planting objective of the Territory of Hawaii Division of Forestry, with Eucalyptus robusta the species of choice (LeBaron, 1970). For the next 50 or so years emphasis of island forestry was placed on forest protection and expansion, and on increasing the watershed to assure adequate water supply for increasing population and agricultural needs (Osgood and Wiemer, 1986). In the late-1970's, due to the high price of imported oil, the potential of trees to provide a renewable source of energy for Hawaii's growing needs regained favor. These investigations included the work of BioEnergy Development Corporation, a C. Brewer company on the island of Hawaii with Eucalyptus and of Dr. J. L. Brewbaker at the University of Hawaii with the nitrogen-fixing tree, Leucaena leucocephala (BioEnergy Development Corp., 1987; Brewbaker et al., 1980).

Hawaii is almost totally dependent on imported petroleum products as an energy source for electrical generation. Periods of rising petroleum prices affect the

basic social well-being as well as the delivery of goods and services throughout the state because electricity is a principal form of energy available. Electrical generation also represents the greatest number of opportunities to use alternate technologies and indigenous, renewable energy resources (Yim, 1979).

Biomass is the most widespread and versatile of the many renewable energy resources. Biomass in the form of fibrous residue from processed sugarcane is called bagasse. The sugar industry in Hawaii makes extensive use of bagasse for the production of electrical energy. The sugar industry has become largely self-sufficient in the production of electrical energy over the past two decades and has sold surplus power to public utilities (BioEnergy Development Corp., 1981). The public utilities have formally contracted a large number of sugar factories to supply electricity on a regular basis (H.S.P.A., 1986). Sugarcane bagasse generated 9.4% of all the electricity produced in the State of Hawaii in 1986 (H.S.P.A., 1987).

A average of 3 million tons of sugarcane bagasse are burnt annually in Hawaii. Total acreage in the production of sugarcane has been declining since the mid-1970's. With increasing electrical demand and the decline in sugarcane acreage, the plantations may not have enough biomass feedstock to provide electricity required under long term contracts with the utility companies.

Short rotation (SR) plantations of fast-growing tropical tree species are considered to be a promising alternative source of renewable biomass energy. (Brewbaker et al., 1981). Energy plantations of fast-growing trees are designed to maximize tree growth. Productivity gains can be made by utilizing practices that are associated with agriculture such as irrigation, fertilization, timely weed control, and high population planting densities (Steinbeck and Thomas, 1984).

This concept of SR forestry has been extended to demands for fuel and fiber products in areas ranging from large industrial plantations (BioEnergy Development Corp., 1985; Brandao, 1984) to small rural fuelwood projects in developing countries (Earl, 1975). The great potential of SR forestry in the tropics results from several factors. First, improved tropical tree species and provenances have become available from expanded yield trials. Secondly, improvements in harvest technology promise more economic chipping of whole trees for biomass energy plantations. Thirdly, very short rotation ages are possible due to the fast growth of selected tropical tree species. Fourth, the coppicing ability of many tropical hardwoods could reduce establishment in later rotations.

The uses of SR plantations in Hawaii for energy has to compete with conversion of wood to fiber for paper pulp or chemicals. Only at high oil prices have biomass plantations

been considered economically viable in Hawaii (Brewbaker et al., 1979). The alternatives depend on the economics of production and the cost of conversion to the respective products. In the following study, economic evaluations were made comparing different markets for Eucalyptus woodchips. The economic viability of the market for energy is compared to the market for paper pulp.

1.2 Tree species for short-rotation energy production

Casuarina equisetifolia (Doran and Hall, 1981) Eucalyptus spp. (FAO, 1979) and Leucaena leucocephala (Brewbaker, 1980; Van Den Beldt, 1983) are a few of the many fast-growing species that have been studied for SR forestry in the tropics. Expanding the knowledge of wood properties and yields of these species and of their environmental and silivicultural requirements is clearly a worthy goal. These three tree species were the experimental core species of this study. Ten additional tree species were also tested but limited to specific sites where growth productivity was thought to have the greatest potential (Brewbaker et al., 1980; Schubert and Whitesell, 1985). A brief discussion of each tree species will follow, but with more detailed discussion of the three core species.

Tropical tree species with the following attributes have been considered as suitable for testing for energy in

Hawaii (MacDicken, 1983; Weisgerer and Hiege, 1988).

- o High biomass production; proven rates of growth that can exceed a mean annual increment of 20 m^3/ha/yr.
- o High capacity for resprouting of harvested stumps even after several rotations, Although, coppice ability and biomass yield are greatly effected by site quality.
- o High resistance to diseases and pests at close spacing.
- o High quality of wood for heating value, density, and fiber lengths optimal for paper and pulp industry.
- o Ease of establishment and adaptation to wide range of environmental conditions.

1.2.1 Casuarina equisetifolia

Casuarina equisetifolia Forst. & Forst. is a moderate to large sized tree growing to a 50 m height, but usually averaging 15-20 m. It is apparently native to a wide region including coastal N and NE Australia, some Pacific islands, Indonesia, Malaysia, India, and Sri Lanka (NAS, 1980). Native environments are characterized by an annual rainfall of about 1000-1500 mm with a 6 to 8 month dry period. The form of a mature tree is arboreal with a open branched canopy. It has a rapid growth rate and wide environmental range, is able to tolerate saline conditions and is wind resistant (NAS, 1980). Further, it is reported

to adapt well to poor sites, although yields are reduced (Doran and Hall, 1981). Casuarinas fix N in root nodules containing actinomycetes of the genus Frankia. Mature trees have a high specific gravity of 0.8 to 1.2 and wood yields that range between 7.5 and 20 m^3 per ha per yr (NAS, 1980). It is known as one of the world's best firewood and makes excellent charcoal with a calorific value of about 4,950 kcal/ kg (Doran and Hall, 1981; NAS, 1980). Casuarinas can be used to make a pulp, but are inferior to eucalyptus and leucaena.

1.2.2 Eucalyptus grandis

Eucalyptus grandis Hill ex Maiden is a fast growing tropical tree native to north-central and coastal Australia. Natural habitats are characterized by rainfall from 1000 to 1800 mm with a 3 month dry season (FAO, 1979). The form of mature trees is usually excellent, reaching heights of 60 m with a wide and spreading crown (NAS, 1980).

E. grandis has performed well on a wide range of soils, but generally prefers moist, well-drained soils of alluvial or volcanic origin (Turnbull and Pryor, 1984). It has performed best in a humid subtropical or warm temperate climate. When planted on a well suited site, it combines very rapid height growth (2-3 m/yr) with a tall, columnar, naturally self-pruning trunk (FAO, 1979). Environmental

factors which limit growth performance are frost, low rainfall, and wind. Poor growth performance is reported on soils deficient in boron (NAS, 1980) and tropical climatic conditions of high temperature and humidity, where it is susceptible to disease. None of the eucalyptus fix nitrogen, and yields are severely limited if they are not fertilized.

Eucalyptus yields of 40 m^3/ha/yr were reported under irrigation in Zimbabwe (NAS, 1980). In Argentina a yield of 50 m^3/ha/yr has been obtained in 14 year old trees. In New South Wales a yield of 22 m^3/ha/yr is common (FAO, 1979). In Brazil, average yields of 33 m^3/ha/year with unimproved seedling and yields as high as 70 m^3/ha/year with selected clonal stock have been recorded (Brandao, 1984). In southern Florida, E. grandis had the highest biomass productivity on two sites with yields of 25 m^3/ha/yr, but extreme freeze terminated the study (Rockwood, 1984). With its high yields and a specific gravity of 0.40-0.55, it makes a good fuelwood species. Other uses are for the production of paper pulp, poles for electrical and telephone lines, wood crates, and occasionally veneer (NAS, 1980).

1.2.3 Leucaena leucocephala

Leucaena leucocephala (Lam.) de Wit is a leguminous tropical tree native to Central America, which is now

distributed throughout the tropics. It fixes nitrogen and may not require additional nitrogen fertilization for acceptable yields. Leucaena is the subject of a annual publication, "Leucaena Research Reports" and several review articles (NAS, 1977; Brewbaker and Hutton 1979; Brewbaker, 1988). The arboreal Salvador type var. K636 has the added advantage of delayed flowering, lower seediness, less branchiness, (Brewbaker, 1980) and some tolerance to the leucaena psyllid Heteropsylla cubana (Sorensson and Brewbaker, 1987).

Leucaena leucocephala is well adapted to low elevations in the tropics but is limited by poorly drained and acid soils (Brewbaker and Hutton, 1979). In Taiwan, average yields of 22.2 m^3/ha/yr at a density of 10,000 stem/ha were reported (Hu and Kiang, 1983). In Hawaii, for a planting that was 2 years old, Van Den Beldt and Brewbaker (1980) found that yields averaged 65 m^3/ha. Further, leucaena has been studied for over 75 years as a fuelwood species (Matthews, 1914). With a specific gravity range of .45-.55, it is in fact excellent fuelwood. In combination, the above properties of leucaena make it a promising species for biomass production.

1.2.4 Other tree species

Acacia mangium is a fast-growing leguminous tree that

is native to NE Australia, Papua New Guinea, and eastern Indonesia. Hot, humid conditions of the lowland tropics favor its establishment and growth, with occurrences reported to elevations of 720 m. In its native habitat, the annual rainfall varies from 1000 mm to more than 4500 mm, indicating a wide environmental range (NAS, 1983). Acacia magium grows to 30 m generally with a straight bole, clear of branches for more than half of its total height. It has the ability to grow on soils with pH as low as 4.2 (NAS, 1983). The species also tolerates calcareous and saline soils. It is a promising biomass species with reported yields of 44 m^3/ha/yr in Sabah, Malaysia (NAS, 1983). With a specific gravity range of 0.4 to 0.56, it is reported to make excellent firewood and produces pulp comparable to eucalyptus in quality.

Acacia mearnsii De Wild. is an Australian acacia well suited to cool, moist environments of tropical highlands. At maturity in its native habitat, A. mearnsii may attain a height of over 20 m. Yields up to 25 m^3/ha/yr and a specific gravity of 0.3-0.5 make it of interest for biomass production (NAS, 1980). A. mearnsii has been pulped for rayon and paper production in South Africa (Sherry, 1971). A. mearnsii clearly merited further testing based on fuelwood trials in Hawaii, where estimated yields ranged from 45 to 107 m^3/ha/yr in unreplicated trials (Brewbaker, 1986; MacDicken, 1983). Since A. mearnsii occurs in

association with eucalyptus in its natural range, A. mearnsii should be a good choice in a mixed plantation with eucalyptus (Sherry, 1971).

Casuarina cunninghamiana Miq. is the largest species of the genus, growing to a height of 35 m on good sites. It is a tree of interest for biomass production in Hawaii because it is suited to drier midland and upper elevations. It is an excellent fuelwood and was formerly used for bakers' ovens (Doran and Hall, 1981). In its native habitat it is found in association with E. camaldulensis (Doran and Hall, 1981).

Over 80 species of Eucalyptus have been grown in Hawaii, on a wide range of sites ranging from hot, dry lowland Vertisols to upland Histosols and Inceptisols that developed on recent lava and ash deposits (FAO,1979).

E. camaldulensis Dehnh. is one of the most widely distributed eucalyptus species in Australia (Turnbull and Pryor, 1984) and one of the most widespread exotic tree species in the world (Zobel et al., 1987). Due to the vast native distribution, there are considerable differences between provenances, and testing for local adaptability is well advised. It is a tree that attains a height of 25-50 m, and noted for its ability to withstand waterlogging and drought and is a vigorous coppicer (FAO, 1979). It has been used for fuel, charcoal, posts and poles. Additionally, it is used for pulp production in

Portugal and Spain (FAO, 1979).

E. citriodora Hook. is a tree for drier, low to mid-elevations sites in Hawaii that can attain a height of 30-40 m and is generally of excellent form. In the Congo a 4 year old trial produced 12 m^3/ha/yr (FAO, 1979). Further, it has a high specific gravity range of 0.75 to 1.10 (Turbull and Pryor, 1984). The wood is utilized for sawtimber, but is considered unsuitable for pulping, while the leaves produce citronella oil which is used in perfume.

E. robusta Sm. is an old favorite in Hawaii, where it occupies many difficult and poorly-drained sites. It will grow where other eucalyptus have failed (BioEnergy Dev. Corp., 1985). It is a medium sized tree up to 30 m in height which has produced mean annual increments of 26 m^3/ha/yr in Hawaii (NAS, 1980). Growth is favored by high rainfall in mid to upper elevations in Hawaii. It is a less preferred pulp species than E. grandis or E. saligna.

E. saligna Sm. is a tree that is adapted well in Hawaii (BioEnergy Dev. Corp.,1985). It is a large tree that can attain a height of up to 55 m with a straight clear bole up to two thirds of total height. In Hawaii, it has been reported to produce 50 m^3/ha/yr (FAO, 1979). With a wood density somewhat greater than E. grandis, it is a favored species for biomass production (FAO, 1979). E. saligna is considered to produce pulp of excellent quality in fast growing plantations.

E. urophylla S.T. Blake is a promising species for biomass or pulp production because it has a slightly denser wood than E. grandis or E. saligna, but similar qualities (FAO, 1979; BioEnegry Dev. Corp., 1985). In addition, it has environmental requirements similar to E. grandis and E. saligna and has high resistance to the stem canker Cryophonectria cubensis (Bruner) Hodges, which affects E. saligna (NAS, 1983). It is a tall tree which can exceed 50 m on favorable sites. Yields of 20-30 m^3/ha/yr have been reported under favorable conditions (NAS, 1983).

Leucaena diversifolia var, K156 is an arboreal upland relative of Leucaena leucocephala reported to have greater cold tolerance and similar wood properties to the lowland species (Brewbaker and Sorensson, 1987). It has produced fresh weight yields ranging from 12 to 90 t/ha/yr in Hawaii (Brewbaker, 1986). Leucaena leucocephala x diversifolia var. K743 is the progeny of L. leucocephala and L. diverifolia that has shown wood properties similar to its parents. It has good growth performance at midland sites (Brewbaker and Sorensson, 1987).

1.3 Thesis objectives

The general objectives of this study were to assess growth performance of selected fast growing trees in five diverse environments in Hawaii to identify the high yielding

tree species at each site.

The specific objectives include:

1. To conduct evaluation trials of superior fuelwood tree species in replicated trials at 5 locations.
2. To develop yield equations for select core species.
3. To conduct economic analysis of Eucalyptus biomass production for fuelwood or pulpwood woodchip markets.

CHAPTER 2

MATERIALS AND METHODS

2.1 Experimental Sites

Five sites were chosen in connection with research imperatives of the Hawaiian Sugar Planters' Association for these performance trials (Table 2.1). The sites were located on four of the Hawaiian islands, and were considered broadly representative of lands that would be available for fuelwood plantations. Two sites (islands of Maui and Molokai) were basically dry lowland sites at which irrigation of sugar is essential. Three sites (on islands of Hawaii and Kauai) were at middle elevations (300-400 m) with high rainfall. Four great soil groups were represented, with pH values ranging from 5.1 to 7.8. As might be expected, vegetation at these sites was greatly different.

The rainfall and light conditions were greatly different from site to site (Table 2.2). The general relationship between rainfall and solar radiation was the lower the elevation of the site, the greater the solar radiation and the higher the elevation of the site the greater the rainfall.

The Hawaii sites are both at higher elevations in high rainfall areas. Mountain View (Fig. 2.1) is a region of very high rainfall on highly leached young soils that

consist of a shallow layer of soil over irregular lava. Ratoon or regrowth sugar cane dominated this site (Fig. 2.2). Honokaa (Fig. 2.1) is at the mauka or high-elevation range of productive sugar lands in an area of moderately high rainfall. A crop of sugarcane was harvested from this site prior to establishment of the experiment.

The Maui site, Puunene (Fig. 2.1) adjoins the HC&S sugar factory at sea level. The factory use this area for dischargiing of mill water effluent. The mill water is delivered through a furrow ditch irrigation system (Fig. 2.3).

The Molokai site, Hoolehua (Fig. 2.1) is a lowland site with low rainfall in an area requiring irrigation (Fig. 2.4) for optimal yields (Brewbaker, 1979). Pineapple plantations formerly occupied this region, characterized by high winds and irregular winter rains.

The Kauai site, Kilohana (Fig. 2.1) is on abandoned sugar lands which was utilized as cattle pasture prior to establishment of experiment. The soils are highly leached oxisols with poor fertility (Fig.2.5) and high rainfall.

2.2 Experimental Designs

The Hawaiian Sugar Planters' Association was contracted in 1986 to initiate a comparative study of biomass yields of grasses and trees. The small plot trial of the present

study was installed at five sites in June of 1986 to compare growth rates of 13 species of fast-growing tropical trees. A core of three species was included at each of the five trial sites. These were:

Casuarina equisetifolia Forst. & Forst.

Eucalyptus grandis Hill ex Maiden

Leucaena leucocephala (Lam.) de Wit.

All trials used the randomized complete block design with eight entries in each of four replications (Fig. 2.6). The three core species were replicated at all sites. Five additional species were planted at each site, differing from site to site according to known site specificities (Table 2.3).

Individual plots were 100 m^2 and included 10 rows of 10 trees each on a 1 x 1 m spacing (10,000 trees/ha). Data were collected from the interior 20 trees which were bordered on all sides by trees of the same species.

A test of growth response of two species to fertilizer was included at each unirrigated site comparing a standard NPK fertilizer treatment vs. the unfertilized control.

2.3 Establishment of Experiments

2.3.1 Seed treatments

Seeds of acacias and leucaena have impervious seed

coats that require treatment to promote uniform germination. With the appropriate treatment, the seed coat becomes permeable, permitting rapid and uniform germination. This is best accomplished for A. mangium and A. mearnsii by pouring boiling water over the seed. A volume ratio of 1 part seed to 10 parts water was used, soaking the seeds for 24 hours (Sherry, 1971; NAS, 1983). A bath of concentrated sulphuric acid for 13 to 15 minutes, followed by a thorough rinsing in water is also an effective treatment for leucaena species.

2.3.2 Nursery methods

Tree seedlings were grown for 3-4 months in Hawaii dibble tubes as described by Walters (1981) at Maunawili, Oahu and Wainaku, Hawaii. The soilless media used was a 1:1 mixture of peat moss and vermiculite. A slow release fertilizer and dolomite were added to promote more vigorous growth in the nursery beds. All nitrogen-fixing tree seedlings were inoculated with species-specific Rhizobium strains provided by the NifTAL Project of the University of Hawaii to enhance biological nitrogen fixation.

2.3.3 Field establishment

Site preparation was accomplished by disk harrowing the

existing vegetation two times to prepare a seedbed suitable for planting. The exception was the Mt. View site where a roller-crusher was used to crush the existing cane, then the tree seedlings were planted into the crushed cane mat. Planting of tree seedlings was with a dibble planting bar designed for use with tree seedlings grown in dibble tubes.

The seedlings were transplanted from dibble tubes into holes prepared in the soil by a dibble bar. Fertilizer was applied at planting at a rate of 50 g per tree of 16:16:16 N:P:K, followed by similar treatments at 6-month intervals throughout the experiment. Annual rates of fertilizer were thus 160 kg N, 70 kg P, and 133 kg K per ha per year. These rates were determined to be optimal for Eucalyptus growth at a varity of sites in Hawaii (BioEnergy Development Corp., 1984).

2.3.4 Weed control

A pre-plant application of the herbicide RoundUp (glyphosate) 1% solution used with Princep (simazine) at 4 lb/A successfully controlled weeds for 2-3 months. This was followed by a second application of herbicide, using Goal (oxyfluorfen) at .05 lb/A and Fusilade (fluazifop) at .05 lb/A. at 3 months after planting. Where necessary a third application was applied at 6, 9, and 12 months.

2.4 Data Collection and Analysis

Heights were measured at 3, 6, 9, 12, 18 and 24 months, and DBH values at 12, 18 and 24 months on all plots. Measurements were collected systematically from 20 sample trees per plot in the same order at each date. Selected trees were harvested for measurements of wood and leaf weights at 24 months. The measurement of height was to the tip of the tallest shoot. Diameter (DBH) was measured at 1.3 m above ground (diameter at breast height), and was over the bark.

Statistical analyses were performed by computer using SAS and QUATTRO. Analysis of variance of heights and diameters was conducted together with the Duncan-Waller test of significance of mean differences. Regression analysis was used for developing allometric equations.

Table 2.1 Sites of fuelwood experiments

Location Island	Elevation	Soil Type
	-m-	
Mountain View Hawaii	389	Lithic Tropofolists, dysic, isohyperthermic
Honokaa Hawaii	305	Hydric Dystrandepts, thixotropic, isothermic
Puunene Maui	10	Typic Torrox, clayey, kaolinitic, isohyperthermic
Hoolehua Molokai	100	Typic Torrox,clayey, kaolinitic, isohyperthermic
Kilohana Kauai	337	Typic Gibbsihumox, clayey, ferritic, isothermic

Table 2.2 Environmental characteristics of sites of fuelwood experiments averaged over 24 months of trial

Location Island	Rain	Temperatures: Max	Min	Avg	Solar Radiation
	-mm-		-o C -		-cal/cm^2/day-
Mountain View Hawaii	4570	---	---	23.8	311
Honokaa Hawaii	2030	26.9	19.5	23.9	390
Puunene Maui	480	---	---	27.9	491
Hoolehua Molokai	700	---	---	25.9	450
Kilohana Kauai	2980	26.5	20.2	23.0	350

Table 2.3 Tree species included in experiments

Species Abbreviation		Seed Source
MAN	Acacia mangium	NFTA
MER	Acacia mearnsii	NFTA
CAS	Casuarina cunninghamiana	HDF
CUN	Casuarina equisetifolia	HDF
ALB	Eucalyptus alba	BDC
CAM	Eucalyptus camaldulensis	BDC
CIT	Eucalyptus citriodora	HDF
GRA	Eucalyptus grandis	HDF
ROB	Eucalyptus robusta	HDF
SAL	Eucalyptus saligna	HDF
URO	Eucalyptus urophylla	BDC
DIV	Leucaena diversifolia	UH, K156
LEU	Leucaena leucocephala	UH, K636
K743	Leucaena leucocephala x diversifolia	UH, K743

* BDC = BioEnergy Development Corp.
HDF = State of Hawaii Dept. of Forestry
NFTA = Nitrogen Fixing Tree Assn.
UH = University of Hawaii

Fig. 2.1 Map of Sites

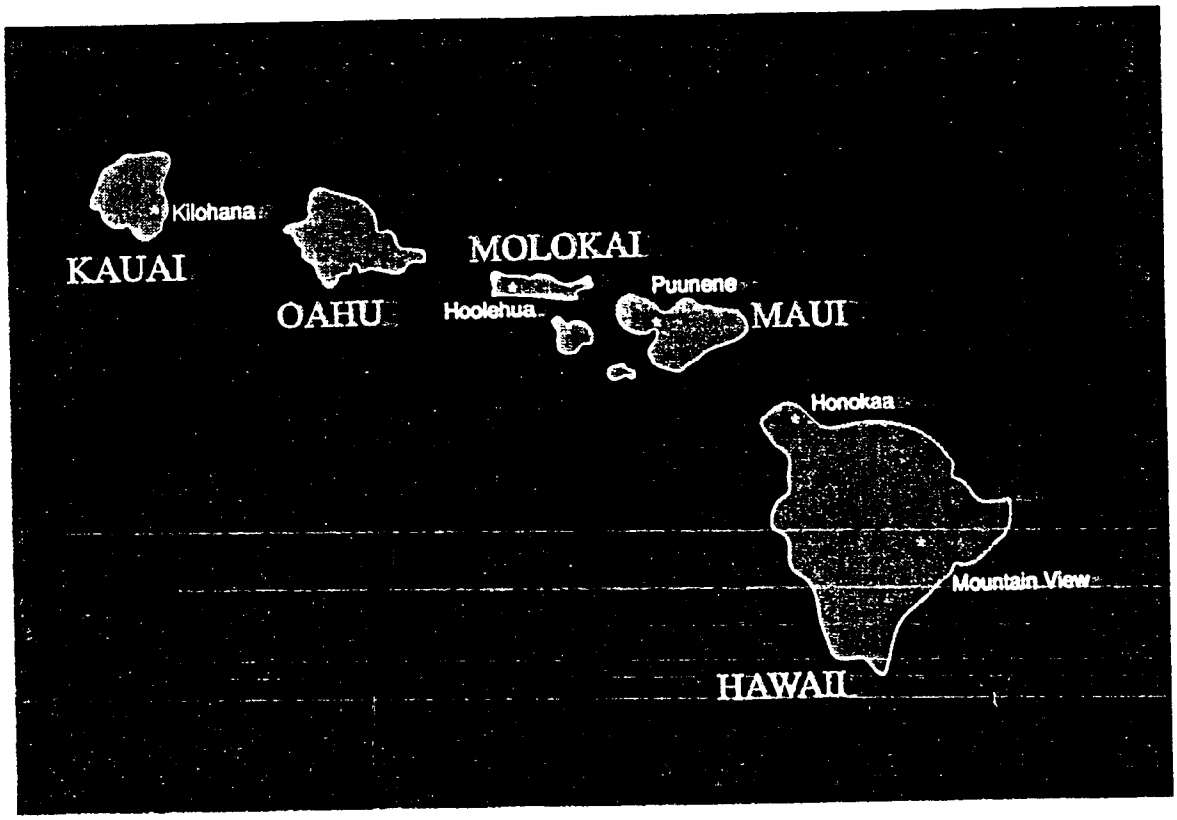

Fig. 2.2 Site Preparation at Mtn. View

Fig. 2.3 Tree Planting at Puunene

Fig. 2.4 Drip Irrigation at Hoolehua

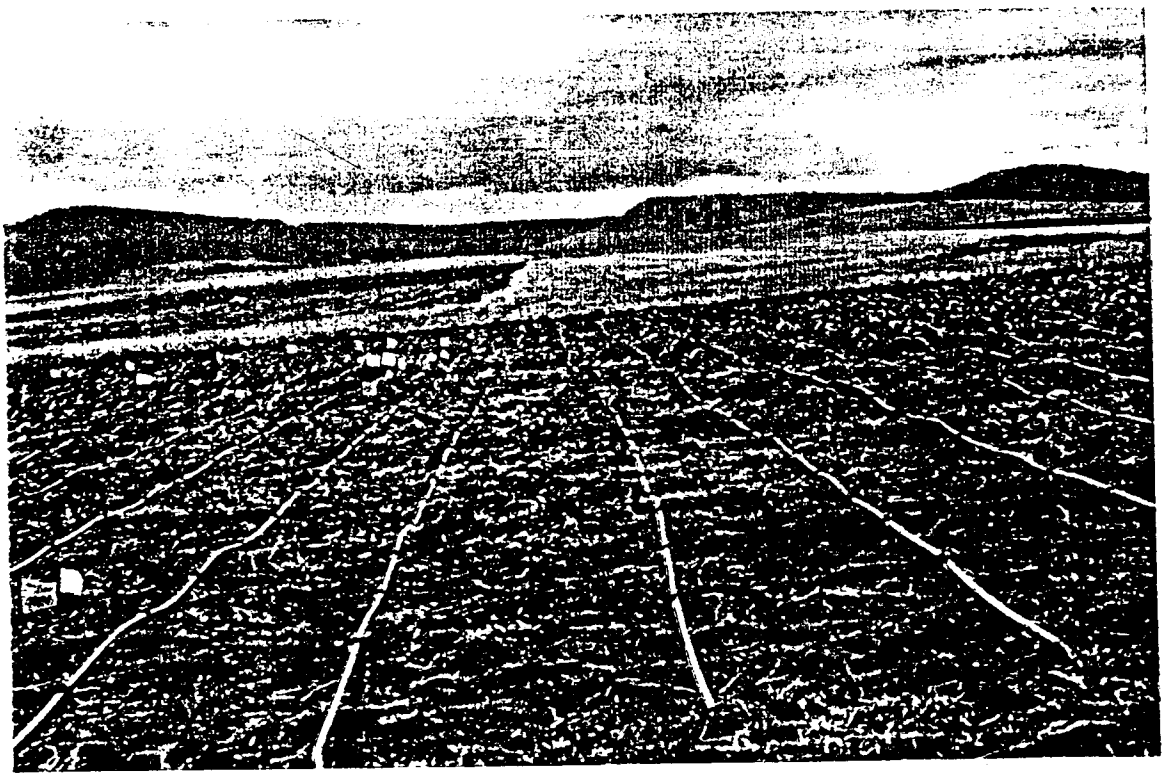

Fig. 2.5 *Eucalyptus grandis* (unfertilized) foreground, *E. grandis* fertilized (background), Kilohana site 12 months after planting

Fig. 2.6 Installing Experiment at Kilohana

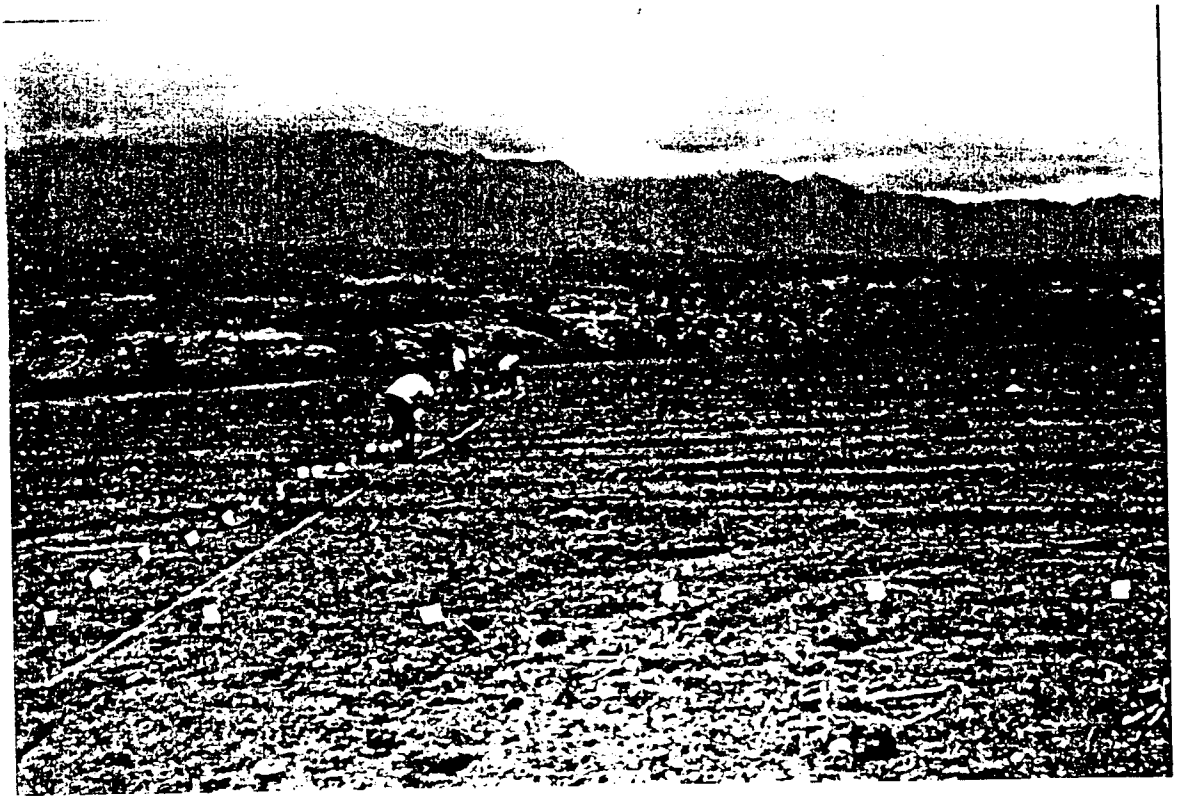

CHAPTER 3

PERFORMANCE OF FAST GROWING TREES

3.1 Introduction and Objectives

Tree crop experiments in Hawaii have identified many promising fast growing species of fuelwood trees (Schubert and Whitesell, 1985; Skolmen, 1986; Brewbaker et al., 1981). Most of these tree species have the potential for utilization as energy, fiber, or feedstock for biochemical conversion. Generally they have not been studied thoroughly in short rotation, intensively cultured plantings, or across the wide range of environments that are available for biomass production in Hawaii. Identifying and matching species to the appropriate site is of obvious importance.

The objective of this study was to test the growth performance over 24 months of 13 fast-growing tree species at five sites on four islands in Hawaii, with special focus on three "core" species included at all sites.

3.2 Tree performance at the five locations

Diameter and height measurements were taken on individual trees at all sites using diameter tapes and measuring rods, often under adverse conditions (rain, wind). Errors in height estimations normally were not too great for trees up to 8 m, even at the 1 x 1 m spacing, but a margin

of error could not be avoided. English was not the first language of some field helpers, which also may have led to some error in recording. However, every precaution was taken to insure accuracy in recording in the field and later transfer to spreadsheets. Data are summarized for the 5 sites in Appendix Tables 1-5, giving averages of the 20 (or fewer) individual tree values taken in each plot.

3.2.1 Mtn. View, Hawaii

The Mountain View ("Mtn. View") site on the island of Hawaii was on the abandoned sugarcane land of Puna Sugar Co. (Amfac). This upland site was cool (23.8 C average) and very wet (4570 mm rainfall) annually (Table 2.1, 2.2). The site was also characterized by extreme variability in soil conditions.

Eucalyptus grandis, E. robusta, E. saligna, and E. urophylla were the tallest species at Mtn. View at every date from 3 mos to 24 mos (App. Table 1). E. urophylla grew fast initially and produced the largest tree up to 18 months when E. grandis overtook it. At final the measurement E. grandis was the tallest (average height 9.2 m) of tree species tested at this site (Table 3.1). Acacia mearnsii began to grow rapidly after a slow start and was clearly the best nitrogen fixing species at this site. Heights of the 8 species showed significant differences by the age of 12 mos

(P<.05). The eucalyptus species achieved their maximum height by 24 mos (mean 8.6 m). They were followed by A. mearnsii (mean 7.0 m). A third group, including Acacia mangium, Casuarina equisetifolia, Leucaena leucocephala (fertilized and unfertilized) and E. grandis (unfertilized) grew poor (mean 4.4 m). At 18 months there was a pronounced plateau in growth suggesting that maxium mean annual increment had been reached at Mtn. View (Fig. 3.1).

Diameter differences between species at Mtn. View were significant (P<.05) at each of the three dates, and generally mimicked the pattern of height data. Relative rankings of the species generally differed little over time (App. Table 1). A. mangium from 12 to 18 months improved relative to other species (App. Table 1). The largest diameter rankings were measured for the eucalptus species and A. mearnsii.

Adverse site conditions at Mtn. View affected the growth of A. mangium, C. equisetifolia, L. leucocephala (fertilized and unfertilized), and E. grandis (unfertilized) significantly. The soils here are superficial and acid (pH 5.4), while the subsoil is a highly acidic and nutrient-poor lava. These soil conditions and climatic factors were evidently important factors for restricting the growth of A. mangium, C. equisetifolia, and L. leucocephala. The poor growth of E. grandis when unfertilized indicates that fertilization is a required for eucalyptus at this site if

optimal growth is to be achieved.

3.2.2 Honokaa, Hawaii

Honokaa is another mid-elevation site on the island of Hawaii. This site was being actively cropped in sugarcane before establishment of this test. It was somewhat drier (avg 2030 mm) and slightly warmer (23.9 C) than Mtn. View, with a deeper soil and greater solar radiation (390 cal/cm^2/day).

The eucalyptus species grew the most rapidly in height at this location (App. Table 2). E. grandis, E. saligna, and E. urophylla grew significantly better then the other tree species tested, averaging 9.4 m in 24 mos. A. mearnsii was the best performing nitrogen-fixing tree, and was actually taller (8 m) than E. robusta at 24 months. There was a significant break between the better performing trees and L. leucocephala (fertilized and unfertilized averaged, 6.2 m), E. grandis (unfertilized, 6.1 m), and C. equisetifolia (3.3 m). The growth trend at Honokaa displayed less striking leveling at 18 months than did the Mtn. View site (Fig. 3.2).

Diameter measurements for this site were very similar to those at Mtn. View. E. saligna and A. mangium, grew at Honokaa and ranked in the same group with the other eucalyptus and A. mearnsii. The diameter growth of C.

equisetifolia, L. leucocephala, and E. grandis was correlated with height growth, which ranked significantly below the acacias and eucalyptus species.

Honokaa was generally a more productive site when compared to Mtn. View. Only C. equisetifolia produced lower mean heights and diameters at 24 months; otherwise all tree species showed better growth at Honokaa.

3.2.3 Puunene, Maui

The Puunene site is on a lowland sugar plantation. The area is irrigated by wastewater from a sugarcane processing mill in a furrow (level-level ditch) irrigation system. Due to irregular rows and spacing (avg 5 ft) of the irrigation furrows, spacing of the trees in rows and plots was adjusted. Because of these differences in experimental design, only the growth performance of core species will be reported. Additionally, data was collected at only 12 and 24 months, as a result no trends were clear (Fig. 3.3).

There was high seedling mortality for the eucalyptus species, this was followed by further mortality due to fungal attack of the tree roots in the water-logged soil. Finally, the high temperature of the wastewater (approx. 40 C) is thought to have contributed to relatively poor growth at this site.

3.2.4 Hoolehua, Molokai

Hoolehua was a mid-elevation drip-irrigated site with hot day temperatures and cool night (avg. 25.9 C) (Table 2.1, 2.2). There was a strong tradewind effect at this site. Leucaena diversifolia and K734 a hybrid of L. leucocephala x L. diversifolia were severely damaged by herbicide soon after planting, so their growth performance was not reported.

The tallest trees at Hoolehua were Eucalyptus grandis, E. camaldulensis, E. saligna, and L. leucocephala, averaging 6.7 m in 24 months as a group (App. table 4). E. camaldulensis grew rapidly and its height was significantly greater compared to species at this location. L. leucocephala recovered from initial herbicide damage and grew about equally compared to E. grandis and E. saligna. The Hoolehua site was the best of the five sites for the growth of C. equisetifolia ranking just below L. leucoephala, E. grandis, and E. saligna. After a slow start, D. cunninghamia grew rapidly from 3 to 9 months, followed by decling growth after 12 months. Eucalyptus and leucaena species exhibited a pronounced plateau in growth at 18 months (Fig. 3.4). In contrast, C. equisetifolia continued to show linear growth until 24 months.

Diameter growth performance varied slightly over the three measurement periods E. camaldulensis grew

significantly better than the other species with an average mean diameter of 4.75 cm. Ranking just below in a cluster were E. grandis, E. saligna, and L. leucocephala, with diameters ranging from 4.27 cm to 4.15 cm. C. equisetifolia followed just below the middle group with a final diameter (3.58 cm).

3.2.5 Kilohana, Kauai

The Kilohana site was also abandoned sugarcane land utilized for cattle pasture prior to installation of the experiment. It was a mid-elevation site with highly weathered soils and moderately high rainfall (2980 mm). Just before the 12 month measurements were taken, cattle from an adjoining pasture broke into the fenced experiment and heavily damaged the leucaena species. As a result, no growth measurements were reported after 9 months for these species. Kilohana was the most productive site especially with favoraable growing conditions for E. grandis and E. urophylla. E. urophylla had the best initial growth; however, by the 12 month measurement, E. grandis was taller than E. urophylla and at 24 months had the greatest average height (10.78 m) of all sites. A. mangium and A. mearnsii were the tallest of the nitrogen-fixing trees at this location. C. equisetifolia grew relatively well at this location when compared to Honokaa and Mt. View. The growth

of unfertilized E. grandis was poor when compared to the fertilized treatment. Patterns of growth at Kilohana were linear for both E. grandis and C. equisetifolia, suggesting that growth was not limited by environmental factors for the first 24 months (Fig. 3.5).

Diameter rankings were similar to height measurements with acasia and eucalyptus species growing well. At final measurement, they were not significantly different, while C. equisetifolia and E. grandis (unfertilized) ranked below the best performing tree species at this location.

3.3 Performance of the three core species

E. grandis was the most productive core species in height and diameter growth at all sites (Table 3.1). At Kilohana, E. grandis attained the greatest height (10.8 m) and diameter (6.6 cm). High rainfall and cooler soil temperatures of upland sites appeared to favor the growth performance of E. grandis. At Puunene, stand mortality was highest for this species. This was probably due to periodic flooding of the level-level ditch system and adverse site conditions. E. grandis prefers well-drained soil and is intolerant of flooded conditions (Turnbull and Pryor, 1984).

Growth performance of L. leucocephala ranked second among the three core species over all sites. This species was severely limited by soil acidity and cool temperatures

of the upland sites at Mountain View and Kilohana (Table 3.1). Poor growth performance of L. leucocephala at cooler sites has been verified by Brewbaker and Sorensson (1987). The best growth performance of L. leucocephala was at Puunene where height and diameter were 7.1 m and 5.5 cm, respectively at 24 months. At Puunene and Honokaa, L. leucocephala growth performance was significantly better than that of C. equisetifolia.

C. equisetifolia showed strong site preference. It did not perform well at Mountain View, Kilohana, or Honokaa (Table 3.1, Fig. 3.1-3.5). However, growth was noticeably better at the sea level and midland irrigated sites of Puunene and Hoolehua. Ranking third among the core species, the growth performance of C. equisetifolia was never greater than L. leucocephala.

The location variation was significant indicating the differences between sites (Table 3.2). The species variation was significant illustrating the differences in growth performance. The location x species interaction was highly significant, reflecting variation in environmental requirements of the five species.

3.4 Summary

Of the core species tested, E. grandis performed well across a range of environmental conditions. Best growth was

recorded at upland sites of Kilohana, Honokaa, and Mtn. View, respectively. C. equisetifolia and L. leucocephala showed strong site preference, performing best at lowland and midland sites of Puunene and Hoolehua under irrigated conditions. Of the augment species, E. urophylla and A. mearnsii growth was outstanding at higher elevations and merits further testing. E. camaldulensis grew well under the demanding conditions of the Hoolehua site.

Kilohana was the most productive site for the eucalyptus species, with linear growth during the period of the study (Fig. 3.5). Honokaa and Mtn. View followed closely, but at 18 months growth appears to plateau (Fig. 3.1, 3.2). This indicates the preference of eucalyptus for cooler, humid locations. Acacias generally displayed the same pattern in terms of site preference as the eucalyptus, suggesting a potential for mixed planting with eucalyptus. L. leucocephala grew best at Puunene and Hoolehua, reflecting its preference for sites that are generally warmer, drier, and have a higher soil pH than sites preferred by eucalyptus and acacias as confirmed by MacDicken (1983), Brewbaker and Sorensson (1987), (Fig.3.3, 3.4). Finally, C. equisetifolia grew best at Puunene and Hoolehua, illustrating the need of site requirements similar to L. leucocephala. For adverse site conditions, such as sandy, infertile, or saline soils, C. equisetifolia still may have potential.

Table 3.1 Height and Diameter Measurements at 24 months after transplanting

	LOCATION					
	Mt. View	Honokaa	Puunene	Hoolehua	Kilohana	Mean
SPECIES			Height (m)			
CAS	4.3b	5.8b	5.6b	5.8b	5.0b	4.9b
LEU	5.0b	6.1b	7.1a	6.1b	4.6d	5.6b
GRA	9.2a	10.1a	7.9a	7.2a	10.8a	8.7a
			DBH (cm)			
CAS	2.5b	1.9c	4.6b	3.6b	2.4b	3.0b
LEU	2.9b	4.0b	5.5a	4.1a	2.0b	3.6b
GRA	5.5a	5.9a	6.4a	4.3a	6.6a	5.6a

NOTE:Values not followed by a common letter are significantly different at p = .05

Table 3.2 Combined ANOVA for DBH of three trees at five locations

SOURCE OF VARIATION	D.F.	S.S.	M.S.	F
LOCATION	4	26.2034	6.550	11.41*
REP W/I LOC	15	8.6116	0.574	
SPECIES	2	74.2990	37.150	9.28*
SPP X LOC	8	32.0056	4.000	13.42*
POOLED ERROR	59	17.5805	0.298	

_____random model was used_____

A combined analysis of variance of diameter growth indicated highly significant differences (P=.01) between locations and species.(Table 2)

Fig. 3.1

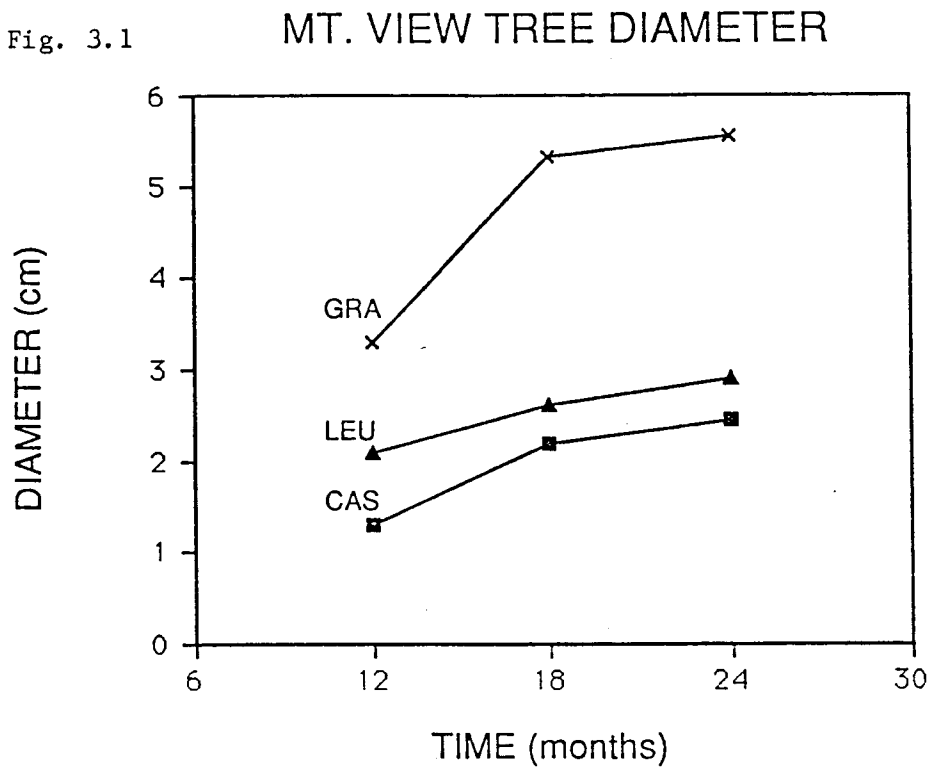
MT. VIEW TREE DIAMETER
DIAMETER (cm)
0
1
2
3
4
5
6
GRA
LEU
CAS
6
12
18
24
30
TIME (months)

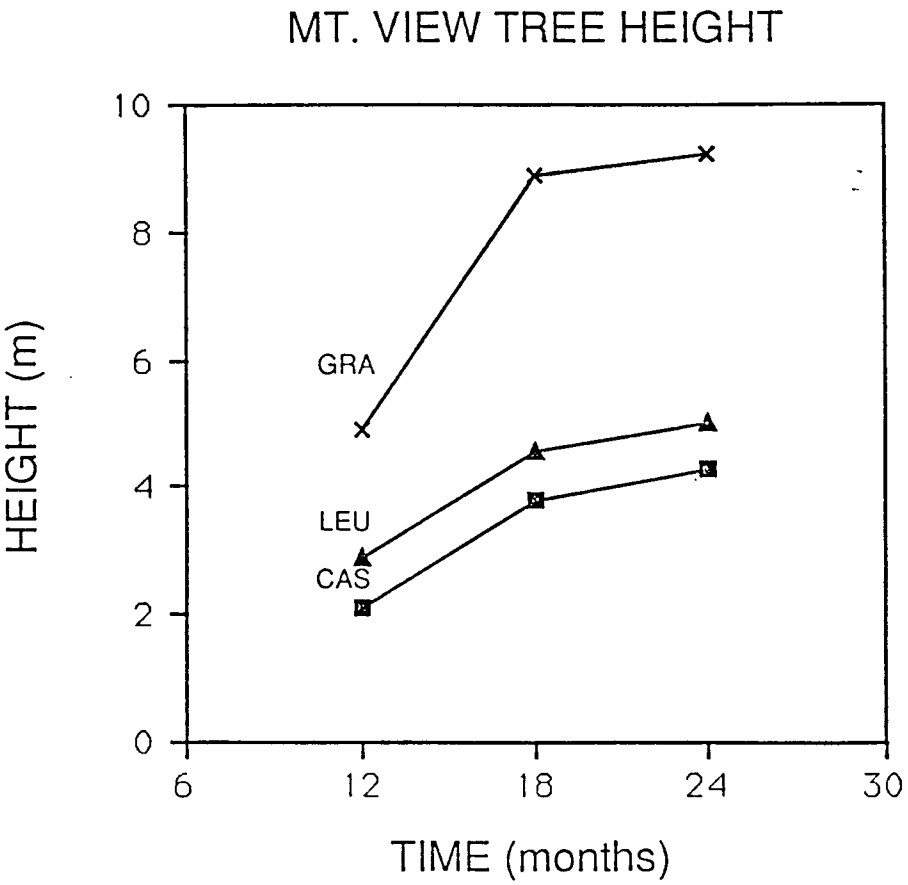
MT. VIEW TREE HEIGHT
HEIGHT (m)
0
2
4
6
8
10
GRA
LEU
CAS
6
12
18
24
30
TIME (months)

Fig. 3.2

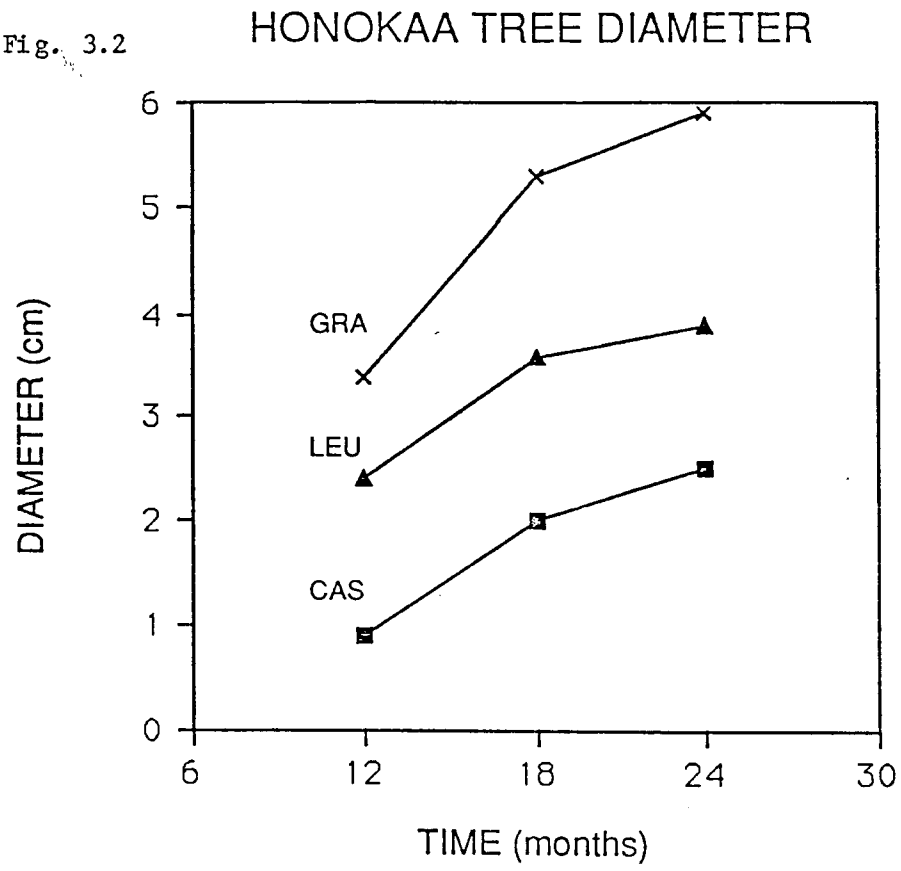
HONOKAA TREE DIAMETER
DIAMETER (cm)
0
1
2
3
4
5
6
GRA
LEU
CAS
6
12
18
24
30
TIME (months)

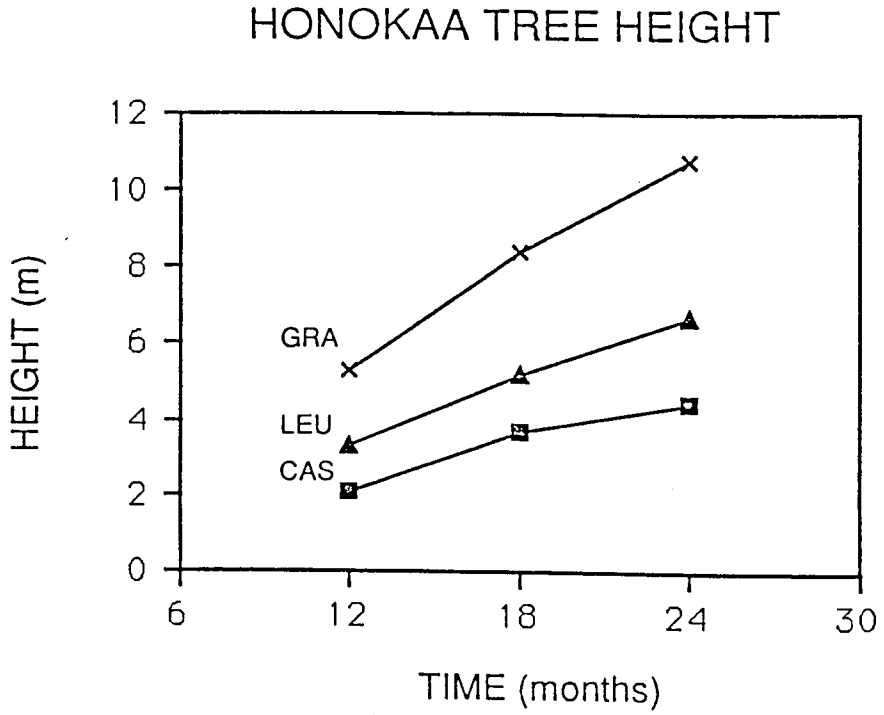
HONOKAA TREE HEIGHT
HEIGHT (m)
0
2
4
6
8
10
12
GRA
LEU
CAS
6
12
18
24
30
TIME (months)

Fig 3.3

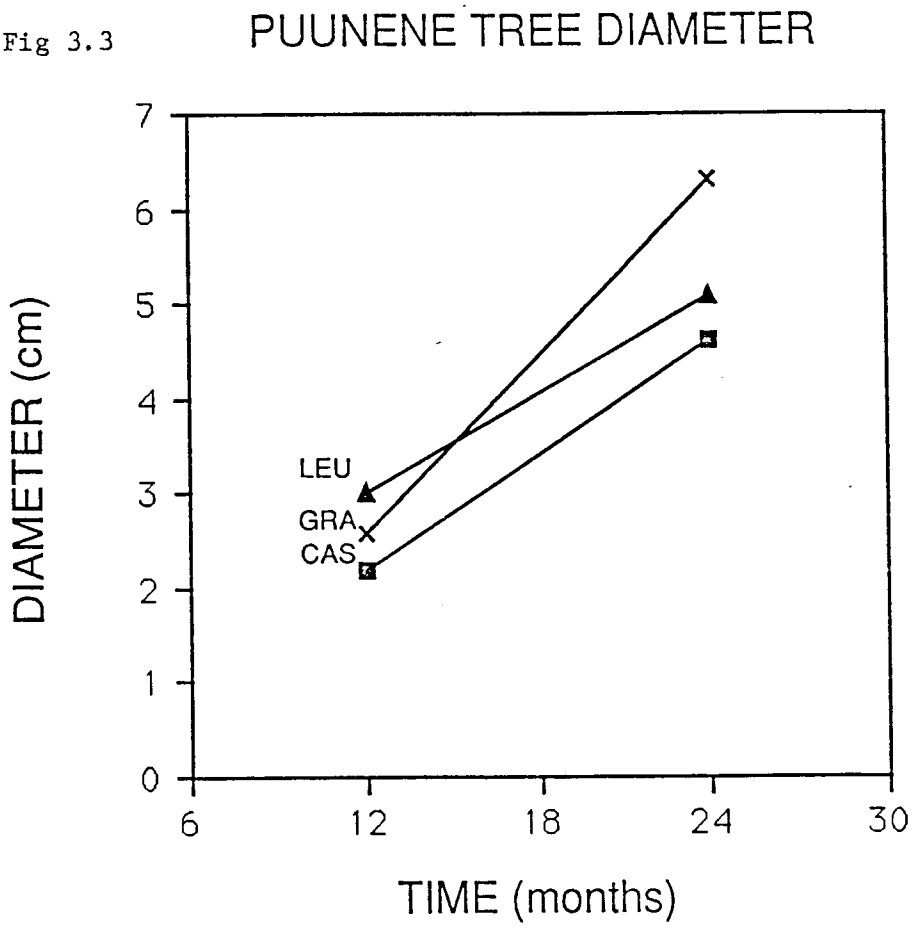
PUUNENE TREE DIAMETER
DIAMETER (cm)
7
6
5
4
3
2
1
0
LEU
GRA
CAS
6
12
18
24
30
TIME (months)

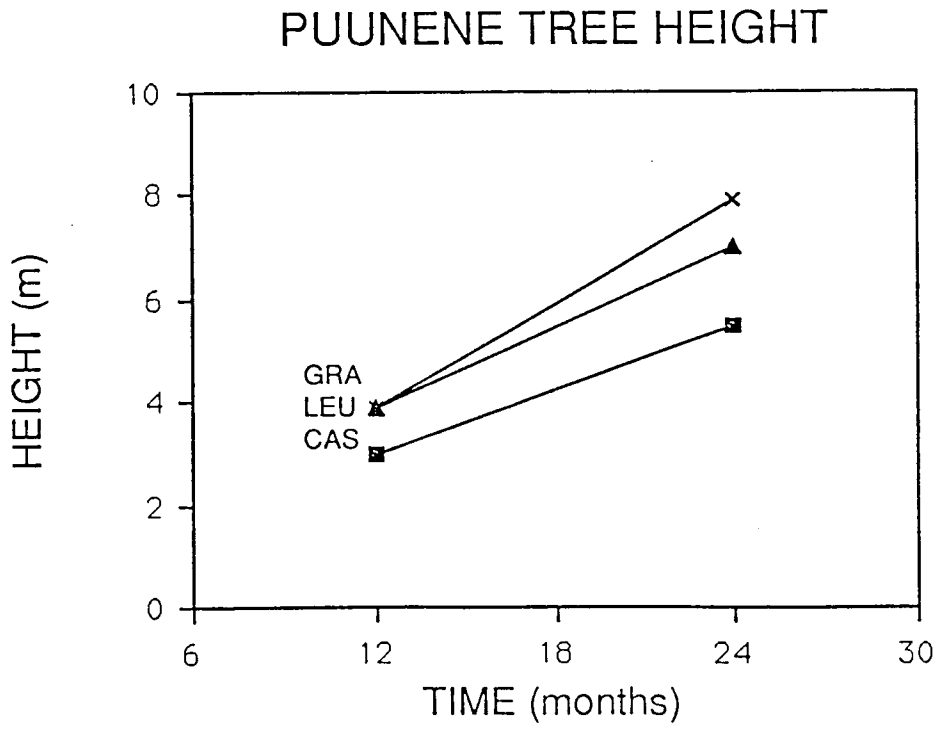
PUUNENE TREE HEIGHT
HEIGHT (m)
10
8
6
4
2
0
GRA
LEU
CAS
6
12
18
24
30
TIME (months)

Fig. 3.4 HOOLEHUA TREE DIAMETER

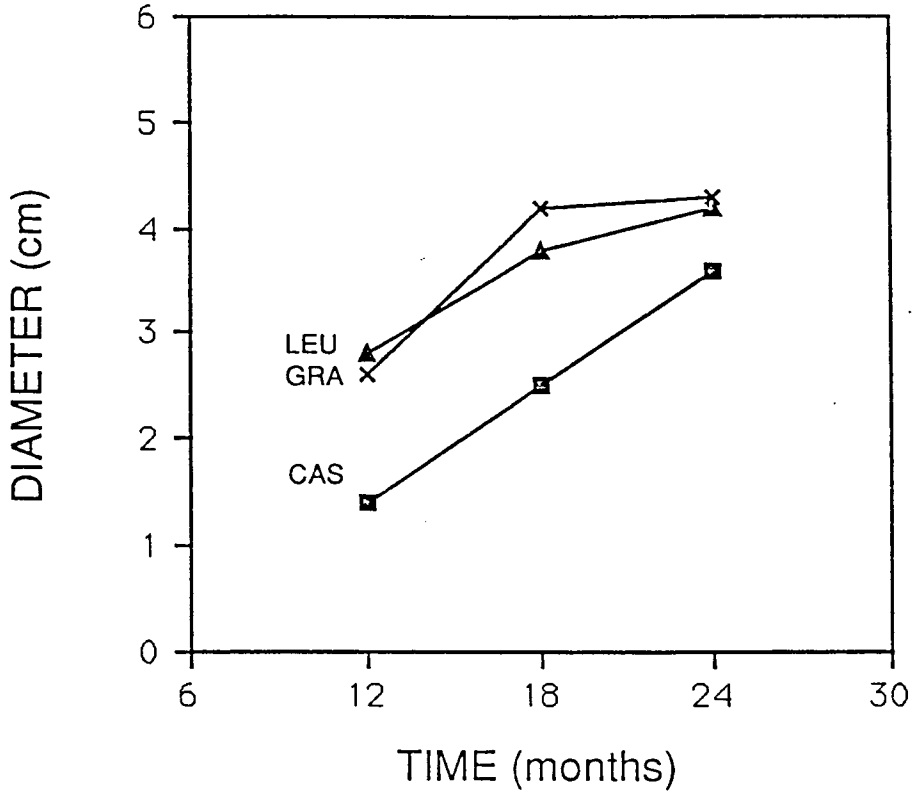

HOOLEHUA TREE HEIGHT

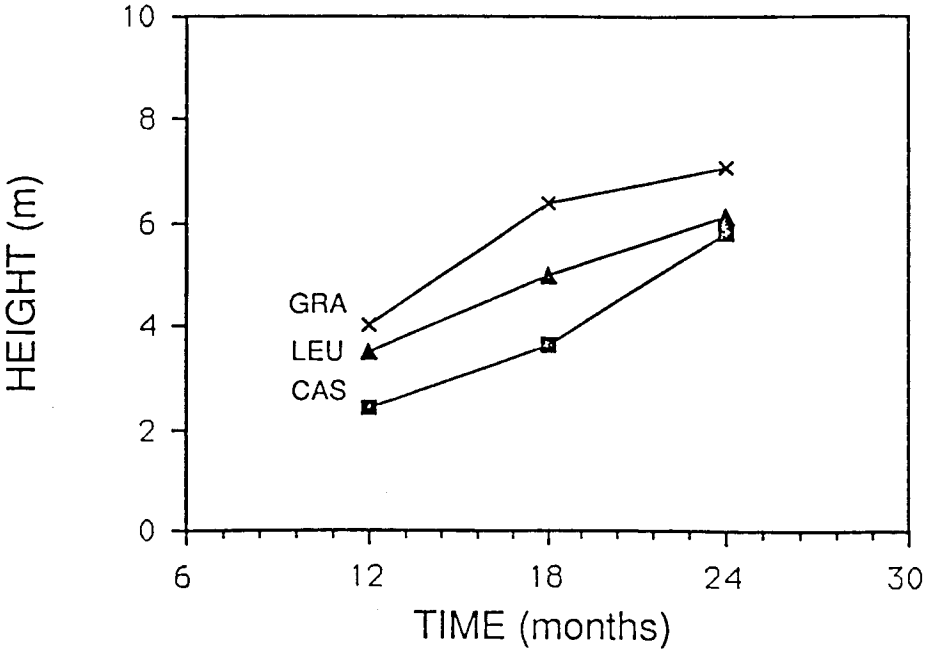

Fig 3.5

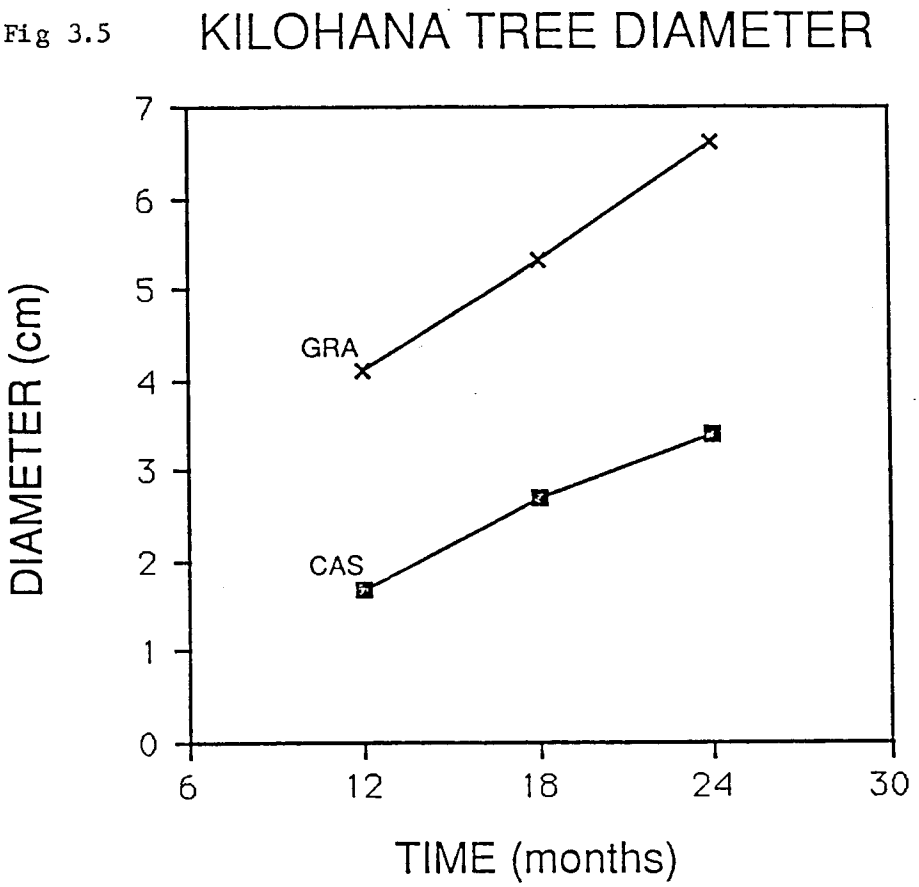
KILOHANA TREE DIAMETER
DIAMETER (cm)
0
1
2
3
4
5
6
7
GRA
CAS
6
12
18
24
30
TIME (months)

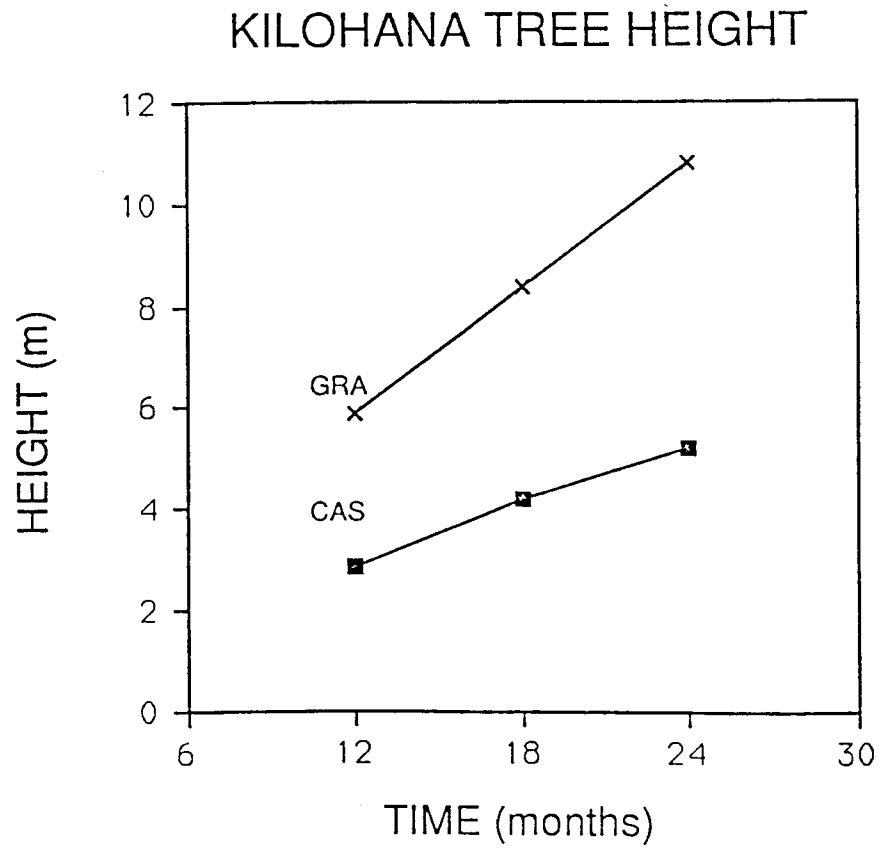
KILOHANA TREE HEIGHT
HEIGHT (m)
0
2
4
6
8
10
12
GRA
CAS
6
12
18
24
30
TIME (months)

CHAPTER 4

ESTIMATING AND PREDICTING WOODY BIOMASS YIELDS

4.1 Introduction

Height and diameter growth reflect relative species performance, but estimates of biomass yields require equations relating biomass to height or diameter. Potentially, biomass yield estimates can be predicted by using existing biomass estimation equations or by developing new equations from harvested sample trees depending on the need for accuracy and budget of project.

Biomass equations are obtained by destructive harvest and regression is one of the most widely used techniques for estimating tree biomass (Baskerville 1965; Bradstock 1981; Sato and Madgwick 1982; Crow 1988, Applegate et al. 1988). Regression is used because of its ease of application and simplicity for determining estimated biomass. Regression analysis relates easily measured growth parameters such as tree height and stem diameter to tree biomass (Baskerville 1972; Madgwick and Satoo 1975).

Existing equations are readily available and their application is clearly the simplest choice. Biomass estimation equations have been derived for Acacia, Eucalyptus, and Leucaena species in Hawaii (Van Den Beldt, 1982; MacDicken, 1983;, Brewbaker, 1987; Schubert et al.,

1988). Additionally, equations from similar stand environments and species are normally applicable over rather wide ranges (Satoo and Magwick 1982; Crow 1983).

There are a number of good reasons to go to the effort to derive site and species specific biomass equations from a small number of trees (15-20). Namely, data from harvested trees provide independent test of precision and accuracy for existing equations. If accurate estimates are needed for a specific tree species at a specific site, then general equations may not be applicable (Crow 1988). For industrial SR plantations accurate estimates of yield data are critical to determine the economic viability of an enterprise. The advantage of reduced field measurement time or increased sample size may be gained using equations based on diameter alone, because height may not explain significant additional variation in tree biomass (Bradstock, 1981; Darrow, 1984; Schubert, 1988). Finally, if published volume equations are used to estimate biomass yield, determination of wood properties is a necessity because density or moisture content may vary among trees and sites.

For trees, yield is usually expressed as biomass accumulation per unit time per unit area (Satoo 1970). Yields of SR plantations are usually expressed as metric tons (t) on a dry weight per unit of land area per year. In addition to biomass per tree, survival rates are needed to convert biomass production to a per land area basis. For

practical as well as economic reasons, the present study will be confined to above-ground tree biomass. The critical problem that emerges is how to determine tree productivity with a non-destructive means in order to estimate tree biomass and utilizable wood. Since there are published equations and wood properties of most of the tree species in this study, it would make sense to test their accuracy against a small destructive harvest that can be applied to a larger tree population.

4.2 Equation comparison

Two approaches were used to determine dry weight yields for six fast growing tropical tree species to determine biomass productivity at the Mtn. View site. The first approach was to use a published equation for each tree species of interest (Published equations). The second approach was to use regression equations generated from the allometric relationship between individual tree dry weight and diameter or diameter and height (Site and species specific equations from harvest data). In this study, the above approaches were used to estimate tree dry matter and will be evaluated for accuracy and ease of measurement.

A biomass estimation equation for Acacia mangium was derived from 29 sample trees that were 6 to 7 years old (Table 4.1), (Halenda, 1988). The mean tree height was 19.7

m and mean tree dbh was 18.7 cm. The range of diameters was from 4.8 cm to over 30 cm. This equation was developed to estimate stem dry weights for plantation grown mangium in Sarawak, Malaysia.

Prediction equations for Eucalyptus grandis and E. urophylla were developed on the island of Hawaii (Table 4.1), (Schubert et al., 1988). Both estimation equations predict dry matter biomass yields, but the E. urophylla equation is based on diameter alone and the E. grandis equation is based on a combination of diameter and height. The parameters for E. grandis were: 39 sample trees; with range of dbh from 1.5 cm to 38.2 cm; and height range was from 4.2 to 29.4 m. For E. urophylla the data ranged from 1.8 to 23.3 cm for diameter. The heights were from 3.6 to 23.8 m. These parameters were developed from a sample of 15 trees.

A stem volume formula was derived by regression analysis for Leucaena leucocephala on Mindanao Island, the Philippines (Table 4.1), (Kanazawa et al., 1982). A simplification of this formula, $V = .5(DBH^2) \times HT$ worked almost as well (Kanazawa et al., 1982). Van Den Belt (1983) validated this equation for L. leucocephala at a number of Hawaiian locations, and recommended the equation for trees at spacings ranging from 5,000-40,000/ha and dbh range from 2.5 to 10.0 cm. Brewbaker (1987) discussed general application of this equation over a wide range of sites and

age classes. Dry weight can be derived by converting wood volume to weight using specific gravity for the species of interest. These values may be available from published information (Sherry 1971; Brewbaker et al 1981, Malan 1988) or can be derived from harvested sample trees.

4.3 Objectives

The purposes of this study: 1) Determine wood properties (moisture content and specific gravity) for a number of fast-growing tree species at two sites. 2) Develop biomass prediction equations for tree species grown at the Mtn. View site for both total biomass and stem only biomass. 3) Determine the relative importance of the variables, height and diameter in developing biomass estimation equations. 4) Compare the Mtn. View equations to published equations for their accuracy in predicting actual dry weight at the Mtn. View site. 5) Test the Mtn. View equations and published equations for their precision in predicting biomass yield at the Kilohana site. 6) Using derived equations, determine when biomass production, as mean annual increment, peaks.

4.4 Materials and Methods

4.4.1 Study area

The sample trees were located at two sites. The first site, Mountain View was located in the Puna district 30 km southwest of Hilo on the windward slopes of Mauna Kea, on the island of Hawaii. The elevation of the Mountain View site was 380 m. The soil at this site was an extremely rocky muck derived from organic matter overlaying a'a lava rock (classified as dysic, isohyperthermic Lithic Tropofolist). Rainfall averaged 4700 mm annually on a 40 year period. Generally, the rainfall was evenly distributed but could vary greatly on a monthly basis. The second site, Kilohana, was located in the Lihue district 9 km northwest of Lihue on the windward slope of Kilohana Crater on the island of Kauai at 337 m elevation. The soil was a gravelly silty clay (classified as clayey, ferritic isothermic Typic Gibbsihumox). Rainfall historically averaged 2980 mm annually, which was evenly distributed over the year.

4.4.2 Destructive Harvest Data Collection

Samples were selected from 2 year old trees growing at both the Mountain View and Kilohana sites in small replicated plots planted at 1 by 1 meter spacing with 100 trees per plot. Five sample trees per plot were randomly

selected from each of 4 replications for a total of 20 sample trees per site. All trees were felled and removed except the randomly selected sample trees. Final height and diameter breast height (DBH) were recorded for each sample tree. The sample trees were then felled and radial slices were removed at the base and at the first live branch for the determination of moisture content and specific gravity. Fresh weights of each sample tree were measured using a field scale (accuracy $\pm$ 0.25 kg). Subsamples of the leaves and branches and wood disks were taken to the laboratory, weighed wet, then dried to a constant weight in drying ovens at 70 C. Final dry weights of each sample tree were calculated in order to generate wood specific gravity and allometric equations for each tree species.

4.4.3 Moisture content and Specific gravity

Specific gravity was determined by dividing the wood dry weight by the fresh (wet) volume of the wood of the stem disks (Husch et al., 1982). Dry weight of each stem disk was obtained by drying a sample of wood at 70 C until a stable weight was reached. The specific gravity for each stem disk was determined using a volume estimate derived from the measured cross sectional area of each disk. This study assumed that wood properties of young trees would not vary significantly from base to the tip of the stem, owing

to lack of heartwood formation in the two year old trees. Regression analysis was performed based on the relationship between specific gravity and diameter (table 4.5).

4.4.4 The choice of regression variables

Bradstock (1981) found that a regression model based on diameter alone was applicable for eucalyptus grown on two sites in New South Wales, Australia. Darrow, (1984) on one site in South Africa used DBH based regression equations to estimate biomass productivity for E. grandis. Schubert et al. (1988) found that biomass equations based on diameter had only small differences in CV and adjusted R^2 when compared to diameter + height models of the same tree species. Diameter accounted for over 90% of the variation in log of biomass for the following tree species: Acacia melanoxylan, Eucalyptus globulus, E. grandis, E. robusta, E. urophylla and Paraserianthes falcataria (Schubert et al., 1988).

4.4.5 Tree biomass equations

Equations were developed for both stem-only and total above ground dry biomass to simulate different harvest scenarios at the Mtn. View site. A small sample of trees (15-20) were used with measurements taken per tree. This

method required destructive harvesting of sample trees. Yields of wood dry weight were derived from allometric relationships between stem dry weight or total dry weight and breast height diameter. The independent variable was tree diameter used singly or in combination with tree height.

Tree biomass models tested in regression analyses were:

$\ln Y = a + b * \ln(D.B.H)$ (D.B.H only)

$Y = a' + b' *(D.B.H)^2 * HT$ (D.B.H. * Height)

where ln = natural logarithm, Y = dry biomass in kg/tree, D.B.H = diameter at breast height (1.3 m) in centimeters, and HT is tree height. Often, the a' values are small for fast-growing trees and do not add significantly to the goodness of fit of the equation (Van Den Belt, 1983).

Log tranformations were used for the following reasons. First, the relationship between tree weight and tree diameter or height is generally greater than 1:1, and therefore requires transformation to become linear (Neter and Wasserman, 1974). Secondly, it homogenizes variances over the range of data. Third, the log tranformation method is the most widely used allometric model in biomass estimation (Crow, 1988). Forth, use of the power function $B = aD^b$ implicitly agrees with the use of predictor variables such as D^2H because H is correlated with D. Because least-squares regression of logarithmic data estimates the geometric mean rather than the arithmetic

mean, a correction factor is necessary (Meyer, 1944; Baskerville, 1972). A correction factor (cf) for each derived logarithmic equation, was calculated using the following formula: $cf = e((RMSE^2)/2)$, in which e = the natural anti-logarithm, and $(RMSE^2)$ is the square of the root mean square error in logarithmic form.

4.5 Results

4.5.1 Tree survival rates

The eucalyptus species generally had survival rates above 90% at 24 months at both Mtn. View and Kilohana (Table 4.2) while the casuarina species had somewhat lower survival. The acacia species had lowest survival rates, 66 to 78 % at both sites. L. leucocephala survived well at Mtn. View but was damaged by cattle at Kilohana.

4.5.2 Wood characteristics

Acacia mearsii, Casuarina equisetifolia, and Eucalyptus urophylla moisture content did not differ significantly between sites (Table 4.3). In contrast, moisture content did differ significantly for E. grandis and A. mangium between sites.

Wood specific gravity did not vary significantly for A.

mangium, A. mearnsii, and C. equisetifolia (Table 4.3). Specific gravity did vary significantly for E. grandis and E. urophylla. E. grandis was found to have highly significant differences in wood specific gravity between trees in Australian locations (Edwards 1973). If environmental factors alone controlled this variation, then one would expect other species to exhibit significant variation in specific gravity.

4.5.3 Regression equations

The allometric or power equations had exponents generally ranging between 2 and 3 (Table 4.4). Linear regression of biomass on D^2H produced equations with slopes which differed little between no-intercept and intercept models (Table 4.5) as previously found by Van Den Belt (1983).

4.5.4 Dry Weight Yields at Mtn. View

The eucalyptus species and A. mearnsii had the greatest mean biomass per tree at 24 months based on mean weights of the harvested sample trees (Table 4.6). The lower survival of A. mearnsii caused the mean production rate to be somewhat lower relative to the eucalyptus species (Table 4.6).

4.5.5 Equation comparison Mtn. View

As expected, the regression equations closely approximated mean biomass of the harvested sample trees (Table 4.7). Acacia mangium estimated average tree weight from harvest data was 3.09 kg. The published equation for A. mangium over-estimated average tree weight by over 70%. The (D^2HT) equation underestimated mean weight by 40%. In contrast, both equations estimated mean weights of A. mearnsii with less than 5% error. C. equisetifolia weight also was well estimated by both approaches. Weight of E. grandis was over predicted by 20% using the published equation. The (D^2H) equation under-estimated weight by 15%. E. urophylla weight was over-estimated by 13% using equations published. The (D^2H) method under-estimated actual weight by about 10%. Mean weight of L. leucocephala slightly under-predicted by 3%.

4.5.6 Equation comparison Kilohana

The independent test using the preliminary equations derived from the Mtn. View harvest to predict tree biomass at Kilohana showed good general agreement (Table 4.7). Mean biomass of A. mangium was slightly over predicted (10%) with the (D) equation, while the (D^2H) equation under-predicted actual biomass (18%). A. mearnsii weight was

under-estimated by both equations, 15% and 25%, respectively. Similarly, C. equisetifloia was slightly underestimated by about 6% using both equations. E. grandis weight was predicted reasonably well with both the Mtn. View (D) and (D^2H) equations. The published equation overestimated weight by about 20%. E. urophylla weight was overestimated by the Mtn. View (D) and the published equation by 27% and 23%, whereas the Mtn. View (D^2H) equation was 4% over.

The difference in estimated biomass by the different equation at Kilohana versus Mtn. View was examined by plotting the wet weights of harvested sample trees against diameter. Wet weights were used to eliminate possible experimental errors in moisture determination. A. mangium trees at the two sites showed a similar pattern (Fig. 4.1), which confirms the good average prediction by the Mtn. View regression equations. A. mearnsii at Kilohana exceeded the range of diameters at Mtn. View (Fig. 4.2), which explains large errors in the regression equations. E. grandis at Kilohana followed the same pattern as Mtn. View (Fig. 4.3) confirming the good fit of the regression equation. Mean weights of E. urophylla was strongly affected by a single large outlier, which caused the Mtn. View equation to over-predict mean biomass (Fig. 4.4). C. equisetifolia at Kilohana followed the same pattern as at Mtn. View, although the three largest trees were outside the range of the Mtn.

View data, contributing to the under-prediction by the Mtn. View equation (Fig4.5).

The differences in wood specific gravity and moisture content between sites (Table 4.3) may also have contributed to errors in using the regression equations from Mtn. View at Kilohana. Furthermore, moisture content was significantly correlated with diameter in A. mangium and E. grandis and specific gravity correlated with diameter in A. mangium and E. urophylla. This finding suggests that the assumption that wood was undifferentiated throughout the stem of the tree may not hold true for these species. Finally, potentially error was introduced in conversion of wet weight to dry weight.

4.5.7 Mean Annual Increment

Mean Annual Increment (MAI) was calculated using the D regression equations developed at Mtn. View and diameter measurements from non-destructive sampling at 12, 18, 24 months. MAI had peaked at 18 months for the following tree species; A. mearnsii, C. equisetifolia, E. grandis, E. robusta, E. saligna, and E. urophylla. Only A. mangium and L. leucocephala did not peak at 18 month at the Mtn. View. The time of peak MAI is a biological criterion for optimal rotation length (Evans, 1982). Optimal productivity at Mtn. View would therefore be obtained by harvesting

between 18 and 24 months.

4.6 Discussion

At the Mtn. View site, E. urophylla had the greatest predicted total biomass and stem only biomass (Table 4.3). E. saligna, E. robusta, and E. grandis were also high yielding. A. mearnsii was the best yielding nitrogen fixing tree at this wet upland site. A. mangium, C. equisetifolia, and L. leucocephala yields did not compare well with the growth of the other tree species at this cool wet site.

In the present study, diameter only (D), and diameter and height (D^2H) equations were used in the biomass regression model. Time spent in the field could be reduced if height were not needed for biomass estimation. Diameter alone explained nearly 90% of the variation in the tree species tested at the Mtn. View site (Table 4.3). However, in some cases height does explain significant variation in addition to diameter (Schubert et al. 1988). This increase in precision must be traded off against the greatly increased measurement time in the field.

In general, the dry weight yields agreed with the growth performance data for the eucalyptus as a group and the nitrogen-fixing A. mearsii. C. equisetifolia, A. mangium, and L. leucocephala grew poorly at the Mtn. View site, reflected in both yield and measurement results. In

terms of biomass, E. urophylla out-yielded E. grandis which was the best performing tree in terms of height and diameter. This difference was due to the fact that E. urophylla had lower moisture content and higher specific gravity.

Performance of the published biomass equations varied. The leucaena volume equation worked well, as has been found previously (Van Den Belt, 1983; Brewbaker, 1987). Published equations for eucalyptus tended to over-predict biomass in this study by 20-25%. The equation for A. mangium performed poorly, probably because it was developed for much larger trees from older stands (Halenda, 1989).

The specific biomass equations worked well for predicting biomass yields at the Mtn. View site as expected. At the Kilohana site, the prediction performance was quite variable. Problems developed when the regression equations generated from a narrow range of tree size were applied beyond their range. These findings illustrate the preliminary nature of these equations and the need for increased sample size which can improve the precision and generality of the estimates. Furthermore, testing and refinement of the equations is suggested before widespread use is recommended.

Table 4.1 Published biomass estimation equation

Species	Biomass equations
Acacia mangium	$\ln SW = -3.212+0.905 \ln(D^2H)$ *
Eucalyptus grandis	$Y = 0.069413 * (D^{2.1472}) * (H^{0.3129})$ **
E. urophylla	$Y = 0.119931 * (D^{2.3610})$ **
Leucaena leucocephala	$Y = .5 (DBH^2)$ X HT X SG ***

SW = stem weight * (Halenda, 1989)

Y = Total above ground biomass ** (Schubert et al.,1989)

SG = Specific gravity ***(Kanazawa et al. 1982)

Table 4.2 Tree survival rates at Mtn. View and Kilohana at 24 months

Species	Mean Percent Survival Mtn. View	Kilohana
Acacia mangium	66.75%	71.25%
A. mearnsii	70.25	77.75%
Casuarina equisetifolia	83.75	77.50
Eucalyptus grandis	93.75	92.75
E. robusta	95.00	-----
E. saligna	91.00	-----
E. urophylla	86.75	95.00
Leucaena leucocephala	94.00	-----

Table 4.3 Wood characteristics

Site	Genus Species	Wood Moisture (%)	Wood Sp. gravity (g/cm)	Wood Sp.gravity (reference)
Mtn. View	Cas	46.06	.53	1.0
Kilohana		46.58	.53	
Mtn. View	Leu	45.81	.50	.52
Mtn. View	Gra	64.07*	.30*	.45
Kilohana		57.75*	.34*	
Mtn. View	Uro	60.65	.34*	NA
Kilohana		59.06	.37*	
Mtn. View	Man	62.51*	.27	.65
Kilohana		59.57*	.30	
Mtn. View	Mer	56.05	.41	.53
Kilohana		53.88	.44	

NOTE: Values in columns followed by a '* ' are significant differences at p = .05 within a species.

(References: Sherry, 1971 = Mer; Brewbaker et al., 1981 =Leu; NAS, 1983 = Man; NAS, 1984 = Cas; FAO, 1979 = Gra.)

Table 4.4 Equations relating biomass to diameter derived from harvest at Mtn. View site. R^2 is from linear regression of log-transformed data.

SPECIES	Regression Equation	R^2
Acacia mangium		
DW stem	$0.02235 * D^{2.736}$	.88
DW total	$0.09815 * D^{2.142}$	.97
A. mearnsii		
DW stem	$0.0572 * D^{2.631}$	.97
DW total	$0.0585 * D^{2.729}$	.97
Casuarina equisetifolia		
DW stem	$0.7839 * D^{3.683}$	.83
DW total	$0.1168 * D^{2.524}$	.93
Eucalyptus grandis		
DW stem	$0.07425 * D^{2.294}$	.94
DW total	$0.06998 * D^{2.439}$	.94
E. robusta		
DW stem	$0.03943 * D^{2.636}$	.96
DW total	$0.04768 * D^{2.756}$	.98
E. saligna		
DW stem	$0.06407 * D^{2.467}$	.94
DW total	$0.08765 * D^{2.443}$	.96
E. urophylla		
DW stem	$0.05836 * D^{2.563}$	.98
DW total	$0.07501 * D^{2.534}$	.98
Leucaena leucocephala c.v. K636		
DW stem	$0.06744 * D^{2.694}$	.86
DW total	$0.10048 * D^{2.391}$	.89

Table 4.5 Mtn. View equations : D^2H

Species	Regression Equation Dry Weight Total	R^2
Acacia mangium		
	$y = -0.12744 + 0.01385 * D^2H$	.97
no-intercept	$y = 0.01328 * D^2H$	.96
Acacia mearnsii		
	$y = -0.4118 + 0.02909 * D^2H$	.96
no-intercept	$y = 0.028165 * D^2H$	.95
Casuarina equisetifolia		
	$y = 0.06063 + 0.04221 * D^2H$	.90
no-intercept	$y = 0.04222 * D^2H$	.89
Eucalyptus grandis		
	$y = -0.43538 + 0.02914 * D^2H$	.95
no-intercept	$y = 0.02816 * D^2H$	.95
E. urophylla		
	$y = -1.13436 + 0.02068 * D^2H$	.97
no-intercept	$y = 0.02068 * D^2H$	.96

Table 4.6 Mt. View equations: Diameter and Height at 24 months from the harvest weights of the sample trees, and accounting for mortality.

Species	Dry Weight Per Tree (kg)	Yield Dry (t/ha/yr)
Acacia mangium		
DW stem	1.88	9.4
DW total	2.86	14.3
A. mearnsii		
DW stem	5.87	20.61
DW total	7.24	25.43
Casuarina equisetifolia		
DW stem	1.7	8.50
DW total	2.9	14.50
Eucalyptus grandis		
DW stem	4.84	22.80
DW total	6.05	28.35
E. robusta		
DW stem	4.1	19.80
DW total	6.91	29.40
E. saligna		
DW stem	5.17	23.85
DW total	6.76	30.76
E. urophylla		
DW stem	6.77	29.36
DW total	8.28	35.91
Leucaena leucocephala var. K636		
DW stem	1.72	8.60
DW total	2.18	10.00

DW stem = Dry weight of stem of tree only
DW total = Dry weight of total tree biomass

Table 4.7 Measured versus estimated mean total dry weight per tree (kg). Measured trees at Mtn. View were those used in determining regressions. Measured trees at Kilohana are independent of the derivation of the equation.

		Equation Type		
Species	Actual	aD^b	D^2H	Pub
Mtn. View				
Acacia mangium	3.09	2.99	1.71	5.36*
A. mearnsii	7.25	7.62	7.41	---
Casuarina equisetifolia	2.90	2.95	2.94	---
Eucalyptus grandis	6.25	6.39	5.32	7.55
E. urophylla	8.29	8.27	7.45	9.47
Leucaena leucocephala	2.26	2.30	---	2.10
Kilohana				
Acacia mangium	4.41	4.89	3.56	---
A. mearnsii	13.16	11.14	9.83	---
Casuarina equisetifolia	3.93	3.67	3.79	---
Eucalyptus grandis	8.83	9.41	8.44	11.07
E. urophylla	9.99	12.75	10.40	12.26

Actual = Dry weight of tree determined from harvest data
D = Diameter equations estimates
D^2H = Diameter and Height equation estimates
Pub = Published equations estimates
* stem-only dry weight

Table 4.8 Mean Annual Increment (t/ha/yr) at Mtn. View

Species	12 months	18 months	24 months
Acacia mangium	2.3	4.7	5.8
A. mearnsii	9.3	25.5	20.3
Casuarina equisetifolia	1.9	12.1	4.9
Eucalyptus grandis	12.1	25.2	22.8
E. robusta	13.9	21.5	20.1
E. saligna	13.8	19.8	19.9
E. urophylla	16.5	26.5	24.4
Leucaena leucocephala c.v. K636	6.2	6.0	6.4

Based on diameter equations with data from appendix 1

Figure 4.1

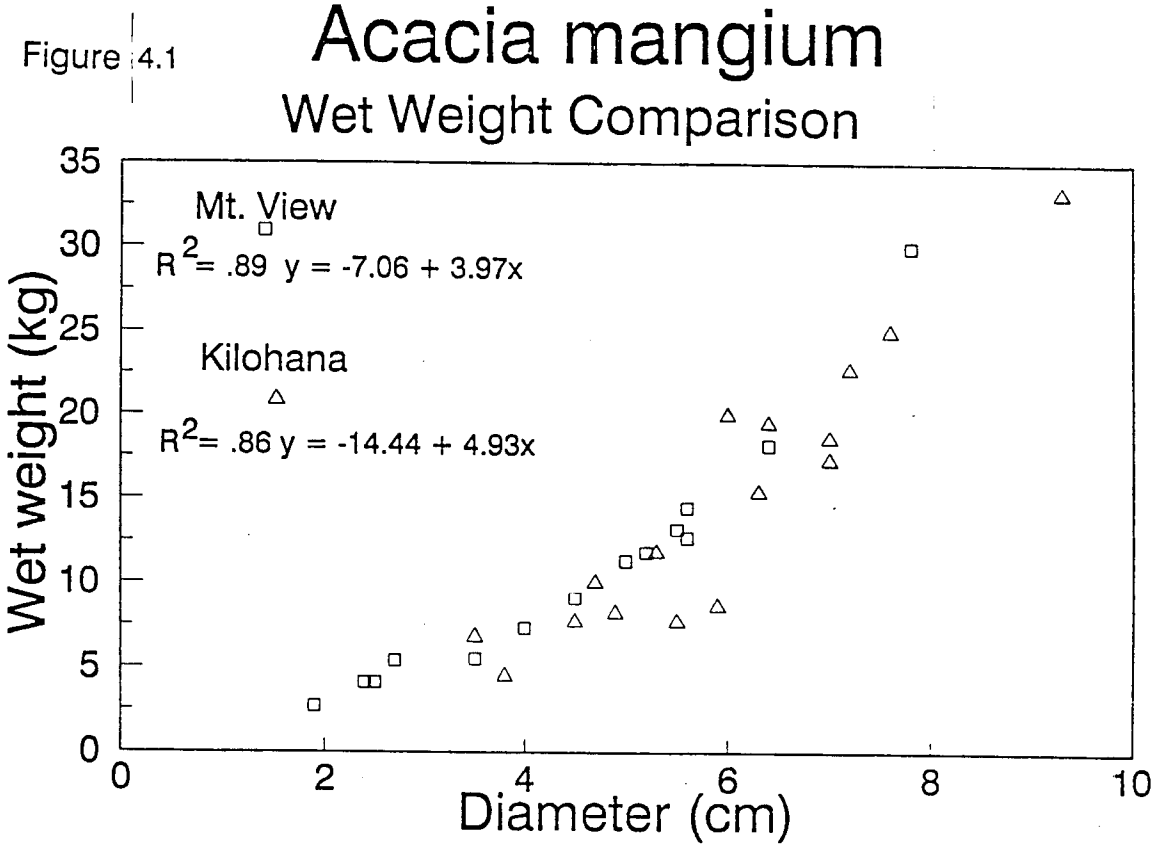

Figure 4.2

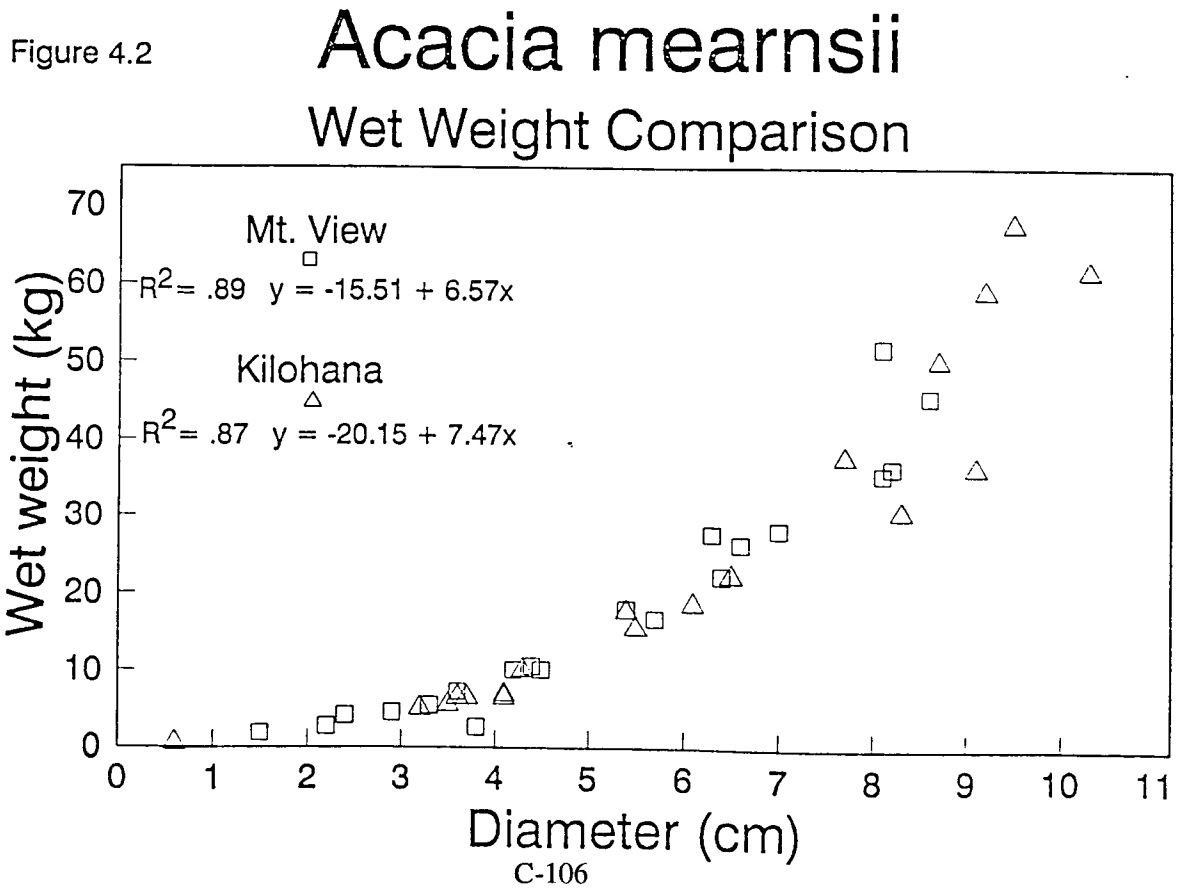

Figure 4.3

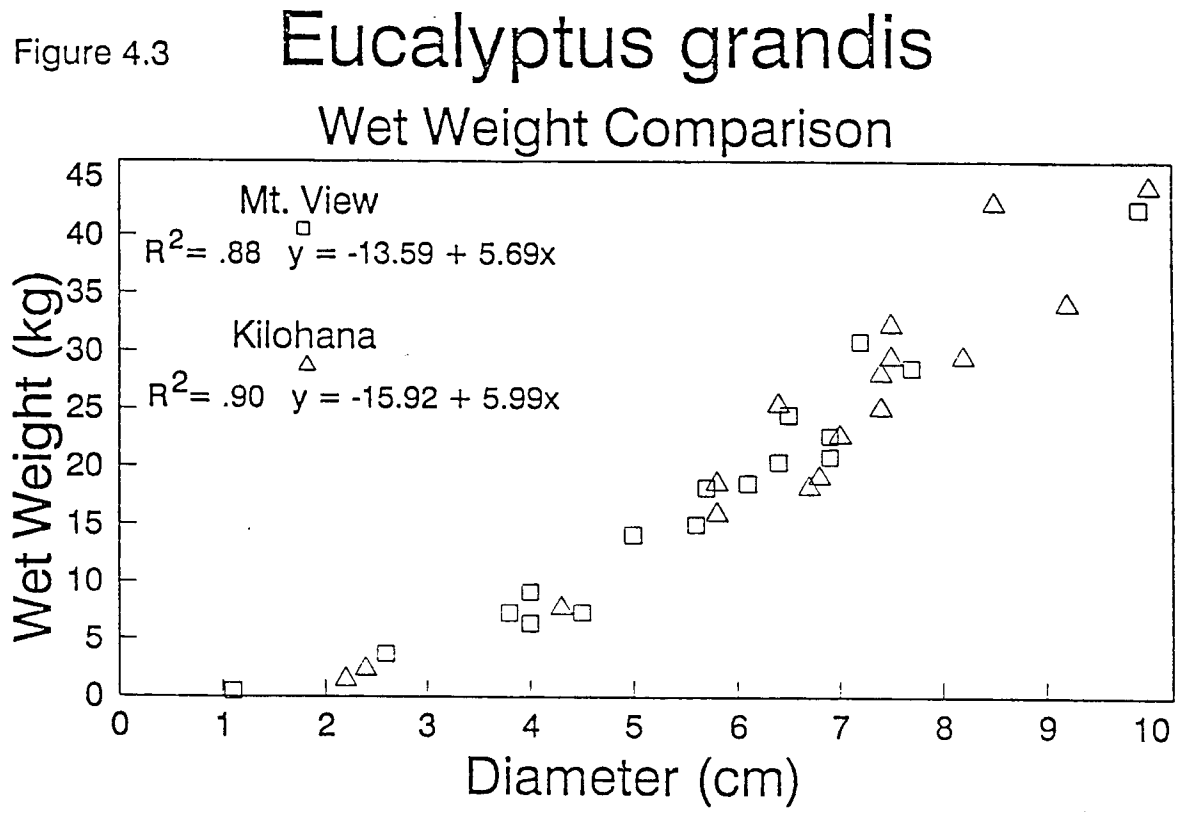

Figure 4.4

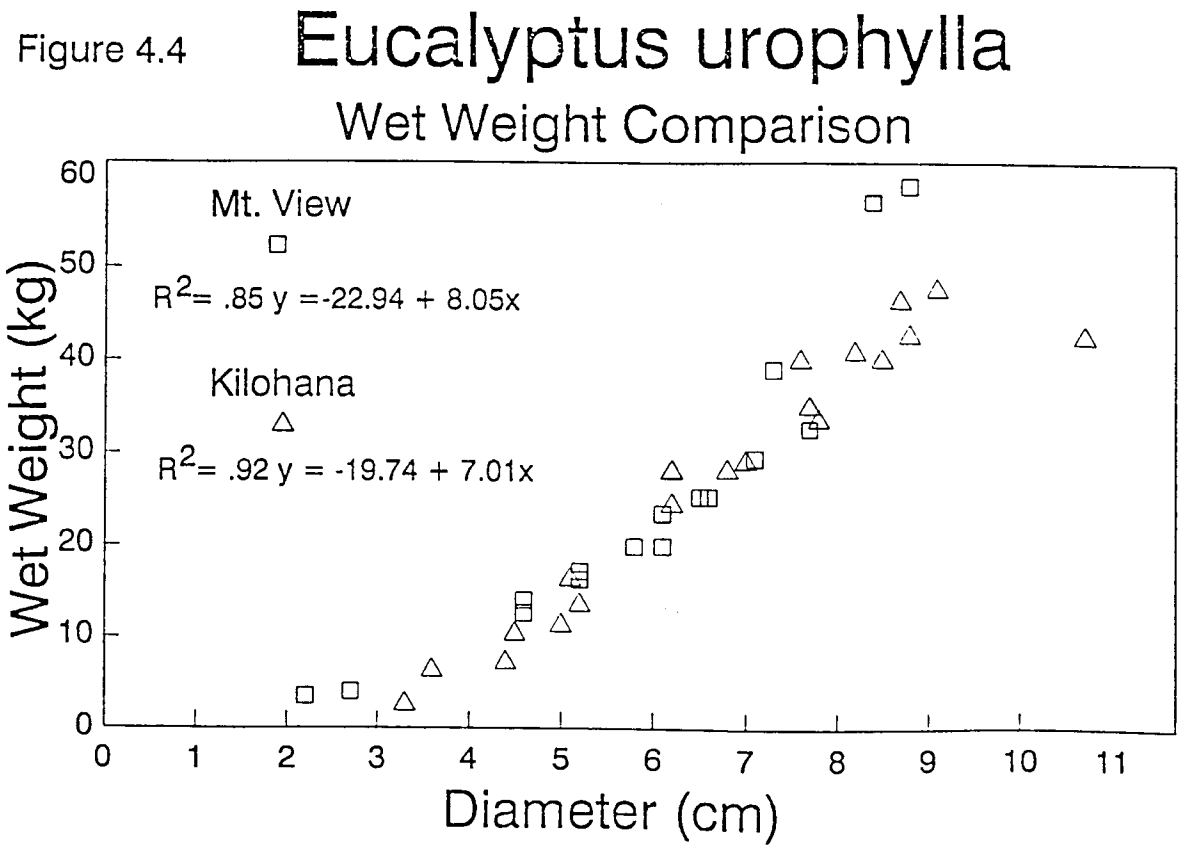

Figure 4.5 Casuarina equisetifolia

Wet Weight Comparison

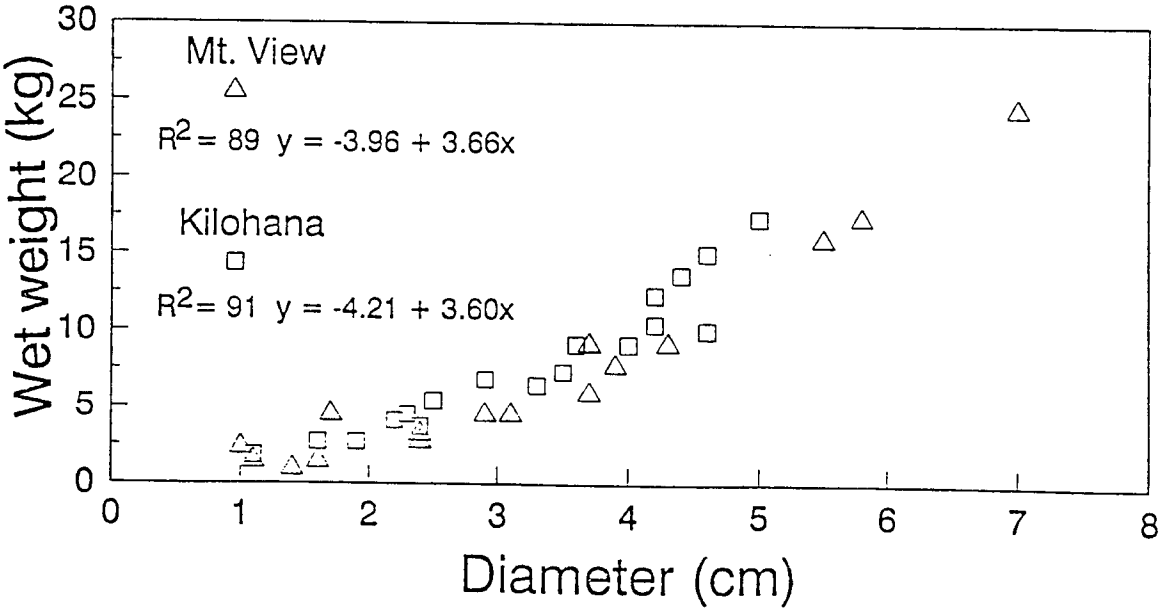

CHAPTER 5

ECONOMIC ASSESSMENT OF EUCALYPTUS FOR WOODCHIP PRODUCTION

5.1. Introduction

Hawaii must import 90 percent of its energy needs because there are no indigenous fossil fuel resources (Phillips, 1989). Approximately 10 percent of the state's energy needs are presently met by burning bagasse the fiberous residue from sugar cane processing to generate electricity (HSPA, 1988).

Eucalyptus plantations in Hawaii have the potential at high oil prices to supplement or replace bagasse as an alternative source of renewable energy in the form of electricity or liquid fuel (Bioenergy Corp.,1983). However, there are at least three competing uses for woodchips from eucalyptus: conversion to electricity, conversion to paper pulp and conversion to lignocellulane derived chemicals (Khamoui,1980). Both alternatives depend on the economics of production and the cost of conversion.

The growing of short rotation (SR) plantations is only experimental in Hawaii. Currently, experimental Hawaiian SR plantation biomass yield per hectare approach some of the highest recorded (Khamoui and Baker,1981) but SR eucalyptus plantations have yet to be grown commercially although a wood chipping facility harvesting standing timber for export operated on the island of Hawaii from 1973 to 1980.

This chapter outlines the economic feasibility of commercial eucalyptus production on abandoned or marginal cane land in Hawaii. Two possible markets for eucalyptus woodchips are examined: fuel for electrical production and feedstock for paper pulp production. In order to evaluate the alternatives this chapter will: 1) assess the production costs of eucalyptus for wood chip production on a ha/yr and ha/rotational basis, 2) compare the price of wood chips in alternative markets for biomass energy production and as a feedstock for paper pulp production, 3) analyze economic feasibility of input costs and output prices at varying discount rates for wood chip markets.

The best economic strategy in tree plantation production is to maximize profit by achieving optimal yields, thus distributing cost over more units of production. The four main components that influence optimal yield are site quality, quality of seedling or clonal nursery stock, sound fertilization practices, and timely weed control. Costs associated with production practices for optimal yield are outlined. (Table 1).

Site quality is an important aspect of obtaining an economically viable level of tree productivity. Good sites produce a greater quantity and usually better quality of biomass yield (Zobel et al.,1987). Furthermore, the rotation age is shorter and returns are greater on sites of high quality. Finally, good sites are usually the most responsive

to management practices.

Within eucalyptus species there is clear evidence of genetic variation (Turnbull and Pryor, 1984). Provenance trials in Australia and Hawaii have demonstrated the importance of selection of provenance when identifying the best adapted seed source for a given site (Skolmen, 1986). After the best seed source has been determined, it is possible to clonally propagate superior trees within this select population for rapid gain in yield (Zobel et al.,1987).

Previous studies of eucalyptus in Hawaii revealed that fertilization was needed to achieve optimal yields and maximize profit (Qureshi,1978; Strand and Whitesell,1989). In this study the standard fertilizer treatment was a uniform rate of 50 grams per tree of 16-16-16 NPK applied twice per year.

In a South African study, the growth of E. grandis was 71% greater when weeds were controlled with glyphosate compared to untreated control plots (Kvitza and Darrow,1983). This finding illustrates the need for timely weed control particularly if maximum yields are to be realized in short rotations.

5.2 Alternate markets

5.2.1 Biomass for energy

Eucalyptus wood chips utilized for energy production must compete with both imported oil, coal and bagasse. At current market prices a bone-dry ton (BDT) of chips for fuel is valued at a maximum of $40.00 delivered to a California electrical plant (Hartsough and Nakamura,1990). The market price fluctuates generally with the price of oil. The current market for biomass feedstock in Hawaii is local in nature and limited to the island where the fuel is produced, reflecting the product's low value and expense of bulk material handling.

5.2.2 Woodchips for paper-pulp

The market for woodchips for paper-pulp production is international in nature. Demand for eucalyptus wood chips exists throughout the Pacific rim, chiefly in the United States and Japan and to a lesser extent in Korea and Taiwan. Khamoui and Baker (1981) reported the export price for woodchips was over $80.00 per BDT in 1980. By 1989, prices had risen as high as $145.00 per BDT delivered in Taiwan (Chen, 1989).

When blended with traditional pulps, eucalyptus pulp

provides opacity, density, printability, and softness, all desirable characteristics in the finished product (Slinn, 1989). Currently, in the United States pulp producers import eucalyptus from Brazil, Spain, and Portugal. Japan's pulp and paper industry uses short fiber tropical hardwood chips for the production of clear white stationary paper and photocopying paper (Clark, 1990). Hawaii's sub-tropical climate is favorable for eucalyptus production due to its frost sensitivity. Potentially, Hawaiian grown eucalyptus wood chips could meet some of the international demand for short fiber hardwood chips.

5.3 Methodology

The windward side of the island of Hawaii has been cited as the most cost effective and potentially the most productive location in the state of Hawaii to grow Eucalyptus (Khamoui and Baker, 1981; Bioenergy Corp., 1980). The site of the current study was located in the Puna district 30 km southwest of Hilo on the island of Hawaii (Table 3.1). The trial was established in June 1986. Eucalyptus yield data utilized for this study was presented in Table 4.3. A loss of 15% was assumed for chips during in field harvest and transportation.

Net Present Value

The economic analysis of eucalyptus for wood chip production was based on net present value (NPV). This calculation assesses the value of a resource at some future date and determines the current value based on a chosen discount (interest) rate. For this study a two year horizon was utilized. To calculate NPV:

$$NPV = \frac{A^1}{(1+r)} + \frac{A^2}{(1+r)^2}$$

NPV was determined for both year 1 and year 2. A represented the future amount to be received in year 2, after income generated from the harvest was divided by 2 and assumed to be equal for both years. The opportunity (interest) rate r, was varied to reflect changes in the cost of capital.

This method will be used to evaluate the different market regimes to determine which is most attractive economically. An enterprise is feasible or break-even if NPV is zero and profitable if NPV is positive.

5.4 Results

Costs were calculated for each management regime (Table 5.1) based on actual costs incurred by the Hawaiian Sugar Planters' Association or from the Annual progress reports of the Bioenergy Development Corporation (Bioenergy Corp., 1985). Land costs were assumed to be zero because FGT plantations would likely be planted on marginal sugar cane

land owned by companies. Growing trees on leased land would substantially increase costs.

Gross revenue is the amount generated by the sales price per BDT of woodchips multiplied by yield per hectare, then discounted 15 percent for losses occurring in handling and transportation (Table 5.2). The net revenue per hectare per year was generated using the difference between gross revenue and the cost of cultural practices and tree seedlings (Table 5.2). Finally, woodchip prices per ton were varied to reflect volatility of world market prices for bulk commodities.

NPV analysis was not performed on data from woodchips for energy production due to negative net revenue (Table 5.3). The energy case was unattractive economically due to unfavorable market conditions reflecting the low value of the end product. Alternatively, net revenue for the paper pulp case was positive at $90.00 and $100.00 per BDT which makes this project feasible economically (Table 5.3). But at $80.00 per BDT the net revenue was negative. This finding illustrates the price sensitivity of this enterprise. Finally, NPV remains positive over a range of discount rates, indicating woodchip production for paper pulp is economically viable (Table 5.4).

5.5 Discussion

Rational plantation management must integrate economics into the biology of tree growth and tree plantation development for meaningful results. The economic potential for SR woodchip production in Hawaii appears to be promising only if utilized for a high value product. The intensive management allows costs to be spread over a greater number of tons per hectare, so costs per unit are reduced.

Alternative woodchip markets were analyzed for eucalyptus. The production of woodchips for energy was not economical under the conditions of this study. The chief contributing factor was the low value of the end product. In contrast, the production of woodchips for the paper pulp market at high prices was economically viable within the parameters of this study reflecting the relatively higher value of the end product and fewer substitutes.

The break even price for wood chips for energy production is estimated to be above $70.00 (BDT), which is the equivalent to $35.00 a wet ton or $35.00 a barrel for oil. It should not be over looked that as oil prices increase, input prices for fertilizers, herbicides, and vehicle operations also increase and therefore result in a higher total cost. The best option for energy production could perhaps be realized with wood chips of inferior quality. This by-product could be utilized as a fuel for

running the woodchip mill. The example of burning bagasse for energy in the Hawaiian sugar industry best illustrates this point.

In intensive tree crop management the use of fertilizers can only be justified if greater revenues significantly off set the cost of the added fertilizer. Furthermore, this increased wood chip yield must be utilized in moderate or high value products for a profitable enterprise.

The scenario could change with input cost fluctuation, as is often the case with fertilizer and bulk commodities. Alternatively, an output price shift might favor one market over another. As raw material, eucalyptus wood chips have substitutes in both energy and paper pulp markets. Currently, the market for wood chips paper pulp production predominates.

Alternative management regimes which would lower input costs and improve the economic attractiveness are possible. Previous research has found that planting fewer trees per hectare and longer rotations between harvests increase total biomass at harvest and decrease harvest costs because fewer trees are handled per unit weight (Hartsough and Nakamura, 1990). Admixtures of nitrogen fixing trees have yielded promising results when interplanted with eucalyptus (DeBell et al., 1988). This technique would have the benefits of lowering costs for purchasing and applying fertilizer.

However, mixed fiber harvest may present processing problems for paper pulp production.

Further value added by processing is beyond the scope of this study although it is thought that additional processing of woodchips into pulp would greatly enhance economic attractiveness. The price per ton of pulp was near $800.00 late in 1988, with an average of $600.00 per ton for the past decade (Embury, 1988).

Presently, the production of wood chips from SR is of experimental interest. At high prices, production of wood chip for paper pulp is economically viable. International bulk commodities markets are volatile when compared to the stability of the Hawaiian sugar market so the opportunity cost of conversion from sugar cane to wood chips would seem high. The problems of market entry, environmental compatibility with tourism, and initial capitalization are significant constraints. If these problems can be worked out then the production of SR plantations in Hawaii might become a reality.

Table 5.1 Production costs for the establishment and maintenance of Eucalyptus plantations for wood chip production

Item	Costs
	$/ha/rotation
Site preparation	$225.00
Herbicides	$147.50
Fertilizer	$577.50
Tree seedlings	$1000.00
Labor	$704.00
Harvest	$900.00
Transportation	$800.00
Total cost	$4353.50

(Appendix 11 contains itemized costs and revenues summary)

Table 5.2 Gross revenue per rotation per hectare at varying prices

Woodchips for paper pulp

Price (BDT)	Yield (BDT)	Gross Revenue (BDT)
$80.00	51	$4080.00
$90.00	51	$4590.00
$100.00	51	$5100.00

Woodchips for energy

Price (BDT)	Yield (BDT)	Gross Revenue (BDT)
$30.00	59.5	$1785.00
$40.00	59.5	$2380.00
$50.00	59.5	$2975.00

Table 5.3 Net revenue per rotation per hectare

Wood chips for paper-pulp

Price (BDT)	Gross Revenue	Total Cost	Net Revenue
-$80.00	$4080.00	$4353.50	-$273.50
$90.00	$4590.00	$4353.50	$236.50
$100.00	$5100.00	$4353.50	$746.50

Wood chips for energy

Price (DBT)	Gross Revenue	Total Cost	Net Revenue
-$30.00	$1785.00	$4353.50	-$2568.50
$40.00	$2380.00	$4353.50	-$1973.50
$50.00	$2975.00	$4353.50	-$1378.50

Table 5.4 Net Present Value per rotation per hectare

Wood chips for paper pulp

		NPV
Discount rate	0%	$746.50
	5%	$694.03
	10%	$647.79
	15%	$606.79

(See appendix 1 for calculations)

LITERATURE CITED

Applegate, G.B., D.A. Gilmour, and B. Mohns. 1988. The use of biomass estimations in the management of forests for fuelwood and fodder production. Commonw. For. Rev. 67:141-147.

Baskerville, G.L. 1965. Estimation of dry weight of tree components and total standing crop in confier stands. Ecol. 46:867-869.

Baskerville, G.L. 1972. Use of logarithmic regression in the estimation of plant biomass. Can. J. For. Res. 2:49-53.

Bradstock, R. 1981. Biomass in an age series of Eucalyptus grandis Plantations. Aust. For. Res. 11:111-127.

Binkley, D. 1987. Forest Nutrition Management. John Wiley and Sons. New York.

BioEnergy Development Corporation. 1984. BioEnergy Development Crop. Annual Report:January 1983-December 1984. 127pp.

_____. 1985. BioEnergy Development Crop. Annual Report:January 1984-December 1985. 119pp.

_____. 1986. BioEnergy Development Crop. Annual Report:January 1985-December 1986. 75pp.

Bradstock, R. 1981. Biomass in an Age Series of Eucalyptus grandis Plantations. Aust. For. Res. 11:111-127pp.

Brandao, L.G., Y.K. Ikemori, and E. Caminhos, Jr. 1984. The new eucalypt forest. p. 1-29. Proc. The Marcus Wallenberg Foundation Symposium, Fallun, Sweden.

Brewbaker, J.L. 1987. Performance of Australian Acaias in Hawaiian Nitrogen-Fixing Tree Trials.p. 180-186. In John Turbull (ed). Australian Acacias in Developing Countires. Australian Centre for International Agricultural Research. Proceedings no.16. Brown Prior Anderson, Victoria, Australia.

_____ . (Editor) 1980. Giant leucaena (koa haole) energy tree farm: An economic feasibility analysis for the Island of Molokai, Hawaii. Hawaii Nat. Energy Institute Pub. No. 80-06.

_____. and E.M. Hutton. 1979. Leucaena: versatile tropical tree legume.p.207-257. In Agricultural Crops. G.A. Ritchie (Ed.) Amer. Assn. Adv. Sci. Westview Press, Boulder, Colo.

_____., K.G. MacDicken and R.J. Van Den Belt. 1981. Nitrogen-Fixing tree resources: Potentialities and Limitations, Paper presented at Conference on Biological Nitrogen Fixation, Cali, Colombia,1981.

_____., and C.T. Sorensson. 1987. Leucaena diversifolia and its Hybrids for the Highlands. Leucaena Research Reports. 8:66-67.

Buongiorno, J., and J.K. Gilless. 1987. Forest Management and Economics. Macmillan. New York.

Campinhos,E. 1980. More wood of better quality through intensive silviculture with rapid growth of improved Brazilian Eucalyptus. Tappi 63 (11):145-147.

Causton, D.R. and Jill Venus. 1981. The biometery of plant growth. Edward Arnold. London.

Chen, H.K. 1989. Vice General Manger, Material Division Chung Hwa Pulp Corp. (Personal Commmunication).

Clark, Earl. 1990. From weed tree to money tree. American Forests 96 (1&2):50-53,70.

Comer, R.N. and E.R. Williams 1982. Biomass and nutrient accumulation in a planted E. globulus (Labill.) fertilizer trial. Australian Journal of Botany 30: 265-278.

Couto, L., and J.C. Nautiyal. 1984. A Nutrient-related Time-dependent Production Function For Eucalyptus grandis Hill ex Maiden in South-eastern Brazil. Aust. For. Res. 14:37-47.

Crow, T.R. 1983. Comparing biomass regression by site and stand age for red maple. Can. J. For. Res. 13:283-288.

Crow, T.R. 1988. A Guide to Using Regression Equations for Estimating Tree Biomass. North. J. Appl. For. 5:15-22. March 1988.

Darrow, W.K. 1984. Biomass production of Eucaluptus grandis in South Africa planted at various close espacements: Two-year results. South Africa Forestry Journal 131:34-39.

DeBell, D.S., C.D. Whitesell and T.H. Schubert. 1985. Mixed plantations of Eucalyptus and leguminous trees enhance biomass production. Res. Paper PSW-175.

Doran,J.C., and N. Hall 1981. Notes on Australian Casurina Species. p.19-56. In S.J. Midley et al.(eds). Casuarina Ecology Management and Utilization, Proc. of an International workshop. Canberra, C.S.I.R.O., Australia.

Earl, E.D. 1975. Forest Energy and Economic Development. Clarendon Press, Oxford, U.K.

Edwards, D.W. 1973. Defects of fast-grown eucalyptus in New South Wales. Proc. Meet. Div. 5. Int. Un. For. Res. Org. South Africa. Vol 2:256-270.

Embury, Lynn. 1988. Market pulp: Industry update. Merrill Lynch Captial Markets Canada Research, Toronto, Ontario, Canada.

Evans, G.C. 1972. The Quantitative Analysis of Plant Growth. University of California Press. Los Angeles, U.S.A.

Evans, J. 1982. Plantation Forestry in the Tropics. Oxford University Press. Oxford, U.K.

FAO. 1979. Eucalyptus for planting. FAO Forestry and Forest Products Studies. No. 11. Rome, Italy.

Fenton, R. 1982. International Wood-Chip Trade and the South Pacfic. Commow. For. Rev. 61(3):181-193.

Ferderick, D.J., H.A.I. Madgwick, G.R. Oliver, and M.F. Jurgensen. 1985. Dry matter and nutrient content of 8-year-old Eucalyptus saligna growing at Taheke Forest. N. Z. J. For. Sci. 15:251-254.

Florence, R.G. 1986. Cultural Problems of Eucalyptus as Exotics. Commonw. For. Rev. 65(2):141-161.

Foote, D., E.L. Hill, S. Nakamura, and F. Stephens. 1972. Soil Survey of Islands of Kauai, Oahu, Maui, Molokai,

Fox, R.L., and R.S. Yost. 1980. Mapping Soil Fertility and Fertilizer Requirements. University of Hawaii, CTAHR research series-No.23-1980.

Geary, T.F., Meskimen, G.F. and Franklin, E.C. 1983. Growing eucalyptus in Florida for industrial wood production. USDA For. Serv. Gen. Tech. Rpt. SE-23, 43pp.

Golob, T.B. 1987. Machinery for Short Rotation Forestry. In D.O. Hall and R.P. Overend (ed.) Biomass:Regenerable Energy. John Wiley & Sons Ltd. Chichester, U.K.

Gomez, K.A. and A.A. Gomez. 1984. Statistical procedures for agricultural research. John Wiley & Sons, Inc. New York.

Goodwin, A.N., and S.G. Candy. 1986. Single-tree and stand growth models for a plantation of Eucalyptus globulus Labill. in Northern Tasmania. Aust. For. Res. 16:131-144.

Grut, M. 1987. Cost-Benefit Analysis of Fuelwood and Forest Projection Projects in Developing Counties. Commonw. For. Rev. 66(1):25-30.

Gunter, J.E., and H.L. Haney, Jr. 1984. Essentials of Forestry Investment Analysis. Orgeron State University Press. Corvallis.

Halenda, Christine. 1989. Biomass estimation of Acacia mangium plantations using allometric regression. NFTRR 7:4951.

Hartsough, B.R., and G. Nakamura. 1990. Harvesting eucalyptus wood chips for fuel chips. Cal. Ag. Vol44 (1):7-8.

Hawaiian Sugar Planters' Association, Experiment Station. 1987. Annual Report 1986. H.S.P.A., Aiea, Hawaii.

1988. Annual Report 1987. H.S.P.A., Aiea, Hawaii.

Hillis, W.E. 1984. Wood quality and utilization. p.259-289 In W.E. Hillis and A.G. Brown (Ed.) Eucalyptus for wood production. Academic Press. Sydney.

Hu, T.W., and T. Kiang. 1983. Leucaena research in Taiwan. In Leucaena Research in the Asia and Pacific Region. Proc. of IDRC/NFTA workshop held in Singapore Nov. 23-26, 1982. IDRC, Ottawa.

Hunt, Roderick. 1978. Plant Growth Analysis. Camelot Press. Southampton, U.K.

Husch, B., C.I. Miller and T.W. Beers 1982. Forest mensuration. John Wiley & Sons. New York.

Kanazawa, Y., A. Santo and R.S. Orsolino. 1982. Above-ground biomass and growth of giant ipip-ipil (Leucaenaleucocephala) plantations in norhtern Mindanao Island, Philippines. JARQ, Japan Agriculutral Res. Quarterly 15 (3):209-217.

Kaumi, S.Y.S. 1983. Four Rotations of a Eucalyptus Fuel Yield trial. Commonw. For. Rev. 62(1):19-24.

Khamoui,T. 1981. An Economic Fesaibility Analysis of Woodchip Production on the Island of Hawaii for export to Japan. Doctoral Dissertation, University of Hawaii.

_____, and H.L. Baker. 1982. An Economic Analysis of Hawaii Eucalyptus woodchip production for Export. College of Tropical Agriculture and Human Resources, University of Hawaii at Manoa. HITAHR Research Series 023.

Kionsky, K. 1988. Economic feasibility of eucalyptus production. Cal. Ag. Vol 42 (6):25-27.

LeBarron, Russell K.1970. The History in Hawaii-from the begining through World War II. Aloha Anina 4:2.

Linder, S. and Rook, D.A. 1984. p.211-234. In G.D. Bowen and E.K.S. Nambiar(ed.) Nutrition of Plantation Forest Academic Press. London.

Lorrain-Smith, R. 1982. Discount Rates and Time Horizons. Commw. For. Rev. 61(4):277-283pp.

Lugo, A.E., S. Brown, and J. Chapman. 1988. An analytical review of production rates and stemwood biomass of tropical forest plantations. For. Ecol. Manage. 23:179-200.

MacDicken, K.G. 1983. Studies on the early growth rates of selected nitrogen-fixing trees. M.S. thesis, University of Hawaii, Agronomy and Soil Science Dept.

Madgwick, H.A.I., and T. Satoo. 1975. On estimating the above ground weight of stands. Ecology 56:1446-50.

Mahilum, B., R.L. Fox, and J.A. Silva. 1970. Residual effects of liming volcanic ash soils in the humid tropics. Soil Sci. 109:102-109.

Malan. F.S. 1988. Wood density variation in four trees of South African grown Eucalyptus grandis (Hill ex Maiden). S. Africa. For. Jour. 144:36-42.

Matthews, D.M. 1914. Ipil-ipil--a firewood and reforestation crop. Philippine Island Dept. of the Interior (Bur. of For.) Bull. #13. Manila. 18pp.

Meyer, H.A. 1944. A correction factor for a systematic error occurring in the application of the logarithmic equation. Penn. State. Sch. Res. Pap. 7:3.

Miller, H.G. 1981. Forest Fertilization:Some Guiding Concepts. Forestry. Vol.54, No. 2:157-167.

Miyasaka, S.C. 1984. Comparison of quick- and slow-release fertilizers in young plantings of Eucalyptus spears. Tree Planter's 35:20-24.

Mullette, K.J., N.J. Hannon and A.G.L. Elliott. 1974. Insoluble phosphorus usage by Eucalyptus. Plant Soil 41:199-205.

National Academy for Sciences. 1984. Casuarina: Nitrogen-Fixing Trees for Adverse Sites. NAS, Wash. D.C.

_____ . 1977. Leucaena - Promising Forage and Tree Crop for the Tropics. NAS, Wash. D.C.

_____. 1980. Firewood Crops, Shrub and Tree Species for Energy Production. NAS, Wash.D.C.

_____. 1984. Leucaena: Promising Forage and Tree Crop for the Tropics,2nd ed. NAS, Wash.D.C.

_____. 1983. Mangium and Other Fast-Growing Acacias for the Humid Tropics. NAS, Wash.D.C.

Neter, J., and W. Wasserman. 1974. Applied linear Statistical Models. Richard D. Irwin, Inc. Homewood, Ill.

Osgood, R. V., and R. D. Wiemer. 1986. Plant Introduction Needs of the Hawaiian Sugar Industry. p.10 Symposium on the Control of Introduced Plants in Hawaii's Native Ecosystem. Honolulu, HI. May 23, 1986. HSPA, Aiea, HI.

Pande, M.C., V.N. Tandon, and M. Negi. 1986. Biomass production and its distribution in an age series plantation of Eucalyptus hybrid and Acacia auriculaeformis in Bihar. Indian Forester. 112:975-985.

Pandey, D. 1987. Yield model of plantations in the tropics. Unasylva 157/158, Vol. 39(3&4):74-75.

Phillips, V. 1989. Hawaii: showcase for methanol-from-biomass. p.32-42 In Proc. third pacific basin biofuels workshop. Waianae, HI. 27-28 Mar. 1989. HENI, Honolulu, HI. U.S.A.

Qureshi, A.H. 1978. Diagnosis of nutritional disorders in Eucalyptus salinga sm. seedlings and their respones to fertilization in forest soils. Dissertation Abstracts International No. 7820436.

Rockwood, D.L. 1984. Genetic improvement of biomass quality and quanity through genetic selection and breeding. Biomass 6:37-45.

Sato, H., W.Ikeda, R. Paeth, R. Smythe, and M. Takehiro,Jr., 1973. Soil Survey of Island of Hawaii, State of Hawaii. U.S. Dept. of Agr.

Satoo, T. 1970. A synthesis of studies by the harvest method. Primary production studies in the temperate deciduous forest of Japan. p.55-73. In D.E. Reichle (ed.), Analysis of Temperate Forest Ecosystem, Springer-Verlag, New York.

_____ , and H.A.I. Madgwick, 1982. Forest Biomass. Martinus Nijhoff/Dr. W. Junk, The Hague.

SAS Institute. 1982. SAS User's Guide: Statistics. SAS Inst. Cary, NC.

Schubert, T.H., and C.D. Whitesell. 1985. Species trials for biomass plantation in Hawaii: a first appraisal. Res. Pap. PSW-176.

_____, R.F. Strand, T.G. Cole, and K.E. MacDuffie. 1988.Equations for predicting biomass of six introduced tree species, island of Hawaii. Res. Note. PSW-401.

Shepard, K.R. and P. Saardavut. 1984. Allometric Relationships between Shoot and Root Development and between Leaf Dry Wieght and Leaf Area in Provenances of Eucalyptus camaldulensis Dehnh. Aust. For. Res. 14:265-270pp.

Sherry, S.P. 1971. The Black Wattle. University of Natal Press. Pietermaritburg.

Skolmen, R.G. 1986. Performance of Australian provenances of Eucalyputs grandis and Eucalytus salinga in Hawaii. Res. Paper PSW-181.

Slinn, R.J. 1989. The impact of industry restructuring on fiber procurment. Jour. of For. 1989-2:17-20.

Sorensson, C.T. and J.L. Brewbaker. 1987. Psyllid resistance of leucaena hybrids and species. Leucaena Research Reports 7 (2):29-34.

Steinbeck, K. 1983. Potentialities of short-rotation forestry for developing countries. Outlook on Agriculture 12:160-164.

_____ and T.M. Skinner. 1984. Growing Short-Rotation Forests in the Southeastern U.S.A. p.63-69. In H.Egneus and A. Ellegard (ed.) Bioenergy 84 vol.II Biomass Resources. Elsevier Applied Science Publishers, Essex, England.

Strand, R.F. and C.D. Whitesell. 1989. Managing Eucalyptus plantations for maximum yield. p 89-95. Proc. third pacific basin biofuels workshop. Waianae, HI. 27-28 Mar. 1989. HNEI, Honolulu, HI. U.S.A.

Streyffert, Thorten. 1968. World pulpwood. Almquist and Wilsells Boktryckeri. Stockholm.

Tischler, K. and R. Karschon. 1983. The Calorific Value of the Biomass of Eucalyptus camaldlensis DENH. Commow. For. Rev. 62(4):265-269.

Turnbull, J.W. and L.D. Pryor. 1984. Choice of species and seed sources. p. 6-65. In W.E. Hillis and A.G. Brown (ed.) Eucalyptus for wood production. Academic Press. Sydney.

Walters, G.A. 1981. Why Hawaii is changing to the dibble-tube system of forestation. J. of For. 79(11): 743-745.

Walters, G.A., and T.H. Schubert. 1969. "Saligna Eucalyptus Growth in a Five-Year-Old Spacing Study in Hawaii." Journal of Forestry, Vol. 67, No.4:232-234.

Whitesell, C.D., S.C. Miyasaka, R.F. Strand, T.H. Schubert, and K.E. McDuffle. 1988. Equations for Predicting Biomass in 2- to 6-year-old Eucalyptus saligna in Hawaii. Res. Note PSW-402.

Van Den Belt, R.J. 1983a. Leucacena leucocephala (Lam.) de Wit for wood production. Ph.D. dissertation, University of Hawaii, Agronomy and Soil Science Dept.

_____ , 1983b. Volumetric models for leucaena. Leucaena Res. Rept. 4:93-95.

_____ , and J.L. Brewbaker. 1980. Leucaena wood production in Hawaii. Leucaena Newsletter. 1:55.

Van Laar, A., and A.P.G. Schonau. 1988. Form Quotients and Stem Form of Eucalyptus grandis. S. Africa. For. Jour. 144:33-35.

Verma. V.P.S., V.N. Tandon, and H.S. Rawat 1987. Biomass production and plant nutrient distribution in different aged plantions of Casuarina equisetifolia in Puri, Orissa. Indian Forester 133:273-280.

Whitesell, C.D., D.S. Debell, and T.H. Schubert. 1987. Six-Year Growth of Eucalyptus Saligns Planting as Affected by Nitrogen and Phosphorus Fertilizer. Res. Pap. PSW-188.

_____ , S.C. Miyasaka, R.F. Strand, T.H. Schubert, K.E. McDuffie. 1988 Equations for predicting biomass in 2 to 6 year old Eucalyptus salinga in Hawaii. Res. Note PSW-402.

Yang, C., et al. (Eds.) 1977. Biomass Energy for Hawaii,Volume IV: Terrestrial and Marine Plantations. Prepared by Sanford University / University of Hawaii Energy Study Team.

Yim, T.C. 1979. Legislative energy RD&D workshop handbook. Hawaii State Senate, Honolulu

Yost, R.S., D.S. Debell, C.D. Whitesell and S.C. Miyasaka. 1987. Early Growth and Nutrient Status of Eucalyptus saliga as affected by Nitrogen and Phosphorus Fertilization. Aust. For. Res. 17:203-214.

Zobel,B.J., G. Van Wyk, and P. Stahl. 1987. Growing Exotic forests. John Wiley & Sons, Inc. New York.

Appendix Table 1. Tree growth data at Mtn. View, Hawaii

Data	Age mos.	Species	Data from Replication: I	II	III	IV	AVG	Range Test	AVG of AVGS
Height (m)	3	Casuarina	0.54	0.71	0.82	0.76	0.71	cde	
		Grandis	0.95	0.96	0.97	0.99	0.97	ab	
		Gra/unf	0.62	0.84	0.91	0.53	0.73	cde	
		Leucaena	0.43	0.51	0.78	0.53	0.56	e	
		Leu/unf	0.51	0.74	0.67	0.94	0.72	cde	
		Mangium	0.27	0.46	0.26	0.28	0.32	f	
		Mearnsii	0.44	0.54	0.86	0.60	0.61	ef	
		Robusta	0.73	0.81	0.90	0.87	0.83	bcd	
		Saligna	1.15	0.86	0.86	0.68	0.89	abc	
		Urophylla	1.23	1.19	0.91	0.92	1.06	a	0.74
	6	Casuarina	1.01	1.26	1.38	1.23	1.22	cd	
		Grandis	1.89	1.57	1.34	2.64	1.86	ab	
		Gra/unf	1.15	1.20	1.81	1.18	1.34	cd	
		Leucaena	0.79	1.44	1.95	1.19	1.34	c	
		Leu/unf	1.15	1.27	1.03	1.74	1.30	c	
		Mangium	0.66	1.02	0.61	0.57	0.72	d	
		Mearnsii	1.53	1.43	1.91	1.87	1.69	bc	
		Robusta	2.09	1.78	1.94	2.53	2.08	ab	
		Saligna	2.62	1.86	1.65	1.46	1.90	ab	
		Urophylla	2.49	2.56	2.67	1.97	2.42	a	1.59
	9	Casuarina	1.51	1.46	1.78	1.54	1.57	c	
		Grandis	2.65	2.86	2.97	4.09	3.14	ab	
		Gra/unf	1.19	1.30	1.30	1.71	1.37	cd	
		Leucaena	1.20	1.05	2.33	1.42	1.50	cd	
		Leu/unf	1.33	1.64	1.23	1.81	1.50	cd	
		Mangium	0.89	1.30	0.71	0.91	0.95	d	
		Mearnsii	2.48	2.08	2.58	3.01	2.54	b	
		Robusta	2.74	2.66	2.71	3.74	2.96	ab	
		Saligna	3.55	2.53	2.72	1.71	2.63	b	
		Urophylla	3.32	3.47	4.09	2.86	3.44	a	2.16
	12	Casuarina	1.9	2.2	2.3	2.1	2.1	e	
		Grandis	4.6	4.5	5.2	5.3	4.9	ab	
		Gra/unf	1.5	1.5	1.5	2.1	1.6	ef	
		Leucaena	2.4	1.7	3.9	3.6	2.9	d	
		Leu/unf	1.3	1.7	1.4	1.9	1.6	ef	
		Mangium	1.2	2.0	1.3	-	1.5	f	
		Mearnsii	3.5	3.6	4.0	4.5	3.9	c	
		Robusta	3.9	4.1	4.2	5.5	4.4	bc	
		Saligna	5.0	4.0	4.4	4.5	4.5	b	
		Urophylla	5.0	4.9	5.5	5.0	5.1	a	3.3

Data	Age mos.	Species	Data from Replication: I	II	III	IV	AVG	Range Test	AVG of AVGS
(m)	18	Casuarina	3.3	3.8	3.9	4.0	3.7	cd	
		Grandis	7.9	8.8	9.3	9.5	8.8	a	
		Gra/unf	3.3	3.6	3.7	5.0	3.9	cd	
		Leucaena	4.2	3.7	5.6	4.9	4.6	c	
		Leu/unf	1.7	2.3	3.2	3.5	2.7	d	
		Mangium	2.4	4.5	3.0	2.7	3.1	d	
		Mearnsii	5.9	6.7	6.4	7.5	6.6	b	
		Robusta	6.5	7.4	7.4	7.8	7.2	b	
		Saligna	9.1	7.1	7.0	6.1	7.3	b	
		Urophylla	7.8	7.8	9.2	6.7	7.9	ab	5.6
	24	Casuarina	4.2	4.3	4.7	4.0	4.3	cd	
		Grandis	8.6	8.9	9.6	9.7	9.2	a	
		Gra/unf	4.6	4.3	5.1	7.1	5.3	d	
		Leucaena	5.2	4.2	5.8	4.9	5.0	d	
		Leu/unf	2.3	2.5	2.9	3.7	2.8	e	
		Mangium	3.5	5.4	4.1	4.5	4.4	d	
		Mearnsii	6.2	6.9	7.1	7.6	6.9	c	
		Robusta	7.8	8.1	8.3	8.7	8.2	ab	
		Saligna	9.8	7.3	7.5	7.3	7.9	bc	
		Urophylla	8.9	8.4	9.8	8.1	8.8	ab	6.3
Dia. (cm)	12	Casuarina	1.2	1.2	1.6	1.1	1.3	cd	
		Grandis	3.2	3.3	3.1	3.6	3.3	a	
		Gra/unf	--	0.7	0.8	1.7	1.1	d	
		Leucaena	1.6	1.3	2.7	2.7	2.1	b	
		Leu/unf	--	1.2	--	1.2	1.2	d	
		Mangium	--	1.8	--	--	1.8	cd	
		Mearnsii	2.8	2.8	3.1	3.7	3.1	a	
		Robusta	3.8	3.1	3.3	3.6	3.4	a	
		Saligna	3.8	2.9	3.0	3.0	3.2	a	
		Urophylla	3.4	3.8	3.7	3.4	3.6	a	2.4
	18	Casuarina	1.6	2.2	2.9	2.0	2.2	bc	
		Grandis	4.9	4.8	5.4	5.9	5.3	a	
		Gra/unf	1.8	2.3	1.9	3.8	2.5	b	
		Leucaena	2.4	1.5	3.0	3.3	2.6	b	
		Leu/unf	0.8	1.4	1.3	2.0	1.4	c	
		Mangium	1.9	3.7	2.1	3.5	2.8	b	
		Mearnsii	4.2	4.5	6.2	5.7	5.4	a	
		Robusta	4.8	4.1	4.6	5.2	4.7	a	
		Saligna	5.1	4.2	4.4	3.7	4.4	a	
		Urophylla	4.8	5.2	5.9	4.1	5.0	a	3.6
	24	Casuarina	2.3	2.4	3.1	2.0	2.5	cd	
		Grandis	5.2	5.4	5.7	6.0	5.6	a	
		Gra/unf	2.4	3.0	2.5	4.3	3.1	b	

Data	Age mos.	Species	Data from Replication: I	II	III	IV	AVG	Range Test	AVG of AVGS
Dia.	24	Leucaena	3.0	2.1	3.1	3.3	2.8	bc	
		Leu/unf	1.1	1.3	1.3	2.1	1.5	d	
		Mangium	3.0	4.3	3.1	4.6	3.8	b	
		Mearnsii	4.2	4.8	6.3	5.8	4.9	a	
		Robusta	5.4	4.6	5.0	5.3	5.1	a	
		Saligna	6.3	4.3	4.5	4.3	4.8	a	
		Urophylla	5.3	5.5	6.3	4.2	5.3	a	3.9

Appendix Table 2. Tree growth data at Honokaa, Hawaii

Data	Age mos	Species	Data from Replication: I	II	III	IV	AVG	Range Test	AVG of AVGS
Height	3	Casuarina	0.54	0.51	0.46	0.37	0.47	e	
	(m)	Grandis	0.79	0.83	0.80	0.82	0.81	ab	
		Gra/unf	0.68	0.86	0.68	0.70	0.73	abc	
		Leucaena	0.53	---	0.91	0.32	0.56	cde	
		Leu/unf	0.31	0.61	0.43	0.48	0.46	e	
		Mangium	0.58	0.45	0.53	0.45	0.51	ed	
		Mearnsii	0.79	0.83	0.91	1.03	0.89	a	
		Robusta	0.62	0.73	0.82	0.67	0.71	bc	
		Saligna	0.76	0.55	0.73	0.61	0.66	bcd	
		Urophylla	0.69	0.69	0.69	0.60	0.67	bcd	0.65
	12	Casuarina	2.0	2.4	2.0	2.1	2.1	d	
		Grandis	5.3	4.1	6.1	5.7	5.3	ab	
		Gra/unf	1.6	3.3	3.9	1.9	2.7	cd	
		Leucaena	3.0	3.7	4.1	2.4	3.3	c	
		Leu/unf	3.3	4.0	2.7	3.3	3.3	c	
		Mangium	2.2	3.0	3.1	2.6	2.7	cd	
		Mearnsii	4.0	4.6	5.1	5.5	4.8	bc	
		Robusta	4.6	5.3	4.9	3.4	4.5	b	
		Saligna	6.1	5.5	6.1	5.1	5.7	a	
		Urophylla	4.7	5.1	5.2	4.0	4.7	ab	3.9
	18	Casuarina	3.6	3.8	3.5	3.7	2.9	d	
		Grandis	8.2	8.3	9.1	8.1	6.7	a	
		Gra/unf	3.4	5.4	6.5	4.3	3.9	c	
		Leucaena	5.8	5.7	5.3	4.0	4.2	c	
		Leu/unf	5.3	5.4	4.1	5.1	3.9	c	
		Mangium	4.5	5.1	5.3	4.2	3.8	cd	
		Mearnsii	5.9	6.4	7.9	6.9	5.4	b	
		Robusta	6.1	7.1	6.8	9.0	5.8	ab	
		Saligna	7.9	8.0	8.7	7.0	6.3	ab	
		Urophylla	8.5	7.7	7.6	7.3	6.2	ab	4.9
	24	Casuarina	4.4	---	4.0	4.8	3.3	e	
		Grandis	10.2	9.9	10.6	9.8	10.1	a	
		Gra/unf	5.3	7.0	6.2	5.9	6.1	e	
		Leucaena	6.9	6.4	6.1	5.1	6.1	ed	
		Leu/unf	6.6	6.4	5.4	6.2	6.2	ed	
		Mangium	6.2	6.0	6.9	4.2	5.8	e	
		Mearnsii	6.8	8.3	8.6	8.3	8.0	bc	
		Robusta	7.7	8.3	7.9	6.6	7.6	dc	
		Saligna	10.0	9.9	9.3	8.0	9.3	ab	
		Urophylla	8.9	9.1	9.4	8.2	8.9	abc	7.1

Data	Age mos	Species	Data from Replication: I	II	III	IV	Range AVG	Test	AVG of AVGS
Dia. (cm)	12	Casuarina	1.0	1.0	0.6	1.0	0.9	e	
		Grandis	3.6	2.4	3.9	3.5	3.3	ab	
		Gra/unf	0.6	1.8	2.3	1.0	1.4	e	
		Leucaena	2.2	3.1	2.8	1.6	2.4	cd	
		Leu/unf	2.2	2.5	1.7	2.2	2.2	d	
		Mangium	1.7	2.7	2.7	2.0	2.3	cd	
		Mearnsii	2.9	3.8	3.8	4.0	3.6	ab	
		Robusta	2.7	3.6	3.3	2.1	2.9	bc	
		Saligna	4.2	3.7	4.1	3.4	3.8	a	
		Urophylla	3.1	3.5	3.3	3.6	3.4	ab	2.6
	18	Casuarina	2.2	2.1	1.6	2.1	2.0	g	
		Grandis	5.7	5.5	5.2	4.8	5.3	ab	
		Gra/unf	1.8	3.0	3.6	2.3	2.6	fg	
		Leucaena	3.9	4.2	3.8	2.4	3.5	de	
		Leu/unf	3.6	3.3	2.4	3.3	3.2	ef	
		Mangium	4.1	4.6	4.8	3.7	4.3	cd	
		Mearnsii	3.7	4.9	5.6	5.0	4.8	bc	
		Robusta	3.9	5.0	4.2	3.3	4.1	cd	
		Saligna	5.8	5.7	5.8	5.0	5.6	a	
		Urophylla	5.0	4.6	4.8	4.6	4.7	bc	4.1
	24	Casuarina	2.9	---	1.7	3.0	1.9	d	
		Grandis	5.9	6.1	6.2	5.3	5.8	a	
		Gra/unf	3.0	3.6	4.3	3.4	3.5	c	
		Leucaena	4.3	4.7	3.8	3.2	4.0	bc	
		Leu/unf	4.2	3.8	2.7	4.1	3.7	c	
		Mangium	5.3	6.5	6.4	4.3	5.6	a	
		Mearnsii	4.4	6.2	5.7	5.8	5.5	a	
		Robusta	4.9	5.8	5.1	4.2	5.0	ab	
		Saligna	6.4	6.5	5.8	5.2	5.9	a	
		Urophylla	5.5	5.7	5.8	5.3	5.6	a	4.7

Appendix Table 3. Tree growth data at Puunene, Maui

Data	Age mos.	Species	Data from Replication: I	II	III	IV	AVG	Range Test	AVG of AVGS
Height (m)	3	Casuarina	0.8	1.1	0.9	0.8	0.9	a	
		Grandis	0.7	0.6	0.6	0.7	0.7	b	
		Leucaena	0.8	0.8	1.3	0.5	0.8	a	0.8
	12	Casuarina	2.5	3.4	3.0	2.9	2.9	b	
		Grandis	3.5	3.8	3.9	3.8	3.87	a	
		Leucaena	3.7	3.9	4.1	3.9	3.9	a	3.5
	24	Casuarina	5.6	5.8	5.5	5.5	5.6	b	
		Grandis	8.9	7.6	7.4	8.3	8.1	a	
		Leucaena	6.5	6.9	6.7	7.7	6.9	ab	6.9
Dia. (cm)	12	Casuarina	2.0	2.6	2.1	2.2	2.2	a	
		Grandis	2.2	2.4	2.7	2.4	2.4	a	
		Leucaena	2.6	3.0	3.3	2.9	2.9	a	2.6
	24	Casuarina	4.2	4.5	4.6	5.2	4.6	b	
		Grandis	7.3	5.3	5.7	6.5	6.2	a	
		Leucaena	4.2	5.0	5.7	5.3	5.1	ab	5.3

Appendix Table 4. Tree growth data at Hoolehua, Molokai

Data	Age mos.	Species	Data from Replication: I	II	III	IV	AVG	Range Test	AVG of AVGS
Height (m)	3	Camaldul	0.97	1.09	0.94	1.01	1.00	a	
		Casuarina	0.56	0.62	0.52	0.88	0.64	cd	
		Cas cun	0.66	0.40	0.54	0.43	0.51	de	
		Grandis	0.78	0.79	0.84	0.79	0.80	b	
		Leucaena	0.29	0.40	0.38	0.34	0.35	f	
		Saligna	0.58	0.54	0.68	0.56	0.59	cd	0.65
	6	Camaldul	1.67	1.81	1.66	1.64	1.69	a	
		Casuarina	1.43	1.26	0.77	1.04	1.12	b	
		Cas cun	0.85	0.87	0.71	1.17	0.90	b	
		Grandis	1.30	1.02	1.02	1.07	1.11	b	
		Leucaena	0.67	0.50	0.59	0.51	0.57	c	
		Saligna	1.06	0.85	0.98	0.87	0.94	b	1.06
	9	Camaldul	2.29	2.60	2.11	2.31	2.33	a	
		Casuarina	1.86	1.66	1.19	1.32	1.50	b	
		Cas cun	0.88	1.43	0.84	1.55	1.17	bcd	
		Grandis	1.86	1.21	1.19	1.51	1.44	b	
		Leucaena	0.83	1.02	1.18	0.64	0.92	cd	
		Saligna	2.01	1.43	1.21	0.97	1.41	b	1.46
	12	Camaldul	4.6	4.6	5.4	4.3	4.7	a	
		Casuarina	3.6	3.2	3.6	3.3	3.4	b	
		Cas cun	2.2	2.0	2.9	2.6	2.4	c	
		Grandis	5.4	2.7	4.3	3.5	3.9	ab	
		Leucaena	4.0	4.2	3.3	2.9	3.6	b	
		Saligna	4.1	3.7	3.1	2.8	3.4	b	3.6
	18	Camaldul	6.4	7.1	6.3	6.6	6.6	a	
		Casuarina	5.0	4.9	3.9	4.6	4.6	b	
		Cas cun	3.1	4.3	3.2	3.8	3.6	c	
		Grandis	7.3	6.3	6.2	5.8	6.4	a	
		Leucaena	4.9	---	5.4	4.8	5.1	b	
		Saligna	5.5	---	4.9	4.6	1.4	b	4.6
	24	Camaldul	7.3	8.1	7.6	6.9	7.5	a	
		Casuarina	6.0	6.0	6.3	5.2	5.9	c	
		Grandis	6.8	7.6	6.2	8.3	7.2	ab	
		Leucaena	6.2	5.4	6.6	6.1	6.1	bc	
		Saligna	6.5	4.8	6.7	6.5	6.1	bc	6.6.

Data	Age mos.	Species	Data from Replication: I	II	III	IV	AVG	Range Test	AVG of AVGS
Dia. (cm)	12	Camaldul	3.1	3.1	3.7	2.7	3.1	a	
		Casuarina	2.3	2.0	2.5	2.0	2.2	b	
		Cas cun	1.0	1.1	1.7	1.6	1.4	b	
		Grandis	3.4	1.8	2.7	2.4	2.6	ab	
		Leucaena	2.8	3.0	2.9	2.4	2.8	ab	
		Saligna	2.8	2.8	2.3	1.7	2.4	b	2.4
	18	Camaldul	4.3	4.7	4.2	4.2	4.4	a	
		Casuarina	3.5	3.8	2.4	3.7	3.4	ab	
		Cas cun	1.6	3.5	2.9	2.0	2.5	b	
		Grandis	4.8	3.9	4.3	3.7	4.2	a	
		Leucaena	3.9	---	4.3	3.2	3.8	a	
		Saligna	4.2	---	3.6	3.2	3.7	a	3.6
	24	Camaldul	4.3	5.1	4.9	4.6	4.7	a	
		Casuarina	4.0	3.5	3.9	3.9	3.6	b	
		Grandis	3.9	4.4	4.1	4.7	4.3	ab	
		Leucaena	4.1	3.5	4.7	4.2	4.2	ab	
		Saligna	4.5	3.3	4.7	4.5	4.3	ab	4.2

Appendix Table 5. Tree growth data at Kilohana, Kauai

Data	Age mos.	Species	Data from Replication: I	II	III	IV	AVG	Range Test	AVG of AVGS
Height (m)	3	Casuarina	0.95	0.90	1.11	0.96	0.98	b	
		Diversi.	1.19	0.74	0.93	0.84	0.93	b	
		Grandis	0.87	0.99	1.51	1.05	1.11	ab	
		Gra/unf	0.77	0.66	0.63	0.64	0.68	cd	
		K743	0.77	0.99	1.19	0.65	0.90	bc	
		Leucaena	0.70	0.90	0.91	0.94	0.86	bc	
		Leu/unf	0.54	0.62	0.50	0.57	0.56	d	
		Mangium	0.58	0.51	0.50	0.44	0.51	d	
		Mearnsii	0.97	0.88	1.15	1.25	1.06	ab	
		Urophylla	1.20	1.21	1.54	1.12	1.27	a	0.89
	9	Casuarina	1.76	1.67	---	1.65	1.69	c	
		Diversi.	1.38	0.94	1.33	1.05	1.17	d	
		Grandis	2.78	2.88	2.78	2.84	2.82	ab	
		Gra/unf	1.24	1.69	0.95	0.87	1.19	d	
		K743	0.95	1.33	0.95	0.92	1.04	de	
		Leucaena	1.07	1.24	1.60	1.42	1.33	cd	
		Leu/unf	0.63	0.73	0.71	0.83	0.73	e	
		Mangium	1.19	1.11	1.14	1.04	1.12	d	
		Mearnsii	2.19	1.93	3.00	2.93	2.51	b	
		Urophylla	2.96	3.02	3.10	2.88	2.99	a	1.66
	12	Casuarina	2.9	---	3.2	2.5	2.87	b	
		Grandis	5.9	6.4	5.7	5.7	5.9	a	
		Gra/unf	3.6	1.9	---	1.1	2.2	b	
		Mangium	2.6	2.4	2.3	2.3	2.4	b	
		Mearnsii	4.0	4.6	5.6	6.3	5.1	a	
		Urophylla	5.9	5.9	5.6	5.8	5.8	a	4.1
	18	Casuarina	4.4	---	3.9	4.2	4.2	c	
		Grandis	8.5	7.8	8.6	8.5	8.4	a	
		Gra/unf	2.8	2.3	---	1.5	2.2	d	
		Mangium	4.0	4.1	4.2	4.4	4.2	c	
		Mearnsii	5.0	5.8	7.3	7.4	6.4	b	
		Urophyll	8.2	7.6	7.8	8.0	7.9	a	5.5
	24	Casuarina	3.7	5.8	5.2	5.4	5.03	d	
		Grandis	10.8	11.5	9.7	11.1	10.78	a	
		Gra/unf	4.9	6.1	---	4.5	5.17	cd	
		Mangium	6.5	6.3	6.6	6.5	6.48	bc	
		Mearnsii	8.8	6.7	8.6	6.1	7.55	b	
		Urophylla	9.8	10.1	10.5	10.0	10.10	a	8.1

Data	Age mos.	Species	Data from Replication: I	II	III	IV	AVG	Range Test	AVG of AVGS
Dia.	12	Casuarina	2.2	---	1.7	1.2	1.7	b	
		Grandis	4.2	4.1	3.9	4.2	4.1	a	
		Gra/unf	2.5	1.1	---	---	1.8	b	
		Mangium	2.2	2.1	1.6	1.8	1.9	b	
		Mearnsii	3.8	3.2	4.2	4.6	4.0	a	
		Urophylla	4.2	3.6	4.0	3.8	3.9	a	2.9
	18	Casuarina	2.5	---	3.0	2.7	2.7	c	
		Grandis	5.3	5.2	5.6	5	5.3	a	
		Gra/unf	1.4	1.1	---	0.8	1.1	d	
		Mangium	3.8	4.0	3.9	3.9	3.9	b	
		Mearnsii	5.6	4.2	5.7	4.7	4.9	a	
		Urophylla	5.1	5.2	5.0	5.0	5.1	a	3.8
	24	Casuarina	1.9	3.1	3.7	4.2	3.2	cd	
		Grandis	6.7	6.7	7.1	5.9	6.6	a	
		Gra/unf	2.0	3.2	---	2.1	2.4	cd	
		Mangium	5.3	6.3	4.8	5.2	5.4	ab	
		Mearnsii	6.4	4.7	5.8	4.8	5.4	ab	
		Urophylla	6.7	6.3	6.1	5.9	6.3	a	4.9

Appendix Table 6. Mtn. View weather data

	Temp max	Temp min	Temp mean	Rain fall	Solar radiation
	-C-			-mm-	cal/cm^2/day
JUN 86			24.2	255.02	367.9
JUL 86			24.8	353.57	430.6
AUG 86			25.1	400.05	360.0
SEP 86			25.3	294.39	310.4
OCT 86			25.1	337.31	302.8
NOV 86			23.8	442.21	195.1
DEC 86			23.1	435.86	264.3
AVG			24.5	359.77	306.8
JAN 87					244.1
FEB 87					295.5
MAR 87					336.5
APR 87					305.7
MAY 87					270.0
JUN 87					338.1
JUL 87					411.4
AUG 87					455.3
SEP 87					284.4
OCT 87					245.8
NOV 87					220.7
DEC 87					180.4
AVG					299.0
JAN 88					199.2
FEB 88					
MAR 88					
APR 88					
MAY 88					326.6
JUN 88					403.4
AVG					309.7

Appendix Table 7. Honokaa weather data

	Temp max	Temp min	Temp mean	Rain fall	Solar radiation
	-C-			-mm-	cal/cm^2/d
FEB 87	25.6	17.2	21.4	175.3	273.2
MAR 87	25.0	17.8	21.5	71.12	286.3
APR 87	25.6	18.3	21.8	378.5	209.4
MAY 87	26.1	18.3	22.2	317.5	237.1
JUN 87	26.7	20.0	23.2	214.4	266.5
JUL 87	27.2	21.1	24.2	157.5	374.5
AUG 87	28.9	21.1	25.1	20.32	403.6
SEP 87	30.0	22.2	26.2	101.6	294.4
OCT 87	28.9	21.7	25.4	160.0	386.0
NOV 87	27.8	20.0	24.0	353.1	397.3
DEC 87	27.2	20.0	23.6	147.3	151.4
AVG	27.2	19.8	23.5	190.6	290.8
JAN 88	26.1	18.9	22.5	456.7	
FEB 88	26.7	18.9	22.8	87.12	
MAR 88	26.7	18.9	22.7	88.65	
APR 88	26.7	18.9	22.7	156.0	
MAY 88	27.2	20.6	23.7	63.75	351
JUN 88	27.8	20.6	24.1	29.72	
JUL 88	27.8	20.6	24.1	82.55	310
AUG 88	28.4	21.7	24.2	95.50	495
SEP 88	28.9	20.6	24.9	60.96	419
OCT 88	29.5	21.1	25.2	139.7	362
NOV 88	27.2	20.6	24.1	106.7	282
DEC 88	27.2	19.5	23.5	167.6	300
AVG	27.6	20.2	23.8	98.02	360
JAN 89	25.6	18.9	22.4	173.7	310.3
FEB 89	26.1	18.3	22.3	177.8	296.2
AVG	25.9	18.6	22.3	175.8	303.25

Appendix Table 8. Puunene weather data

	Temp			Rain	Solar
	max	min	mean	fall	radiation
		-C-		-mm-	cal/cm^2/day
AUG 86			29.9	6.858	590.3
SEP 86			30.1	5.842	542.6
OCT 86			29.4	18.54	467.5
NOV 86			27.8	55.63	403.1
DEC 86			26.2	57.4	354.9
AVG			28.7	28.85	471.7
JAN 87	27.0	16.6	21.8	75.95	352.6
FEB 87	25.5	15.3	20.4	45.72	393.6
MAR 87	27.6	15.9	21.7	12.95	483.1
APR 87	27.7	16.4	22.1	102.9	447.3
MAY 87	26.0	17.1	21.5	100.6	443.1
JUN 87	28.5	17.2	22.9	0	
JUL 87	29.2	18.3	23.8	63.25	475.4
AUG 87	29.6	17.7	23.7	3.302	460.0
SEP 87	23.8	13.2	18.5	32.00	400.5
OCT 87	27.7	16.4	22.0	0.508	354.6
NOV 87	27.7	18.1	22.9	65.02	390.8
DEC 87	26.1	18.7	22.4	139.4	267.6
AVG	27.2	16.5	21.9	641.6	406.2
JAN 88	25.4	17.1	21.2	204.0	344.2
FEB 88	25.0	16.0	21.0	19.05	277.3
MAR 88	29.2	18.6	23.9	22.86	
APR 88	27.3	17.0	22.1	30.23	
MAY 88	28.7	17.6	23.2	0	
JUN 88	30.4	18.0	24.2	0	
JUL 88	28.6	16.7	22.6	0	
AUG 88	28.7	16.6	22.6	3.556	
AVG	27.9	17.2	22.6	34.96	310.6

Appendix Table 9. Hoolehua weather data

	Temp max	Temp min -C-	Temp mean	Rain fall -mm-	Solar radiation cal/cm^2/day
SEP 86	30.9	21.5	26.2	21.59	
OCT 86	30.0	21.5	25.7	46.99	
NOV 86	28.6	20.1	24.4	15.49	
DEC 86	26.4	17.8	22.2	53.34	
AVG	29.0	20.2	24.6	34.35	
JAN 87	24.7	16.5	20.6	55.63	
FEB 87	23.9	14.6	19.2	130.6	
MAR 87	25.9	21.5	20.5	22.86	
APR 87				102.4	
MAY 87				73.66	
JUN 87				9.144	
JUL 87				6.858	
AUG 87				3.302	
SEP 87				59.69	
OCT 87				7.366	
NOV 87				45.97	
DEC 87				278.6	
AVG				66.34	
JAN 88				106.2	
FEB 88				24.64	
MAR 88				43.43	
APR 88				17.02	
MAY 88				6.858	
JUN 88				2.79	
JUL 88				8.636	
AUG 88				13.72	
SEP 88					
AVG				27.91	

Appendix Table 10. Kilohana weather data

	Temp max	Temp min -C-	Temp mean	Rain fall -mm-	Solar radiation cal/cm^2/day
JUN 86	26.9	20.9	23.9	189.0	367.3
JUL 86	27.5	21.8	24.7	276.4	340.5
AUG 86	28.1	21.1	24.6	289.8	331.1
SEP 86	28.5	20.1	24.3	240.8	296.6
OCT 86	28.1	21.4	24.7	147.3	277.4
NOV 86	27.5	19.2	23.4	311.1	216.9
DEC 86	25.3	16.1	20.7	166.9	
AVG	27.4	20.1	23.7	231.6	304.9
JAN 87	23.7	16.7	20.2	44.45	260.5
FEB 87	24.5	16.8	20.7	104.9	304.9
MAR 87	24.6	17.5	21.0	84.33	317.5
APR 87	23.6	17.5	20.5	242.6	273.6
MAY 87	24.1	17.1	20.6	216.7	299.8
JUN 87	26.0	19.2	22.6	170.7	350.6
JUL 87	27.0	21.2	24.1	275.3	335.4
AUG 87	27.9	21.7	24.8	196.3	355.5
SEP 87	27.6	21.6	24.6	224.3	
OCT 87	26.7	21.4	24.0	299.7	228.6
NOV 87	25.4	20.5	22.9	355.3	225.8
DEC 87	23.0	19.6	21.3	711.5	194.6
AVG	25.3	19.2	22.2	2926	286.0
JAN 88	24.6	19.7	22.2	341.4	221.2
FEB 88	26.6	21.7	24.2	174.2	262.2
MAR 88	27.4	21.2	24.3	302.3	280.9
APR 88	27.9	21.8	24.8	170.4	271.7
MAY 88	27.1	21.6	24.4	342.9	227.2
JUN 88	26.6	21.7	24.2	87.12	295.9
AVG	26.7	21.3	24.0	236.4	259.8

Appendix 11. Illustrative Costs and Calculations for woodchip production

---

Item

Site preparation per hectare per 2 year rotation

1.Rental of Machinery $75.00 per/hr X 3hrs = $225.00

2.Cost of seedling $0.10 x 10,000 = $1000.00

3.Planting Labor: $8.00 per/hr X 40hrs = $320.00

Fertilization:

4.(N)16-(P)16-(K)16: $0.385 per kg x 1500kg per rotation = $577.50

5.Fertilizer application labor: $8.00 per/hr X 8 hrs per application X 3 applications per rotation = $192.00

Weed control:

6.Glyphosate (Roundup) per liter:$25.00 X 2.5 liter x 1 application = $62.50

7.Fluazifop-P (fusilade) per liter:$70.00

8.Oxyflurfen (Goal) per liter:$15.00

9.Weed control application labor: $8.00 per/hr X 8hrs/application X 3 applications per rotation = $192.00

10.Harvest Cost per wet ton = $9.00

11.Transportation Cost per green ton per 20 mile trip = $8.00

12.Predicted yield Eucalyptus harvest ha/rotation with estimated loss of 15 percent:

12.1 Energy (Total biomass utilization) ha/59.5 B.D.T

12.2 Pulp (Tree stem only utilization) ha/51 B.D.T

Appendix 12. Illustrative NPV calculations assuming $100.00 per BDT for pulp woodchips

---

$$\text{at 5\% NPV} = \frac{373.25}{(1+.05)} + \frac{373.25}{(1+.05)^2} = 355.48 + 338.55 = \$694.03$$

$$\text{at 10\% NPV} = \frac{373.25}{(1+.10)} + \frac{373.25}{(1+.10)^2} = 339.32 + 308.47 = \$647.79$$

$$\text{at 15\% NPV} = \frac{373.25}{(1+.15)} + \frac{373.25}{(1+.15)^2} = 324.23 + 282.23 = \$606.79$$

Appendix D

Fundamental Solvolysis Research

Productive and Parasitic Pathways in Dilute Acid-Catalyzed Hydrolysis of Cellulose

William Shu-Lai Mok and Michael Jerry Antal, Jr.
Department of Mechanical Engineering and the
Hawaii Natural Energy Institute
University of Hawaii at Manoa
Honolulu, Hawaii 96822

and

Gabor Varhegyi
Research Laboratory for Inorganic Chemistry
Hungarian Academy of Sciences
Budapest, Hungary

ABSTRACT

Cellulose hydrolysis experiments were conducted in a percolating reactor at 34.5MPa. A glucose yield of 71% of the theoretical maximum was obtained at 215°C with 0.05% by weight of sulfuric acid in the percolating solution. The classical model of glucose formation from cellulose followed by secondary sugar degradation did not describe the reaction chemistry under these conditions. A parasitic pathway which leads to the formation of non-hydrolyzable oligomer was discovered in the absence of acid. In the presence of acid, kinetic modelling of the measured, temperature dependent rates of glucose evolution indicates that an acid-catalyzed parasitic pathway operates in competition with the glucose production pathway. No chemical changes were detected in the solid phase during the course of reaction.

INTRODUCTION

Although the acid-catalyzed hydrolysis of cellulosic materials was industrialized almost a century ago (Harris, 1949), the underlying chemistry is still a focus of research interest today. Three approaches characterize the state-of-the-art technology. Dilute acid hydrolysis processes employ flow reactors which only accept a finely ground feedstock. Typical glucose yields of about 55% can be achieved with acid concentrations below 3% and a residence time of a few seconds (Thompson and Grethlein, 1979; Church and Wooldridge, 1981; Brenner and Rugg, 1981). Somewhat higher yields are obtained with percolator reactors at the cost of reduced reaction rates, batch operation, and the dilution of sugar products (Faith, 1945; Harris and Beglinger, 1946; Gilbert et al., 1952). Finally, low temperature, concentrated acid processes are sometimes employed (Moore and Barrier, 1987; Dunning and Lathrop, 1945). In most cases, the yield of glucose is considerably less than 100%. The goal of this research was to elucidate the underlying chemistry which limits the yield of glucose from cellulose.

The classical explanation for the low yield of glucose was first enunciated by Saeman (1945), and employed more recently by McParland et al. (1982) and Conner et al. (1985). It posits the role of secondary degradation reactions in reducing the yield of glucose as the sole primary product of cellulose hydrolysis: cellulose -> glucose -> degradation products. Contradicting this classical picture, important recent work by Abatzoglou et al.

(1986) has shown that the initial products of cellulose hydrolysis are primarily soluble oligosaccharides. Moreover, in the presence of 40mM H_2SO_4 at 190°C, Bouchard et al. (1989) detected very significant alterations in the chemical structure of the unconverted "cellulose" after 30 min at reaction conditions. However, Bouchard et al. (1989) did not actually measure the rate of glucose formation from cellulose; consequently they could not employ the powerful tools of kinetic analysis to scrutinize the chemistry. Also, they did not examine the hydrolyzability of the soluble oligosaccharides, which are important contributors to the ultimate yield of glucose. Finally, screening studies led us to emphasize considerably lower acid concentrations (5mM) and a somewhat higher temperature (215°C) than they employed in their work. Our results thus complement theirs, and together they offer considerable insight into the limitations of high temperature, dilute acid hydrolysis of cellulose as a source of glucose.

EXPERIMENTAL APPARATUS AND PROCEDURES

Acid-catalyzed hydrolysis experiments were conducted in a semi-batch flow reactor described in a preliminary report of this work (Mok and Antal, 1989). Further details of the reactor system design can be found in Antal et el. (1990a). A HPLC pump delivered solvent (water/acid) first into an annular preheater, composed of an outer 6.4mm OD x 4.6mm ID tube, and an inner tube of 1.6mm OD x 0.76mm ID, both fabricated from Hastelloy C-276 tubing. This material was chosen because of its strength at elevated

temperatures, corrosion resistance, and commercial availability. In the annular section, the solvent was heated to the desired solvolysis temperature by two independently controlled electric heaters. The inner tube accommodated a fixed thermocouple located immediately before the flow entered the solid phase reactor. This thermocouple measured the final fluid temperature. Solid samples were held in a 7.6cm section (same diameter as the outer tube of the heat up section) capped at both ends with 10 μ Hastelloy frits. A secondary reaction chamber, with variable volume to control the liquid phase residence time, was installed after the solid phase reactor. The effluent exiting the reactor was quenched and directed to the sampling system. For some experiments, the secondary reaction chamber was removed to minimize liquid phase reactions.

Two modes of sampling were employed. In the differential mode, samples of the effluent were withdrawn as the reaction progressed using a 10 port sampling valve, which contains two 1 mL sampling loops. At any moment, a 1 mL sample of the effluent was trapped in one loop while the product stream flowed through the other. The minimal sampling interval is the time required for the effluent to completely flush at least twice the loop volume. Employing the differential sampling mode, rates of product formation as a function of time were measured. To determine more accurately the glucose yield and obtain mass balances, the integral collection method was used during some of the experiments. Under this scheme, the entire effluent stream was collected in a product

accumulator for analysis.

The experimental procedure begins with loading a known weight of sample into the solid phase section. The various sections of the reactor are then assembled and flushed with water to remove air. After the proper flow and pressure are obtained, heat is applied. Control experiments showed that a negligible amount of reaction occurs during the heat up stage (about 10 minutes), when no acid is present. After the operating temperature is reached, the pump is switched to feed the acid solution, which is premixed to the desired operating strength. The instant at which the switching occurs is defined to be time "zero". When the differential mode is employed, the first sample is taken at this time. At the end of an experiment, the flow is again switched back to pure water, and heat is shut off. After the system returns to room temperature, the reactor is depressurized and the amount of solid residue washed, dried, and weighted.

The liquid products were analyzed by HPLC using polymeric cation exchange columns in either the Pb^+ or H^+ form. For some experiments, an additional post-hydrolysis (described later) was applied to the effluent to analyze the oligomeric products. The solid residue was quantitatively saccharified (described later) to determine its glucose content.

Whatman #1 and #42 filter papers were used as the sample material. The moisture content of the samples was determined by drying at 105°C until constant weight was obtained. The ash contents of the two filter papers were determined by the

manufacturer. The glucose contents of the sample and reaction residues were measured by the method adopted by the Forest Product Laboratory (Saeman et al., 1945; Moore and Johnson, 1967), with slight modification. Approximately 0.01g of the sample was placed in a 30mL glass vial, and about 1 cc of 72% sulfuric acid was added. The vial was then heated at 30°C (±1°C) in a water bath with frequent stirring for 1 hour. Water was then added to the bottle until a 4% acid solution was obtained. The vial was then loosely capped and placed inside a pressure vessel, which was subsequently charged with argon to 0.3MPa. The pressure vessel was then heated in an oil bath maintained at 120°C (±3°C). Approximately 90 minutes was required before the center of the vessel reached the temperature of the bath. Afterwards, the vessel was kept for another 60 minutes at 120°C and quenched with cold water. The solution was re-weighted to determine the loss due to evaporation (typically about 0.1% of the weight of solution). The concentration of the sugar in solution was measured by HPLC, and corrected by dilution factors to determine the sugar content on a dry sample basis. When this procedure was applied to Avicel PH105 cellulose, 106% by weight of the original dry sample was obtained. Since this is 96% of the theoretical maximum, a correction factor (commonly used to compensate for sugar decomposition) of 1.04 was applied to subsequent sample analyses.

The post hydrolysis procedure, which was used to analyze the oligomeric reaction products, follows the second half of the quantitative saccharification procedure, beginning with the

preparation of 4% acid solution from the reactor effluent.

The values of moisture, ash and glucose contents of the two cellulose substrates are tabulated in Table I. All subsequent data concerning glucose yield are referenced to the glucose content of the starting material given in Table I, while the yields of other products are reported on a sample dry weight basis. The sample size for the experiments was about 0.35g. Experiments were conducted at 34.5MPa, the upper pressure limit of the reactor.

Thermogravimetric studies were executed using a Perkin-Elmer TGS-2/System 4 thermobalance. Samples weighing about 2mg were housed in an open platinum crucible purged continuously with high purity dry argon (140mL/min), and heated linearly at 10°C/min from 25 to 750°C. FTIR spectra were taken by a Perkin-Elmer Model 1710 instrument using a DTGS detector, and a Perkin-Elmer DRIFT accessory with microsampling. The original sample was measured as is in paper form, while partially hydrolyzed samples were ground to powders (and analyzed without dilution by KBr). All spectra were analyzed from 4000 to 450 cm^{-1} with 50 scans at 2 cm^{-1} resolution.

RESULTS AND DISCUSSION

SCREENING STUDIES. Several series of exploratory experiments were run to determine the experimental conditions which resulted in favorable glucose yields. Whatman #1 paper was used in these experiments, which employed the differential sampling mode and a 1mL secondary reaction chamber. Since it was not feasible at this early stage to carry each experiment to completion (because the

reaction rate at the lower temperatures was very slow), the experiments were all terminated after one hour. Consequently, the final glucose yield was not measured directly. Instead, the best-fitting exponential decay curve (more discussion of this curve later) for each experiment was used to project the rate of glucose production, and by integration obtain a projected final glucose yield. Accurate final yields were obtained later from integral experiments which carry the reaction to completion.

The first series of experiments was conducted to study the effect of temperature. A 2mL/min flow of 5mM (at NTP, <0.05% by weight) H_2SO_4 solution was used. The yield of 5-hydroxy-methyl-furfural (HMF), the major decomposition product of glucose, was always less than 10%, and less then 5% below 220°C. Levoglucosan and cellobiose were also detected at low levels (<5%). The solid residues at lower temperatures were white, retaining the shape of the original sample. At higher temperatures, the residues resembled a mixture of char and ash. Plots of the rate of glucose formation vs. time are shown in Figure 1. The 5 to 10 minute delay before the sudden onset of glucose formation reflects the transit time for the acid to travel from the pump to the solid sample, and the products to reach the sampling system. As expected, increasing temperature increases the rate of glucose formation. A sudden change in the reaction behavior can be observed when the temperature was increased from 212 to 215°C. This discontinuity may be explained by physical changes in the solid sample matrix, rendering the material more accessible to acid. Similar plots for

a second series of experiments, employing a 4mL/min flow, are shown in Figure 2. No obvious discontinuity as a function of temperature was observed. The initial delay was noticeably shortened as a result of the increased flow.

The projected glucose yields from the first two series of experiments are shown in Figure 3. A temperature range of 212-215°C resulted in favorable glucose yields. Increased yields were consistently observed when a higher percolating flow was employed.

The effect of acid concentrations at two selected temperatures and flows can be seen in Figure 4. Increased concentration of acid decreased the glucose yield.

In the third series of experiments, the liquid phase reaction volume was varied to seek further improvements in sugar yields. The classical reaction model discussed earlier (Saeman, 1945) implies that the glucose yield should increase when the liquid phase reaction volume is reduced to shorten the time available for the secondary, liquid phase degradation reactions. However, results contrary to expectation were obtained, as shown in Figure 5. At 225°C a reduction in the liquid phase reaction volume from 1mL to 0.6 and 0.2mL reduced the projected yield of glucose, instead of increasing it! To explain this negative result, we speculated that cellulose produces significant amounts of soluble intermediate oligomers, which further hydrolyze in the liquid phase to produce glucose. In this scenario, sufficient time in the liquid phase must be provided to permit complete hydrolysis of oligomer. Two sets of experiments were then performed to study the

effect of increased reaction volume, and the results are also displayed in Figure 5. Small but significant increases in the glucose yield were observed with increasing liquid phase residence time at both 200 and 215°C. This data supports the findings of Abatzoglou et al. (1986) concerning the formation of soluble oligomer. Furthermore, since short residence time is not advantageous, we infer that the increased yield obtained with a higher flow probably results from the more rapid removal of soluble products from the solid matrix, which helps to suppress parasitic reactions.

CHARACTERIZATION OF REACTION PATHWAYS. Results of the screening studies indicated that favorable sugar yields can be obtained at around 215°C, employing a high percolating flow of weak (5mM or less at NTP) acid and allowing sufficient liquid phase reaction time for complete hydrolysis of oligomeric intermediates. To gain further insight into the various parasitic pathways and to accurately measure the true glucose yield, two series of experiments were executed using the integral sampling method. In the first series, a long (4mL) secondary reaction chamber was installed to ensure complete hydrolysis of the intermediate oligomer. In the second series, the secondary chamber was completely removed to minimize secondary, liquid phase decomposition; while post hydrolysis (discussed earlier) was applied to the effluent to ensure complete hydrolysis of oligomer. Whatman paper #42 was used in these experiments. The reaction time was varied from 20 min to 120 min (required for complete

solubilization of the solid sample) at 215°C with 4mL/min flow of 5mM acid.

Results of these experiments are displayed in Figure 6. Looking at the three different determinations of the glucose yield, it can be seen that the results from the two types of experiments (with a 4mL secondary reaction chamber or with post hydrolysis) are essentially the same, and that the measured glucose yields enjoy good agreement with the yields obtained by integrating the differential sampling data obtained earlier. The final maximum glucose yield was about 70% of the sugar content. The data in Figure 6 also suggest that the sugar content of the unreacted sample, and the relative glucose yield (weight of glucose / sugar content of solubilized fraction of the sample) remains fairly constant during the course of the reaction. This result implies that no significant parasitic reaction occurred in the solid phase which rendered the sample less hydrolyzable.

To search for some indication of the solid phase degradation reactions detected by Bouchard et al. (1989), Thermogravimetry Mass Spectrometry (TG-MS) (Varhegyi et al., 1988) was used to analyze the original sample and two partially hydrolyzed samples (44% and 69% weight loss) at 210°C with 5mM acid. The samples evidenced very similar DTG behavior (see Figure 7). The shift to a lower decomposition temperature exhibited by the partially hydrolyzed samples may be explained by changes in the macro-molecular structure, perhaps a loss of crystallinity. No significant difference in the gaseous product composition was observed. The

residual char yields in these experiments were less than 10% at 500°C, which is typical for cellulose. These results are dramatically different than those of Bouchard et al. (1989), who reported char yield as large as 35% from their partially hydrolyzed cellulosic residuals after oxidative thermogravimetric analysis (TGA) in air at 10°C/min to 500°C. In our experience, oxidative TGA of cellulose leaves negligible char at 500°C. Certainly, the residuals they examined by TGA did not evidence cellulosic behavior.

Comparative analysis by FTIR revealed no major changes in the chemical structure of the solid as reaction progressed from 0 to 80% conversion (see Figure 8). Minor differences in the spectra were attributed to differences in the degree of hydrogen bonding. Although Bouchard et al. (1989) concluded that major structural changes occur in the solid residue as hydrolysis progresses, their FTIR data indicated major changes only in the case of low temperature strong acid hydrolysis process. The changes occurring during the high temperature, dilute acid process were comparatively minor. Moreover, their dilute acid process employed 40mM of sulfuric acid, which catalyzes char formation (Antal et al., 1990b). Our minimal use of sulfuric acid (5mM) may have helped to avoid acid- catalyzed parasitic reactions in the solid phase.

To verify the effect of acid concentration, four experiments were conducted, each at 215°C with a 4mL/min flow, and sufficient reaction time to ensure reaction completion. The results, shown in Table II, confirm that 5mM acid is close to optimal. Stronger acid

leads to increased formation of glucose decomposition products (e.g. HMF).

The foregoing results led us to conclude that neither a chemical alteration in the unhydrolyzed cellulosic residue, nor secondary acid-catalyzed degradation reactions of the glucose limited the yield of glucose achieved at 215°C with 5mM acid. These findings prompted us to examine the nature of the soluble oligomers born by the hydrolysis reactions. Since it was not possible to dry down the acidic effluent to measure its solute content, an experiment was conducted without acid at 215°C with a 4mL/min flow. Due to the slow rate of reaction, it was not feasible to carry the reaction to completion. After 7.5 hours, the amount of soluble products (obtained by drying the effluent) was 64% by weight of the dry sample, while the amount of solid residue was 42%. The mass balance exceeds 100% due to hydrolytic addition of water. The glucose content of the effluent was 14% of the initial cellulose, and 36% after post-hydrolysis of the effluent. This data clearly shows the presence of a pathway leading to solubilized products which cannot be hydrolyzed to glucose. The sugar content of the residue was 100%, again suggesting only minimal change in the solid phase.

The primary objective of this research was to gain insight into the reaction pathways which influence sugar formation; consequently conditions were employed which offered sugar concentrations in the effluent of less than 0.07% by weight. This concentration can be improved by increasing acid concentration;

thereby reducing the time of reaction and reducing the amount of percolating flow. An experiment was performed with 0.38g of sample and 0.5mL/min flow of 20mM acid, resulting in a reaction time of 30min. The glucose yield was 44% by weight of the dry sample, giving an overall effluent glucose concentration of 1.1%. Additional increases may be possible by improving sample loading, and applying stirring to overcome mass diffusion problems associated with a low flow. Furthermore, since glucose decomposition is not severe at 215°C, it may be possible to recirculate the effluent to obtain even higher concentration of sugar in the final product solution.

KINETIC MODELING. As we noted earlier, the rate curves obtained from the differential sampling experiments can be described by exponential curves. Several different mechanisms can lead to exponential curves under the applied experimental conditions. One of them is the commonly assumed model for hydrolysis, which involves two consecutive first order reactions:

Cellulose —> glucose —> decomposition products (1)

In this mechanism, the fraction of cellulose not reacted at time t is:

$$c(t) = \exp(-k_{hydr} (t-t_0)) \qquad (2)$$

Keeping in mind that the glucose decomposition takes place only during a fixed liquid phase residence time τ, we find:

$$dg/dt = k_{hydr} \exp(-k_{hydr}(t-t_0)) * \exp(-k_{decomp} \tau) \qquad (3)$$

where g(t) is the amount of glucose formed at time t, normalized by the initial sample mass of cellulose, and k_{hydr} and k_{decomp} are the

rate constants of the cellulose hydrolysis and glucose decomposition at a given acid concentration.

Another possible mechanism involves two competing reactions, one of which leads to glucose and the other to some non-hydrolyzable by-products. Denoting the two rate constants respectively by k_1 and k_2, we have:

$$-dc/dt = (k_1+k_2)\ c \qquad (4)$$

$$dg/dt = k_1\ c \qquad (5)$$

Solving (4) and (5) for dg/dt gives:

$$dg/dt = k_1\ \exp(-(k1+k2)(t-t_0)) \qquad (6)$$

From a mathematical point of view, equations (3) and (6) are equivalent exponential curves having the form:

$$dg/dt = a\ \exp(\ -b\ (t-t_0)\ ) = a'\ \exp\ (\ -bt\ ) \qquad (7)$$

The difference between the two models lies only in the interpretation of the two constants, a and b. Note, that t_0 is also unknown since the reactions do not start at a well defined point of time (see Figures 1 and 2). Since equation (7) is obviously not valid during the transition period, t_0 can be chosen in such a way that the measured formation of glucose $[g^{obs}(t)]$ would be equal to the g(t) value calculated from equation (7) at some arbitrary time t_1 shortly after the transition period.

The calculation of the unknown parameters was carried out by the method of least squares. Plots of the logarithm of the rate constants versus 1/T are shown in Figures 9 and 10. Figure 9 indicates that k_{decomp} is very insensitive to temperature. This suggests that the model defined by equations (1)-(3) does not

apply. On the other hand, Figure 10 shows reasonable temperature dependence: the corresponding activation energies are 144 and 100 kJ/mol for k_1 and k_2, respectively. This observation supports the validity of equations (4) and (5) in accordance with the chemical evidence for competing parasitic reactions discussed earlier. The influence of acid on k_1 and k_2 is shown in Figure 11. Both k_1 and k_2 display a saturation type dependence on acid concentration.

Finally we wish to note that a simple scheme of two competing pathways cannot fully describe the complex set of reactions taking place. However, the experimental curves do not permit the determination of more then two parameters for each curve. Since the amount of decomposition products is small, equations (4)-(6) provide a reasonable approximation for the experimental results.

CONCLUSIONS

Throughout this study, insights concerning the chemical pathways of hydrolysis were gathered. We summarize them here and present an overall reaction model.

- The classical model of two sequential reactions does not adequately describe cellulose hydrolysis at temperatures below 220°C.
- Glucose is formed via an oligomeric intermediate. Glucose may also be formed directly from the solid phase, but our studies have revealed no evidence to support this speculation.
- Quantitative saccharification of the residue indicates little chemical change occurring in the solid phase during hydrolysis

at 215°C in the presence of 5mM acid.

- Neither TG-MS nor FTIR analysis of the cellulosic residue indicate any significant difference between it and pure cellulose.
- There exists a competing pathway (observed in a non-acid catalyzed hydrolysis experiment) which solubilizes cellulose to unknown products that cannot be hydrolyzed to glucose. This could be a major cause for the imperfect glucose yield at low (<220°) temperatures in the presence of acid.
- Kinetics analysis suggests that there exists a acid-catalyzed parasitic pathway which competes with the acid-catalyzed hydrolysis pathway and is the major cause for the imperfect glucose yield at low (<220°C) temperatures.

While we have not established whether the two parasitic pathways are in fact the same, the reaction network of Figure 12 is consistent with all our observations. Our other findings include:

- A good glucose yield of 70% can be obtained by dilute acid hydrolysis. This yield is comparable to conventional percolating reactors, although a much lower concentration of acid (0.05% by weight) in the solvent is required.
- The best glucose yield is obtained at 215°C. Increasing temperature initially favors glucose formation, but glucose decomposition becomes significant above 220°C.
- The glucose concentration in the effluent can be increased at the expense of yield, by increasing acid concentration to reduce reaction time, and by lowering the percolating flow.

ACKNOWLEDGEMENTS

This work was supported by the Solar Energy Research Institute (subcontract no. XK-8-18000-1) and the Coral Industries Endowment. Dr. Borbala Zelei and Dr. Piroska Szabo (Research Laboratory for Inorganic Chemistry, Hungarian Academy of Sciences) performed the FTIR and TG-MS analyses of the hydrolysis residue. The authors wish to thank Dr. Ralph Overend (SERI) and Dr. E. Chornet (University of Sherbrooke) for insightful discussions, Dr. Victor Philips (UH) for administrative support, and Ben Respicio (UH) for assistance in reactor fabrication.

REFERENCES

Abatzoglou, N.; Bouchard, J.; Chornet, E. Dilute Acid Depolymerization of Cellulose in Aqueous Phase: Experimental Evidence of the Significant Presence of Soluble Oligomeric Intermediates. Can. J. of Chem. Engineering **1986**, 64, 781-786.

Antal, M.J.; Mok, W.S.; Richards, G.N. Mechanism of formation of 5-(hydroxymethyl)-2-furaldehyde from D-fructose and sucrose. Carbohy. Res., **1990**a, 91-109.

Antal, M.J.; Mok, W.S.; Varhegyi, G.; Szekely, T. Review of Methods for Improving the Yield of Charcoal from Biomass. Energy and Fuels, **1990**b, 4, 221-225.

Bouchard, J.; Abatzoglou, N.; Chornet, E.; Overend, R.P. Characterization of depolymerized cellulosic residues. Wood Science and Technology **1989**, 23, 343-355.

Brenner, W.; Rugg, B. High Temperature Dilute Acid Hydrolysis of Waste Cellulose: Batch and Continuous Processes. Report to the Environmental Protection Agency, report no. EPA/600/S2-85/137, **1985.**

Church, J.; Wooldridge, D. Continuous High-Solids Acid Hydrolysis of Biomass in a 1½-in. Plug Flow Reactor. Ind. Eng. Chem. Prod. Res. Dev. **1981,** 20(2), 371-378.

Conner, A.H.; Wood, B.F.; Hill, D.G.; Harris, J.F. Kinetic model for the dilute sulfuric acid saccharification of lignocellulose. J. Wood Chem. Technol. **1985**, 5, 461-489.

Dunning, J.W.; Lathrop, E.C. The saccharification of Agricultural Residues. Ind. Eng. Chem. **1945,** 37(1), 24-29.

Faith, W.L. Development of the Scholler Process in the United States. Ind. Eng. Chem **1945,** 37(1), 9-11.

Gilbert, N.; Hobbs, I.A.; Levine, J. Hydrolysis of Wood. Ind. Eng. Chem. **1952,** 44, 1712-1720.

Harris, Elwin E. Wood Saccharification. Advances in Carbohydrate Chemistry **1949**, 4, 153-188.

Harris, E.; Beglinger, E. Madison Wood Sugar Process. Ind. Eng. Chem **1946,** 38(9),890-895.

McParland, J.J.; Grethlein, H.E., Converse, A. O. Kinetics of Acid Hydrolysis of Corn Stover. Solar Energy **1982**, 28, 55-63.

Mok, W. W.; Antal, M.J. Dilute Acid Hydrolysis of Biopolymers in a Semi-Batch Flow Reactor At Supercritical Pressure. Proceedings

of the IGT Conference on Energy from Biomass and Wastes, New Orleans, 1989.

Moore, E.W.; Johnson, D.B. Procedures for the Chemical Analysis of Wood and Wood Products. Forest Products Laboratory, Forest Service, U. S. Dept. of Agriculture, 1967.

Moore, M.; Barrier, J. Ethanol from Cellulose Residues and Crops. Tennessee Valley Authority Report no. TVA/NFDC-89/4, **1987.**

Saeman, J.F.; Bubl, J.L.; Harris, E.E. Quantitative Saccharification of Wood and Cellulose. Ind. Eng. Chemistry, **1945**, 17(1), 35-37.

Saeman, J.F. Kinetics of Wood Saccharification Ind. Eng. Chem. **1945**, 37(1), 43-52.

Thompson, D.; Grethlein, H.E. Design and Evaluation of a Plug Flow Reactor for Acid Hydrolysis of Cellulose. Ind. Eng. Chem. Prod. Res. Dev. **1979,** 18(3), 166-169.

Varhegyi, G.; Antal, M.J.; Szekely, T.; Till, F.; Jakab, E. Simultaneous Thermogravimetric-Mass Spectrometric Studies of the Thermal Decomposition of Biopolymers. 1. Avicel Cellulose in the Presence and Absence of Catalysts. Energy & Fuels, **1988**, 2, 267-272.

Table I. Sample Characteristics

	Whatman Paper #1	Whatman Paper #42
Moisture Content (% wet basis)	4	4
Ash Content (% dry wt. basis)	0.06	0.01
Glucose Content (% dry wt. basis)	92	108

Table II. Effect of Acid Concentration on Glucose Yield. Experiments conducted using the integral collection method at 215°C and 34.5 MPa, with flow rate of 4mL/min until the reaction was complete.

Acid Conc. (mM at NTP)	Reaction Time (min)	Glucose Yield (%)	HMF Yield (%)
2	300	65	1
5	120	71	0
10	80	69	4
20	60	67	5

LIST OF FIGURES

1) Rate of glucose production vs. reaction time. Data obtained from differential sampling experiments conducted with a 2mL/min flow of 5mM acid (at NTP).

2) Rate of glucose production vs. reaction time. Data obtained from differential sampling experiments conducted with a 4mL/min flow of 5mM acid (at NTP).

3) Projected glucose yield vs. temperature, at various flow rates of 5mM acid.

4) Projected glucose yield vs. acid concentration at various temperature and flow rates.

5) Effect of secondary reaction volume on the projected glucose yield at various temperature and flow rates with 5mM acid.

6) Glucose yields from integral sampling experiments with either post-hydrolysis (□) or long secondary reaction chamber (○), compared with the integrated glucose yields from a differential sampling experiment (bold line). Also plotted are the glucose content of the solid residue and relative glucose yield (from all integral experiments) as a function of reaction time. Dotted lines are linear regression lines to show trend. Experiments carried out at 215°C with a 4mL/min flow of 5mM acid.

7) DTG behavior of an original sample of Whatman paper #42 (A) and partially hydrolyzed samples (B: 44% conversion after 30 min,; C: 69% conversion after 60 min.).

8) FTIR spectra of an original sample of Whatman paper #42 (A), and partially hydrolyzed samples (B: 44% conversion after 30 min.; C: 69% conversion after 60 min.; D: 80% conversion after 80 min.)

9) Arrhenius plots assuming a simple model of two sequential reactions: k_{hydr} leading to glucose formation followed by k_{decomp} leading to decomposition products.

10) Arrhenius plots assuming a simple model of two competitive reactions, k_1 leading to glucose and k_2 to non-hydrolyzable products.

11) Effect of acid concentration on the rate of reaction, assuming a simple model of two competitive reactions.

12) A proposed network of reactions governing cellulose hydrolysis based on the evidence collected in this study.

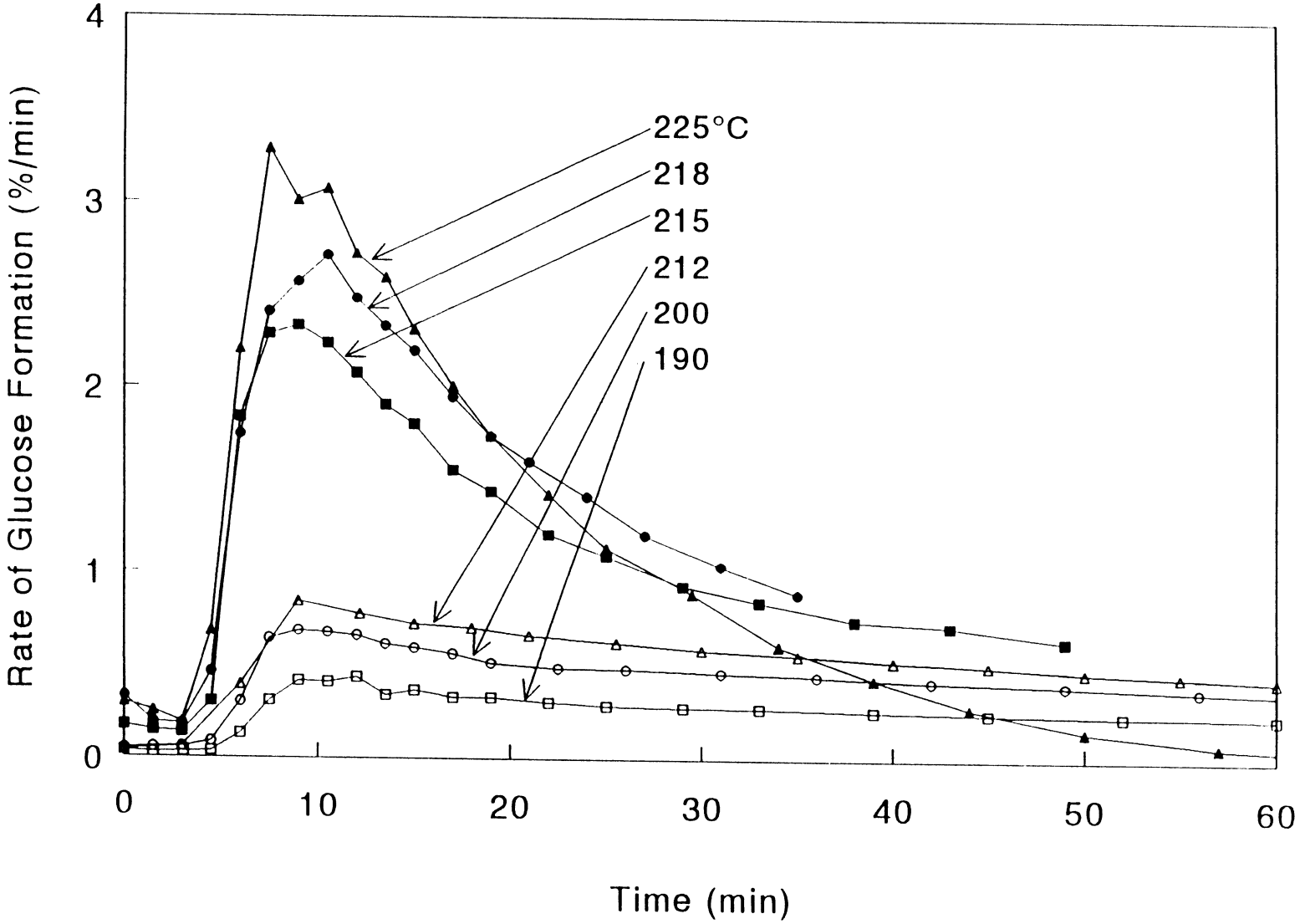

Figure 1. Rate of glucose production vs. reaction time. Data obtained from differential sampling experiments conducted with a 2mL/min flow of 5mM acid (at NTP).

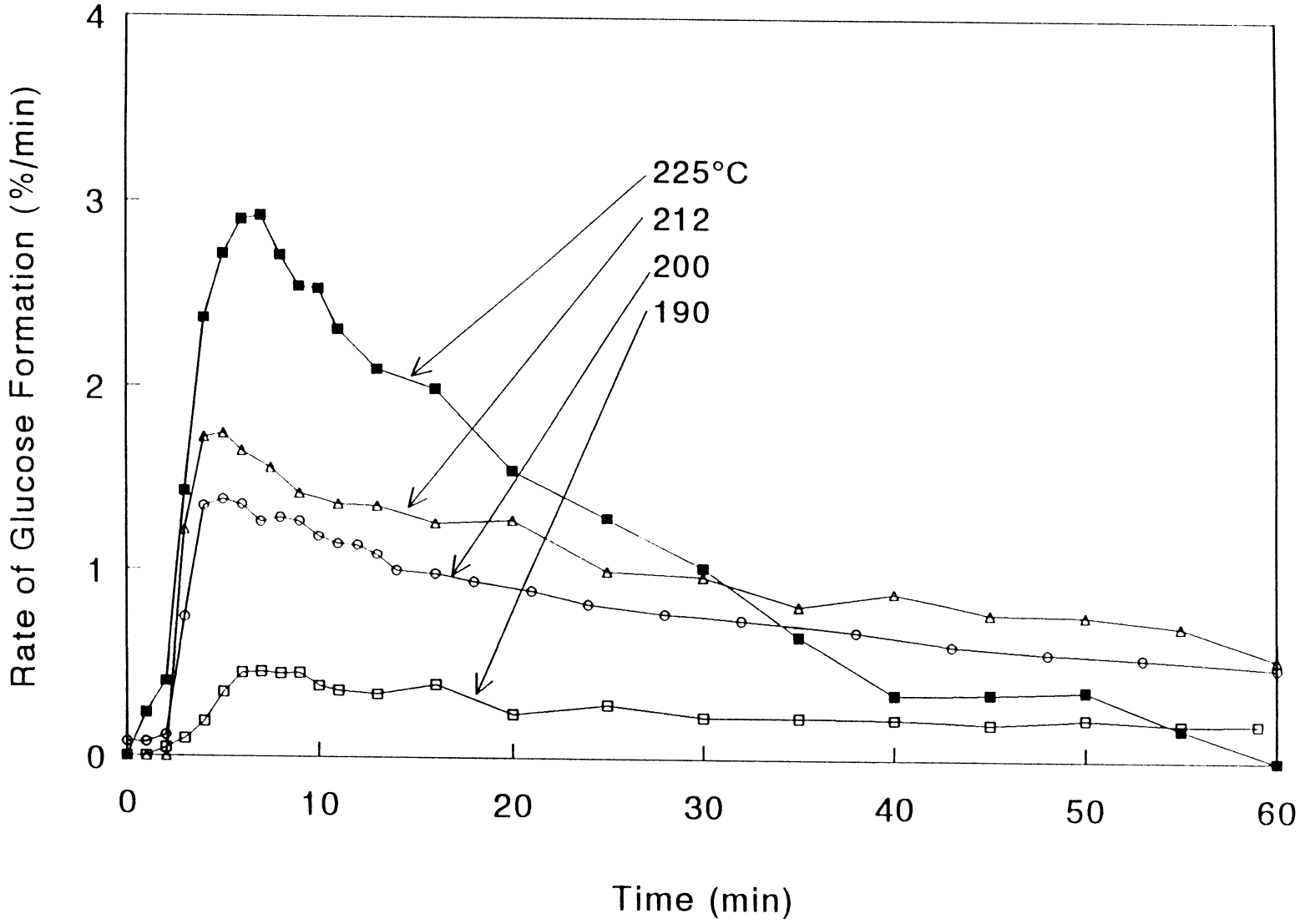

Figure 2. Rate of glucose production vs. reaction time. Data obtained from differential sampling experiments conducted with a 4mL/min flow of 5mM acid (at NTP).

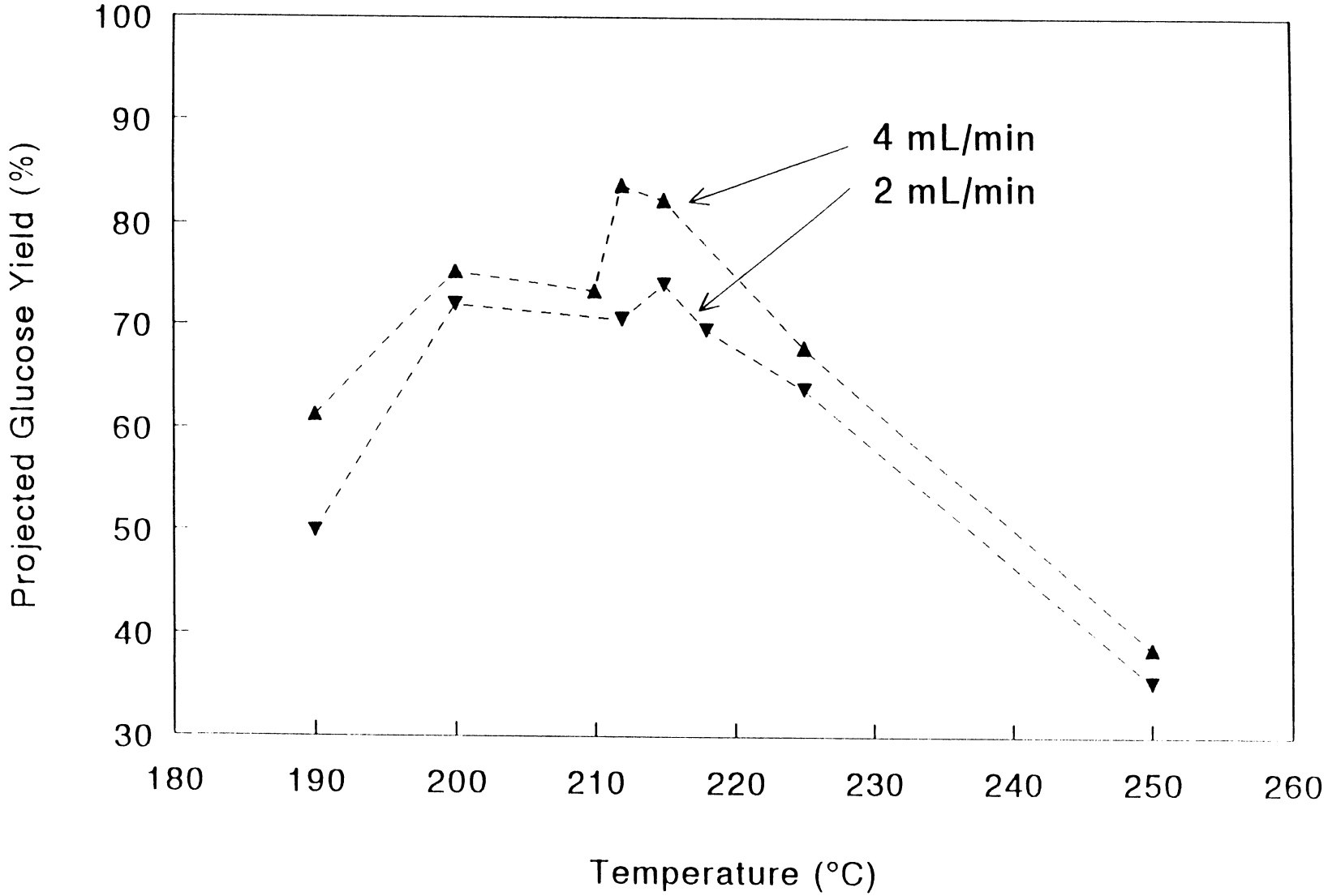

Figure 3. Projected glucose yield vs. temperature, at various flow rates of 5mM acid.

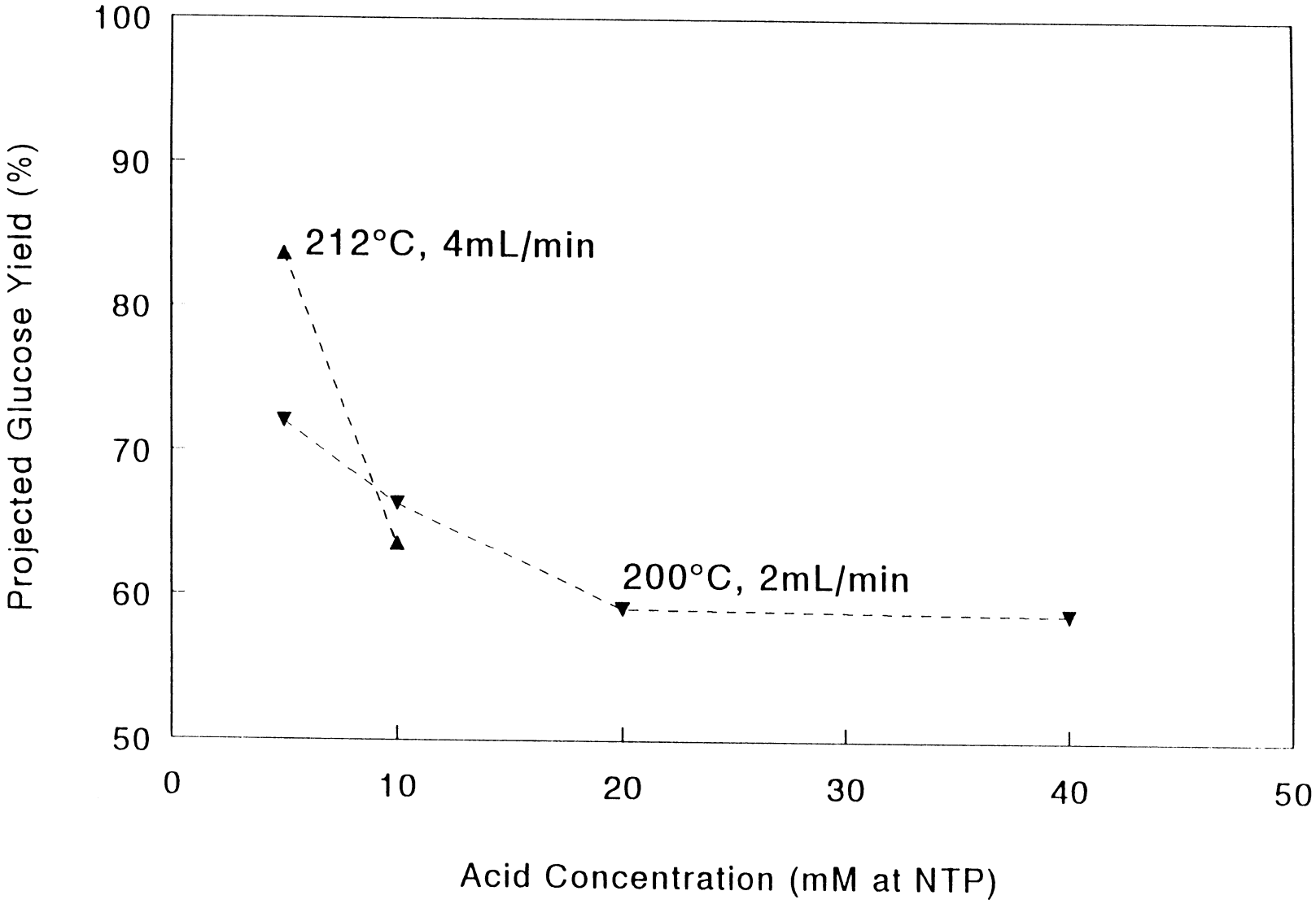

Figure 4. Projected glucose yield vs. acid concentration at various temperature and flow rates.

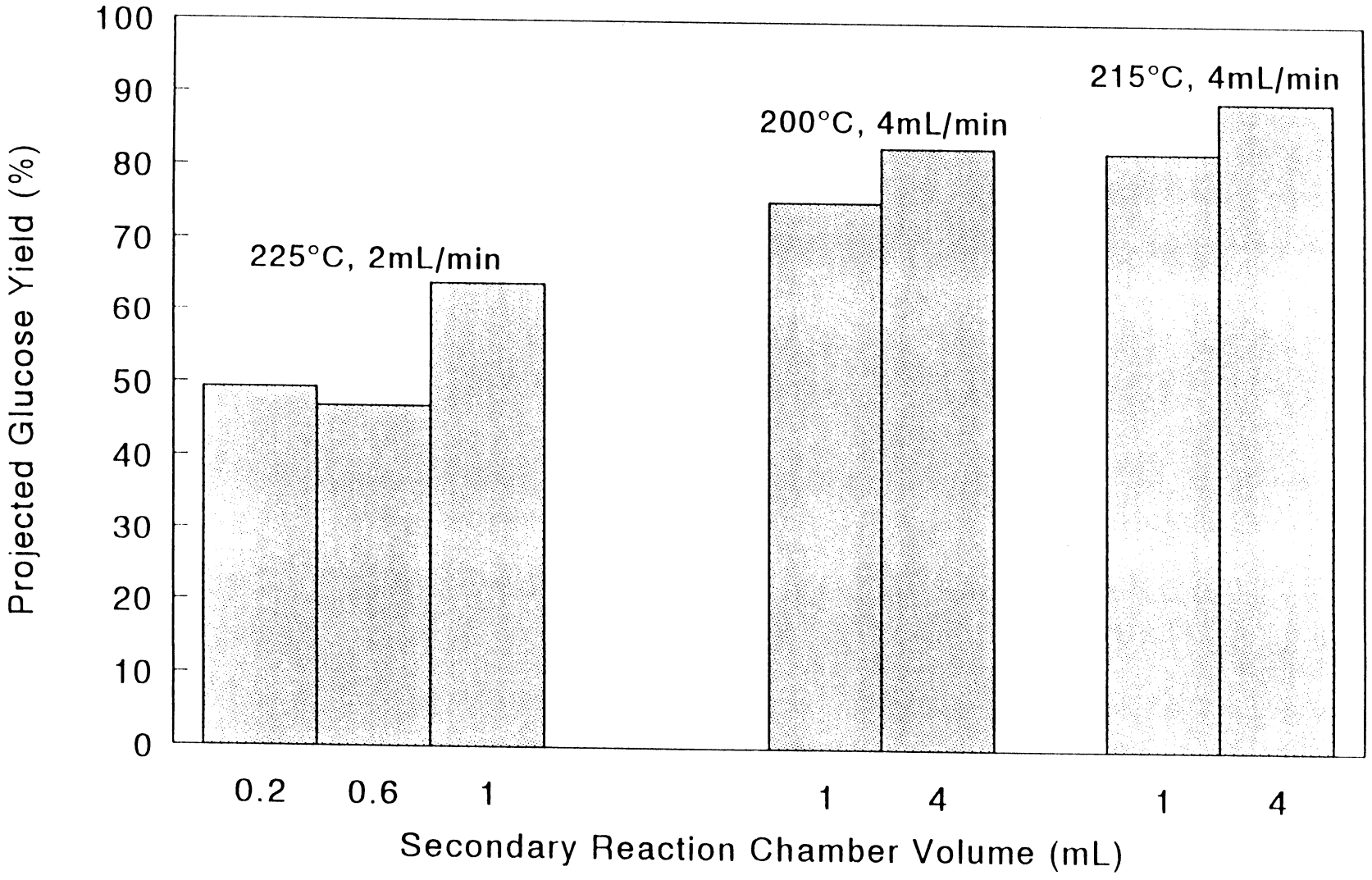

Figure 5. Effect of secondary reaction volume on the projected glucose yield at various temperature and flow rates with 5mM acid.

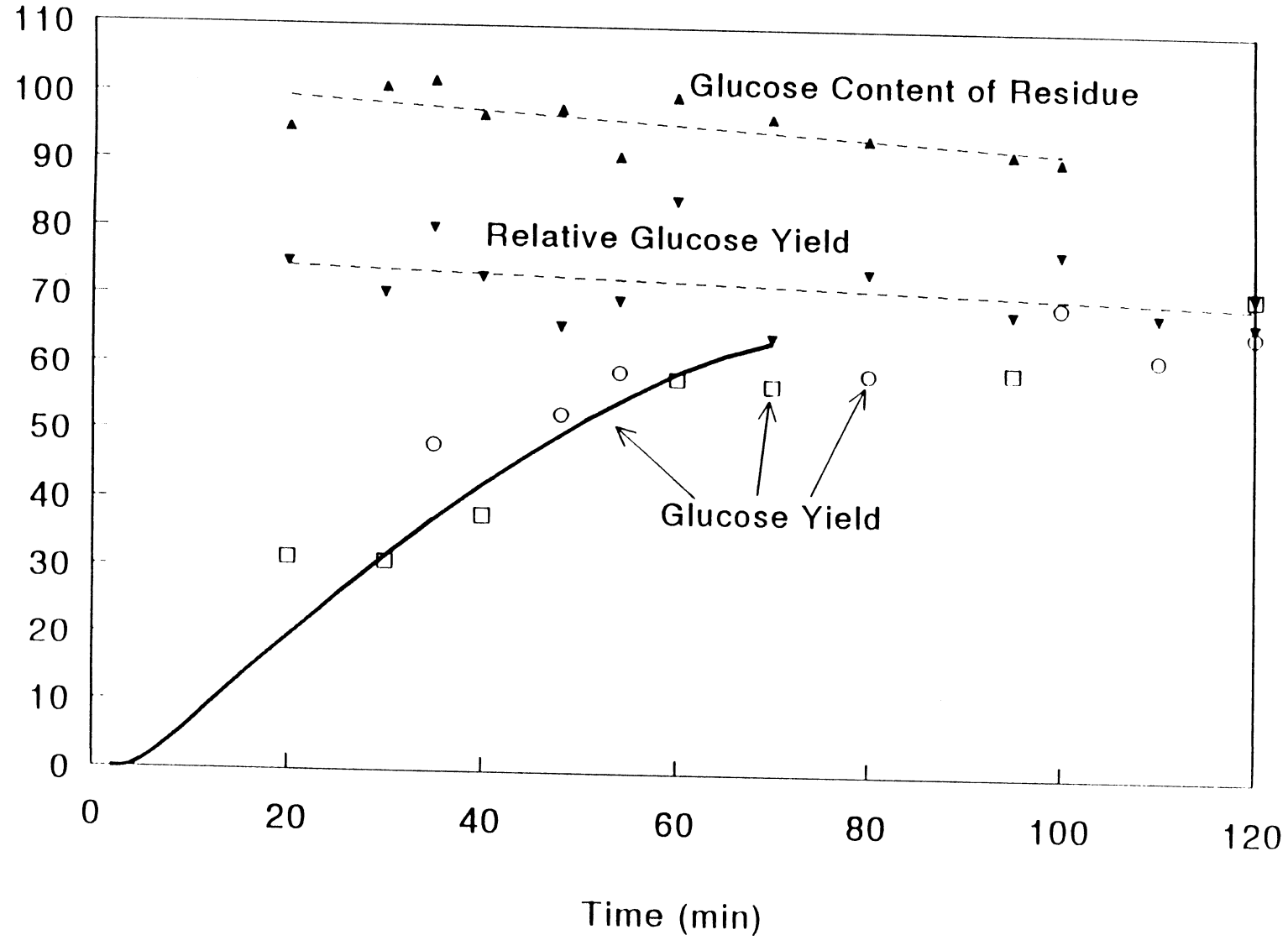

Figure 6. Glucose yields from integral sampling experiments with either post-hydrolysis (□) or long secondary reaction chamber (○), compared with the integrated glucose yields from a differential sampling experiment (bold line). Also plotted are the glucose content of the solid residue and relative glucose yield (from all integral experiments) as a function of reaction time. Dotted lines are linear regression lines to show trend. Experiments carried out at 215°C with a 4mL/min flow of 5mM acid.

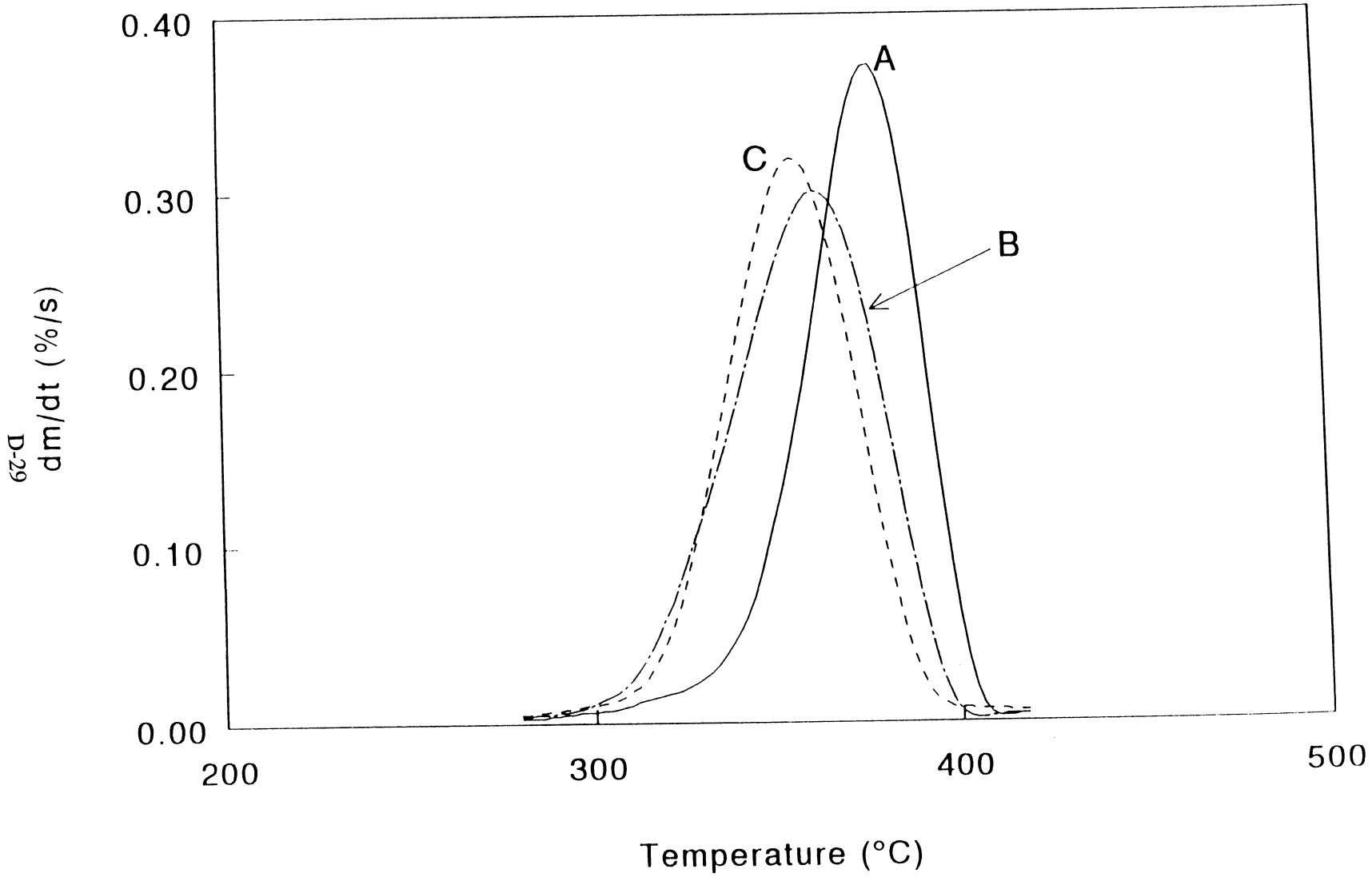

Figure 7. DTG behavior of an original sample of Whatman paper #42 (A) and partially hydrolyzed samples (B: 44% conversion after 30 min,; C: 69% conversion after 60 min.).

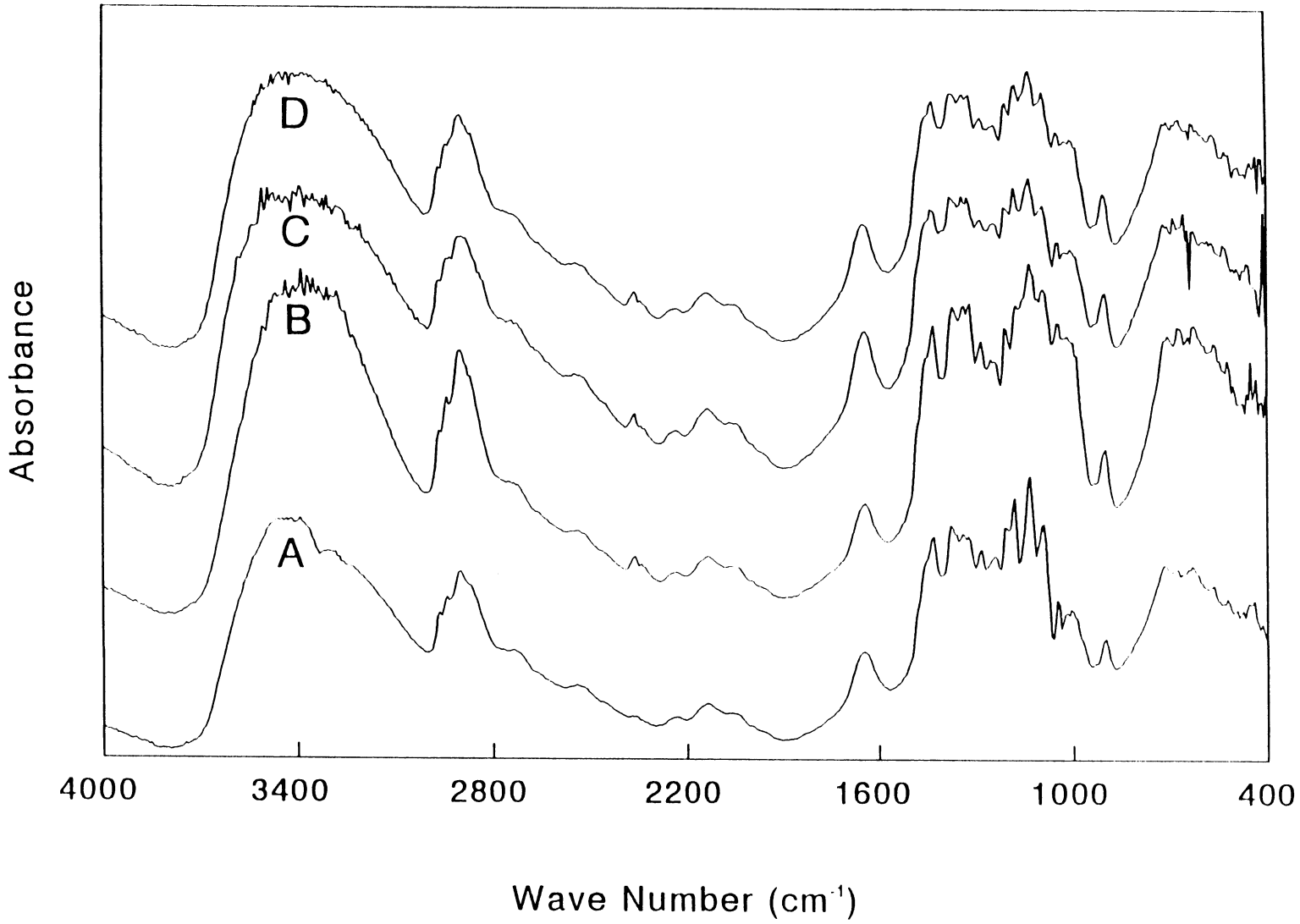

Figure 8. FTIR spectra of an original sample of Whatman paper #42 (A), and partially hydrolyzed samples (B: 44% conversion after 30 min.; C: 69% conversion after 60 min.; D: 80% conversion after 80 min.)

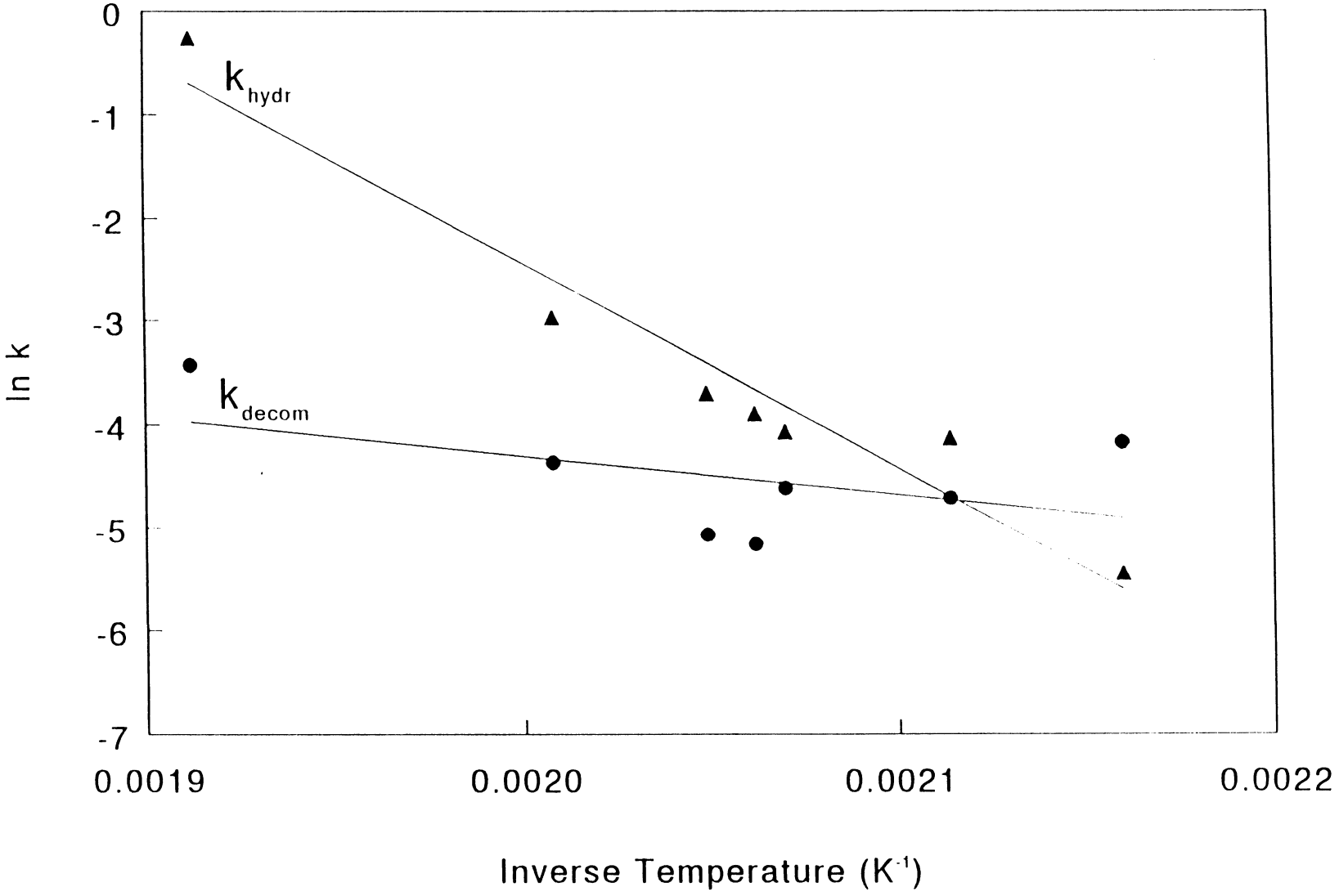

Figure 9. Arrhenius plots assuming a simple model of two sequential reactions: k_{hydr} leading to glucose formation followed by k_{decomp} leading to decomposition products.

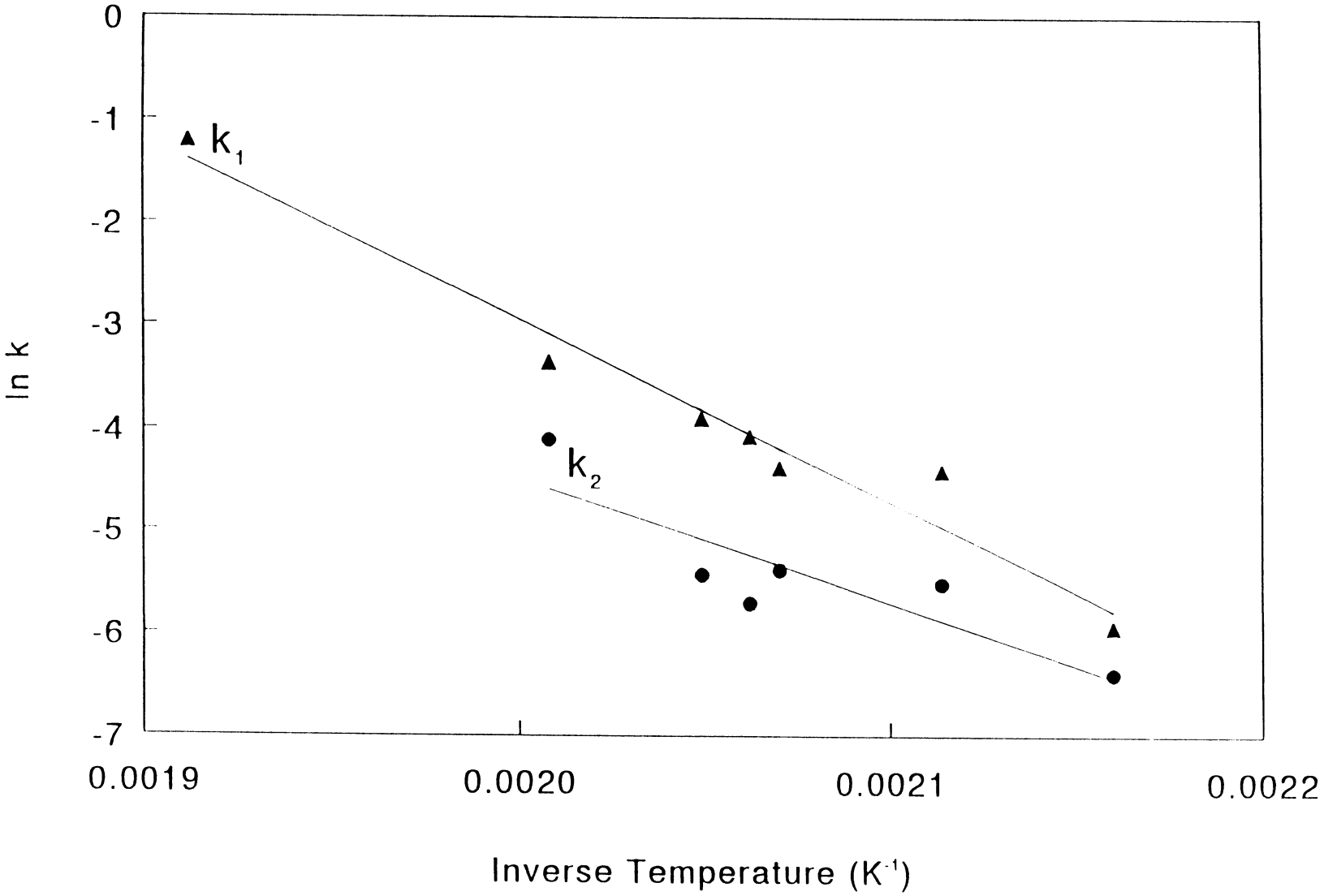

Figure 10. Arrhenius plots assuming a simple model of two competitive reactions, k_1 leading to glucose and k_2 to non-hydrolyzable products.

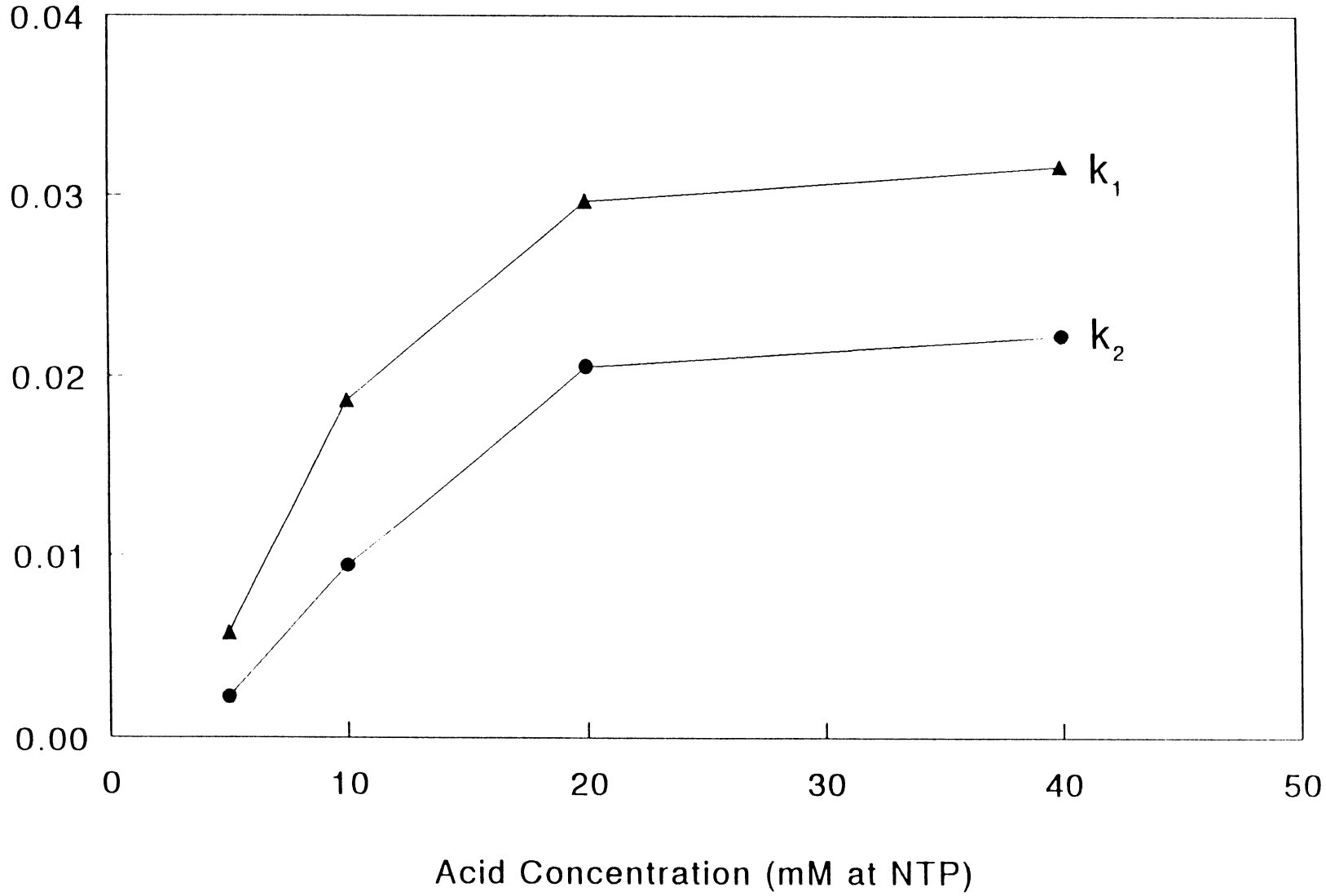

Figure 11. Effect of acid concentration on the rate of reaction, assuming a simple model of two competitive reactions.

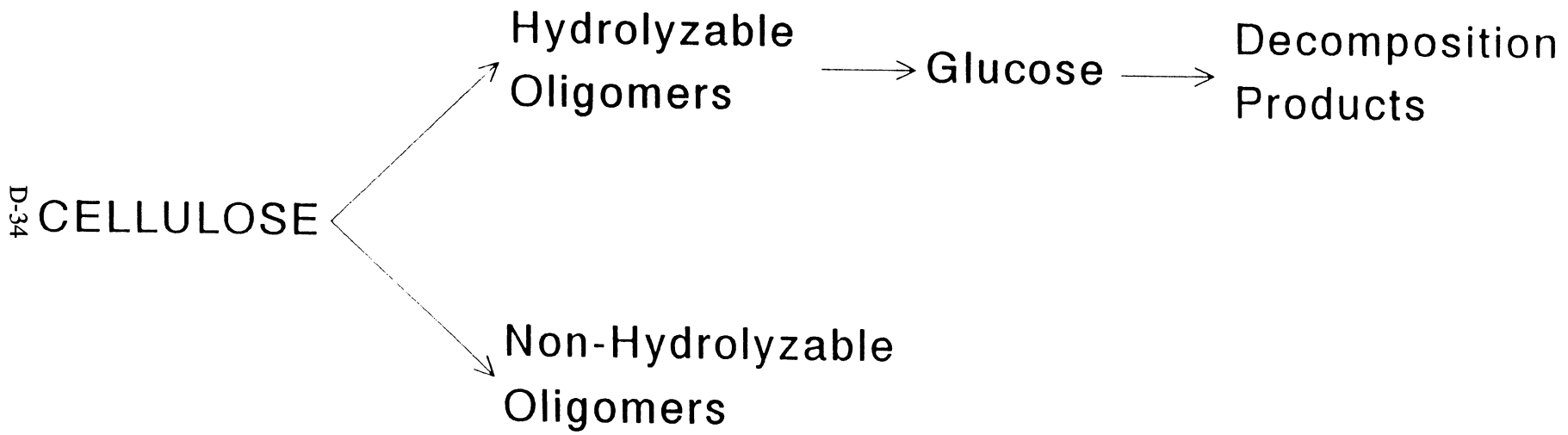

Figure 12. A proposed network of reactions governing cellulose hydrolysis based on the evidence collected in this study.

Uncatalyzed Solvolysis of Whole Biomass Hemicellulose by Hot Compressed Liquid Water

William Shu-Lai Mok and Michael Jerry Antal, Jr.
Department of Mechanical Engineering and the
Hawaii Natural Energy Institute
University of Hawaii at Manoa
Honolulu, Hawaii 96822

ABSTRACT

Samples of six woody and four herbaceous biomass species were washed with compressed, liquid water at 200°-230°C to determine the extent of hemicellulose solvolysis. In the case of sweet gum, 100% of the hemicellulose was solubilized in one minute at 230°C, and was completely recoverable as sugar after post hydrolysis. Concurrently, as much as 20% of the cellulose and 40% of the lignin were also solubilized. These values were almost invariant within a wide range of temperatures and residence times. In most other cases, over 90% of the hemicellulose was solubilized and was recoverable as sugar. High lignin content somewhat reduced the effectiveness of the solvolysis process.

INTRODUCTION

Component fractionation is playing an increasingly important role in the complete and efficient utilization of biomass. In this approach, the hemicellulose, cellulose and lignin components of biomass are each recognized as a chemical resource, with inherent chemical value exceeding their combined heating value. Industrial applications include the removal of hemicellulose for production of xylitol and furfural, and as a pretreatment for enzymatic hydrolysis (Hormeyer et al., 1988; Heitz et al., 1991). Alternatively, the residual cellolignin can be used to manufacture biodegradable films and fibers (Excoffier et al., 1988), or further delignified to produce a high quality cellulose for pulp and paper applications (Aravamuthan et al., 1989; Heitz et al., 1991).

Hemicellulose can be easily removed from biomass by treatment with dilute acid (Grohmann et al., 1986; Abatzoglou et al., 1990), but this same goal can be achieved by water alone. Bobleter et al. (1976) pioneered the technique of hydrothermolysis mainly as a pretreatment for subsequent enzymatic hydrolysis. Applying the technique of steam explosion, Pou-Llinas et al. (1990) succeeded in removing over 90% of the hemicellulose from almond shells after 135s at 227°C, but the actual recovery of xylose was much lower. The ability of pure water (without acid) to solubilize hemicelluloses at temperatures of 200° to 230°C was noted in the recent paper by Abatzoglu et el. (1990), but they did not report the extent of solubilization, nor did they determine the effect of feedstock identity on solubilization behavior. Heitz et al. (1991)

reported a maximum 65% recovery of pentosans from a hardwood using the STAKE II technology.

Because no quantitative information is available concerning the ability of hot, liquid water to fractionate biomass, the primary goal of this work was to quantitate hemicellulose removal, sugar recovery, the co-solubilization of cellulose and lignin, and the composition of the residue obtained by washing various biomass samples with hot, compressed, liquid water. A secondary goal of this work was to determine the effects of biomass composition on the solvolysis chemistry. We were particularly anxious to learn if some biomass feedstocks can be solubilized more easily than others.

EXPERIMENTAL APPARATUS AND PROCEDURES

A tubular percolating reactor (Mok et al., 1991) was employed in this work. To begin an experiment, approximately 0.3g of 1mm mesh sample was loaded into the tubular solvolysis section of the reactor (Hastelloy C-276 tubing, 6.4mm OD x 4.6mm ID x 7.6cm long). This section was then connected to a solvent preheater, flushed with cold water to purge it of air, and pressurized. A HPLC pump delivered water to the reactor system at the prescribed rate, and heat was applied. The time at which the system reached 1°C below its set point was arbitrarily taken as time zero. Two thermocouples monitored the system temperature. The first was in contact with the percolating water immediately before the flow entered the solvolysis section. The second was located on the wall of the solvolysis section. After steady state was achieved, the

two thermocouple readings differed by less than 3°C. The effluent from the solvolysis section was immediately quenched and directed to a pressurized storage tank. The flow of water into the tank displaced air in a tank through a back pressure regulator, which controlled the system pressure. When the heaters were turned off to terminate the experiment, the flow of water was increased to accelerate quenching and flush any remaining solubilized products into the storage tank. To facilitate comparison of these results with other ongoing work in the laboratory, experiments were conducted at 34.5 MPa.

The contents of the effluent tank were collected and weighted. An aliquot of the effluent was dried under vacuum at 56°C until weight loss ceased. The solute content of the effluent was thus determined. Another aliquot was post-hydrolyzed (described later) to obtain the monomeric sugar content of the effluent. The entire solid residue in the solvolysis section was washed into a glass vial, dried at 105°C, cooled in a desiccator and weighted. A sample of the solid residue was ground and quantitatively saccharified.

The quantitative saccharification (QS) method employed in this work was developed by Saeman (1945) and Moore et al. (1967) and adapted by Mok et al. (1991). Briefly, it consists of preliminary soaking of the solid sample in 72% sulfuric acid at 30°C for one hour with constant stirring, followed by dilution to a 4% acid solution and heating for another hour at 120°C. The post hydrolysis procedure (applied to the effluent of the solvolysis

experiments) was essentially the second half of the QS procedure, starting with the addition of acid to the liquid sample to prepare a 4% acid solution. The sugar contents of a sample were obtained by HPLC analysis of the hydrolysate (see later). The solid residue of the QS procedure was filtered, washed many times with de-ionized water until neutral, dried and weighted. The amount of this dry residue (relative to the sample size) was reported as the "Klason" lignin content. This procedure was also used to analyze the original biomass samples.

When the hydrolyzate from the QS procedure was analyzed by HPLC (Hewlett Packard model 1050 pump, Waters model 201 refractive index detector, Interaction ION-300 column operated at 80°C with 0.05mL/min flow of 2mM H_2SO_4, Perkin-Elmer LC600 autosampler, Hewlett-Packard ChemStation data system), two main peaks were observed. The first corresponded to glucose, and the second embodied a mixture of xylose, mannose and galactose. Arabinose, if present, was below the limit of detection. The glucan content of the sample was determined by correcting the amount of glucose by a multiplicative factor of 1.04 (determined by applying QS to a pure cellulose) to account for sugar decomposition during QS (Moore et al., 1967), and a multiplicative factor of 0.9 to account for hydrolytic addition of water. Assuming contributions from hemi-cellulose were small, the glucan content was used as an estimate of the cellulose content. Similarly, the ratio of glucans found in the solvolysis effluent to those contained in the original sample was used to estimate the fraction of cellulose solubilization.

Since xylose, mannose and galactose had the same RI response factor by weight, the total amount of hemicellulose derived sugar was quantified from their combined HPLC peak. Because similar procedures were applied to the original sample, effluent and residue, no correction factor was needed to determine the fraction of hemicellulose solubilization (which is the ratio of hemicellulose sugar recovered by post hydrolysis of the effluent to those obtained by QS of the original sample). To estimate the hemicellulose content, we assumed pentoses to be its principal component (which is true for all hard woods (Wenzl, 1971)), and applied a multiplicative factor of 0.88 to the combined (xylose/mannose/galactose) content to account for hydrolytic addition of water.

A total of 10 biomass species, 6 woody and 4 herbaceous, were tested. The samples were prepared by the Solar Energy Research Institute (SERI). A Pyrolysis-Mass-Spectrometry technique employed by SERI indicated that these samples are characteristic of a wide spectrum of biomass material (Agblevor et al., 1989). A simplified summative analysis of each species is given in Table 1. The data are reported on a dry weight, but not extractive free, basis. The material balances for the herbaceous samples are particular low, as would be expected for species with a high extractive content.

RESULTS AND DISCUSSION

Because sweet gum has the highest hemicellulose content among the ten samples tested, it was used in the first stage of this work

to determine the preferred condition for hemicellulose solvolysis. The results are summarized in Figure 1, which shows the fractional solubilization of each component, as well as the total percentage of solubilization by weight. At first glance, few differences as a function of reaction time and temperature are observed. This finding suggests that uncatalyzed solvolysis of biomass by hot, compressed water enjoys the advantage of being tolerant to changing operating conditions. Upon closer examination, the expected increase in solubilization of all components with increasing temperature is evident. The amount of each component solubilized increases with the solid's retention time at 210°C. However, a slight drop in sugar recovery (but not the amount of sample solubilized) can be observed with increasing heating time at 230°C. This can be explained by decomposition of a small amount of sugars trapped in the reactor. At 230°C, the hemicellulose is completely removed and recoverable as monomers (after post hydrolysis), even with a nominal reaction time of zero (i.e. the reaction was complete during the 5 minute warm-up time). Approximately 20% of the cellulose and 40% of the lignin was solubilized with the hemicellulose during the process. Note that the solubilization of cellulose and lignin does not increase significantly with time, despite the fact that much of each component remains in the solid. In the case of cellulose, this result agrees with the well known concept of an amorphous region which solubilizes easily, and a crystalline region which is resistant to attack by pure water. Apparently lignin responds in a similar manner to attack by water.

Figure 2 displays the yield of solid residue from sweet gum at various reaction conditions. Also displayed are the cellulose and lignin contents of the residue, showing averages of 71% and 20% respectively. The mass balances (sum of the solubilized and residual solid fractions) average 100% (although the theoretical maximum could be slightly higher due to hydrolytic addition of water). The average cellulose balance, obtained by summing the fraction of cellulose solubilized and fraction of cellulose remaining in the residue, is 95%. Since the cellulose content was measured by hydrolysis to glucose, this shows that the hydrothermal treatment preserves the hydrolyzability of the cellulose contained in the sample.

Since the hydrothermal process did not appear to be critically dependent upon the operating parameters, a reaction condition of 2min at 230°C with 1mL/min flow of water was chosen to conduct the survey of all ten biomass samples. No effort was made to optimize the process for each material.

Figure 3 summarizes the results of the survey. Each bar chart displays the woody species on the left, and the four herbaceous species on the right. Within each of the two groups, the species are ordered by the percentage of hemicellulose solubilized. Few differences were observed. With the exception of Eucalyptus Gummifera, the amount of hemicellulose solubilized ranges from 85 to 99%. These values should be compared to the maximum pentosan recovery of 65% from hardwood Populus Tremuloides achieved by Heitz et al. (1990) using a steam explosion process. Evidently the hot,

compressed liquid water wash process employed in this work results in less degradation of the pentosans than steam explosion. A negative correlation with a level of significance of 0.01 (Frefund, 1972) was observed between the lignin content of the sample and the solubilization of hemicellulose. Apparently, a high lignin content somewhat inhibits hemicellulose solvolysis and/or sugar recovery. This trend is best exemplified by Eucalyptus Gummifera, which has the highest lignin content and the lowest hemicellulose solubilization measured.

Large variations in the fractional solubilization of cellulose were observed, but these variations were not correlated with the composition of the substrate. Perhaps these variations are related to variations in the crystallinity of the cellulose contained in each species. The changes in lignin solubilization are also not dependent on the substrate composition, but the amount of total eluant is correlated (at the 0.01 level of significance) with the hemicellulose content of each sample. As expected, higher hemicellulose content leads to higher fraction of sample solubilization. In a recent paper, Heitz et al. (1991) employed a severity parameter $R_o = t \exp([T-100]/14.75)$, where t is time (min) and T is temperature (°C), to optimize steam pretreatment conditions using STAKE II steam explosion equipment. They obtained a maximum recovery of pentosans with $\log_{10}R_o = 3.8$. Data displayed in Figure 3 were all obtained at severity $\log_{10}R_o = 4.1$, which is close to the optimum condition identified by Heitz et al. (1991). However, the highest percentage of solubilization achieved by Heitz

et al. (1991) was 26%; whereas the lowest percentage of solubilization displayed in Figure 3 is 39%, and the highest is 56%. Evidently, pretreatment using hot, compressed liquid water solubilizes considerably more of the biomass substrate than steam explosion.

The mass balances for these survey experiments are displayed in Figure 4. During the initial flush of cold water (required to remove air) a visible amount of colored extractive was observed from the herbaceous samples. These extractives were not collected. Consequently the herbaceous species evidenced lower mass balances than the woody species. The total mass recovery for the woody species was well over 90%. The cellulose and lignin contents of the residues are also plotted in Figure 4, and show average values of 71% and 19% respectively.

CONCLUSIONS

This study has shown that hot, compressed liquid water can effectively solubilize hemicellulose from whole biomass. Of the ten biomass species studied, hemicellulose solubilization and subsequent monomeric sugar recovery ranged from 85% to 99%. In the case of sweet gum, 100% of the hemicellulose was solubilized in 1 minute at 230°C, and the entire amount was recoverable as sugar after post hydrolysis. A fraction of the cellulose and lignin constituents, dependent more on the species composition than the operating condition, was also solubilized during the process. The

solid residue consisted of at least 70% cellulose and 20% lignin. Because of its relative insensitivity to reaction conditions, this hot water solubilization process should be amenable to scaleup without undue attention to the control of temperature or solids residence time in the reactor. In light of the results obtained using a wide variety of biomass species, the process should also be insensitive to the identity of the biomass feedstock; thereby permitting (in most cases) the recovery of more than 90% of the hemicellulose as sugar without optimization for each species fed. On a finer scale, there is a correlation between hemicellulose solubilization and the lignin content of the sample, with the latter inhibiting the former.

ACKNOWLEDGEMENT

This work was supported by the Solar Energy Research Institute (subcontract no. XN-0-19164-1). The authors wish to thank Dr. Helena Chum and Dr. Foster Agblevor (SERI) for supplying the ten biomass substrates used in this work, Dr. Ralph Overend (SERI) for many stimulating discussions of hydrolysis chemistry, Dr. Victor Phillips (UH) for administrative support, Ben Respicio (UH) for assistance in reactor fabrication, and Supaporn Manaruson (UH) for her help in conducting the experiments. The text of this paper was written during a visit to the Research Laboratory for Inorganic Chemistry of Hungarian Academy of Sciences. The hospitality of the Hungarians, particularly Dr. Tamas Szekely, Dr. Gabor Varhegyi and Dr. Piroska Szabo, were appreciated.

REFERENCES

Abatzoglou, N.; Koeberle, P .G.; Chornet, E.; Overend, R.P.; Koukios, E.G., Dilute Acid Hydrolysis of Lignocellulosics: An application to medium consistency suspensions of hardwoods using a plug flow reactor. Can. J. Chem. Eng., **1990**, 68, 627-638.

Agblevor, F. A.; Evans, R.J.; Milne, T.A.; Antal, M.J., "Multivariate Data Analysis of Biomass Feedstocks Using Pyrolysis Mass Spectrometry", presented at the International Chemical Congress of Pacific Basin Societies, December 1989.

Aravamuthan, R.; Chen, W.; Zargarian, K.; April, G., Chemicals from Wood: Prehydrolysis/Organosolv Methods. Biomass, **1989**, 20, 263-276.

Bobleter, O.; Niesner, R.; Rohr, M., The Hydrothermal Degradation of Cellulosic Matter to Sugars and their fermentative Conversion to Protein. J. Appl. Polym. Sci. **1976**, 20, 2083-2093.

Excoffier, G.; Peguy, A.; Rinaudo, M.; Vignon, M.R., Evolution of Lignocellulosic Components During Steam Explosion: Potential Applications. International Workshop on Steam Explosion Technique, October 1988, Milan, Italy.

Frefund, J. E. "Mathematical Statistics". 2nd Edition, Prentice/Hall International, Inc., **1972**, p.382.

Grohmann, K.; Torget, R.; Himmel, M., Dilute Acid Pretreatment of Biomass at High Solids Concentration. Biotechnology and Bioengineering Symp. **1986**, 17, 135-151.

Heitz, M.; Capek-Menard, E.; Koeberle, P.G.; Gange, J., Chornet, E.; Overend, R.P.; Taylor, J.D.; Yu, E., Fractionation of Populus tremuloides at the Pilot Plant Scale: Optimization of Steam Pretreatment Conditions using the STAKE II Technology. Bioresource Technology, **1991**, in press.

Hormeyer, H.F.; Schwald, W.; Bonn, G.; Bobleter O., Hydrothermolysis of Birch Wood as Pretreatment for Enzymatic Saccharification. Holzforschung **1988**, 42, 95-98.

Mok, W.; Antal, M. J.; Varhegyi, G., Productive and Parasitic Pathways in Dilute Acid-Catalyzed Hydrolysis of Cellulose. submitted to Ind. Eng. Chem. Res., 1991.

Pou-Llinas, J.; Driguez, H.; Excoffier, G.; Vignon, M.; Canellas, J., Steam pretreatment of almond shells for xylose production. Carbohydrate Research, **1990**, 207, 126-130.

Moore, J.F.; Johnson, D.B. "Procedures for the Chemical Analysis of Wood and Wood Products", Forest Products Laboratory, Forest Service, U.S. Dept. of Agriculture, 1967.

Saeman, J. F.; Bubl, J. L.; Harris, E. E., Quantitative Saccharification of Wood and Cellulose. Industrial and Engineering Chemistry 1945, 17, 35-37.

Wenzl, H. F. J., "The Chemical Technology of Wood", Academic Press, New York and London, 1970.

Table I. Brief summative analysis of ten biomass species studied in this work. All data in % on dry weight basis.

Sample	Hemi-cellulose	Cellulose	Lignin	Total*
Eucalyptus Gummifera	13	38	37	88
Luecaena hybrid KX-3	14	43	25	82
Populus Deltoides	17	39	26	82
Eucalyptus Saligna	12	45	25	82
Silver Maple	19	40	22	81
Sweet Gum	19	40	19	78
Switch Grass	17	30	23	70
Sweet Sorghum	15	36	16	67
Sugar Cane Bagasse	14	35	17	66
Energy Cane	14	37	15	66

*Extractives and ash content were not determined

LIST OF FIGURES

Figure 1. Percentage solubilization of the original sample mass, hemicellulose, cellulose, and lignin from Sweet Gum as a function of the solid sample's residence time in a 1mL/min percolating flow of water at the indicated temperature and 34.5 MPa.

Figure 2. Percentage yield of solid residue (by weight) from Sweet Gum as a function of the solid sample's residence time at the indicated temperature. Also displayed are the cellulose and lignin contents of the residue. All experiments were conducted with a 1mL/min percolating flow of water at 34.5MPa.

Figure 3. Percentage solvolysis of the original sample mass, hemicellulose, cellulose and lignin for ten biomass species. Solvolysis was conducted with a nominal 2 min reaction time at 230°C and a percolating 1mL/min flow of water at 34.5MPa.

Figure 4. Mass balances of the solvolysis experiments described in Figure 3. Also displayed are the cellulose and lignin contents of the residue.

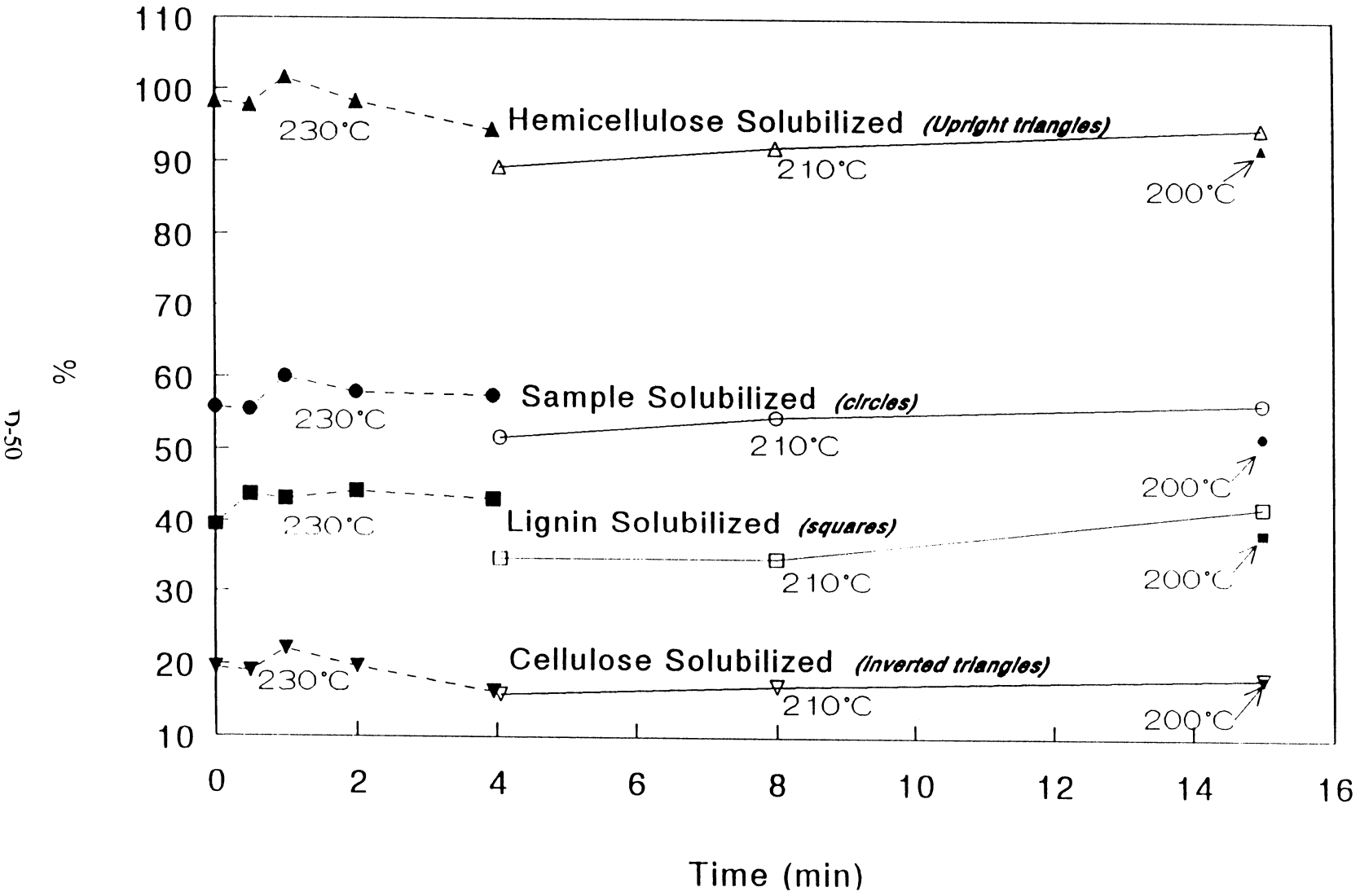

Figure 1. Percentage solubilization of the original sample mass, hemicellulose, cellulose, and lignin from Sweet Gum as a function of the solid sample's residence time in a 1mL/min percolating flow of water at the indicated temperature and 34.5 MPa.

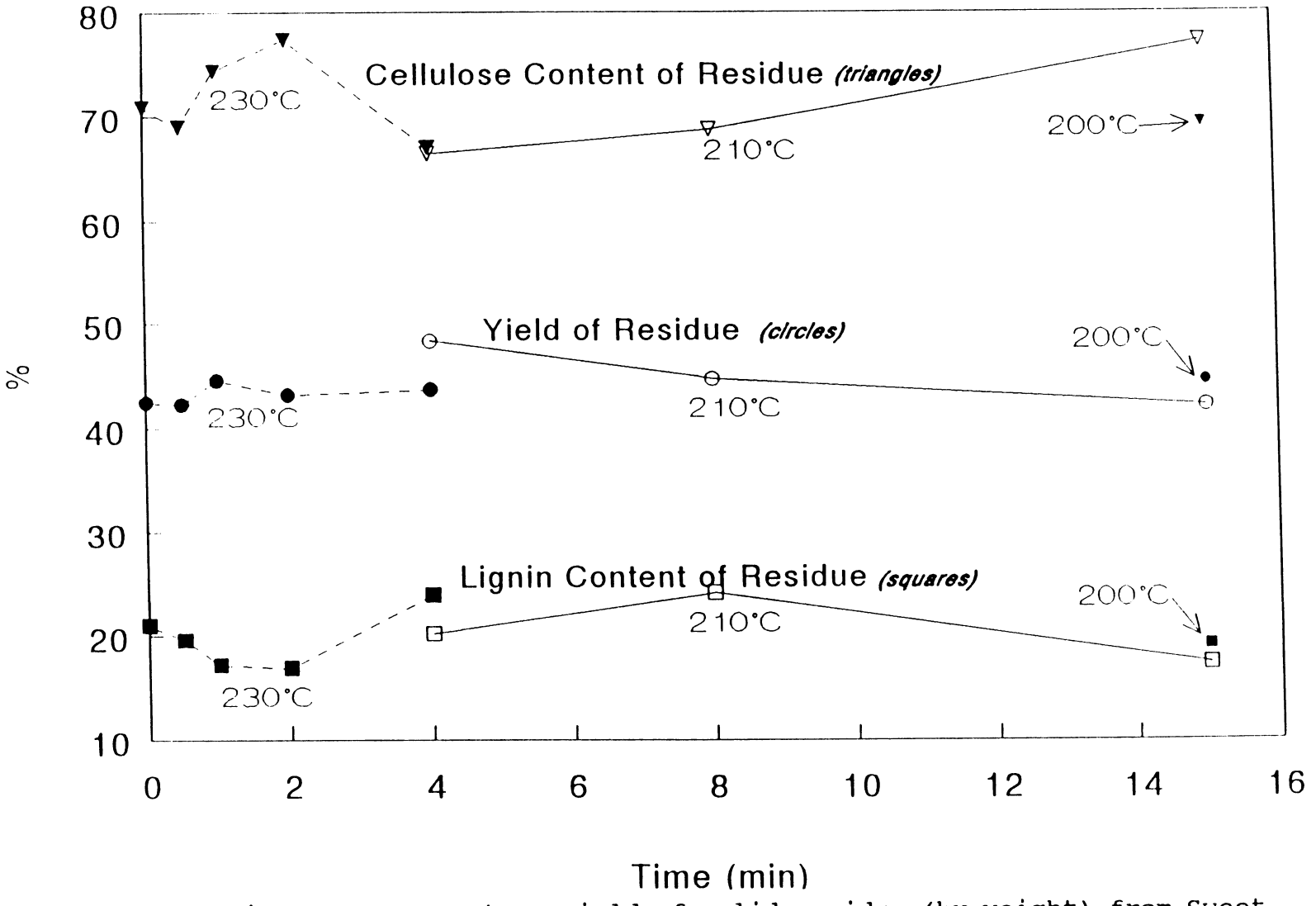

Figure 2. Percentage yield of solid residue (by weight) from Sweet Gum as a function of the solid sample's residence time at the indicated temperature. Also displayed are the cellulose and lignin contents of the residue. All experiments were conducted with a 1mL/min percolating flow of water at 34.5MPa.

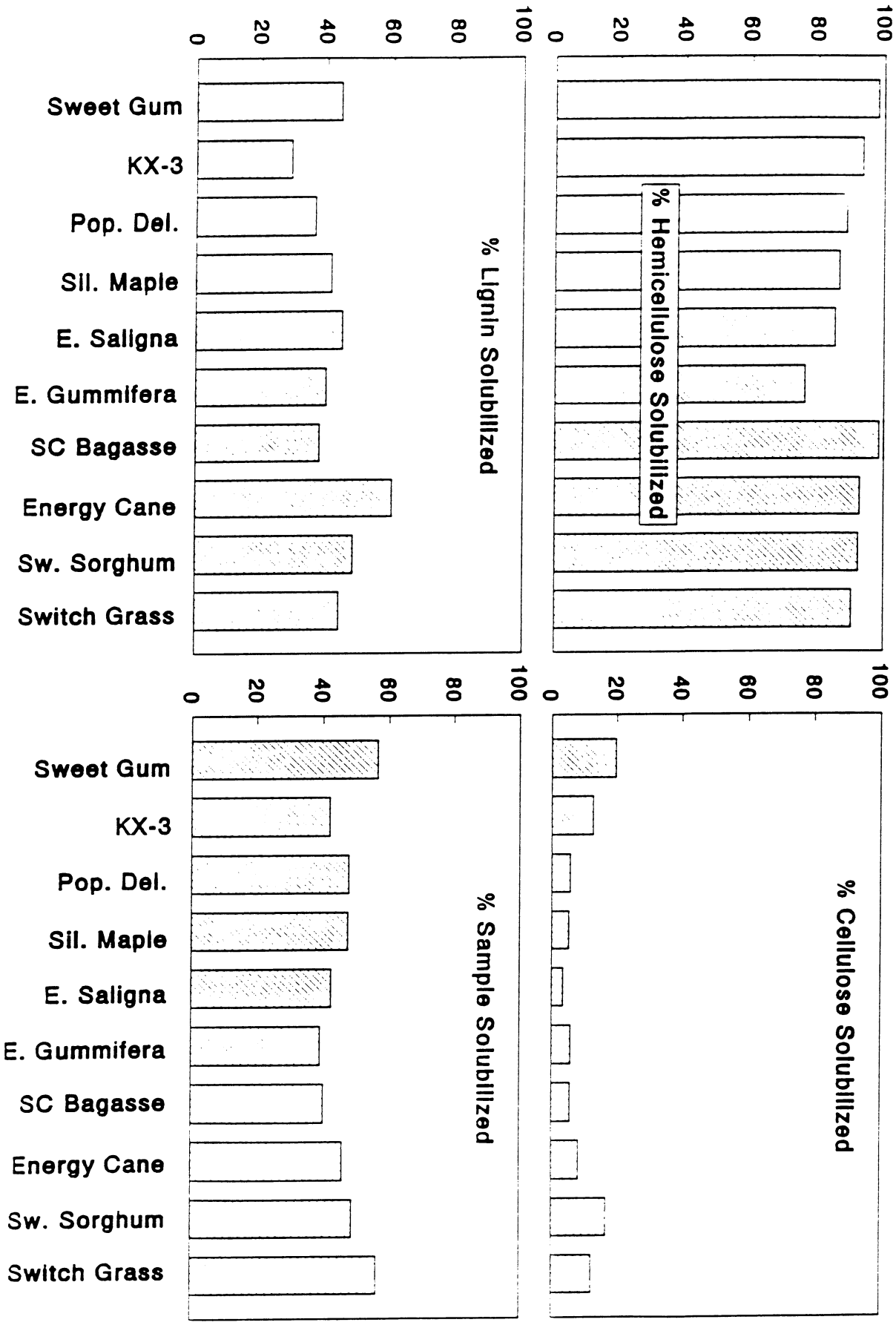

Figure 3. Percentage solvolysis of the original sample mass, hemicellulose, cellulose and lignin for ten biomass species. Solvolysis was conducted with a nominal 2 min reaction time at 230°C and a percolating 1mL/min flow of

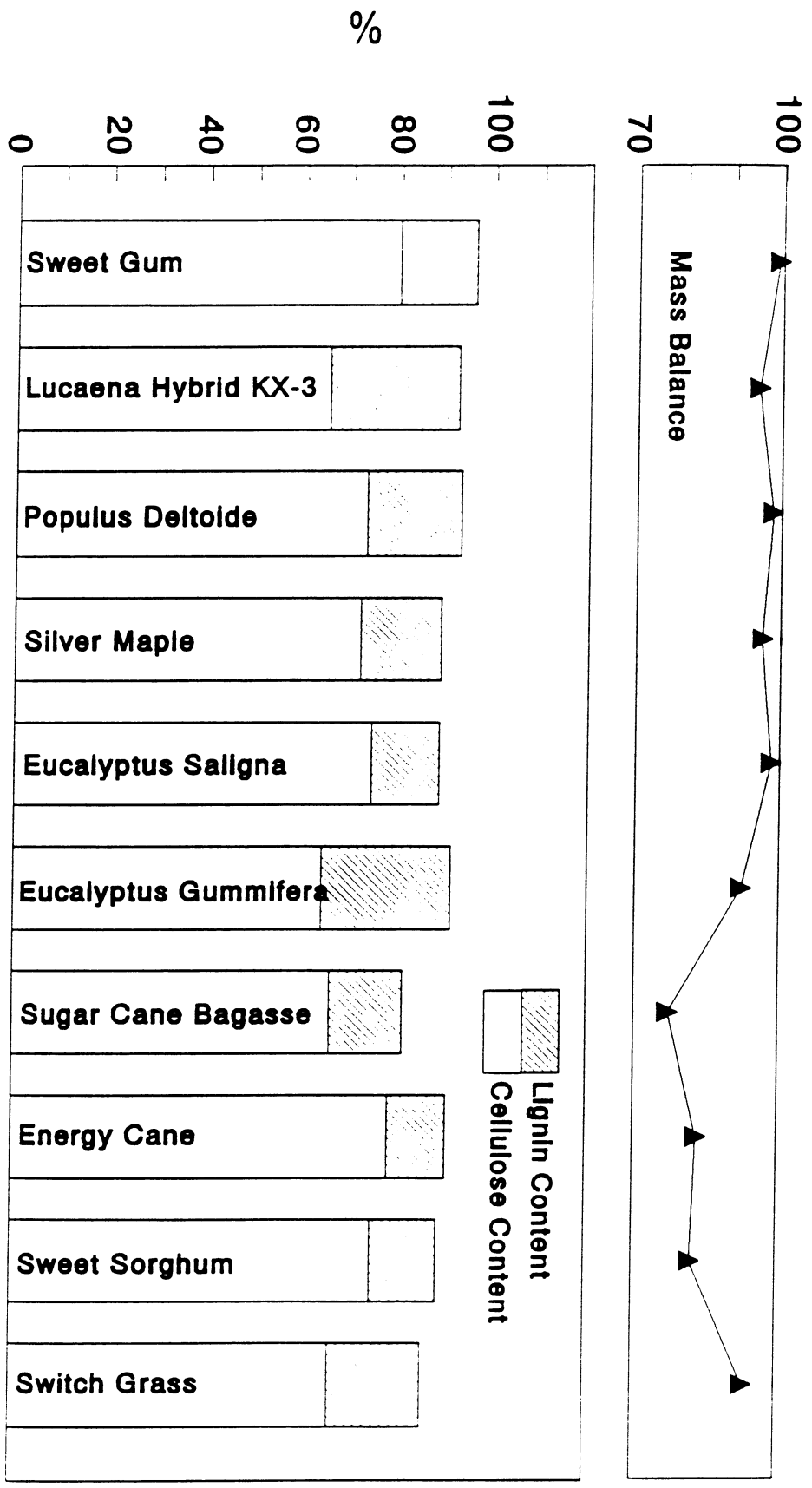

Figure 4. Mass balances of the solvolysis experiments described in Figure 3. Also displayed are the cellulose and lignin contents of the residue.

Appendix E

Feedstock and Process Testing

Energy Sources, Volume 13, 361–368
Printed in the UK.

0090-8312/91 $3.00 + .00

Chemical Equilibrium Computations for Gasification of Biomass to Produce Methanol

CHARLES M. KINOSHITA
YUE WANG
PATRICK K. TAKAHASHI

Hawaii Natural Energy Institute
University of Hawaii
Honolulu, Hawaii 96822

Abstract *Gasification of biomass into synthesis gas is the first step in producing methanol from biomass. Catalytic conversion of the gas produced by the gasifier into methanol is strongly affected by the composition of the product gas. It is thus important to know what the gas composition would be under different gasification conditions and to be able to identify those conditions that would be optimal for methanol production. A computer program is developed to determine the equilibrium composition of biomass gasification products under various conditions. The theoretical influence of temperature, pressure, moisture, and equivalence ratio on gasification is analyzed. The equilibrium computations are used to define appropriate gasification conditions for methanol production and related gasification parameters. By judiciously adjusting certain gasification parameters, it appears that one can optimize the gas generated from biomass for subsequent synthesis into methanol. Energy balances and theoretical methanol yields are examined. Theoretical computations are compared with published experimental data.*

Keywords biomass, equilibrium, gasification, methanol, synthesis gas

Introduction

Gasification of biomass is the primary step in producing methanol from biomass. Catalytic conversion of the gas produced by the gasifier into methanol is strongly affected by the composition of the product gas. It is thus important to know what the gas composition would be under different gasification conditions and to be able to identify those conditions that would be optimal for methanol production. A computer program is developed to determine the equilibrium composition of biomass gasification products under various conditions. The equilibrium computations are used to define appropriate gasification conditions for methanol production and related gasification parameters. The theoretical computations are compared with published experimental data.

Basis for Computation

A general chemical equation for biomass gasification is

$$\begin{aligned} CH_\alpha O_\beta + yO_2 + zN_2 + wH_2O = {} & x_1C + x_2H_2 + x_3H_2O + x_4CO + x_5CO_2 \\ & + x_6CH_4 + x_7C_2H_2 + x_8C_2H_4 \\ & + x_9O_2 + x_{10}N_2 \end{aligned} \quad (1)$$

where $CH_\alpha O_\beta$ is the chemical representation of biomass and y, z, w, and x_i are the molar numbers of various components. A group of nonlinear equations can be formulated in accordance with stoichiometry and minimization of the Gibbs Free Energy as the latter applies to chemically reacting mixtures in equilibrium. These can be recast in the following functional form.

$$f(\alpha, \beta, p, T, w_t, \text{ER}, \mathbf{X}) = 0 \tag{2}$$

where p and T denote pressure and temperature, respectively; w_t is the moisture (per unit mass of dry feedstock) in the fuel and from any added steam; ER is the equivalence ratio (here defined as the mass of oxidant actually supplied per unit mass of dry feedstock divided by the oxidant stoichiometrically required per unit mass of dry feedstock); and $\mathbf{X}$ represents the composition of the gasification products, i.e., $\mathbf{X} \equiv (x_1, x_2, \ldots, x_{10})$. Thus, the composition of the product gas $\mathbf{X}$ depends on the type of biomass (through α and β); gasification conditions (p and T); moisture in the reactants w_t; and the equivalence ratio ER.

The energy shortfall associated with the gasification reaction can be described in terms of an Energy Input Ratio ϵ defined as

$$\epsilon \equiv (\Sigma_{\text{products}}\, x_i h_i - \Sigma_{\text{reactants}}\, y_j h_j)/E_B \tag{3}$$

where h_i is specific enthalpy; y_j denotes the molar numbers of biomass, oxidant, and any added steam; and E_B is the energy content of the biomass feedstock, calculated as its lower heating value. Here, positive ϵ indicates that input of energy from an external source is necessary to sustain the gasification reaction under the prescribed conditions, while $\epsilon < 0$ indicates that the gasification process liberates energy in excess of that needed to sustain the overall reaction and thus can occur without expending energy from an external source. $\epsilon = 0$ represents adiabatic gasification. This is of special interest since most gasification systems are not externally heated, and, in such cases, the adiabatic process could be used as a standard against which actual performance could be compared.

Once the composition of the gasification products has been established, the theoretical amount of methanol producible can be computed as per the following reaction:

$$CO + 2H_2 = CH_3OH \tag{4}$$

Also considered is the option of increasing the yield of methanol by steam reforming of methane:

$$CH_4 + H_2O = CO + 3H_2 \tag{5}$$

and by adjusting the H_2:CO ratio of the product gas via the water gas shift reaction:

$$CO + H_2O = CO_2 + H_2 \tag{6}$$

Computational Results

A computer program was developed to solve the previous equations and perform related computations. Using the program, equilibrium computations were performed for differ-

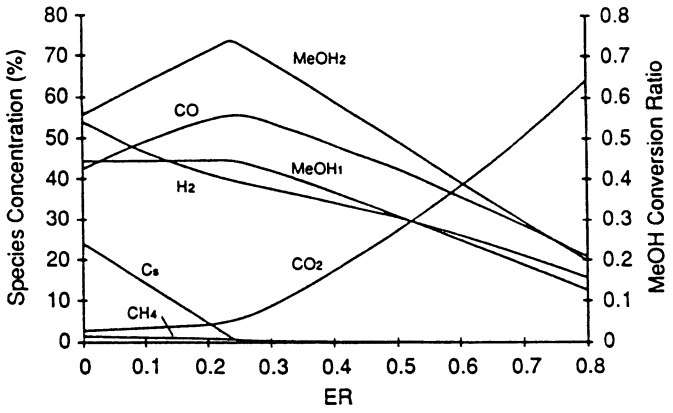

Figure 1. Equilibrium product composition and methanol conversion versus equivalence ratio for $T = 800°C$, $p = 1$ atm, and $w_t = 0$. All gaseous species are presented on a dry, volumetric basis; char (C_S) and methanol conversions are presented on a dry-feedstock, mass basis.

ent values of parameters ER, p, T, w_t, α, and β. Select results are presented for gasification with oxygen and steam, with $\alpha = 1.4$ and $\beta = 0.59$.

Figure 1 presents the equilibrium composition of the dry product gases and solid carbon (char) C_S and the theoretical yields of methanol as functions of ER for fixed T, p, and w_t. The concentration of hydrogen decreases monotonically as ER increases. Carbon monoxide increases with increasing ER in the interval $0.0 < ER < 0.24$ but decreases at higher ER. Carbon dioxide increases with increasing ER as the combustion reaction becomes more prevalent. Methane is present in relatively low concentrations and decreases as ER increases. Here, as in most equilibrium conditions of interest in this study, other hydrocarbon species, such as C_2H_2 and C_2H_4, and oxygen are present only in minute concentrations ($< 10^{-4}\%$). (Since those species did not appear in significant quantities in any of the computations of interest in this study, they will not be included in further discussions.) Solid carbon disappears when ER reaches 0.26.

Two theoretical yields of methanol are shown in Figure 1, both given as mass of methanol per unit mass of dry feedstock. The lower curve, designated by $MeOH_1$, represents the yield stoichiometrically obtainable via conversion of only the hydrogen and carbon monoxide present in the equilibrium product gas (i.e., via Eq. 4 only) and the higher curve ($MeOH_2$) represents the yield stoichiometrically obtainable by also employing steam reforming of methane (Eq. 5) and the water gas shift reaction (Eq. 6) to supply additional hydrogen or carbon monoxide, whichever is limiting the amount of methanol in the lower yield. In the interval $0.0 < ER < 0.24$, the reduction in hydrogen concentration is approximately offset by an increase in gas produced per unit of feedstock (accompanying the decrease in remaining char and increase in oxidant), thus the total amount of hydrogen in the product gas remains roughly constant. As a result, the lower yield of methanol per unit of feedstock ($MeOH_1$) is nearly constant over the interval $0.0 < ER < 0.24$. The higher methanol yield ($MeOH_2$) increases in that same interval by taking advantage of the increasing amount of carbon monoxide present to increase the hydrogen available for methanol synthesis via the water gas shift reaction. For $ER > 0.24$, the yields of methanol decrease in response to decreasing concentrations of hydrogen and carbon monoxide in the product gas.

Figure 2 illustrates the influence of T on the equilibrium composition and on methanol yields. Hydrogen increases in the range $T < 800°C$ then decreases slightly for $T >$

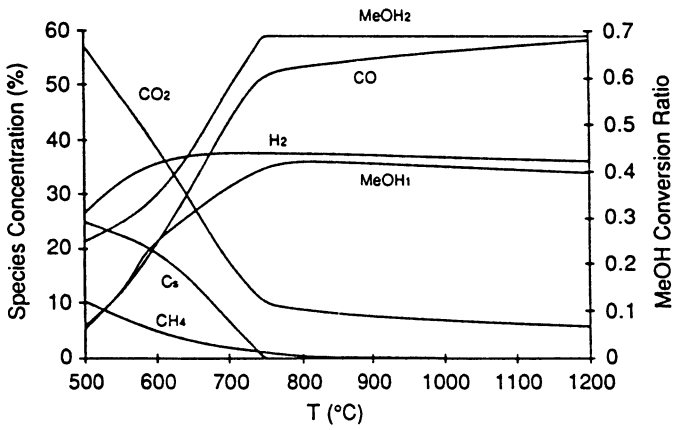

Figure 2. Equilibrium product composition and methanol conversion versus temperature for $p = 1$ atm, ER = 0.3, and $w_t = 0$.

800°C. Carbon monoxide increases and carbon dioxide decreases as T increases. Methane decreases steadily as T increases. Solid carbon disappears at moderate gasification temperatures provided there is sufficient oxidant. At very low temperatures ($T < 600$°C) the lower yield of methanol ($MeOH_1$) closely tracks carbon monoxide concentration, which is the limiting component in that temperature range, while at higher temperatures the yield tracks the then-limiting hydrogen concentration. Although not apparent from the figure, the number of moles (per unit of feedstock) of hydrogen and carbon monoxide combined is nearly constant in the range $T > 800$°C; therefore, by adjusting the hydrogen to carbon monoxide ratio via the water gas shift reaction (Eq. 6), the higher methanol yield ($MeOH_2$) likewise remains nearly constant in the same temperature range.

Figure 3 illustrates the effect of w_t on the product gas composition and on methanol yields. Solid carbon decreases as the moisture content increases and disappears when w_t reaches 0.40; at this point, hydrogen reaches a minimum and carbon monoxide a maximum. Carbon dioxide increases and methane decreases as w_t increases. At low w_t, $MeOH_1$ is limited by poor carbon conversion; at higher w_t, $MeOH_1$ increases with the

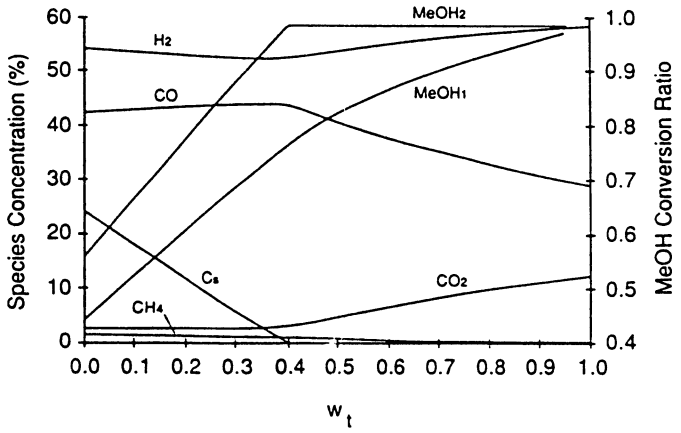

Figure 3. Equilibrium product composition and methanol conversion versus moisture in reactants for $T = 800$°C, $p = 1$ atm, and ER = 0.

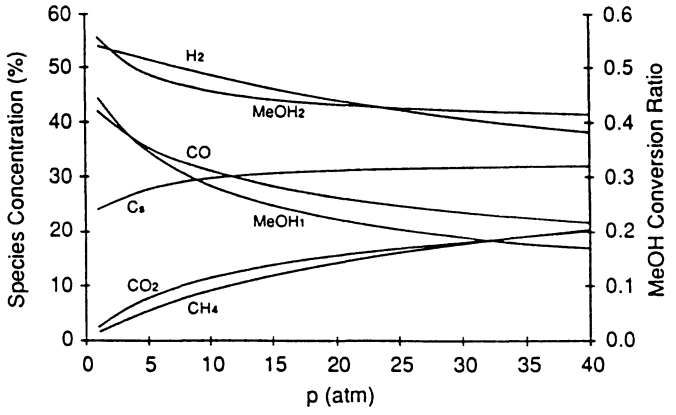

Figure 4. Equilibrium product composition and methanol conversion versus pressure for T = 800°C, ER = 0, and w_t = 0.

increasing hydrogen content in the gas. At w_t = 1, the ratio of hydrogen to carbon monoxide is approximately equal to 2.0, and, therefore, $MeOH_1 \approx MeOH_2$.

Solid carbon, carbon dioxide, and methane generally increase while the other gaseous products decrease as p increases (Fig. 4). Both methanol yields decrease as p increases because of lower carbon conversion; $MeOH_1$ is especially affected at high pressures by the high concentration of methane.

Optimization for Methanol Synthesis

The methanol synthesis reaction listed previously indicates that, for methanol production, a product gas with a H_2:CO ratio of approximately 2.0 is advantageous since this would allow for relatively high yield without the need to perform the shift reaction. Hence, equilibrium gas compositions and related data were computed with H_2:CO fixed at 2.0 to investigate biomass gasification conditions targeted to methanol synthesis. In these computations, it was assumed that no solid carbon remains.

Figure 5 displays the equilibrium gas composition for select conditions with the H_2:CO ratio fixed at 2.0 and indicates the amount of moisture required to maintain that

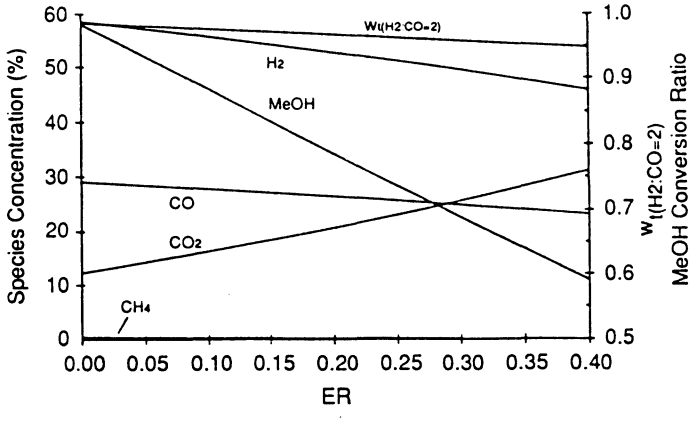

Figure 5. Gas composition, input moisture required, and methanol conversion versus equivalence ratio with H_2:CO = 2.0 for T = 800°C and p = 1 atm.

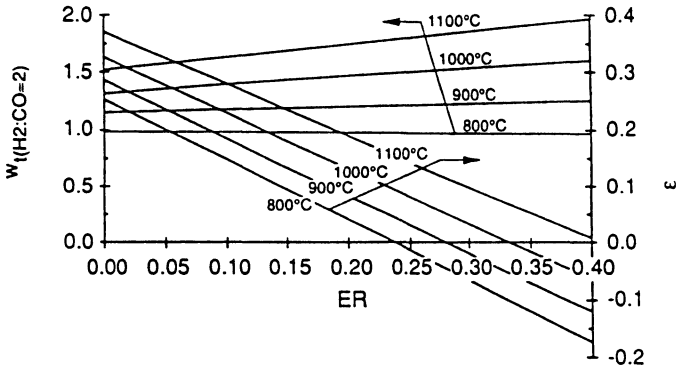

Figure 6. Moisture and energy inputs required versus equivalence ratio with H_2:CO = 2.0 and p = 1 atm for different gasification temperatures. In the ϵ computations, the moisture in the reactants is assumed to originate from injected steam (i.e., the feedstock is assumed to have zero moisture content) as saturated vapor at 1 atm.

ratio, $w_{t(H_2:CO=2)}$. All of the dependent variables plotted in Figure 5 vary almost linearly with ER.

The amount of moisture required to maintain H_2:CO equal to 2.0, $w_{t(H_2:CO=2)}$; and the Energy Input Ratio ϵ are plotted in Figure 6 as functions of ER for various T. The variable $w_{t(H_2:CO=2)}$ is not highly dependent on ER (for fixed T) and increases as T increases. Additional computations indicate that in the range of temperatures shown in Figure 6, the dry gas composition is not much different from that shown in Figure 5. ϵ decreases with increasing ER as the exothermic combustion reaction becomes more prevalent and increases with increasing T as more energy is needed to support the gasification process at elevated temperatures. The results of Figure 6 show that under certain conditions $\epsilon \leq 0$, in which case a gas with H_2:CO = 2.0 could be produced without relying on energy from an external source.

The gasification temperature, amount of steam required, and the theoretical methanol yield are plotted as functions of equivalence ratio in Figure 7 for adiabatic gasification of dry biomass to a gas with a H_2:CO ratio of 2.0. The adiabatic temperature and the

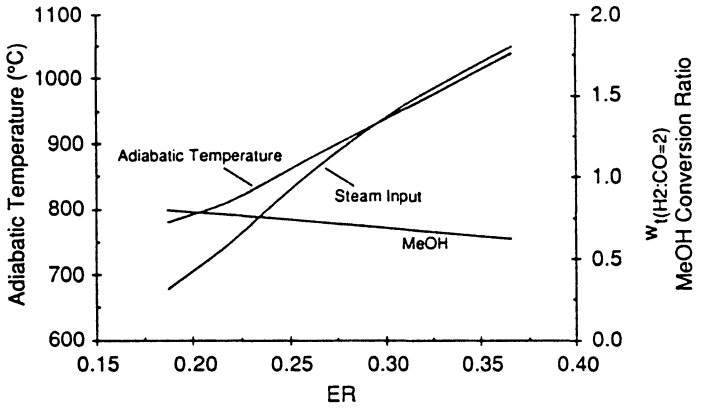

Figure 7. Gasification temperature, steam input required, and methanol conversion versus equivalence ratio in adiabatic gasification with H_2:CO = 2.0 and p = 1 atm. Feedstock moisture content assumed to be zero and injected steam assumed to be saturated vapor at 1 atm.

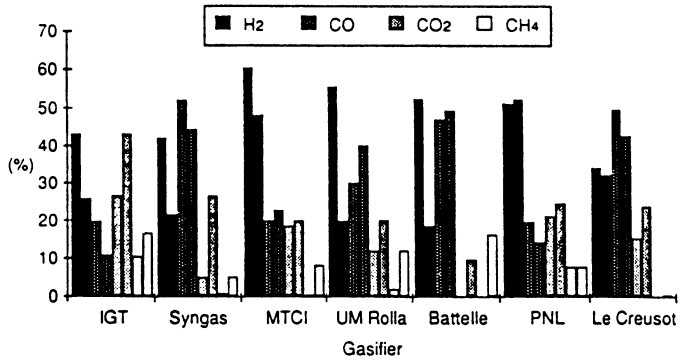

Figure 8. Comparison of theoretical (left of paired columns) versus actual (right of paired columns) gas compositions for different biomass gasification systems (inert-free basis). Data primarily from references: Evans et al. 1987 (IGT—pressurized fluid bed); Reed et al. 1987 (Syngas—downdraft); Durai-Swamy et al. 1989 (MTCI—indirectly fired); Flanigan and Sitton 1985 (UM Rolla—indirectly fired); Paisley et al. 1987 (Battelle-circulating bed); Baker et al. 1983 (PNL—catalytic steam gasification); and Chrysostome and Lemasle 1984 (Le Creusot—fluidized bed with secondary oxygen reforming).

amount of steam required to maintain H_2:CO = 2.0 both increase substantially with increasing ER. The methanol yield remains nearly constant over the range of ER presented in Figure 7, decreasing only slightly as ER and, consequently, the extent of combustion that occurs increase.

Comparison of Theoretical and Actual Data

Theoretical (equilibrium) computations are compared with actual (published experimental) data for different gasification systems in Figure 8. In most cases, the differences between the actual and theoretical results are substantial. The processes that most nearly approach equilibrium compositions are a catalytic-gasification process (PNL) and a secondary oxygen-reforming process (Le Creusot). For the production of methanol synthesis gas, it is assumed that one or more of several available gas processing and upgrading schemes such as those described elsewhere (Baker et al. 1983; Chrysostome and Lemasle 1984; Institute of Gas Technology 1989; Institute of Gas Technology 1985; Strom and Sjostrom 1984) can be employed to produce a gas of near equilibrium composition that is essentially free of oils, tars, and light hydrocarbons.

Summary

A computer program was developed to determine the equilibrium composition of biomass gasification and related information. The influences of ER, T, p, and w_t on biomass gasification were analyzed. The program was also used to determine the methanol theoretically obtainable under prescribed gasification conditions. The computations show that a gas with a H_2:CO ratio of 2.0, which is appropriate for methanol synthesis, can be obtained adiabatically by adjusting certain gasification parameters. The theoretical gas compositions were compared with experimentally obtained data. The comparisons were generally poor except for gasification processes that employed reforming schemes.

Acknowledgments

The authors wish to thank the U.S. Department of Energy, the Solar Energy Research Institute, and the State of Hawaii for partially funding this work.

References

Baker, E.G., D.H. Mitchell, L.K. Mudge, and M.D. Brown. 1983. Methanol synthesis gas from wood gasification. *Energy Progress* 3(4): 226–228.

Chrysostome, G., and J.-M. Lemasle. 1984. Syngas production from wood by oxygen gasification under pressure. *Bioenergy 84 Vol. 3 Biomass Conversion*, 73–79.

Durai-Swamy, K., D.W. Warren, B. Aghamahommadi, and M.N. Mansour. 1989. Pulse-assisted gasification of black liquor and organic wastes for medium-Btu gas. Presented at IGT Symposium on Energy from Biomass and Wastes XIII.

Evans, R.J., R.A. Knight, M. Onischak, and S.P. Babu. 1987. *Development of biomass gasification to produce substitute fuels*. Prepared for the U.S. Department of Energy under contract No. B-C5821-A-Q. March.

Flanigan, J., and O.C. Sitton. 1985. *Commercial design of an indirect fired fluid bed gasifier system*. Prepared for the U.S. Department of Energy under contract No. B-C5866A-Q. November.

Institute of Gas Technology. 1985. *Evaluation of coal conversion catalysts*. Contract No. 5014-322-0139. 1978–1985. Sponsored by Gas Research Institute.

Institute of Gas Technology. 1989. *Cooperative development of direct methanation technology*. Contract No. 5085-222-1159. 1986–1989. Sponsored by Gas Research Institute.

Paisley, M.A., H.F. Feldmann, and H.R. Appelbaum. 1987. Scale-up of a high-throughput gasifier to produce medium-Btu gas (500 Btu/scf) from wood. Presented at IGT Symposium on Energy from Biomass and Wastes XIII.

Reed, T.B., B. Levie, and M.S. Graboski. 1987. *Fundamentals, development and scaleup of the air-oxygen stratified downdraft gasifier*. Prepared for the U.S. Department of Energy under Contract No. DE-AC02-83CH10093. August.

Strom, E. and K. Sjostrom. 1984. Gasification of biomass in the MINO-process. *Bioenergy 84 Vol. 3 Biomass Conversion*, 57–64.

1991 SOLAR WORLD CONGRESS

VOLUME 1, PART II

Proceedings of the Biennial Congress of
the International Solar Energy Society,
Denver, Colorado, USA, 19-23 August 1991

Edited by
M.E. ARDEN
SUSAN M.A. BURLEY
MARTHA COLEMAN
American Solar Energy Society, Inc.,
Boulder, Colorado, USA

PERGAMON PRESS
OXFORD • NEW YORK • BEIJING •
FRANKFURT • SEOUL • SYDNEY • TOKYO

PARAMETRIC BENCH-TESTING OF AN INDIRECTLY HEATED, STEAM/OXYGEN-BLOWN BIOMASS GASIFIER

Y. Wang* and C.M. Kinoshita**

*Agricultural Engineering Department, University of Hawaii at Manoa, Honolulu, Hawaii
**Hawaii Natural Energy Institute, University of Hawaii at Manoa, 2540 Dole Street, Holmes 246, Honolulu, Hawaii 96822

ABSTRACT

Parametric tests are performed on an indirectly-heated, fluidized bed biomass gasifier. The test system allows feedstock, oxygen, nitrogen, and steam flow rates, and temperature to be controlled independently. Gas residence time, temperature, equivalence ratio, and steam:biomass ratio are varied, and product gas composition and select gasification parameters are evaluated and compared with theoretical predictions.

KEYWORDS

Gasification; biomass; methanol; indirect heating; fluidization; residence time; equivalence ratio; steam:biomass ratio.

INTRODUCTION

Substantial research on biomass gasification has been performed during the past decade, employing different gasifier configurations, oxidants, and modes of heating (e.g., Baker and coworkers 1983; Chrysostome and Lemasle 1984; Evans and coworkers 1987; Flanigan and Sitton 1985; Paisley, Feldmann, and Appelbaum 1987; Reed, Levie, and Graboski 1987). However, most of the biomass gasification studies performed to date have focused on the production of direct-combustion gases, not on the production of a synthesis gas for subsequent conversion into methanol. Thus, important information that could significantly impact the design and operation of biomass gasifiers and, ultimately, the yield and cost of producing methanol from biomass is largely lacking. This experimental work attempts to fill that void by correlating actual gasification behavior with theoretical predictions, with the overall goal of optimizing the conversion of biomass into methanol.

PROCEDURE

The experiments in this study were performed on a bench-scale, indirectly-heated, fluidized bed gasifier (Fig. 1) fabricated specifically to conduct experiments relating to biomass-to-methanol production. Oxygen and nitrogen streams entering the gasifier are adjusted independently with two mass flow controllers. The steam pressure is regulated to the desired value at the outlet of the steam generator and the flow rate is adjusted with a calibrated metering valve. A 10 kW electric heater is used to maintain the internal temperature of the gasifier at a specified level (up to 1100°C) via a temperature controller with PID mode.

The gasifier has an inside diameter of 89 mm and a overall height of 2500 mm. The disengagement section at the top of the vessel consists of a larger diameter (152 mm ID) pipe which reduces the gas velocity to prevent carry-over of the fluidization medium (alumina beads). A gas distributor, comprised of staggered perforated plates mounted at the bottom of the vessel, provides a uniform gas flow field to ensure thorough fluidization. Biomass is control-fed into the gasifier by a calibrated screw feeder which enters the vessel 250 mm above the gas distributor. The feeder is

sealed and pressurized with the dry inlet gases to prevent tars and steam from flowing back into the feeder. Nitrogen is used as a trace gas or as a diluent to vary the residence time of the gas in the vessel. Gas temperature is measured at several locations in the gasifier by thermocouples connected to an A/D board in the microcomputer. The product gas is cooled and cleaned, and then sampled and analyzed with a gas chromatograph.

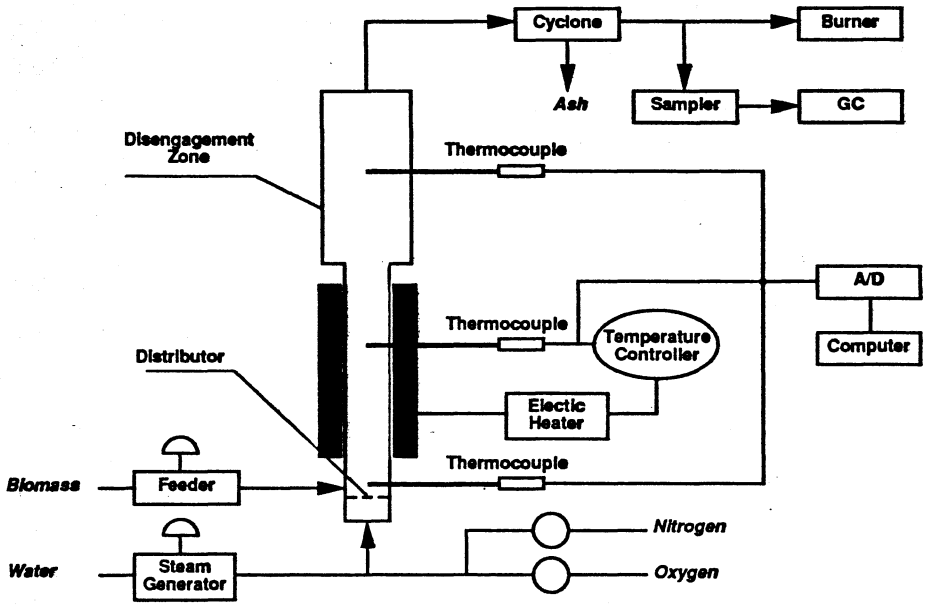

Fig. 1. Schematic of biomass gasifier test system.

Parametric biomass gasification tests, varying residence time, equivalence ratio (ER), temperature (T), and steam:biomass ratio (w_{st}), were performed at approximately atmospheric pressure using sawdust as the feedstock (with 7.8% moisture content, dry-matter basis).

The flow rates of product gas and water vapor at the gasifier outlet and the amount of carbon converted into dry gases are calculated from balances on trace gas (in this case, nitrogen), oxygen, and carbon, respectively. Three important indices of gasifier performance can be computed from the experimental data: (1) carbon conversion efficiency (ratio of carbon converted into dry gases divided by the total carbon in biomass), η_C; (2) volumetric gross heating value of the inert-free product gas, HHV; and (3) gas yield (volume of dry, inert-free gas produced per unit mass of fuel), GY.

RESULTS AND DISCUSSION

Residence Time

Residence time is varied in this test system by adjusting the nitrogen flow rate while fixing the oxygen flow, biomass feed rate, and temperature. Multiple gases and steam enter into or are evolved in the reactor and are entrained with the fluidization medium and char (solid carbon), and the gas flow rates and the temperature vary throughout the gasifier. These complications make the precise determination of residence time difficult. The residence time mentioned in this study is based on the superficial velocity of the input gases and steam, adjusted for expansion due to temperature elevation in the gasifier.

The inert-free gas composition is plotted as a function of residence time in Fig. 2a. (No steam was injected in those runs in which residence time was varied.) The trends in Fig. 2a show that, as expected, the longer the residence time, the more the product gas composition approaches equilibrium — hydrogen and carbon monoxide increase, and methane and other light hydrocarbons decrease. The influence of residence time on gasifier performance is presented in Fig. 2b. Carbon conversion efficiency and gas yield increase, and gross heating value remains approximately constant as residence time increases.

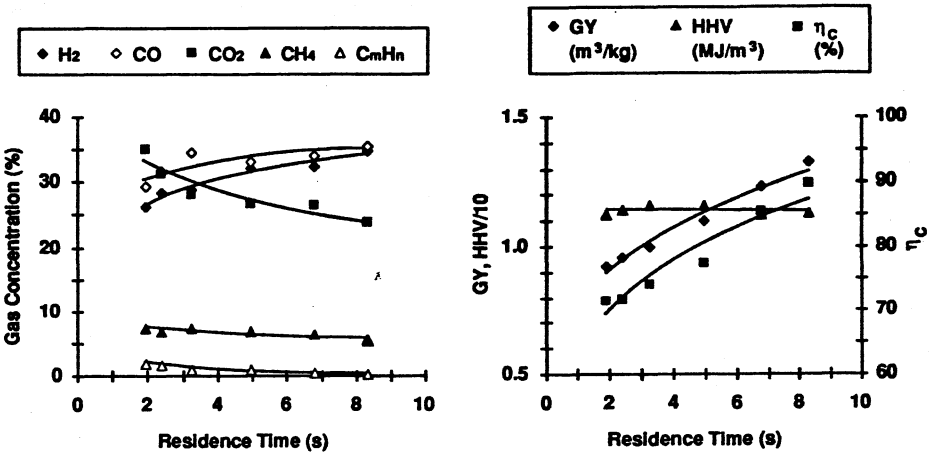

Fig. 2. (a) Inert-free product gas composition and (b) gasifier performance versus residence time (ER=0.30, T=800°C, w_{st}=0).

Equivalence Ratio

Equilibrium computations indicate that gasification is optimal at equivalence ratios between 0.2 and 0.4, a range in which most current gasification systems operate. The product gas composition is plotted in Fig. 3a as a function of equivalence ratio. (In these runs, T=800°C and no steam was injected.) Carbon monoxide and hydrogen decrease, and carbon dioxide increases as equivalence ratio increases. Methane and other light hydrocarbons remain virtually the same over all equivalence ratios tested. The trends exhibited are quite similar to those predicted by theory (Kinoshita, Wang, and Takahashi 1991), but the methane and carbon monoxide concentrations differ slightly from theoretical predictions — under equilibrium conditions, carbon monoxide reaches a maximum at ER=0.27 (at which point complete carbon conversion is achieved) and methane decreases with increasing equivalence ratio; these were not observed in the experiments.

Figure 3b illustrates the effect of equivalence ratio on gasifier performance. Carbon conversion efficiency increases due to decreased char formation, gross heating value decreases due to increased combustion (formation of carbon dioxide), while gas yield remains approximately constant, as equivalence ratio increases.

Temperature

The product gas composition is plotted as a function of temperature in Fig. 4a. (In these runs, ER=0.3 and no steam was injected.) The gas composition approaches equilibrium — hydrogen and carbon monoxide increase, while carbon dioxide, methane and other light hydrocarbons decrease, as temperature increases. Figure 4b illustrates the effect of temperature on gasifier performance. Gross heating value decreases as temperature increases due to decreases in the concentrations of methane and other light hydrocarbons which have relatively large heating values. Carbon conversion

efficiency increases markedly with increasing temperature due to accelerated chemical reaction, and gas yield increases significantly with increasing temperature due to reduced char formation and conversion of polyatomic hydrocarbons into greater molar quantities of diatomic species such as carbon monoxide and hydrogen.

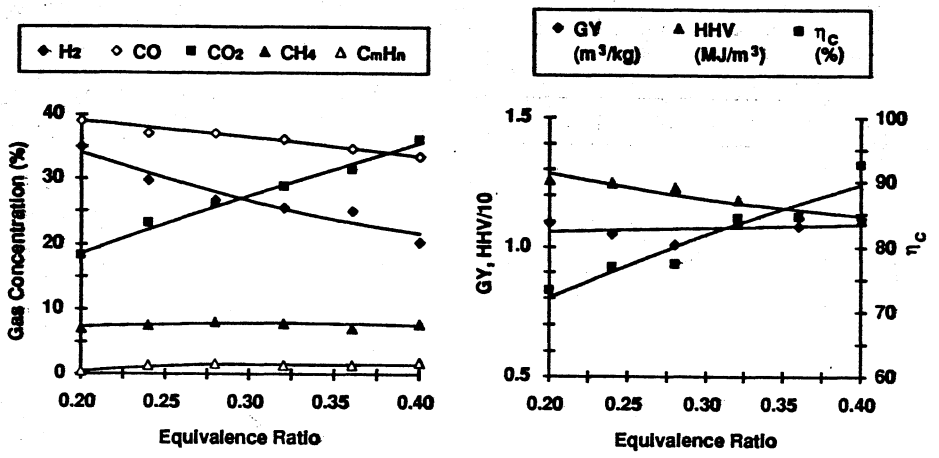

Fig. 3. (a) Inert-free product gas composition and (b) gasifier performance versus equivalence ratio (T=800°C, w_{st}=0).

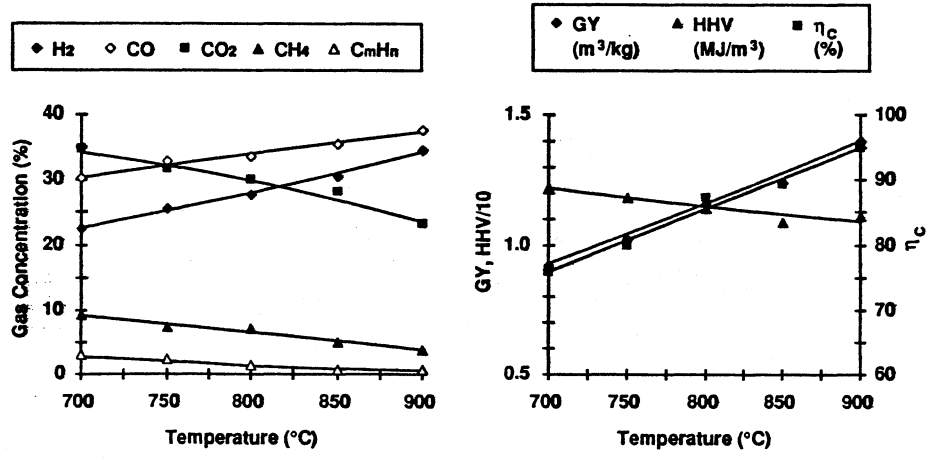

Fig. 4. (a) Inert-free product gas composition and (b) gasifier performance versus temperature (ER=0.30, w_{st}=0).

Equilibrium computations predict that char disappears and the concentrations of carbon monoxide and carbon dioxide change abruptly at 750°C, and that the gas composition changes very little at temperatures above 750°C. However, such trends were not observed in these experiments. All gaseous components vary monotonically with temperature indicating the existence of non-equilibrium gasification conditions even at relatively high (~900°C) temperatures.

Steam:Biomass Ratio

Steam gasification was tested under fairly low equivalence ratio (ER = 0.2) at a fixed gasification temperature (800°C). The steam:biomass ratio can be changed either by varying the input steam flow rate (while fixing the biomass feed rate) or by varying the biomass feed rate (while fixing the steam flow rate). The latter was adopted in this experiment because of its smaller effect on residence time.

The inert-free gas composition is plotted against steam:biomass ratio in Fig. 5a. In the range of steam:biomass ratios tested, hydrogen increases, carbon monoxide decreases slightly, and carbon dioxide remains roughly the same as the amount of steam increases, while the amounts of methane and other light hydrocarbons produced decrease slightly as the steam:biomass ratio increases. The influence of steam:biomass ratio on gasifier performance is presented in Fig. 5b. Carbon conversion efficiency and gas yield increase as the steam:biomass ratio increases. The gross heating value decreases due to reductions in methane and other light hydrocarbons produced as the steam:biomass ratio increases.

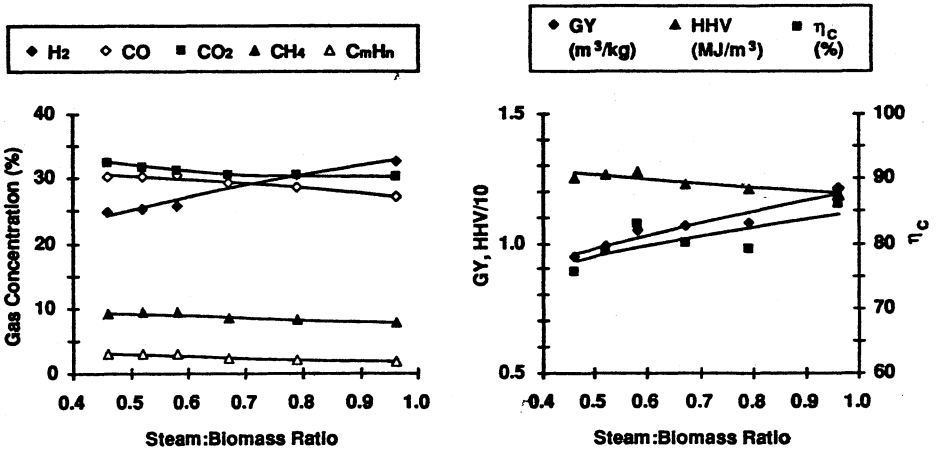

Fig. 5. (a) Inert-free product gas composition and (b) gasifier performance versus steam:biomass ratio (ER=0.20, T=800°C).

The trends in the steam gasification tests agree fairly well with equilibrium computations for most species except carbon dioxide. Under equilibrium conditions, carbon dioxide increases as the steam:biomass ratio increases. Such was not the case in these experiments. As under equilibrium conditions, hydrogen increases with increasing steam:biomass ratio. However, if the steam:biomass ratio were increased at fixed biomass feed rate, then the residence time would decrease. This could result in the production of less hydrogen (see Fig. 2a). Thus, the actual hydrogen concentration is influenced by competition between residence time versus the amount of steam injected. Indeed, increasing the steam:biomass ratio could result in less, not more, hydrogen, if the effect of residence time dominates that of steam injection.

SUMMARY AND CONCLUSIONS

An indirectly-heated fluidized bed biomass gasifier was designed and fabricated. Biomass feedstock, oxygen, nitrogen, and steam flow rates, and temperature are controlled in the test system. Gas residence time, temperature, equivalence ratio, and steam:biomass ratio were varied in parametric tests, and product gas composition and select gasification parameters were evaluated.

The product gas approaches equilibrium composition (i.e., hydrogen and carbon monoxide increase, and methane and other light hydrocarbons decrease), and carbon conversion and gas yield increase,

as residence time increases. Hydrogen, carbon monoxide, and gross heating value decrease, and carbon dioxide and carbon conversion efficiency increase, as equivalence ratio increases. Hydrogen, carbon monoxide, carbon conversion, and gas yield increase, and carbon dioxide, hydrocarbons, and heating value decrease, as temperature increases. Hydrogen, gas yield, and carbon conversion increase, and carbon monoxide, hydrocarbons, and heating value decrease, as steam:biomass ratio increases.

Presently, the data collected in this study are being reviewed to assess deviations of actual behavior from theoretical predictions and to evaluate the effects of varying select parameters on methanol production. Future planned and/or recommended work includes measurement and analysis of the tars and oils produced in the gasifier, evaluation of catalysts to determine whether they might be used more successfully than in previous tests to facilitate the production of methanol synthesis gas, and development of a simplified kinetic model which links actual and theoretical behavior so that the performance of gasification systems can be determined *a priori*.

ACKNOWLEDGEMENTS

The authors wish to thank Dr. Michael Antal, Jr., Coral Industries Professor of Renewable Energy Resources, and Mr. William Mok, Chemical Research Engineer, of the Hawaii Natural Energy Institute, for providing the biomass feeder and the steam generator used in this experiment and for offering valuable assistance and guidance. The authors also thank the U.S. Department of Energy, the Solar Energy Research Institute, and the State of Hawaii for funding this work; and Dr. Victor Phillips, Manager of the Hawaii Integrated Biofuels Research Program, for his support in this project.

REFERENCES

Baker, E.G., D.H. Mitchell, L.K. Mudge, and M.D. Brown. (1983). Methanol synthesis gas from wood gasification. *Energy Progress 3(4)*, 226-228.

Chrysostome, G. and J.-M. Lemasle. (1984). Syngas production from wood by oxygen gasification under pressure. *Bioenergy 84 Vol. 3 Biomass Conversion*, 73-79.

Evans, R.J., R.A. Knight, M. Onischak, and S.P. Babu. (1987). *Development of biomass gasification to produce substitute fuels.* Prepared for the U.S. Department of Energy under contract No. B-C5821-A-Q. March.

Flanigan, J. and O.C. Sitton. (1985). *Commercial design of an indirect fired fluid bed gasifier system.* Prepared for the U.S. Department of Energy under contract No. B-C5866A-Q. November.

Kinoshita, C.M., Y. Wang, and P.K. Takahashi. (1991). Chemical equilibrium computations for gasification of biomass to produce methanol. *Energy Sources 13*, 361-368.

Paisley, M.A., H.F. Feldmann, and H.R. Appelbaum. (1987). Scale-up of a high-throughput gasifier to produce medium-Btu gas (500 Btu/scf) from wood. Presented at IGT Symposium on Energy from Biomass and Wastes XIII.

Reed, T.B., B. Levie, and M.S. Graboski. (1987). *Fundamentals, development and scaleup of the air-oxygen stratified downdraft gasifier.* Prepared for the U.S. Department of Energy under Contract No. DE-AC02-83CH10093. August.

Y. Wang[1]

C. M. Kinoshita
Researcher.

Hawaii Natural Energy Institute,
University of Hawaii at Manoa,
Honolulu, HI 96822

Temperature Field and Reaction Zones in Biomass Gasification

A method used to measure and validate the temperature field in an experimental downdraft biomass gasifier and reformulate the discrete test data into continuous mathematical functions is described. The reformulated temperature field is analyzed to identify different reaction zones within the gasifier. Distinct endothermic and exothermic regions, separated by rather complicated boundaries, are found.

Introduction

Biomass gasification is a complicated thermochemical process which involves pyrolysis, combustion, and reduction. Since the directions and rates of these reactions are highly dependent on temperature, analysis of the temperature field within a gasifier would contribute to the fundamental understanding and the engineering of biomass gasifiers.

Although much basic and applied research has been performed on downdraft biomass gasifiers during the past decade (Walawender, Chern, and Fan 1986; Graboski and Brogan, 1987; Reed and Das, 1988; Reed, Levie, and Graboski, 1988; Schiefelbein, 1989), very little work has been conducted on measuring the temperature distribution and identifying the different reaction zones within such gasifiers. This study was established to address those issues. Here, discrete temperatures in a specially fabricated downdraft gasifier are measured; surface-fitting techniques are used to reduce the discrete temperature data to continuous analytical functions; and then the reformulated temperature field is analyzed to identify the endothermic and exothermic zones.

Test System, Data Collection, and Processing

The experimental system—downdraft gasifier and temperature measurement and data processing system—is illustrated in Fig. 1. The 90-cm diameter gasifier was specially fabricated with access holes for thermocouple measurements. Temperature measurements were performed within the 45 cm (radial direction) × 72 cm (axial direction) shaded region—the reaction zone, where most of the important reactions occur—during steady-state operation. The 100 measurement locations were distributed uniformly within the shaded region in a 10 × 10 array. Whether the individual thermocouple readings reflect the temperatures of particle surfaces or the gas stream is unknown; however, it is believed that any differences between the temperature of particle surfaces and the temperature of the adjacent gas stream would be negligible (Reed, Levie, and Graboski, 1988). Air was preheated in an air jacket and then injected into the reaction zone through nine circumferentially located nozzles and one central nozzle (the tube leading to the central nozzle is not shown in Fig. 1). The feedstock used in the test was prepared corn cobs (≤ 70 mm, ~ 10 percent moisture content), and the feed rate was controlled nominally at 400 kg/h and the equivalence ratio at approximately 0.3.

Data Validation. The temperature field is relatively stable overall when the gasifier operates at steady state; however, the temperatures at individual points fluctuate. To expedite data collection and ensure precision in the temperatures measured

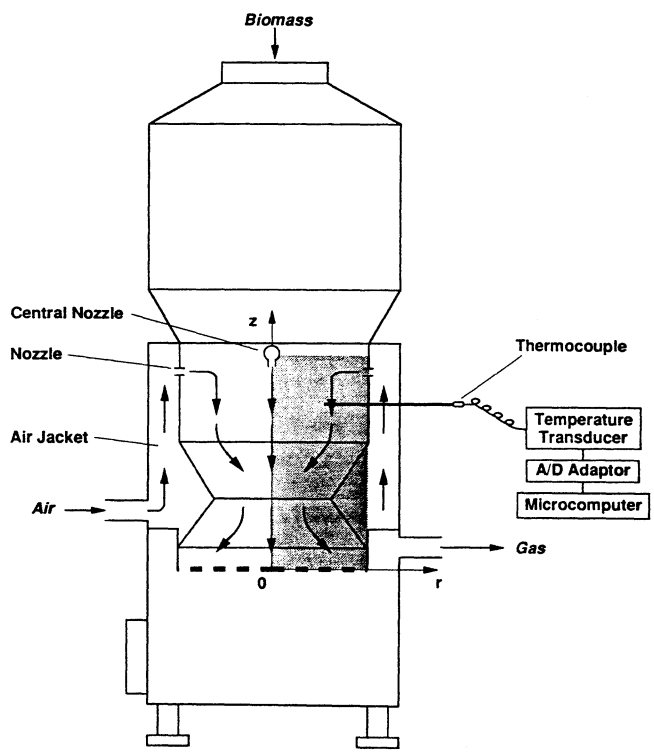

Fig. 1 Downdraft biomass gasifier test system (shaded region represents reaction zone, where temperature measurements were made)

[1] Visiting Researcher from the Energy and Power Institute, Chinese Academy of Agricultural Mechanication Sciences.

Contributed by the Solar Energy Division of THE AMERICAN SOCIETY OF MECHANICAL ENGINEERS for publication in the JOURNAL OF SOLAR ENERGY ENGINEERING. Manuscript received by the ASME Solar Energy Division, Oct. 11, 1990; final revision, June 24, 1991.

during the experiments, the statistical hypothesis test described below was employed in the data acquisition computer program.

Consider the null hypothesis (H_O): $\mu_1 = \mu_0$ and the alternate hypothesis (H_A): $\mu_1 \neq \mu_0$, where μ_0 and μ_1 are the population means of two consecutive statistical samples. H_O is rejected at the confidence level $1-\alpha$ whenever

$$|T_1 - T_0| > Z_{\alpha/2} S_w (1/n_1 + 1/n_0)^{0.5} \quad (1)$$

where T_0 and T_1 are the means of the two consecutive samples of sizes n_0 and n_1, respectively, Z is a random variable with a standard normal distribution, and $S_w = \{((n_1-1)S_1^2 + (n_0-1)S_0^2)/(n_0+n_1-2)\}^{0.5}$, in which S_0 and S_1 are the standard deviations of the two samples. Equation (1) represents the criterion used in the data acquisition computer program to determine whether individual data samples collected in the experiment were statistically valid.

Determination of Appropriate Sample Size. Two types of errors can occur in hypothesis testing (Rice, 1988). The probability of committing a Type I error (i.e., rejecting a true H_O) is equal to α. If the probability of committing a Type II error (retaining a false H_O) is denoted by β (Fig. 2), it can be shown that, for prescribed α, β, and error, $|\mu_1 - \mu_0|$, the sample size, n, should be

$$n \geq \{(Z_\alpha + Z_\beta) S/(\mu_1 - \mu_0)\}^2 \quad (2)$$

where S is the standard deviation. Thus, the probabilities of committing either error can be maintained below α and β by securing a satisfactorily large sample. The sample size used in the experiment, 200, easily satisfies Eq. (2) for $\alpha = \beta = 0.005$ and $|\mu_1 - \mu_0| = 5°C$.

Data Reformulation. The temperature measurements made with the computerized data acquisition and validation system were stored as a two-dimensional array, $T_{ij} = T(r_i, z_j)$. Surface fitting techniques were then used to convert the discrete temperature data, T_{ij}, into continuous analytic functions, $T_s(r, z)$, which, within the boundaries of the gasifier, have the same concave-convex pattern as T_{ij} and agree with T_{ij} to within a prescribed tolerance, $\epsilon \geq |T_s(r_i, z_j) - T(r_i, z_j)|$.

Analysis of Temperature Field

The following energy balance expression can be derived from relationships presented by Williams (1965) for a flowing, reacting system:

$$q''' = -\nabla \cdot (k/c_p \nabla h) + \rho \mathbf{V} \cdot \nabla h \quad (3)$$

where q''' is the thermal energy released per unit time and per unit volume, $\mathbf{V}$ is the mass-averaged velocity, and h, k, c_p, and ρ denote the mass-averaged sensible enthalpy, thermal conductivity, specific heat, and density, respectively. Roughly speaking, the two terms on the right side of Eq. (3) represent, respectively, thermal energy conducted and convected out of an elemental volume per unit time and per unit volume, and $q''' > 0$ indicates the presence of an energy source (i.e., an exothermic reaction) and $q''' < 0$ indicates the presence of an energy sink (i.e., an endothermic reaction).

Adequate for the purposes of this study—to determine what zones in the gasifier are exothermic versus endothermic—the thermal conductivity and specific heats are assumed to be fixed within the reaction zone. Equation (3) can then be rewritten as:

$$q''' = -k\nabla^2 T + \rho c_p \mathbf{V} \cdot \nabla T. \quad (4)$$

The conduction term in Eq. (4) can be determined from the temperature field, $T_s(r, z)$, and properties data. The convection term, however, depends not only on the temperature field and properties, but on the velocity field $\mathbf{V}$ (with components V_r and V_z) as well, which makes its determination more difficult. However, as described later, its contribution to thermal energy transfer within the gasifier can be assessed roughly, and in so doing, the exothermic and endothermic regions might be identifiable.

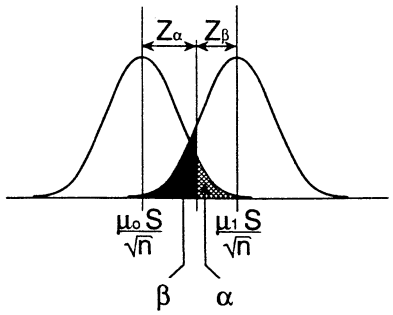

Fig. 2 Probability distributions of two normal samples

Experimental Results and Identification of Reaction Zones

The transformed temperature field, $T_s(r, z)$, in the reaction zone of the experimental downdraft biomass gasifier is presented in a contour map and three dimensionally in Fig. 3(*a*) and 3(*b*), respectively ($\epsilon = 5°C$). Although symmetry dictates that the temperature gradient at the centerline ($r = 0$) should be zero, the computer software employed to obtain the surface fit does not permit the imposition of that boundary condition—hence the nonperpendicular intersections of the temperature contour lines with the centerline. In spite of that deficiency, it is believed that the temperature field is accurately represented.

Figure 3 shows that presence of two temperature peaks—one below the center nozzle ($r < 15$ cm, $z > 40$ cm), with temperatures ranging from 900°C to 1100°C, and the other inside of the peripheral nozzles (10 cm $< r <$ 30 cm, 30 cm $< z <$ 50 cm), with temperatures exceeding 900°C. The temperature gradients along the flow paths of the air streams approaching the peak temperature centers are significantly higher than elsewhere, suggesting the presence of highly exothermic reactions.

An order of magnitude comparison of the two terms on the right side of Eq. (4) indicates that for biomass gasification the second (convection) term is several orders of magnitude greater than the first (conduction) term. Therefore, only the convec-

Nomenclature

- c_p = specific heat
- h = sensible enthalpy
- H_A = alternate hypothesis
- H_O = null hypothesis
- k = thermal conductivity
- n = sample size
- q''' = energy generation rate per unit volume
- r = coordinate, radial direction
- S = standard deviation
- T = temperature
- T_s = continuous temperature field obtained by fitting the discrete data
- $\mathbf{V}$ = velocity vector
- V_i = velocity component in i direction ($i = r, z$)
- z = coordinate, axial direction
- z_t = axial coordinate of gasifier throat
- Z = random variable with standard normal distribution
- α = probability of Type I error
- β = probability of Type II error
- ϵ = fitting tolerance
- μ = population mean
- ρ = density

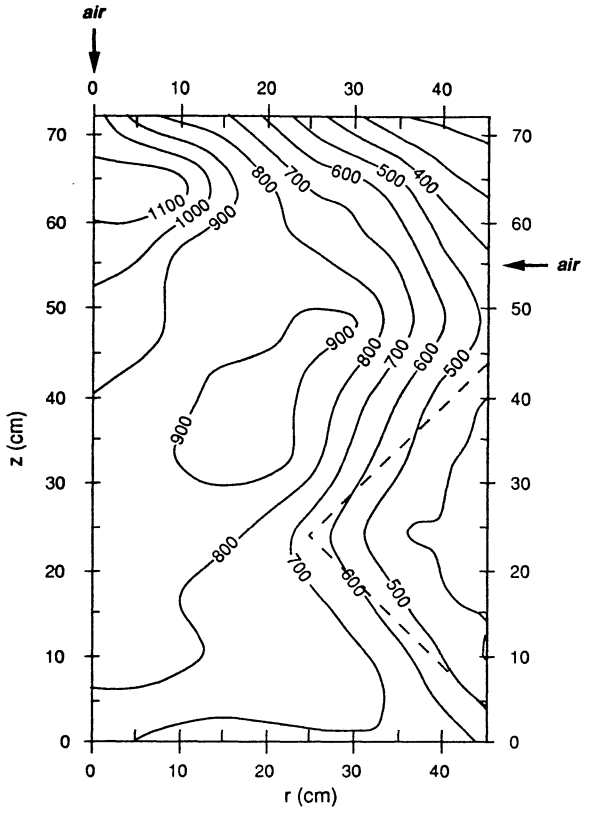

Fig. 3(*a*) Temperature contour map (dashed lines designate throat section of gasifier)

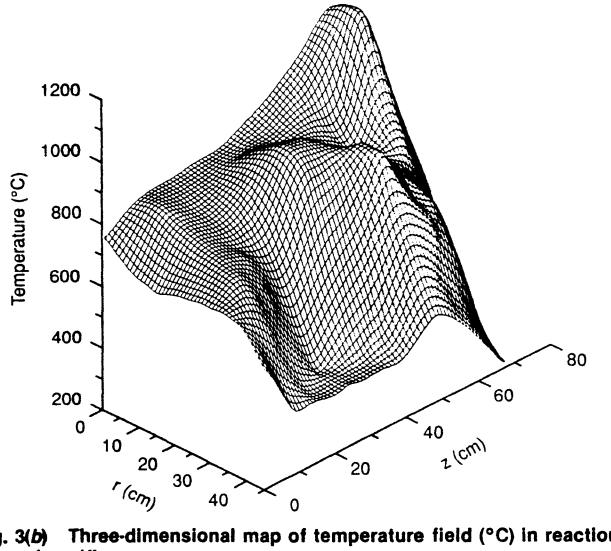

Fig. 3(*b*) Three-dimensional map of temperature field (°C) in reaction zone of gasifier

tion term is considered in the following discussion. It was assumed that above the throat section (i.e., above the minimum area section located at z_t; here, $z_t = 24$ cm) of the gasifier, the radial component of the mass-averaged velocity is inward (i.e., $V_r < 0$ for $z > z_t$, while below the throat, it is outward (i.e., $V_r > 0$ for $z < z_t$). The axial velocity was assumed to be downward throughout the gasifier (i.e., $V_z < 0$ for $z > 0$). The assumed flow path, which conforms to the geometry of the gasifier, is illustrated in Fig. 1.

Figure 4 shows the various zones within the gasifier based on substitution of the temperature field and the assumed local flow directions into Eq. (4). In the regions marked predominantly by "+" in Fig. 4, $\partial T/\partial r < 0$ and $\partial T/\partial z < 0$ for $z > z_t$, or $\partial T/\partial r > 0$ and $\partial T/\partial z < 0$ for $z < z_t$. The region near the entrance of the reaction zone with $T > 600°C$ contains exothermic, combustion reactions. Temperatures in that region increase along the direction of flow to a maximum of ~1200°C. Although the region above the peripheral nozzles is also labeled as exothermic, the temperature is quite low (<600°C) and relatively little air passes through that region; hence, that region more likely contains pyrolysis reactions. In the regions marked predominantly by "−" in Fig. 4, $\partial T/\partial r > 0$ and $\partial T/\partial z > 0$ for $z > z_t$, or $\partial T/\partial r < 0$ and $\partial T/\partial z > 0$ for $z < z_t$. Those regions, mostly near the throat of the gasifier, are endothermic reduction zones. Temperatures in those regions are mostly in the 700 to 900°C range. In the regions marked by "0," the above conditions do not hold, thus implying that the convection of thermal energy along the two coordinate directions (r and z) oppose each other in those regions. Little can be concluded on the exothermic or endothermic nature of the reactions within those regions without performing more detailed computations. Throughout much of the region near the centerline and above the throat ($z > z_t$) but below the exothermic zone, $\partial T/\partial r < 0$ and $\partial T/\partial z > 0$, hence that region is designated as neither exothermic nor endothermic (marked by "0"). Since in that region $|V_r| \ll |V_z|$, the radial convection term is dominated by the axial term. Hence, that region should more appropriately be designated as endothermic ("−"). The temperature near the bottom of the gasifier is relatively low—600 to 700°C. That region, composed primarily of char, is largely inert.

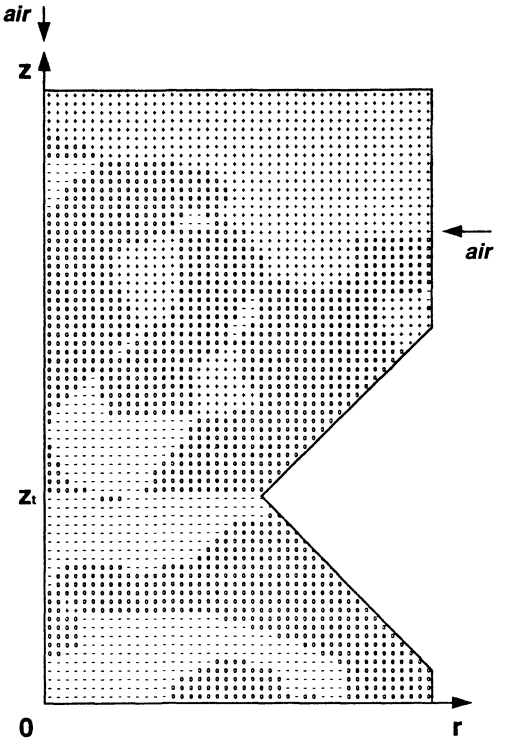

Fig. 4 Reacting zones within the gasifier that appear to be exothermic ("+") or endothermic ("−"); zones marked by "0" are not obviously exothermic or endothermic

Summary and Conclusions

The temperature field within an experimental downdraft biomass gasifier was measured. A computerized system, employing statistical hypothesis testing, was used in the experiment to collect and validate the temperature data. Surface fitting techniques were used to convert the discrete temperature data into continuous fitting functions which enabled further mathematic manipulation of the data. Different reaction zones

were identified based on the resultant temperature field and its apparent relationship with the thermal energy transfer mechanisms occurring within the gasifier. Quite distinct endothermic and exothermic regions were found; however, the regions are separated by rather complicated boundaries instead of the simple, horizontal boundaries often described in the literature.

Acknowledgments

The authors wish to thank the U.S. Department of Energy, the Solar Energy Research Institute, and the State of Hawaii for partially funding this work.

References

Graboski, M. S., and Brogan, T. R., 1987, "Development of a Downdraft Modular Skid Mounted Biomass/Waste Gasification System," Energy from Biomass and Wastes, XI.

Reed, T. B., and Das, A., 1988, "Handbook on Biomass Downdraft Gasifier Energy Systems," SERI/SP-271-3022, DE88001135, Mar.

Reed, T. B., Levie, B., and Graboski, M. S., 1988, "Fundamentals, Development and Scaleup of the Air-Oxygen Stratified Downdraft Gasifier," SERI/PNL-6600, June.

Rice, J. A., 1988, *Mathematical Statistics and Data Analysis*, Wadsworth & Brooks/Cole Advanced Books & Software, Pacific Grove, Calif., p. 270.

Schiefelbein, G. F., 1989, "Biomass Thermal Gasification Research: Recent Results from the United States DOE's research program," *Biomass*, Vol. 19, pp. 145-159.

Walawender, W. P., Chern, S. M., and Fan, L. T., 1986, "Influence of Operating Parameters on the Performance of a Wood-Fed Downdraft Gasifier," Energy from Biomass and Wastes, X.

Williams, F. A., 1965, *Combustion Theory: The Fundamental Theory of Chemically Reacting Flow Systems*, Addison-Wesley, Reading, Mass.

EXPERIMENTAL ANALYSIS OF BIOMASS GASIFICATION WITH STEAM AND OXYGEN

Y. Wang and C.M. Kinoshita

Hawaii Natural Energy Institute
University of Hawaii at Manoa
2540 Dole Street, Holmes Hall 246
Honolulu, Hawaii 96822

ABSTRACT

Parametric tests are performed on an indirectly-heated, fluidized bed biomass gasifier. The test system allows feedstock, oxygen, nitrogen, and steam flow rates, and temperature to be controlled independently. Gas residence time, temperature, equivalence ratio, and steam:biomass ratio are varied, and product gas composition and select gasification parameters are evaluated and compared with theoretical predictions.

INTRODUCTION

Methanol, produced via biomass gasification, has the potential to contribute substantially to future supplies of renewable transportation fuels. Technoeconomic analyses (e.g., Ref. [1]) have indicated that gasification of biomass for methanol synthesis can be economically feasible where biomass can be grown and processed efficiently and in sufficient quantities. Substantial research on biomass gasification has been performed during the past decade, employing different gasifier configurations, oxidants, and modes of heating [2–7]. However, most of the biomass gasification studies performed to date have focused on the production of direct-combustion gases, not on the production of a synthesis gas for subsequent conversion into methanol. Moreover, very little experimental research has been performed to analyze the influence of gasification parameters on product gas composition and gasifier performance. Thus, important information that could significantly impact the design and operation of biomass gasifiers and, ultimately, the yield and cost of producing methanol from biomass is largely lacking. This experimental work

attempts to fill that void by correlating actual gasification behavior with theoretical predictions, with the overall goal of optimizing the conversion of biomass into methanol.

PROCEDURE

The experiments in this study were performed on a bench-scale, indirectly-heated, fluidized bed gasifier (Fig. 1) fabricated specifically to conduct experiments relating to biomass-to-methanol production. Oxygen and nitrogen streams entering the gasifier are adjusted independently with two mass flow controllers. The steam pressure is regulated to the desired value at the outlet of the steam generator and the flow rate is adjusted with a calibrated metering valve. A 10 kW electric heater is used to maintain the internal temperature of the gasifier at a specified level (up to 1100° C) via a temperature controller with PID mode.

The gasifier has an inside diameter of 89 mm and an overall height of 2500 mm. The disengagement section at the top of the vessel consists of a larger diameter (152 mm ID) pipe which reduces the gas velocity to prevent carry-over of the fluidization medium (alumina beads). A gas distributor, comprised of staggered perforated plates mounted at the bottom of the vessel, provides a uniform gas flow field to ensure thorough fluidization. Biomass is control-fed into the gasifier by a calibrated screw feeder which enters the vessel 250 mm above the gas distributor. The feeder is sealed and pressurized with the dry inlet gases to prevent tars and steam from flowing back into the feeder. Nitrogen is used as a trace gas or as a diluent to vary the residence time of the gas in the vessel. Gas temperature is measured at several locations in the gasifier by thermocouples connected to an A/D board in the microcomputer. The product gas is cooled and cleaned, and then sampled and analyzed with a gas chromatograph.

Parametric biomass gasification tests, varying residence time, equivalence ratio (ER), temperature (T), and steam:biomass ratio (w_{st}), were performed at approximately atmospheric pressure using sawdust as the feedstock (with 7.8% moisture content, dry-matter basis).

The flow rates of product gas and water vapor at the gasifier outlet and the amount of carbon converted into dry gases are calculated from balances on trace gas (in this case, nitrogen),

oxygen, and carbon, respectively. Three important indices of gasifier performance can be computed from the experimental data: (1) carbon conversion efficiency (ratio of carbon converted into dry gases divided by the total carbon in biomass), η_C; (2) volumetric gross heating value of the inert-free product gas, HHV; and (3) gas yield (volume of dry, inert-free gas produced per unit mass of fuel), GY.

RESULTS AND DISCUSSION

Residence Time

Residence time is varied in this test system by adjusting the nitrogen flow rate while fixing the oxygen flow, biomass feed rate, and temperature. Multiple gases and steam enter into or are evolved in the reactor and are entrained with the fluidization medium and char (solid carbon), and the gas flow rates and the temperature vary throughout the gasifier. These complications make the precise determination of residence time difficult. The residence time mentioned in this study is based on the superficial velocity of the input gases and steam, adjusted for expansion due to temperature elevation in the gasifier.

The inert-free gas composition is plotted as a function of residence time in Fig. 2a. (No steam was injected in those runs in which residence time was varied.) The trends in Fig. 2a show that, as expected, the longer the residence time, the more the product gas composition approaches equilibrium — hydrogen and carbon monoxide increase, and methane and other light hydrocarbons decrease. The influence of residence time on gasifier performance is presented in Fig. 2b. Carbon conversion efficiency and gas yield increase, and gross heating value remains approximately constant as residence time increases.

Equivalence Ratio

Equilibrium computations indicate that gasification is optimal at equivalence ratios between 0.2 and 0.4, a range in which most current gasification systems operate. The product gas composition is plotted in Fig. 3a as a function of equivalence ratio. (In these runs, T=800° C and no

steam was injected.) Carbon monoxide and hydrogen decrease, and carbon dioxide increases as equivalence ratio increases. Methane and other light hydrocarbons remain virtually the same over all equivalence ratios tested. The trends exhibited are quite similar to those predicted by theory [8], but the methane and carbon monoxide concentrations differ slightly from theoretical predictions — under equilibrium conditions, carbon monoxide reaches a maximum at ER=0.27 (at which point complete carbon conversion is achieved) and methane decreases with increasing equivalence ratio; these were not observed in the experiments.

Figure 3b illustrates the effect of equivalence ratio on gasifier performance. Carbon conversion efficiency increases due to decreased char formation, gross heating value decreases due to increased combustion (formation of carbon dioxide), while gas yield remains approximately constant, as equivalence ratio increases.

Temperature

The product gas composition is plotted as a function of temperature in Fig. 4a. (In these runs, ER=0.3 and no steam was injected.) The gas composition approaches equilibrium — hydrogen and carbon monoxide increase, while carbon dioxide, methane, and other light hydrocarbons decrease — as temperature increases. Figure 4b illustrates the effect of temperature on gasifier performance. Gross heating value decreases as temperature increases due to decreases in the concentrations of methane and other light hydrocarbons which have relatively large heating values. Carbon conversion efficiency increases markedly with increasing temperature due to accelerated chemical reaction, and gas yield increases significantly with increasing temperature due to reduced char formation and conversion of polyatomic hydrocarbons into greater molar quantities of diatomic species such as carbon monoxide and hydrogen.

Equilibrium computations predict that char disappears and the concentrations of carbon monoxide and carbon dioxide change abruptly at 750° C, and that the gas composition changes very little at temperatures above 750° C. However, such trends were not observed in these experiments.

All gaseous components vary monotonically with temperature indicating the existence of non-equilibrium gasification conditions even at relatively high (~900° C) temperatures.

Steam:Biomass Ratio

Steam gasification was tested under fairly low equivalence ratio (ER=0.2) at a fixed gasification temperature (800° C). The steam:biomass ratio can be changed either by varying the input steam flow rate (while fixing the biomass feed rate) or by varying the biomass feed rate (while fixing the steam flow rate). The latter was adopted in this experiment because of its smaller effect on residence time.

The inert-free gas composition is plotted against steam:biomass ratio in Fig. 5a. In the range of steam:biomass ratios tested, hydrogen increases, carbon monoxide decreases slightly, and carbon dioxide remains roughly the same as the amount of steam increases, while the amounts of methane and other light hydrocarbons produced decrease slightly as the steam:biomass ratio increases. The influence of steam:biomass ratio on gasifier performance is presented in Fig. 5b. Carbon conversion efficiency and gas yield increase as the steam:biomass ratio increases. The gross heating value decreases due to reductions in methane and other light hydrocarbons produced as the steam:biomass ratio increases.

The trends in the steam gasification tests agree fairly well with equilibrium computations for most species except carbon dioxide. Under equilibrium conditions, carbon dioxide increases as the steam:biomass ratio increases. Such was not the case in these experiments. As under equilibrium conditions, hydrogen increases with increasing steam:biomass ratio. However, if the steam:biomass ratio were increased at fixed biomass feed rate, then the residence time would decrease. This could result in the production of less hydrogen (see Fig. 2a). Thus, the actual hydrogen concentration is influenced by competition between residence time versus the amount of steam injected. Indeed, increasing the steam:biomass ratio could result in less, not more, hydrogen, if the effect of residence time dominates that of steam injection.

Comparison of Theoretical and Actual Performance

Theoretical (equilibrium) data, computed as described in Ref. [8], are compared with experimental data from selected test runs in Fig. 6. Under most conditions tested in this study, the differences between the actual gas composition and the equilibrium gas composition are substantial. This is not surprising as earlier comparisons of equilibrium versus actual performance data for other gasification systems indicate that none of the existing gasification systems can produce a gas with near-equilibrium composition without employing catalysts or secondary oxygen-reforming [8].

The actual gas composition in Test RT6 (longest residence time) is significantly closer to the equilibrium gas composition than in Test RT1 (shortest residence time), as increasing residence time improves the extent of gasification reactions. The hydrogen in test RT6 is almost the same as the equilibrium level; however, carbon monoxide, carbon dioxide, and methane in Test RT6 still differ substantially from equilibrium.

Theoretical computations indicate that the equilibrium gas composition changes very little at temperatures above 750° C [8]. The data for T2 (T=750° C) and T5 (T=900° C) are selected to test the theory. The actual gas composition in Test T5 is closer to equilibrium than in Test T2, indicating that under the conditions of these experiments, increasing the temperature improves the extent of gasification reactions well above 750° C. At the highest temperature tested (Test T5), the hydrogen concentration is quite close to the equilibrium value; however, carbon monoxide, carbon dioxide, and methane concentrations still differ substantially from equilibrium levels.

The differences between actual and equilibrium compositions for ER1 (ER=0.2) and ER6 (ER=0.4) are about the same. This suggests that equivalence ratio, by itself, does not significantly influence the extent of gasification reactions. Similarly, the actual compositions in Test W1 (w_{st}=0.46) and Test W6 (w_{st}=0.96) both deviate about equally from their equilibrium compositions, indicating that the extent of gasification reactions also is not affected significantly by the steam:biomass ratio.

In all cases, the actual concentrations of hydrogen and carbon monoxide are lower than

theoretically predicted, while the actual concentrations of carbon dioxide and methane are higher than theoretically predicted. This can be explained by the reaction zone hypothesis [7]. Biomass enters the Flaming Pyrolysis Zone (the region above the distributor and below the level of the screw feeder, see Fig. 1) and is converted into volatiles at about 1000° C. Intensive combustion takes place when the volatiles meet the input oxidant, producing char, water vapor, and carbon dioxide. A small part of the volatiles is also converted into methane in the Flaming Pyrolysis Zone. The products of the Flaming Pyrolysis Zone then move into the Char Reduction Zone (the region above the level of the screw feeder and below the disengagement section) where char reacts with carbon dioxide and water vapor to form carbon monoxide and hydrogen, and methane is reformed into hydrogen and carbon monoxide. Since the reactions are not complete given the limited residence time, the product gas would have higher concentrations of carbon dioxide and methane, and lower concentrations of hydrogen and carbon monoxide than equilibrium.

SUMMARY

An indirectly-heated, fluidized bed biomass gasifier was designed and fabricated. Biomass feedstock; oxygen, nitrogen, and steam flow rates; and temperature are controlled in the test system. Gas residence time, temperature, equivalence ratio, and steam:biomass ratio were varied in parametric tests, and product gas composition and select gasification parameters were evaluated.

Actual gas compositions for selected test runs are compared with equilibrium compositions under different gasification conditions. There are substantial differences between the actual gas compositions and the theoretical predictions. The comparison indicates that longer residence time and higher temperature improve the extent of gasification reactions, and therefore, result in gas compositions closer to equilibrium.

ACKNOWLEDGEMENTS

The authors wish to thank Dr. Michael Antal, Jr., Coral Industries Professor of Renewable

Energy Resources, and Mr. William Mok, Chemical Research Engineer, of the Hawaii Natural Energy Institute, for providing the biomass feeder and the steam generator used in this experiment and for offering valuable assistance and guidance. The authors also thank the U.S. Department of Energy, the Solar Energy Research Institute, and the State of Hawaii for funding this work.

REFERENCES

1. Takahashi, P.K., D.R. Neill, V.D. Phillips, and C.M. Kinoshita. Hawaii: An International Model for Methanol from Biomass. *Energy Sources 12*, 421-428. 1990.

2. Baker, E.G., D.H. Mitchell, L.K. Mudge, and M.D. Brown. Methanol synthesis gas from wood gasification. *Energy Progress 3(4)*, 226-228. 1983.

3. Chrysostome, G. and J.-M. Lemasle. Syngas production from wood by oxygen gasification under pressure. *Bioenergy 84 Vol. 3 Biomass Conversion*, 73-79. 1984.

4. Evans, R.J., R.A. Knight, M. Onischak, and S.P. Babu. *Development of biomass gasification to produce substitute fuels.* Prepared for the U.S. Department of Energy under contract No. B-C5821-A-Q. March 1987.

5. Flanigan, J. and O.C. Sitton. *Commercial design of an indirect fired fluid bed gasifier system.* Prepared for the U.S. Department of Energy under contract No. B-C5866A-Q. November 1985.

6. Paisley, M.A., H.F. Feldmann, and H.R. Appelbaum. Scale-up of a high-throughput gasifier to produce medium-Btu gas (500 Btu/scf) from wood. Presented at IGT Symposium on Energy from Biomass and Wastes XIII. 1987.

7. Reed, T.B., B. Levie, and M.S. Graboski. *Fundamentals, development and scaleup of the air-oxygen stratified downdraft gasifier.* Prepared for Pacific Northwest Laboratory under Contract No. DE-AC06-76RL0 1830 with the U.S. Department of Energy. June 1988.

8. Kinoshita, C.M., Y. Wang, and P.K. Takahashi. Chemical equilibrium computations for gasification of biomass to produce methanol. *Energy Sources 13*, 361-368. 1991.

FIGURE CAPTIONS

Fig. 1. Schematic of biomass gasifier test system.

Fig. 2. (a) Inert-free product gas composition and (b) gasifier performance versus residence time (ER=0.30, T=800° C, w_{st}=0).

Fig. 3. (a) Inert-free product gas composition and (b) gasifier performance versus equivalence ratio (T=800° C, w_{st}=0).

Fig. 4. (a) Inert-free product gas composition and (b) gasifier performance versus temperature (ER=0.30, w_{st}=0).

Fig. 5. (a) Inert-free product gas composition and (b) gasifier performance versus steam:biomass ratio (ER=0.20, T=800° C).

Fig. 6. Comparison of theoretical (left of paired columns) versus actual (right of paired columns) gas compositions for selected tests.

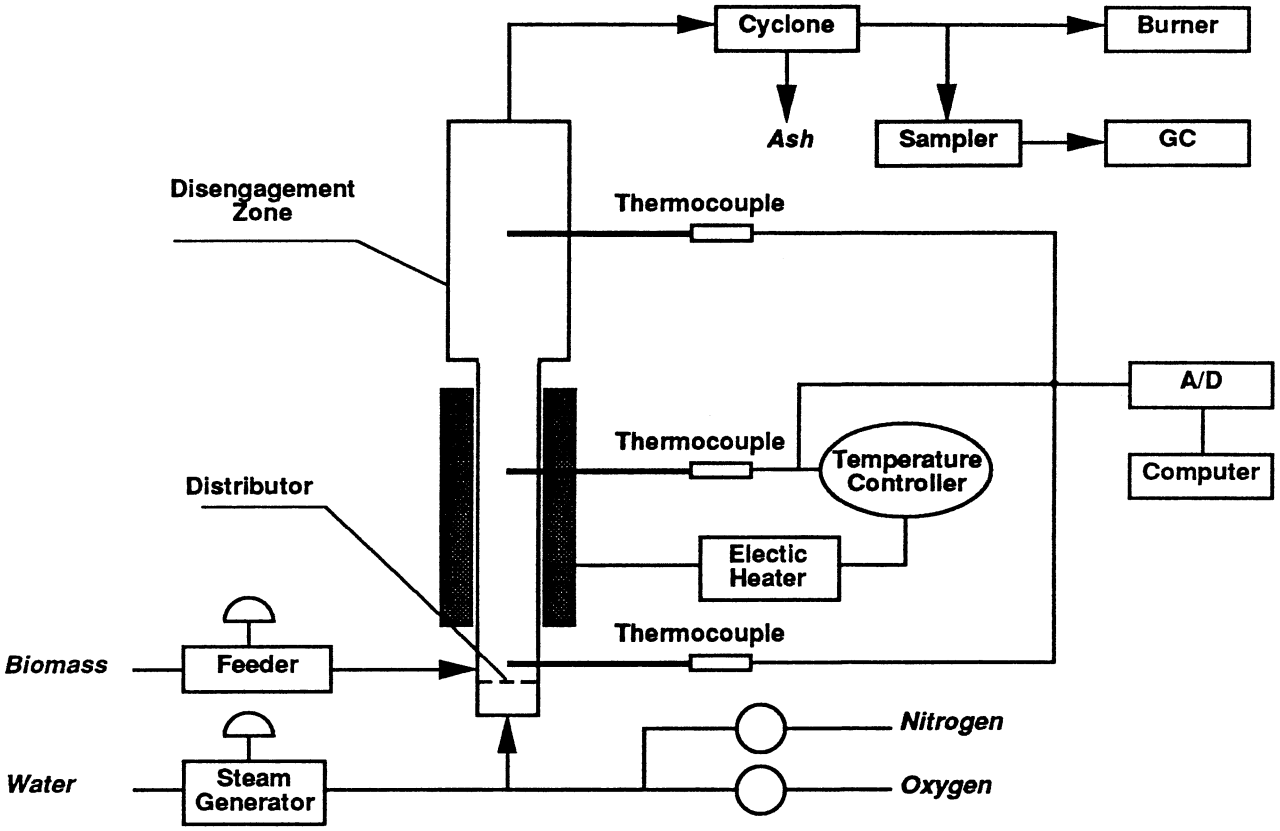
Cyclone
Burner
Ash
Sampler
GC
Disengagement Zone
Thermocouple
A/D
Thermocouple
Temperature Controller
Computer
Distributor
Electic Heater
Thermocouple
Biomass
Feeder
Nitrogen
Water
Steam Generator
Oxygen

Fig. 1

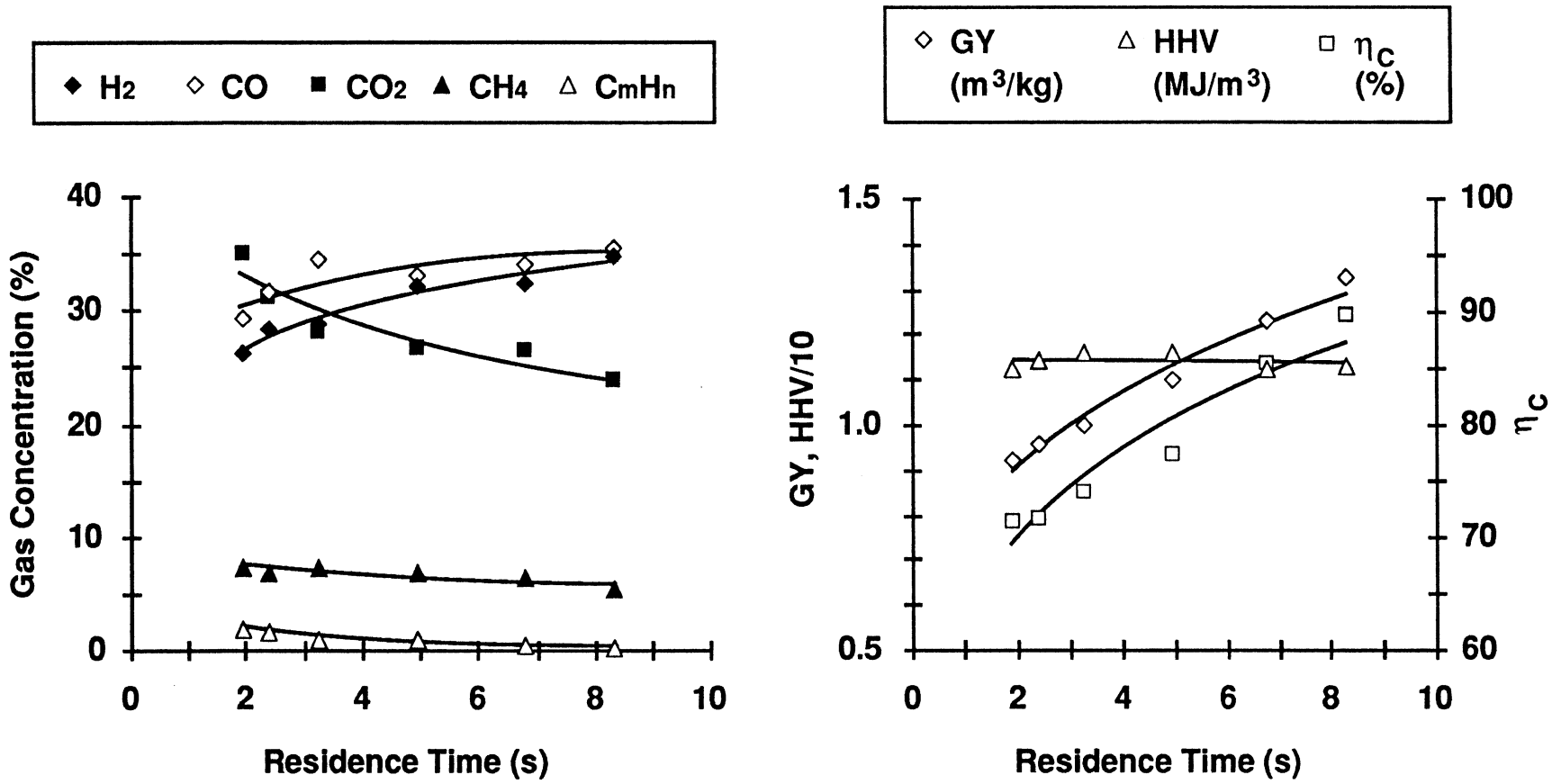
H2
CO
CO2
CH4
CmHn
Gas Concentration (%)
40
30
20
10
0
0
2
4
6
8
10
Residence Time (s)
GY (m3/kg)
HHV (MJ/m3)
ηC (%)
GY, HHV/10
1.5
1.0
0.5
100
90
80
70
60
ηC
0
2
4
6
8
10
Residence Time (s)

Fig. 2

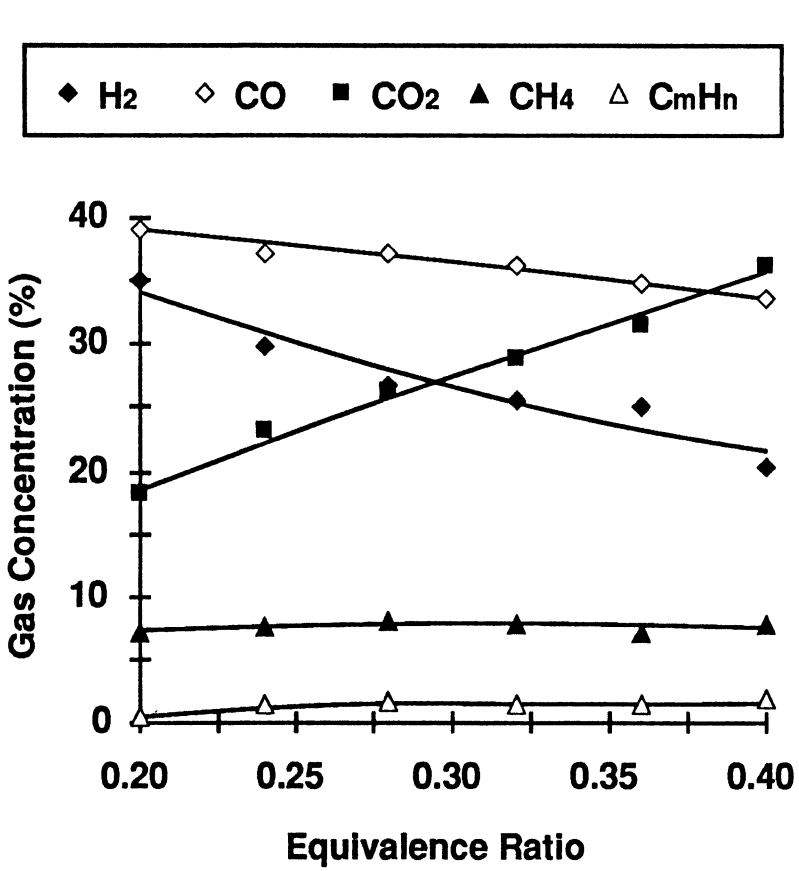
H2
CO
CO2
CH4
CmHn
Gas Concentration (%)
40
30
20
10
0
0.20
0.25
0.30
0.35
0.40
Equivalence Ratio

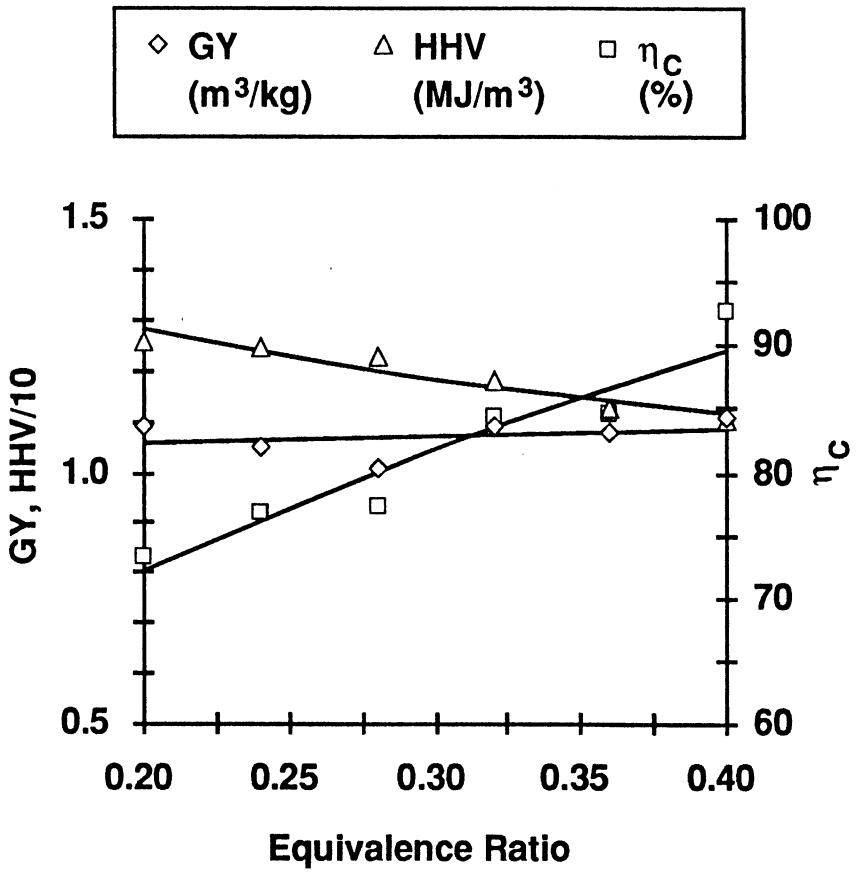
GY (m3/kg)
HHV (MJ/m3)
ηC (%)
GY, HHV/10
1.5
1.0
0.5
100
90
80
70
60
ηC
0.20
0.25
0.30
0.35
0.40
Equivalence Ratio

Fig. 3

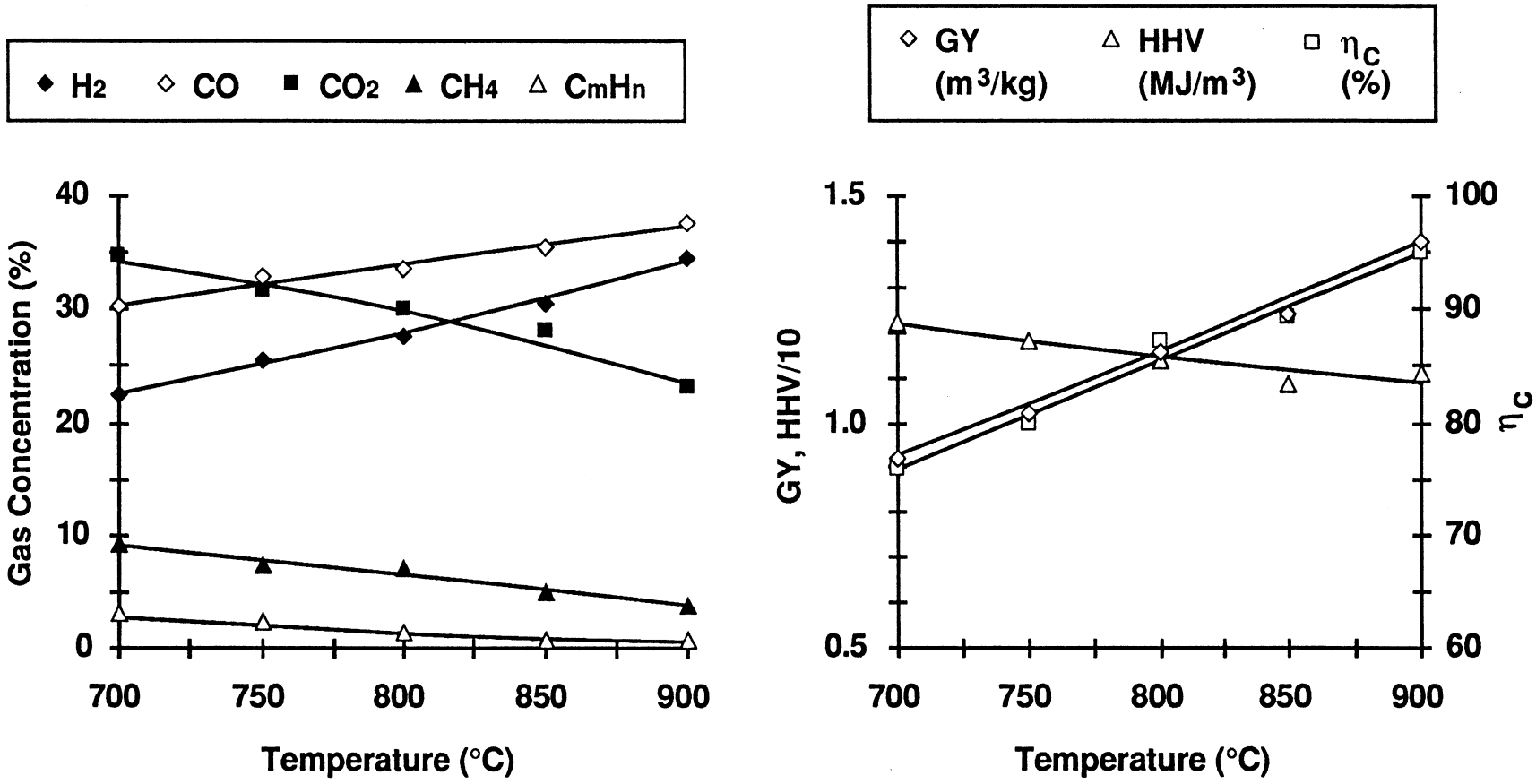
H2
CO
CO2
CH4
CmHn
Gas Concentration (%)
40
30
20
10
0
700
750
800
850
900
Temperature (°C)
GY (m3/kg)
HHV (MJ/m3)
ηC (%)
GY, HHV/10
1.5
1.0
0.5
100
90
80
70
60
ηC
700
750
800
850
900
Temperature (°C)

Fig. 4

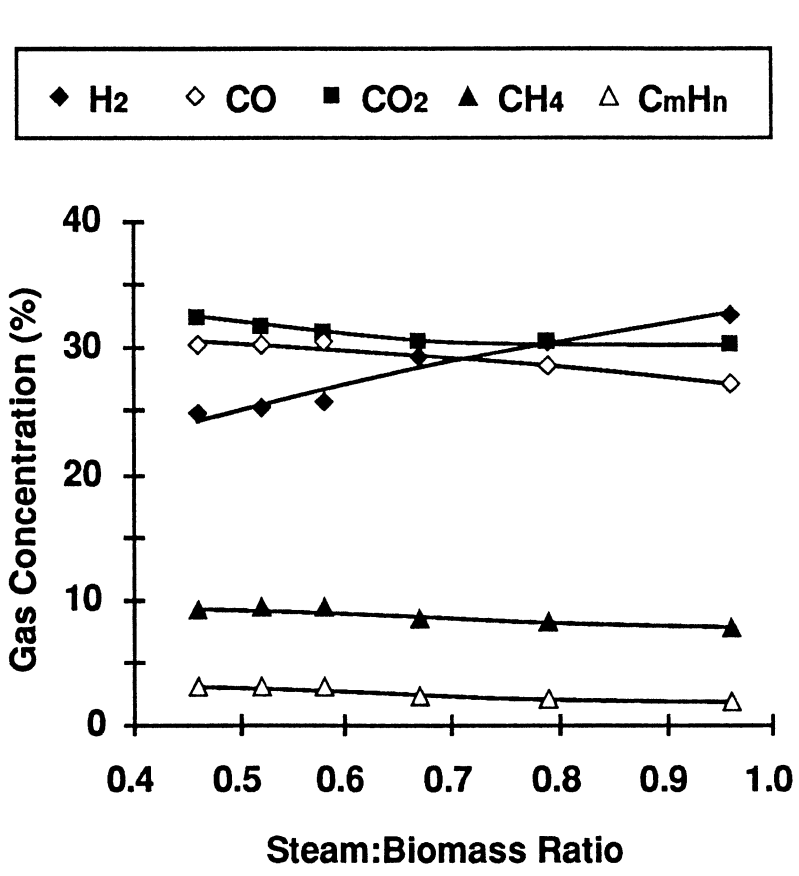
H2
CO
CO2
CH4
CmHn
Gas Concentration (%)
40
30
20
10
0
0.4
0.5
0.6
0.7
0.8
0.9
1.0
Steam:Biomass Ratio

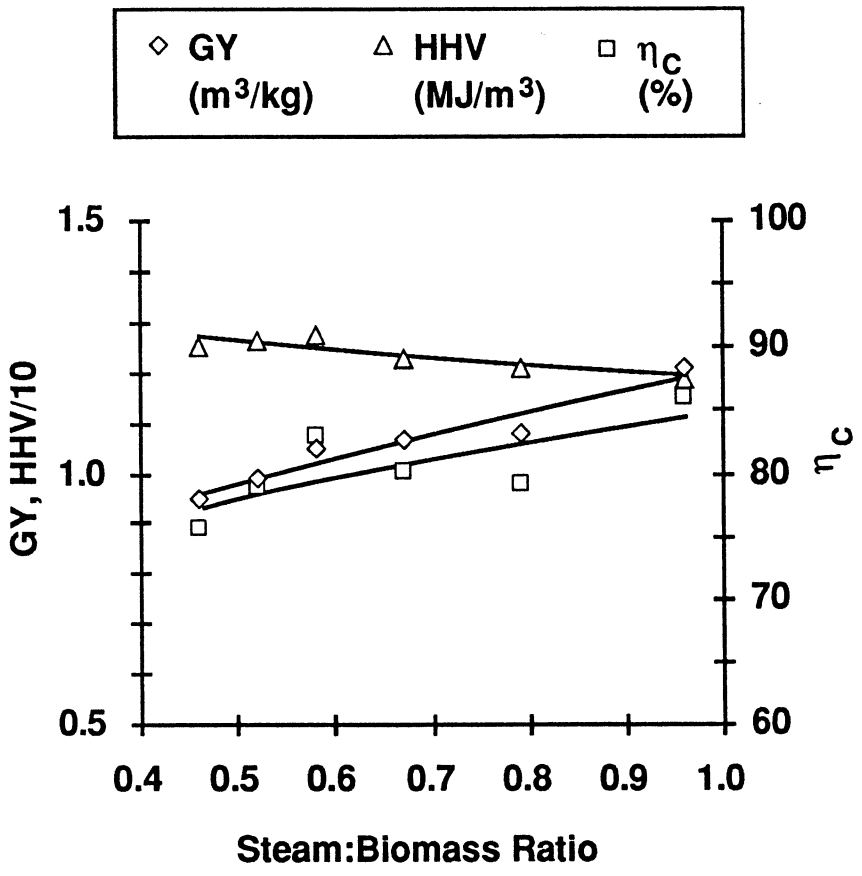
GY (m3/kg)
HHV (MJ/m3)
ηC (%)
GY, HHV/10
1.5
1.0
0.5
100
90
80
70
60
ηC
0.4
0.5
0.6
0.7
0.8
0.9
1.0
Steam:Biomass Ratio

Fig. 5

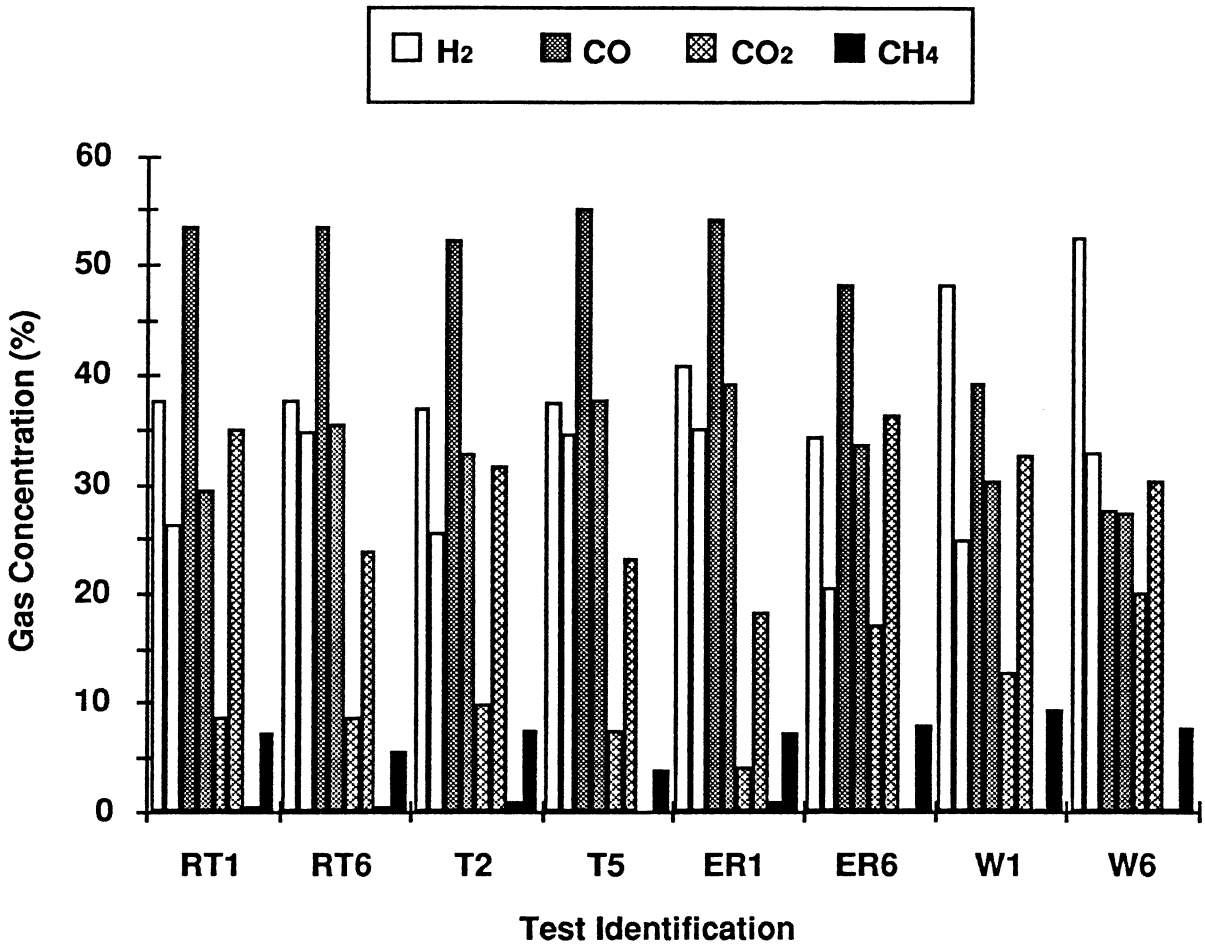
H2
CO
CO2
CH4
60
50
40
30
20
10
0
Gas Concentration (%)
RT1
RT6
T2
T5
ER1
ER6
W1
W6
Test Identification

Fig. 6

Appendix F

Gasification of Wet Biomass in Supercritical Water

PYROLYTIC GASIFICATION OF GLUCOSE AND WET BIOMASS IN SUPERCRITICAL WATER TO PRODUCE HYDROGEN

A THESIS SUBMITTED TO THE GRADUATE DIVISION OF THE UNIVERSITY OF HAWAII IN PARTIAL FULFILLMENT OF THE REQUIREMENTS FOR THE DEGREE OF

MASTER OF SCIENCE

IN

MECHANICAL ENGINEERING

MAY 1991

By

Supaporn Manarungson

Thesis Committee:

Michael J. Antal, Jr., Chairman
Bruce E. Liebert
Takahashi K. Patrick

We certify that we have read this thesis and that, in our opinion, it is satisfactory in scope and quality as a thesis for the degree of Master of Science in Mechanical Engineering.

THESIS COMMITTEE

Chairman

ACKNOWLEDGEMENTS

Throughout the course of my study in Hawaii, a number of people have given and lent me their support, assistance and advice. I would like to express my sincere gratitude and appreciation for their dedication and good will in the guidance and support I received.

I am extremely grateful to Professor Michael Antal, Jr., for his ceaseless guidance, encouragement, and support. Without his perserverance and concern about my progress, this thesis would not be successful. I gratefully acknowledge and thank him for giving me the opportunity to do this research. His kindness and valuable advice are gratefully appreciated.

I would like to acknowledge and thank my thesis committee members, Professor Bruce Liebert and Professor Patrick Takahashi, for their support.

My special appreciation and thanks go also to Mr. William Mok for his assistance and advice to resolve a number of problems arose during the research process. Also, I would like to thank my colleagues; Sunil Sinha and Sheldon Xu for the help extended to me.

I wish to offer my sincere appreciation to HNEI staffs for their assistance in official work. I would like to acknowledge all Mechanical Engineering graduate students, faculty members and staffs for having made my stay in Hawaii a pleasant.

My sincere gratitude is also extended to Ms. Irene Kanda for her kindly encouragement and assistance. I wish to express my sincere thanks to Ms. Meg Rakow, one of my best friends, for her time and efforts in editing the draft of this thesis.

My special gratitude goes to my family for their constant support and concern about my academic development.

My most special thanks is offered to Apichai Therdthianwong for his immeasurable patience, support, and inspiration throughout my study here.

Finally, I wish to thank all unnamed supporters for their kindness and spiritual support.

This research was supported by the Solar Energy Research Institute under Contract No. XN-0-19164-1.

ABSTRACT

Two different types of reactor, a supercritical annulus flow reactor and a supercritical coil flow reactor were employed to study the gasification of glucose and wet biomass respectively. Glucose was employed as a model fuel, operated using supercritical annulus flow reactor, to determine practical conditions for wet biomass gasification in SCW. High hydrogen yield was obtained at high temperature, long residence time and low initial reactant concentration. Supercritical coil flow reactor was employed to study wet biomass gasification in SCW at higher temperature and longer residence time than that of glucose gasification. The factors influencing the conversion and gas yields of wet biomass gasification are temperature, residence time, and types of feedstock. Steam gasification was observed in both glucose and wet biomass gasification in SCW.

TABLE OF CONTENTS

ACKNOWLEDGEMENTS		iii
ABSTRACT		v
LIST OF TABLES		vii
LIST OF FIGURES		ix
LIST OF SYMBOLS		xii
CHAPTER 1	INTRODUCTION	1
CHAPTER 2	LITERATURE REVIEW	7
CHAPTER 3	APPARATUS AND EXPERIMENTAL PROCEDURE	21
CHAPTER 4	RESULTS AND DISCUSSION	47
CHAPTER 5	CONCLUSIONS AND RECOMMENDATIONS	105
APPENDIX A	MASS BALANCE CALCULATION	107
APPENDIX B	NONDIMENSIONAL ANALYSIS PROGRAM	120
APPENDIX C	GAS ANALYSIS QUANTIFICATION PROGRAM	127
APPENDIX D	CALCULATION OF ENTHALPY OF GLUCOSE REACTION IN SCW	131
APPENDIX E	CALCULATION OF FRACTIONAL POTENTIAL HYDROGEN YIELD	133
APPENDIX F	DATA FROM GASIFICATION OF GLUCOSE AND WET BIOMASS IN SCW USING SCAFR & SCCFR	136
APPENDIX G	QUALITATIVE ANALYSIS OF ALGAE AND KELP USING X-RAY DIFFRACTION	153
REFERENCES		156

LIST OF TABLES

Table		Page
3.1	Elemental analysis of reactants.....	22
3.2	Values for calculation of non-dimensional numbers and characteristic times for SCAFR.....	29
3.3	Non-dimensional numbers and characteristic times for SCAFR.....	30
3.4	Values for calculation of non-dimensional numbers and characteristic times for SCCFR.....	34
3.5	Non-dimensional numbers and characteristic times for SCCFR.....	35
4.1	The effect of temperature on glucose gasification in SCW.....	63
4.2	The effect of residence time on glucose gasification.....	64
4.3	The effect of reactant on glucose gasification in SCW.....	65
4.4	The effect of oxygen on glucose gasification in SCW.....	66
4.5	The effect of reactant types on gasification in SCW.....	67
4.6	The effect of residence time on soluble starch gasification in SCW.....	68
4.7	Comparison of gas compositions from this work to others.....	69

Table Page

4.8 Carbon balances and absolute gas yields from algae gasification in SCW..... 70

4.9 Carbon balances and absolute gas yields from gasification of wet biomass in SCW..... 71

4.10 Carbon balances and absolute gas yields from sewage sludge gasification in SCW..... 72

4.11 Effect of feeding system..... 83

4.12 Effect of temperature and residence time on wet biomass gasification in SCW..... 84

4.13 Effect of quenching system on wet biomass gasification in SCW..... 85

4.14 Effect of initial reactant concentration on wet biomass gasification in SCW..... 86

4.15 Effect of reactant types on wet biomass gasification in SCW..... 87

F.1 Elemental balances and absolute gas yields for oxidation and pyrolysis reactions in SCW using the SCAFR..... 137

F.2 Carbon balances and gas yields from wet biomass gasification in SCW using the SCCFR..... 142

LIST OF FIGURES

Figure		Page
1.1	Ion products of water at different temperature and pressure.....	6
2.1	Thermal gasification of biomass and their products.....	15
3.1	Supercritical annulus flow reactor scheme.....	25
3.2	Supercritical coil flow reactor scheme.....	27
3.3	Sampling system of the SCFR.....	40
3.4	Configuration of sampling valve.....	40
4.1	Gas yields from 0.01M glucose gasification in SCW vs temperature	73
4.2	Elemental balance from 0.01M glucose gasification in SCW vs temperature.....	74
4.3	Gas yields from 0.05M glucose gasification in SCW vs residence time.....	75
4.4	Elemental balance from 0.05M glucose gasification in SCW vs residence time.....	76
4.5	Gas yields from 0.01M glucose gasification in SCW vs residence time.....	77
4.6	Elemental balance from 0.01M glucose gasification in SCW vs residence time.....	78
4.7	Gas yields from glucose gasification in SCW vs initial concentration.....	79
4.8	Elemental balance from glucose gasification in SCW vs initial concentration.....	80

Figure Page

4.9 Effect of oxygen on hydrogen yield from glucose gasification in SCW..... 81

4.10 Effect of oxygen on carbon balance from glucose gasification in SCW..... 82

4.11 Gas yields from 0.7 g/l algae gasification in SCW with different feeding system..... 88

4.12 Elemental balance from 0.7 g/l algae gasification in SCW with different feeding systems..... 89

4.13 Gas yields from 0.7 g/l algae gasification in SCW vs residence time at 550°C..... 90

4.14 Gas yields from 0.78 g/l algae gasification in SCW vs residence time at 600°C..... 91

4.15 Gas yields from 0.78 g/l algae gasification in SCW vs residence time at 650°C..... 92

4.16 C-balance from 0.7 g/l algae gasification in SCW vs residence time (at various temperatures) 93

4.17 Hydrogen yield from 0.7 g/l algae gasification in SCW vs residence time (at various temperatures) 94

4.18 CO_2 yield from 0.7 g/l algae gasification in SCW vs residence time (at various temperatures).... 95

4.19 CO yield from 0.7 g/l algae gasification in SCW vs residence time (at various temperatures).... 96

4.20 CH_4 yield from 0.7 g/l algae gasification in SCW vs residence time (at various temperatures) 97

Figure Page

4.21 C_2H_4 yield from 0.7 g/l algae gasification in SCW vs residence time (at various temperatures) 98

4.22 C_2H_6 yield from 0.7 g/l algae gasification in SCW vs residence time (at various temperatures) 99

4.23 Effect of immediate quenching on gas yields.... 100

4.24 Effect of immediate quenching on elemental balance..... 101

4.25 Gas yields vs initial algae concentration..... 102

4.26 Elemental balances vs initial algae concentration 103

4.27 Effect of reactant types on gas yields and elemental balances..... 104

LIST OF SYMBOLS

T = Temperature

Re.No. = Reynolds number

Pr.No. = Prandtl number

Sc.No. = Schmidt number

Pe.No. = Peclet number

DA. = Damkohler number

k = Rate constant

E_a = Activation energy

A = pre-exponential factor

R = Universal gas constant

Subscripts

fc = forced convection

sd = species diffusion

td = thermal diffusion

md = momentum diffusion

ck = chemical kinetic

CHAPTER 1

INTRODUCTION

Interest in biomass as an alternative to fossil energy resources has increased since the crude oil price escalation started in 1973. Utilization of biomass for producing energy, and liquid and gaseous fuels (ie. hydrogen) is one alternative. Biomass can only be considered as an energy feedstock, however, if there is an adequate amount of crops and plants, and their efficient conversion to products is achieved. Although high moisture biomass (wet biomass) such as aquatic plants is one of the world's largest available feedstocks, it rarely has been regarded as a potential fuel source because of its high moisture content and the high cost of water removal. Therefore, it would be advantageous to develop a suitable thermochemical conversion process in order to utilize high moisture biomass in its wet form as a fuel.

Aquatic plants have some advantages over terrestrial plants. For example, the optimum photosynthetic efficiency of land-based plants is limited by water availability for growing (Vaclav, 1983). Moreover, the rate of production of aquatic plants is many times greater than that of land-biomass (Vaclav, 1983). Spencer Burrett has noted that water hyacinth, Eichhornia crassipes, and kariba weed, Salvina molesta, the most noxious aquatic weeds, have inflicted wide

destruction on waterways all over the world because they are able to grow and multiply rapidly and uncontrollably (Spencer, 1989). Two water plants can reproduce 1200 plants within four months.

Among synthetic fuels (hydrogen, methane, methanol, ethanol, ammonia hydrazine, etc.), hydrogen is considered the best fuel for the future energy needs of mankind (Veziroglu, 1990). It is an ideal fuel which is clean and non-polluting. Also, hydrogen has the highest utilization diversity and can be used in every application where fossil fuels are used nowadays, including domestic heating, automotive and air transportation, powering industry, and electricity generation (Veziroglu, 1990; Johnson, 1975; Gregory, 1973).

There are four principal commercial processes for hydrogen manufacture: catalytic steam reforming and oxidation of hydrocarbons, coal gasification and water electrolysis (Mark et al., 1978). In the United States, steam reforming of natural gas is employed to produce hydrogen. However, the present day hydrogen production processes are too expensive and consume too much of the fossil fuels, natural gas and coal.

Unlike fossil fuels, biomass materials have not been converted to more useful chemicals and fuels by efficient and

selective thermochemical processes, because of the non-specificity of high temperature pyrolysis reactions involving biopolymer substrates (Antal, 1984a, 1984b, 1985). For example, a good control of complex pyrolysis reaction is not accomplished by variations of the conventional engineering parameters.

Fortunately, supercritical fluids have been found to have unique thermophysical and chemical properties (Paulaitis et al., 1983) which may make them especially suitable for gasification process. These properties include the solvent's dielectric constant (Franck, 1970), electrolyte conductance (Quist, 1970; Marshall, 1968), ion product (Marshall, 1981; Quist et al., 1965), transport properties (ie. viscosity (Bruges, 1969), diffusivities (Lamb et al., 1981), ion mobilities (Franck et al., 1968)), hydrogen bonding characteristics (Franck, 1970) and solute/solvent enhancement factor (Franck, 1983). With these unusual properties, the reaction rates may be enhanced while maintaining the selectivity and it may be possible to dissolve reactants and catalyst in a single, homogeneous fluid phase so that interphase mass transfer is limited (Subramanlam and McHugh, 1986). For instance supercritical water, which is water at a temperature above 374°C (705°F) and pressure above 3200 psi (22.1 MPa), behaves like a dense gas and has a high solubility for organics (Connolly, 1966), high diffusivities (Lamb et

al., 1981) and low solubility of inorganics.

For chemical reaction involving a polar solute, the solvent's ion product is the most important property (Franck, 1970; Antal et al., 1987). Under near-critical and supercritical condition (high dielectric constant and ion product) water retains its ionic properties and behaves as a liquid-like solvent even at elevated temperature. However, as temperature increases above a certain temperature, water can lose its ionic properties (see Figure 1.1).

Work by Antal and coworkers holds promise as a new means to improve utilization of the vast biopolymer resource, especially wet biomass (Antal et al., 1987). In their studies of ethanol dehydration to ethylene in supercritical water, they found that when the ion product was greater than 10^{-14}, heterolytic (ionic) reactions were favored, whereas with $K_w << 10^{-14}$, SCW behaves as a high-temperature gas and a homolytic (free-radical) reaction predominated.

Studies of the pyrolytic chemistry of water-soluble biomass substrates in supercritical water in the R^3L was initiated with glycerol in 1985 (Antal et al., 1985). The pyrolysis products were mostly gases, consisting mainly of CO_2 and H_2. It was found that at higher temperatures, free-radical chemistry plays the dominant role; whereas at lower

temperatures, heterolytic reactions involving a carbonium ion intermediate can be catalyzed to selectively by produce acrolein.

With this background, I initiated studies of the pyrolytic gasification of wet biomass in supercritical water to produce a useful fuel, hydrogen.

The objectives of my study were:

1. Modify existing supercritical flow reactor to accept high moisture content biomass as a feedstock.

2. Identify an appropriate range of and study the influences of temperatures, residence times, oxygen, and initial reactant concentrations using glucose as a model fuel.

3. Apply the selected operating condition obtained from the first stage to the study of wet biomass.

Figure 1.1 Ion products of water at different temperature and pressure

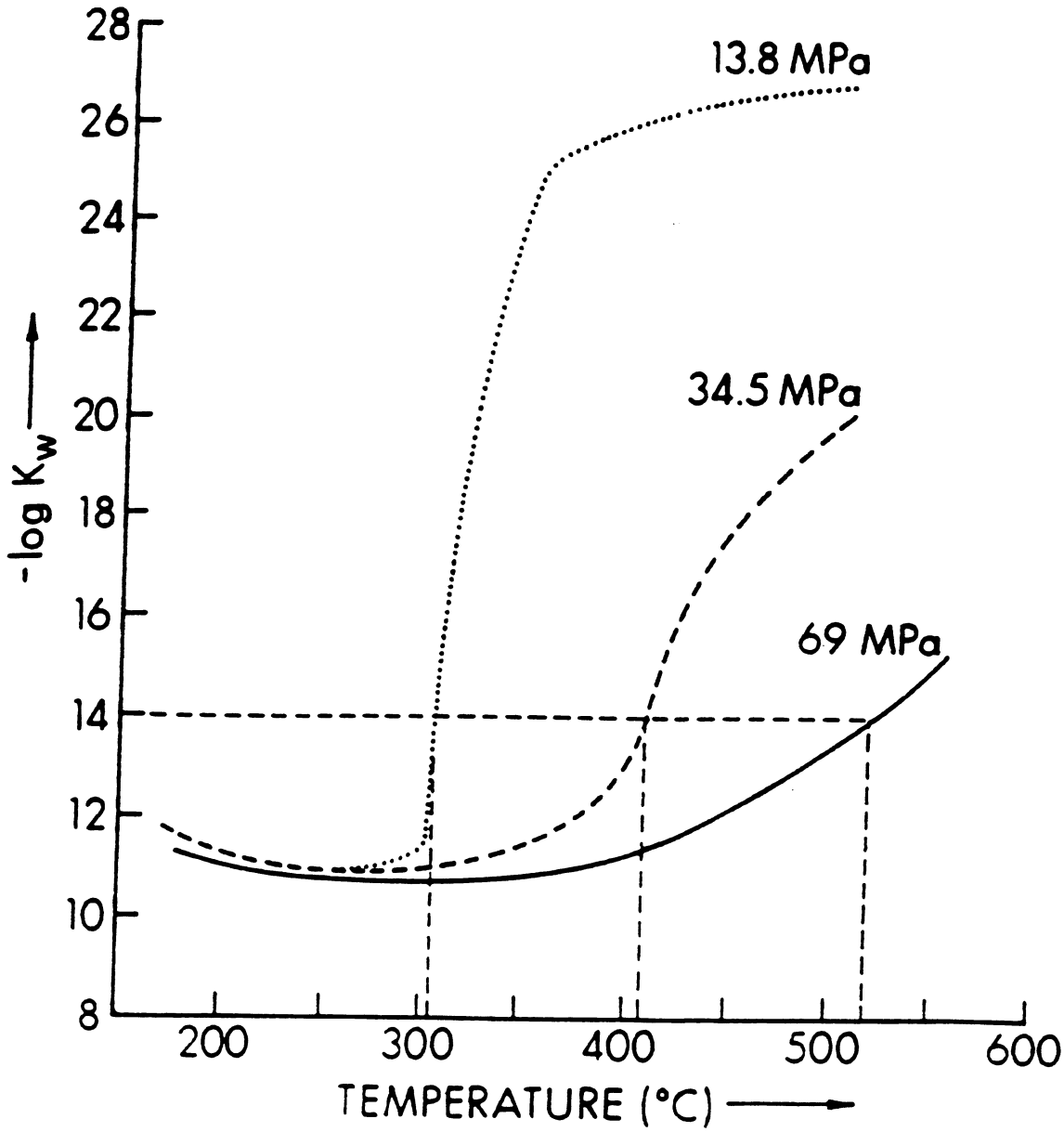

CHAPTER 2

LITERATURE REVIEW

2.1 Introduction

Due to their unique thermophysical and chemical properties, supercritical fluids have been widely used in many areas including food, pharmaceuticals, petroleum, hazardous waste and environmental control (Eckert et al., 1986; Buelow et al., 1981). The most promising applications are in synfuels processes, improved separation methods and as non toxic solvents. The following is a review of some uses and studies of supercritical fluids.

2.2 Oxidation in the Aqueous Phase

2.2.1 Wet Air Oxidation

The concept of wet air oxidation (WAO) is the reaction of organic materials with dissolved oxygen in an aqueous phase at temperature between 100°C and the critical temperature of water (374°C), and pressures between 100 - 150 atm. WAO is a process that combines destruction and detoxification of dilute and toxic hazardous organic waste streams.

The WAO process, originally developed by Zimmermann and also known as the Zimmermann process, was applied to the waste disposal field (Zimmermann, 1961). The destruction efficiency was improved (from 15% to 95%) with increased temperature

(from 100 to 300°C). Several researchers (Welhelmi and Zimpro, 1979; Flynn and Flemington, 1979; Baillod et al., 1985; DeAngelo and Wilhelmi, 1983) reported the economics and application of WAO comparative to conventional incineration in treating hazardous waste such as by products from steel production, sewage, individual hydrocarbons, and spent caustic liquors in hydrocarbon plants. Dietrich et al. also reported a full-scale performance study of the ability of WAO to destroy various hazardous wastes containing phenols, pesticides, and herbicides greater than 99% (Dietrich et al., 1985).

At higher WAO temperature, the reaction becomes increasingly more oxidative and causes considerable amounts of fragmentation and oxidation of biomass. For example, a study of biomass conversion with high-temperature WAO was performed by McGinnis et al. (McGinnis et al., 1983). Three types of biomass (pine, black oak, and a mixture of hard wood) were used and operated at the temperature of 171 - 227°C, 240 - 480 psi and residence time of 30 minutes. High yields of acetic (28%) and formic acid (14%), an insoluble product, carbon dioxide and traces of methanol were obtained. No gas product was observed.

2.2.2 Oxidation in SCW

The supercritical water oxidation (SCWO) concept is

similar to WAO. Organics, oxidant and water are brought together in a mixture above the critical condition. Parameters governing the demarcation between WAO and SCWO are critical temperature, critical pressure, and oxidant (which can be air, oxygen, hydrogen peroxide, etc). SCWO is practiced at conditions above the critical temperature and pressure of water. Operating at supercritical condition provides some advantages over WAO such as (Modell, 1989):

1. Higher reaction rate in SCWO than in WAO.
2. Shorter residence time in SCWO than in WAO.
3. No interphase mass transfer limiting the reaction rate because of the presence of only a homogeneous single phase at SC condition.

The technology and application of SCWO have been demonstrated by several authors. Modell is a pioneer in the study and application of SCWO to hazardous waste treatment plants (Modell et al., 1982; Staszak et al., 1987). In the MODAR process (Thomason and Modell,1989; Staszak et al., 1987), operated at or above 374°C (which later goes to 550 - 650°C due to the exothermic oxidation reaction), Modell et al. used a bench-scale SCWO system to study the oxidation of a variety of model compounds including DDT, trichlorobenzene, trichloroethane, ethylene dichloride, biphenyl, and PCB. The destruction efficiencies in all cases were reported to exceed 99.99% (Modell et al. 1982; Thomason and Modell, 1984).

Currently, the chemistry and kinetics of SCWO for hazardous chemical waste destruction processes are being investigated and conducted by several researchers. Studies of the oxidation of simple compounds such as CH_4, CO, NH_3, CH_3OH, and C_2H_5OH in SCW were conducted by Tester and coworkers (Webley and Tester, 1989; Helling and Tester, 1987; Webley and Tester, 1988), and Rofer and Streit (Rofer and Streit, 1988; Rofer, 1989). Most of their interest was in modelling oxidation chemistry in SCW. The oxidation reaction was found to be first order and independent of oxygen concentration. Gas phase free-radical oxidation was observed as a dominant pathway mechanism in this study.

For CO-oxidation operated in an isothermal continuous flow reactor, Helling and Tester (Helling and Tester, 1987) determined the reaction to be first order in CO and zero order in oxygen, with an activation energy of 120 ± 7.7 kJ/mol and a preexponential factor of $10^{7.25\pm0.53}s^{-1}$. They assumed the reaction was zero order in water. A major product during the oxidation reaction was hydrogen, which was produced by the water-gas shift reaction. The water-gas shift reaction was much faster, while the direct oxidation of carbon monoxide was much slower than predicted by existing models. They discussed the reaction pathways and explained the influence of solvent (water) cage on the reaction by surrounding reactive solutes, promoting the water-gas shift reaction between solvent and

solute, and retarding the direct oxidation reactions. However, they were not able to simulate the formation of hydrogen using the water-gas shift reaction.

Webley and Tester (Webley and Tester, 1988) completed oxidation studies of methane in the temperature range 640 - 700°C and a pressure of 242 atm (24.5 MPa) and 5.6 to 11.1 seconds residence time. Unlike the oxidation of CO in SCW, the parallel water-gas shift reaction was found to be negligible in the oxidation of methane. Also, neither elementary nor global reaction models could quantitatively predict oxidation in SCW.

Fundamental kinetics of methanol oxidation in SCW over the temperature range 450 - 550°C at 250 bar and residence time of order 8.4 - 11.4 seconds were investigated by Webley and Tester (Webley and Tester, 1989). Global kinetic expressions were presented and a free-radical gas-phase chemistry was suggested as a reaction mechanism. However, the observed conversion data could not be predicted. The model of the oxidation kinetics represented a first-order approximation in methanol which is independent of oxygen.

Rofer and Streit have been interested in modelling SCWO using simple, one-carbon compounds such as CO, CH_4 and CH_3OH (Rofer and Streit, 1988; Rofer, 1989). Three different

operating conditions, temperature at 400 - 543°C at a pressure of 24.5 MPa, temperature at 640 - 700°C at a pressure of 24.5 MPa, and temperature at 450 - 550°C at a pressure of 24.6 MPa, were conducted for CO, CH_4 and CH_3OH respectively. A global first-order rate expression was determined for methane oxidation with the assumption of O_2 concentration independence. However, pathway information was not reported. Also, the reaction mechanisms were presumed to be a gas-phase free-radical oxidation.

Finally, the kinetics of uncatalyzed and homogeneously catalyzed oxidation of p-chlorophenol in water at subcritical and supercritical condition were studied by Yang and Eckert (Yang and Eckert, 1988). They accomplished the experiment in a flow reactor system at conditions ranging from 310 - 400°C and 75 - 240 atm. The rate of oxidation at both conditions appeared to be first order at low concentrations, second order at high concentrations, and independent of the oxygen concentration in both cases. Free-radical oxidation was offered as a feasible reaction chemistry which was consistent with the observed kinetics. Nevertheless, there was no direct experimental verification of the postulated mechanisms. In the reactor effluent stream, metals were detected, which were assumed to be corrosion products from the 316 stainless steel and Inconel, materials which were used to construct the reactor system. These metals also affect the uncatalyzed

oxidation reactions. For catalyzed oxidation, it was postulated that the catalyst only facilitates certain steps in the uncatalyzed oxidation without altering the pathway.

2.3 Pyrolysis and Gasification

2.3.1 Conventional Gasification Process

Pyrolysis is an incomplete thermochemical decomposition in the absence of oxygen resulting in char, condensable liquids or tars and gaseous products. The gasification process is a combination of pyrolysis followed by heating at high temperature of the char, tars and primary gases to yield mainly low molecular weight gaseous products and some condensable liquids (Reed, 1981). Its application has been reviewed elsewhere (Schiefelbein, 1989). Figure 2.1 displays a number of useful products produced from biomass by gasification.

Steam can be added with air in some gasification units to promote the overall process to form carbon monoxide and hydrogen (Mark et al., 1978). The steam gasification of wood involves three types of reactions (Mudge et al., 1985): 1) pyrolysis to produce gaseous products (CO_2, CO, CH_4, and some heavier hydrocarbons), tar, water-soluble organics (acetic acid, methanol, acetone, esters, and aldehydes), char; 2) reaction of char from reaction 1 with H_2O, CO_2, and H_2 to produce H_2, CO, CH_4, and CO_2; and 3) reforming and condensation

of the products from reaction 1 and 2 to produce additional gas products, tars, and char.

A study of the production of hydrogen-rich syngas by gasification of biomass in a pilot plant involving both moving and entrained bed reactors was conducted successfully by Lucchesi et al. (Lucchesi et al., 1988). In the temperature range 650 - 750°C fast pyrolysis of biomass was obtained and the conversion was 70%. The steam gasification process achieves a significant rate at temperatures above 800°C. Hydrogen and carbon monoxide were the major gas products. However, conventional gasification processes generally cannot utilize feedstocks with moisture content higher than 50% wt.

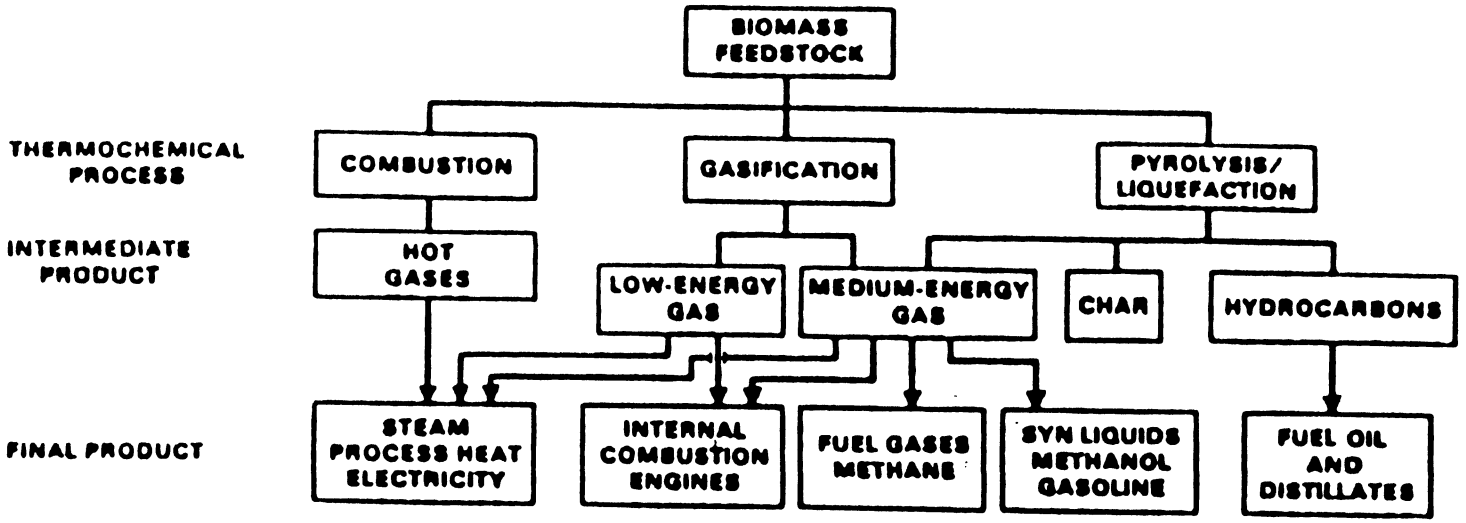

Figure 2.1 Thermal gasification of biomass and their products (Schiefelbein, 1989).

2.3.2 Gasification in SCW

Water at high temperature and pressure has been used originally as a solvent for coal (Towne et al., 1985; Maddocks and Gibson 1977, 1979) and as a media for reaction (Subramanlam and McHugh, 1986). Like other media solvents, SCW acts as a carrier solvent for the feed material and reaction products. Furthermore, a few investigators found that operating in SCW has two apparent effects. First, SCW can eliminate char formation from pyrolysis of materials such as glucose, cellulose, and maple sawdust (Modell, 1982), poplar wood (Beckman and Boocock, 1983; Boocock and Sherman, 1985) and 1,3-butanediol (West and Gray, 1987) by suppressing dehydration reactions or by preventing recombination reactions within the solid. Second, SCW reacts with and breaks down organic substances into low molecular weight products (ie. liquid organics and gases) (Modell et al., 1978; Amin et al., 1975) which is similar to conventional gasification.

Initially, glucose, used as a representative of the carbohydrate in spacecraft waste, was gasified in an aqueous phase at subcritical and supercritical condition by Amin (Amin et al., 1975). The products were entirely liquid organics and a gaseous mixture of CO, H_2, CO_2, and CH_4. Similarly, he found that no solids (presumably char) were formed at SC condition. Also an increase in the yield of H_2 with increased temperature was discovered. The water gas shift reaction was suggested as

the possible reason.

Later, Modell studied the reaction of glucose, cellulose, and maple sawdust in subcritical and supercritical water and his results also showed that SCW may prevent char formation either with or without catalyst (Modell, 1982). Work done by Boocock and coworkers also indicated the high potential of interaction between wood components and SCW (Beckman and Boocock, 1983; Boocock and Sherman, 1985).

West and Gray studied the pyrolysis of 1,3-butanediol, as a model reaction for wood liquefaction, in SCW (425°C, 21.5 MPa and 30 minutes residence time) in a tubing bomb reactor (West and Gray, 1987). A variety of products including higher molecular weight than butanediol, lower molecular weight and oxygenated species were products of the reaction. They reported that dehydration and char formation reactions were prevented by SCW. The reactant conversion was strongly affected by water density and pressure. The presence of water shifted the product selectivity according to the ionic properties of SCW. Also, traces of oxygen in the reaction mixture were an important inhibitor, particularly in dilute solution.

Very few researchers have studied the gasification of wet biomass in SCW. A catalytic gasification process operated in

near critical and supercritical water was originally applied to convert high-moisture biomass feedstocks to useful gas and liquid products by the Pacific-Northwest Laboratory (PNL) (Sealock et al., 1988; Butner et al., 1985; Elliott et al., 1989). The operating condition was temperature between 400 - 450°C and pressure up to 5000 psi. Ni-metal and alkali carbonate were employed as catalyst. A number of experiments were conducted in both a batch system (Sealock et al., 1988; Butner et al., 1985, 1989) and a continuous system (Elliott et al., 1989; Butner et al., 1989). With Ni catalyst, the major gas products were 40% CH_4, 45 - 55% CO_2 and 15 - 25% H_2. A high carbon conversion (about 95%) was obtained. But the carbon conversion was very low (18 - 33%) in the experiment without the catalyst. There was some qualitative experimental evidence that the catalyst role is similar to a steam-reforming catalyst in the steam cracking and reforming of hydrocarbons.

In general, the underlying chemical reactions for biomass gasification in SCW are complex, non-specific, and not well understood. With the simplicity of model compound structures and spectra of products, the fundamental reaction chemistry of biopolymer substrate can be hypothesized (Simmons and Klein, 1985). The thermal reactions of coal and coal compounds in SCW have been examined by several researchers (Deshpande et al., 1987; Ross et al., 1987; Abraham and Klein, 1987;

Townsend et al., 1988, Townsend and Klein, 1985). It was found that water both actively participates as a reactant in most of those reactions, and it also acts as an inert solvent. Consequently, thermal reactions in SCW involved parallel pyrolysis and solvolysis reactions pathways. For example, studies of the reaction of dibenzyl ether (Townsend and Klein, 1985) and benzyl phenylamine (Abraham and Klein, 1985) in dense water elucidated two reaction pathways: pyrolysis and hydrolysis and selective generation of pyrolysis increased with water density.

Abraham and Klein (Abraham and Klein, 1987) studied solvent effects during the reaction of the coal model compound in SCW and found that as the water density increased, system density increased from a gas-like to a liquid-like value, with a minimum in reactant conversion observed. They concluded that these results were consistent with two mechanistic interpretations. First, each reaction pathway (hydrolysis and pyrolysis) involved a pressure-dependent rate constant. Second, each reaction pathway allowed solvent cage formation to suppress the pyrolysis reaction by trapping free-radicals, and resulted in increase in solvent density.

The work of Townsend et al. (Townsend et al., 1988) also involved solvent effects during reaction of a set of heteroatom-containing diaryls in SCW. She reported that the

selectivity of the hydrolysis path increased with an increase in water density. Since increasing the water density raised the water dielectric constant, she suggested that the reaction proceeded through the polar hydrolysis transition state which was more polar than the reactants.

The identification and implications of a polar transition state during hydrolysis in SCW were further studied by Huppert et al. (Huppert et al., 1989). The ionic strength of the solvent was varied by adding salt. They concluded that the hydrolysis rate can be manipulated to be either ionic chemistry or free-radical chemistry by changing the density of SCW, and through the addition of salts.

CHAPTER 3

APPARATUS AND EXPERIMENTAL PROCEDURES

3.1 Apparatus

The experimental apparatus consists of five major systems. Their descriptions are given below:

3.1.1 Reactants and Feed Preparation

In the early stages of my work, dihydroxy acetone (DHA), glucose, and soluble starch were used as reactants to mimic the reaction chemistry of wet biomass. Initially, hydrogen peroxide was employed as an oxidizer. Wet biomass such as algae (Gracilaria bursapastoris), kelp (Macrocystis pyrifera), sewage sludge and water hyacinth (Eichornia crassipes) were chosen as representative biomass materials. The chemical composition of each material is shown in Table 3.1.

Wet biomass was blended by a 600 W Hamilton Beach Blender to ensure that the biomass particles in the feed slurry were homogeneous and small enough to be fed to the reactor.

Table 3.1 Elemental Analysis of Reactants

Materials	Elemental analysis (%)		
	C	H	O
Algae [a]	42.91	6.60	40.02
Kelp [a]	23.22	2.96	40.13
Sewage sludge [b]	38.9	5.8	23.4
Water hyacinth [c]	43.0	5.8	29.5

a: analyzed by independent laboratory

b: data from reference (Urban and Antal, 1982)

c: data from reference (Sealock et al., 1988)

3.1.2 Supercritical Flow Reactor

Two different configurations of the supercritical flow reactor (SCFR) were used in this study: supercritical annulus flow reactor (SCAFR) and supercritical coil flow reactor (SCCFR). Each reactor is described in the following sections:

a) Supercritical Annulus Flow Reactor

A schematic diagram of the annulus flow reactor is shown in Figure 3.1. A 4.572 mm ID Hastelloy C-276 tube is the outer annulus of the reactor, and a 3.175 mm OD sintered alumina tube is the inner annulus, giving a 3.2 mm effective

hydraulic diameter to the reactor. The alumina tube accommodates a movable type K thermocouple which provides for the measurement of axial temperature gradients along the reactor length. Radial temperature gradients are measured as the differences between the centerline temperature and the wall temperature measured at ten fixed positions along the outer wall of the reactor. The location of the movable thermocouple inside the reactor is measured with a retractable measuring tape with an estimated accuracy of 0.25 inches. An isothermal condition is maintained by controlling the reactor wall temperature with OMEGA 6001-K-DC-A1 temperature controllers, a Transtemp Infrared Furnace, an entrance heater and an exit heat guard. Cooling water jackets on both ends of the reactor enable the desired sharp drop in temperature outside the reactor length.

b) Supercritical Coil Flow Reactor

The reactor is 6.19 m of 0.3175 mm OD x 0.1397 ID (1/8" x 0.055 in.) coiled Hastelloy C-276 tubing, immersed in a fluidized sand bath (Techne SBL-2D) for temperature control. The reaction temperature is measured via a type K thermocouple placed within the fluidized sand bath. A rapid drop in temperature of the reactor effluent is provided by an outlet cooling jacket. It is configured as shown in Figure 3.2.

Figure 3.1 Supercritical Annulus Flow Reactor Scheme

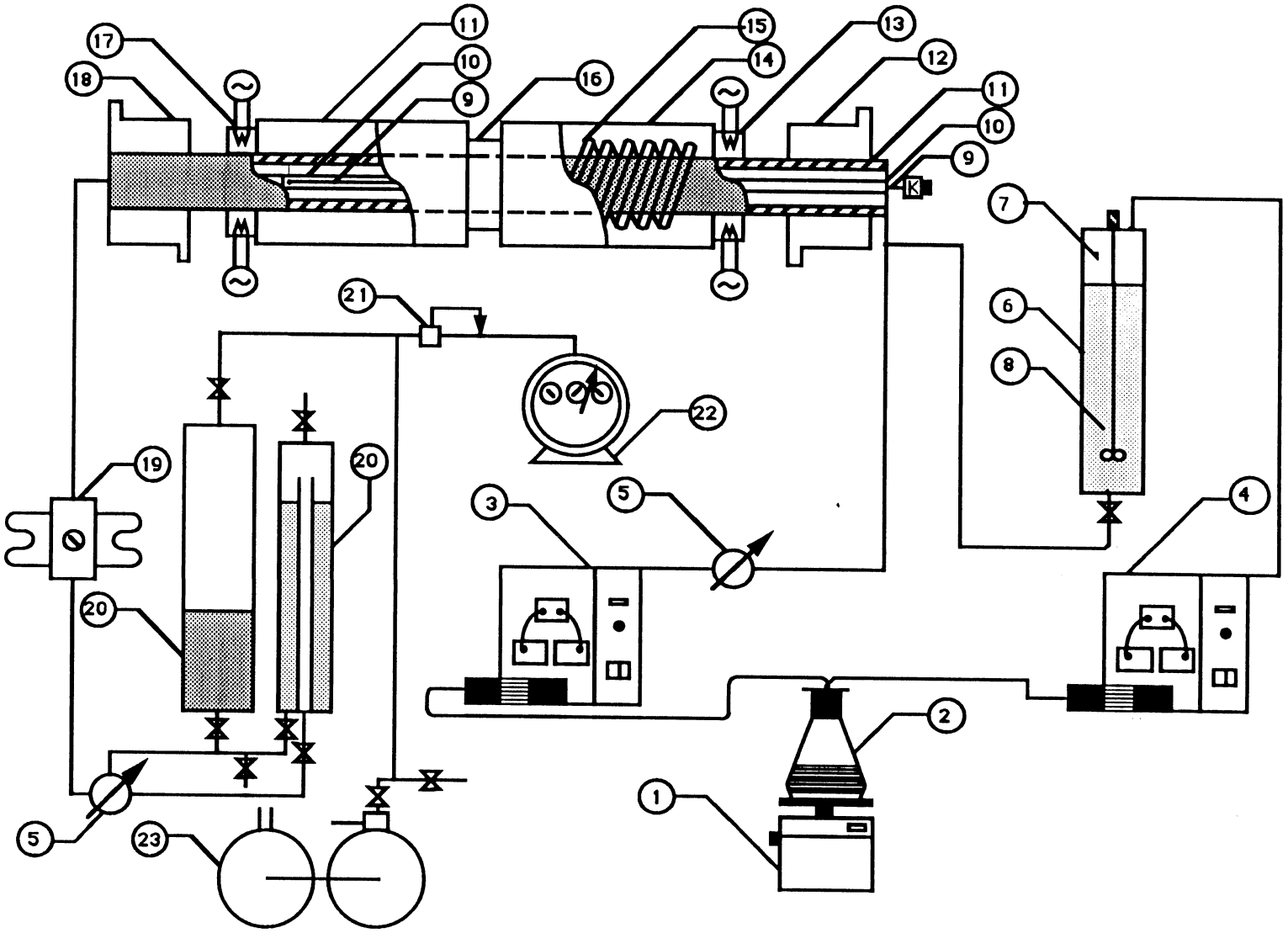

Figure 3.2 Supercritical Coil Flow Reactor Scheme

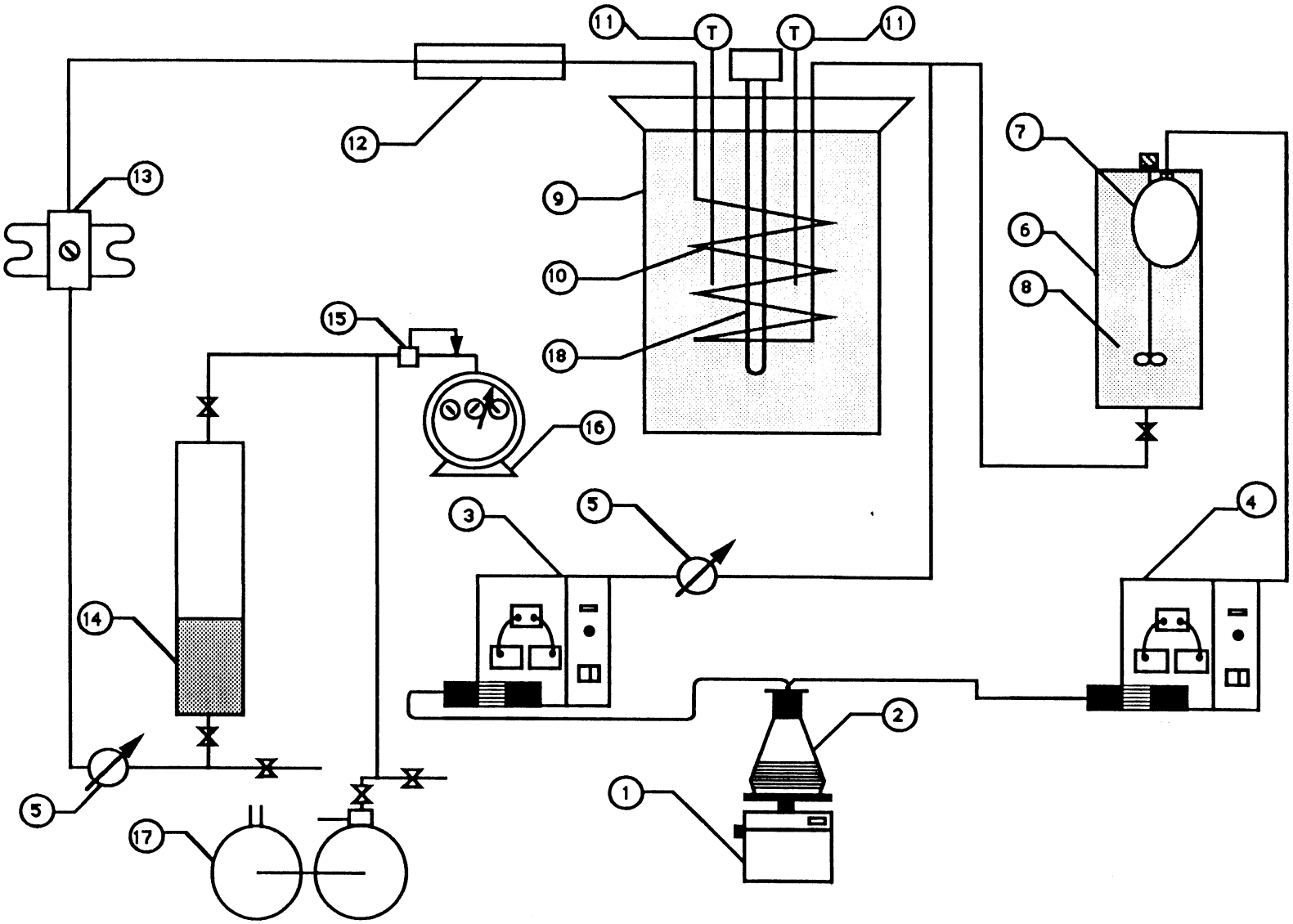

The computer program given in Appendix B was used to calculate the non-dimensional numbers and characteristic times which describe the two reactors used in this work. The values shown in Table 3.2 and 3.4 were used to calculate both the non-dimensional numbers and characteristic times for SCAFR and SCCFR respectively. Methanol was employed as a representative reactant for calculation. The values obtained in the right hand column of Table 3.3 for SCAFR and Table 3.5 for SCCFR are compared with the criteria taken from the literature. It is clear that both reactors and reacting conditions are well within the criteria established for the plug flow idealization. The references cited adjacent to the criteria in this section can be found in reference (Ramayya, 1987).

Table 3.2 Values for calculation of non-dimensional numbers and Characteristic times for SCAFR

'METHANOL'	!NAME OF THE REACTANT
823.	!OPERATING TEMPERATURE(K)
345.	!OPERATING PRESSURE(BARS)
45.72	!EFFECTIVE REACTOR LENGTH(CMS)
0.457	!REACTOR OUTER DIAMETER(CMS)
0.317	!REACTOR INNER DIAMETER(CMS)
53.	!RESIDENCE TIME(S)
121.	!THERMAL CONDUCTIVITY(MILLIWAT/M.K)
8.494	!SPECIFIC VOLUME(CM**3/G)
3.935	!SPECIFIC HEAT AT CONST PRESS(KJ/KG K)
353.3	!DYNAMIC VISCOSITY(MICROPOISE)
32.	!REACTANT MOLECULAR WEIGHT
513.2	!REACTANT CRITICAL TEMPERATURE(K)
79.5	!REACTANT CRITICAL PRESSURE(BARS)
18.	!SOLVENT MOLECULAR WEIGHT
647.4	!SOLVENT CRITICAL TEMPERATURE(K)
218.3	!SOLVENT CRITICAL PRESSURE(BARS)
0.86	!COMPRESSIBILITY FOR REACTANT
1.	!FLOW RATE(ML/MIN)
0.135	!RATE CONSTANT(1/SEC) from reference (Webley and Tester, 1989).

Table 3.3 Non-dimensional numbers and characteristic times for SCAFR

NAME OF THE REACTANT	METHANOL
OPERATING TEMPERATURE (DEG KELVIN)	823.000000
OPERATING PRESSURE (BARS)	345.000000
EFFECTIVE REACTOR LENGTH (CM)	45.720000
REACTOR OUTER DIAMETER (CM)	4.570000E-01
REACTOR INNER DIAMETER (CM)	3.170000E-01
RESIDENCE TIME (SEC)	53.000000
THERMAL CONDUCTIVITY (MILLIWAT/M DEG.K)	121.000000
SPECIFIC VOLUME (CM**3 / GRMS)	8.494000
SPECIFIC HEAT AT CONST PRESS (KJ/KG DEG.K)	3.935000
DYNAMIC VISCOSITY (MICROPOISE)	353.300000
REACTANT MOLECULAR WT.	32.000000
REACTANT CRITICAL TEMP. (DEG. K)	513.200000
REACTANT CRITICAL PRESS. (BARS)	79.500000
SOLVENT MOLECULAR WT.	18.000000
SOLVENT CRITICAL TEMP. (DEG. K)	647.400000
SOLVENT CRITICAL PRESS. (BARS)	218.300000
COMPRESSIBILITY FOR REACTANT	8.600000E-01
FLOW RATE (ML / MIN)	1.000000
RATE CONSTANT	1.350000E-01
HYDRAULIC RADIUS (CM)	1.645904E-01
BULK VELOCITY (CM / SEC)	8.626415E-01
THERMAL DIFFUSIVITY (CM**2 / SEC)	2.611878E-03
KINEMATIC VISCOSITY (CM**2 / SEC)	3.000930E-03
DIFFUSIVITY-->NONPOLAR, VAPOR (CM**2/SEC)	2.321410E-03
T. DIFFUSIVITY-->NONPOLAR, VAPOR (CM**2/SEC)	1.832373E-01
DIFFUSIVITY-->POLAR , VAPOR (CM**2/SEC)	3.692728E-03
T. DIFFUSIVITY-->POLAR , VAPOR(CM**2/SEC)	1.174243E-01
DIFFUSIVITY-->LIQUID (CM**2/SEC)	6.927065E-04
T. DIFFUSIVITY-->LIQUID (CM**2/SEC)	6.069810E-01

DIFFUSION->NON-POLAR, VAPOR (BIRDS FORMULA)

CHARACTERISTIC TIMES (SEC)

TFc,R	=	1.907981E-01
TFc,L	=	53.000000
TSd,R	=	11.669630
TSd,L	=	11407.720000
Ttd,R	=	10.371850
Ttd,L	=	800312.400000
Tmd	=	9.027200
Tck	=	7.407407

Table 3.3 Continued

NON-DIMENSIONAL NUMBERS

RE.NO.	(Tmd / Tfcr) =	47.312830
PR.NO.	(Ttdr / Tmd) =	1.148955
SC.NO.	(Tsdr / Tmd) =	1.292719
Pesd.NO.	(Tsdr / Tfcr) =	61.162190
Petd.NO.	(Ttdr / Tfcr) =	54.360310
DA.	(Tsdr / Tck) =	1.575400

NEGLIGIBLE AXIAL DIFFUSION

NAME	CRITERIA	VALUE
DICKENS ETAL, 1960 AZATYAN, 1972 HOWARD, 1979 FURUE AND PACEY, 1980	Tfcr**2/Tck*Tsdr < 0.1	4.211385E-04
MULCATY AND PETHARD,1963	Tfcl/Tsdl < 0.015	4.645978E-03
DANG AND STEINBERG, 1980	Tfcr/Tsdr < 0.02	1.634997E-02
FURUE AND PACEY, 1980	Tfcr**2/Tsdr*Tck + Tsdr/48*Tck << 1	3.324198E-02
	Tfcl/Tck << 2	7.155000

NEGLIGIBLE POISEUILLE FLOW

NAME	CRITERIA	VALUE
CLELAND AND WILHEM, 1956	Tsdr/Tfcl < 0.5	2.201817E-01
MULCAHY AND PETHARD,1963	Tsdr/Tfcl << 14.29	2.201817E-01
WALKER, 1961	Tsdr/Tck << 10	1.575400
POIRIER AND CARR, 1971	Tsdr/Tck << 2	1.575400
OGRER, 1975	Tsdr/Tck << 1.0	1.575400
BROWN, 1978	Tfcr/Tck < 0.05	2.575775E-02

Table 3.3 Continued

NEGLIGIBLE NON-ISOTHERMALITY

NAME	CRITERIA	VALUE
GILBERT, 1958	Ttdr/Tfcl << 3.7	1.956952E-01
MULCAHY AND PETHARD,1963	Ttdr/Tfcl << 1.0	1.956952E-01
FURUE AND PACAY, 1980	Ttdr/Tfcl << 1.0	1.956952E-01

DIFFUSION->POLAR, VAPOR (BIRDS FORMULA)

CHARACTERISTIC TIMES (SEC)

TFc,R	=	1.907981E-01
TFc,L	=	53.000000
TSd,R	=	7.336039
TSd,L	=	17801.410000
Ttd,R	=	10.371850
Ttd,L	=	800312.400000
Tmd	=	9.027200
Tck	=	7.407407

NON-DIMENSIONAL NUMBERS

RE.NO.	(Tmd / Tfcr) =	47.312830
PR.NO.	(Ttdr / Tmd) =	1.148955
SC.NO.	(Tsdr / Tmd) =	8.126594E-01
Pesd.NO.	(Tsdr / Tfcr) =	38.449210
Petd.NO.	(Ttdr / Tfcr) =	54.360310
DA.	(Tsdr / Tck) =	9.903652E-01

Table 3.3 Continued

NEGLIGIBLE AXIAL DIFFUSION

NAME	CRITERIA	VALUE
DICKENS ETAL, 1960 AZATYAN, 1972 HOWARD, 1979 FURUE AND PACEY, 1980	Tfcr**2/Tck*Tsdr < 0.1	6.991610E-04
MULCATY AND PETHARD,1963	Tfcl/Tsdl < 0.015	2.977292E-03
DANG AND STEINBERG,1980	Tfcr/Tsdr < 0.02	2.600833E-02
FURUE AND PACEY, 1980	Tfcr**2/Tsdr*Tck + Tsdr/48*Tck << 1	2.130252E-02
	Tfcl/Tck << 2	7.155000

NEGLIGIBLE POISEUILLE FLOW

NAME	CRITERIA	VALUE
CLELAND AND WILHEM, 1956	Tsdr/Tfcl < 0.5	1.384158E-01
MULCATY AND PETHARD,1963	Tsdr/Tfcl << 14.29	1.384158E-01
WALKER, 1961	Tsdr/Tck << 10	9.903652E-01
POIRIER AND CARR, 1971	Tsdr/Tck << 2	9.903652E-01
OGRER, 1975	Tsdr/Tck << 1.0	9.903652E-01
BROWN, 1978	Tfcr/Tck < 0.05	2.575775E-02

NEGLIGIBLE NON-ISOTHERMALITY

NAME	CRITERIA	VALUE
GILBERT, 1958	Ttdr/Tfcl << 3.7	1.956952E-01
MULCAHY AND PETHARD,1963	Ttdr/Tfcl << 1.0	1.956952E-01
FURUE AND PACAY, 1980	Ttdr/Tfcl << 1.0	1.956952E-01

Table 3.4 Values for calculation of non-dimensional numbers and Characteristic times for SCCFR

'METHANOL'	!NAME OF THE REACTANT
823.	!OPERATING TEMPERATURE(K)
345.	!OPERATING PRESSURE(BARS)
600.	!EFFECTIVE REACTOR LENGTH(CMS) 20 ft
0.140	!REACTOR OUTER DIAMETER(CMS)
0.000	!REACTOR INNER DIAMETER(CMS)
53.	!RESIDENCE TIME(S)
121.	!THERMAL CONDUCTIVITY(MILLIWAT/M.K)
8.494	!SPECIFIC VOLUME(CM**3/G)
3.935	!SPECIFIC HEAT AT CONST PRESS(KJ/KG K)
353.3	!DYNAMIC VISCOSITY(MICROPOISE)
32.	!REACTANT MOLECULAR WEIGHT
513.2	!REACTANT CRITICAL TEMPERATURE(K)
79.5	!REACTANT CRITICAL PRESSURE(BARS)
18.	!SOLVENT MOLECULAR WEIGHT
647.4	!SOLVENT CRITICAL TEMPERATURE(K)
218.3	!SOLVENT CRITICAL PRESSURE(BARS)
0.86	!COMPRESSIBILITY FOR REACTANT
1.	!FLOW RATE(ML/MIN)
0.135	!RATE CONSTANT(1/SEC) from reference (Webley and Tester, 1989).

Table 3.5 Non-dimensional numbers and characteristic times for SCCFR

NAME OF THE REACTANT	METHANOL
OPERATING TEMPERATURE (DEG KELVIN)	823.000000
OPERATING PRESSURE (BARS)	345.000000
EFFECTIVE REACTOR LENGTH (CM)	600.000000
REACTOR OUTER DIAMETER (CM)	1.400000E-01
REACTOR INNER DIAMETER (CM)	0.000000E+00
RESIDENCE TIME (SEC)	53.000000
THERMAL CONDUCTIVITY (MILLIWAT/M DEG.K)	121.000000
SPECIFIC VOLUME (CM**3 / GRMS)	8.494000
SPECIFIC HEAT AT CONST PRESS (KJ/KG DEG.K)	3.935000
DYNAMIC VISCOSITY (MICROPOISE)	353.300000
REACTANT MOLECULAR WT.	32.000000
REACTANT CRITICAL TEMP. (DEG. K)	513.200000
REACTANT CRITICAL PRESS. (BARS)	79.500000
SOLVENT MOLECULAR WT.	18.000000
SOLVENT CRITICAL TEMP. (DEG. K)	647.400000
SOLVENT CRITICAL PRESS. (BARS)	218.300000
COMPRESSIBILITY FOR REACTANT	8.600000E-01
FLOW RATE (ML / MIN)	1.000000
RATE CONSTANT	1.350000E-01
HYDRAULIC RADIUS (CM)	7.000000E-02
BULK VELOCITY (CM / SEC)	11.320760
THERMAL DIFFUSIVITY (CM**2 / SEC)	2.611878E-03
KINEMATIC VISCOSITY (CM**2 / SEC)	3.000930E-03
DIFFUSIVITY-->NONPOLAR, VAPOR (CM**2/SEC)	2.321410E-03
T. DIFFUSIVITY-->NONPOLAR, VAPOR(CM**2/SEC)	5.638099
DIFFUSIVITY-->POLAR, VAPOR (CM**2/SEC)	3.692728E-03
T. DIFFUSIVITY-->POLAR, VAPOR (CM**2/SEC)	3.546588
DIFFUSIVITY-->LIQUID (CM**2/SEC)	6.927065E-04
T. DIFFUSIVITY-->LIQUID (CM**2/SEC)	18.887410

DIFFUSION->NON-POLAR, VAPOR (BIRDS FORMULA)

CHARACTERISTIC TIMES (SEC)

TFc,R	=	6.183333E-03
TFc,L	=	53.000000
TSd,R	=	2.110786
TSd,L	=	63851.310000
Ttd,R	=	1.876045
Ttd,L	=	1.378319E+08
TMd	=	1.632827
Tck	=	7.407407

Table 3.5 Continued

NON-DIMENSIONAL NUMBERS

RE.NO.	(Tmd / Tfcr) =	264.069100
PR.NO.	(Ttdr / Tmd) =	1.148955
SC.NO.	(Tsdr / Tmd) =	1.292719
Pesd.NO.	(Tsdr / Tfcr) =	341.367100
Petd.NO.	(Ttdr / Tfcr) =	303.403500
DA.	(Tsdr / Tck) =	2.849562E-01

NEGLIGIBLE AXIAL DIFFUSION

NAME	CRITERIA	VALUE
DICKENS ETAL, 1960 AZATYAN, 1972 HOWARD, 1979 FURUE AND PACEY, 1980	Tfcr**2/Tck*Tsdr < 0.1	2.445315E-06
MULCATY AND PETHARD,1963	Tfcl/Tsdl < 0.015	8.300534E-04
DANG AND STEINBERG, 1980	Tfcr/Tsdr < 0.02	2.929398E-03
FURUE AND PACEY, 1980	Tfcr**2/Tsdr*Tck + Tsdr/48*Tck << 1	5.939032E-03
	Tfcl/Tck << 2	7.155000

NEGLIGIBLE POISEUILLE FLOW

NAME	CRITERIA	VALUE
CLELAND AND WILHEM, 1956	Tsdr/Tfcl < 0.5	3.982616E-02
MULCATY AND PETHARD,1963	Tsdr/T << 14.29	3.982616E-02
WALKER, 1961	Tsdr/Tck << 10	2.849562E-01
POIRIER AND CARR, 1971	Tsdr/Tck << 2	2.849562E-01
OGRER, 1975	Tsdr/Tck << 1.0	2.849562E-01
BROWN, 1978	Tfcr/Tck < 0.05	8.347500E-04

Table 3.5 Continued

NEGLIGIBLE NON-ISOTHERMALITY

NAME	CRITERIA	VALUE
GILBERT, 1958	Ttdr/Tfcl << 3.7	3.539707E-02
MULCAHY AND PETHARD,1963	Ttdr/Tfcl << 1.0	3.539707E-02
FURUE AND PACAY, 1980	Ttdr/Tfcl << 1.0	3.539707E-02

DIFFUSION->POLAR, VAPOR (BIRDS FORMULA)

CHARACTERISTIC TIMES (SEC)

TFc,R	=	6.183333E-03
TFc,L	=	53.000000
TSd,R	=	1.326932
TSd,L	=	101506.000000
Ttd,R	=	1.876045
Ttd,L	=	1.378319E+08
TMd	=	1.632827
Tck	=	7.407407

NON-DIMENSIONAL NUMBERS

RE.NO.	(Tmd / Tfcr)	=	264.069100
PR.NO.	(Ttdr / Tmd)	=	1.148955
SC.NO.	(Tsdr / Tmd)	=	8.126594E-01
Pesd.NO.	(Tsdr / Tfcr)	=	214.598200
Petd.NO.	(Ttdr / Tfcr)	=	303.403500
DA.	(Tsdr / Tck)	=	1.791359E-01

Table 3.5 Continued

NEGLIGIBLE AXIAL DIFFUSION

NAME	CRITERIA	VALUE
DICKENS ETAL, 1960 AZATYAN, 1972 HOWARD, 1979 FURUE AND PACEY, 1980	Tfcr**2/Tck*Tsdr < 0.1	3.889827E-06
MULCATY AND PETHARD,1963	Tfcl/Tsdl < 0.015	5.221365E-04
DANG AND STEINBERG, 1980	Tfcr/Tsdr < 0.02	4.659871E-03
FURUE AND PACEY, 1980	Tfcr**2/Tsdr*Tck + Tsdr/48*Tck << 1	3.735887E-03
	Tfcl/Tck << 2	7.155000

NEGLIGIBLE POISEUILLE FLOW

NAME	CRITERIA	VALUE
CLELAND AND WILHEM, 1956	Tsdr/Tfcl < 0.5	2.503646E-02
MULCAHY AND PETHARD,1963	Tsdr/Tfcl << 14.29	2.503646E-02
WALKER, 1961	Tsdr/Tck << 10	1.791359E-01
POIRIER AND CARR, 1971	Tsdr/Tck << 2	1.791359E-01
OGRER, 1975	Tsdr/Tck << 1.0	1.791359E-01
BROWN, 1978	Tfcr/Tck < 0.05	8.347500E-04

NEGLIGIBLE NON-ISOTHERMALITY

NAME	CRITERIA	VALUE
GILBERT, 1958	Ttdr/Tfcl << 3.7	3.539707E-02
MULCAHY AND PETHARD,1963	Ttdr/Tfcl << 1.0	3.539707E-02
FURUE AND PACAY, 1980	Ttdr/Tfcl << 1.0	3.539707E-02

3.1.3 Sampling System

The system consists of a ten-port dual sampling loop valve (Valco Instruments Co.Inc.), two sealed, evacuated test tubes (VACUTAINER No.6430 for 10 cm^3 and No.6433 for 20 cm^3 volume) and a vacuum pump as shown in Figure 3.3. The test tubes are connected by a needle bridge. They are weighed before and after use. The ten-port sampling loop is able to capture a 5.0 ml sample, while the continuous flow of products from the reactor bypass through an alternative route. The possible system configuration is shown in Figure 3.4.

Figure 3.3 Sampling system of the SCFR (Leesomboon, 1988; DeAlmeida, 1986)

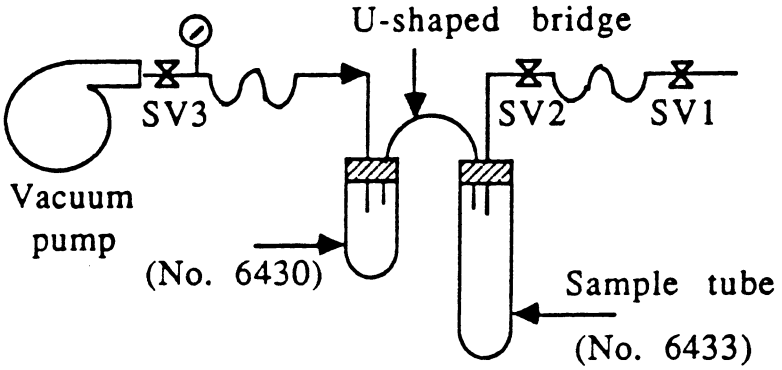

Figure 3.4 Configuration of sampling valve (Leesomboon, 1988; DeAlmeida, 1986)

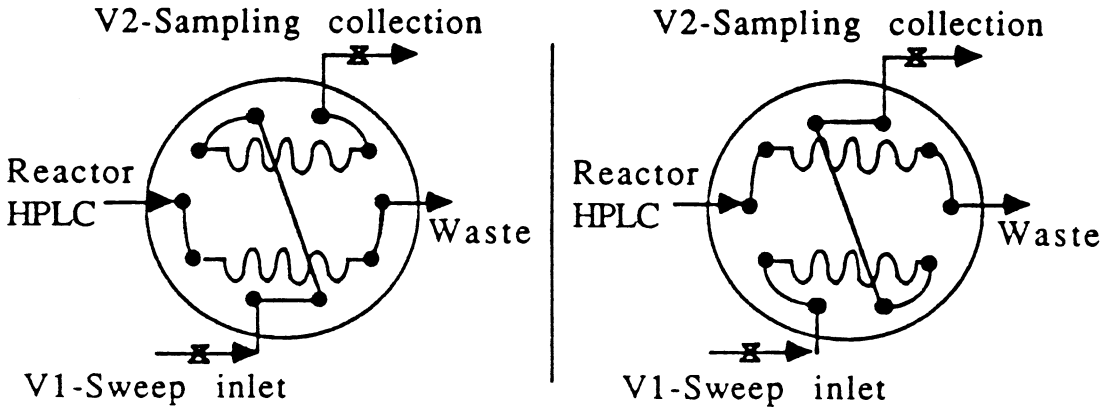

3.1.4 Slurry Feeding System

A HPLC pump was employed for glucose gasification experiments. For the wet biomass gasification experiments, in which the reactant is heterogeneous, an extra feeding system was required. Initially, a 500 ml stainless steel vessel was used. Because the feed slurry settled in the vessel and became inhomogeneous at high reactant concentration, it was replaced by a 500 ml capacity, high pressure and temperature vessel, series 4570/80, equipped with a A1120HC magnetic drive (Parr Instrument Company). The entrance of the feeding tank was connected to an HPLC pump and the exit to the supercritical flow reactor. Two feeding methods, a diesel oil feeding system and a balloon feeding system, were designed to operate with the heterogeneous mixture (wet biomass slurry). The description for each system is given below:

a) Diesel Oil Feeding System

This system requires diesel oil, insoluble in water, to force wet biomass slurry through the reactor. First of all, wet biomass slurry was placed in the feeding vessel prior to the initiation of the experiment. Diesel oil was pumped into the feeder to replace the biomass slurry. Wet biomass slurry, thus, was fed into the reactor continuously. At the beginning, this system was designed and used with earlier experiments involving a low reactant concentration. Later we designed a balloon feeding system in order to provide the

higher speeds of agitation necessary for higher concentrations of biomass slurry. We also found that the balloon system was preferable to the diesel oil system, in terms of ease of use and cleaning.

b) Balloon Feeding System

A 10 gm meteorological balloon (Weather Measure Company) was placed in the feeder filled with wet biomass slurry. Water was pumped into the balloon, the volume of which replaced the wet biomass slurry.

3.1.5 Chemical Analysis Instrument

A Hewlett Packard model 5830A Gas Chromatography, equipped with thermal conductivity and flame ionization detectors and Carbosieve S-II (Supelco, Inc.) column is employed to analyze gas composition.

3.2 Experimental Procedures

The experimental procedures for both reactors are explained together:

1. The system is brought up to operating pressure by an air compressor.

2. Afterwards, the HPLC pump forces deaerated, deionized water to flow through the system. The flow of products into

the accumulator displaces air through a back-pressure regulator and into a wet test meter.

3. For wet biomass gasification, an extra feeding tank filled with wet biomass slurry is brought up to desired operating pressure either by diesel oil (for diesel oil feeding system) or water (for balloon feeding system), as explained previously.

4. The water flow is rapidly heated to reaction temperature by an entry heater, temperature controllers and an exit heat guard (for SCAFR), and by immersed and bottom heaters (for SCCFR).

5. During a run, the mass flow rate of the feed solution into the reactor is constantly measured using a Mettler E2000 balance, while the outflow can be measured using the wet test meter. For experiments involving a biomass slurry, the flow rate of diesel oil to the feeder is measured.

6. Once the operating conditions are reached, the desired feed solution is pumped directly through the reactor, for glucose gasification. In case of wet biomass slurry, either a diesel oil or a balloon feeding system was employed, as mentioned earlier.

For the diesel oil feeding system (used in the beginning with low reactant concentration experiments), diesel oil was pumped into the feeder to replace the wet biomass slurry. Wet biomass slurry, thus, was fed into the reactor continuously. For the balloon system, instead of diesel oil, water was pumped into the balloon placed in the feeder to replace the wet biomass slurry feeding through the reactor. The latter system was used with high concentrations of biomass, and later displaced the diesel oil feeding system, for reasons already mentioned.

7. A comprehensive temperature profile, including the centerline and wall temperatures, is recorded when steady state operation is established (for SCAFR). The bath temperature is recorded for SCCFR.

8. The effluent from the reactor, cooled to an ambient temperature by the water-cooling jacket, flows through a 20 micron filter to one of the dual sampling loops. The filter is employed to prevent large particles from entering the loop sampling system. A product sample volume, 5 ml, which exceeds the reactor's functional volume, is trapped in the sample loop, assuring a representative sample of the product stream.

9. The captive sample containing the products at reaction pressure is isolated by valve SV3 (see Figure 3.3) from an

evacuated sampling system. When the sample loop is opened to the evacuated system, the products are projected into the larger 20 ml test tube. The pressure rise within the evacuated system measures the amount of gaseous products collected in the sample loop. Subsequently, the sample loop is purged with an injection of 20 ml water from the syringe through valve SV1. The water fills the large tube and displaces the gases into the small (10 ml) tube through the needle bridge. Usually, triplicate samples are taken for a particular set of reaction conditions, and subject to triplicate analyses. In some experiments, more than three samples are taken.

The composition of gaseous products is analyzed and quantified using a GC. Fixed gases H_2, O_2, N_2, CO, CH_4, CO_2, C_2H_2, C_2H_4 and C_2H_6 were separated by a 3.2 mm x 2.44 m 100/200 mesh Carbosieve S-II column using an 8.5 % hydrogen in helium carrier with a flow rate of 30 ml/min, and temperature program of 6 min at 50°C, followed by a 30°C/min rise to 190°C. A known calibration gas mixture, 12.9 % H_2, 9.8 % Ar, 38.75 % CO, 7.92 % CH_4, 8.97 % CO_2, 1.78 % C_2H_2, 15.2 % C_2H_4 and 0.92 % C_2H_6, was used to determine response factors for the thermal conductivity detector (TCD) and flame ionization detector (FID). The composition of gas sample was calculated using computer program GCN (see Appendix C). The computer program MBSUGAR (see Appendix A) which accurately accounts for the

effects of the various fluid compressibilities, the mass and elemental balances for each experiment was employed to calculate the elemental balances and absolute gas yields of each experimental results.

The liquid samples were not analyzed since most HPLC peaks could not be identified.

CHAPTER 4

RESULTS AND DISCUSSION

The experimental results of this study are presented in Tables 4.1 through 4.10 for the supercritical annular flow reactor and Tables 4.11 through 4.14 for the supercritical coil reactor. Figures 4.1 through 4.23 are related to these tables. These studies of glucose and wet biomass gasification in SCW to produce hydrogen have been carried out under various reaction conditions: temperature, residence time, initial reactant concentration and oxygen were all varied in a systematic manner. The influence of these parameters on the carbon balance (that is, the ratio of carbon in gas phase to carbon in reactant) and the yield of gaseous products, which are the major products of reaction, were studied using the SCAFR and the SCCFR.

4.1 Gasification in Supercritical Annulus Flow Reactor

4.1.1 Glucose Gasification in SCW

For glucose gasification in supercritical water, the influences of temperature, residence time, initial reactant concentration and oxygen on the carbon balance and the gaseous product yields were studied, in order to obtain information about the practical condition for wet biomass gasification. Amin et al. (Amin et al., 1975) discovered that in water at critical condition glucose decomposes to liquid and volatile

gases. In my study, in supercritical water, the products are also gas and liquid. However, the gas yield was much higher than the liquid yield. The major gas products were H_2, CO_2, CO and CH_4, and the minor products were C_2H_4 and C_2H_6.

a) Effect of Reaction Temperature

The chosen temperature range lies between 400 - 550°C at 25 - 34.5 MPa. The effect of temperature is shown in Table 4.1 and Figures 4.1 - 4.2. Increasing the temperature of the reaction increases the carbon balance and yields of CO_2 and H_2 while CO remains constant over the temperature range of 460 - 550°C.

From the Arrhenius rate law, the dependency of the rate constant k on temperature follows the relationship:

$$k = Ae^{-Ea/RT}$$

where A is a pre-exponential factor, E_a is activation energy, R is universal gas constant, and T is absolute temperature. The reaction rate is predominantly influenced by temperature. Also, the enthalpy of the overall reaction (discussion of overall reaction is in section 4.1.3) shows that this reaction is an endothermic reaction (See Appendix D), favored by a high temperature.

b) Effect of Residence Time

Table 4.2 and Figures 4.3 - 4.6 illustrate the effect of

residence time. Similar to the temperature effect, at long residence time, high carbon conversion and yields of CO_2, H_2, and CO are obtained.

c) Effect of Initial Reactant Concentration

Table 4.3 and Figures 4.7 - 4.8 display the effect of reactant concentration, comparing the results of 0.01M to 0.05M glucose at both 500°C and 550°C. The carbon balance and CO_2, H_2, and CH_4 yields decrease as the initial concentration of reactant increases. The slight increase of CO_2 observed when the concentration increases from 0.005M to 0.01M at 28 seconds residence time is probably not significant. These results indicate that the kinetics of gasification of glucose are neither first order nor second order. For a first order reaction, the rate of reaction is not affected by the initial concentration of reactant.

The following equation shows the relationship

$$r = dC/dt = k_A(C_0 - C)^n$$

where C = concentration of A that has been consumed

C_0-C = concentration of A at time t

C_0 = initial concentration of reactant

n = order of reaction

If it is a second order reaction, conversion will increase rapidly as the initial concentration increases (Levenspiel, 1972; Laidler, 1987). Therefore, the gas production was less

than first order in glucose concentration.

d) Effect of Oxygen

The effect of oxygen was examined with dihydroxyacetone (DHA) and glucose as the reactants and hydrogen peroxide (H_2O_2) as the oxidizer. Hydrogen peroxide decomposes in the reactor to provide free oxygen. Table 4.4 contains the data of the experiment with 0.005M and 0.01M DHA and 0.005M glucose, with and without hydrogen peroxide. Figures 4.9 and 4.10 are related to these tables. The presence of oxygen increases the carbon balance and CO_2 yield, but decreases the yield of hydrogen. These results suggest that oxygen selectively attacks and oxidizes the gaseous products, lowering the yield of hydrogen gas but raising the yield of CO_2. Because of this negative effect, no further studies of partial oxidation were conducted.

e) Effect of Reactant Type

As a next step towards more complicated feedstocks, soluble starch was studied as a reactant. This material was chosen because its solubility permits the preparation of a homogeneous polymeric feed solution. Gas yield for soluble starch experiments is defined the same as that of glucose and the chemical formula of soluble starch is assumed as $C_6H_{10}O_5$. Comparing the gasification of soluble starch and glucose, soluble starch gives higher carbon balance and CO, but lower

CO_2 and H_2 than glucose at the same reaction condition. The results are shown in Table 4.5. In Table 4.6, results of a study of residence time effect on starch gasification are displayed. As in the case of glucose, higher yields of gas and carbon balance are observed with increasing residence time.

4.1.2 Comparing These Results with Prior Work on Glucose Gasification in SCW

Comparing my result at 400°C and 34.5 MPa to the work done at 374°C and 22.9 MPa by Amin et al. (Amin et al., 1975), the percentage of carbon in gas phase from my work (28%) is higher than in their work (8%), (see Table 4.7). This is probably the effect of temperature, as higher temperature produces a higher fraction of carbon in the gas phase. Gas composition in Amin's work is 25.8% H_2, 34.4% CO_2, 35.5% CO, and 1.3% CH_4 while in my work, the gas composition is 40.7% H_2, 44.4% CO_2, 13.5% CO, 0.6% CH_4 and 0.8% C_{2+}.

4.1.3 The Global Reaction of Glucose Gasification in SCW

The experimental results show that the CO_2 yield is higher than CO, and the ratio of H_2 to CO_2 is close to 2, as shown in Figure 4.7. The expected primary reaction for glucose gasification in SCW is the pyrolysis of glucose:

$C_6H_{12}O_6$ -----> 6 CO + 6 H_2 Strong Endothermic

Reaction ____(4.1)

Moreover, H_2O is involved in the reaction of CH_3OH in SCW (Webley and Tester, 1988). Therefore, H_2 and CO_2 must be formed from the water-gas shift reaction (Webley et al., 1989; Amin et al., 1975):

CO + H_2O -----> CO_2 + H_2 Exothermic

Reaction ____(4.2)

The above equation derives from the study of CO oxidation in SCW (Helling and Tester, 1987; Webley and Tester, 1988) and is suggested to be a possible reaction in increasing H_2 yield in glucose gasification in SCW (Modell, 1982; Amin et al., 1975).

Therefore, the overall reaction (reaction (4.1) + (4.2)), steam gasification, is suggested as a global reaction for glucose gasification as follows:

$C_6H_{12}O_6$ + 6 H_2O -----> 12 H_2 + 6 CO_2 Endothermic

Reaction___(4.3)

4.1.4 <u>The Selected Operating Condition for Wet Biomass Gasification</u>

Experiments with model compounds indicate that high

yields (up to 500% molar yield) of hydrogen can be obtained from gasification in SCW. Yields are improved at high temperature (>500°C); long residence time (>1 minute); and low reactant concentration (ie. 0.9 g/l). Based on these preliminary results, the following practical conditions for wet biomass gasification were determined: 480 - 550°C; 34.5 MPa; and residence time longer than 28 seconds.

4.1.5 Wet Biomass Gasification

From the study of gasification of glucose in SCW, a practical condition of 550°C and 34.5 MPa was chosen to study the gasification of wet biomass in SCW to produce hydrogen. The influences of the reactant and reactant concentration on carbon balance and gaseous products were determined. The carbon balance and yields of gas (ratio of mole of gas to mole of carbon in reactant) from wet biomass are calculated by using the chemical compositions determined by an independent laboratory (See Table 3.1). The primary gas products in every experiment are H_2 and CO_2, but the ratio of the two gases varies.

The first experiment was gasification of algae in SCW. Carbon balance and the yields of gases from a solution of 1.12 g of algae/l at a residence time of 28 seconds are shown in Table 4.8. The ratio of H_2 and CO_2 is about 2.2:1.0. The estimated carbon conversion is in the range of 74 to 87%,

which is higher than that from the glucose experiment (66 to 71%) in the same condition.

The results of algae gasification experiments at higher concentration are also displayed in Table 4.8. The algae concentration in the second experiment is about three times that of the previously-mentioned experiment (3.34 g algae / 1 of solution). The operating condition was 520°C, 31.7 MPa, and 25 seconds residence time. The effects of initial reactant concentration and temperature on carbon balance and gas yields of this experiment are the same as in the glucose gasification experiment. The carbon balance and gas yields are lower when the initial reactant concentration increases but temperature decreases. The ratio of H_2 to CO_2, the two major products, is about 2.5:1.0.

A third algae experiment was conducted at 550°C, 34.5 MPa, and 49 seconds residence time. The results of sample no.M1 are obviously different from the other two. The carbon balance and gas yields of sample no.M1 are very much lower than those of the others. Some of the algae passing through the reactor settled and accumulated on the bottom of the reactor, resulting in a non-homogeneous mixture. The changing concentration with respect to time would account for the large variations in observed gas yields.

For kelp gasification, the operating condition was 550°C, 34.5 MPa, and 49 seconds residence time. Two initial concentrations, 7.78 and 17 g kelp/l of solution, were studied. The results are shown in Table 4.9. In the experiment of 17 g/l, the total amount of gas product was collected from the accumulator. The carbon balance and gas yields for kelp, compared to those of algae gasification, are lower.

Gasification of sewage sludge was also studied. In this case, the chemical composition of sewage sludge is assumed to be the same as that of raw sewage sludge reported and given in Table 3.1 (Urban et al., 1982). Carbon balance and gas yields of this experiment are generally lower than those of the above (See Table 4.10).

As can be seen, the higher yield of H_2 is obtained at higher temperature and longer residence time. Because the temperature and residence time limitation of the supercritical annulus reactor (550°C and 1 minute respectively), and the inhomogeneity of reactant fed to the reactor resulted in inconsistent data, a new supercritical coil reactor was equipped with a new feeder system and employed to further study the gasification of wet biomass in SCW.

4.2 Gasification of Wet Biomass in the New Supercritical Coil Flow Reactor

4.2.1 Effect of the Feeding System

In the beginning of the study of wet biomass gasification in SCW using SCCFR, a diesel oil feeder system was employed for feeding the wet biomass slurry. The experimental results are tabulated in Table 4.11.

To ensure that the diesel oil did not enter the reactor and interfere with the reaction, experiments employing the same conditions (550°C, 34.5 MPa and 33 - 134 seconds residence time) using a balloon feeder system were performed. The results are also shown in Table 4.11 and Figures 4.11 - 4.12. The changes of gas yields (H_2, CO_2, CH_4, CO and C_{2+}) and carbon gasified for both experiments are similar. These results illustrate that diesel oil does not affect the reaction chemistry of wet biomass. In spite of these positive results, we decided to substitute the balloon feeding system for the diesel oil feeding system when the agitator was operated at high speeds for use with high concentrations of wet biomass.

4.2.2 Effect of Reaction Conditions

The influences of temperature, residence time and initial reactant concentration on gas yields and carbon conversion of wet biomass gasification in SCW were also studied. However,

the operating temperature range (550 - 650°C) was higher than that of the SCAFR (400 - 550°C). Residence time also increased about two times from 26 - 53 seconds to 26 - 118 seconds. The gas yields (at various temperatures) are plotted vs residence time in Figures 4.13 - 4.15. Similar to glucose gasification, the products are mostly gaseous. The major products are, H_2 and CO_2, and minor products are CO, CH_4 and C_{2+}. The influence of each parameter on gas yield and carbon balance is discussed as follows:

a) Effect of Temperature

The effects of temperature on the carbon balance (the fraction of carbon gasified) of wet-biomass gasification in this reactor are tabulated in Table 4.12. They are similar to those of glucose gasification in SCAFR; the higher the temperature, the higher the carbon balance. Increasing the temperature from 550°C to 650°C, increases carbon balance by about 10 - 30%, depending on residence time as shown in Figure 4.16.

Gas yields, H_2, CO_2, CO, CH_4, and C_{2+}, are also increased by increasing temperature (see Figures 4.17 - 4.22). However, at higher temperature, ie. 650°C, the residence time predominantly effects the gas yields, as discussed in the next section.

b) Effect of Residence Time

Table 4.12 also illustrates the influence of residence time on carbon balance and yields of gas. At longer residence times, a larger fraction of the biomass carbon was converted to gas products, as seen in the increasing carbon balance.

It is obvious from Figures 4.17 and 4.18 that there are two contradictory effects of residence time on the gas yields of H_2 and CO_2. In the temperature range of 550°C to 600°C, longer residence time enhanced H_2 and CO_2 formation, but inhibited the formation of CH_4 and CO. Conversely, at 650°C, longer residence time suppressed the formation of H_2 and CO while CH_4 and CO_2 formation were promoted. The reason for the decrease in H_2 yield at longer residence time and higher temperature (650°C) probably involves the CH_4 and CO_2 formation as follows:

$$CO + 3\ H_2 \text{ -----> } CH_4 + H_2O \quad \text{_____(4.5)}$$

$$2\ CO + 2\ H_2 \text{ -----> } CH_4 + CO_2 \quad \text{_____(4.6)}$$

These two reactions took place after wet biomass were gasified by :

the steam reforming reaction for algae (see Appendix E)

$$(C_{1.79}H_{3.30}O_{1.25})_n + 0.54\ n\ H_2O \text{ -----> } 1.79\ n\ CO + 2.19\ n\ H_2 \quad \text{_____(4.4)}$$

and the water-gas shift reaction

$$CO + H_2O \text{ -----> } H_2 + CO_2 \quad \text{_____(4.2)}$$

The overall reaction ((4.2)+(4.4)) for H_2 formation is endothermic (favored by high temperature). The reduction of H_2 occurred because the product was not quenched promptly, and resulted in formations of CH_4 and CO_2 by (4.5) and (4.6). These two reactions were insignificant at lower temperatures (550°C and 600°C). More explanation is given in the next section.

c) Effect of the Immediate Quenching System

Previously, products exited the reactor into an about 0.4 ml tube before passing through the quenching system. Since the two possible reactions (4.5) and (4.6) presumably needed longer residence time and higher temperatures, the possibility of a reaction occurring in the 0.4 ml tube was investigated by quenching the products immediately after they exited the reactor. A study of this effect was performed at 650°C, 34.5 MPa and residence time of 26 - 106 seconds with 0.78 - 0.89 g/l algae. These results are displayed in Table 4.13 and Figures 4.23 - 4.24.

The H_2 yield increased from 31% to 43%, and CH_4 decreased from 24% to 19% at 650°C and a residence time of 106 seconds with the use of the immediate quenching system. This confirms that reactions (4.5) and (4.6) were inhibited when the product was rapidly quenched. It also shows the effect of residence time on a continuous tubular reactor and the importance of abrupt quenching in high temperature condition. Therefore, this immediate quenching system was connected to the outlet of reactor for the rest of the study.

d) Effect of Initial Reactant Concentration

Table 4.14 and Figures 4.25 - 4.26 show the effect of initial reactant concentration on gas yields and carbon balance respectively. At 650°C and 53 seconds, the carbon balance and gas yields are about the same. It seems that initial reactant concentration, in the range of 0.7 - 4.0 g/l, does not influence the carbon balance, H_2 and CO_2 yields at this temperature and residence time.

e) Effect of Type of Feedstock

Other than algae, other types of wet biomass, such as water hyacinth and kelp, can be used as raw materials for H_2 production. The results in Table 4.15 and Figure 4.27 show that water hyacinth can be gasified to gas products similar to those of algae. Nevertheless, carbon balance and H_2 yield results of kelp gasification are about twice as high as those

from water hyacinth and algae. This is probably caused by the difference of minerals in feedstocks, as follows:

Feedstocks	Minerals
Algae[a]	Crystobalite (SiO_2)
Kelp[a]	Apatite (KCl), Halite (NaCl), Zeolite

a : Analyzed using X-ray diffraction by Eric Decarlo, Geophysics Department, University of Hawaii (see the results in Appendix G).

4.2.3 Potential Hydrogen Yield

The overall reaction for wet biomass gasification in SCW is assumed to be steam reforming reaction as follows:

$$C_xH_yO_z + (2x-z)\ H_2O \text{ -----> } x\ CO_2 + \{2x+(y/2)-z\}\ H_2 \quad (4.7)$$

Theoretically, the potential hydrogen yields per mole of carbon in reactant of algae, water hyacinth and kelp are 2.22, 2.29 and 1.47 respectively. From the experimental hydrogen yields, the fractions of potential hydrogen yield ($H_{2,t}/H_{2,p}$), shown in Tables 4.12 - 4.15 and calculated in Appendix E, are about 0.20 for algae, 0.27 for water hyacinth, and 0.78 for kelp. These fractions for algae and water hyacinth were quite small because the wet biomass was not completely gasified and was gasified to other hydrocarbon gases, including CH_4 and C_{2+}.

But kelp was gasified more than algae and water hyacinth; hence the higher fraction of potential hydrogen yield with kelp. Furthermore, CO in the gas product of kelp gasification is small as a result of converting of CO to H_2 and CO_2.

In addition to the steam reforming reaction, CO and CH_4 produced from the gasification of wet biomass can further react with water, yielding in H_2. The fractions of potential hydrogen yield (including H_2 from CO and CH_4) displayed in Tables 4.12 - 4.15, are about 0.50 for algae, 0.46 for water hyacinth, and 1.23 for kelp. This difference is also because of the difference of minerals in feedstocks.

Table 4.1 The effect of temperature on glucose gasification in SCW
Reactant : 0.01M Glucose, P = 34.5MPa

	Temperature, C					
	400~ 112 sec.	460* 43 sec.	480** 38 sec.	500+ 34 sec.	520^ 31 sec.	550@ 28 sec.
C-Balance	0.275	0.634	0.644	0.703	0.685	0.727
H-Balance	0.200	0.558	0.700	0.663	0.773	0.856
O-Balance	0.468	0.964	0.930	1.043	0.975	1.026
CO2 yield	1.22	2.41	2.29	2.6	2.37	2.58
H2 yield	1.11	2.60	3.20	3.00	3.50	3.72
CO yield	0.37	0.97	1.01	1.07	1.10	1.00
CH4 yield	0.02	0.27	0.36	0.35	0.41	0.51
C2+ yield	0.02	0.07	0.10	0.09	0.10	0.13
H2/CO2	0.91	1.08	1.40	1.15	1.48	1.44

~ The average of exp. no. 37, 38 and 39
* The average of exp. no.21 and 22
**The average of exp. no. 23, 24 and 25
+ The average of exp. no. 30 and 31
^ The average of exp. no. 32 and 33
@ The average of exp. no. 34, 35 and 36

Table 4.2 The effect of residence time on glucose gasification in SCW
Condition : T = 550 C, P = 34.5 MPa

	0.01M Glucose		0.05M Glucose	
	Residence time (sec)		Residence time (sec)	
	28*	56**	28***	53****
C-Balance	0.727	0.798	0.644	0.686
H-Balance	0.856	1.064	0.739	1.118
O-Balance	1.026	1.024	0.922	0.887
CO2 yield	2.58	2.51	2.48	2.40
H2 yield	3.72	4.27	2.93	4.54
CO yield	1.00	1.14	0.57	0.51
CH4 yield	0.51	0.77	0.41	0.87
C2+ yield	0.13	0.19	0.11	0.14
H2/CO2	1.44	1.70	1.18	1.89

* The average of exp. no.34, 35 and 36
** The average of exp. no. 46, 47 and 48
*** The data of exp. no. 13
**** The average of exp. no. 18 and 19

Table 4.3 The effect of reactant concentration on glucose gasification in SCW
Condition : T = 500 and 550 C, P = 34.5 MPa

	T = 550 C, t = 28s			T = 500 C, t = 34s	
	0.005M*	0.01M**	0.05M***	0.01M @	0.05M^
C-Balance	0.695	0.727	0.570	0.703	0.419
H-Balance	1.123	1.064	0.586	0.663	0.352
O-Balance	0.982	1.024	0.699	1.043	0.568
CO2 yield	2.43	2.58	1.45	2.60	1.21
H2 yield	5.45	3.72	2.34	3.00	1.57
CO yield	1.04	1.00	1.30	1.07	1.00
CH4 yield	0.47	0.51	0.41	0.35	0.18
C2+ yield	0.11	0.13	0.12	0.06	0.09
H2/CO2	2.24	1.44	1.61	1.15	1.30

* The average data of exp. no. 43, 44 and 45
** The average data of exp. no. 34, 35 and 36
*** The average data of exp. no. 57 and 58
^ The average data of exp. no. 30 and 31
@ The average data of exp. no. 55 and 56

Table 4.4 The effect of oxygen on glucose gasification in SCW
Reactants : 0.01M DHA and 0.005M Glucose

	0.005M DHA at 480 C, 25 MPa, 6s		0.01M DHA at 480 C, 25 MPa, 24s		0.005M GLUCOSE at 550 C, 34.5MPa, 28s	
	No H2O2@	+0.01M H2O2#	No H2O2*	+0.01M H2O2**	No H2O2^	+0.005M H2O2~
C-Balance	0.602	0.937	1.097	1.217	0.695	0.785
H-Balance	0.556	0.487	1.305	1.373	1.123	1.045
O-Balance	0.942	1.609	1.459	1.778	0.982	1.120
CO2 yield	1.18	2.17	1.72	2.25	2.43	2.79
H2 yield	1.34	1.14	2.86	3.02	5.45	4.83
CO yield	0.47	0.48	0.95	0.84	1.04	1.15
CH4 yield	0.16	0.16	0.39	0.50	0.47	0.54
C2+ yield	0.00	0.00	0.12	0.03	0.11	0.11
H2/CO2	1.14	0.53	1.66	1.34	2.24	1.73

@ The data of exp. no. 1
# The average data of exp. no. 2 and 3
* The average data of exp. no. 28 and 29
** The average data of exp. no. 26 and 27
^ The average data of exp. no. 43, 44 and 45
~ The average data of exp. no. 40, 41 and 42

Table 4.5 The effect of reactant types on gasification in SCW
Reactants : 0.9 g/l glucose and 0.9 g/l soluble starch
Condition : T = 550 C, P = 34.5 MPa, t = 28 s

	Glucose *	Soluble starch **
C-Balance	0.695	0.732
H-Balance	1.123	1.041
O-Balance	0.982	1.161
CO2 yield	2.43	2.19
H2 yield	5.45	3.83
CO yield	1.04	1.42
CH4 yield	0.47	0.50
C2+ yield	0.11	0.15
H2/CO2	2.24	1.75

* The average data of exp. no. 43, 44 and 45
** The average data of exp. no. 52, 53 and 54

Table 4.6 The effect of residence time on soluble starch gasification in SCW
Reactant : 0.9 g/l of soluble starch at 550 C, 34.5 MPa

	28 s **	56 s *
C-Balance	0.732	0.883
H-Balance	1.041	1.266
O-Balance	1.161	1.394
CO2 yield	2.19	2.94
H2 yield	3.83	4.31
CO yield	1.42	1.10
CH4 yield	0.50	0.67
C2+ yield	0.15	0.27
H2/CO2	1.75	1.47

* The average data of exp. no. 49, 50 and 51
** The average data of exp. no. 52, 53 and 54

Table 4.7 Comparison of gas compositions from this work to others

% gas	This work at 400 C, 34.5 MPa	Work of Amin et al. at 374 C, 22.9 MPa
H2	40.7	25.8
CO2	44.4	34.4
CO	13.5	35.5
CH4	0.6	1.3
C2+	0.8	-

Table 4.8 Carbon balances and absolute gas yields from algae gasification in SCW

Reactant	Samp No.	Reaction Condition	C balance	H balance	O balance	Absolute Yield* CO2	H2	CO	CH4	C2H4	C2H6	H2/CO2
1.121 g/l Algae	G1	550 C 34.5 MPa	0.866	1.700	1.701	0.549	1.171	0.092	0.138	0.019	0.024	2.04
	G2	28 s	0.839	1.773	1.606	0.531	1.201	0.061	0.154	0.023	0.023	2.35
	G3		0.739	1.594	1.332	0.441	1.042	0.049	0.151	0.029	0.019	2.50
3.336 g/l Algae	I1	520 C 31.7 MPa	0.367	0.482	0.500	0.101	0.260	0.148	0.051	0.020	0.013	2.78
	I2	25 s	0.444	0.669	0.619	0.145	0.368	0.144	0.072	0.025	0.017	2.92
	I3		0.455	0.757	0.651	0.170	0.425	0.116	0.080	0.025	0.019	2.53
25 g/l Algae	M1	550 C 34.5 MPa	0.372	0.396	0.778	0.263	0.209	0.018	0.051	0.009	0.011	1.09
	M2	49 s	1.280	2.910	1.193	0.338	1.324	0.158	0.424	0.046	0.133	4.17
	M3		1.103	2.070	1.337	0.416	0.912	0.103	0.300	0.040	0.102	2.32

* Mole of gas product/Mole of carbon in reactant (dry, ash-free basis)

Table 4.9 Carbon balances and absolute gas yields from gasification of wet biomass in SCW
Condition : 550 C, 34.5 MPa and 49 seconds residence time

Reactant	Samp No.	C balance	H balance	O balance	Absolute Yield* CO2	H2	CO	CH4	C2H4	C2H6	H2/CO2
7.78 g/l of kelp	J1	0.576	1.565	0.601	0.381	0.866	0.018	0.128	0.009	0.016	2.04
	J2	0.559	1.478	0.589	0.375	0.813	0.015	0.125	0.008	0.014	2.04
17 g/l of kelp	N1**	0.284	0.966	0.242	0.151	0.513	0.007	0.09	0.007	0.015	3.40

* Mole of gas product/Mole of carbon in reactant (dry, ash-free basis)
** Gas product was collected from accumulator

Table 4.10 Carbon balances and absolute gas yields from sewage sludge gasification in SCW
Condition : 550 C, 34.5 MPa and 49 seconds residence time

Reactant	Samp No	C balance	H balance	O balance	Absolute Yield* CO2	H2	CO	CH4	C2H4	C2H6	H2/CO2
2.42 g/l of Sewage sludge	L1	0.413	0.335	1.617	0.352	0.246	0.026	0.012	0.008	0.004	0.88
	L2	0.396	0.428	1.477	0.321	0.306	0.025	0.017	0.01	0.006	0.95
	L3	0.273	0.342	0.982	0.212	0.242	0.019	0.014	0.009	0.005	1.50

* Mole of gas product/Mole of carbon in reactant (dry, ash-free basis)

Figure 4.1 Gas yields from 0.01M glucose gasification in SCW vs temperature

Residence time : 28 - 112 seconds

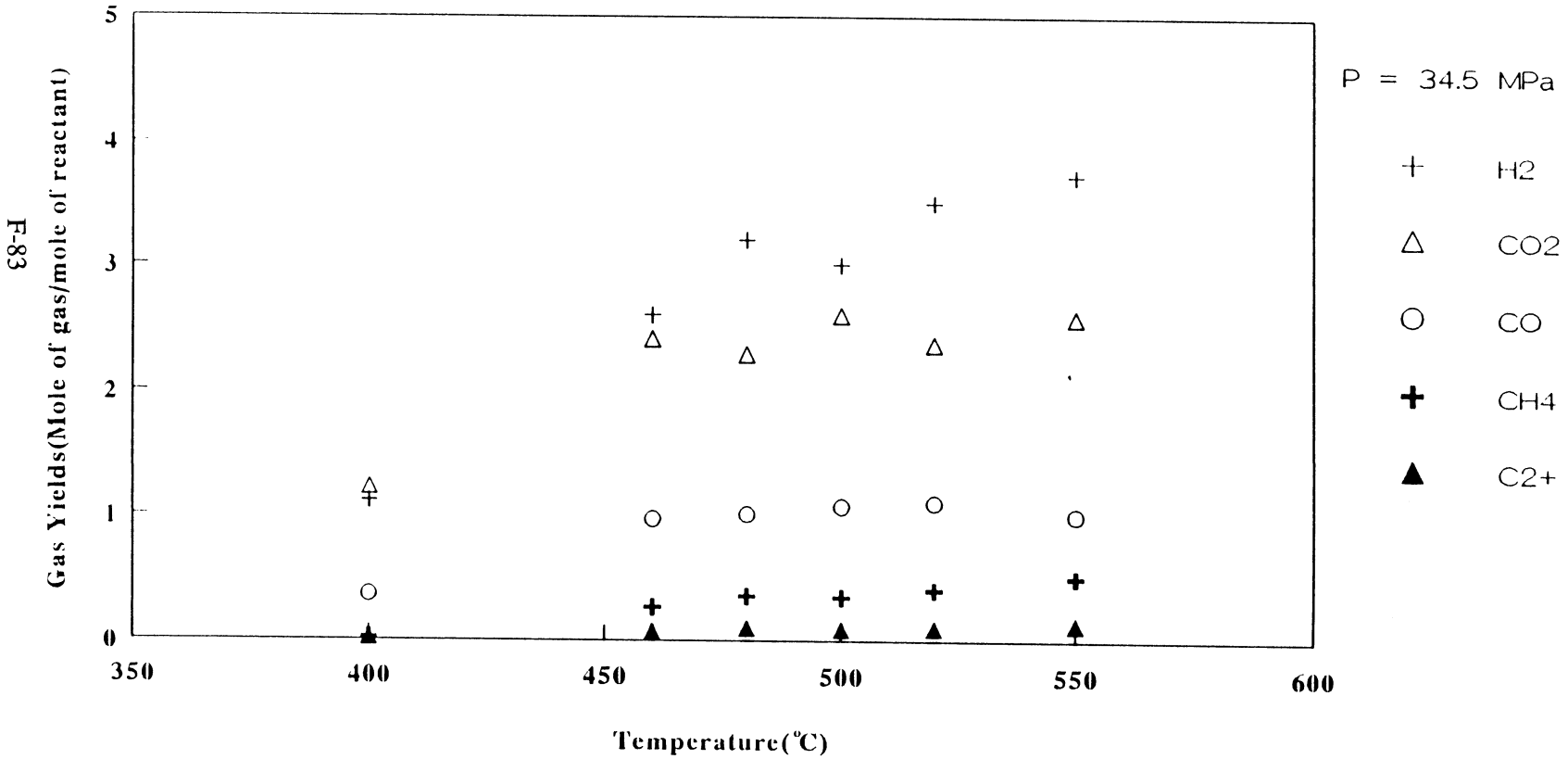

Figure 4.2 Elemental balance from 0.01M glucose gasification in SCW vs temperature

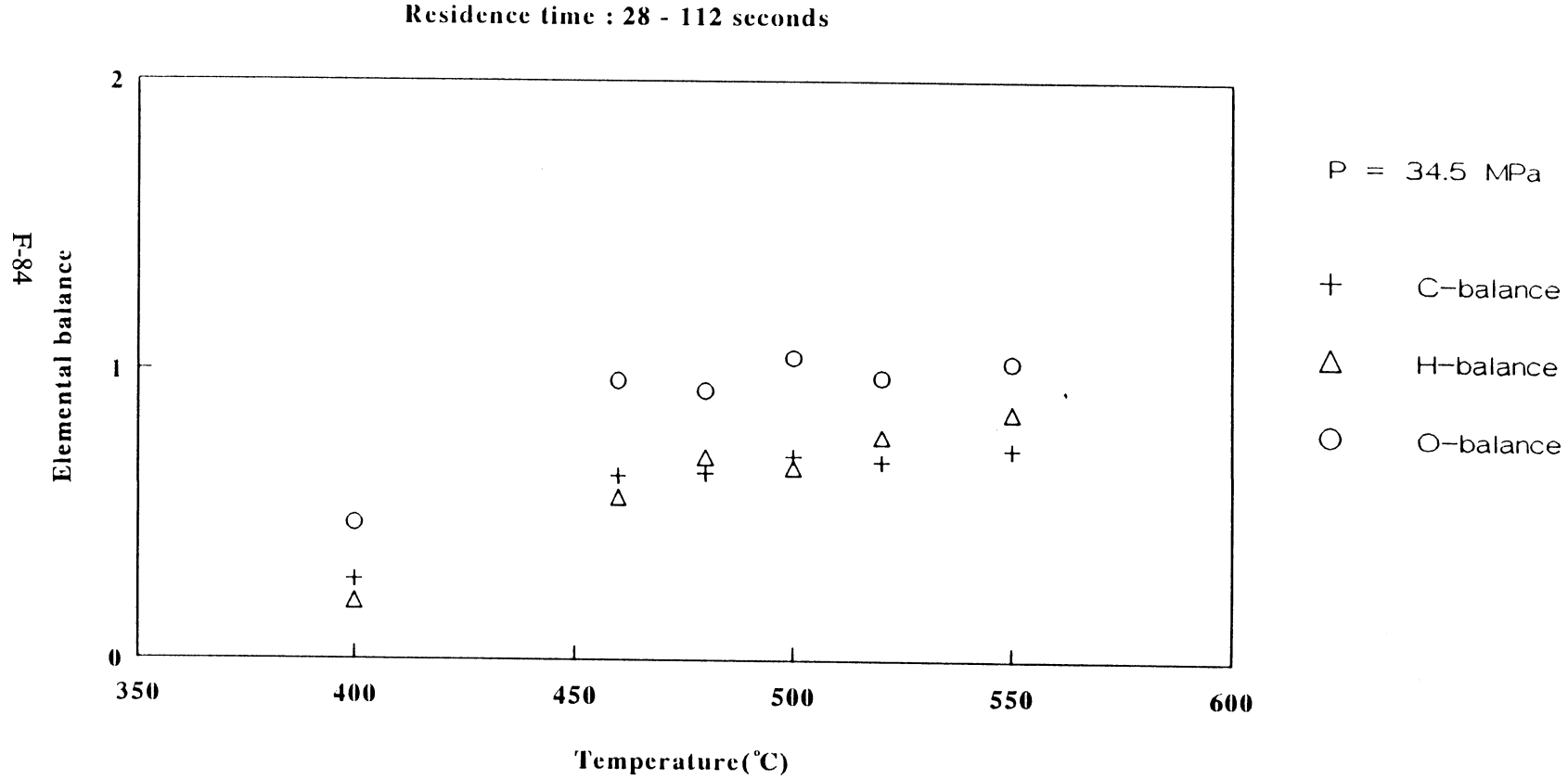

Figure 4.3 Gas yields from 0.05M glucose gasification in SCW vs residence time

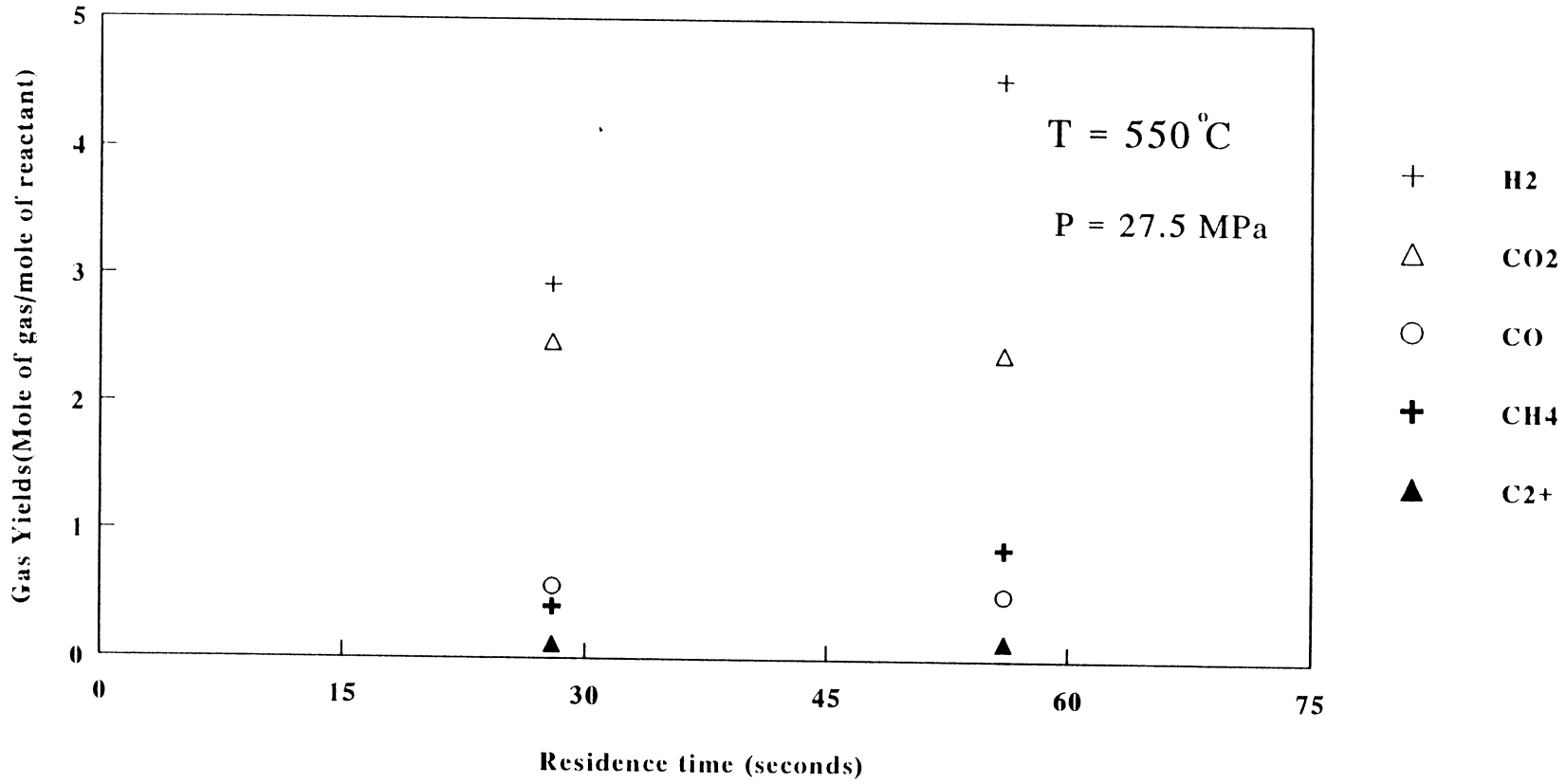

Figure 4.4 Elemental balance from 0.05M glucose gasification in SCW vs residence time

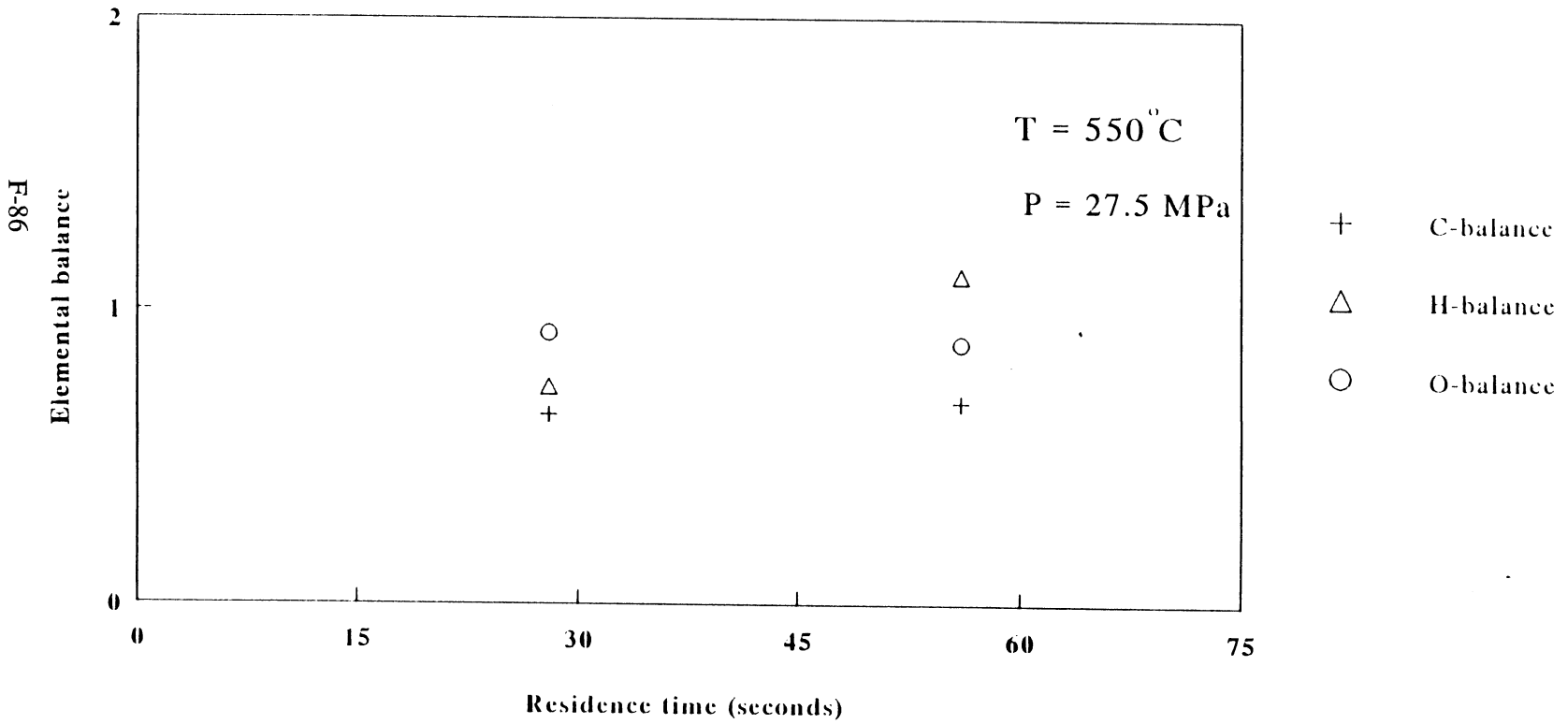

Figure 4.5 Gas yields from 0.01M glucose gasification in SCW vs residence time

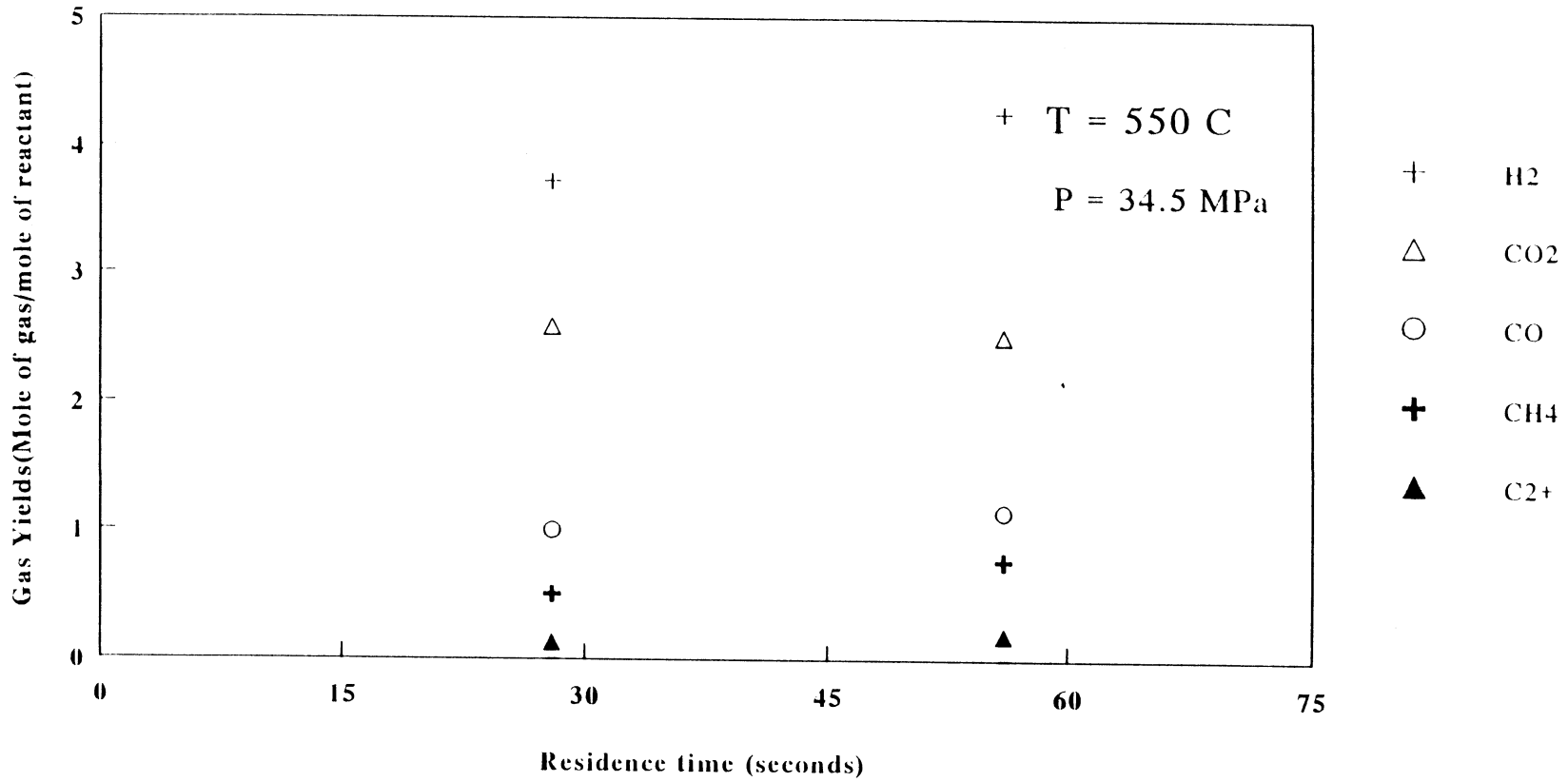

Figure 4.6 Elemental balance from 0.01M glucose gasification in SCW vs residence time

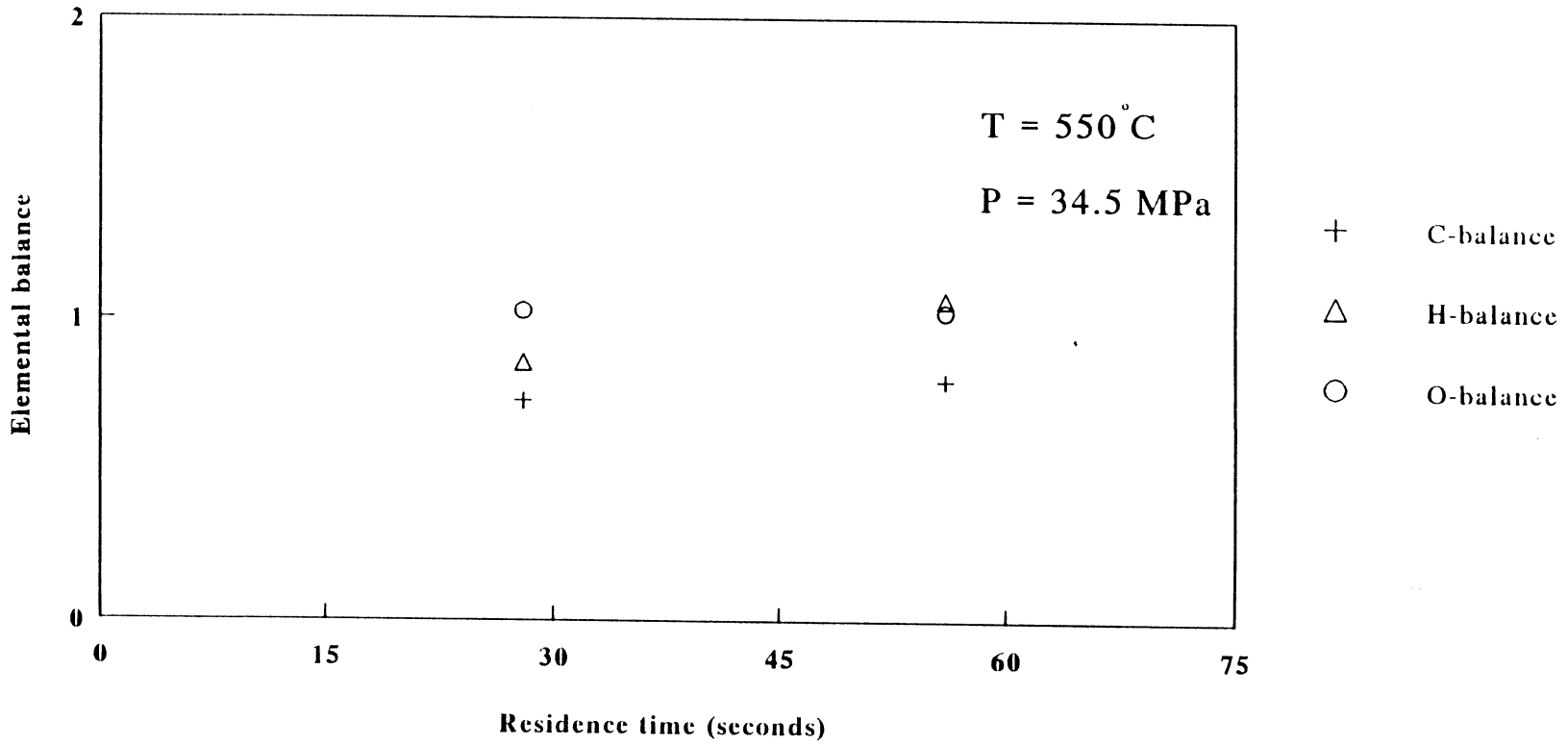

Figure 4.7 Gas yields from glucose gasification in SCW vs initial concentration

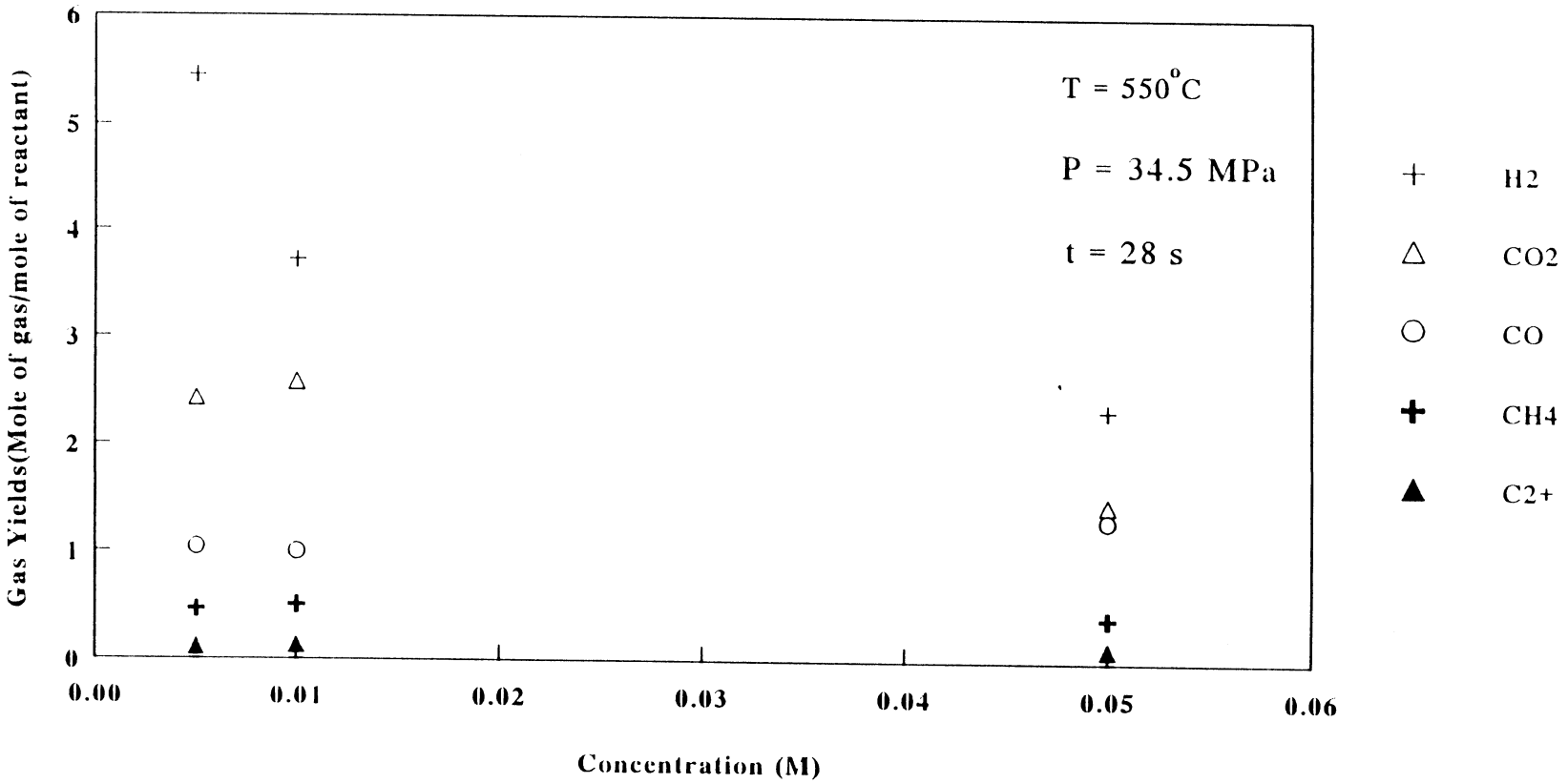

Figure 4.8 Elemental balance from glucose gasification in SCW vs initial concentration

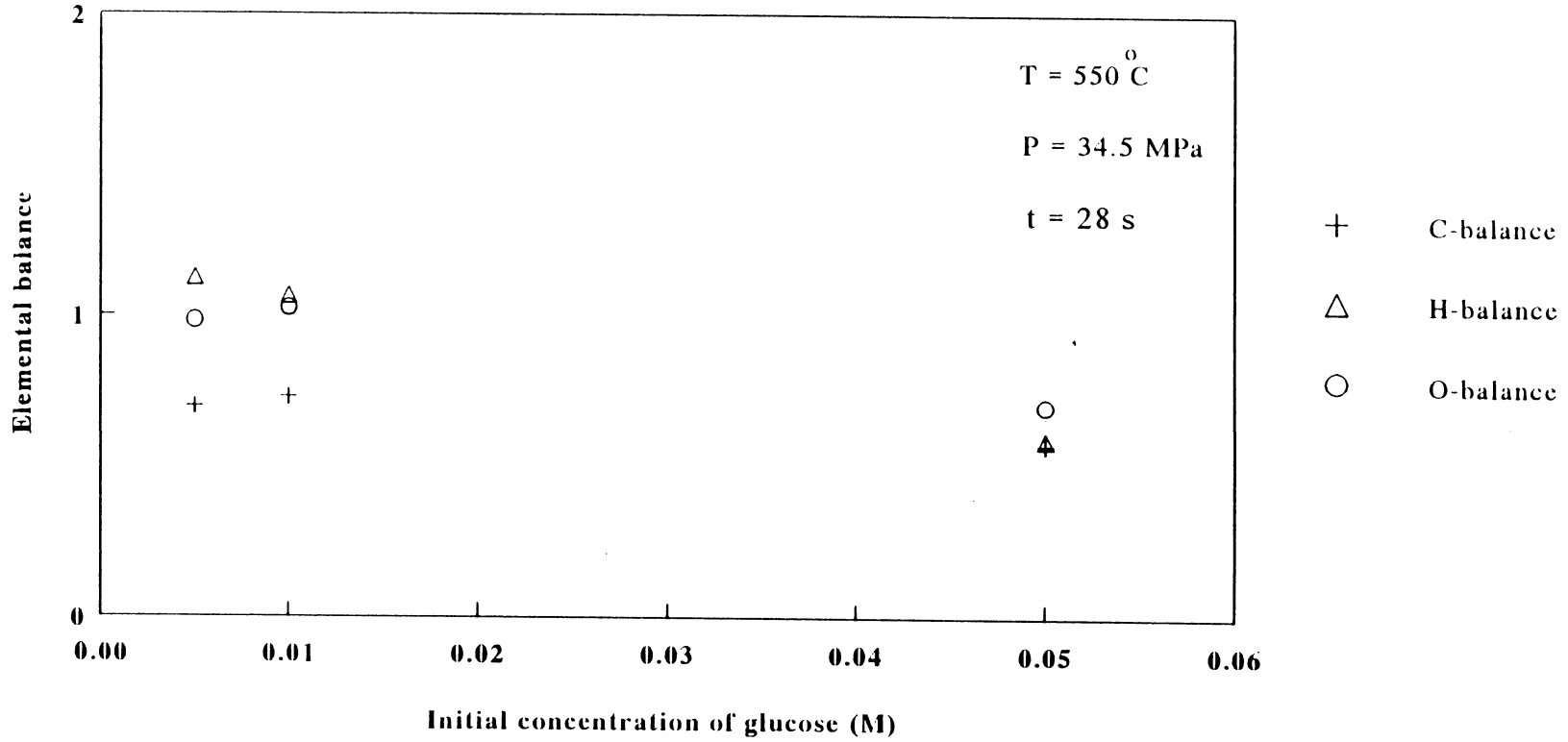

Figure 4.9 Effect of oxygen on hydrogen yield from glucose gasification in SCW

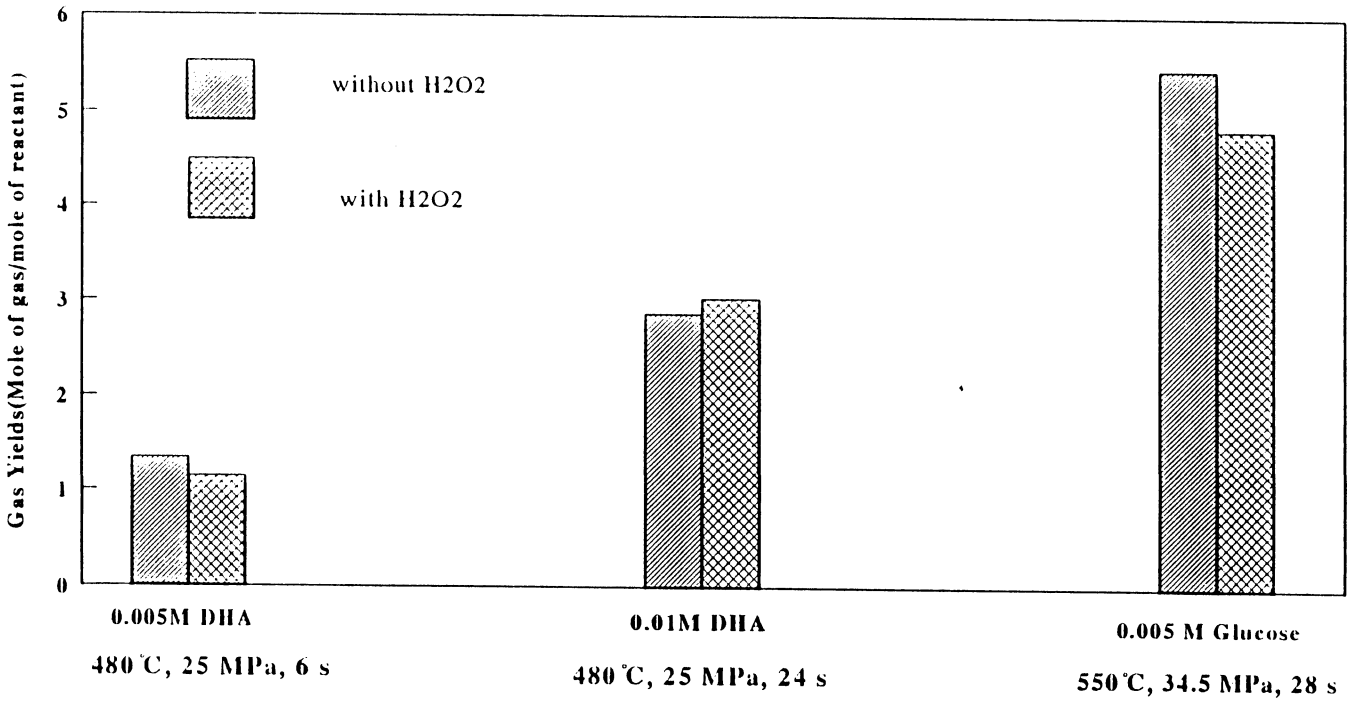

Figure 4.10 Effect of oxygen on carbon balance from glucose gasification in SCW

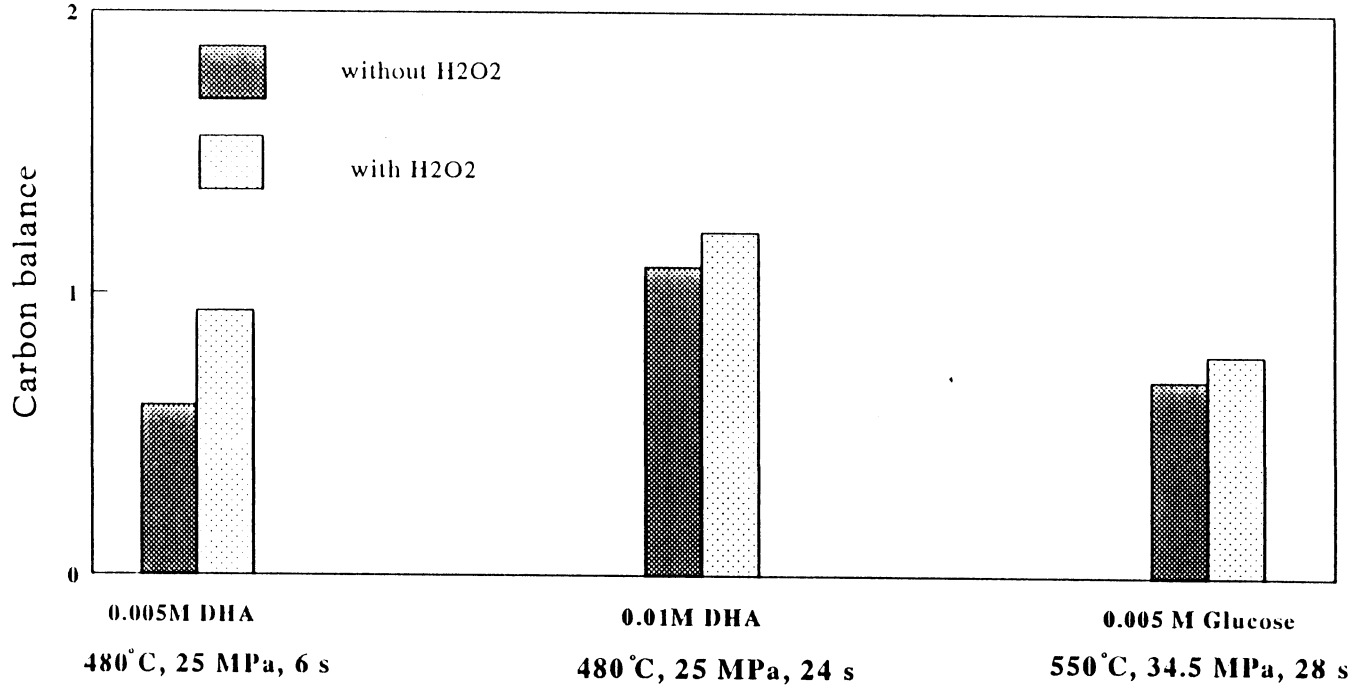

Table 4.11 Effect of feeding system

Reactant	Samp.No.	Reaction Condition	C balance	H balance	O balance	Absolute Yield (Moles of Gas/Moles of Carbon in Reactant) CO2	H2	CO	CH4	C2H4	C2H6	H2/CO2	H2,pot**	H2,t/ H2,p(*)
Diesel Oil Feeding System														
0.7 g/l Algae	D1 - D3	550 C 134 s	0.591	0.780	0.864	0.209	0.399	0.188	0.099	0.026	0.022	1.91	0.44	0.18
	D4 - D6	550 C 67 s	0.496	0.644	0.752	0.175	0.363	0.177	0.066	0.023	0.016	2.09	0.36	0.16
	D7 - D9	550 C 33 s	0.454	0.504	0.689	0.148	0.278	0.186	0.052	0.022	0.013	1.88	0.30	0.13
Balloon Feeding System														
0.7 g/l Algae	E1 - E3	550 C 134 s	0.602	0.845	0.985	0.272	0.474	0.145	0.094	0.024	0.022	1.74	0.45	0.21
	E4 - E6	550 C 67 s	0.499	0.704	0.817	0.210	0.429	0.151	0.061	0.022	0.016	2.05	0.37	0.19
	E7 - E9	550 C 33 s	0.422	0.565	0.733	0.195	0.358	0.123	0.044	0.018	0.011	1.84	0.30	0.16

* Fraction of Potential Hydrogen Realized

** Fraction of Potential Hydrogen Realized including H2 from CO and CH4

Table 4.12 Effect of temperature and residence time on wet biomass gasification in SCW

Reactant	Reaction Condition	Samp.No.	C balance	H balance	O balance	Absolute Yield (Moles of Gas/Moles of Carbon in Reactant) CO2	H2	CO	CH4	C2H4	C2H6	H2/CO2	H2,pot**	H2,t/ H2,p(*)
0.70 g/l Algae	550 C 134 s	D1 - D3	0.591	0.780	0.864	0.209	0.399	0.188	0.099	0.026	0.022	1.91	0.44	0.18
	550 C 67 s	D4 - D6	0.496	0.644	0.752	0.175	0.363	0.177	0.066	0.023	0.016	2.09	0.36	0.16
	550 C 33 s	D7 - D9	0.454	0.504	0.689	0.148	0.278	0.186	0.052	0.022	0.013	1.88	0.30	0.13
0.78 g/l Algae	600 C 117 s	B4 - B6	0.715	1.219	0.982	0.302	0.588	0.083	0.167	0.044	0.035	1.95	0.60	0.26
	600 C 59 s	B1-3, A4	0.732	0.876	0.929	0.197	0.352	0.255	0.141	0.038	0.032	1.79	0.53	0.16
	600 C 29 s	B7 - B9	0.662	0.839	0.934	0.246	0.379	0.162	0.116	0.042	0.023	1.54	0.45	0.17
0.78 g/l Algae	650 C 106 s	C1 - C3	0.889	1.077	1.244	0.388	0.309	0.094	0.238	0.052	0.032	0.80	0.61	0.14
	650 C 53 s	C4 - C6	0.759	1.110	1.050	0.321	0.468	0.093	0.179	0.051	0.028	1.46	0.57	0.21
	650 C 26 s	C7 - C9	0.744	1.088	0.987	0.260	0.489	0.171	0.166	0.045	0.029	1.89	0.60	0.22

* Fraction of Potential Hydrogen Realized

** Fraction of Potential Hydrogen Realized including H2 from CO and CH4

Table 4.13 Effect of quenching system on wet biomass gasification in SCW

Reactant	Reaction Condition	Samp.No.	C balance	H balance	O balance	Absolute Yield (Moles of Gas/Moles of Carbon in Reactant) CO2	H2	CO	CH4	C2H4	C2H6	H2/CO2	H2,pot**	H2,t/ H2,p(*)
0.78 g/l Algae	650 C 106 s	C1 - C3	0.889	1.077	1.244	0.388	0.309	0.094	0.238	0.052	0.032	0.80	0.61	0.14
	650 C 53 s	C4 - C6	0.759	1.110	1.050	0.321	0.468	0.093	0.179	0.051	0.028	1.46	0.57	0.21
	650 C 26 s	C7 - C9	0.744	1.088	0.987	0.260	0.489	0.171	0.166	0.045	0.029	1.89	0.60	0.22
With Immediate Quenching														
0.89 g/l Algae	650 C 106 s	F1 - F3	0.753	1.072	1.129	0.366	0.429	0.058	0.190	0.035	0.034	1.17	0.56	0.19
	650 C 53 s	F4 - F7	0.728	1.126	1.073	0.339	0.507	0.072	0.175	0.037	0.037	1.50	0.58	0.23
	650 C 26 s	F8 - F11	0.662	1.083	0.941	0.271	0.546	0.115	0.146	0.038	0.026	2.01	0.56	0.25

* Fraction of Potential Hydrogen Realized

** Fraction of Potential Hydrogen Realized including H2 from CO and CH4

Table 4.14 Effect of initial reactant concentration on wet biomass gasification in SCW

Reactant	Reaction Condition	Samp.No.	C balance	H balance	O balance	Absolute Yield (Moles of Gas/Moles of Carbon in Reactant) CO2	H2	CO	CH4	C2H4	C2H6	H2/CO2	H2,pot**	H2,t/ H2,p(*)
0.89 g/l Algae	650 C 53 s	F4 - F7	0.728	1.126	1.073	0.339	0.507	0.072	0.175	0.037	0.037	1.50	0.58	0.23
1.85 g/l Algae	650 C 53 s	G12 - G14	0.605	1.058	0.927	0.312	0.520	0.025	0.145	0.025	0.037	1.67	0.51	0.23
4.34 g/l Algae	650 C 53 s	I4 - I5	0.666	1.045	1.131	0.365	0.540	0.061	0.134	0.013	0.040	1.50	0.52	0.25

* Fraction of Potential Hydrogen Realized

** Fraction of Potential Hydrogen Realized including H2 from CO and CH4

Table 4.15 Effect of reactant types on wet biomass gasification in SCW

Reactant	Reaction Condition	Samp.No.	C balance	H balance	O balance	Absolute Yield (Moles of Gas/Moles of Carbon in Reactant) CO2	H2	CO	CH4	C2H4	C2H6	H2/CO2	H2,pot**	H2,t/ H2,p(*)
1.85 g/l Algae	650 C 53 s	G12 - G14	0.605	1.058	0.927	0.312	0.520	0.025	0.145	0.025	0.037	1.67	0.51	0.23
1.5 g/l Water Hyacinth	650 C 53 s	K1 - K6	0.413	1.128	0.963	0.242	0.627	0.012	0.103	0.010	0.018	2.59	0.46	0.27
1.98 g/l Kelp	650 C 53 s	M1 - M10	0.742	2.089	0.765	0.492	1.156	0.006	0.162	0.016	0.025	2.35	1.23	0.78

* Fraction of Potential Hydrogen Realized

** Fraction of Potential Hydrogen Realized including H2 from CO and CH4

Figure 4.11 Gas yields from 0.7 g/l algae gasification in SCW with different feeding system

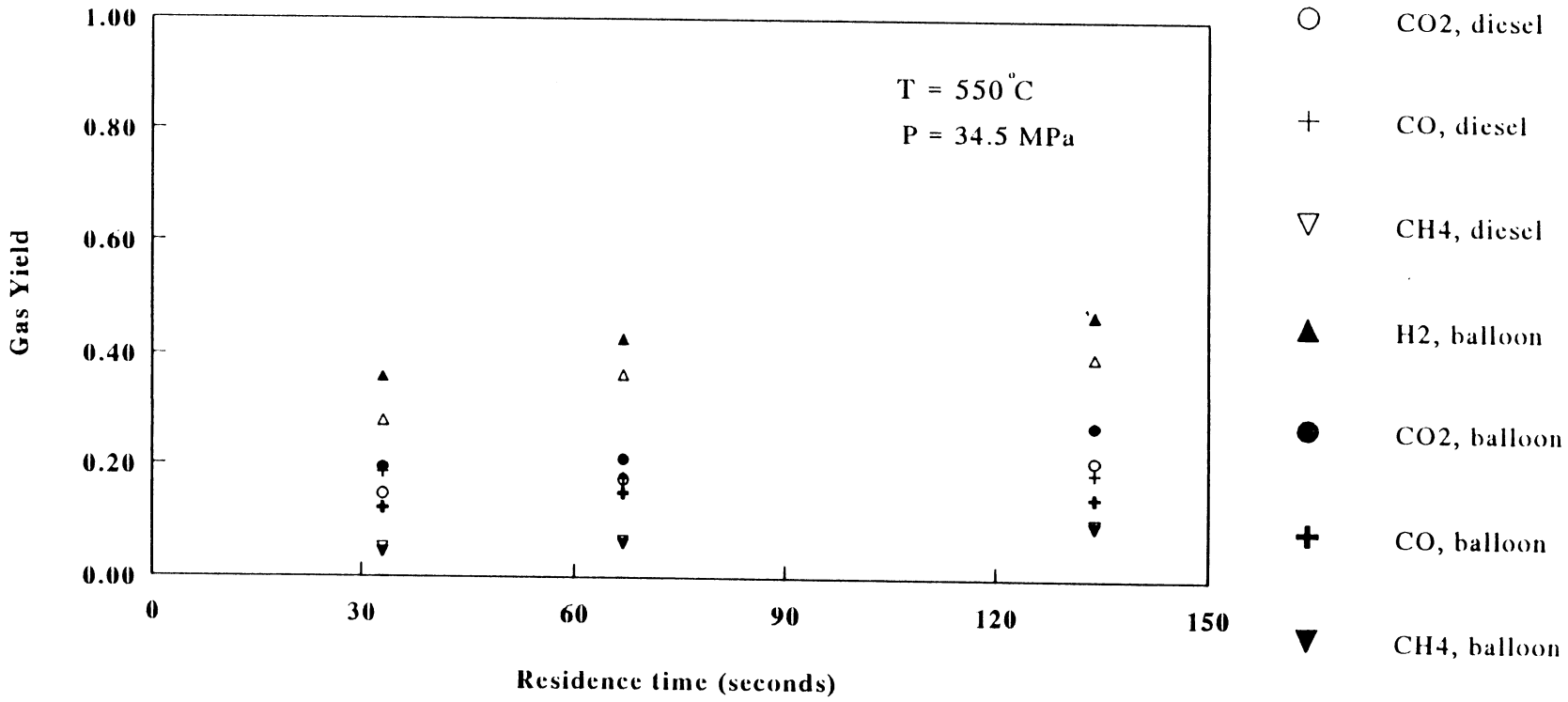

Figure 4.12 Elemental balance from 0.7 g/l algae gasification in SCW with different feeding systems

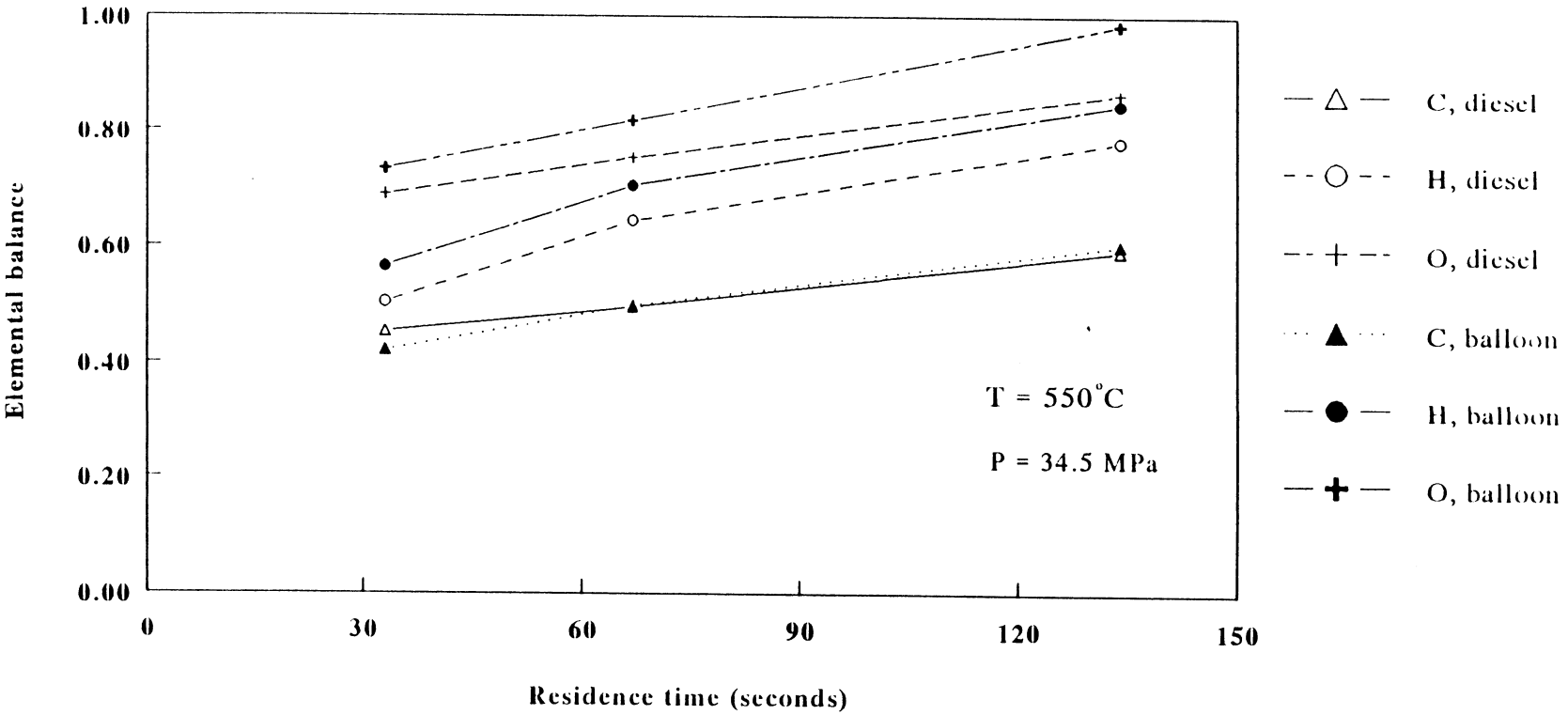

Figure 4.13 Gas yields from 0.7 g/l algae gasification in SCW vs residence time at 550 °C

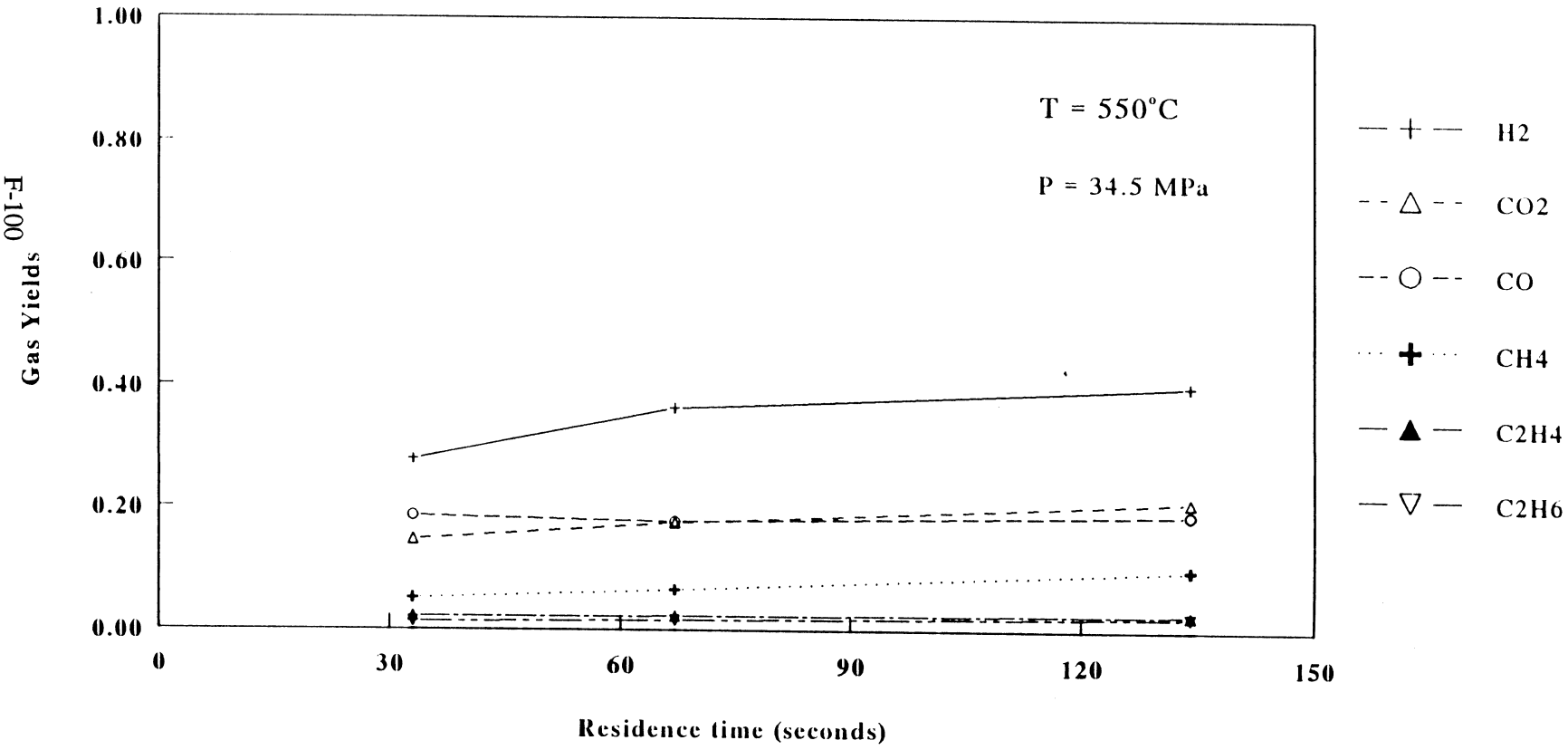

Figure 4.14 Gas yields from 0.78 g/l algae gasification in SCW vs residence time at 600°C

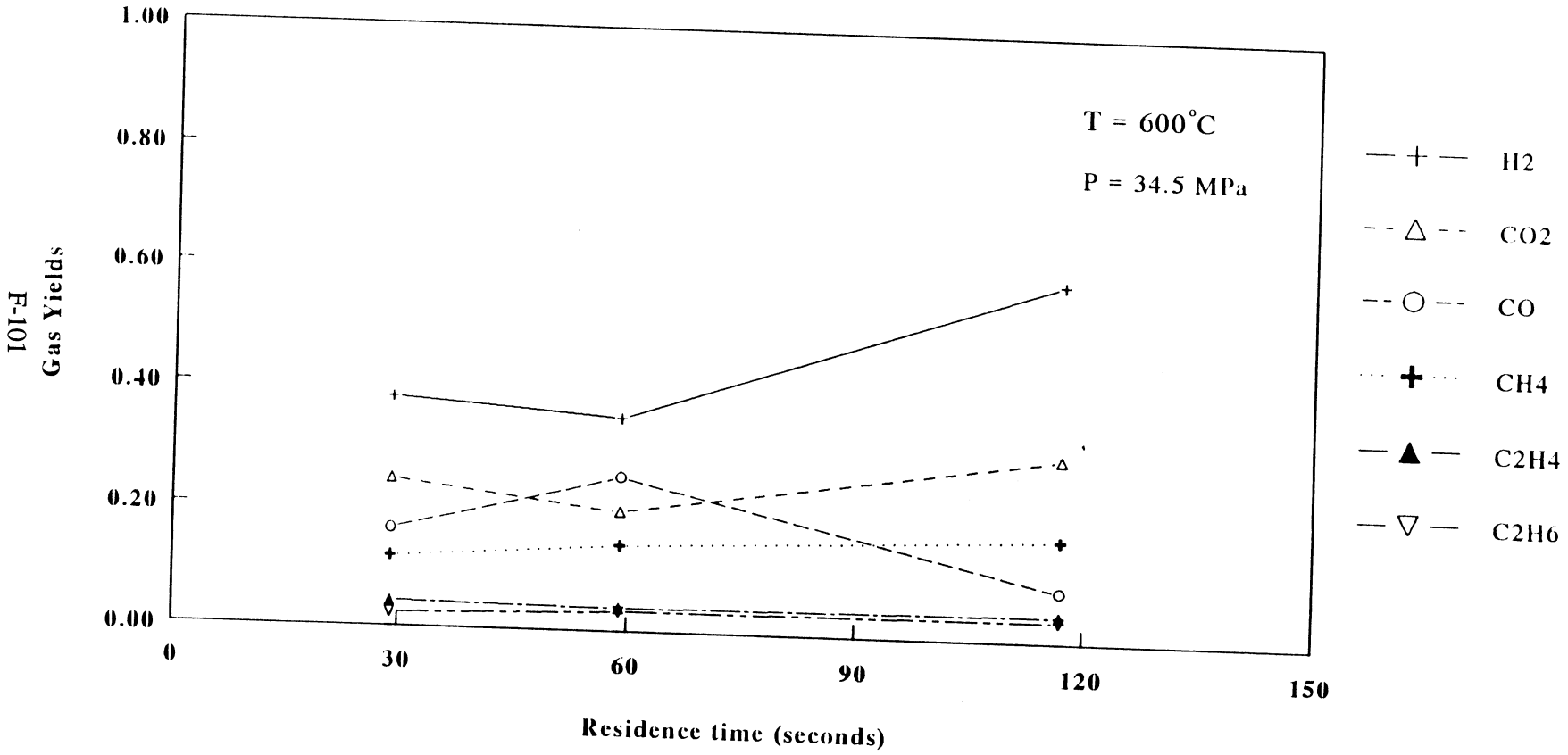

Figure 4.15 Gas yields from 0.78 g/l algae gasification in SCW vs residence time at 650 ℃

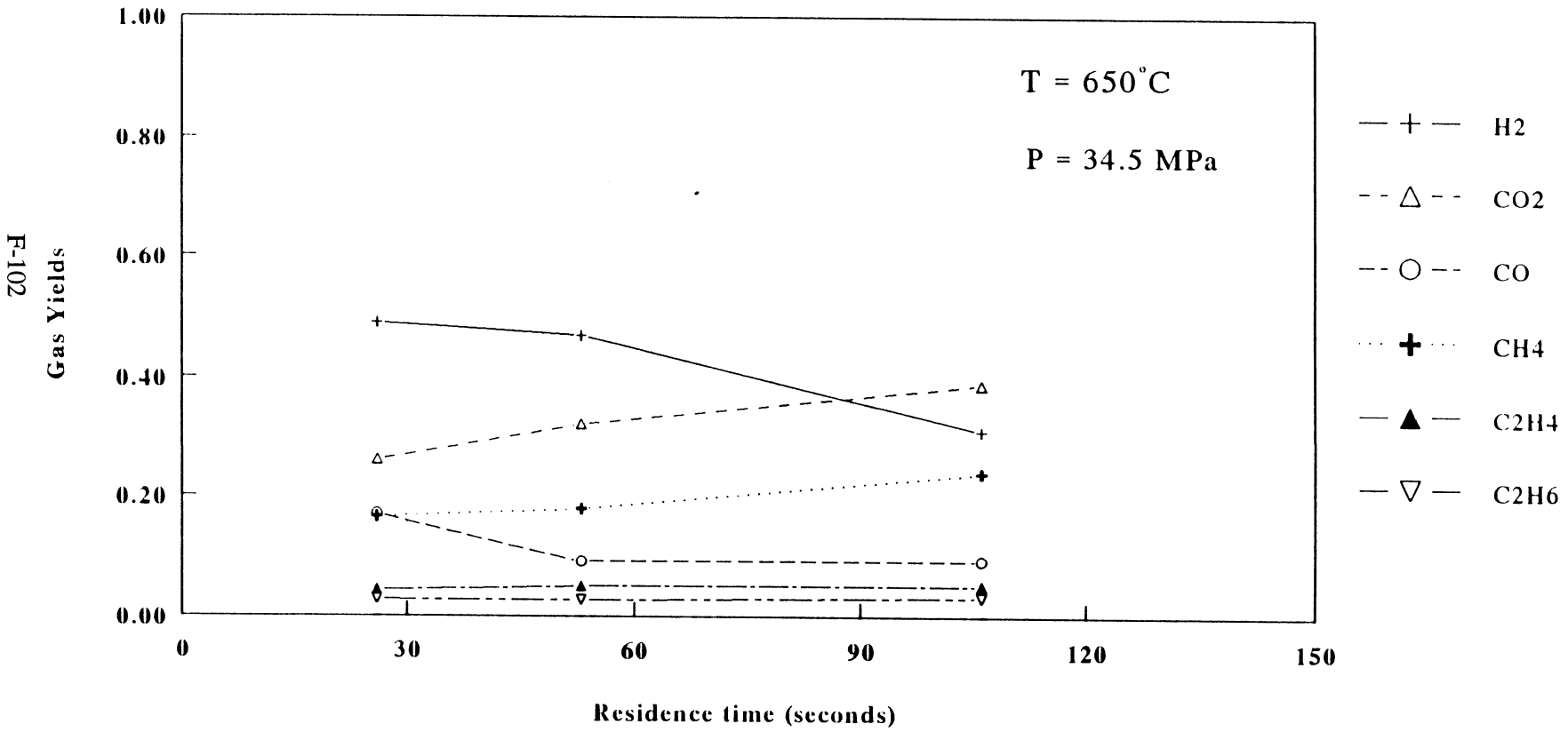

Figure 4.16 C-balance from 0.7 g/l algae gasification in SCW vs residence time (at various temperatures)

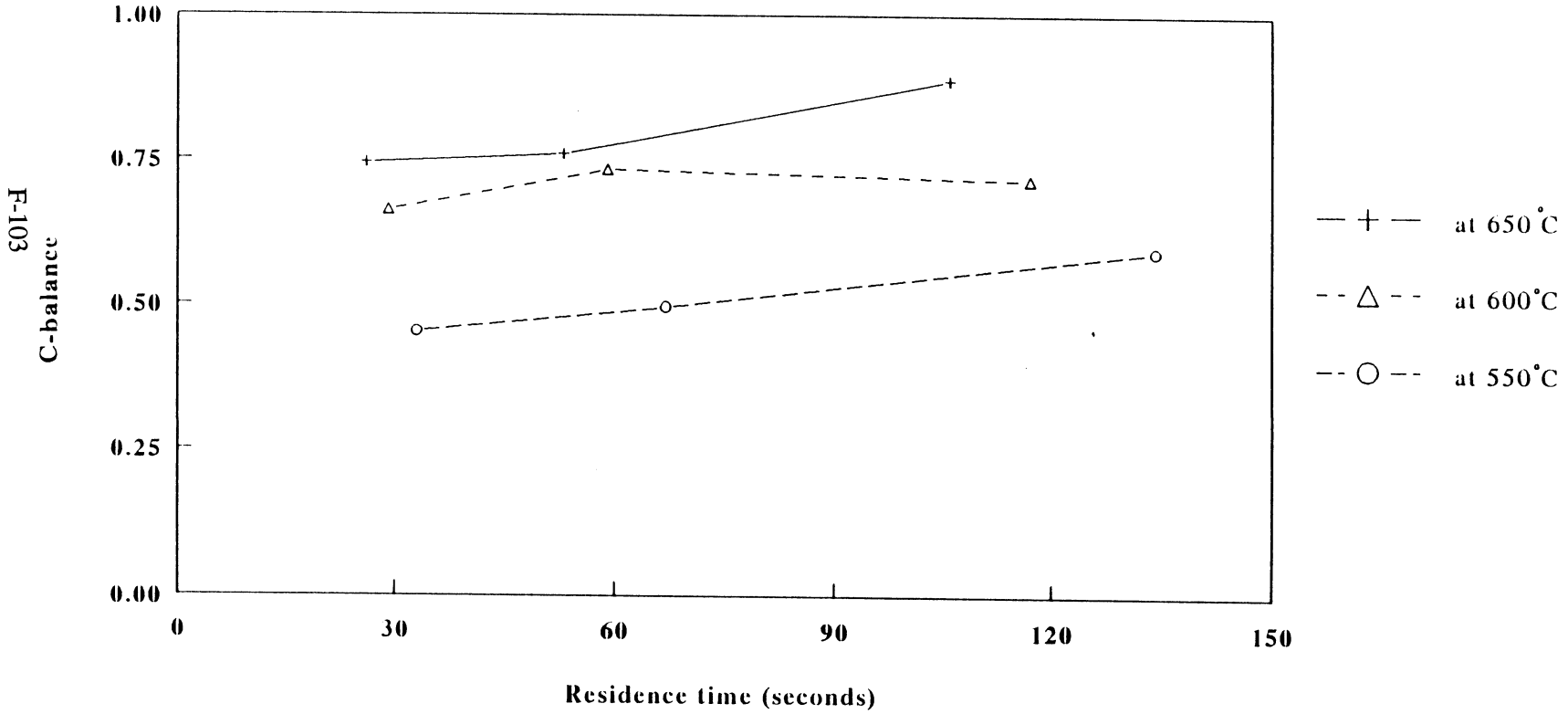

Figure 4.17 Hydrogen yield from 0.7 g/l algae gasification in SCW vs residence time (at various temperatures)

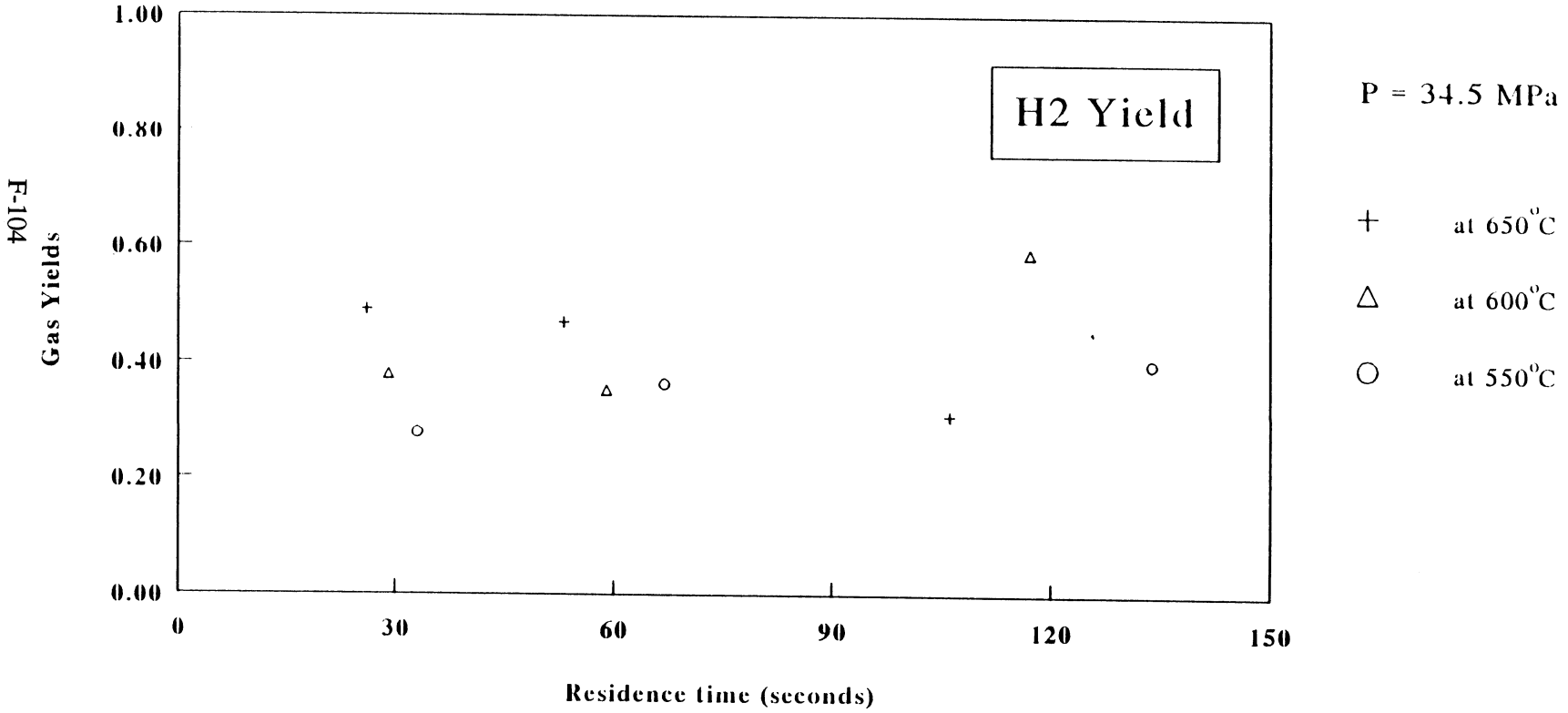

Figure 4.18 CO2 Yield from 0.7 g/l algae gasification in SCW vs residence time (at various temperatures)

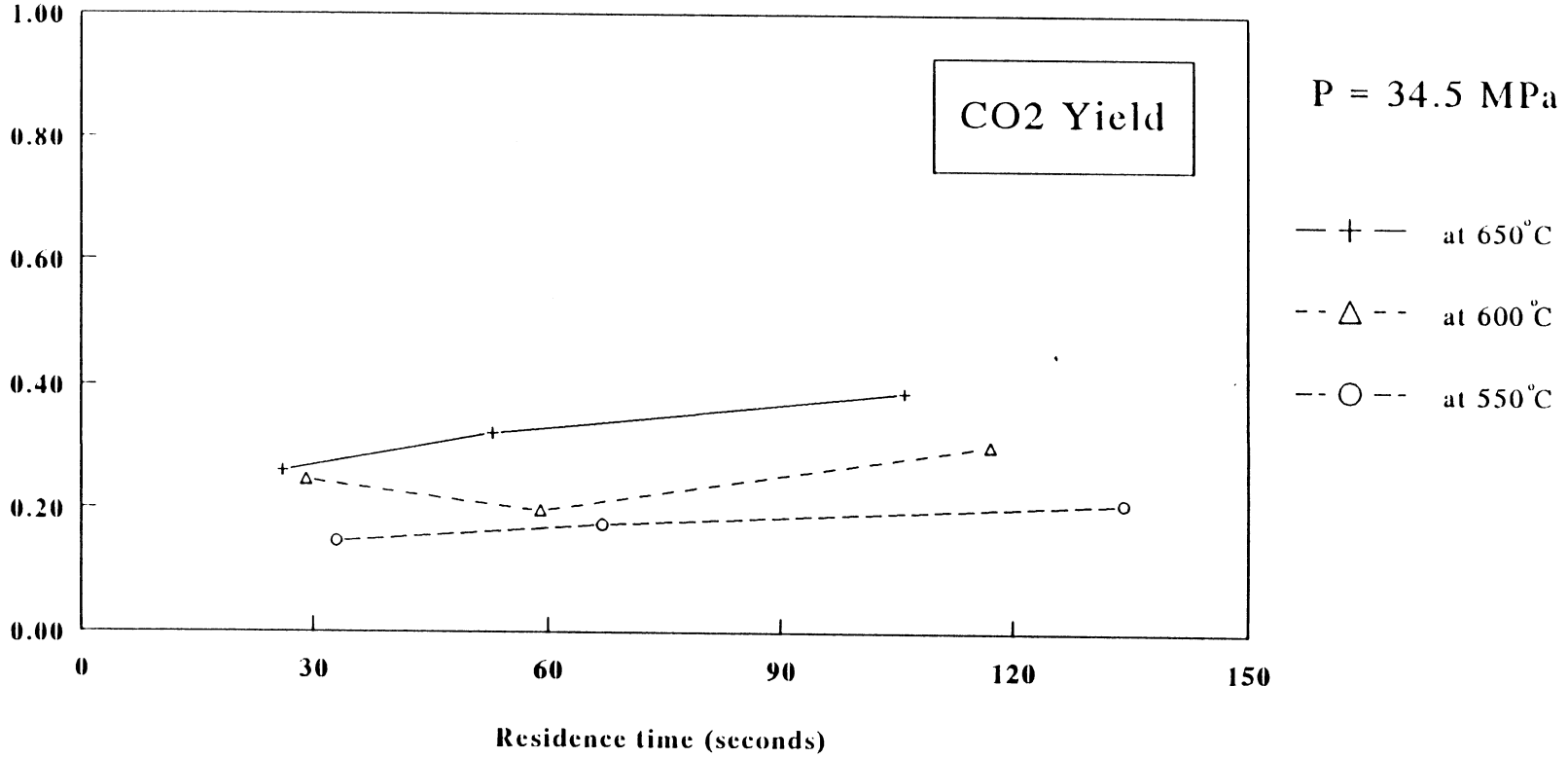

Figure 4.19 CO Yield from 0.7 g/l algae gasification in SCW vs residence time (at various temperatures)

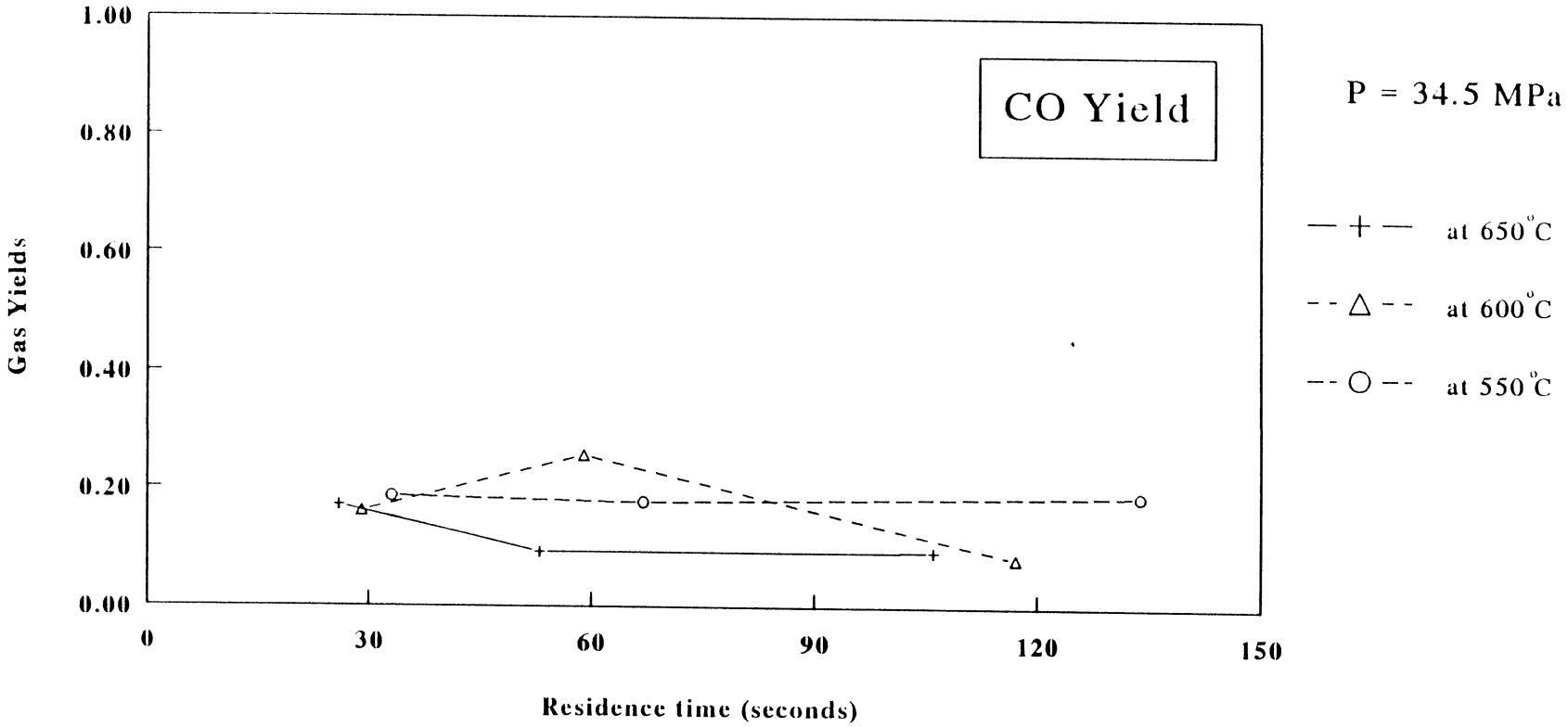

Figure 4.20 CH4 Yield from 0.7 g/l algae gasification in SCW vs residence time (at various temperatures)

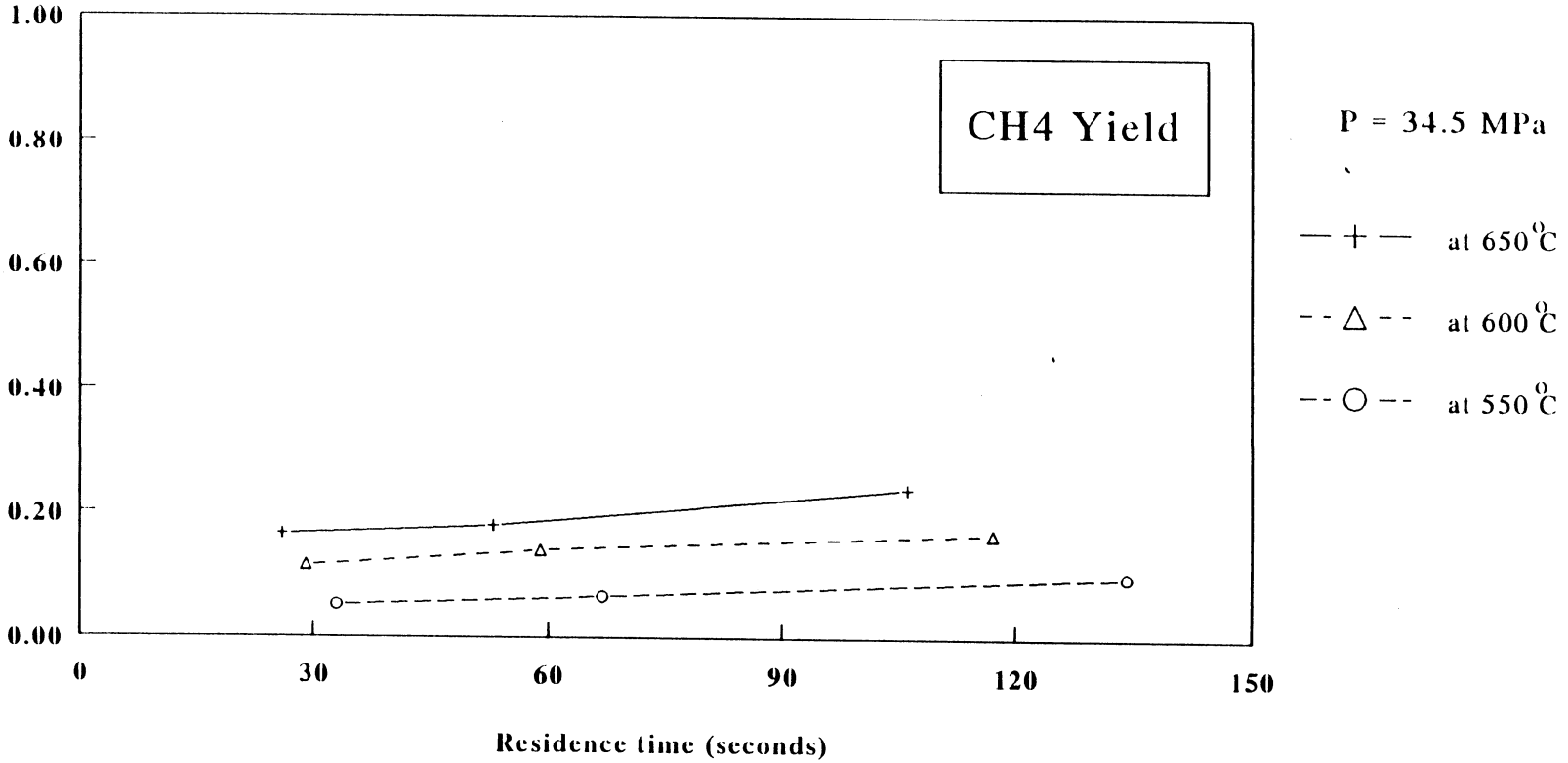

Figure 4.21 C2H4 Yield from 0.7 g/l algae gasification in SCW vs residence time (at various temperatures)

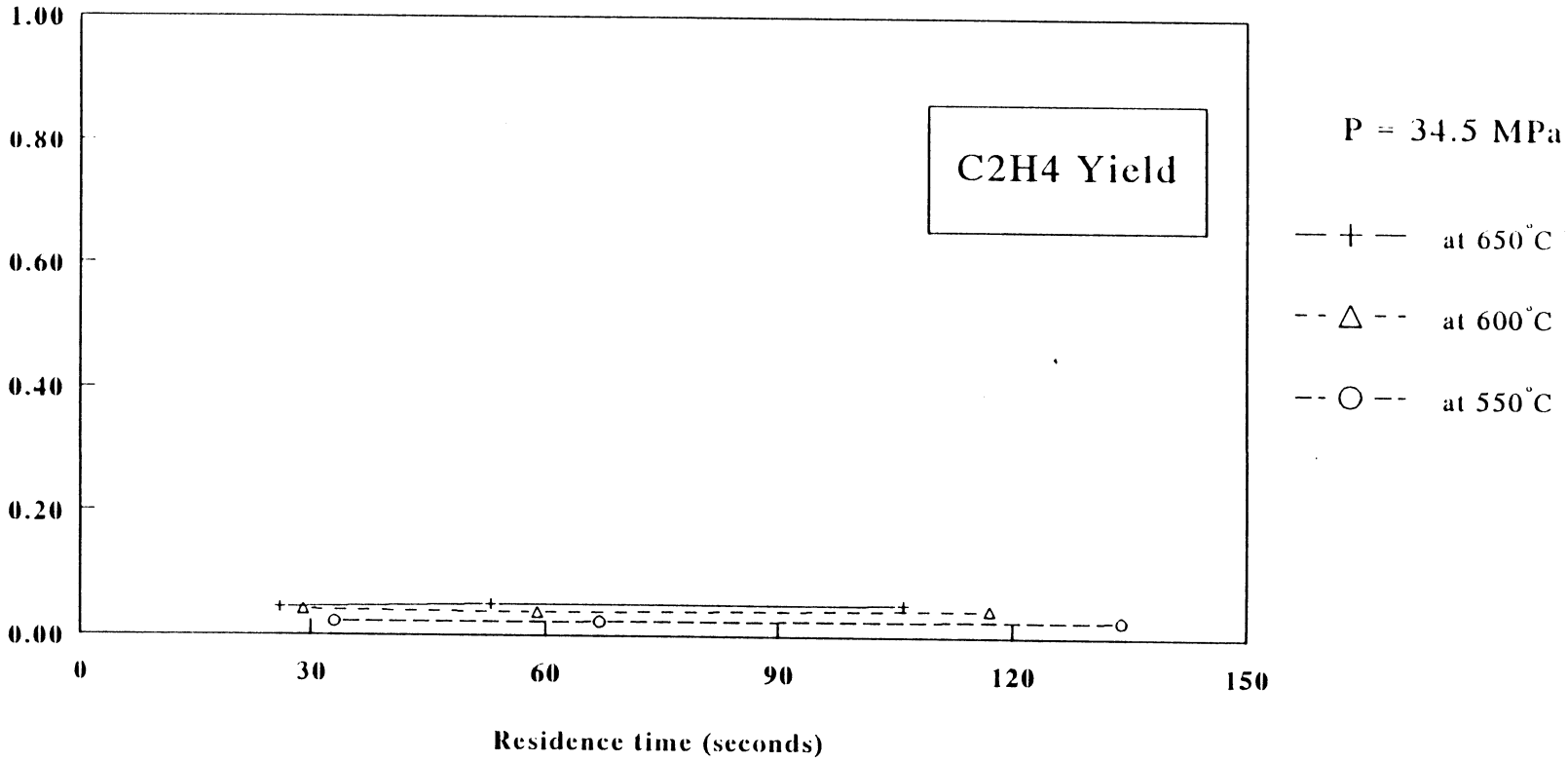

Figure 4.22 C2H6 Yield from 0.7 g/l algae gasification in SCW vs residence time (at various temperatures)

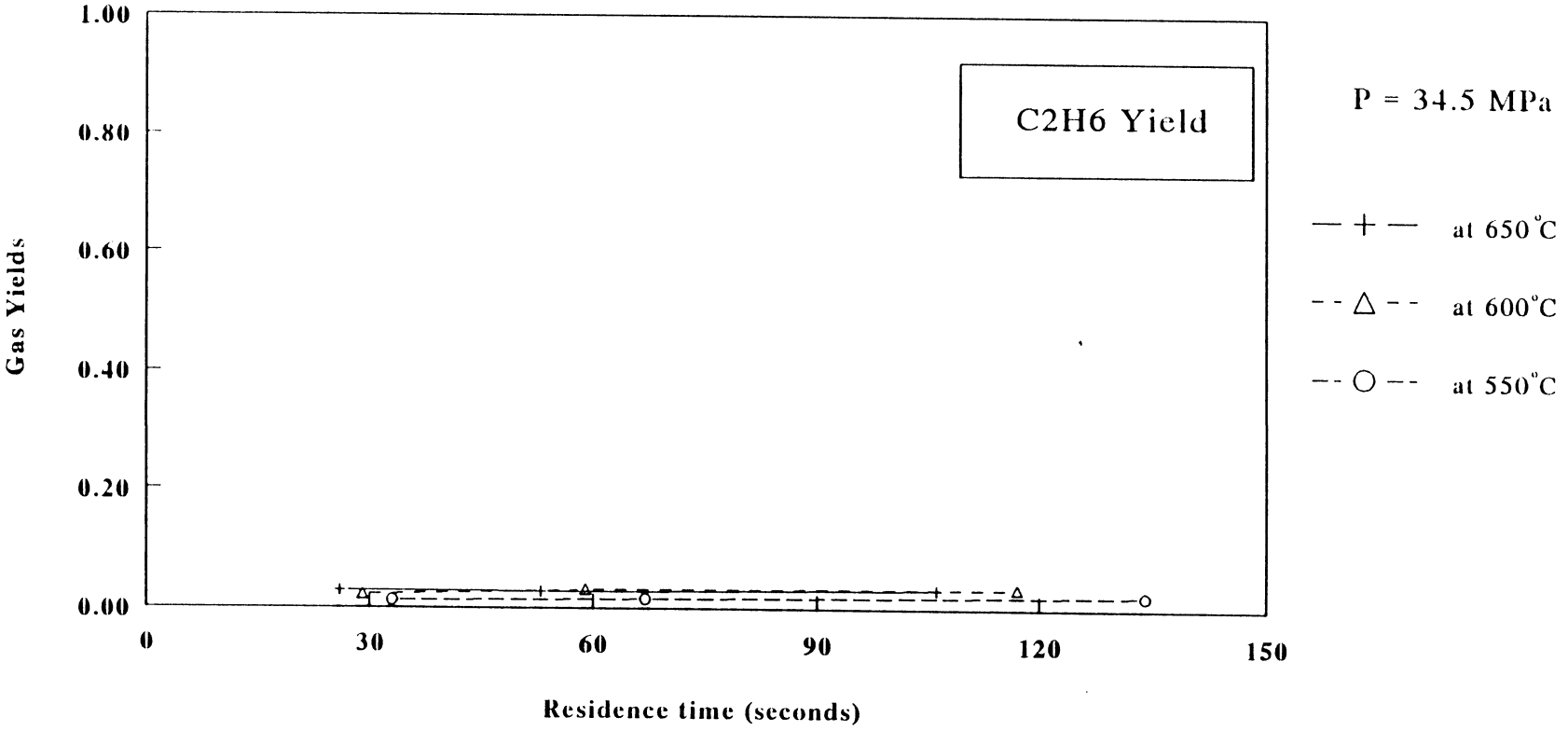

Figure 4.23 Effect of immediate quenching on gas yields

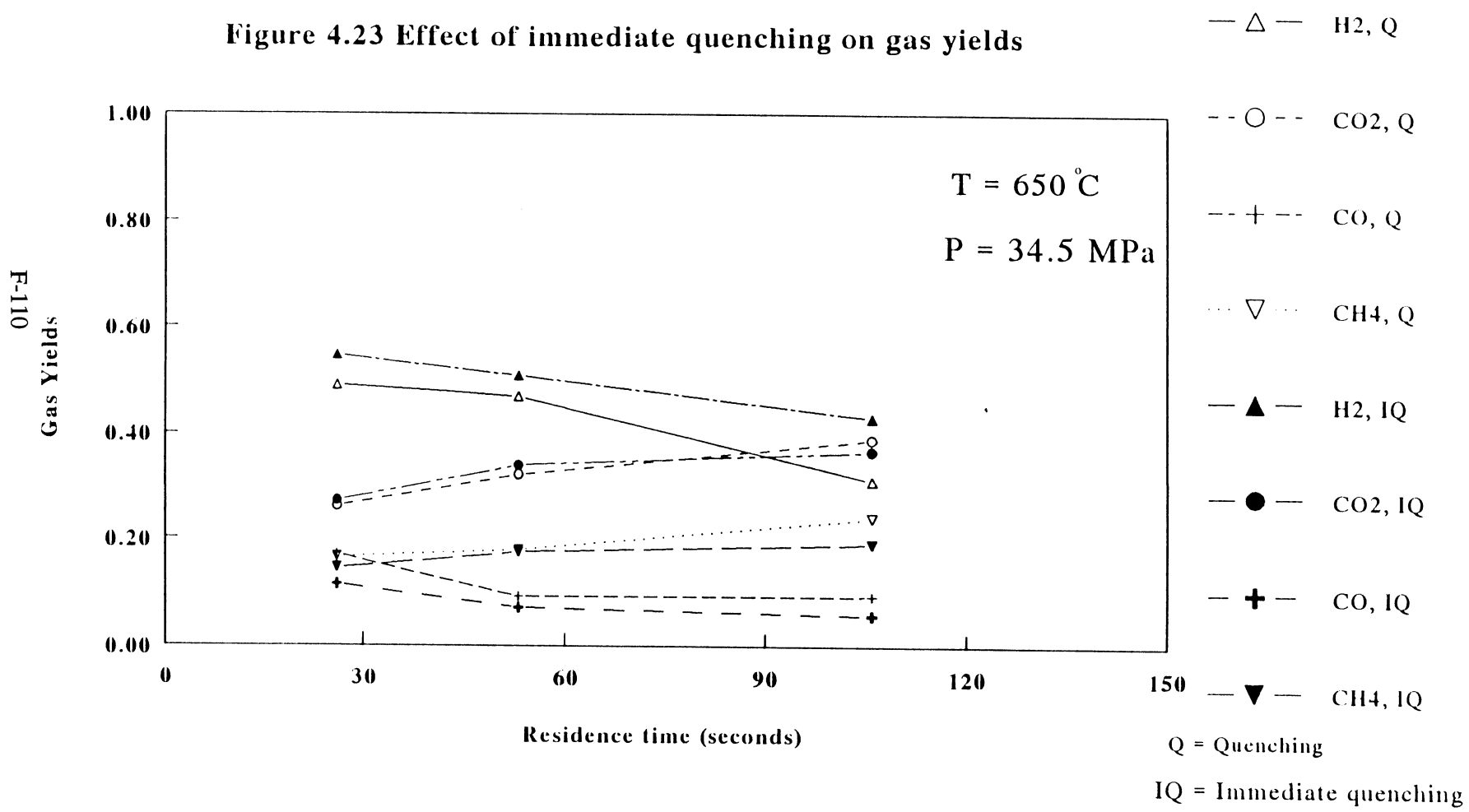

Figure 4.24 Effect of immediate quenching on elemental balance

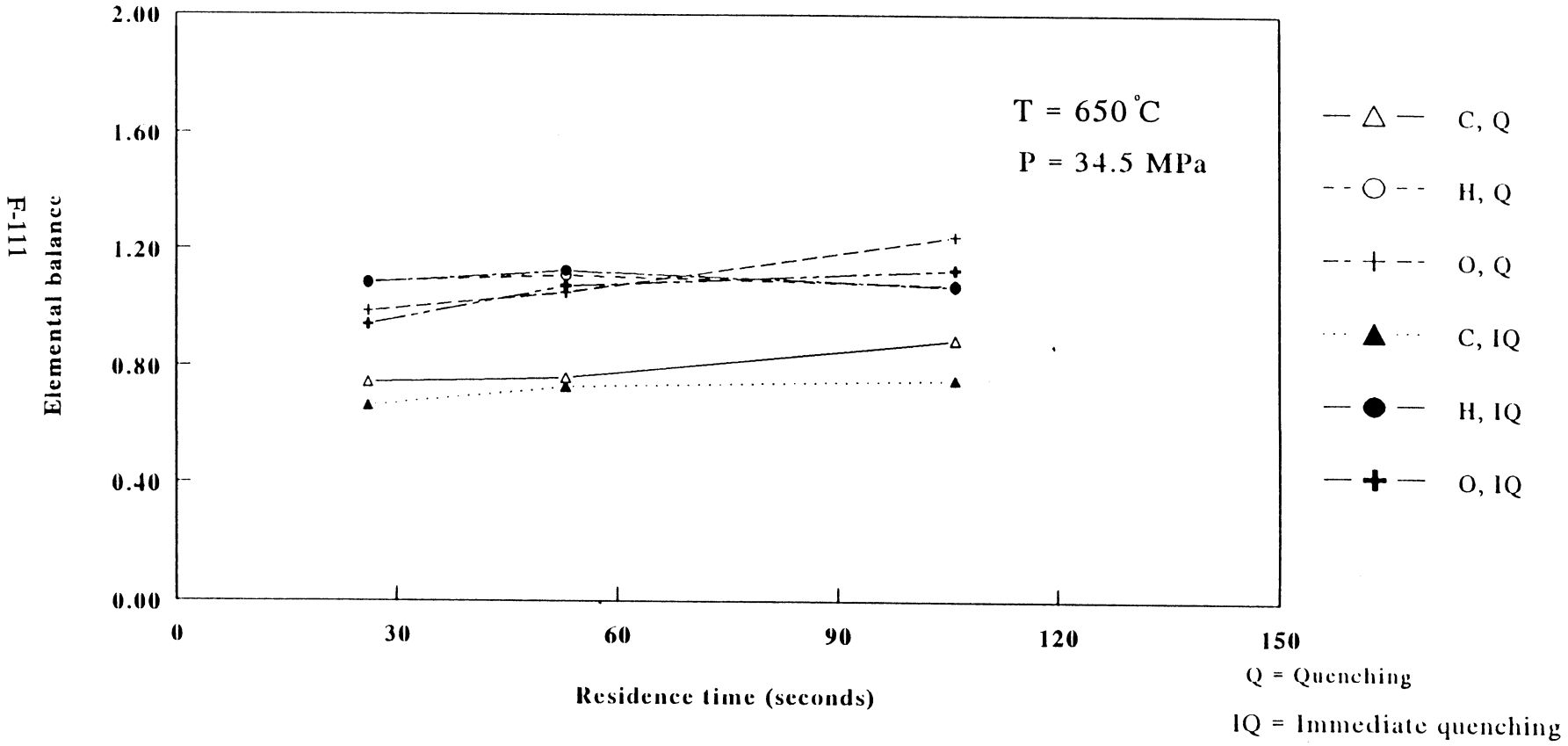

Figure 4.25 Gas yields vs initial algae concentration

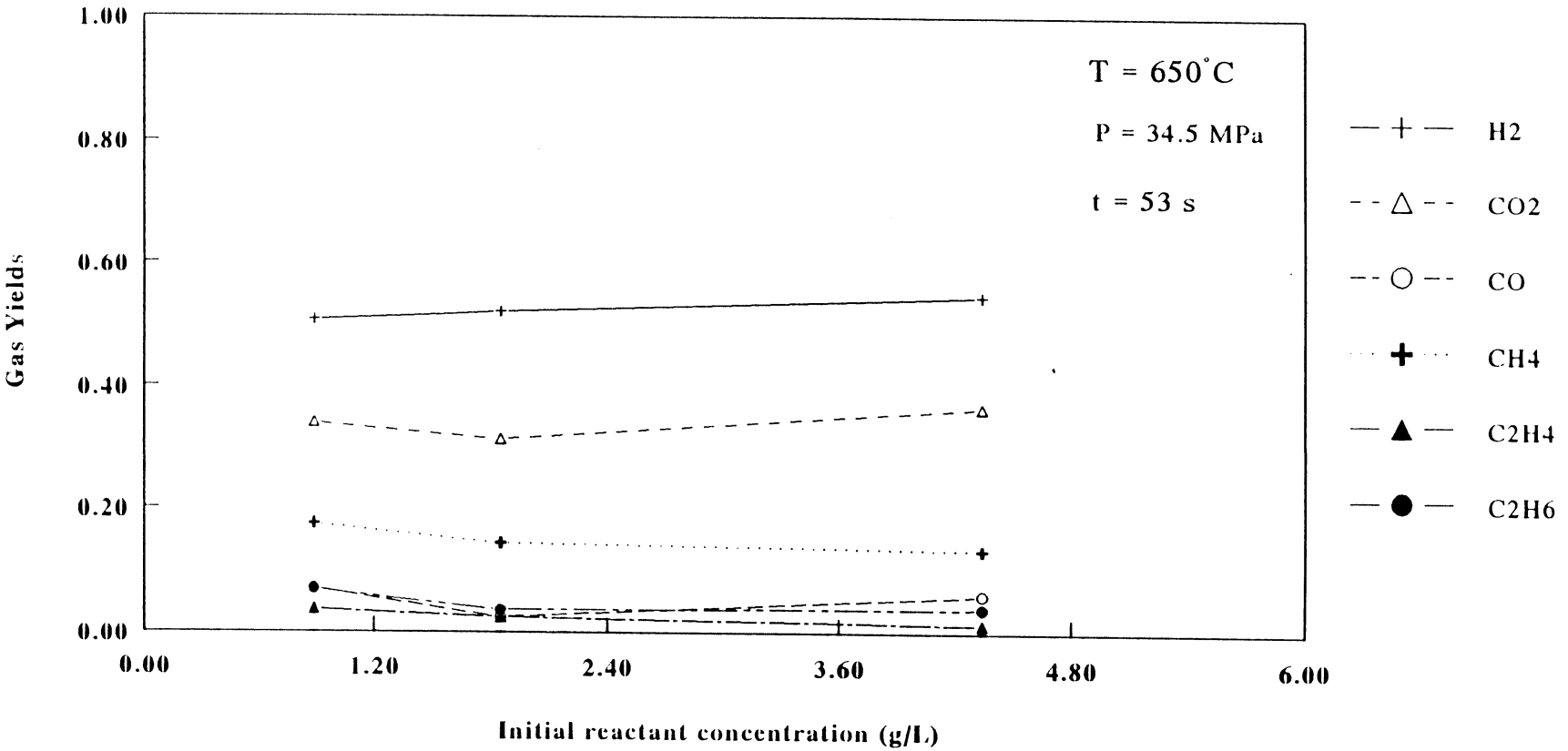

Figure 4.26 Elemental balances vs initial algae concentration

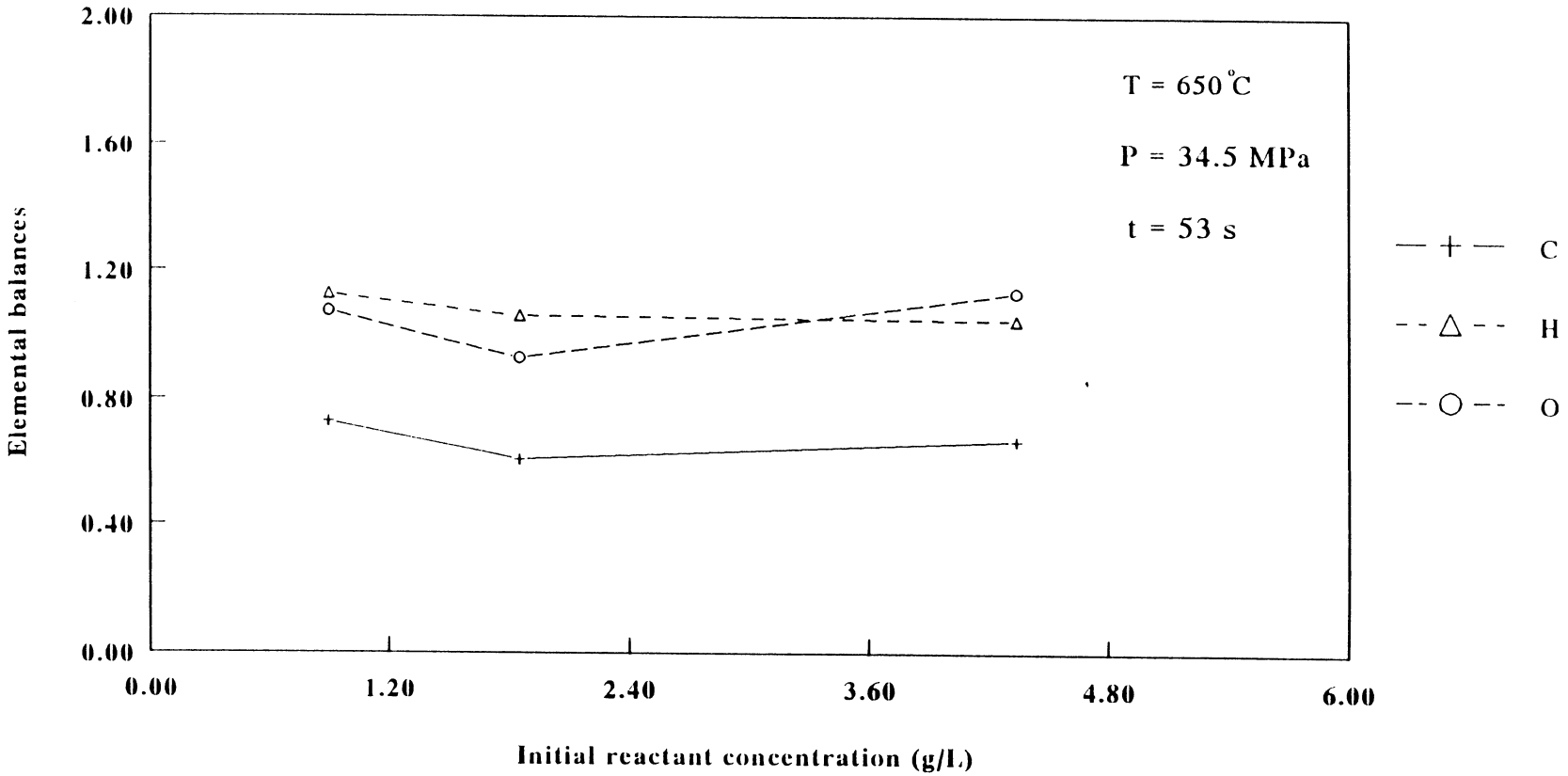

Figure 4.27 Effect of reactant types on gas yields and elemental balances

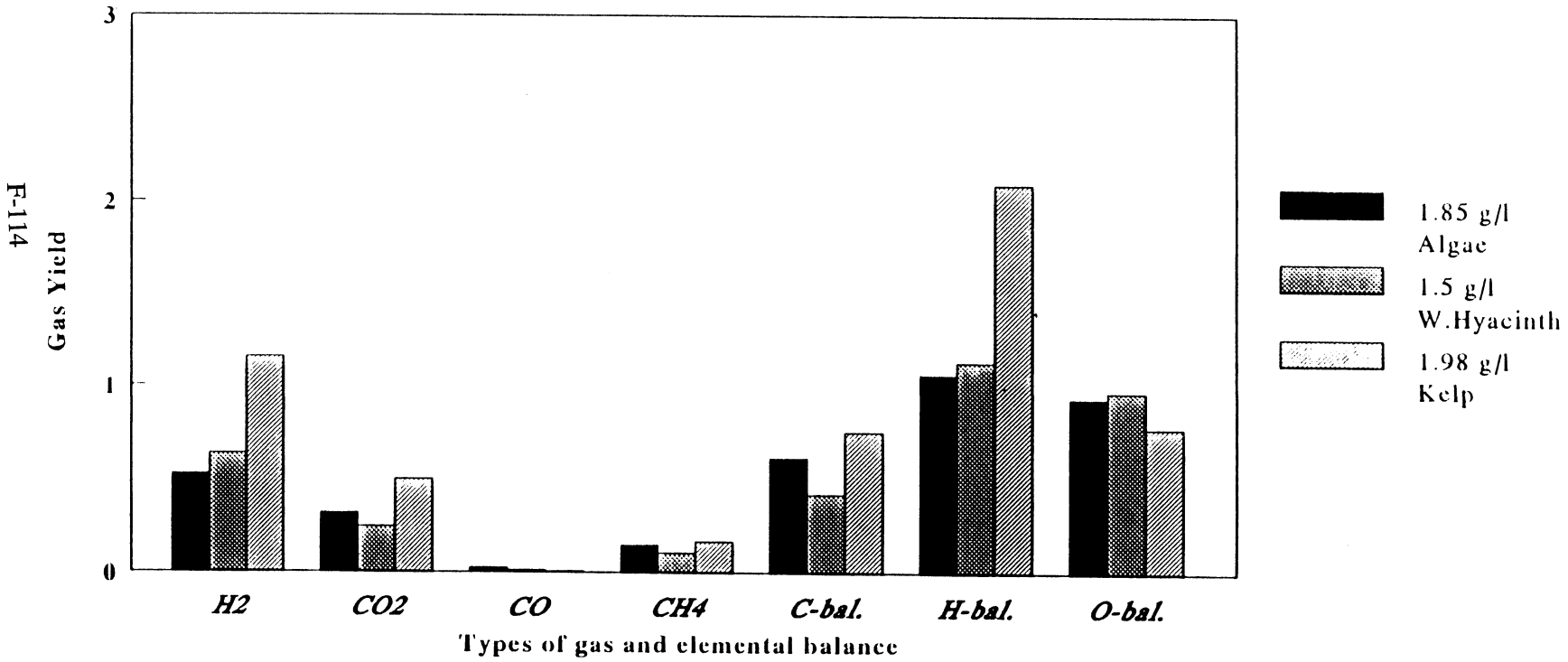

CHAPTER 5

CONCLUSIONS AND RECOMMENDATIONS

5.1 Conclusions

From the study of glucose gasification in SCW, the following conclusions are drawn:

1. A high hydrogen yield (545 mol%) and percentage of gasification (70%) were obtained when high temperatures and long residence time were employed.

2. No solid products were formed.

3. Steam gasification was observed:

$$C_6H_{12}O_6 + 6\ H_2O \text{ -----> } 6\ CO_2 + 12\ H_2$$

4. Traces of oxygen increased the percentage of carbon gasified while reducing the yield of hydrogen.

The following summarizes my studies of wet biomass gasification in SCW :

1. A high percentage of the carbon contained in algae can be gasified at high temperature and long residence time.

2. A high hydrogen yield from algae was obtained at high temperature and short residence time.

3. The initial reactant concentration has an insignificant effect on carbon balance and hydrogen yield.

4. The types of reactant also affected the carbon balance

and hydrogen yield. Among three types of biomass (algae, water hyacinth and kelp) kelp produces the highest percentage of hydrogen and carbon gasified. Algae and water hyacinth give about the same amount of hydrogen and carbon balance.

5.2 Recommendations for future work:

1. Perform additional experiments at higher temperatures to determine the conditions which produce a maximum yield of hydrogen; and at lower temperatures, employing catalyst, to consume less energy.

2. Analysis of liquid products should be done.

3. According to the effect of reactant types, more experiments should be performed with a variety of feedstocks.

4. Modify the reactor to enable it to operate with higher concentrations.

5. An economic assessment should be made to study the feasibility of building the system on a larger scale to function as a commercial plant.

APPENDIX A

MASS BALANCE COMPUTER PROGRAM

```
* RENEWABLE RESOURCES RESEARCH LAB * MBSUGAR * January'90 *
*                                                          *
************************************************************
*                                                          *
*    MBSUGAR : Algorithm of mass balance calculation in a  *
*              chemical reaction                           *
*                                                          *
*    Programmer : Michael J. Antal, Jr.                    *
*                 William S. Mok                           *
*                 Supaporn Manarungson                     *
*                                                          *
************************************************************
*                                                          *
*                  PROGRAM DESCRIPTION                     *
*                                                          *
*      This program calculates mass balance of sugar and   *
* biomass reaction in flow reactor.  This program reads    *
* data from data file named 'FOR20.DAT' if the solvent is  *
* water else 'FOR21.DAT'.                                  *
*                                                          *
************************************************************
*                                                          *
*                VARIABLE DEFINITION                       *
*                                                          *
* a) COMP  : Compressibility of the solvent                *
* b) SVABWT: Specific volume of water at ambient condition *
* c) RFLO  : Reactant mass flow rate                       *
* d) PFLO  : Product mass flow rate                        *
* e) VPFLO : Volumetric product flow rate                  *
* f) PGASVN: Product gas volume normalized to STP          *
* g) RAREA : Crossectional area of reactor                 *
* h) TMP   : Ambient temperature of the day                *
* i) PRES  : Absolute pressure of the gas in system        *
* j) RESDT : Residence time in seconds                     *
* k) SVRPRS: Specific volume of solvent @ reaction T and P*
* l) RCONC : Concentration of reactant                     *
* m) PGM   : Product gas mass flow rate                    *
* n) PGVCP : Product gas volume percent                    *
* o) PGDENS: Product gas density at STP                    *
* p) SVOL  : Sample loop volume                            *
* q) PLM   : Product liquid mass flow rate                 *
* r) SOLV  : Type of solvent                               *
* s) PLCONC: Product liquid concentration from HPLC        *
* t) RTM   : Reactant mass flow                            *
* u) RMT   : Total reactant mass flow rate                 *
* v) CONFIG: Reactor configuration                         *
* w) RPRES : Operating pressure                            *
```

```
* x) RL    : Reactor length                                        *
* y) PGMW  : Molecular weight of gas species                       *
* z) RDENS : Density of solution at STP                            *
*                                                                  *
********************************************************************


      PROGRAM MBSUGAR

      INTEGER DTG,LNUM(10),IPRODL,IPRODG,GNUM(10),ANSRAT,CONFIG
      CHARACTER*28 RNAM(10)
      CHARACTER*22 PLNAM(22)
      CHARACTER*9 PGNAM(20)
      REAL PGMWR(20),GMASR(20),NGASMR(20),LMASR(22),NLMASR(22)
      REAL RCONC(5),RMW(5),RCFRAC(5),RHFRAC(5),ROFRAC(5)
      REAL PGVPC(20),PLCONC(22),PGDENS(20),PGO(20),PGH(20)
      REAL PGRAT(20,20),PLRAT(22,22),PGLRAT(22,22),GMOLR(20)
      REAL LMOLR(22),PRCONC(5),PGC(20),CALIB,SVAMB,PMT
      REAL NGMOLR(20),NLMOLR(22),NRMOLC,NRMOUT,NRMC,DELTAP,PMTR
      DOUBLE PRECISION PLM(22),PLMOL(22),PLMW(22),PLC(22),PLOF(22)
      DOUBLE PRECISION PGCF(20),PGOF(20),PGHF(20),PLCF(22),PLO(22)
      DOUBLE PRECISION PGM(20),PGMOL(20),PGMW(20),PLHF(22),PLH(22)
      REAL MB,SVABWT,SVRPRA(15),SVARPA(3),SVRPRS,SVARP,TINDEX
      REAL SVPRSA(14),SVPRES,SVAMBS,RMOLC,RMIN,RMOUT,RMC,PCCONV,RL
      INTEGER SOLV,INDR,INDP,IREAC
      REAL RAREA(4),GMASS(20),PGCM(20),PGHM(20),PGOM(20),GMOLC(20)

* Provide Library of known values which are often used in
  calculations

      DATA RAREA/0.085,0.1642,0.00456,0.01533/
      DATA SVABWT/1.00615/
      DATA SVPRSA/0.99335,0.99292,0.99250,0.99208,0.99166,0.99124,
     * 0.99082,0.99040,0.98999,0.98958,0.98916,0.98875,0.98834,
     * 0.98793/
      DATA PGNAM/'CO2','H2','N2','AR','CO','O2','CH4','C2H2',
     * 'C2H4','C2H6','C3H6','C3H8','N-C3H8O','I-C3H8O','C4H8',
     * 'C4H10','CH3OCH3','(C2H5)2O','C2H5OH','CH3CHO'/
      DATA PLNAM/'Hydroxymethylfurfural','Furfural','Lactic Acid',
     * 'D-Mannose','D-Fructose','Water','Glucose','Acetol',
     * 'Methylglyoxal','Glycolaldehyde','Dihydroxyacetone',
     * 'Glycerol','Levoglucosan','Levulinic acid','Formic Acid',
     * 'Glyceraldehyde','Xylose','Arabinose','Lyxose','Ribose',
     * 'Cellobiose','DP-2'/
      DATA PGMW/44.0098,2.016,28.0134,39.948,28.0104,31.9988,
     * 16.043,26.038,28.054,30.07,42.081,44.097,60.0964,60.0964,
     * 56.044,58.124,46.069,74.12,46.07,44.0534/
      DATA PGCF/0.2729,0.,0.,0.,0.4288,0.,0.74867,0.92257,0.85627,
     * 0.79887,0.85627,0.81713,0.59959,0.59959,0.85726,0.82658,
     * 0.5214,0.6482,0.5214,0.54529/
```

```
      DATA PGOF/0.727,0.,0.,0.,0.57119,1.,0.,0.,0.,0.,0.,0.,
     * 0.26623,0.26623,0.,0.,.3472,0.2159,0.3473,0.36318/
      DATA PGHF/0.,1.,0.,0.,0.,0.,0.25132,0.07742,0.14372,0.20113,
     * 0.14372,0.18287,0.13418,0.13418,0.14389,0.17342,.1312,
     * 0.1360,0.1313,0.09152/
      DATA PLMW/126.00,96.00,90.00,180.00,180.00,18.00,180.00,
     * 74.00,72.00,120.10,90.00,92.00,162.14,116.0,46.0,90.08,
     * 150.0,150.0,150.0,150.0,342.0,342.0/
      DATA PLCF/0.5714,0.625,0.4000,0.400,0.4000,0.0,0.4000,
     * 0.6202,0.5000,0.3997,0.4000,0.3916,0.4444,0.5172,0.2609,
     * 0.3996,0.4000,0.4000,0.4000,0.4000,0.42,0.42/
      DATA PLHF/0.0476,0.0417,0.0667,0.0667,0.0667,0.1119,0.0667,
     * 0.1042,0.0560,0.0666,0.0671,0.0877,0.0622,0.069,0.0435,
     * 0.0666,0.0667,0.0667,0.0667,0.0667,0.0648,0.0648/
      DATA PLOF/0.3810,0.3333,0.3556,0.5333,0.5333,0.8881,0.5333,
     * 0.2756,0.4440,0.5329,0.5329,0.5217,0.4934,0.4134,0.6956,
     * 0.5328,0.5333,0.5333,0.5333,0.5333,0.5142,0.5142/
      DATA PGDENS/1.9768,0.0898,1.2507,1.7828,1.2501,1.4289,
     * 0.7167,1.1708,1.2644,1.3567,1.9148,2.0153,2.72029,2.72029,
     * 2.5368,2.6310,2.0853,0.2564,0.1510,0.788/

      OPEN (20, FILE= 'FOR20.DAT')
      OPEN (5, FILE = 'CON')
      OPEN (30, FILE= 'MASS.DAT')
C     * Read necessary data from file 'FOR20.DAT'

      READ(20,98)CONFIG
      READ(20,98)SOLV
      READ(20,100)DTG
      READ(20,101)TMP
      READ(20,101)DELTAP
      READ(20,101)T1
      READ(20,101)T2
      READ(20,101)RL
      READ(20,101)RPRES
      READ(20,101)RDENS
      READ(20,101)RFLO
      READ(20,98)IREAC

C     * Input data about the reactants
C     * This loop gathers info about each reactant
C     * See file 'FOR20.DAT' for meaning of the variables

      DO 110 I=1,IREAC

      READ(20,99)RNAM(I)
      READ(20,101)RCONC(I)
      READ(20,103)RMW(I)
      READ(20,101)RCFRAC(I)
      READ(20,101)RHFRAC(I)
      READ(20,101)ROFRAC(I)
```

```
110 CONTINUE

    READ(20,102)IPRODG
    READ(20,101)CALIB

C * Read in volume percentage of each product gas

    IF (IPRODG .EQ. 0) GOTO 90
    READ(20,101)(PGVPC(I),I=1,IPRODG)


C * Read No. of liq. prods., sample loop vol.
C * Read concentration of each liquid product

90  READ(20,102)IPRODL
    READ(20,101)SVOL
    READ(20,101)(PLCONC(I),I=1,IPRODL)

98  FORMAT(I1)
99  FORMAT(A28)
100 FORMAT(I10)
101 FORMAT(F10.4)
102 FORMAT(I2)
103 FORMAT(F10.2)

    SVAMBS= SVABWT

C *  If Solvent is not water, user must provide the following
C *  values using file 'FOR21.DAT'

    IF (SOLV.NE.1)THEN
    READ(21,101)SVRPRS
    READ(21,101)SVPRES
    READ(21,101)SVAMBS
    GO TO 700
    END IF


c* change pressure from psi to bar
    RPRES=RPRES*6.894/100

    IF ((RPRES .GE. 220) .AND. (RPRES .LE. 349)) THEN

    L=(RPRES-220) / 10
    M=RPRES-220-L*10
    SVPRES= SVPRSA(L+1)+(SVPRSA(L+2)-SVPRSA(L+1))/10*M

    ELSE

    WRITE(5,*)'Pressure does not fall within the catalogued
 *  range.'
```

```
      WRITE(5,*)'Enter Spec.Vol.of H2O @RPRES & Amb.Temp.(cm3/g)'
      WRITE(30,*)'ENTER SPEC.VOL.OF H2O @PRES & AMB.TEMP.(CM3/G)'
      WRITE(5,*)
      READ(*,*)SVPRES

      END IF

      WRITE(5,*)'Enter Spec. Vol. for H2O @RPRES & T2 (cm3/g)'
      WRITE(30,*)'ENTER SPEC. VOL. FOR H2O @RPRES & T2 (CM3/G)'
      READ(*,*)SVRPRS

700   CONTINUE

      COMP= SVPRES/SVAMBS
      VPFLO= RFLO*SVPRES
      PGASVN= DELTAP/CALIB
      RESDT= (RL*2.54*RAREA(CONFIG)*60.)/(SVRPRS*RFLO)


      DO 115 I=1,IREAC
      RCONC(I)= (RCONC(I)*1.E-3)*(1/COMP)
115   CONTINUE

      PGCT=0.
      PGOT=0.
      PGHT=0.
      PLCT=0.
      PLOT=0.
      PLHT=0.
      PGMT=0.

      IF (IPRODG.NE.0) THEN

C * Calculate all variables related to prod. gas
C * See printout statements at end of program for definition
C * of the variables calculated below

      DO 120 I=1,IPRODG
      PGM(I)=PGASVN*PGVPC(I)*(PGDENS(I)*1.E-3)*(VPFLO/SVOL)
      PGMOL(I)=PGM(I)/PGMW(I)
      PGC(I)=PGCF(I)*PGM(I)
      PGH(I)=PGHF(I)*PGM(I)
      PGO(I)=PGOF(I)*PGM(I)
      PGMT=PGMT+PGM(I)
      PGCT=PGCT+PGC(I)
      PGHT=PGHT+PGH(I)
      PGOT=PGOT+PGO(I)
120   CONTINUE

      END IF
```

```
C * Calculate all values related to liq. prods.
C * See printout statements for definition of
C * variables

      PLMT=0.

      DO 130 I=1,IPRODL
      PLM(I)=(PLCONC(I)*1.E-3)*VPFLO
      PLMOL(I)=PLM(I)/PLMW(I)
      PLC(I)=PLCF(I)*PLM(I)
      PLH(I)=PLHF(I)*PLM(I)
      PLO(I)=PLOF(I)*PLM(I)
      PLMT=PLMT+PLM(I)
      PLCT=PLCT+PLC(I)
      PLOT=PLOT+PLO(I)
      PLHT=PLHT+PLH(I)
130   CONTINUE

C * Calculate all values related to reactants
C * See printout statement for definition of
C * variables

      RCT=0.
      RHT=0.
      ROT=0.
      RMT=0.

      DO 200 I= 1,IREAC
      RTM=RFLO*SVPRES*RCONC(I)
      RMT=RMT+RTM
      RCT=RCT+RTM*RCFRAC(I)
      RHT=RHT+RTM*RHFRAC(I)
      ROT=ROT+RTM*ROFRAC(I)
200   CONTINUE

C * Calculate all appropriate fractions and totals
C * Calculate mass and elemental balances for reaction

      PMT=PGMT+PLMT
      PMTR= PMT-PLM(6)
      PCT=PGCT+PLCT
      PHT=PGHT+PLHT
      POT=PGOT+PLOT
      FMG=PGMT/RMT
      FML=PLMT/RMT
      FCG=PGCT/RCT
      FCL=PLCT/RCT
      FHG=PGHT/RHT
      FHL=PLHT/RHT
      FOG=PGOT/ROT
      FOL=PLOT/ROT
```

```
      MB=FMG+FML
      CB=FCG+FCL
      HB=FHG+FHL
      OB=FOG+FOL


C THE FOLLOWING IS NOT ACTUALLY USED, BUT INCLUDED AS A DUMMY
C READ IN ORDER NOT TO CHANGE THE FORMAT OF THE INPUT DATA
C FILE
      READ (20,98) ANSRAT

      NGRAT=0
      NLRAT=0
      NGLRAT=0

      IF (IPRODG.NE.0)THEN

C * Read how many gases will be compared, and their
C * appropriate numbers within the catalogued array

      READ(20,102)NGRAT
      READ(20,102)(GNUM(I),I=1,NGRAT)


      END IF

C * Here the above procedure is done with liq. prods.

      READ(20,102)NLRAT
      READ(20,102)(LNUM(I),I=1,NLRAT)

C * Calculate all values related to conversion

      READ(20,102)INDR
      READ(20,102)INDP

      RMIN= RFLO*SVPRES*RCONC(INDR)
      RMOUT= VPFLO*(PLCONC(INDP)*1.E-3)
      NRMOUT= RMOUT/MB
      RMC= RMIN - RMOUT
      NRMC= RMIN - NRMOUT
      RMOLC= RMC/RMW(INDR)
      NRMOLC= NRMC/RMW(INDR)
      PCCONV= (1.- (RMOUT/RMIN))*100.

      IF (IPRODG.EQ.0)THEN
      GO TO 298
      END IF
```

```
C * Calculate ratios between mass of CHO in each gas and
C * mass of CHO in reactants

      DO 277 I=1, NGRAT
      PGCM(I)=PGC(GNUM(I))/RCT
      PGHM(I)=PGH(GNUM(I))/RHT
      PGOM(I)=PGO(GNUM(I))/ROT
277   CONTINUE

C * Calculate molar and mass ratios between react. converted
  * and prods.

      DO 251 I= 1,NGRAT
      GMOLR(I)= (PGMOL(GNUM(I))/RMOLC)
      NGMOLR(I)= (PGMOL(GNUM(I))/MB)/NRMOLC
      GMASS(I)= (PGM(GNUM(I))/RMC)
      GMOLC(I)= (PGMOL(GNUM(I))/(RCT/12.))
251   CONTINUE

298   DO 253 J= 1,NLRAT
      LMOLR(J)= (PLMOL(LNUM(J))/RMOLC)
      NLMOLR(J)= (PLMOL(LNUM(J))/MB)/NRMOLC
      LMASR(J)= LMOLR(J)*PCCONV*0.01
253   CONTINUE



      WRITE(30,*)
      WRITE(30,*)'*********************************************'
      WRITE(30,300) DTG,PGASVN,TMP,DELTAP
300   FORMAT('DTG= ',I10,21X,'S.T.P. Gas Vol.=',F10.2,1X,'cc'/
     * 'Loop Temp.=',F10.2,1X,'deg K',9X,'Gas Reading=',F10.2,
     * 1X,'mV')
      WRITE(30,305) T1,T2
305   FORMAT('Pre-Heat Temp.= ',F10.2,1X,'deg C',4X,
     * 'Reactor Temp.= ',F10.2,1X,'deg C')
      WRITE(30,310) RPRES,SVPRES
310   FORMAT('Reactant Pres.= ',F10.2,1X,'bar',6X,
     * 'Spec Vol @ press= ',F10.5,1X,'ml/g')
      WRITE(30,315) RFLO,VPFLO
315   FORMAT('React. flow (STP)= ',F7.2,1X,'mg/min',3X,
     * 'Prod Flow (@press)= ',F10.3,'ml/min')
      WRITE(30,*)
      WRITE(30,*)'*********************************************'
      WRITE(30,327)RESDT
327   FORMAT('Residence Time = ',F10.4,' sec.')
      WRITE(30,*)
      WRITE(30,*)'*********************************************'
      WRITE(30,*)
      WRITE(30,*)'Composition of Products in Loop @ high pressure'
```

```
      WRITE(30,*)

      IF (IPRODG.EQ.0)THEN
      GO TO 385
      END IF

  385 WRITE(30,358)
  358 FORMAT(' ',25X,'Prod. Liq. Conc.(mg/ml)')


      DO 359 I=1,IPRODL
      IF (PLCONC(I).NE.0.0000)THEN
      WRITE(30,360)PLNAM(I),PLCONC(I)
      END IF
  359 CONTINUE
  360 FORMAT(' ',5X,A22,10X,F10.4)
      WRITE(30,*)
      WRITE(30,*)'***********************************************'
      WRITE(30,*)
      WRITE(30,393) PCCONV
  393 FORMAT(' ',18X,'Conversion = ',F6.2,' %')
      WRITE(30,*)
      WRITE(30,*)'***********************************************'
      WRITE(30,*)
      WRITE(30,*)'                Fractional Elemental Balances'
      WRITE(30,*)
      WRITE(30,*)'             Carbon   Hydrogen   Oxygen   Mass'
      WRITE(30,430) FCG,FHG,FOG,FMG
  430 FORMAT(' ',5X,'Gas',7X,4(F7.4,2X))
      WRITE(30,435) FCL,FHL,FOL,FML
  435 FORMAT(' ',5X,'Liq.',6X,4(F7.4,2X))
      WRITE(30,440) CB,HB,OB,MB
  440 FORMAT(' ',5X,'Balance',3X,4(F7.4,2X))


      WRITE(30,*)
      WRITE(30,*)'***********************************************'
      WRITE(30,*)
      WRITE(30,*)' Relative Yield (Gas Prods./Converted React.)'
      WRITE(30,*)
      WRITE(30,*)'                       Actual     Normalized'
      WRITE(30,*)
      WRITE(30,252)(PGNAM(GNUM(I)),GMOLR(I),NGMOLR(I),I=1,NGRAT)
  252 FORMAT(' ',5X,A9,5X,F7.3,5X,F7.3)
      WRITE(30,*)
      WRITE(30,*)
      WRITE(30,*)'Relative Yield (Liq. Prods./Converted React.)'
      WRITE(30,*)
      WRITE(30,*)'                         Actual     Normalized'
```

```
      WRITE(30,*)
      WRITE(30,255)(PLNAM(LNUM(J)),LMOLR(J),NLMOLR(J),J=1,NLRAT)
  255 FORMAT(' ',5X,A22,5X,F7.3,5X,F7.3)
      WRITE(30,*)
      WRITE(30,*)
      WRITE(30,*)'*********************************************'
      WRITE(30,*)
      WRITE(30,*)'  Absolute Yield (Liq. Prods./Reactant Input)'
      WRITE(30,*)
      WRITE(30,256)(PLNAM(LNUM(J)),LMASR(J),J=1,NLRAT)
  256 FORMAT(' ',5X,A22,5X,F7.3)
      WRITE(30,*)
      WRITE(5,*)
      WRITE(30,*)
      WRITE(30,*)'*********************************************'
      WRITE(30,*)
      WRITE(5,*)'     Gas Products, PGM         '
      WRITE(30,*)'       Gas Products, PGM        '
      WRITE(30,*)
      WRITE(5,*)
      WRITE(30,*)

      WRITE(5,511)(PGNAM(GNUM(I)),PGM(I),I=1,NGRAT)
      WRITE(30,511) (PGNAM(GNUM(I)),PGM(I),I=1,NGRAT)
  511 FORMAT(' ',5X,A22,5X,F7.3)
      WRITE(30,*)
      WRITE(5,*)
      WRITE(30,*)
      WRITE(5,*)'*********************************************'
      WRITE(30,*)'*********************************************'
      WRITE(5,*)
      WRITE(30,*)
      WRITE(5,*)'    Absolute Yield(Gas product/Reactant Input)'
      WRITE(30,*)
      WRITE(30,*)'   ABSOLUTE YIELD(GAS PRODUCT/REACTANT INPUT)'
      WRITE(30,*)
      WRITE(5,521)(PGNAM(GNUM(I)),GMASS(I),I=1,NGRAT)
      WRITE(30,521)(PGNAM(GNUM(I)),GMASS(I),I=1,NGRAT)
  521 FORMAT(' ',5X,A22,5X,F7.4)
      WRITE(5,*)
      WRITE(30,*)
      WRITE(5,*)'*********************************************'
      WRITE(30,*)'*********************************************'
      WRITE(30,*)
      WRITE(5,*)'Mole of gas products/Mole of carbon in reactant'
      WRITE(30,*)'                ABSOLUTE YIELD                 '
      WRITE(30,*)'MOLE OF GAS PRODUCTS/MOLE OF CARBON IN REACTANT'
      WRITE(5,*)
      WRITE(30,*)
      WRITE(5,522)(PGNAM(GNUM(I)),GMOLC(I),I=1,NGRAT)
      WRITE(30,522)(PGNAM(GNUM(I)),GMOLC(I),I=1,NGRAT)
```

```
522 FORMAT(' ',5X,A22,5X,F7.4)
    WRITE(5,*)
    WRITE(30,*)
    STOP

    END
```

```
 * DATA FILE 'FOR20.DAT' *

 4          1-Large annular, 2-Large (no annulus), 3-Micro,
*           4-Coil
 1          1 If solvent = H2O, 2 if other
*           (if 2 update FOR21.DAT)
 1319100000DateTimeGroup
 298.       Temperature of sample loop, (deg K)= ?
 32.        Change of Pressure in loop, (mV) = ?
 650.       Pre-Heat temp. (deg C) = ?
 650.       Reactor temp. (deg C) = ?
 243.8      Estimated Reactor Length (inches) = ?
 5000.      Reaction pres. (psi)= ?
 1.00       Reactant density @ ambient conditions (g/ml)= ?
 0.5        Measured mass flow rate into reactor (g/min)= ?
 1          Number of reactants = ?
*           DO I=1,IREAC Input data about reactants
 0.01 M Glucose   --------->  ! Name of reactant ',I,' is ?
 0.72       Concentration of reactant I,@ ambient conditions
*           is(mg/ml) ?
 180.2      The Mol. Weight of reactant ',I,' is(g) ?
 0.4291     The Carbon Fraction of reactant ',I,' is ?
 0.0660     The Hydrogen Fraction of reactant ',I,' is ?
 0.4002     The Oxygen Fraction of reactant ',I,' is ? END DO
 10         Number of actual gaseous product highest on list=?
 6.7        The calibration for transducer gas pres.
*           (large bott 1.3848)regu 6.7
 0.2262     CO2  Enter all product gas concentration
 0.6042     H2
 0.         N2
 0.         AR
 0.0104     CO
 0.         O2
 0.1163     CH4
 0.0000     C2H2
 0.0123     C2H4
 0.0306     C2H6
 22         Number of actual liquid product highest on list=?
 5.0        The product liquid volume is(ml) ?
 0.         HMF,Enter all product liquid concentrations(mg/ml)
 0.0         Furfural
 0.0         Lactic Acid
 0.0         Mannose
 0.          Fructose
 0.          water
 0.          Glucose
 0.          Acetol
 0.          Methylglyoxal
 0.          Glycolaldehyde
 0.          Dihydroxyacetone
 0.          Glycerol
```

```
 0.          Levoglucosan
 0.          Levulinic Acid
 0.          Formic Acid
 0.          Glyceraldehyde
 0.          Xylose
 0.          Arabinose
 0.          Lyxose
 0.          Ribose
 0.0         Cellobiose
 0.0         DP-2
 1           Compare the products by means of MOLAR ratios?
*            Yes=1,No=2
 7           How many gases will be compared ?
 1           Enter all gases list numbers one @ a Time.
*            (From Gas Lists)
 2
 5
 7
 8
 9
10
 1          How many liquids will be compared?
 7          Enter all liquid list numbers one @ a time.
 1          Enter reactant # from reactant list for
*           conversion base
 7          Enter reactant # from liq. prod. list
```

APPENDIX B

COMPUTER CODE FOR EVALUATION OF NONDIMENSIONAL NUMBERS

```
       * RENEWABLE RESOURCES RESEARCH LAB *

        * NONDIM : VERSION 2.0 * AUG 85 *

*************************************************************
*                                                           *
* NONDIM  : :  Algorithm to calculate charateristic times   *
*              and non-dimensional numbers                  *
*                                                           *
* Programmer:                                               *
*              Michael Jerry Antal, Jr                      *
*              Sundaresh Venkat Ramayya                     *
*                                                           *
*************************************************************
*                                                           *
*                    PROGRAM DESCRIPTION                    *
*                                                           *
*          This porgram calculates charateristic times and  *
* and non-dimensional numbers for a tubular flow reactor    *
* at given operating conditions.  This program is run using *
* the data form the data file for21.dat.  Using these       *
* charectiristic times it checks the reactor for negligible *
* non-isothermality, negligible axial diffusion and         *
* negligible poiseuille flow.  These criteria are varified  *
* using the emperical correlations put forth by earlier     *
* researchers                                               *
*                                                           *
*************************************************************
*                                                           *
*                    VARIABLE DEFINITION                    *
*                                                           *
* (a) REACNE : Name of the reactant                         *
* (b) TEMP   : Operating temperature                        *
* (c) PRESS  : Operating pressure                           *
* (d) EFFLEN : Effective reactor length                     *
* (e) REACOD : Reactor outer diameter                       *
* (f) REACID : Reactor inner diameter                       *
* (g) RESTIM : Resedence time                               *
* (h) THRCON : Thermal conductivity of the solvent          *
* (i) SPVOL  : Specific volume of the solvent               *
* (j) SPHEAT : Specific heat at cons. press. of the solvent *
* (k) DYVISC : Dynamic viscosity of the solvent             *
* (l) REMOL  : Reactant molecular weight                    *
* (m) RECRTM : Reactant critical temperature                *
* (n) RECRPR : Reactant critical pressure                   *
```

```
* (o) SLMOL  : Solvent molecular weight                          *
* (p) SLCRTM : Solvent critical temperature                      *
* (q) SLCRPR : Solvent critical pressure                         *
* (r) COMPRS : Compresibility factor for the reactant            *
* (s) FLRATE : Flow rate of the reactant mixture                 *
* (t) ECONST : Rate constant of the reaction occuring            *
* (u) HYDRAD : Hydraulic radius of the reactor                   *
* (v) BLKVEL : Bulk velocity  of the mixture                     *
* (w) THRDIF : Thermal diffusivity of the solvent                *
* (x) KIVISC : Kinematic viscosity of the solvent                *
* (y) DIFFUS : Species diffusivity                               *
* (z) RMLVOL : Reactant molar volume                             *
*                                                                *
******************************************************************

 REAL TEMP,PRESS,EFFLEN,REACOD,REACID,RESTIM,THRCON,SPVOL
 REAL SPHEAT,DYVISC,REMOL,RECRTM,RECRPR,SLMOL,SLCRTM,SLCRPR
 REAL COMPRS,FLRATE,ECONST
 REAL HYDRAD,BLKVEL,THRDIF,KIVISC,PRNO,DIFFUS(3),G(3)
 REAL Tfcr,Tfcl,Tsdr,Tsdl,Ttdr,Ttdl,Tmd,Tck
 REAL Re,Pr,Sc,PeSd,Petd,Da
 REAL EQUA1,EQUA2,EQUA3,EQUA4,EQUA5,EQUA6,EQUA7,EQUA8,EQUA9
 REAL A,B,C,D,RMLVOL
 CHARACTER*20 REACNE
 CHARACTER*1 ANS

 OPEN (20, FILE = 'FOR21.DAT')
 OPEN (5, FILE = 'CON')

 READ (20,*) REACNE
 READ (20,*) TEMP
 READ (20,*) PRESS
 READ (20,*) EFFLEN
 READ (20,*) REACOD
 READ (20,*) REACID
 READ (20,*) RESTIM
 READ (20,*) THRCON
 READ (20,*) SPVOL
 READ (20,*) SPHEAT
 READ (20,*) DYVISC
 READ (20,*) REMOL
 READ (20,*) RECRTM
 READ (20,*) RECRPR
 READ (20,*) SLMOL
 READ (20,*) SLCRTM
 READ (20,*) SLCRPR
 READ (20,*) COMPRS
 READ (20,*) FLRATE
 READ (20,*) ECONST
```

```
      WRITE(5,*)'NAME OF THE REACTANT                    ',REACNE
      WRITE(5,*)'OPERATING TEMPERATURE ( DEG KELVIN )    ',TEMP
      WRITE(5,*)'OPERATING PRESSURE    ( BAR)            ',PRESS
      WRITE(5,*)'EFFECTIVE REACTOR LENGTH                ',EFFLEN
      WRITE(5,*)'REACTOR OUTER DIAMETER   ( CM)          ',REACOD
      WRITE(5,*)'REACTOR INNER DIAMETER   ( CM )         ',REACID
      WRITE(5,*)'RESIDENCE TIME           ( SEC )        ',RESTIM
      WRITE(5,*)'THERMAL CONDUCTIVITY (MILLIWAT/M DEG.K)',THRCON
      WRITE(5,*)'SPECIFIC VOLUME      ( CM**3 / GRMS )   ',SPVOL
      WRITE(5,*)'SPECIFIC HEAT AT CONST PRESS(KJ/KG DEG.K)',
     * SPHEAT
      WRITE(5,*)'DYNAMIC VISCOSITY        ( MICROPOISE )',DYVISC
      WRITE(5,*)'REACTANT MOLECULAR WT.                  ',REMOL
      WRITE(5,*)'REACTANT CRITICAL TEMP.  ( DEG. K )     ',RECRTM
      WRITE(5,*)'REACTANT CRITICAL PRESS. ( BARS )       ',RECRPR
      WRITE(5,*)'SOLVENT MOLUCULAR WT.                   ',SLMOL
      WRITE(5,*)'SOLVENT CRITICAL TEMP.   ( DEG. K )     ',SLCRTM
      WRITE(5,*)'SOLVENT CRITICAL PRESS.  ( BARS )       ',SLCRPR
      WRITE(5,*)'COMPRESSIBILITY FOR REACTANT            ',COMPRS
      WRITE(5,*)'FLOW RATE                ( ML / MIN )   ',FLRATE
      WRITE(5,*)'RATE CONSTANT                           ',ECONST


      HYDRAD = 0.5*((REACOD**2-REACID**2)**0.5)

      BLKVEL = EFFLEN/RESTIM

      THRDIF = ((THRCON*SPVOL)/SPHEAT)/100000.

      KIVISC = (DYVISC*SPVOL)/1000000.

      PRNO   = (KIVISC/THRDIF)

      A = (TEMP/((RECRTM*SLCRTM)**0.5))

      B = ((RECRPR*SLCRPR)**0.3333)

      C = ((RECRTM*SLCRTM)**0.4167)

      D = (((1/REMOL) + (1/SLMOL))**0.5)/PRESS

      DIFFUS(1) = 0.0002745*(A**1.823)*B*C*D
      G(1)  = DIFFUS(1) + ((HYDRAD*BLKVEL)**2)/(48*DIFFUS(1))

C     POLAR
      DIFFUS(2) = 0.000364 *(A**2.334)*B*C*D
      G(2)  = DIFFUS(2) + ((HYDRAD*BLKVEL)**2)/(48*DIFFUS(2))

      RMLVOL = (COMPRS*8314.34*TEMP)/(PRESS*100)
```

```
      DIFFUS(3) = (13.26/100000.)*((DYVISC/10000.)**(-1.4))
     * 1*(RMLVOL**(-0.589))
      G(3)   = DIFFUS(3) + ((HYDRAD*BLKVEL)**2)/(48*DIFFUS(3))

      WRITE(5,*)'HYDRAULIC RADIUS       ( CM )            ',HYDRAD
      WRITE(5,*)'BULK VELOCITY          ( CM / SEC )      ',BLKVEL
      WRITE(5,*)'THERMAL DIFFUSIVITY    ( CM**2 / SEC )   ',THRDIF
      WRITE(5,*)'KINEMATIC VISCOSITY    ( CM**2 / SEC )   ',KIVISC
      WRITE(5,*)'DIFFUSIVITY-->NONPOLAR,VAPOUR ( CM**2/SEC) ',
     * DIFFUS(11)
      WRITE(5,*)'T.DIFFUSIVITY-->NONPOLAR,VAPOUR(CM**2/SEC)',G(1)
      WRITE(5,*)'DIFFUSIVITY-->POLAR,VAPOUR (CM**2/SEC)',
     * DIFFUS(21)
      WRITE(5,*)'T. DIFFUSIVITY-->POLAR,VAPOUR( CM**2/SEC)',G(2)
      WRITE(5,*)'DIFFUSIVITY-->LIQUID   ( CM**2/SEC) ',DIFFUS(31)
      WRITE(5,*)'T. DIFFUSIVITY-->LIQUID     ( CM**2/SEC) ',G(3)

      DO 100 I = 1,3
     C READ (5,10) ANS
    10 FORMAT(A1)
      WRITE(5,*)
      WRITE(5,*)
      WRITE(5,*)'-------------------------------------------'
      IF(I.EQ.1)WRITE(5,*)'DIFFUSION->NON-POLAR,VAPOUR
     * (BIRDS FORMULA)'
      IF(I.EQ.1)WRITE(5,*)'--------------------------
     * ----------------'
      IF(I.EQ.2)WRITE(5,*)'DIFFUSION->POLAR , VAPOUR
     * (BIRDS FORMULA)'
      IF(I.EQ.2)WRITE(5,*)'--------------------------
     * ----------------'
      IF(I.EQ.3)WRITE(5,*)'DIFFUSION->LIQUID
     * (HAYDUK-LAUBIE CORR)'
      IF(I.EQ.3)WRITE(5,*)'--------------------------
     * ----------------'
      WRITE(5,*)
      WRITE(5,*)

      Tfcr = HYDRAD / BLKVEL

      Tfcl = EFFLEN / BLKVEL

      Tsdr = (HYDRAD**2) / DIFFUS(I)

      Tsdl = (EFFLEN**2) / G(I)

      Ttdr = (HYDRAD**2) / THRDIF

      Ttdl = (EFFLEN**2) / THRDIF
```

```
Tmd  = (HYDRAD**2) / KIVISC

Tck  = ( 1 / ECONST )

RENO = ( Tmd / Tfcr )

PRNO = ( Ttdr / Tmd )

SC   = ( Tsdr / Tmd  )

PeSd = ( Tsdr / Tfcr )

Petd = ( Ttdr / Tfcr )

Da   = ( Tsdr / Tck )

EQUA1 = ( Tfcr * Tfcr )/(Tck*Tsdr)

EQUA2 = ( Tfcl / Tsdl )

EQUA3 = ( Tfcr / Tsdr )

EQUA4 = ( Tsdr / (Tck*48)) + EQUA1

EQUA5 = ( 1 / (Tfcl * Tck) )

EQUA6 = (Tsdr / Tfcl )

EQUA7 = ( Tsdr / Tck )

EQUA8 = ( Tfcr / Tck )

EQUA9 = ( Ttdr / Tfcl )

WRITE(5,*)
WRITE(5,*)
WRITE (5,*) '       CHARACTERISTIC TIMES  ( SEC )'
WRITE (5,*) '       --------------------  '
WRITE (5,*)
WRITE (5,*) '      TFc,R   =  ', Tfcr
WRITE (5,*) '      TFc,L   =  ', Tfcl
WRITE (5,*) '      TSd,R   =  ', Tsdr
WRITE (5,*) '      TSd,L   =  ', Tsdl
WRITE (5,*) '      Ttd,R   =  ', Ttdr
WRITE (5,*) '      Ttd,L   =  ', Ttdl
WRITE (5,*) '      TMd     =  ', Tmd
WRITE (5,*) '      Tck     =  ', Tck

WRITE(5,*)
WRITE (5,*) '       NON-DIMENSIONAL NUMBERS '
WRITE (5,*) '       ----------------------- '
```

```
      WRITE (5,*)
      WRITE (5,*) '       RE.NO.   ( Tmd / Tfcr ) =  ', RENO
      WRITE (5,*) '       PR.NO.   ( Ttdr / Tmd ) =  ', PRNO
      WRITE (5,*) '       SC.NO.   ( Tsdr / Tmd ) =  ', SC
      WRITE (5,*) '       Pesd.NO.( Tsdr / Tfcr) =  ', PeSd
      WRITE (5,*) '       Petd.NO.( Ttdr / Tfcr) =  ', PeTd
      WRITE (5,*) '       DA.      ( Tsdr / Tck ) =  ', Da

      WRITE(5,*)
      WRITE (5,*) '        NEGLIGIBLE AXIAL DIFFUSION '
      WRITE (5,*) '        -------------------------- '
      WRITE (5,*)
      WRITE (5,*) '            NAME                CRITERIA       '
     * 1,'                     VALUE'
      WRITE (5,*) '            ----                --------       '
     * 1,'                     -----'
      WRITE (5,*)
      WRITE (5,*) '      DICKENS ETAL, 1960   Tfcr**2/Tck*Tsdr '
     * 1,'< 0.1                ',EQUA1
      WRITE (5,*) '      AZATYAN , 1972 '
      WRITE (5,*) '      HOWARD ,  1979 '
      WRITE (5,*) '      FURUE AND PACEY , 1980 '
      WRITE (5,*)
      WRITE (5,*)
      WRITE (5,*) '      MULCATY AND PETHARD,1963  Tfcl/Tsdl    '
     * 1,'< 0.015              ',EQUA2
      WRITE (5,*)
      WRITE (5,*) '    DANG AND STEINBERG ,1980  Tfcr/Tsdr      '
     * 1,'< 0.02               ',EQUA3
      WRITE (5,*)
      WRITE (5,*) '  FURUE AND PACEY , 1980  Tfcr**2/Tsdr*Tck '
      WRITE (5,*) '                                + Tsdr/48*Tck     '
     * 1,'<< 1                 ',EQUA4
      WRITE (5,*) '                                  1/Tfcl*Tck      '
     * 1,'<< 2                 ',EQUA5
      WRITE (5,*)
      WRITE (5,*)
      WRITE (5,*)
      WRITE (5,*)
      WRITE (5,*)
      WRITE (5,*)
      WRITE (5,*)
      WRITE (5,*) '       NEGLIGIBLE POISEUILLE FLOW '
      WRITE (5,*) '       -------------------------- '
      WRITE (5,*)
      WRITE (5,*) '           NAME                  CRITERIA      '
     * 1,'                    VALUE'
      WRITE (5,*) '           ----                  --------      '
     * 1,'                    -----'
```

```
      WRITE (5,*)
      WRITE (5,*) '     CLELAND AND WILHEM , 1956 Tsdr/Tfcl   '
     * 1,'< 0.5          ',EQUA6
      WRITE (5,*) '     MULCAHY AND PETHARD ,1963 Tsdr/Tfcl   '
     * 1,'<< 14.29        ',EQUA6
      WRITE (5,*)
      WRITE (5,*) '     WALKER , 1961             Tsdr/Tck    '
     * 1,'<< 10           ',EQUA7
      WRITE (5,*) '     POIRIER AND CARR ,1971   Tsdr/Tck     '
     * 1,'<<  2           ',EQUA7
      WRITE (5,*) '     OGRER , 1975          Tsdr/Tck        '
     * 1,'<< 1.0          ',EQUA7
      WRITE (5,*)
      WRITE (5,*)
      WRITE (5,*) '     BROWN ,1978           Tfcr/Tck        '
     * 1,'< 0.05          ',EQUA8
      WRITE (5,*)
      WRITE (5,*)
      WRITE (5,*) '       NEGLIGIBLE NON-ISOTHERMALITY '
      WRITE (5,*) '       ---------------------------- '
      WRITE (5,*)
      WRITE (5,*) '          NAME                CRITERIA     '
     * 1,'           VALUE'
      WRITE (5,*) '          ----                --------     '
     * 1,'           -----'
      WRITE (5,*)
      WRITE (5,*) '     GILBERT , 1958            Ttdr/Tfcl   '
     * 1,'<< 3.7          ',EQUA9
      WRITE (5,*) '     MULCAHY AND PETHARD,1963 Ttdr/Tfcl    '
     * 1,'<< 3.7          ',EQUA9
      WRITE (5,*) '      FURUE AND PACAY , 1980  Ttdr/Tfcl    '
     * 1,'<< 1.0          ',EQUA9
  100 CONTINUE

      STOP
      END
```

APPENDIX C

GAS ANALYSIS QUANTIFICATION PROGRAM

```
10      ' GAS ANALYSIS QUANTIFICATION PROGRAM
15      '
16      KEY OFF
18      DIM CALI(10), SCOUNT(4,10)
19      '
        ' gases
20      G$(1)="H2"  : G$(2)="Ar"  : G$(3)="O2"  : G$(4)="N2":
        G$(5)="CO"  : G$(6)="CH4" : G$(7)="CO2" : G$(8)="C2H2":
        G$(9)="C2H4": G$(10)="C2H6"
21      '
        'gas densities at STP in gm/liter
22      RHO(1)=0.08988 : RHO(2)=1.7832 : RHO(3)=1.429 :
        RHO(4)=1.25057 : RHO(5)=1.2504 : RHO(6)=0.7168 :
        RHO(7)=1.9769  : RHO(8)=1.1708 : RHO(9)=1.2604 :
        RHO(10)=1.3566
23      '
        ' gas molecular weights
24      MW(1)=2 : MW(2)=40 : MW(3)=32 : MW(4)=28 : MW(5)=28 :
        MW(6)=16 : MW(7)=44 : MW(8)=26 : MW(9)=28 : MW(10)=30
25      print : INPUT "Enter Standards ? ", Z$ :
        IF Z$="N" OR Z$="n" THEN INPUT "Enter calibration
        file: ", F$: BLOAD F$, VARPTR(CALI(0)) : GOTO 300
26      '
27      ' Here to determine new calibration file
28      '
30      STD(1)=.129  : STD(2)=9.800001E-02  : STD(3)=.79 :
        STD(4)=.21   : STD(5)=.3875  : STD(6)=.0792  :
        STD(7)=.0897 : STD(8)=.0178  : STD(9)=.152 :
        STD(10)=9.199998E-03
40      '
50      INPUT "Enter number of standard injections ", N
55      PRINT
60      FOR I=1 TO N
70              PRINT "Injection "; I
75              INPUT "Enter injection volume"; VOL(I):
                IF VOL(I)=0 THEN VOL(I)=.3
80              FOR J=1 TO 10
90                   IF J=3 OR J=4 HEN GOTO 120
100                  PRINT "Enter counts for "; G$(J) :
                     INPUT COUNT(I,J)
101                  IF COUNT(I,J)=-1 THEN J=J-1: GOTO 90
102                  IF COUNT(I,J)=-2 THEN GOTO 70
103                  IF COUNT(I,J)=-3 THEN N=N-1: GOTO 70
104                  IF COUNT(I,J)=-4 THEN GOTO 50
120             NEXT J
125     PRINT
130     NEXT I
```

```
140     '
200     FOR J=1 TO 10
205        IF J=3 OR J=4 THEN GOTO 230
210        T C O U N T = 0 :    F O R    I = 1    T O    N    :
           TCOUNT=TCOUNT+COUNT(I,J)/VOL(I) : NEXT I
220        CALI(J)=STD(J)/(TCOUNT/N)
230     NEXT J
231     '
232     INPUT "Enter extra (overriding) calibration points";
        Z$: IF Z$<>"Y" AND Z$<>"Y" THEN GOTO 250
234     PRINT: FOR J=1 TO 10: PRINT J;"-";G$(J), : NEXT J
235     INPUT "Enter gas #: "; I%:
        IF I%<1 THEN GOTO 250
236     INPUT "Enter volume (room condition) injected: "; V :
        INPUT "Enter percentage: "; P :
        INPUT "Enter count: "; COUNT
237     CALI(I%)=p/100*V/COUNT : GOTO 234
240     '
250     INPUT "Saved this calibration file "; Z$
260     IF Z$="Y" OR Z$="Y" THEN INPUT "Enter file name: ";F$:
        BSAVE F$, VARPTR(CALI(0)),44
300     '
        ' here to obtain sample data
        '
310     PRINT : INPUT "Recall old injection files <n> "; Z$
315     IF Z$="Y" OR Z$="Y" THEN INPUT "Enter injection file:",
        F$ : BLOAD F$, VARPTR(SCOUNT(0,0)): N=SCOUNT(0,1) :
        TVOL=SCOUNT(0,2) : FOR I=1 TO N : SVOL(I)=SCOUNT(I,0)
        : NEXT I : PRINT : GOTO 600
320     '
499     '
500     '
        ' here to enter GC counts for multiple injections
        of each sample ", N
        '
507     INPUT "Enter number of injection for this sample ", N
509     REM total is sum of all injections of each gas
            tconc is sum of all gases in each injection
510     FOR I=1 TO N
512             TCONC(I)=0
515             PRINT
520             PRINT "Injection "; I
530             INPUT "Enter injection volume (ml) "; SVOL(I)
540             FOR J=1 TO 10
550                  PRINT "Enter counts for "; G$(J) :
                     INPUT SCOUNT(I,J)
555                  IF SCOUNT(I,J)=-1 THEN J=J-1: GOTO 550
556                  IF SCOUNT(I,J)=-2 THEN GOTO 530
557                  IF SCOUNT(I,J)=-3 THEN I=I-1 : GOTO 515
558                  IF SCOUNT(I,J)=-4 THEN GOTO 502
580             NEXT J
590     NEXT I
```

```
591     '
592     PRINT :INPUT "Saved this injection file "; Z$
593     IF Z$="Y" OR Z$="Y" THEN INPUT "Enter file name: ";F$:
        FOR I=1 TO N:SCOUNT(I,0)=SVOL(I):NEXT I: SCOUNT(0,1)=N:
        SCOUNT(0,2)=TVOL: BSAVE F$, VARPTR(SCOUNT(0,0)), 224
595     '
600     '
        ' here to calculate concentrations
        '
604     PRINT : PRINT "Enter report heading" :
        INPUT "", TITLE$ : PRINT
605     FOR I=1 TO N
607        FOR J=1 TO 10
609             CONC(I,J)=SCOUNT(I,J)/SVOL(I)*CALI(J)
615             TCONC(I)=TCONC9I)+CONC(I,J)
620        NEXT J
630     NEXT I
640     '
650     GOSUB 1500      ' calculate average
660     GOSUB 1600      ' print out
699     '
700     END
900     '
        '
1500    '
        ' subroutine to calculate average and totals
        '
1510    '
1520    TMCONC=0
1530    FOR J=1 TO 10
1540       TOTAL=0 :
           FOR I=1 TO N : TOTAL=TOTAL+CONC(I,J) : NEXT I :
           MCONC(J)=TOTAL/N
1560    TMCONC=TMCONC+MCONC(J)
1570    NEXT J
1580    NTOTAL=TMCONC-MCONC(4)   ' total excluding N2
1585    FOR J=1 TO 10: NCONC(J)=MCONC(J)/NTOTAL*100: NEXT J:
        NCONC(4)=0
1599    RETURN
1600    '
        ' subroutine to print
        '
1601    PRINT: PRINT TITLE$ : PRINT
1605    PRINT "Total volume collected for this sample is ";
        TVOL; " cc"
1610    P$="  ###.####"
1620    PRINT "Concentration of gases in vol%: " : PRINT
1630    PRINT "gas  ";: FOR I=1 TO N : PRINT USING "  sample#";
        I; : NEXT I: PRINT "     Mean    Norm w/out N2" :PRINT
1640    FOR J=1 TO 10
1645       PRINT USING "\     \"; G$(J);
1647       FOR I=1 TO N: PRINT USING P$; CONC(I,J)*100,  :
```

```
          NEXT I
1650      PRINT USING P$;MCONC(J)*100;NCONC(J)
1655    NEXT J
1660    PRINT : PRINT "Total: ";
1665    FOR I=1 TO N: PRINT USING P$; TCONC(I)*100,: NEXT I
1667    PRINT USING P$;TMCONC*100
1670    RETURN
```

APPENDIX D

CALCULATION OF ENTHALPY OF GLUCOSE REACTION IN SCW

The steam gasification reaction:

$$C_6H_{12}O_6 + 6H_2O \text{ --------> } 12H_2 + 6CO_2$$

Condition for calculation: 823 K, 34.5 MPa

$$H_{R,823\ K,34.5MPa} = n_{C6H1206}\{h_f^0 + \Delta h\}_{C6H1206} + 6\{h_f^0 + h_{823K,34.5MPa} - h_{298K,0.1MPa}\}_{H2O}$$

$$= 1\{h_{f,298}^0 + C_p\Delta T\}_{C6H1206} + 6\{h_{f,298}^0 + h_{823K,34.5MPa} - h_{298K,0.1MPa}\}_{H2O}$$

$$= 1\{-1,274,500 + 226(823-298)\} + 6\{-285818 + 18(4065 - 104.9)\}$$

$$= -1,155,850 - 1,287,217$$

$$= -2,443,067 \text{ kJ/kmol} \quad \text{(1)}$$

$$H_{P,823\ K,34.5MPa} = n_{H2}\{h_f^0 + \Delta h\}_{H2} + n_{CO2}\{h_f^0 + \Delta h\}_{CO2}$$

$$= 12\{h_{f,298}^0 + C_p\Delta T\}_{H2} + 6\{h_{f,298}^0 + C_p\Delta T - 40T_c\}$$

$$= 12\{0 + 52.90(525)\} + \{-393,522 + 44.33(525) - 40(304.2)\}$$

$$= -1,961,230 \text{ kJ/kmol} \quad \text{(2)}$$

$$\Delta H_{Reac,823\ K,34.5MPa} = H_P - H_R = -1,961,230 - (-2,443,067)$$

$$= 481,836 \text{ kJ/kmol ; Endothermic}$$

Notation:

$h_{f,i}^{0}$ = enthalpy of formation of species i at reference state, the data for H_2O and gas species obtained from Van Wylen et al. (Van Wylen, 1976), and that of $C_6H_{12}O_6$ from Stull et al. (Stull et al., 1969)

h_i = enthalpy of species i at one state

n_i = number of moles of species i

H_P, H_R = enthalpy of products and reactants respectively

$C_{P,i}$ = heat capacity of species i

h = enthalpy difference between at any given state and at 298 K, 0.1 MPa

H_{Reac} = enthalpy of reaction

APPENDIX E

CALCULATION OF FRACTION OF POTENTIAL HYDROGEN YIELD REALIZED

From Steam Reforming equation :

$$C_xH_yO_z + (2x-z)\ H_2O \text{ -------> } x\ CO_2 + \{2x+(y/2)-z\}\ H_2 \quad \text{(E-1)}$$

From Table 3.1, the Elemental Analysis of Algae is:

C = 42.91 %, H = 6.60 %, O = 40.02 %

or in terms of mole

x = 1.79, y = 3.30, z = 1.25

By substituting x, y, z into equation (E-1)

$$CH_{1.84}O_{0.70} + 1.30\ H_2O \text{ -------> } CO_2 + 2.22\ H_2$$

Therefore, Fraction of Potential Hydrogen Yield Realized, x_{H2}, for Algae is $x_{H2} = H_{2,t} / H_{2,p}$, or

$$\mathbf{x_{H2} = H_{2,t} / 2.22}$$

where $H_{2,t}$ = Experimental mole of hydrogen per mole of carbon in reactant

$H_{2,p}$ = Theoretical mole of hydrogen per mole of carbon in reactant

Similarly, for Kelp the Elemental Analysis (see Table 3.1) is

C = 23.22 %, H = 2.96 %, O = 40.13 %

or in terms of mole

x = 1.935, y = 2.96, z = 2.508

By substituting x, y, z terms into equation (E-1)

$$CH_{1.53}O_{1.30} + 0.70\ H_2O \text{ ------> } CO_2 + 1.47\ H_2$$

Therefore, Fraction of Potential Hydogen Yield Realized, x_{H2}, for Kelp is

$$\mathbf{x_{H2} = H_{2,t} / 1.47}$$

From Table 3.1, the Elemental Analysis of Water Hyacinth is

C = 43.0 %, H = 5.8 %, O = 29.5 %

or in terms of mole

x = 3.583, y = 5.8, z = 1.844

By substituting x, y, z terms into equation (E-1)

$$CH_{1.62}O_{0.51} + 1.49\ H_2O \text{ ------> } CO_2 + 2.29\ H_2$$

Therefore, Fraction of Potential Hydogen Yield Realized, x_{H2}, for Water Hyacinth is

$$\mathbf{x_{H2} = H_{2,t} / 2.29}$$

Calculation of Fraction of Potential Hydrogen Yield including Hydrogen from CO and CH_4:

Hydrogen is easily produced from CH_4 by steam reforming:

$$CH_4 + 2\ H_2O \text{ -----> } 4\ H_2 + CO_2$$

Also, hydrogen can be easily produced from CO by the water-gas shift reaction:

$$CO + H_2O \text{ -----> } H_2 + CO_2$$

Therefore,

$$H_{2,ta} = H_{2,t} + 4\ CH_{4,t} + CO_t$$

$$H_{2,pot} = H_{2,ta}/H_{2,p}$$

where $H_{2,ta}$ = Experimental mole of hydrogen including hydrogen from CH_4 and CO per mole of carbon in reactant

$H_{2,pot}$ = Fraction of potential hydrogen yield including hydrogen from CH_4 and CO

$CH_{4,t}$ = Experimental mole of CH_4 per mole of carbon in reactant

CO_t = Experimental mole of CO per mole of carbon in reactant

APPENDIX F

DATA FROM GASIFICATION OF GLUCOSE AND WET BIOMASS IN SCW USING SCAFR AND SCCFR

Table F.1 Elemental balances and absolute gas yields for oxidation and pyrolysis reactions in SCW using the SCAFR

Exp.date	Reactant	Exp.No. (Sam.No.)	Temp. /C	Pressure /MPa.	Residence time,/sec	C balance	H balance	O balance	Absolute Yield(Mole of Product/ Mole of Reactant Feed) CO2	H2	CO	CH4	C2H4	C2H6
3/31/89	0.005M DHA	1(N3)	480	25	6	0.6020	0.5556	0.9423	1.18	1.34	0.47	0.16	0.00	0.00
	0.005M DHA+0.01M H2O2	2(N5)	480	25	6	0.8917	0.5398	1.5047	2.01	1.27	0.50	0.17	0.00	0.00
		3(N7)				0.9820	0.4339	1.7134	2.34	1.01	0.46	0.14	0.00	0.00
4/14/89	0.05M XYLOSE	4(Q1)	480	25	6	0.3989	0.3157	0.5157	0.94	1.03	0.69	0.16	0.05	0.04
	0.05M GLUCOSE	5(Q2)	480	25	6	0.4185	0.3190	0.5581	1.18	1.31	1.00	0.22	0.03	0.03
		6(Q3)				0.4104	0.2644	0.5602	1.25	0.99	0.87	0.19	0.03	0.05
	0.05M FRUCTOSE	7(Q4)	480	25	6	0.3369	0.2419	0.4416	0.94	0.90	0.77	0.20	0.03	0.03
		8(Q5)				0.3149	0.2620	0.4138	0.89	1.06	0.71	0.19	0.03	0.02
	0.05M DHA	9(Q6)	480	25	6	0.3886	0.3830	0.5012	0.53	0.80	0.45	0.15	0.01	0.01
		10(Q7)				0.3850	0.4043	0.4963	0.52	0.86	0.44	0.15	0.01	0.01

Table F.1 Continued

Exp.date	Reactant	Exp.No. (Sam.No.)	Temp. /C	Pressure /MPa.	Residence time,/sec	C balance	H balance	O balance	Absolute Yield(Mole of Product/ Mole of Reactant Feed) CO2	H2	CO	CH4	C2H4	C2H6
5/8/89	0.05M DHA	11(R1)	480	27.5	26	0.4780	0.5422	0.6499	0.76	1.20	0.44	0.16	0.02	0.02
		12(R2)				0.4884	0.5120	0.6782	0.80	1.12	0.43	0.16	0.02	0.02
	0.05M GLUCOSE	13(R3)	480	27.5	26	0.6441	0.7385	0.9223	2.48	2.93	0.57	0.41	0.03	0.08
		14(R4)				0.4717	0.5280	0.6111	1.36	2.25	0.95	0.33	0.05	0.05
		15(R5)				0.5250	0.4686	0.6995	1.61	1.84	0.98	0.34	0.05	0.05
5/17/89	0.05M GLUCOSE	16(S1)	480	27.5	53	0.3901	0.3085	0.5608	1.32	1.34	0.73	0.17	0.03	0.03
		17(S2)				0.4348	0.4294	0.5982	1.32	1.97	0.94	0.20	0.03	0.04
5/18/89	0.05M GLUCOSE	18(S3)	480	27.5	53	0.7145	0.9312	1.0608	3.04	3.84	0.29	0.71	0.03	0.07
		19(S4)				0.6583	1.3046	0.7125	1.77	5.23	0.73	1.02	0.08	0.11
		20(S5)				0.3609	0.3346	0.5059	1.13	1.56	0.79	0.15	0.02	0.03
5/31/89	0.01M GLUCOSE	21(T1)	460	34.5	43	0.6712	0.5177	1.0182	2.54	2.32	1.04	0.28	0.04	0.04
		22(T2)				0.597	0.5985	0.9105	2.28	2.87	0.90	0.26	0.04	0.03
		23(T3)	480	34.5	38	0.7161	0.6242	1.0599	2.64	2.72	1.08	0.37	0.05	0.05
		24(T4)				0.6232	0.7550	0.8906	2.18	3.54	1.00	0.36	0.05	0.05
		25(T5)				0.5939	0.7209	0.8380	2.04	3.33	0.95	0.34	0.06	0.05

Table F.1 Continued

Exp.date	Reactant	Exp.No. (Sam.No.)	Temp. /C	Pressure /MPa.	Residence time,/sec	C balance	H balance	O balance	Absolute Yield(Mole of Product/ Mole of Reactant Feed) CO2	H2	CO	CH4	C2H4	C2H6
6/5/89	0.01M DHA +0.01M H2O2	26(U1)	480	25.5	24	1.2464	1.2431	1.8189	2.30	2.64	0.85	0.47	0.03	0.02
		27(U2)				1.1871	1.5021	1.7366	2.19	3.40	0.83	0.53	0.00	0.01
	0.01M DHA	28(U3)	480	25.5	24	1.1279	1.2733	1.4031	1.66	2.55	0.89	0.39	0.20	0.02
		29(U4)				1.0656	1.3360	1.5154	1.77	3.16	1.01	0.39	0.00	0.02
6/14/89	0.01M GLUCOSE	30(V2)	500	34.5	34	0.6370	0.6371	0.9414	2.33	2.92	0.99	0.33	0.04	0.04
		31(V3)				0.7683	0.6890	1.1442	2.86	3.07	1.15	0.38	0.05	0.05
		32(V4)	520	34.5	31	0.6726	0.7708	0.9645	2.37	3.50	1.05	0.41	0.05	0.06
		33(V5)				0.6970	0.7760	0.9851	2.38	3.50	1.16	0.41	0.06	0.06
6/28/89	0.01M GLUCOSE	34(W1)	550	34.5	28	0.7367	0.8323	1.0313	2.58	3.54	1.03	0.52	0.06	0.08
		35(W2)				0.7530	0.8814	1.0633	2.67	3.83	1.04	0.53	0.06	0.08
		36(W3)				0.6906	0.8535	0.9819	2.48	3.80	0.93	0.48	0.05	0.07
		37(W4)	400	34.5	112	0.2819	0.1927	0.4809	1.25	1.07	0.38	0.02	0.02	0.00
		38(W5)				0.2705	0.2054	0.4559	1.18	1.14	0.38	0.02	0.02	0.00
		39(W6)				0.2725	0.2015	0.4681	1.23	1.13	0.35	0.02	0.02	0.00

Table F.1 Continued

Exp.date	Reactant	Exp.No. (Sam.No.)	Temp. /C	Pressure /MPa.	Residence time,/sec	C balance	H balance	O balance	Absolute Yield(Mole of Product/ Mole of Reactant Feed) CO2	H2	CO	CH4	C2H4	C2H6
7/6/89	0.005M GLUCOSE + 0.005M H2O2	40(X1)	550	34.5	28	0.7848	1.0308	1.1121	2.74	4.75	1.20	0.54	0.04	0.07
		41(X2)				0.8103	1.0559	1.1580	2.88	4.86	1.19	0.56	0.04	0.08
		42(X3)				0.7601	1.0489	1.0910	2.74	4.89	1.07	0.53	0.04	0.07
	0.005M GLUCOSE	43(X4)	550	34.5	28	0.7136	1.1385	1.0088	2.49	5.52	1.07	0.48	0.05	0.06
		44(X5)				0.6632	1.0879	0.9348	2.31	5.29	1.00	0.45	0.05	0.06
		45(X6)				0.7091	1.1435	1.0023	2.48	5.55	1.05	0.48	0.06	0.06
7/12/89	0.01M GLUCOSE	46(Y1)	550	34.5	56	0.8082	1.0778	1.0324	2.52	4.30	1.16	0.79	0.03	0.16
		47(Y2)				0.7825	1.0682	1.0008	2.44	4.32	1.12	0.76	0.03	0.15
		48(Y3)				0.8035	1.0465	1.0384	2.54	4.19	1.14	0.76	0.04	0.15
7/31/89	SOLUBLE STARCH	49(Z1)	550	34.5	56	0.9410	1.2679	1.4994	3.18	4.29	1.14	0.69	0.14	0.11
		50(Z2)				0.8797	1.3112	1.3057	2.73	4.29	1.07	0.65	0.27	0.14
		51(Z3)				0.8268	1.2202	1.3765	2.90	4.35	1.09	0.66	0.04	0.12
		52(Z4)	550	34.5	28	0.7348	1.0206	1.1665	2.20	3.73	1.44	0.51	0.04	0.09
		53(Z5)				0.7561	1.0535	1.2011	2.28	3.85	1.45	0.51	0.05	0.10
		54(Z6)				0.7046	1.0495	1.1142	2.10	3.92	1.37	0.49	0.05	0.09

Table F.1 Continued

Exp.date	Reactant	Exp.No. (Sam.No.)	Temp. /C	Pressure /MPa.	Residence time,/sec	C balance	H balance	O balance	Absolute Yield(Mole of Product/ Mole of Reactant Feed) CO2	H2	CO	CH4	C2H4	C2H6
8/24/89	0.05M GLUCOSE	55(A1)	500	34.5	34	0.4186	0.3496	0.5683	1.21	1.55	1.00	0.19	0.02	0.04
		56(A2)				0.4183	0.3534	0.5679	1.20	1.58	1.00	0.18	0.02	0.04
		57(A3)	550	34.5	28	0.5758	0.5780	0.7122	1.49	2.27	1.29	0.42	0.03	0.09
		58(A4)				0.5650	0.5942	0.6851	1.40	2.40	1.31	0.41	0.04	0.08

Table F.2 Carbon balance and gas yields from wet biomass gasification in SCW using the SCCFR
Condition : 550-650 C, 34.5 MPa

Reactant	Samp.No.	Reaction Condition	C balance	H balance	O balance	Absolute Yield (Moles of Gas/Moles of Carbon in Reactant) CO2	H2	CO	CH4	C2H2	C2H4	C2H6	H2/CO2	H2,pot**	H2,t/ H2,p(*)
1 g/l Algae	A1	580 C 62 s	0.816	0.831	0.959	0.165	0.308	0.341	0.115	0.004	0.061	0.032	1.87	0.50	0.14
	A2	600 C 59 s	0.787	0.959	0.993	0.215	0.39	0.265	0.151	0.002	0.044	0.032	1.81	0.57	0.18
	A3	605 C	0.953	1.121	1.251	0.294	0.423	0.287	0.188	0	0.046	0.045	1.44	0.66	0.19
	A4	600 C 59 s	0.703	0.883	0.934	0.211	0.389	0.231	0.131	0	0.036	0.029	1.84	0.51	0.17
	Average (600 C)		0.745	0.921	0.964	0.213	0.39	0.248	0.141	0.001	0.040	0.031	1.83	0.54	0.18

Table F.2 Continued

Reactant	Samp.No.	Reaction Condition	C balance	H balance	O balance	Absolute Yield (Moles of Gas/Moles of Carbon in Reactant) CO2	H2	CO	CH4	C2H2	C2H4	C2H6	H2/CO2	H2,pot**	H2,t/ H2,p(*)
0.78 g/l Algae	B4	600 C 117 s	0.709	1.114	0.931	0.274	0.503	0.103	0.163	0.01	0.043	0.032	1.84	0.57	0.23
	B5		0.664	1.259	0.967	0.304	0.672	0.068	0.157	0	0.034	0.033	2.21	0.62	0.30
	B6		0.773	1.284	1.048	0.328	0.59	0.077	0.18	0.001	0.054	0.039	1.80	0.62	0.27
	Average		0.715	1.219	0.982	0.302	0.588	0.083	0.167	0.004	0.044	0.035	1.95	0.60	0.26
	B1	600 C 59 s	0.746	0.809	0.945	0.184	0.307	0.293	0.137	0.001	0.036	0.029	1.67	0.52	0.14
	B2		0.840	0.976	0.977	0.194	0.328	0.296	0.178	0	0.047	0.039	1.69	0.60	0.15
	B3		0.697	0.825	0.849	0.172	0.310	0.250	0.141	0	0.038	0.029	1.80	0.51	0.14
	Average		0.761	0.870	0.924	0.183	0.315	0.280	0.152	0	0.040	0.032	1.72	0.54	0.14
	B7	600 C 29 s	0.631	0.815	0.900	0.240	0.376	0.149	0.109	0.002	0.041	0.023	1.57	0.43	0.17
	B8		0.716	0.883	1.021	0.269	0.389	0.177	0.129	0.004	0.041	0.025	1.45	0.49	0.18
	B9		0.638	0.818	0.882	0.229	0.372	0.159	0.110	0.005	0.043	0.021	1.62	0.44	0.17
	Average		0.662	0.839	0.934	0.246	0.379	0.162	0.116	0.004	0.042	0.023	1.54	0.45	0.17

Table F.2 Continued

Reactant	Samp.No.	Reaction Condition	C balance	H balance	O balance	Absolute Yield (Moles of Gas/Moles of Carbon in Reactant) CO2	H2	CO	CH4	C2H2	C2H4	C2H6	H2/CO2	H2,pot**	H2,t/ H2,p(*)
0.78 g/l Algae	C1	650 C 106 s	0.813	1.004	1.103	0.331	0.301	0.109	0.214	0	0.047	0.031	0.91	0.57	0.14
	C2		0.997	1.189	1.386	0.434	0.322	0.103	0.270	0	0.059	0.037	0.74	0.68	0.15
	C3		0.857	1.038	1.242	0.400	0.304	0.069	0.230	0	0.05	0.029	0.76	0.58	0.14
	Average		0.889	1.077	1.244	0.388	0.309	0.094	0.238	0	0.052	0.032	0.80	0.61	0.14
	C4	650 C 53 s	0.794	1.113	1.048	0.323	0.436	0.087	0.182	0.010	0.063	0.028	1.35	0.56	0.20
	C5		0.710	1.088	1.001	0.302	0.491	0.097	0.167	0	0.043	0.028	1.63	0.57	0.22
	C6		0.773	1.129	1.102	0.338	0.478	0.096	0.188	0	0.046	0.029	1.41	0.60	0.22
	Average		0.759	1.110	1.050	0.321	0.468	0.093	0.179	0.003	0.051	0.028	1.46	0.57	0.21
	C7	650 C 26 s	0.820	1.145	1.088	0.289	0.483	0.184	0.185	0	0.048	0.033	1.67	0.63	0.22
	C8		0.681	1.008	0.908	0.237	0.467	0.161	0.149	0	0.041	0.026	1.97	0.55	0.21
	C9		0.731	1.111	0.964	0.253	0.516	0.168	0.165	0	0.045	0.027	2.04	0.60	0.23
	Average		0.744	1.088	0.987	0.260	0.489	0.171	0.166	0	0.045	0.029	1.89	0.60	0.22

Table F.2 Continued

Reactant	Samp.No.	Reaction Condition	C balance	H balance	O balance	Absolute Yield (Moles of Gas/Moles of Carbon in Reactant) CO2	H2	CO	CH4	C2H2	C2H4	C2H6	H2/CO2	H2,pot**	H2,t/ H2,p(*)
0.7 g/l Algae	D1	550 C 134 s	0.606	0.782	0.862	0.201	0.387	0.202	0.103	0	0.027	0.024	1.92	0.45	0.17
	D2		0.580	0.788	0.846	0.205	0.409	0.183	0.099	0	0.025	0.022	2.00	0.44	0.18
	D3		0.588	0.771	0.885	0.220	0.401	0.180	0.095	0	0.025	0.021	1.82	0.43	0.18
	Average		0.591	0.780	0.864	0.209	0.399	0.188	0.099	0	0.026	0.022	1.91	0.44	0.18
	D4	550 C 67 s	0.473	0.627	0.696	0.157	0.351	0.174	0.065	0	0.023	0.016	2.24	0.35	0.16
	D5		0.521	0.646	0.798	0.187	0.357	0.184	0.069	0	0.024	0.017	1.91	0.37	0.16
	D6		0.494	0.659	0.762	0.180	0.382	0.173	0.065	0	0.022	0.016	2.12	0.37	0.17
	Average		0.496	0.644	0.752	0.175	0.363	0.177	0.066	0	0.023	0.016	2.09	0.36	0.16
	D7	550 C 33 s	0.451	0.495	0.658	0.133	0.265	0.195	0.053	0	0.022	0.013	1.99	0.30	0.12
	D8		0.476	0.523	0.740	0.164	0.292	0.189	0.053	0	0.022	0.013	1.78	0.31	0.13
	D9		0.436	0.495	0.670	0.148	0.278	0.173	0.049	0	0.021	0.012	1.88	0.29	0.13
	Average		0.454	0.504	0.689	0.148	0.278	0.186	0.052	0	0.022	0.013	1.88	0.30	0.13

Table F.2 Continued

Reactant	Samp.No.	Reaction Condition	C balance	H balance	O balance	Absolute Yield (Moles of Gas/Moles of Carbon in Reactant) CO2	H2	CO	CH4	C2H2	C2H4	C2H6	H2/CO2	H2,pot**	H2,t/ H2,p(*)
0.7 g/l Algae "BALLOON"	E1	550 C 134 s	0.625	0.866	1.000	0.272	0.472	0.155	0.100	0	0.024	0.024	1.74	0.46	0.22
	E2		0.618	0.857	1.006	0.276	0.475	0.152	0.098	0	0.025	0.022	1.72	0.46	0.21
	E3		0.562	0.811	0.949	0.269	0.474	0.127	0.084	0	0.022	0.019	1.76	0.42	0.21
	Average		0.602	0.845	0.985	0.272	0.474	0.145	0.094	0	0.024	0.022	1.74	0.45	0.21
	E4	550 C 67 s	0.486	0.730	0.772	0.198	0.444	0.144	0.064	0	0.023	0.017	2.24	0.38	0.20
	E5		0.489	0.716	0.805	0.213	0.440	0.137	0.062	0	0.022	0.016	2.07	0.37	0.20
	E6		0.523	0.665	0.873	0.219	0.403	0.172	0.058	0	0.021	0.016	1.84	0.36	0.18
	Average		0.499	0.704	0.817	0.210	0.429	0.151	0.061	0	0.022	0.016	2.05	0.37	0.19
	E7	550 C 33 s	0.425	0.537	0.748	0.199	0.337	0.125	0.043	0	0.018	0.011	1.69	0.28	0.15
	E8		0.432	0.604	0.736	0.193	0.384	0.130	0.047	0	0.020	0.012	1.99	0.32	0.17
	E9		0.409	0.554	0.715	0.193	0.354	0.114	0.043	0	0.017	0.011	1.83	0.29	0.16
	Average		0.422	0.565	0.733	0.195	0.358	0.123	0.044	0	0.018	0.011	1.84	0.30	0.16

Table F.2 Continued

Reactant	Samp.No.	Reaction Condition	C balance	H balance	O balance	Absolute Yield (Moles of Gas/Moles of Carbon in Reactant) CO2	H2	CO	CH4	C2H2	C2H4	C2H6	H2/CO2	H2,pot**	H2,t/ H2,p(*)
0.89 g/l Algae "QUENCH"	F1	650 C 106 s	0.749	1.073	1.105	0.352	0.433	0.070	0.189	0	0.036	0.033	1.23	0.57	0.20
	F2		0.767	1.065	1.153	0.372	0.417	0.062	0.191	0	0.035	0.035	1.12	0.56	0.19
	F3		0.743	1.079	1.130	0.374	0.437	0.042	0.191	0	0.034	0.033	1.17	0.56	0.20
	Average		0.753	1.072	1.129	0.366	0.429	0.058	0.19	0	0.035	0.034	1.17	0.56	0.19
	F4	650 C 53 s	0.815	1.260	1.152	0.358	0.545	0.090	0.202	0	0.042	0.040	1.52	0.65	0.25
	F5		0.730	1.100	1.081	0.338	0.495	0.079	0.170	0.002	0.037	0.033	1.46	0.56	0.22
	F6		0.691	1.066	1.046	0.337	0.488	0.058	0.164	0.001	0.035	0.030	1.45	0.54	0.22
	F7		0.676	1.076	1.011	0.324	0.501	0.060	0.163	0	0.035	0.030	1.55	0.55	0.23
	Average		0.728	1.126	1.073	0.339	0.507	0.072	0.175	0	0.037	0.037	1.50	0.58	0.23
	F8	650 C 26 s	0.670	1.087	0.960	0.277	0.548	0.118	0.145	0	0.037	0.028	1.98	0.56	0.25
	F9		0.677	1.136	0.960	0.279	0.587	0.114	0.145	0.002	0.041	0.027	2.10	0.58	0.26
	F10		0.628	1.073	0.872	0.250	0.546	0.109	0.144	0	0.037	0.025	2.18	0.55	0.25
	F11		0.673	1.035	0.970	0.279	0.502	0.120	0.148	0	0.038	0.025	1.80	0.55	0.23
	Average		0.662	1.083	0.941	0.271	0.546	0.115	0.146	0	0.038	0.026	2.01	0.56	0.25

Table F.2 Continued

Reactant	Samp.No.	Reaction Condition	C balance	H balance	O balance	Absolute Yield (Moles of Gas/Moles of Carbon in Reactant) CO2	H2	CO	CH4	C2H2	C2H4	C2H6	H2/CO2	H2,pot**	H2,t/ H2,p(*)
1.85 g/l Algae	G1	600 C 117 s	0.621	0.956	0.912	0.272	0.447	0.095	0.140	0	0.024	0.034	1.64	0.50	0.20
	G2		0.547	0.881	0.825	0.251	0.434	0.074	0.123	0	0.020	0.029	1.73	0.45	0.20
	G3		0.515	0.864	0.808	0.258	0.443	0.050	0.115	0	0.019	0.027	1.72	0.43	0.20
	G4		0.545	0.956	0.867	0.286	0.496	0.034	0.124	0	0.020	0.031	1.73	0.46	0.22
	Average		0.557	0.914	0.853	0.267	0.455	0.063	0.126	0	0.021	0.030	1.70	0.46	0.20
	G5	600 C 58 s	0.511	0.925	0.799	0.242	0.525	0.074	0.103	0	0.021	0.025	2.17	0.46	0.24
	G6		0.493	0.883	0.772	0.232	0.501	0.075	0.100	0	0.020	0.023	2.16	0.44	0.23
	G7		0.505	0.892	0.777	0.235	0.491	0.074	0.107	0	0.020	0.024	2.09	0.45	0.22
	G8		0.509	0.922	0.800	0.243	0.526	0.074	0.103	0	0.021	0.024	2.16	0.46	0.24
	Average		0.505	0.906	0.787	0.238	0.511	0.074	0.103	0	0.021	0.024	2.15	0.45	0.23

Table F.2 Continued

Reactant	Samp.No.	Reaction Condition	C balance	H balance	O balance	Absolute Yield (Moles of Gas/Moles of Carbon in Reactant) CO2	H2	CO	CH4	C2H2	C2H4	C2H6	H2/CO2	H2,pot**	H2,t/ H2,p(*)
1.85 g/l Algae	G9	650 C 106 s	0.655	1.041	0.968	0.333	0.428	0.011	0.168	0	0.025	0.047	1.29	0.50	0.19
	G10		0.638	0.986	0.958	0.329	0.402	0.012	0.161	0	0.024	0.044	1.22	0.48	0.18
	G11		0.626	0.988	0.941	0.324	0.411	0.011	0.161	0	0.023	0.042	1.27	0.48	0.19
	Average		0.640	1.005	0.956	0.329	0.414	0.011	0.163	0	0.024	0.044	1.26	0.49	0.19
	G12	650 C 53 s	0.634	1.079	0.974	0.327	0.520	0.028	0.152	0	0.026	0.038	1.59	0.52	0.23
	G13		0.585	1.034	0.890	0.301	0.506	0.021	0.142	0	0.024	0.036	1.68	0.49	0.23
	G14		0.595	1.062	0.917	0.307	0.535	0.027	0.141	0	0.024	0.036	1.74	0.51	0.24
	Average		0.605	1.058	0.927	0.312	0.520	0.025	0.145	0	0.025	0.037	1.67	0.51	0.23

Table F.2 Continued

Reactant	Samp.No.	Reaction Condition	C balance	H balance	O balance	Absolute Yield (Moles of Gas/Moles of Carbon in Reactant) CO2	H2	CO	CH4	C2H2	C2H4	C2H6	H2/CO2	H2,pot**	H2,t/ H2,p(*)
4.34 g/l Algae	I1	600 C 58 s	0.612	0.806	1.026	0.287	0.435	0.144	0.097	0	0.017	0.025	1.52	0.44	0.20
	I2		0.551	0.716	0.866	0.223	0.374	0.160	0.092	0	0.016	0.022	1.68	0.41	0.17
	I3		0.516	0.717	0.872	0.248	0.398	0.114	0.083	0	0.014	0.021	1.60	0.38	0.18
	Average		0.560	0.746	0.921	0.253	0.402	0.139	0.091	0	0.016	0.023	1.60	0.41	0.18
4.34 g/l Algae	I4	650 C 53 s	0.675	1.057	1.136	0.365	0.546	0.064	0.135	0	0.013	0.042	1.50	0.52	0.25
	I5		0.656	1.033	1.125	0.364	0.543	0.059	0.133	0	0.013	0.037	1.49	0.51	0.24
	I6		0.878	1.399	1.484	0.478	0.730	0.081	0.177	0	0.015	0.055	1.53	0.68	0.33
	Average		0.736	1.163	1.248	0.402	0.606	0.068	0.148	0	0.014	0.045	1.51	0.57	0.27

Table F.2 Continued

Reactant	Samp.No.	Reaction Condition	C balance	H balance	O balance	Absolute Yield (Moles of Gas/Moles of Carbon in Reactant) CO2	H2	CO	CH4	C2H2	C2H4	C2H6	H2/CO2	H2,pot**	H2,t/ H2,p(*)
1.5 g/l Water Hyacinth	K1	650 C 53 s	0.421	0.928	0.968	0.240	0.461	0.019	0.106	0	0.012	0.017	1.92	0.39	0.20
	K2		0.488	1.113	1.088	0.271	0.549	0.019	0.123	0	0.014	0.023	2.03	0.46	0.24
	K3		0.430	1.142	0.995	0.250	0.624	0.013	0.106	0	0.011	0.020	2.50	0.46	0.27
	K4		0.388	1.150	0.911	0.230	0.661	0.010	0.097	0	0.008	0.017	2.87	0.46	0.29
	K5		0.357	1.183	0.857	0.218	0.713	0.005	0.090	0	0.007	0.015	3.27	0.47	0.31
	K6		0.391	1.250	0.960	0.244	0.753	0.006	0.093	0	0.008	0.016	3.09	0.49	0.33
	Average		0.413	1.128	0.963	0.242	0.627	0.012	0.103	0	0.010	0.018	2.59	0.46	0.27

Table F.2 Continued

Reactant	Samp.No.	Reaction Condition	C balance	H balance	O balance	Absolute Yield (Moles of Gas/Moles of Carbon in Reactant) CO2	H2	CO	CH4	C2H2	C2H4	C2H6	H2/CO2	H2,pot**	H2,t/ H2,p(*)
1.98 g/l Kelp	M1	650 C 53 s	0.706	1.707	0.736	0.471	0.906	0.012	0.146	0	0.016	0.022	1.92	1.02	0.62
	M2		0.780	1.944	0.816	0.525	1.042	0.007	0.161	0	0.017	0.026	1.98	1.06	0.71
	M3		0.755	2.135	0.759	0.486	1.170	0.012	0.167	0	0.017	0.028	2.41	1.26	0.80
	M4		0.789	2.281	0.812	0.524	1.272	0.005	0.172	0	0.016	0.028	2.43	1.34	0.86
	M5		0.730	2.276	0.745	0.481	1.293	0.004	0.163	0	0.015	0.026	2.69	1.32	0.88
	M7		0.728	2.276	0.743	0.479	1.294	0.005	0.164	0	0.014	0.026	2.7	1.33	0.88
	M8		0.719	2.096	0.736	0.475	1.166	0.004	0.162	0	0.015	0.024	2.45	1.32	0.79
	M9		0.770	2.029	0.814	0.525	1.115	0.005	0.163	0	0.016	0.022	2.12	1.20	0.76
	M10		0.704	2.056	0.722	0.466	1.145	0.004	0.160	0	0.015	0.022	2.46	1.22	0.78
	Average		0.742	2.089	0.765	0.492	1.156	0.006	0.162	0	0.016	0.025	2.35	1.23	0.78

(*) Fraction of Potential Hydrogen Realized

(**) Fraction of Potential Hydrogen Realized including H2 from CO and CH4

APPENDIX G

QUALITATIVE ANALYSIS OF ALGAE AND KELP USING X-RAY DIFFRACTION

Source of analysis: Eric Decarlo, Geophysics Department, University of Hawaii

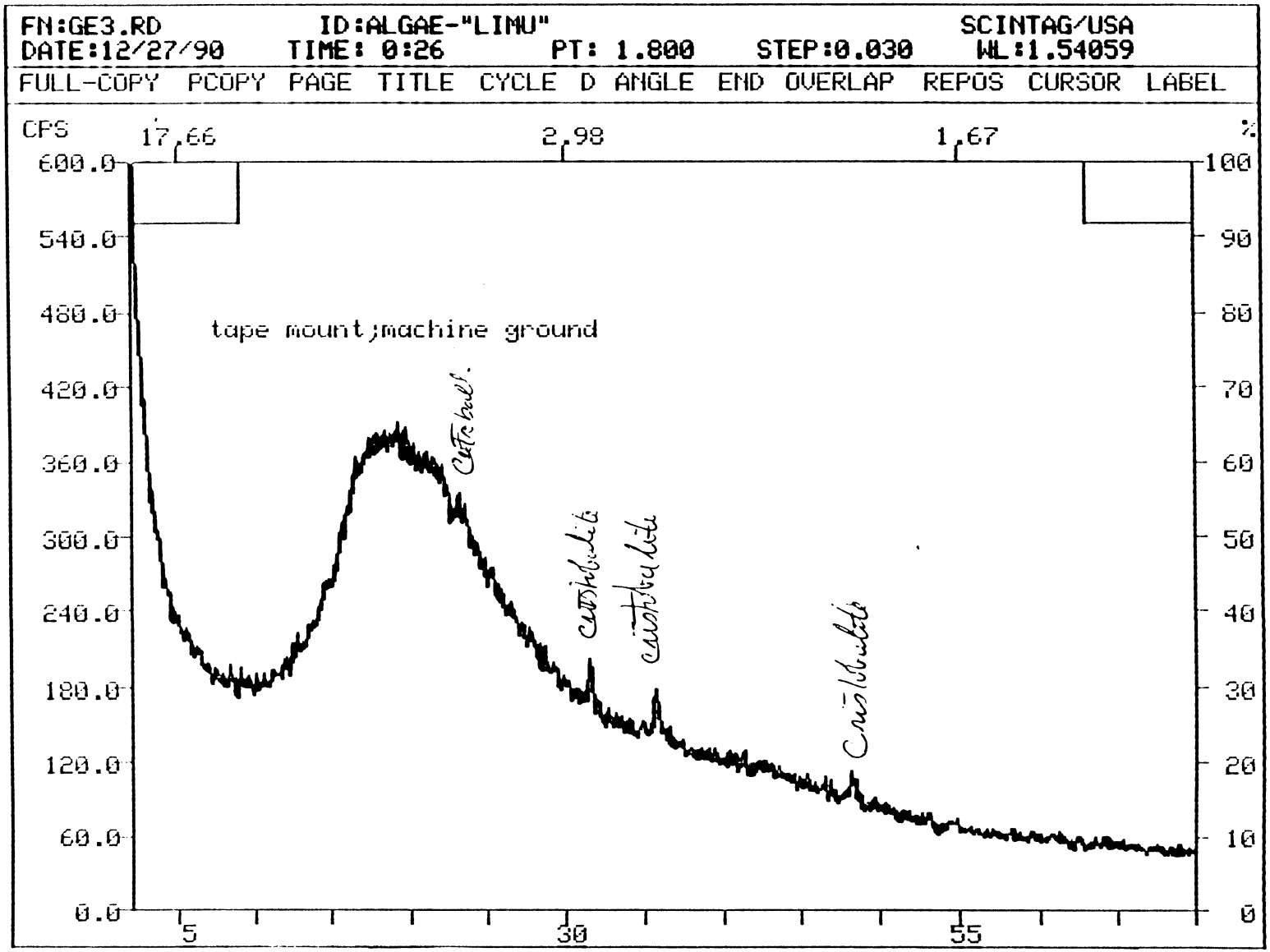
FN:GE3.RD
ID:ALGAE-"LIMU"
SCINTAG/USA
DATE:12/27/90
TIME: 0:26
PT: 1.800
STEP:0.030
WL:1.54059
FULL-COPY PCOPY PAGE TITLE CYCLE D ANGLE END OVERLAP REPOS CURSOR LABEL
CPS
17.66
2.98
1.67
%
600.0
540.0
480.0
420.0
360.0
300.0
240.0
180.0
120.0
60.0
0.0
100
90
80
70
60
50
40
30
20
10
0
5
30
55
tape mount;machine ground

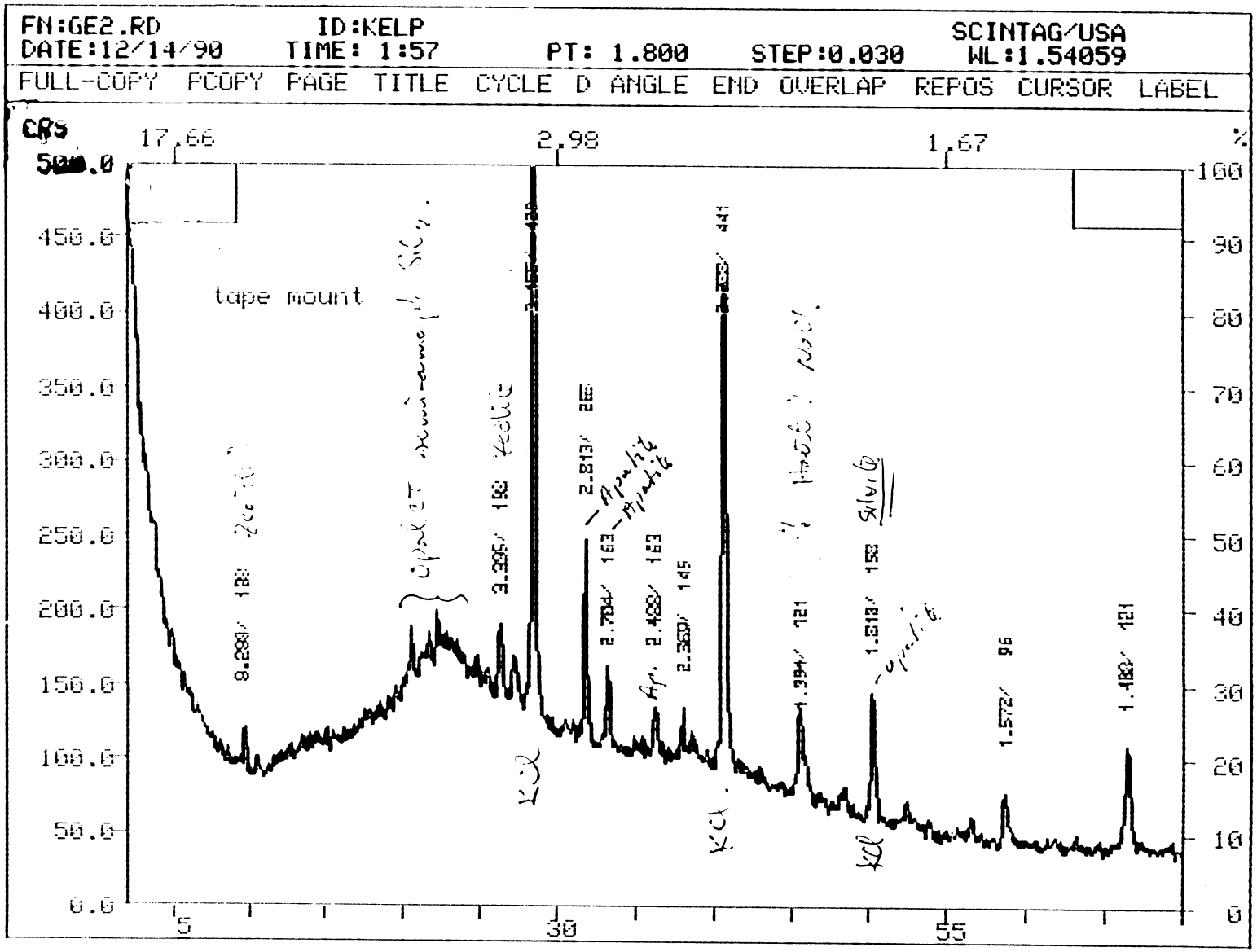
FN:GE2.RD
ID:KELP
SCINTAG/USA
DATE:12/14/90
TIME: 1:57
PT: 1.800
STEP:0.030
WL:1.54059
FULL-COPY PCOPY PAGE TITLE CYCLE D ANGLE END OVERLAP REPOS CURSOR LABEL
CPS
17.66
2.98
1.67
%
tape mount
8.288
3.395
2.813
2.784
2.488
2.359
1.394
1.572
1.488
441
183
163
153
145
121
96
450.0
400.0
350.0
300.0
250.0
200.0
150.0
100.0
50.0
0.0
100
90
80
70
60
50
40
30
20
10
0
5
30
55

REFERENCES

Abraham, M. A. and Klein, M. T., Pyrolysis of Benzyl Phenyllamine Neat and Tetralin, Methanol and Water Solvent, Ind. Eng. Chem. Prod. Res. Dev., 24, 1985, pp.300-306.

Abraham, M. A. and Klein, M. T., Solvent Effects During the Reaction of Coal Model Compounds, Supercritical Fluids, ACS Symposium Series No.329, 1987.

Amin, S., Reid, R. C. and Modell, M., Reforming and Decomposition of Glucose in Aqueous Phase, Presented at the Intersociety Conference on Environmental Systems, San Francisco, 21-24 July 1975.

Antal, M. J., Jr., Biomass Pyrolysis, A Review of the Literature. Part 1: Carbohydrate Pyrolysis, Advances in Solar Energy (Eds Boer, K. W. and Duffie, J. A.) vol.1, American Solar Energy Society, New York, 1984.

Antal, M. J., Jr., Brittain, A., De Almeida, C., Ramayya, S. and Roy, J. C., Heterolysis and Homolysis in Supercritical Water, ACS Symposium Series No.329, 1987.

Antal, M. J., Jr., Biomass Engineering: Thermochemical Conversion Research Needs, Hawaii Natural Energy Institute, University of Hawaii, Honolulu, 1984.

Antal, M. J., Jr., Biomass Pyrolysis, A Review of the Literature. Part 2: Lignocellulose Pyrolysis, Advances in Solar Energy (Eds Boer, K. W. and Duffie, J. A.) vol.2, Plenum Press, New York, 1985.

Antal, M. J., Jr., Mok, W. S. L., Roy , J. C., T-Raissi, A. and Anderson, D. G. M., Pyrolytic Sources of Hydrocarbons from Biomass, J. Anal. App. Pyrolysis, 8, 1985, pp.291-303.

Baillod, C. R., Lamparter, R. A., and Barna, B. A., Wet Oxidation for Industrial Waste Treatment, Chem. Eng. Prog., 1985, pp.52-56.

Beckman, D. and Boocock D. G., Liquefaction of Wood by Rapid Hydropyrolysis, Can. J. Chem. Eng., 61, 1983, pp.80-86.

Boocock, D. G. B. and Sherman, K. M., Future Aspects of Powdered Poplar Wood Liquefaction by Aqueous Pyrolysis, Can. J. Chem. Eng., 63, 1985, pp.627-633.

Bruges, E. A. and Gibson, M. R., J. Mech. Eng. Sci., 11, 1969, pp.189-205.

Buelow, S. J., Dyer, R. B., Rofer, C. K., Atencio, J.H. and Wander J. D., Advanced Techniques for Soil Remediation: Destruction of Propellant Components in Supercritical Water, Proceedings of the Workshop on the Alternatives to Open Burning/Open Detonatoion of Propellants and Explosives, Los Alamos National Laboratory, New Mexico, 1981.

Butner, R. S., Elliott, D. C. and Sealock, L. J., Jr., Development of Water-slurry Gasification Systems for High-Moisture Biomass, Energy from Biomass and Wastes IX, presented at Lake Buena Vista, Florida, Jan.-Feb.,1985.

Butner, R. S., Sealock, L. J., Jr., Elliott, D. C. and Neuenschwander, G. G., Thermochemical Conversion of High-Moisture Biomass Feedstocks, Thermochemical Conversion Program, Annual Review Meeting at the Solar Energy Research Institute, June 21-22, 1989.

Connolly, J. F., Solubility of Hydrocarbon in Water near the Critical Solution Temperature, J. Chem. Eng. Data, 11, 1966, pp. 13-16.

De Almeida, C. P., Sulfuric Acid Catalyzed Ethanol Dehydration in SCW, M.S.Thesis, University of Hawaii, 1986.

DeAngelo, D. J., and Wilhelmi, A. R., Wet Air Oxidation of Spent Caustic Liquors, Chem. Eng. Prog., March 1983, pp.68-73.

Deshpande, G. V., Holder, G. D. and Shah, Y. T., Effect of Solvent Density on Coal Liquefaction Kinetics, Supercritical Fluids, ACS Symposium Series No.329, 1987.

Dietrich, M. J., Randall, T. L. and Canney, P. J., Wet Air Oxidation of Hazardous Organics in Wastewater, Environmental Progress, 4(3), 1985, pp.171-177.

Eckert, C. A., Van Alsten, J. G. and Stoicos, T., Supercritical Fluid Processing, Environmental Science & Technology, 20(4), 1986, pp.319-325.

Elliott, D. C., Sealock, L. J., Jr., Baker, E. G., Butner, R. S. and Neuenschwander, G. G., Low Temperature Conversion of High-Moisture Biomass Continuous Reactor System Results, Pacific Northwest Laboratory, October 1989.

Flynn, B. L., Jr. and Flemington, W. Va., Wet Air Oxidation of Waste Streams, Chem. Eng. Prog., 1979, pp.66-69.

Franck, E. U., Water and Aqueous Solutions at High Pressures and Temperatures, Pure Appl. Chem., 24(1), 1970, pp.13-30.

Franck, E. U., Thermophysical properties of Supercritical Fluids within Special Consideration of Aqueous Systems, Fluid Phase Equilibrium, 10(2-3), 1983, pp.211-222.

Franck, E. U., Hartmann, D. and Hensel, F., Proton Mobility in Water at High Temperatures and Pressures, J. Phys. Chem., 72, 1968, pp.200-206.

Franck, E. U., Supercritical Water, Endeavor, 27, 1968, pp. 55-59.

Gregory, D. P., The Hydrogen Economy, Scientific American, 228(1), 1973, pp.13-21.

Helling, R. K. and Tester, J. W., Oxidation Kinetics of Carbon Monoxide in Supercritical Water, Energy & Fuels, 1(5), 1987, pp.417-423.

Houser, T. J., Tsao, C., Dyla, J. E., Van Attan, M. K. and McCarville, M. E., The Reactivity of Tetrahydroquinoline, Benzylamine and Dibenzyl with Supercritical Water, Fuel, 68, 1989, pp.323-327.

Huppert, G. L., Wu, B. C., Townsend, S. H., Klein, M. T. and Paspek, S. C., Ind. Eng. Chem. Res., 28, 1989, pp.161-165.

Johnson, J. E., An Economic Perspective on Hydrogen fuel, Plenum Press, New York, 1975, pp.299-308.

Koufopanos, C., Mashio, G., Paci, M. and Lucchesi, A., Some Kinetic Aspects of the Pyrolysis of Biomass Components, Energy from Biomass: 3rd. EC Conference (Eds. Palz, W., Coombs, J. and Hall, D. O.), Elsevier Applied Science Publishers, London, 1985, pp.837-841.

Laidler, K. J., Chemical Kinetics, 3rd ed., Harper & Row Publishing, New York, 1987.

Lamb, W. J., Hoffman, G. A. and Jonas, J., Self-Diffusion in Compressed Supercritical Water, J. Chem. Phys., 74 (12), 1981, pp.6875-6880.

Leesomboon, T., A study of Catalytic Reaction Chemistry of Five and Six Carbon Sugars in Near-Critical Water, M.S.Thesis, University of Hawaii, 1988.

Levenspiel, O., Fundamental of Chemical Reactor Engineering, 2nd ed., John Wiley & Sons, New York, 1972.

Lucchesi, A., Maschio, G., Rizzo, C. and Giusto, S., A Pilot Plant for the Study of the Production of Hydrogen-rich Syngas by Gasification of Biomass, Res. Thermochem. Convers., Elsvier London, 1988, pp.642-654.

Lucchesi, A. and Maschio, G., Study on the Pyrolysis of Agricultural Wastes Proceedings of the Workshop and EC Contractors' Meeting, Energy from Biomass, 1983, Series E, Volume 5, Eds. Palz, W. and Pirrwitz, D. and Redel, D. Publishing Company, Dordrecht, 1984, pp.289-296.

Maddocks, R. R. and Gibson, J., Supercritical Extraction of Coal, Chem. Eng. Prog., 73, 1977, pp.55-63.

Maddocks, R. R., Gibson, J. and Williams, D. F., Supercritical Extraction of Coal, Chem. Eng. Prog., 1979, pp.49-55.

Mark, H. F., Othmer, D. F., Overberger, C. G. and Seaborg, G. T., Encyclopedia of Chemical Technology, vol. 12, 3rd. ed., John Wiley & Sons, 1978.

Marshall, W. L., Rev. Pure Appl. Chem., 18, 1968, pp.167-168.

Marshall, W. L. and Franck, E. U., Ion Product of Water Substance, 0-1000°C, 1-10,000 Bars New International Formulation and Its Back Ground, J. Phys. Chem. Ref.

Data, 10 (2), 1981, pp.295-304.

Marshall, W. L., Water at High Temperatures and Pressures, Chemistry, 48(2), 1975, pp.6-12.

McGinnis, G. D., Wilson, W. W., Prince, S. E. and Chen, C. C., Conversion of Biomass into Chemicals with High-Temperature Wet Oxidation, Ind. Eng. Chem. Prod. Res. Dev., 22, 1983, pp.633-636.

Modell, M., Gaudet, G. G., Simmon, M., Hong, G. T. and Biemann, K., Supercritical Water Testing Reveals Process Holds Promise, Solid Waste Management, 1982.

Modell, M., Gasification and Liquefaction of Forest Products in Supercritical Water, Fundamentals of Thermochemical Biomass Conversion, Elsevier Applied Science Publishers, 1982, pp.95-119.

Modell, M., Standard Handbook of Hazardous Waste Treatment and Disposal, Ed. Freeman, H. M., Section 8.11, McGraw Hill, 1989.

Modell, M., Reid, R. C. and Amin, S., Gasification Process, U.S. Patent 4, 113, 446, September 12, 1978.

Mudge, L. K., Baker, E. D., Mitchell, D. H. and Brown, M. D., Catalytic Steam Gasification of Biomass for Methanol and Methane Production, Journal of Solar Energy Engineering, 107, 1985, pp.88-92.

Padmapriya, R., Gadgil, K., Dastidar M. G. and Sarkar, M. K., Steam Pyrolysis of Biomass, Indian Journal of Technology, 27, 1989, pp.35-38.

Paulaitis, M. E., Penninger, J. M. L., Gray, R. D., Jr. and Davidson, P., Chemical Engineering at Supercritical Fluid Conditions, Ann Arbor Science, Ann Arbor, 1983.

Quist, A. S., The Ionization Constant of Water to 800° and 4000 Bars, J. Phys. Chem., 74(18), 1970, pp.3396-3402.

Quist, A. S., Marshall, W. L. and Jolley, H. R., J. Phys. Chem., 69, 1965, pp.2726-2735.

Ramayya, S. V. et al., Acid Catalyzed Dehydration of Alcohols in SCW, Fuel, 66, 1987, pp.1364-1371.

Reed, B. T., Gasification Principles and Technology, Noyes Data Corporation, New Jersey, 1981.

Rofer, C. K., Oxidation of Hydrocarbons and Oxygenates in Supercritical Water, Los Alamos Report LA-11700-MS, 1989, DOE/HWP-90.

Rofer, C. K. and Streit, G. E., Kinetics and Mechanism of Methane Oxidation in Supercritical Water, Los Alamos Report LA-11439-MS, 1988, DOE/HWP-64.

Rofer C. K., Kinetics Experiments and Bench-Scale System; Background, Design and Preliminary Experiments, Los Alamos National Laboratory, New Mexico, 1987.

Rofer, C. K. and Wander, J. D., Proceedings of the Workshop on Supercritical Fluid Processing of High Risk Wastes, Los Alamos Natural Laboratory, New Mexico, 1989.

Ross, D. S., Hum, G. P., Miin, T. C. and Mansani, R., Isotope Effects in Supercritical Water: Kinetic Studies of Coal Liquefaction, Supercritical Fluids, ACS Symposium Series No 329, 1987, pp.242-250.

Samir, S. S. and Oskar, R. Z., Biomass Conversion Processes for Energy and Fuels, Plenum Press, New York, 1981.

Schiefelbein, G. F., Biomass Thermal Gasification Research Program, Biomass, 19, 1989, pp.145-159.

Sealock, L. J., Jr., Elliott, D. C., Butner, R. S. and Neuenschwander, G. G., Low-Temperature Conversion of High-Moisture Biomass, Topical Report Jan. 1984 - Jan. 1988, October 1988.

Simmons, M. B. and Klein, M. T., Free-Radical and Concerted Reaction Pathways in Dibenzyl Ether Thermolysis, Ind. Eng. Chem. Fundam., 24, 1985, pp.55-60.

Spencer, B. C. H., Waterweed Invasions, Scientific American, October 1989.

Staszak, C. N., Malinowski, K. C. and Killilea, W. R., The Pilot-Scale Demonstration of the MODAR Oxidation Process for the Destruction of Hazardous Organic Waste Materials, Environmental Progress, 6(1), February 1987, pp.39-43.

Subramanlam, B. and McHugh M. A., Reactions in Supercritical Fluids-A Review, Ind. Eng. Chem. Process. Des. Dev., 25(1), 1986, pp.1-12.

Thomason, T. B. and Modell, M., Supercritical Water Destruction of Aqueous Wastes, Hazardous Waste, 1(4), 1984, pp.453-467.

Towne, S. E., Shah, Y. T. Holder, G. D., Deshpande, G. V. and Cronauer, D. C., Liquefaction of Coal Using Supercritical Fluid Mixtures, Fuel, 64(5), 1985, pp.883-889.

Townsend, S. H., Abraham, M. A., Huppert, G. L., Klein, M. T. and Paspek, S. C., Ind. Eng. Chem. Res., 27, 1988, pp.143-149.

Townsend, S. H. and Klein, M. T., Dibenzyl Ether as a Probe into the Supercritical Fluid Solvent Extraction of Volatiles from Coal with Water, Fuel, 64(5), 1985, pp.635-638.

Tsang, W. and Huie, R. E., Chemical Kinetics in Supercritical Water, Chemical Kinetics Division, National Institute of Standards and Technology, Gaithersbury, Maryland 20899.

Urban, D. L. and Antal, M. J., Jr., Study of the Kinetics of Sewage Sludge Pyrolysis using DSC and TGA, Fuel, 61, September, 1982.

Vaclav, S., Biomass Energies, Plenum Press, New York, 1983.

Van Wylen, G. J. and Sonntag, R. E., Fundamentals of Classical Thermodynamics, Second edition, John Wiley and Sons, 1978.

Veziroglu, T. N., The Future Energy System: Hydrogen Economy, WHEC TREK '90 WORLD HYDROGEN CONFERENCE #8, July 22-27, 1990.

Webley, P. A. and Tester, J. W., Fundamental Kinetics of Oxidation in Supercritical Water, 1989.

Webley, P. A. and Tester, J. W., Fundamental Kinetics and Mechanistic Pathways for Oxidation Reactions in Supercritical Water, SAE Technical Paper Series, 18th Intersociety Conference on Environmental Systems, San Francisco, California, July 11-13, 1988.

Welhelmi, A. R. and Zimpro, P. V., Wet Air Oxidation - An Alternative to Incineration, Chem. Eng. Prog., 1979, pp.46-52.

West, A. B. and Gray, M. R., Pyrolysis of 1,3-Butanediol as a Model Reaction for Wood Liquefaction in Supercritical Water, Can. J. Chem. Eng., 65, 1987, pp.645-650.

Yang, H. H. and Eckert, C. A., Homogeneous Catalysis in the Oxidation of p-chlorophenol in Supercritical Water, Ind. Eng. Res., 27, 1988, pp.2009-2014.

Zimmermann, F. J., Wet Air Oxidation, Industrial Water & Wastes, July-August, 1961, pp.102-106.

HYDROGEN PRODUCTION BY GASIFICATION OF GLUCOSE AND WET BIOMASS IN SUPERCRITICAL WATER

Supaporn Manarungson, William S. Mok and Michael J. Antal, Jr.
Department of Mechanical Engineering, University of Hawaii,
Honolulu, Hawaii, 96822, U.S.A.

Abstract

Glucose was used as a model reactant to determine practical conditions for wet biomass gasification in supercritical water. The factors influencing the conversion and gas yields of wet biomass gasification are temperature, residence time, initial concentration, and the feedstock. The primary gas products of both glucose and wet biomass gasification are H_2 and CO_2. The estimated carbon conversion of glucose (66-71%) is lower than that of wet biomass (74-87%) at 550°C and 28 seconds. The ratio of H_2 to CO_2 for glucose and wet biomass gasification are 1.6:1.0 and 2.2:1.0 respectively at the same conditions. For glucose, molar H_2 yield in excess of 500 % was achieved. Higher yield can be expected with further increases in temperature and residence time. The result agrees with global reaction for steam gasification of carbohydrate:

$$C_6H_{10}O_5 + 7\ H_2O \quad ----> \quad 6\ CO_2 + 12\ H_2$$

1. INTRODUCTION

Land biomass has always been used to produce energy and fuels. However, aquatic biomass, which constitutes one of the world's largest available biomass feedstock, has not been regarded as a potential fuel source because of its high moisture content and the high cost of water removal. Supercritical fluid, such as supercritical water (SCW), plays an important role as a solvent media in both chemical reactions and extraction processes. Currently, in the MODAR process, SCW is applied with the gasification process to oxidize organic wastes to destroy toxic substances [1]. Pyrolytic gasification is a high temperature thermochemical process, which converts biomass to fuels and other useful organic materials. The objective of this project is to use this biomass, in its wet form, to produce hydrogen gas by a pyrolytic gasification process in SCW.

2. PREVIOUS RESEARCH

Pyrolytic gasification has been used to yield either fuel gases or liquid products. Very few investigaters have studied the

gasification of biomass in SCW. Modell studied the gasification of forest products in SCW to produce liquid and gaseous fuels [2]. In US Patent No. 4,113,446, it was revealed that the products of the reaction of some organic material include CO, H_2, CO_2, CH_4 and light hydrocarbons and liquid organics at 374°C and 218 atm [3]. Also, there is no char formation at that condition. The effect of oxygen on the reactant conversion in SCW has been studied by a few investigators. Webley and Tester modeled and presented the independence of methanol conversion on oxygen in global kinetic expressions [4]. Eckert and Lemarn studied the kinetics of the uncatalyzed and homogeneously catalysed oxidation of p-chlorophenol in water near the critical point [5]. They found that the rate of disappearance of p-chlorophenol is unaffected by oxygen concentration. Helling and Tester also found that the rate of global expression for the oxidation of CO in SCW is zeroth order for oxygen [6].

3. EXPERIMENTAL APPARATUS AND PROCEDURES

The supercritical fluid reactor, decribed in an earlier publication [7],[8] was modified to accomodate a slurry feed reservoir for this study (see Figure 1). Initially, glucose was used as a reactant model. For the wet biomass gasification experiment, algae (Gracilaria sp.), kelp and sewage sludge were chosen as representative materials.

4. RESULTS AND DISCUSSION

Glucose Gasification in Supercritical Water

The gasification of glucose in SCW to produce hydrogen was studied over the temperature range 400-550°C at 25.0-34.5 MPa. The influences of temperature, reactant concentration and oxygen on the carbon balance and the gaseous product yields were studied.

The effect of temperature is shown in Table I. Increasing the temperature of the reaction increases the carbon balance and yields of CO_2 and H_2 while CO remains constant over the temperature range of 460-550°C. Tables II and III display the effect of residence time. Time affects the carbon balance and CO_2, H_2, and CO in the same way as temperature.

Table IV displays the effect of reactant concentration, comparing the results of 0.01M to 0.05M glucose at both 550 and 500°C. The carbon balance, CO_2, H_2, and CH_4 decrease when the concentration of reactant increases. The slight increase of CO_2 observed when the concentration increases from 0.005 to 0.01 M at 28 seconds residence time is probably not significant.

The effect of oxygen was examined with dihydroxyacetone (DHA) and glucose as the reactants and hydrogen peroxide (H_2O_2) as the oxidizer. Hydrogen peroxide decomposes in the reactor to provide

free oxygen. Table V contains the data of experiment with 0.005M and 0.01M DHA and 0.005M glucose, with and without hydrogen peroxide. The presence of oxygen increases the carbon balance and CO_2, but decreases the yield of hydrogen. These results suggest that oxygen selectively attacks and oxidizes the gaseous products, lowering the yield of hydrogen gas. Because of this negative effect, no further studies of partial oxidation was conducted.

As a next step towards more complicated feedstock, soluble starch was studied as a reactant. This material was chosen because its solubility permits the preparation of a homogeneous polymeric feed solution. Comparing the gasification of soluble starch and glucose, soluble starch gives higher carbon balance and CO, but lower CO_2 and H_2 than glucose at the same reaction condition. The results are shown in Table VI. In Table VII, results of a study of residence time effect on starch gasification are displayed. As in the case of glucose, the higher yields of gas and carbon conversion are observed with increasing residence time.

Experiment with model compounds indicate that high yields (up to 500% molar yield) of hydrogen can be obtained from gasification in SCW. Yields are improved at high temperature (>500°C); long residence time (>1 minute); and low reactant concentration (0.9 gm/liter). Base on these preliminary results, the following practical condition for wet biomass gasification was determined: 480-550°C; 34.5 MPa; and 28 seconds residence time.

Wet Biomass Gasification

From the study of gasification of glucose in SCW, a practical condition of 550°C and 34.5 MPa was chosen to study the gasification of wet biomass in SCW to produce hydrogen. The influences of the reactant and reactant concentration on carbon balance and gaseous products were determined. The carbon balance and yields of gas from wet biomass are calculated by using the chemical compositions determined by an independent laboratory (see Table VIII). The primary gas products in every experiment are H_2 and CO_2, but the ratio of the two gases varies.

The first experiment was gasification of algae in SCW. Carbon balance and the yields of gases from a solution of 1.121 gm algae/liter at a residence time of 28 seconds is shown in Table IX. The ratio of H_2 and CO_2 is about 2.2:1.0. The estimated carbon conversion is in the range of 74 to 87%, which is higher than that from the glucose experiment (66 to 71%) at the same condition.

The second experiment was a control experiment. The purpose of this experiment was to see if there is any reaction between water and the wall of reactor at the reactant condition. Little amount of gas product (less than 5% of H_2 gas yield from the algae experiment) was obtained. This shows that the reaction between H_2O and the carbon deposits on the inside wall of the reactor does not

contribute significantly to the gas yields of the algae experiment.

The results of the algae gasification at higher concentration are also displayed in Table IX. The algae concentration is about three times the previously-mentioned experiment (3.336 gm algae/liter of solution). The operating condition is 520°C, 31.7 MPa, and 25 seconds residence time. The effects of initial reactant concentration and temperature on carbon balance and gas yields of this experiment are the same as the glucose gasification experiment. The carbon balance and gas yields are lower when initial reactant concentration increases but temperature decreases. The ratio of H_2 and CO_2, which are major products, is about 2.5:1.0.

A third algae experiment was conducted at 550°C, 34.5 MPa, and 49 seconds residence time. The results of sample no.M1 are obviously different from the other two. The carbon balance and gas yields of sample no.M1 are very much lower than those of the others. Some of the algae feeding and passing through the reactor settled and accumulated on the bottom of the reactor, resulting in non-homogeneous mixture. The changing concentration with respect to time would account for the large variations in observed gas yields.

For kelp gasification, the operating condition was 550°C, 34.5 MPa, and 49 seconds residence time. Two initial concentrations, 7.78 and 25.0 gm kelp/liter of solution, were studied. The results are shown in Table X. In the experiment of 25.0 gm/liter, the total amount of gas product was collected from the accumulator. The carbon balance and gas yields for kelp, compared to those of algae gasification, are lower.

In the case of sewage sludge gasification, the chemical composition of sewage sludge was assumed to be the same as that of raw sewage sludge reported by Urban and Antal [9] (see Table VIII). Carbon balance and gas yields of this experiment are generally lower than those of the above (see Table XI).

5. CONCLUSION

In supercritical water with temperature equal or higher than 500°C and residence time equal or longer than 30 seconds steam gasification of biomass is observed. Noting that the hydrogen balance based only on the organic reactant exceeds unity, and that H_2 to CO_2 product ratio close to 2:1 was observed, the global stoichiometry of the governing reaction appears to be :

$$C_6H_{10}O_5 + 7\ H_2O \text{ -----> } 6\ CO_2 + 12\ H_2$$

Hydrogen and carbon dioxide products exiting the reactor are available at 5000 psi and high temperature which is ideal for the synthesis of methanol. Alternatively, the gas can be quenched at

high pressure, and seperated to generate pure hydrogen without extra cost by a controlled reduction of pressure.

REFERENCES

1. Modell, M., G.G. Gaudet, M. Simson, G.T. Hong and K. Biemann, 1982, "Supercritical Water; Testing Reveals New Process Holds Promise", Solid Wastes Management, August.
2. Modell, M. 1982, "Gasification and Liquefaction of Forest Products in Supercritical Water", Fundamentals of Thermochemical Biomass Conversion", Elsvier Applied Science Publishers, pp.95- 119.
3. Modell, M., R.C. Reid and S.I. Amin, 1978, "Gasification Process", US Patent 4,113,446, September 12.
4. Webley, P.A., and J.W. Tester, Report on the Fundamental Kinetics of Oxidation in Supercritical Water.
5. Eckert, C.A., and G.W. Leman, Homogeneous Catalysis for Wet Oxidation Design and Economic Feasibility of a Mobile Detoxification Unit, Final Report.
6. Helling, R.K., and J.W. Tester, 1987, "Oxidation Kinetics of Carbon Monoxide in Supercritical Water", J.Energy and Fuels: vol.1, no. 5, pp. 417-423.
7. Mok, S.W., M.J. Antal, Jr., and M. Jones, Jr., 1989, "Formation of Acrylic acid from Lactic Acid in Supercritical Water", J. Org. Chem.: vol.54. no.19, pp.4956-4602.
8. Ramayya, S., A. Brittain, C. DeAlmeida, W. Mok and M.J. Antal, Jr., 1987, "Acid-Catalysed Dehydration of Alcohols in Supercritical Water", Fuel, vol.66, October, pp.1363-1370.
9. Urban, L.D.,and M.J. Antal, Jr., 1982, "Study of the Kinetics of Sewage Sludge Pyrolysis Using DSC and TGA", Fuel, vol.61, September, pp.799-806.

Document Control Page	1. NREL Report No. TP-230-4634	2. NTIS Accession No. DE9210583	3. Recipient's Accession No.

4. Title and Subtitle
Hawaii Integrated Biofuels Research Program Final Subcontract Report: Phase III

5. Publication Date
May 1992

6.

7. Author(s)
Hawaii Natural Energy Institute

8. Performing Organization Rept. No.

9. Performing Organization Name and Address

Hawaii Natural Energy Institute
University of Hawaii
Holmes Hall 246
2540 Dole Street
Honolulu, HI 96822

10. Project/Task/Work Unit No.
BF251010

11. Contract (C) or Grant (G) No.

(C)

(G)

12. Sponsoring Organization Name and Address

National Renewable Energy Laboratory
1617 Cole Blvd.
Golden, CO 80401

13. Type of Report & Period Covered
Technical report

14.

15. Supplementary Notes

16. Abstract (Limit: 200 words)
The U. S. Department of Energy's (DOE) Hawaii Biofuels Program is focused on providing a technology data base for converting biomass feedstocks indigenous to Hawaii to liquid fuels or electricity. This report is a compilation of studies done to develop an integrated set of strategies for the production of energy from renewable resources in Hawaii. Because of the close coordination between this program and other ongoing DOE research, the work will have broad-based applicability to the entire United States.

17. Document Analysis

a. Descriptors
biomass, feedstocks, liquid fuels, electricity, renewable energy technologies

b. Identifiers/Open-Ended Terms

c. UC Categories 243

18. Availability Statement
National Technical Information Service
U.S. Department of Commerce
5285 Port Royal Road
Springfield, VA 22161

19. No. of Pages
548

20. Price
A23

Form No. 0069E (6-30-87)